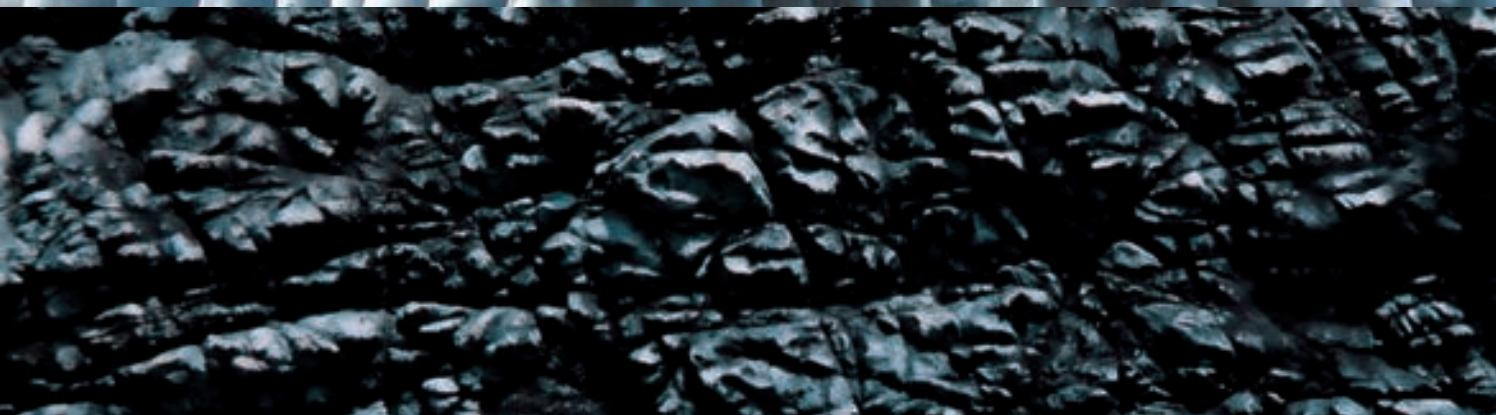


# KARST ROCK FEATURES KARRREN SCULPTURING

Editors: Angel Ginés, Martin Knez, Tadej Slabe, Wolfgang Dreybrodt



# C A R S O L O G I C A

---

KARST ROCK FEATURES • KARREN SCULPTURING  
Editors: Angel Ginés, Martin Knez, Tadej Slabe, Wolfgang Dreybrodt



## Carsologica 9

Urednik zbirke / Series Editor Franci Gabrovšek

Angel Ginés, Martin Knez, Tadej Slabe, Wolfgang Dreybrodt (Eds.)  
KARST ROCK FEATURES – KARREN SCULPTURING

Recenzenta / Reviewed by Andrej Kranjc in/and Rajko Pavlovec  
Jezikovni pregled /  
Language review Alenka Možina, Trevor Shaw, Wayne Tuttle  
Oblikovanje in prelom /  
Design and typesetting Brane Vidmar  
Oblikovanje ovitka / Cover design Barbara Hiti  
Risane priloge / Drawing Iztok Sajko  
Obdelava fotografij / Photo editing Marko Zaplatil

Izdajatelj / Issued by Inštitut za raziskovanje krasa ZRC SAZU, Postojna /  
Karst Research Institute ZRC SAZU, Postojna

Zanj / Represented by Tadej Slabe

Založnik / Published by Založba ZRC / ZRC Publishing, Ljubljana  
Za založnika / For the publisher Oto Luthar  
Glavni urednik / Editor-in-Chief Vojislav Likar

Tisk / Printed by Littera picta d. o. o., Ljubljana  
Naklada / Printrun 600

Izdajo knjige je podprla Javna agencija za raziskovalno dejavnost RS  
Subsidized by Slovenian Research Agency

Digitalna verzija (pdf) je pod pogoji licence <https://creativecommons.org/licenses/by-nc-nd/4.0/>  
prosto dostopna: <https://doi.org/10.3986/9789610502968>.

CIP - Kataložni zapis o publikaciji  
Narodna in univerzitetna knjižnica, Ljubljana

551.44(082)

KARST rock features = Karren sculpturing / editors Angel Ginés  
... [et al.] ; [risane priloge Iztok Sajko]. - Ljubljana : Založba ZRC =  
ZRC Publishing, 2009. - (Carsologica ; 9)

ISBN 978-961-254-161-3

1. Vzp. stv. nasl. 2. Ginés, Angel  
248380928

© 2009, Založba ZRC, ZRC SAZU.

All rights reserved. No part of this publication may be reproduced, stored in a retrieval system or transmitted, in any form or by any means, electronic, mechanical, photocopying, recording or otherwise, without the prior permission of the publisher.

# **KARST ROCK FEATURES**

# **KARREN SCULPTURING**

Editors:

**Angel Ginés**

**Martin Knez**

**Tadej Slabe**

**Wolfgang Dreybrodt**

**Postojna – Ljubljana 2009**



# FOREWORD

Rock forms are important traces of the formation and development of surface karst features. On various karren their record is especially rich, revealing to us the many factors that in diverse conditions formed the karst surface on various carbonate and other rock.

We have tried to present the most characteristic rock forms and through them the most important factors and processes in the formation of the karst surface, the methods of studying them, and the most outstanding examples.

Forty-nine contributing authors offer a wide spectrum of content and examples of rock forms from many karst regions around the world.

During the preparation of the book, many new and interesting discoveries emerged that strongly encouraged further research into this extremely indicative and often aesthetically attractive part of our karst natural heritage.

The Editors



# CONTENTS

## ROCK FORMS

1	Karrenfield landscapes and karren landforms .....	13
	Angel Ginés	
2	Physics and chemistry of dissolution on subaerially exposed soluble rocks by flowing water films .....	25
	Wolfgang Dreybrodt and Georg Kaufmann	
3	Biokarstic processes associated with karren development .....	37
	Heather Viles	
4	Karren simulation with plaster of Paris models .....	47
	Tadej Slabe	
5	The problem of rillenkarrren development: a modelling perspective .....	55
	Matija Perne and Franci Gabrovšek	
6	Some methodologies on karren research .....	63
	Gábor Tóth	
7	Microrills .....	73
	Lluís Gómez-Pujol and Joan J. Fornós	
8	Cavernous weathering .....	85
	Andrew S. Goudie	
9	Kluftkarren or grikes as fundamental karstic phenomena .....	89
	Helen S. Goldie	
10	Subsoil shaping .....	103
	Anikó Zseni	
11	Significant subsoil rock forms .....	123
	Tadej Slabe and Hong Liu	
12	Kamenitzas .....	139
	Franco Cucchi	
13	Trittkarren .....	151
	Márton Veress	
14	Corrosion terraces, a meगाausgleichsfläche or a specific landform of bare glaciokarst .....	161
	Jurij Kunaver	



15	<b>Rainpits: an outline of their characteristics and genesis</b> .....	169
	Angel Ginés and Joyce Lundberg	
16	<b>Rillenkarrén</b> .....	185
	Joyce Lundberg and Angel Ginés	
17	<b>Rinnenkarrén</b> .....	211
	Márton Veress	
18	<b>Meanderkarrén</b> .....	223
	Márton Veress	
19	<b>Wandkarrén</b> .....	237
	Márton Veress	
20	<b>Coastal karrén</b> .....	249
	Joyce Lundberg	

### **CASE STUDIES**

21	<b>Limestone pavements in the British Isles</b> .....	267
	Peter Vincent	
22	<b>Case studies of grikes in the British Isles</b> .....	275
	Helen S. Goldie	
23	<b>The karrénfields of the Muota valley: type localities of the main karrén types after the nomenclature by Alfred Bögli</b> .....	291
	Michel Monbaron and Andres Wildberger	
24	<b>The nature of limestone pavements in the central part of the southern Kanin plateau (Kaninski podi), Western Julian Alps</b> .....	299
	Jurij Kunaver	
25	<b>Karrén features in the Dachstein mountain</b> .....	313
	Gábor Tóth	
26	<b>Glaciokarst landforms of the lower Adige and Sarca valleys</b> .....	323
	Ugo Sauro	
27	<b>Karrén in Patagonia, a natural laboratory for hydroaeolian dissolution</b> .....	329
	Richard Maire, Stéphane Jaillet and Fabien Hobléa	
28	<b>Cutters and pinnacles in the Salem limestone of Indiana</b> .....	349
	Arthur N. Palmer	
29	<b>Types of karrén and their genesis on the Velebit mountain</b> .....	359
	Dražen Perica and Tihomir Marjanac	
30	<b>Mid-mountain karrénfields at Serra de Tramuntana in Mallorca island</b> .....	375
	Joaquín Ginés and Angel Ginés	
31	<b>Tropical monsoon karrén in Australia</b> .....	391
	Ken G. Grimes	
32	<b>The tsingy karrénfields of Madagascar</b> .....	411
	Jean-Noël Salomon	
33	<b>The pinnacle karrénfields of Mulu</b> .....	423
	Mick Day and Tony Waltham	
34	<b>Arête and pinnacle karst of Mount Kaijende</b> .....	433
	Paul W. Williams	

35	<b>Lithological characteristics, shape, and rock relief of the Lunan stone forests</b> .....	439
	Martin Knez and Tadej Slabe	
36	<b>Two important evolution models of Lunan shilin karst</b> .....	453
	Linhua Song and Fuyuan Liang	
37	<b>Solution rates of limestone tablets and climatic conditions in Japan</b> .....	461
	Kazuko Urushibara-Yoshino, Naruhiko Kashima, Hiroyuki Enomoto, Takehiko Haikawa, Masahiko Higa, Zenshin Tamashiro, Tokumatsu Sunagawa and Eisyo Ooshiro	
38	<b>The rock cities of Rosso Ammonitico in the Venetian Prealps</b> .....	469
	Ugo Sauro	
39	<b>Coastal eogenetic karren of San Salvador island</b> .....	475
	John E. Mylroie and Joan R. Mylroie	
40	<b>Coastal karren in the Balearic islands</b> .....	487
	Lluís Gómez-Pujol and Joan J. Fornós	
41	<b>Coastal and lacustrine karren in western Ireland</b> .....	503
	David Drew	
42	<b>Solution pipes and pinnacles in syngenetic karst</b> .....	513
	Ken G. Grimes	
43	<b>The karren landscapes in the evaporitic rocks of Sicily</b> .....	525
	Giuliana Madonia and Ugo Sauro	
<b>REFERENCES</b> .....		535



# **ROCK FORMS**



# KARRENFIELD LANDSCAPES AND KARREN LANDFORMS

Angel GINÉS

Karren is used today as a generic term for typical sculpturing features on surfaces of exposed soluble rock. As a whole, their outstanding variety of shapes constitutes the kind of solutional exokarst-landforms of smaller size, spanning from millimetres to more than 10 metres. But on the other hand, quite large extensions of rocks sculpted by karren spread over many square kilometres showing in many cases a characteristic pattern of furrows and grooves, separated by sharp ridges or crests, that stands out in the landscape.

Older references on karren description (Heim, 1878; Chaix, 1895; Eckert, 1902) were in the beginning related geographically to the Alpine karsts from Glattalp-Muotatal (Schwyz, Switzerland), Désert de Platé (Savoie, France) and Gottesackerplateau (Allgäu, Germany) respectively. Terms as *Karrenfeld*, *Karren*, *lapiaz* and *lapiés*, that are today present in karst descriptions, appear therefore in the literature, at the end of the 19<sup>th</sup> century, as a particular expression of high mountain karst.

Later on, in parallel with growing speleological research in Europe, the words *lapiés* and *karren* were early incorporated as synonyms through the karst literature after the Martel's (1921) and Cvijić's (1924) publications, including also several mid-mountain locations as Var (Provence, France) and Velebit (Dalmatia, Croatia). But subsequently, especially under the influence of new research developed by Bögli (1951, 1960a) in the classical

area of Glattalp-Muotatal, the international literature on karst geomorphology (Trimmel, 1965; Monroe, 1970; Jennings, 1971; Sweeting, 1972) favoured progressively the change from *lapiés* to *karren*, even though introducing new connotations in the term. Indeed Sweeting (1972) explains that "the name *karren* was originally used to describe solution runnels cut into limestones, but it is now used for the whole complex of micro-forms that occur on outcrops of karst limestones". More precisely, White (1988) introduces his section on solutional sculpturing pointing out that "direct rainfall, sheet wash, channelized flow, and percolating flow under various kinds of mantle materials produce a myriad of small sculpturings on the bedrock surface of soluble rocks", and then states that "these forms, as a class, are called *karren*, a German term that has come into general usage in English". Looking back today over the evolution of *karren* terminology, the choice made during the seventies of an anglicized version of the Bögli's terms seems to be successful in avoiding the uncontrolled burst of new terms.

*Karren* landforms develop not only on limestone outcrops. They occur in bare carbonate, gypsum and salt rocks (Figures 1, 2, 3) or under soil cover. The presence of *karren* is widespread wherever karstic rocks are exposed, but sometimes many significant – but not especially conspicuous – forms are ignored or neglected. Right up for the



**Figure 1:** Rillenkarren features developing on micritic limestones at Serra de Tramuntana karrenfields (Mallorca, Spain).



**Figure 2:** Rillenkarren features developing on gypsum blocks, after one century of exposure to rainfall, at the Minoan Knossos Palace (Crete, Greece). Width of view is 15 cm.



**Figure 3:** Rillenkarren features developing on salt rock at Cardona mountain (Catalonia, Spain).

present time, the history of karren and karrenfield description has been strongly biased towards the most striking karren landforms: for instance, rillenkarren and spectacular solution runnels (Figure 4), as well as the scenic karrenfield landscapes of alpine and tropical environments (Figures 5, 6), are very much better documented than rainpits and monotonous karrenfield surfaces related to arid environments.

According to A. Ginés (1995) and Fornós and Ginés (1996), karren features are, probably even more than dolines, the most widespread karstic landform. This is obviously unquestionable if the term karren turns to be applied to any small-sized solutional sculpturing, as it is done in the more recent literature, because nearly every karstic terrain exposed to surface erosion contains karren forms. Some of them are even microscopic solutional and biokarstic features related to the highly specific limestone weathering processes. Others remain hidden under soil or buried by clastic sediments, as happens with the typical subcutaneous karren features or cryptolapiaz. Finally, there is a great variety of karren forms – the better known, being exposed to open air so that their current growth and development remain basically under the control of atmospheric precipitations – which become integrated as complex karren assemblages into larger karstic features called *karrenfields*; that is, the former *Karrenfelder*. In many cases the role of such karrenfields in the autogenic recharge of karst aquifers could be even more important than karst depressions or dolines.

Classification of karren landforms is obviously an open debate. Since it is a matter of natural forms – and therefore it is characterized by inherent difficult description and intermingling origin – several different criteria can be considered as sound bases for classification. Probably the better option is to move from one classification to another depending on the approach to the problem that is being studied. One useful analysis of karren landforms we are suggesting here relies on a three-level approach, based on the following scale of decreasing size and complexity: karrenfield

landscapes, karren assemblages and elementary karren features.

## Karrenfield landscapes

Interest in karrenfields started in the second half of 19<sup>th</sup> century, probably due to the increased appreciation of the wilderness and scenic values of alpine landscapes. Significantly, the two oldest German descriptions of karren areas appeared in journals edited by alpine societies (Schweizer Alpenclub and Deutscher und Österreichischer Alpenverein) and both include the word *Karrenfeld* in their titles. Ancient literature on karren landforms was clearly caught by the description of bizarre shapes and impressive landscapes. The most conspicuous karren landforms were reported during this time in the geographical literature, with special emphasis on *rillenkarren*, *rinnenkarren*, *kamenitzas* and *trittkarren*-features. In this way, the term *karrenfeld* became progressively associated with high mountain landscapes.

Additional descriptions of bare limestone outcrops gradually demonstrated the existence of large areas of karren landscapes in the form of the so-called limestone pavements of the British Isles as well as by occupying many barren and deforested limestone mid-mountains around the Mediterranean basin. Their particular scenic value focused again the interest on the strange forms, but at the same time these descriptive studies allowed to some kind of wider generalization promoting the use of a revisited concept of karrenfield as it is implicitly postulated in Sweeting (1972).

All through the seventies and the eighties a remarkable number of tropical and equatorial karst settings have been described over the world; namely in New Guinea (*arête* and *pinnacle karst* of Mount Kaijende), northern Australia (Chillagoe, Queensland), Borneo (Gunung Mulu, Sarawak), southern China (stone forest of Lunan) and Madagascar (Bemaraha *tsingy*), among others. Many of them are in fact giant karrenfields, as assumed in Ford and Williams (2007). Once again



**Figure 4:** Conspicuous solution runnels on the sides of a jagged limestone pinnacle, 8 metres tall, called *Es Camell de Lluc* (Serra de Tramuntana, Mallorca, Spain).



**Figure 5:** A typical mountain-karrenfield, with plenty of wall solution runnels related to snow melting, at 4,500 metres a.s.l. in Yulong mountain (Yunnan, China).



**Figure 6:** Extremely dissected pinnacles and pillars in the subtropical karrenfield type-locality of Lunan Stone Forest (Yunnan, China).



**Table 1:** Classification of karren forms. Yellow areas enclose elementary karren features. Green areas enclose complex large-scale landforms, namely karren assemblages and karrenfield types (after Ginés 2004, slightly modified).

SOLUTIONAL AGENT	KARREN FORMS								SYNONYMS
BIOKARSTIC	BORINGS								
WETTING		IRREGULAR ETCHING							
TINY WATER FILMS		MICRORILLS							RILLENSTEINE
STORM SHOWERS			RAINPITS						SOLUTION PITS
DIRECT RAINFALL			RILLENKARREN						SOLUTION FLUTES
CHANELLED WATER FLOW					SOLUTION RUNNELS				RINNENKARREN
						WALL KARREN			WANDKARREN
					DECANTATION RUNNELS				
					MEANDERING RUNNELS				MÄANDERKARREN
STANDING WATER				KAMENITZAS				SOLUTION PANS	
SHEET WASH WATER FLOW				SOLUTION BEVELS					AUSGLEICHSFÄCHEN
				TRITTKARREN					HEELSTEPS
		COCKLING PATTERNS							
			SOLUTION RIPPLES						
SNOW MELTING				TRICHTERKARREN					FUNNEL KARREN
				SHARPENED EDGES					LAME DENTATES
					DECANTATION RUNNELS				
					MEANDERING RUNNELS				
ICE MELTING						MEANDERING RUNNELS		MÄANDERKARREN	
INFILTRATION					GRIKES			KLUFTKARREN	
SOIL PERCOLATION WATER					RUNDKARREN				ROUNDED RUNNELS
				SMOOTH SURFACES					
				SUBSOIL TUBES					
				SUBSOIL HOLLOWES					
					CUTTERS				
COMPLEX PROCESSES					UNDERCUT RUNNELS				HOHLKARREN
					CLINTS				FLACHKARREN
					PINNACLES				SPITZKARREN
							PINNACLE KARRENFIELD		KARRENFIELD
							LIMESTONE PAVEMENT		
								STONE FOREST	
							ARÊTE KARST		
	0-1mm	1mm-1cm	1-10cm	10cm-1m	1m-10m	10-100m	100m-1km	1km-	LAPIÉS

these impressive labyrinths of pinnacles and vertical pillars are mainly appreciated in the geomorphological literature by their striking landscapes rather than by being extreme examples of karrenfields. Nowadays, it is not enough to describe in a detailed manner such spectacular landscapes: further studies on the role of karrenfields in karst hydrology as well as on the genesis and development of the continuum karrenfield-epikarst call for a new approach to this topic. Having this in mind, probably it could be useful to redefine and enlarge the term karrenfield in order to embrace whatever large surface of exposed soluble rock, sculpted by karren and showing topographic characteristics comprised between two significant end members

represented by limestone pavements and stone forests (Table 1).

In his “Glossary of Karst Terminology”, Monroe (1970) defines Karrenfeld as “an area of limestone dominated by karren”. More especially, Bögli (1980) states that “karren fields appear as bare karst and consist of the sum of exposed and half-exposed karren, and occasionally also of covered karren which have become exposed”; moreover, he points out that “they attain the size of a few hectares to a few hundred square kilometers”. Ginés (1999a) suggests attaining a minimum of 50% of exposed bare rock – extended over large limestone outcrops – to be considered karrenfields; but obviously there exists a clear hydro-



**Figure 7:** The most significant karren assemblages from the mid-mountain karst of Serra de Tramuntana (Mallorca, Spain) usually include rillenkarren, trittkarren-heelsteps and cockling patterns from which collected water is drained into wider solution runnels.



**Figure 8:** Funnel shaped trichterkarren from an alpine limestone outcrop at 2,050 metres a.s.l. in the Vallon des Morteys (Fribourg, Switzerland). Width of view is 15 cm.



**Figure 9:** Sharpened edges, topped with their characteristic flat facets, are found in many alpine karrenfields like this karren-wall at 1,750 metres a.s.l. in Böldmeren (Schwyz, Switzerland).

logical continuity along exposed and soil-covered rocks and – following these pathways downwards – subsoil karren features appear as direct links towards the most efficient epikarst drains. Since the complexity of karst subsurface poses many challenges to understanding the transition between karren landforms and the epikarst (Williams, 1983; Klimchouk, 2000c; Jones et al., 2004; Williams, 2008), special attention must be paid in the future to describe in detail this subcutaneous part of the exokarst. The growing interest on subsoil karren assemblages (Slabe, 1999) could focus additional research on the overall evolution of karrenfields and epikarst.

## Karren landform assemblages

Karrenfields are in fact major recharge areas feeding the epikarst, but at the same time karrenfields are vast bare rock areas dominated by little-scale karren sculpturing. Filling this remarkable size-gap, in his explanation on “the genetic system of karren forms”, Bögli (1980) states an intermediate stage of integration gathering the so called *single karren forms* into greater *complex karren forms* and indicating clints and pinnacles as examples of such level of classification. Indeed, limestone pavements in alpine or glaciated karst are characterized by a clint and grike topography, defined initially as Flachkarren (Bögli, 1951, 1960a), in the same manner than intertropical stone forests are characterized by a pinnacle and trench topography, defined initially as Spitzkarren (Bögli, 1951, 1960a). For this reason, I personally think that the old distinction between Flachkarren and Spitzkarren yet remains a very useful criterion, especially suitable for landform modelling.

Clints and/or pinnacles become dissected and sculpted by characteristic karren assemblages (Figure 7) whose distribution patterns over the rock faces have not been sufficiently studied until recently (Tóth, 2007). On the one hand, it can be expected that association of karren features reflects the many factors that interact in the par-

ticular shaping of different homogeneous rock outcrops subjected to the agents that cause karren development. On the other hand, increasing knowledge on karren assemblages could provide information on the genetical processes involved in the formation of each type of elementary karren features, particularly on the base of their frequency of appearance as well as on their correlation (positive or negative) with other elementary karren features (Ginés, 1996a). For instance, there can be found in mountain or cold climate areas typical karren assemblages related to snow melting, that are characterized by trichterkarren (Figure 8) and sharpened edges (Figure 9) as diagnostic features (Perna and Sauro, 1978). Reshaping of subsoil karren after deforestation and rock exposure to direct rainfall also produces a definite assemblage of forms showing vertical gradation downwards, from the top of the rising rocks to the soil surface.

Table 1 identifies as follows the main solutional agents responsible for karren growth: biokarstic corrosion, wetting by dew, tiny water films drawn by capillary tension, direct rainfall, channelled water flow, sheet wash water flow, short but intense storm showers, still-stand water, snow melting, glacier ice melting, direct infiltration and slow soil water percolation. It appears that many of them are strongly controlled by environmental factors, mainly climate-dependent conditions. This explains most of the hydrological integration, from the upper part of the rock outcrops downwards, shown by several types of karren assemblages (e.g. from the splashing of raindrops to the collection of water into channelled water flow). Even, on the contrary, the apparent lack of hydrological connection between karren features that is exhibited by some karren assemblages related to arid or semiarid climates indicates juxtaposition of etching elements rather than efficient water drainage. Coastal influence, wind orientation, sun exposure, frost action, dampness, frequent dew formation, etc. could favour or hinder the development of specific karren assemblages. An environmental and statistical approach to the karren

assemblages along climatic gradients and/or between different lithologies is therefore justified, taking into account the complex frame of factors determining the array of forms able to result overprinted on the rock.

## Elementary karren features

Karren is a complex group of small to medium-sized karstic landforms showing a great variety of characteristic shapes. Some of them can be considered as elementary karren features, since they seem associated to definite genetic factors and they become frequently integrated in wider-scale karren assemblages. The bewildering diversity of karren is difficult to summarize. A brief description of the most documented elementary karren features is stated below, and is presented as a simplified diagram in Table 1:

**Biokarstic borings:** Nanokarren features produced or promoted by microorganisms (bacteria, cyanobacteria, algae and fungi), lichens or roots. Pits, boreholes, trenches and tunnels, generally smaller than 1 mm in size are their most common appearances through microscopic examination with SEM.

**Irregular etching:** Nanokarren and microkarren features constituted by a wide variety of pitting and differential, non-oriented, etching forms, commonly showing protrusions and hollows lesser than 1 cm. Rock surfaces affected by these rough shapes show no clear directional trends and are characterized by a chaotic and coarse microtopography.

**Microrills (= Rillensteine):** Microkarren features characterized by rock surfaces showing several different patterns formed by tiny channels and/or micro-spikes, rarely surpassing 1 mm in width. They have been typically described as about 1 mm wide rills, round bottomed and packed together with characteristic tightly sinuous to anastomosing plan view patterns on gentle slopes, becoming more parallel and straighter with increasing slope.

**Rainpits** (= **solution pits**): Small, hollowed cup-like karren features, subcircular in plan and nearly parabolic or tapering in cross section, whose diameter ranges from 1 cm to 5 cm, and exceptionally exceeding 2 cm in depth. Frequently appear clustered in groups and can coalesce to give irregular and carious appearance to the rock surfaces.

**Rillenkarren** (= **solution flutes**): Small, straight, narrow, closely packed, parallel solutional furrows, that head at the crest of bare rock slopes and extinguish downslope. Their dimensions in limestone outcrops are typically 1.2–2.5 cm in width, 2–6 mm in depth and 10–30 cm in length. Individual flutes are parabolic in cross-section and are separated by sharply pronounced cusp lines. In plan view, they may form a simple suite of parallel flutes showing remarkable regularity of form and dimension. Their development to either side of a crest often produces a typical herringbone pattern.

**Solution runnels** (= **Rinnenkarren**): Mesokarren features consisting of linear channels or furrows that generally show increased width and depth downslope. Threads of runoff water, pouring down the flanks of the rocks, are collected into channels to create solution runnels which width and depth range from 5 to 50 cm, being very variable in length (commonly from 1 to 10 m, but in some cases exceeding 30 m long). Owing to the great diversity of topographic conditions and the kind of water supply feeding their channelized flow, they have a remarkable variety in cross section and plan pattern (including tributaries).

**Wall karren** (= **Wandkarren**): Straight furrows that are often found on sub-vertical outcrops as a result of water flowing down rock walls. They are in many cases real makarren features because they can attain lengths close to 100 metres. There is frequent overlapping between wall karren and some types of decantation runnels.

**Decantation runnels**: Channels generated by water released steadily, that start from an up-slope point-located store (e.g. a patch of moss) or

from a diffuse or linear source (e.g. a bedding plane) situated upwards. Generally their cross-sections are largest close to the input of water and diminish downslope.

**Meandering runnels** (= **Mäanderkarren**): Small winding channels that are cut directly into the rock surface or within a larger runnel. This special kind of karren channels exhibits meander forms with typical undercutting and slip-off slopes. There is frequent overlapping between meandering karren and some types of decantation runnels.

**Kamenitzas** (= **solution pans**): Dish-shaped depressions, 1 cm to 0.5 m deep, 5 cm to 5 m wide and mostly elliptical or circular to highly irregular in plan. Usually they have flat and nearly horizontal bottoms that are floored by a thin layer of soil, vegetation or algal remains which decay enhances further dissolution. Their borders are frequently overhanging and may have small overspill outlets.

**Solution bevels** (= **Ausgleichsflächen**): Flat, smooth surfaces, 0.2 to 1 m long, usually found as plane sub-horizontal belts developed below the level of rillenkarren-flutes extinction.

**Trittkarren** (= **heelsteps**): Conspicuous karren features that form arcuate headwalls, which flat floors are open in downslope direction. The single trittkarren consists of a flat tread-like surface, 10 to 40 cm in diameter, and a sharp back-slope or riser, 3 to 30 cm in height. Their typical appearance is as groups of heel prints excavated as steps on the rock outcrops. They seem to be the result of complex solutional processes involving both horizontal and headward corrosion generated by the thinning of water sheets flowing upon small slope falls.

**Cockling patterns**: Solutional concave shapes undulating the rock surfaces randomly or, in some cases, producing a regularly crinkled pattern and a characteristic horizontally-lined appearance to the rock slopes.

**Solution ripples**: Wave-like forms, transverse to downward water movement under gravity. Their rhythmic forms suggest that periodic

pulses of flow or chemical changes are important in their development.

**Trichterkarren** (= *funnel karren*): Concave karren forms that resemble trittkarren in shape and dimensions, differing from such karren type in their much rounded cross section which lacks the characteristic horseshoe appearance and the stepped pattern. There is frequent overlapping between genuine trichterkarren and trittkarren, but the former seem to be exclusively associated with snow melting.

**Sharpened edges** (= *lame dentate*): Mesokarren features delimiting a sharp and straight edge on the flanks of steep rocks. Their upper part shows a characteristic and almost triangular flat facet. They seem to be exclusively associated with snow melting.

**Grikes** (= *Kluftkarren*): Deep clefts, from 1 cm to 0.5 m across and up to several metres deep. They are one of the most typical mesokarren features, normally from 1 m to 10 m in length, formed through the simple solutional enlargement of joints or cracks. Their linear trends are determined by major structural directions as joint sets or faulting. Owing to the fact that such slots cut in the bedrock are merely the visible surface expression of the fissures crisscrossing the karstifiable rocks, grikes constitute a significant component of the epikarst.

**Rundkarren** (= *rounded runnels*): Channels or furrows developed beneath a soil cover, which troughs and ribs become smoothed by the more active corrosion associated with soil waters that produces their characteristic rounded cross-sections.

**Subsoil smooth surfaces** (= *subcutaneous karren forms*): A whole array of characteristic rounded and smooth rock surfaces appear clearly related to subsoil corrosion. Smoothing and bleaching of subsoil karren-forms is evident when it is compared with the sharpening and grey appearance of exhumed karren forms. Subsoil smoothing can be considered a consequence of specific nanokarren features developed in contact with the sponge action of acidic soil water.

**Subsoil tubes** (= *subcutaneous karren pipes*): Perforating tubes and rock holes, formerly filled with soil, which diameter range from a few centimetres to less than 1 m. They show rounded cross sections as well as branching and complex tridimensional patterns that penetrate deeply into the rock. Subsoil tubes are a significant part of the epikarst in many well developed karrenfields.

**Subsoil hollows** (= *subcutaneous hollow-forms*): Subsoil hollows showing different shapes and sizes are frequently exposed in road cuts and quarry walls. They are also common at the foot of karren pinnacles. In addition to pockets, niches and recesses, great subsoil wells and small subsoil pitting and scallop-like features are frequently found.

**Cutters**: Great solution crevices similar to grikes but generally larger than 1 m in wide and filled with regolith or soil. They appear much widened at the top and tapering to narrow cracks with depth and are generated by vertical solution along fractures beneath a thick soil.

**Undercut runnels** (= *Hohlkarren*): Mesokarren furrows transformed by organic debris or partial soil filling because their side walls have been hollowed under by enhanced biogenic carbon dioxide concentration. Typical bag-like cross sections, wider at the bottom than at the top, are generated in this way.

**Clints** (= *Flachkarren*): Tabular intervening blocks or slabs isolated by grikes. They are flat or gently inclined outcropping rocks which become divided into straight-sided blocks by the solutional widening of fissures. These bare plane surfaces of limestone, generally parallel to the bedding, are the main constituent of limestone pavements.

**Pinnacles** (= *Spitzkarren*): Vertical solution along joints and fractures lowers the intervening rock flanks and produces isolated spires or pinnacles that can reach a few metres or tens of metres in height. Usually the side walls are deep grikes with runnels cutting across one another to form sharp ridges and peaks. They could



**Figure 10:** Winding rib remnants that are exclusively found between some rillenkarren flutes developed on salt rock (Cardona, Catalonia, Spain). Width of view is 12 cm.

be considered as a particularly mature form of karren and in many cases are the result from sharpening of subsoil pinnacles after being exhumed by soil removal.

This is necessarily a simplified overview on the elementary karren features that are enclosed in Table 1 (based in Ginés, 2004), and corresponds to some extent with the so called *single forms* from Bögli (1980). It stands out that some of these elementary karren features accumulate a very uneven amount of bibliographical references (for instance, many references about rillenkarren in comparison with very few on trichterkarren). Furthermore, some of them can be considered as the end members from a continuum of related forms (this is the reason for the choice of the complementary term *runnel*, which embraces a wide array of forms, including the formerly spelled Rinnenkarren, Wandkarren, Mäanderkarren, Rundkarren and Hohlkarren as well as many decantation forms). Finally, there are elementary karren features easy to delimit (as, for example, the rainpits), but many others show clear overlapping (this seems to be the case for the transitional forms between trittkarren and trichterkarren).

A broad discussion about so complex terminology would be tedious in this merely introductory chapter. During the seventies, the wide use of the terminology adapted from Bögli (1951, 1960a) into the international karst literature proved to



**Figure 11:** Eogenetic karren formed on Miocene reef rocks of south-eastern Mallorca (Balearic islands, Spain). Recent soil removal allows us to recognize the characteristic differences existing between the upper rough and grey formerly exposed rock and the smooth and whitish appearance of freshly exhumed subsoil sculpturing. Width of view is 1.5 m.

**Figure 12:** Great subsoil-shaped pinnacles arise after iron mining in the palaeokarst of Cerro del Hierro (Seville province, Andalusia, Spain).



be a successful decision. But today, in my opinion, such tendency has outlived its usefulness. For example, and from a strictly personal point of view, let me suggest avoiding the future expansion of germanized new terms as recently occurred with the excellent paper from Simms (2002) on lacustrine Röhrenkarren.

### Looking forward to karren research strategies

Among the major issues faced by the researchers on karren landforms in the next years are: the use of modelling techniques for a better explanation of the genesis of specific elementary karren features; the accurate morphometrical description of the most significant karren landforms; and the application of statistical methods in order to compare karren locations differing in lithology and/or climate conditions.

The formation of the different types of karren features can be largely understood in terms of the mobility of solutes along the rock surfaces. This approach constitutes the base for the experiments

carried out by Petterson (2001) and Dreybrodt and Kaufmann (2007) on the solution by flowing water films on sloped blocks. Experimental work in the laboratory, using plaster of Paris (artificial gypsum) block-models, were previously initiated with success by Glew and Ford (1980) for rillenkarren, and subsequently were developed by Dzulyński et al. (1988) and Slabe (2005), trying to embrace also the kluftkarren, solution runnels and subcutaneous stone-teeth formation. Furthermore simulation of rillenkarren flutes by Slabe (2005) has been especially successful in obtaining by means of plaster models the expected downward sequence on the typical karren assemblage consisting of rillenkarren, ausgleichsfläche and solution runnels.

There is an increasing literature on morphometry of elementary karren features though not all the measurements of karren types are substantiated by large sampling nor are they easily comparable with another karren locations. Valuable field data on rillenkarren are gathered in Belloni and Orombelli (1970), Lundberg (1977a, b), Heinemann et al. (1977), Dunkerley (1979), Goudie et al. (1989), Stenson and Ford (1993), Mottershead (1996a) and Ginés (1996b), while measurements



of clints and grikes are documented in Goldie and Cox (2000). The references on morphometry of rainpits are limited to Lundberg (1977a) and Ginés (1998b), and only scant quantitative data are reported from meandering runnels in Zeller (1967), Hutchinson (1996) and Veress and Tóth (2004). Morphometric characteristics of trittkarren-trichterkarren features are discussed by Vincent (1983a) on the base of six morphological variables. Belloni and Orombelli (1970) provide also measurements of kamenitzas and solution runnels. In this way, an important recent trend in exokarst studies lies in the greater application of morphometric techniques to karren descriptions. Further research would be encouraged as long as available measurements of elementary karren forms on different karstic locations continue to grow. A combined and cautious use of morphometry and terminology is recommended in order to clarify and simplify the overwhelming amount of karren terms.

It has long been recognized that several factors may control karren development: lithology, topography, climate, biological activity and time. The effects of climatic differences on karren development tend to be apparent at a global overlook, both at the scale of karrenfields and at the scale of individual elementary karren features. Most of the diversity in karren landforms can be easily explained as a direct consequence of variation in

precipitation and temperature. Correlation with macroflora is not quite congruent because karren is obviously defined as predominantly bare rock-surfaces and landscapes. But correlation with weathering and soil-forming processes could be useful. Topography would be significant, especially regarding soil removal and exposure to sun radiation. Furthermore, it can be expected that lithology influences the nature and rate of karren growth in two major ways: mineralogy and texture. Correlations between forms and environmental factors along gradients as well as multifactor analysis including rock properties (Figure 10) have presumably good application to karren research owing to such complex causation. Statistical methods (e.g. principal component analysis) and integrated geomorphological and ecological studies (e.g. transects) are being introduced gradually with this purpose, as suggest the contributions from Goudie et al. (1989), Ginés (1996a, 1999a) and Veress et al. (2001a). Finally, time is also important in relation to karren because these landforms are subjected to evolution at different chronological scales, ranging from decades or centuries of deforestation and subsequent soil removal (Figure 11) to very old burying under sediments for millions of years until produce in some cases palaeokarst ore-deposits (Figure 12).

# PHYSICS AND CHEMISTRY OF DISSOLUTION ON SUBAERIALY EXPOSED SOLUBLE ROCKS BY FLOWING WATER FILMS

Wolfgang DREYBRODT and Georg KAUFMANN

Karren is the generic term for dissolution features on exposed soluble rock surfaces. Because of their variety of shapes and also their regularity karren have been a fascinating object of interest for geomorphologists. Although a large body of observations and descriptions of karren has been accumulated, knowledge on the physical and chemical processes on their formation by dissolution is scarce. In this paper we will focus on processes occurring on bare rock surfaces such as limestone or gypsum exposed to the atmosphere, and covered by flowing water films. Two basic ingredients control the dissolution process, the hydrodynamics of thin water films flowing down inclined surfaces, and the dissolution kinetics of the CO<sub>2</sub>-containing rainwater on limestone or gypsum rock surfaces. After discussion of these two topics, we will use this for an interpretation of the data of Glew and Ford (1980), who performed experimental simulations on the formation of rillenkarren on inclined surfaces of plaster of Paris exposed to artificial rainfall.

Using these results an interpretation of existing field data on lengths of rillenkarren is presented.

Also recent data by Petterson (2001) on dissolution on rillenkarren from plaster of Paris will be discussed. Finally the dissolution kinetics of limestone will be used to explain surface denudation on bare limestone surfaces.

## The fluid dynamics of water films on smooth and rough surfaces

When rain with intensity  $q$  (cm s<sup>-1</sup>, 1 mm/hour = 2.8 · 10<sup>-5</sup> cm s<sup>-1</sup>) falls onto an inclined smooth surface with slope angle  $\gamma$ , a thin layer of water is established (see Figure 1). Its flow rate  $Q$  in cm<sup>3</sup>/s per unit width is given in cm<sup>2</sup>/s. After distance  $x' = l$  down the surface of the rock  $Q$  is

$$Q = x \cdot q = l q \cos \gamma, \tag{1}$$

The thickness  $h$  (in cm) of the water film is related to flow  $Q$  (Myers, 2002) by

$$Q = \frac{\rho g h^3}{3\eta} \sin \gamma, \tag{2}$$

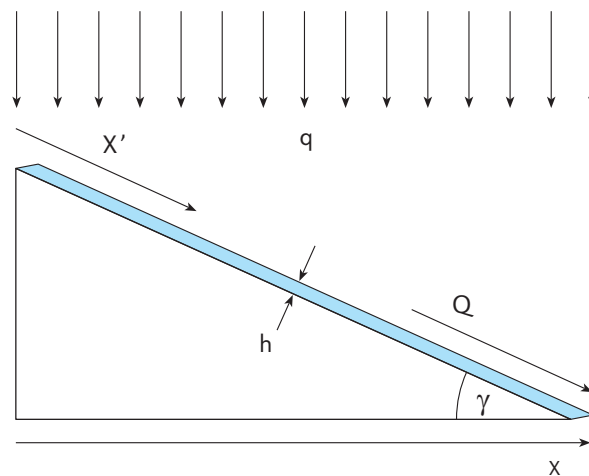


Figure 1: Water film on inclined rock surface.

where  $g$  is earth's gravitational acceleration,  $\rho$  is the density of water, and  $\eta$  its viscosity. By using eqns. 1 and 2, we obtain the film thickness

$$h = \sqrt[3]{\frac{3\eta q \ell}{\rho g \tan \gamma}}. \quad (3)$$

For rainfall intensities of 1 mm/hour onto a surface sloping with  $45^\circ$  and at a distance  $l = 50$  cm, a fairly thin film of  $h = 3.6 \cdot 10^{-3}$  cm develops. For 40 mm/hour rainfall intensity as used by Glew and Ford (1980), the film thickness  $h$  is  $1.2 \cdot 10^{-2}$  cm.

The flow velocity  $u$  (in  $\text{cm s}^{-1}$ ) is obtained from  $u \cdot h = Q$  by inserting eqns. 2 and 3 and one finds

$$u = \sqrt[3]{\frac{\rho g Q^2 \sin \gamma}{3\eta}} = \sqrt[3]{\frac{\rho g q^2 l^2 \cos^2 \gamma \sin \gamma}{3\eta}}. \quad (4)$$

Note that the velocity increases with flow distance  $l$ . Assuming a rainfall of 10 mm/hour, a flow distance of 1 m, and a slope angle of  $45^\circ$ , the velocity is  $2.1 \text{ cm s}^{-1}$ . If rainfall is reduced to 1 mm/hour one finds  $0.5 \text{ cm s}^{-1}$ . These velocities are of importance because they give the time of residence during which a water parcel can dissolve bedrock.

When the surface is rough a correction factor must be introduced (Myers, 2002), which is given by

$$f_c = \left[ 1 - 0.25 \left( \frac{k}{h} \right)^{1.28} \right], \quad (5)$$

where  $k$  is the roughness of the surface and  $h$  the film thickness of the layer on a smooth surface, as given by eqn. 3 (Phelps, 1975). This dimensionless factor relates the flow velocities  $u$  and  $u_r$  of the smooth to the rough surfaces respectively:

$$u_r = f_c \cdot u. \quad (6)$$

Because  $u \cdot h = Q$  the film thickness values are related by

$$h_r = \frac{1}{f_c} h. \quad (7)$$

For  $k/h = 2$ , a reasonable number, we obtain  $f_c \approx 0.4$ , and flow velocities are lower. Film thickness values are higher by a factor of 2.5.

## Dissolution kinetics

### Gypsum

By use of rotating disc experiments Jeschke et al. (2001) have found that the surface reaction rates of gypsum (in  $\text{mmol cm}^{-2} \text{ s}^{-1}$ ) are given by

$$R_s = k_s (1 - c_s / c_{eq}) = \alpha_s (c_{eq} - c_s) \quad (8)$$

with

$$\alpha_s = k_s / c_{eq} = 6.5 \cdot 10^{-3} \text{ cm/s}.$$

Here,  $c_s$  is the calcium-concentration at the surface and the rate constant is  $k_s = 1.1 \cdot 10^{-4} \text{ mmol cm}^{-2} \text{ s}^{-1}$ . The equilibrium concentration  $c_{eq}$  with respect to gypsum is  $15.4 \cdot 10^{-3} \text{ mmol cm}^{-3}$ .  $\text{Ca}^{2+}$  and  $\text{SO}_4^{2-}$  ions released from the mineral surface are transported away from the surface into the solution by molecular diffusion. Therefore concentration gradients exist and the surface concentration  $c_s$  differs from the concentration  $c$  in the bulk. The transport rate  $R_D$  by molecular diffusion is given by

$$R_D = k_D (1 - c / c_{eq}) = \alpha_D (c_{eq} - c) \quad (9)$$

with

$$\alpha_D = k_D / c_{eq}$$

where  $k_D$  is the transport constant and  $c$  is the average concentration of the bulk solution. Since due to mass conservation  $R_s$  must be equal to  $R_D$ , one finds an effective rate law (Dreybrodt, 1988).

$$R = k_{eff} (1 - c / c_{eq}) \quad (10)$$

with

$$k_{eff} = \frac{k_s \cdot k_D}{k_s + k_D},$$

or

$$R = \alpha_{eff} (c_{eq} - c)$$

with

$$\alpha_{eff} = \frac{\alpha_s \cdot \alpha_D}{\alpha_s + \alpha_D}.$$

When  $k_s \gg k_D$ ,  $k_{eff}$  becomes close to  $k_D$  and rates are controlled by diffusion. On the other hand if  $k_s \ll k_D$ ,  $k_{eff}$  becomes close to  $k_s$  and the rates are surface controlled. In the region where  $k_s$  and  $k_D$  are of similar magnitudes both processes control dissolution.

For a laminar water film of thickness  $h$ ,  $k_D$  is given by (Beek and Muttzall, 1975)

$$k_D = 2Dc_{eq} / h \quad (11)$$

or

$$\alpha_D = 2D/h,$$

where  $D$  is the coefficient of diffusion ( $1 \cdot 10^{-5} \text{ cm}^2 \text{ s}^{-1}$ ). For  $h = 0.01 \text{ cm}$  one obtains  $\alpha_D = 2 \cdot 10^{-3} \text{ cm s}^{-1}$  and the rates are controlled by diffusion. However, raindrops impinging on the water film may cause mixing, which could increase the effective diffusion constant. Only a factor of 10 suffices to obtain surface control and a value of  $\alpha_{eff} \approx 7 \cdot 10^{-3} \text{ cm s}^{-1}$ .

To convert the rates from  $\text{mmol cm}^{-2} \text{ s}^{-1}$  into retreat of rock in  $\text{cm/year}$  for gypsum one has to multiply by a factor of  $2.3 \cdot 10^6$ .

## Limestone

Water films running down rock surfaces under natural rainfall conditions have a comparatively small depth of a few tenths of a millimetre. In contrast to gypsum, where dissolution rates are determined by surface reaction and molecular diffusion, the situation on limestone is more complex. Figure 2 schematically depicts three regimes of dissolution rates. For highly undersaturated solutions,  $0 < c \leq c_{app}$ , rates are high and decline steeply with slope  $\alpha_1$  to an apparent equilibrium concentration  $c_{app} = 0.3 \cdot c_{eq}$ , where  $c_{eq}$  is the true equilibrium concentration with respect to calcite. The values of  $\alpha_1$  are almost independent on the film thickness  $h$  for  $0.005 \text{ cm} < h < 0.03 \text{ cm}$ , and  $\alpha_1 = 5 \cdot 10^{-4} \text{ cm s}^{-1}$  (Kaufmann and Dreybrodt, 2007).

To a good approximation the rates found by theoretical modelling can be expressed by

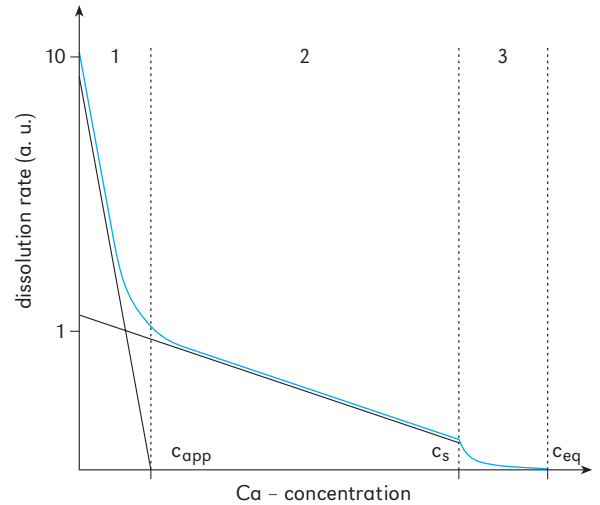


**Figure 2:** Dissolution rates of limestone by  $\text{CO}_2$ -containing water. Three regimes of very fast (region 1), moderate (region 2), and inhibited dissolution rates (region 3) are clearly distinguishable. Only the fast dissolution rate in region 1 is relevant in this paper.

$$R_l = \alpha_1 (c_{app} - c) \quad (12)$$

for

$$c \leq 0.3 c_{eq}$$

For higher calcium concentrations a second linear region with significantly lower slope  $\alpha_2$  arises, until close to equilibrium in region 3 for  $c \geq c_{sw}$ , above the switch concentration  $c_{sw} = 0.9 c_{eq}$  inhibition occurs and the rates are controlled by slow surface reactions.

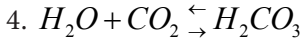
The dissolution rates in regions 2 and 3 are well understood (Plummer et al., 1978; Buhmann and Dreybrodt, 1985; Svensson and Dreybrodt, 1992).

Three basic chemical reactions control the dissolution of  $\text{CaCO}_3$ :

1.  $H^+ + CaCO_3 \rightleftharpoons Ca^{2+} + HCO_3^-$
2.  $H_2CO_3 + CaCO_3 \rightleftharpoons Ca^{2+} + 2HCO_3^-$
3.  $CaCO_3 + H_2O \rightleftharpoons Ca^{2+} + CO_3^{2-} + H_2O \rightleftharpoons Ca^{2+} + HCO_3^- + OH^-$

For all three reactions  $\text{CO}_2$  dissolved in the solu-

tion must be hydrated into carbonic acid, which rapidly reacts to  $H^+ + HCO_3^-$ .



The pH-values of the solution in region 2 are between 7.5 and 8.3. For such pH-values conversion of  $CO_2$  is slow (Usdowski 1982, Dreybrodt 1988) and for thin films below 0.02 cm control by  $CO_2$ -conversion limits the rates. For film thickness between 0.01 cm up to 0.04 cm slope values are about  $\alpha_2 = 3 \cdot 10^{-5} \text{ cm s}^{-1}$ , lower by about one order of magnitude than  $\alpha_1 = 5 \cdot 10^{-4} \text{ cm s}^{-1}$ .

The reason for the high rates in region 1 are reactions (1) and (3). When no calcite has yet been dissolved the initial pH of the solution in equilibrium with  $CO_2$  in the atmosphere is 5.7. Since reaction (1) is very fast protons are rapidly consumed by dissolving calcite.

Furthermore dissolution of calcite produces  $OH^-$  ions. Therefore pH increases to values of about 11. Because of the high concentration of  $OH^-$ , conversion of  $CO_2$  is fast by reaction 5. With increasing Ca-concentration pH drops, and consequently slow conversion of  $CO_2$  by reaction (4) takes over in controlling the rates. As a conclusion we state that for low concentrations  $c$  the rates are given by the relation

$$R = \begin{cases} \alpha_1 (0.3 c_{eq} - c); & 0 < c < 0.3 c_{eq} \\ \alpha_2 (c_{eq} - c); & c > 0.36 < 0.9 c_{eq} \end{cases} \quad (13, 14)$$

## Experimental determination of dissolution rates in region 1

When a thin water layer of width  $W$  flows down a smooth, plane limestone surface with inclination angle  $\gamma$  it dissolves calcite and the concentration  $c(x)$  of calcium along its flow path increases. The amount of calcite dissolved during one second between positions  $x$  and  $x + dx$  is given by  $\alpha_1 (c_{app} - c(x)) \cdot dx \cdot W$ . Due to mass conservation this must

be equal with  $Q_{total} dc$ , where  $dc$  is the increase in concentration from  $x$  to  $x + dx$ , and  $Q_{total}$  is the total flow rate in  $\text{cm}^3 \text{ s}^{-1}$ . From this a differential equation is found

$$\frac{dc}{dx} = \frac{\alpha_1 \cdot W}{Q_{total}} (c_{app} - c). \quad (15)$$

Its solution is

$$c(x) = c_{app} \left( 1 - \exp \left( -\frac{\alpha_1}{Q} x \right) \right), \quad (16)$$

where  $Q = Q_{total}/W$  is the amount of flow in one cm width of the film.

We use eqn. 16 to determine  $\alpha_1$  experimentally. To this end, we have constructed a channel of 5 cm width and 1.2 m length by employing acryl rims fixed to a plate of limestone. The inclination is  $\gamma = 3.2^\circ$ . At the end of the channel a funnel of acryl-glass channels the water into a hole from where it runs into a bottle. The experiment is illustrated in Figure 3 (at the top), which provides a view from above. To guide the water into a stable film the channel at its upper end is blocked by a piece of acryl-glass, which leaves a narrow space of a few tenths of a millimetre between the limestone surface and its lower plane face (see Figure 3, below). Distilled water in equilibrium with the  $p_{CO_2}$  in the atmosphere by use of a peristaltic pump is introduced into the upper compartment, and a film of constant thickness moves down in laminar flow at ambient temperature of  $20^\circ\text{C}$ . This film is established by drawing down the water along the limestone surface by use of a wet paper strip as wide as the film is desired to be. The water film does not touch the acryl walls but is kept by surface tension. It does not change its shape, even when its depth varies by a factor of three. The surface of the film is absolutely plain as can be seen by a mirror like reflection of light. The flow rate  $Q$  is measured by collecting 10 ml of water at the outlet hole at the end of the channel, and measuring the time needed. The calcium concentration  $c_{end}$  of this sample is then measured for various values of  $Q$ . Furthermore, water in equilibrium with atmospheric  $p_{CO_2}$  and calcite is used to measure  $c_{eq}$ . The

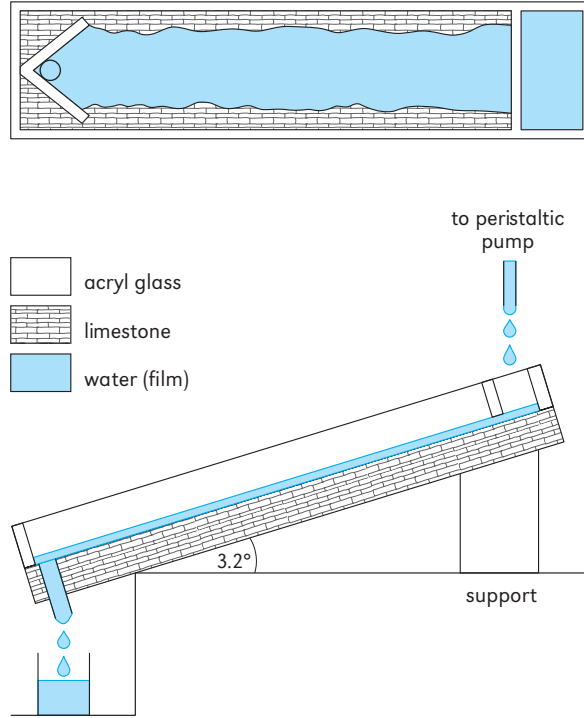


**Figure 3:** Experimental set up to measure limestone dissolution rates in region 1 (top and side view). Length  $l$  of channel 120 cm, width of channel 5 cm, average width  $W$  of water film 4 cm.

calcium concentrations are determined by measuring electrical conductivity, which for such low concentrations is linear with calcium concentration. The experiment was performed at 25°C.

Eqn. 16 can be rewritten to

$$-\ln\left(1 - \frac{c_{end}}{c_{app}}\right) = \frac{\alpha_1 \cdot l \cdot W}{Q_{total}} \quad (17)$$

Figure 4 shows the plot of the experimental data in terms of  $\ln(1 - c_{end}/c_{app})$  versus  $1/Q_{total}$ . This can be fitted with a straight line by using  $c_{app} = 0.3$   $c_{eq} = 0.17$  mmol/cm<sup>3</sup>. From the slope 0.129 of the line one finds  $\alpha_1 = 2.6 \cdot 10^{-4}$  cm s<sup>-1</sup>, which is in reasonable agreement to the theoretical predictions of  $\alpha_1^{th} = 5 \cdot 10^{-4}$  cm s<sup>-1</sup> and  $c_{app}^{th} = 0.36 \cdot c_{eq}$ .

## Dissolution on bare rock surfaces

When rain falls onto an inclined surface the flow

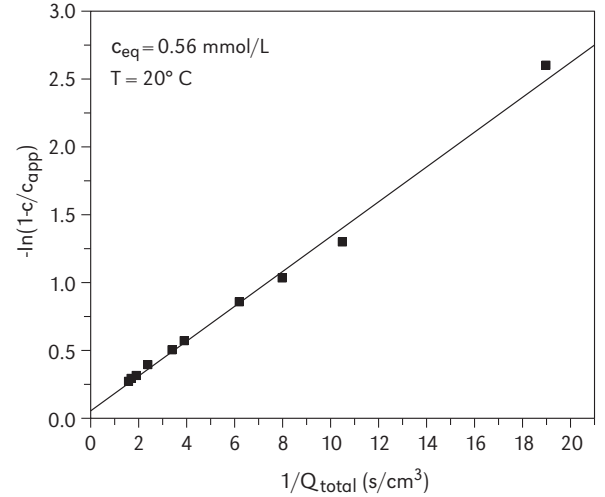


**Figure 4:** Calcium concentration versus inverse of flow rate for experimental data (squares).  $Q_{total}$  is the total flow rate of the film. The straight line is a least square fit to the data.

rate downstream increases (see Figure 1). If at  $x'=0$  the flow rate is  $Q_0$ ; then at a later position  $x'$  it is given by

$$Q = Q_0 + q' x' \cos \gamma = Q_0 + q' x' \quad (18)$$

Mass conservation demands that

$$\begin{aligned} W(Q_0 + q' x')c + W \tilde{\alpha} \cdot (c_{eq} - c) dx' &= \\ = W(Q_0 + q' x' + q' dx')(c + dc), \end{aligned} \quad (19)$$

where  $c$  is the average concentration at position  $x'$ , and  $W$  is the width of the film.  $\tilde{\alpha} \approx \alpha \cdot f_\alpha$ , where  $f_\alpha$  is a correction factor considering the roughness of the rock surface. If one assumes that the rock surface consists of small half spheres densely packed, instead of a smooth plane, the surface area available for dissolution will increase by  $f_\alpha = 2$ . This gives an estimation on the order of magnitude of  $f_\alpha$ . Equation 19 states that the outflow of calcium at position  $x' + dx'$  is given by the inflow at position  $x'$  plus the amount of calcium ions dissolved per time between  $x'$  and  $x' + dx'$ . Neglecting terms with  $dx' \cdot dc$  one finds a differential equation

$$\frac{dx'}{Q_0 + q' x'} = \frac{dc}{\tilde{\alpha}(c_{eq} - c) - q' c} \quad (20)$$

with solution

$$c(x') = \frac{\tilde{\alpha} c_{eq}}{q' + \tilde{\alpha}} \left[ 1 - \left( 1 + \frac{q' x'}{Q_0} \right)^{-\frac{q'}{q' + \tilde{\alpha}}} \right]. \quad (21)$$

For large values of  $x'$  the concentration approaches the value

$$c_\infty = \frac{\tilde{\alpha}}{q' + \tilde{\alpha}} c_{eq}. \quad (22)$$

90% of this value is reached at a distance

$$x'_{0.9} = \frac{Q_0}{q'} \left[ 10^{\frac{q'}{q' + \tilde{\alpha}}} - 1 \right]. \quad (23)$$

For  $Q_0 = 0$  the concentration  $c_\infty$  is established immediately. Therefore dissolution rates are uniform downstream if one assumes that  $\tilde{\alpha}$  is independent of the thickness of the water sheet. This is not true for gypsum. A reasonable approximation is to use average values. For gypsum  $\alpha$  is maximal  $7.1 \cdot 10^{-3} \text{ cm s}^{-1}$  if the rates are controlled by surface reactions and at a sheet thickness of 0.1 mm it is  $1.56 \cdot 10^{-3} \text{ cm s}^{-1}$  (see eqn. 10). At a sheet thickness of 0.5 mm one finds  $\alpha = 3.8 \cdot 10^{-4} \text{ cm s}^{-1}$ .

## Rillenkarrren

### Experiments on formation of rillenkarrren on gypsum

Glew and Ford (1980) experimentally simulated the formation of rillenkarrren on gypsum by exposing inclined surfaces of plaster of Paris to a rainfall intensity of 38 mm/hour, which lasted for 500 h. They obtained well developed rillenkarrren. Their average length from the crest to the “Ausgleichsfläche” was dependent on the angle of inclination, as shown in Figure 5. Ford and Glew argued that the “Ausgleichsfläche” could form only when the water film exceeds a critical thickness  $h_c$ , which should be higher than the roughness  $k$  of the rock. With this assumption by use of eqns. 1 and 2 one finds

$$l = \frac{\rho g}{3\eta q} h_c^3 \tan \gamma. \quad (24)$$

Therefore, by plotting  $l$  versus  $\tan \gamma$  one should find a straight line. This indeed is the case for the Glew and Ford’s (1980) data, as shown by Figure 5. The slope of this line is 14 cm, from which one finds a critical thickness  $h_c = 7.7 \cdot 10^{-3} \text{ cm}$  if one assumes a smooth surface. For a rough surface with  $k = h_c$  one finds a value of  $10^{-2} \text{ cm}$ . Glew and Ford measured a value below  $(1.5 \pm 0.5) \cdot 10^{-2} \text{ cm}$ , which is in good agreement. They also measured dissolution rates of  $4 \cdot 10^{-3} \text{ cm/h}$ . For their experimental data one finds  $c_\infty \approx 0.66 c_{eq}$  from eqn. 17.

The amount of flow leaving a rock of width  $W$  at  $x'$  is equal to the amount of rainfall which falls to the area  $W \cdot x$ . It carries away the mass of rock  $q \cdot c_\infty \cdot x$  which is dissolved from the rock’s surface area  $Wx' = Wx/\cos \gamma$ . Converting the mass of dissolved material to its volume one finds the retreat of rock

$$R_D = c_\infty \cdot q \cdot \cos \gamma / \rho_g, \quad (25)$$

where  $\rho_g = 2.3 \text{ g/cm}^3$  is the density of gypsum. With the experimental conditions of Glew and Ford one finds  $R_D = 2.7 \cdot 10^{-3} \cdot \cos \gamma \text{ (cm/h)}$ . This fits reasonably well into their data set. However, it rep-

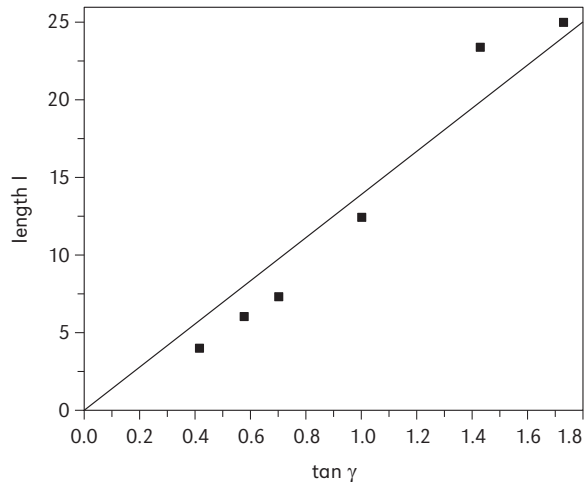


**Figure 5:** Length of experimental rillenkarrren versus slope,  $\tan \gamma$ . The squares are experimental data from Glew and Ford (1980). The line represents eqn. 24 with  $h_c = 7.7 \cdot 10^{-3} \text{ cm}$ .

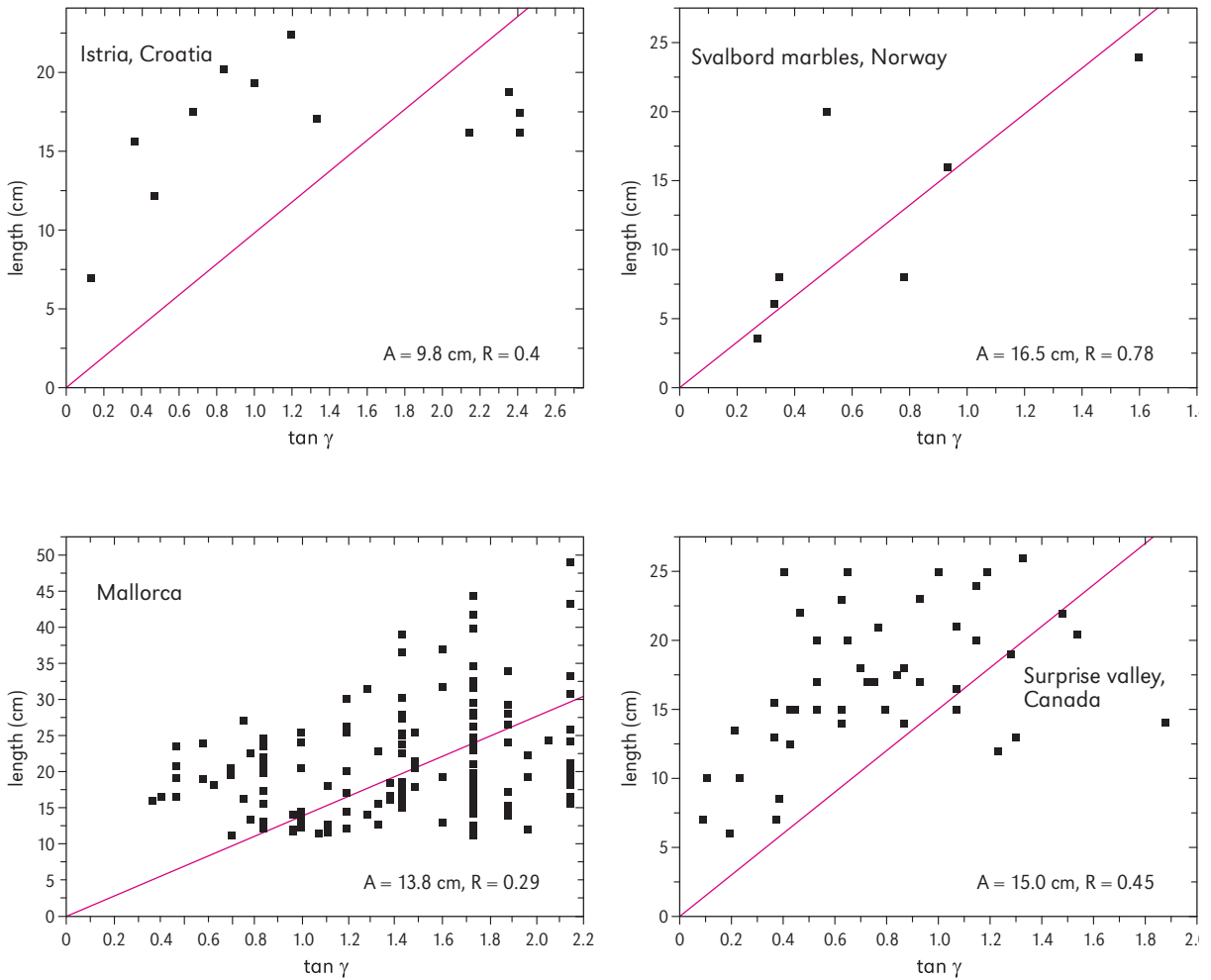


**Figure 6:** Length of natural rillenkarren on limestone versus slope  $\tan \gamma$ . From J. Lundberg and A. Ginés, personal communication. The straight lines are fits to  $l = A \cdot \tan \gamma$ .

resents a lower limit because one assumes laminar flow. Splashing raindrops may disturb this flow and cause mixing of the solution by which the effective diffusion constants increase. A factor of 10 is sufficient to rise  $c_{\infty}$  to  $0.9 c_{eq}$ .

In a recent work Petterson (2001) has exposed rillenkarren channels modelled from real limestone rillenkarren by plaster of Paris, to artificial rain of 115 mm/hour intensity. By using an optical technique he measured the thickness of the laminar flowing water films along the karren rills. The thickness of these films, measured at a distance of 5 cm to 40 cm from the upper edge, range from 0.2 mm up to 0.8 mm, when the karren model was

tilted by 30°. Water samples collected from the karren at various distances from the crest were used to measure the calcium concentration profile along the karren. Petterson found an almost linear increase from 75 mg/l of calcium at 5 cm to a value of 105 mg/l at 40 cm. The average value was  $90 \text{ mg/l} \pm 15 \text{ mg/l}$ .

With an average film thickness of 0.5 mm one finds  $\bar{\alpha} = 7.6 \cdot 10^{-4} \text{ cm s}^{-1}$ . With a rainfall intensity of 115 mm/h =  $3.2 \cdot 10^{-3} \text{ cm s}^{-1}$  by use of eqn. 22 one obtains a value  $c_{\infty} = 118 \text{ mg/l}$ . In view of the approximations this can be regarded as good agreement to experiment and proves our theoretical considerations.



### Interpretation of field data of rillenkarrren

A large body of data has been collected, which relates the lengths of rillenkarrren to the slope of the rock surface where they grow. From eqn. 24 one expects a linear relation of length and slope.

$$l = A \cdot \tan \gamma \quad (26)$$

with

$$A = \frac{\rho g}{3\eta q} h_c^3.$$

Figure 6 shows average lengths of rillenkarrren versus slope ( $\tan \gamma$ ) for several areas (Ginés and Lundberg, personal communication, 2006). The straight line represents a least square fit by the relation  $l = \text{const} \cdot \tan \gamma$  to the data points with  $\gamma \leq 64^\circ$  ( $\tan \gamma \leq 2$ ).

Although the scatter of points, which could be caused by differing values of precipitation  $q$  at different sites and times is significant one finds  $A = 12.6 \pm 3 \text{ cm}$  for all plots. From this by use of eqn. (26) one obtains  $h_c^3/q = (3.9 \pm 0.2) \cdot 10^{-4} \text{ cm}^2\text{s}$ .

Figure 7 shows the relationship of length with mean annual temperature as reported by Lundberg and Ginés (personal communication, 2006). The data can be fitted by a relation  $l = 0.5T + 12.6 \text{ (cm)}$ , where  $T$  is in  $^\circ\text{C}$ . The variation of  $l$  in temperature could result from the temperature dependence of  $\eta$  which can be presented with an accuracy within 2% by the empirical relation

$$1/\eta = 53.8 + 2.76 T \left[ \frac{\text{cm s}}{\text{g}} \right], \quad (27)$$

that is valid between  $0^\circ\text{C}$  and  $25^\circ\text{C}$ .

Introducing this into eqn. 26 one finds using  $h_c^3/q = 6.11 \cdot 10^{-4} \text{ cm}^2\text{s}$  and  $\tan \gamma = 1$

$$l = 12 + 0.52 \cdot T \quad [\text{cm}]. \quad (28)$$

The value of  $h_c^3/q$  is close to that found from the dependence of length on slope in the previous example.

As a final example we discuss the data presented in Figure 8 which relates the average lengths of

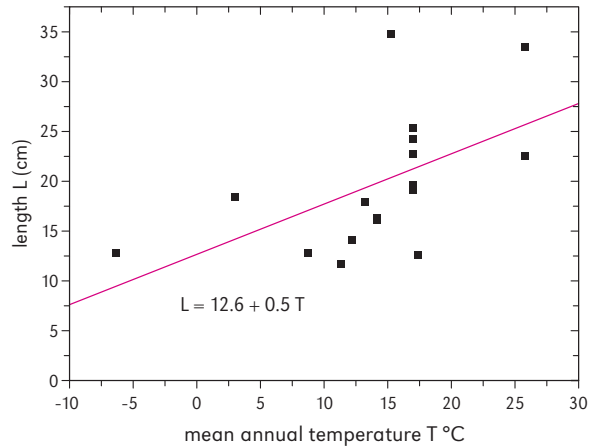


**Figure 7:** Length of natural rillenkarrren on limestone versus mean annual temperature. From J. Lundberg and A. Ginés, personal communication.

rillenkarrren in Serra de Tramuntana as a function of altitude above sea level, taken from Lundberg and Ginés (personal communication, 2006).

There is a clear decrease of length with altitude  $h$ , which can be caused by two reasons. First there is a linear relation between altitude and temperature. The up most abscissa shows the corresponding temperature given by

$$T = 17 - 0.0065 h \text{ (}^\circ\text{C)}, \quad (29)$$

where the altitude  $h$  is in m.

Furthermore mean annual precipitation  $q_{av}$  is related to altitude  $h$  by

$$q_{av} = 461 + 0.4h \text{ [mm/year]}. \quad (30)$$

See upper abscissa in Figure 8.

We now assume that the actual rainfall to the rock is related to  $q_{av}$  by  $q = f_q \cdot q_{av}$ , where  $f_q$  is a constant.

Both  $q$  and viscosity  $\eta$  depend on altitude. Using eqns. 26, 27, 29 and 30 one can calculate the length as a function of altitude. With  $h_c^3/q$  as a fitting parameter one obtains the curve in Figure 8.

The curve underestimates the large lengths, but shows the general trend. Whether it is a reasonable estimation must be judged from the value

of  $h_c^3/q(h)$ . If one assumes that 1000 mm/year correspond to an average actual precipitation of 10 mm/hour one obtains  $h_c = 0.005$  cm and correspondingly  $h_c^3/q(h) = 6.7 \cdot 10^{-4}$  cm<sup>2</sup>s. This value is also close to those found in the previous examples. Assuming an average actual precipitation of 10 mm/h dominant in the formation of karren one finds  $h_c = 0.0059$  cm from the length-slope relation and  $h_c = 0.0065$  cm from the length-temperature relation.

In all three examples we have assumed an average precipitation of about 10 mm/hour during the formation of rillenkarren. This is a value, which seems possible. For higher precipitation the length would be smaller and would be overprinted by lower precipitation yielding longer karren. At low precipitation rates (1mm/hour) the karren become very long (2 m) and will form very slowly, such that they may not be detected.

In summary, Glew's and Ford's idea that karren length is determined by a critical thickness  $h_c$  of the down flowing water film can be used to explain field data. One should keep in mind that at a precipitation rate of 10 mm/h a film thickness of 0.006 cm is attained after 27 cm on a smooth rock surface inclined by 45°.

We do not know at present the physical reason, why this critical thickness avoids further growth of rillenkarren. This requires experimental observations of flow rates and chemical composition of the water flowing on natural karren on limestone during rain storms of various intensities.

## Denudation rates in the field

### Gypsum

Denudation rates on subaerial exposed gypsum samples have been reported by Cucchi et al. (1996). In an observation station close to Triest (Italy) with a yearly rainfall of 1,350 mm they found 0.9 mm/year as an average during an observation time of eight years.

At rainfall intensities of 40 mm/hour the solu-

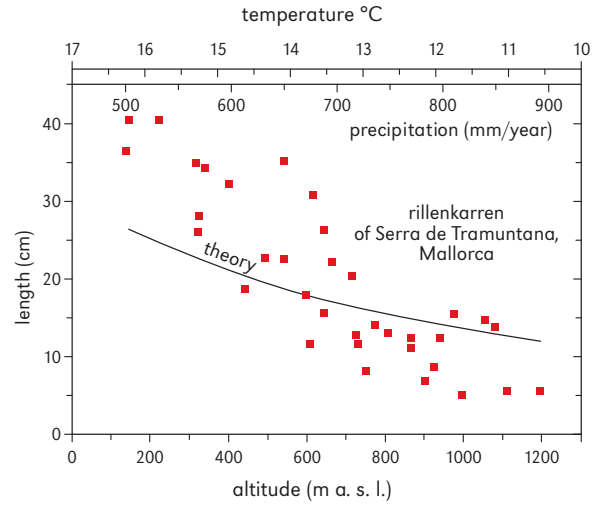


**Figure 8:** Length of natural rillenkarren on limestone (Mallorca) versus altitude above sea level. From J. Lundberg and A. Ginés, personal communication. The curve represents the fit discussed in the text.

tion running off the rock has a concentration of  $0.5 c_{eq}$ . At lower rainfall intensities of 4 mm/hour one finds  $c = 0.9 c_{eq}$ . Therefore it is reasonable to take an average value  $c = 0.75 c_{eq}$  for all the water during one year's rainfall. From this one finds a denudation rate of 1 mm/year.

### Limestone

For dissolution under linear kinetics with a rate law

$$R = \alpha(c_{eq} - c), \quad (31)$$

the time  $T$ , which is needed until a volume element with initial concentration zero attains concentration of  $0.63 c_{eq}$  is given by

$$T = h / \alpha. \quad (32)$$

For limestone with a film thickness of 0.2 mm one finds  $T_1 = 10^{-2} / \tilde{\alpha}_1 = 20$  s to attain  $c = 0.64 c_{app}$ . In the slower region 2,  $\tilde{\alpha}_2 = 2 \cdot 10^{-5}$  cm s<sup>-1</sup> and the time to reach  $c = 0.63 c_{eq}$  is  $T_2 = 500$  s. Under natural rainfall flow velocities are on the order of 1 cm s<sup>-1</sup>. Therefore dissolution will be effective only in region 1. Even when the water dissolved limestone

in region 2, the dissolution rates were about two orders of magnitude lower. In other words, all the water, which falls to the rock surface, will leave it with concentration  $c_{\infty}$  derived from dissolution in region 1.

With  $\tilde{\alpha}_1 = 10^{-3} \text{ cm s}^{-1}$  one finds

$$c_{\infty} = \frac{10^{-3}}{10^{-3} + 2.8 \cdot 10^{-5} \cdot p \cdot \cos \gamma} \cdot c_{app}, \quad (33)$$

where  $p$  is the rainfall intensity in mm/h.

At low slope angles ( $\cos \gamma \approx 1$ ) and for rainfall intensities of 1 mm/h,  $c_{\infty} = 0.97 c_{app} = 0.29 \text{ mmol/l}$ . At 10 mm/h,  $c_{\infty} = 0.24 \text{ mmol/l}$ , and for extreme intensities of 40 mm/h  $c_{\infty} = 0.14 \text{ mmol/l}$ .

Cucchi et al. (1996), by using micrometers, measured surface denudation rates on a huge number of limestone samples with slope angles of about 15 degrees in the karst of Triest. They found average dissolution rates sampled over eight years of  $0.015 \pm 0.01 \text{ mm/year}$ . At an average rainfall of 1,350 mm/year in this region one needs an average run-off concentration  $c_{\infty} = 0.97 c_{eq}$  to explain this number. A closer inspection of the distribution of rainfall-depth distribution is therefore necessary to verify this number. Anyway, our findings support that denudation on bare rock by the dissolutional action of rainwater is caused by fast dissolution in region 1 of Figure 2.

We have performed a first attempt to measure concentrations of rainwater flowing from the surface of a karren formation of limestone from Lipica, Slovenia, exhibited in front of the Postojna cave. After two days of heavy rainfalls, cleaning the rock from dust, water was collected during a medium strong rainfall of a few millimeters/h by use of an aluminum foil attached to the rock. Figure 9 shows the experimental situation. The water had flown on top of the formation, which exhibits only a slight inclination of about  $10^\circ$  degree for about one meter, then down one half meter, almost vertically, where it was channelled by the foil and collected into a beaker. This flowpath is depicted by the grey line. Measures were taken to prevent dilution of the sample by rainwater dripping into it. In parallel a sample of rainwater was collect-

ed. The specific conductivities were measured in the field. The conductivity of rain water was  $6 \mu\text{S/cm}$ , whereas the water from the karren exhibited  $57 \mu\text{S/cm}$ . Analysis for calcium in the lab yielded a value of  $0.25 \text{ mmol/liter}$ , 38% of the saturation value of  $65 \text{ mmol/liter}$  at  $10^\circ\text{C}$ , the temperature during collection of the sample. This result is in good agreement to what one expects from eqn. 33.

## Discussion and conclusion

We have presented some basic principles of flow dynamics of thin water films that can approximate flow on natural rock surfaces under rainfall conditions. Although these approximations are crude they can be used for realistic estimations.

To understand the formation of geomorphologic features on rock surfaces basic knowledge of the dissolution rates by flowing water sheets is needed. Water in equilibrium with the  $p_{\text{CO}_2}$  of the atmosphere dissolves limestone quickly up to a concentration of  $c_{app} \approx 0.3c_{eq}$ . For higher concentrations the dissolution rates drop rapidly. The time to reach the concentration  $c_{app}$  under natural rainfall conditions is on the order of 10 seconds, sufficiently short, that all dissolution will be affected in this regime of concentrations. Even if the solution would reach concentrations higher than  $c_{app}$ , then dissolution rates drop to such low values that they become insignificant. We have presented experimental data, which confirm this behaviour. It is also possible to understand from these kinetics denudation rates of limestone measured in the field.

For gypsum dissolution rates are controlled by mixed kinetics of surface reactions and molecular diffusion. Therefore, the rates become dependent on the thickness of the flowing water sheet. It is possible, however, to predict denudation rates on gypsum, as obtained from field data. Furthermore experimental findings on rillenkarren can be explained.

It should be noted that we have neglected temperature dependence and have used  $20^\circ\text{C}$  as stan-

**Figure 9:** Karren formation, from which water was collected. The grey line marks the flow path. The water was collected at the end of this line.



dard. Since many of the constants used depend on temperature, however, some temperature dependence on the denudation rates is expected. In view of the many approximations this is not of high significance.

We have not addressed the issue of rillenkarren formation. At present one may only speculate. The surface of the rocks acts to flow like a two-dimensional porous medium. In such an inhomogeneous

environment channelling can occur and parallel flow paths can arise, where the flow rates are higher. For limestone then the concentration  $c_{\infty}$  decreases and dissolution rates correspondingly increase. In gypsum the solution is close to saturation and therefore the amount of dissolved rock is proportional to the volume of the flowing water. One therefore could imagine that rillenkarren could only originate at rough rocks. This issue

can be handled experimentally by simulating karren formation experimentally on polished and rough samples of plaster of Paris.

An object of further research should be to measure flow velocities on limestone surfaces under natural conditions in dependence of rainfall intensity, and also to take samples of the water at various locations on that surface to obtain calcium concentrations. Such experimental data could

be of utmost use for a better understanding. One of the purposes of this work is to stimulate such research.

## **Acknowledgement**

We thank Joyce Lundberg and Angel Ginés for providing their field data in Figures 6, 7 and 8.

# BIOKARSTIC PROCESSES ASSOCIATED WITH KARREN DEVELOPMENT

Heather VILES

Karren features in many environments are covered with a variety of organisms, and many authors have suggested that microorganisms, plants and animals may contribute to surface weathering of limestone and other soluble rocks and the development of karst features. In this chapter I review the evidence for biological contributions to karren development, starting with a consideration of the types of organisms found on soluble rock surfaces.

## Organisms found on limestone surfaces

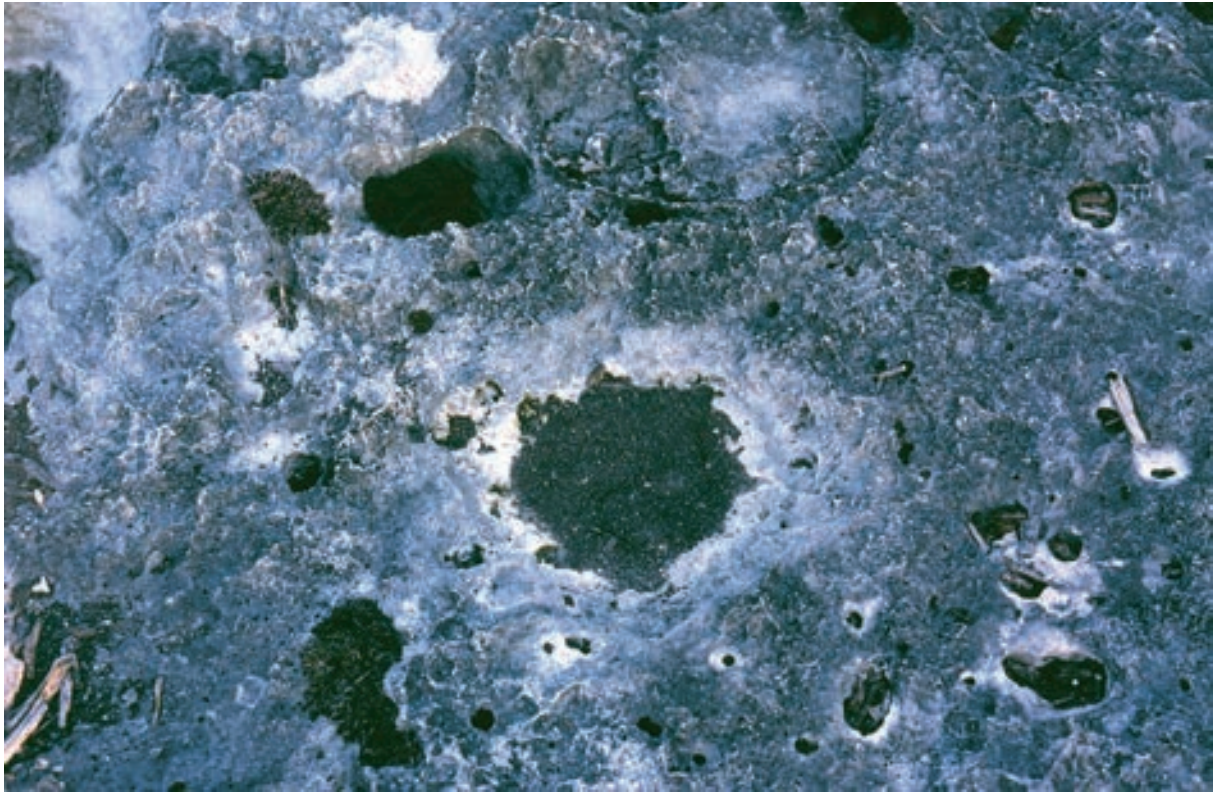
Most bare rock surfaces are discoloured by a layer of microorganisms, which together make up a biofilm. Such biofilms contain a mixture of microorganisms, including fungi, cyanobacteria (also known as blue-green algae) and lichens as well as associated extracellular products which create a slimy surface. Biofilms have been observed on many limestone surfaces, creating a grey to black patina where they are dominated by cyanobacteria and fungi and a multicoloured patchwork where dominated by lichens.

Figure 1 shows a characteristic biofilm on a limestone surface. Such biofilms can be several millimetres thick. Research by Viles et al. (2000) illustrates the speed at which surfaces can become

colonized by biofilms. On terrestrial limestone surfaces on Aldabra Atoll, Indian Ocean, they found that a cyanobacteria-dominated biofilm recolonized cleared squares on the surface within 16 years at many sites. Colonization was found to be rather patchy, however, with some particularly dry or hard sites experiencing very little recolonization even after over a decade. Many biofilms growing on carbonate rocks or building stones are highly biodiverse, as indicated by the findings of Tomaselli et al. (2000) from a survey of European buildings.

Higher plants can also be key components of rock surface flora, although their growth is in many cases limited by the absence of soils. Limestone pavements, for example, often contain a wide range of plants, many endemic to karst areas and of great conservation value (Ward and Evans, 1976; Webb, 1995). Animals also commonly range over and inhabit bare limestone surfaces, especially along coastal exposures where a whole suite of sessile and motile animals have been found to occur. Some animals are capable of extracting nutrients directly from the rock surface, whilst others make use of the rock surface biofilm as a source of food.

Organisms inhabit a range of rock surface niches, as shown in Figure 2. The terminology presented in Figure 2, which derives from the work of Golubić and others, has been applied



**Figure 1:** Mixed cyanobacterial biofilm on Quaternary age limestones from Aldabra Atoll, Indian Ocean. Width of view is 1 m.

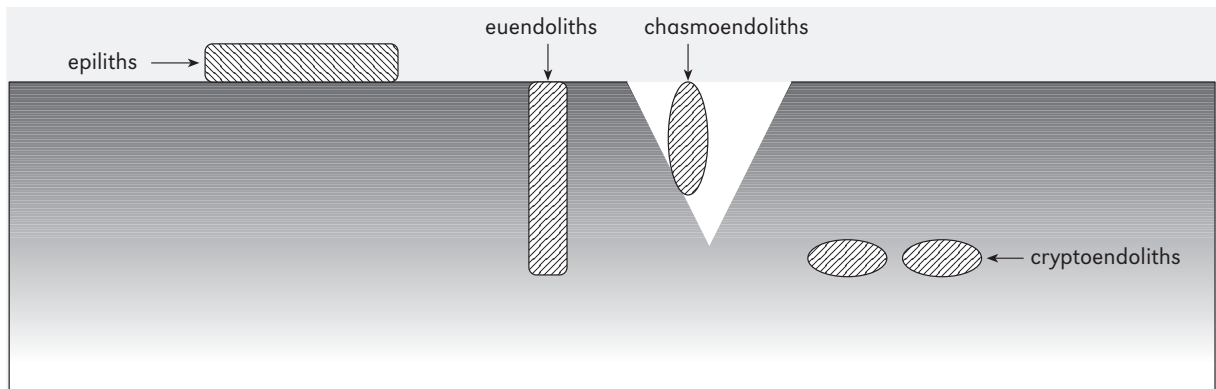


**Figure 2:** Rock surface niche terminology (from Golubić et al., 1981).

mainly to microorganisms but can also be applied to higher plants and animals. At the simplest level organisms growing on a rock surface are termed “epilithic”. Those that live under the surface are referred to as “endolithic”. There are

several different types of endolithic niche. Organisms which actively penetrate into the surface are called “euendolithic” whereas those that inhabit preformed fractures and cavities connected to the surface are called “chasmoendolithic” and those



**Figure 3:** Lichens growing on marble in the central Namib desert. The west-facing slopes (left side of image) are characterized by luxurious lichen growths, and the east facing ones with thin crustose forms.

that live in a subsurface layer within pores etc. are called “cryptoendolithic”. Finally, organisms which live under stones on the surface are called “hypolithic”.

The community of microorganisms, plants and animals found on bare limestone surfaces and the niches that they inhabit, varies according to climate and the nature of the environment. In particular cases carbonate island terrains support unusual plant and animal communities, such as those on Aldabra Atoll dominated by the Giant Tortoise *Geochelone gigantea*. In general the major controls are light and rainfall levels. On terrestrial karst surfaces, for example, there are gross differences between temperate, semi-arid and humid tropical communities. Studies from around the world indicate fairly similar biofilm communities across most environments, although the arid and cold extremes are characterized by unusual

and often species-poor assemblages. Coastal limestone exposures support a diverse suite of organisms tolerant of marine conditions including gastropods and algae, but with few lichens or higher plants. Finally, rock surfaces in cave environments are populated by highly specialized communities – especially in areas well away from light where non-phototropic organisms dominate. Viles (1995) proposed that at the macroscale across a gradient of decreasing rainfall, biofilms would change from being dominated by epilithic forms to endolithic ones.

At the more local level, rock surface communities are influenced by smaller scale variations in light and water availability. For example, on many inland limestone scarp slopes water flow paths become concentrated in some areas, producing fertile grounds for thick, rich biofilms (often called *Tintenstriche*, because they look like a streak of ink



running down the scarp face). In other drier areas biofilms are thinner and less species rich. Similar microenvironmental differences are found in arid terrains. On marble exposures in the central Namib desert, in southern Africa, for example, well developed lichen communities with foliose and fruticose forms common are found on the west-facing slopes which receive high amounts of fog, whereas on the east-facing slopes which experience the full force of the desiccating east winds only a thin cover of crustose lichens is found (see Figure 3). Endolithic forms are found more commonly on the harsher, east-facing surfaces. Both plants and rock-dwelling animals will tend to inhabit depressions and fractures within the rock surface, where there is more moisture, shade and soil development.

## Weathering and erosive action of organisms on limestone surfaces

It has commonly been found that the microorganisms, plants and animals inhabiting karst terrain play active roles in denuding the surface. Both biophysical and biochemical processes are involved, and organisms inhabiting both epilithic and endolithic niches can cause weathering and erosion. Looking firstly at biofilms, many studies have shown the biochemical weathering effect of epilithic biofilms that produce acid exudations which can contribute to calcite dissolution. When biofilms are removed from limestone surfaces the underlying surface is often found to be etched and pitted (Viles, 1987). Euendolithic microorganisms produce similar biochemical weathering, but in this case focused on producing the holes and tunnels which the organisms then inhabit. In some cases a networks of euendolithic boreholes is produced stretching several millimetres into the rock. This produces an altered near surface layer with high porosity. Cryptoendolithic biofilms may also contribute to exfoliation of limestone surfaces, as suggested recently for the Hirao-dai karst in Japan (Darabos, 2003). Many organisms pro-

duce quite complicated effects. For example, fungi have been found to produce spicily etched calcite as well as sparmicritization in experiments by Jones and Pemberton (1987). Some lichens, for example, produce different patterns of etching and boreholes under different parts of the thallus as evidenced by studies from Jerusalem which indicate pinhead pits caused by apothecia or perithecia of endolithic lichens and microgrooves formed by dissolution at the meeting point of lichen thalli (Danin et al., 1983). Figure 4 shows fungal hyphae from the base of crustose lichens growing on marble in the central Namib desert boring their way into the rock. Lichens can also have a biophysical weathering effect on limestone surfaces, as demonstrated in the pioneering experiments of E. Jennie Fry in the 1920s (e.g. Fry, 1927) and more recently by Moses and Smith (1993). Lichens are capable of absorbing an enormous amount of water relative to their size and weight, and on wetting and drying of lichens partially attached to limestone through hyphae at the base of the thallus considerable stresses are put onto the limestone, causing flaking and granular disintegration. Similar biophysical effects have been ascribed to chamoendolithic cyanobacteria which can expand by 300% on wetting and dislodge calcite crystals from the sides of fissures (Danin and Caneva, 1990). Many organisms can produce both biochemical and biophysical effects as evidenced by studies on lichens from the genus *Xanthoparmelia* growing on sandstone in Arizona (Paradise, 1997). Paradise found that biophysical weathering dominated under the centre of the lichen cortex, with biochemical weathering predominant towards the edge of the thallus. Synergistic associations of biological weathering processes with dissolution and physical weathering may also occur. Papida et al. (2000), for example, found enhanced physical weathering of limestones to occur under experimental conditions when inoculated with mixed microbial populations, in comparison with fresh limestone samples.

Plant roots can have endolithic growth forms, producing tunnels in limestone surfaces through

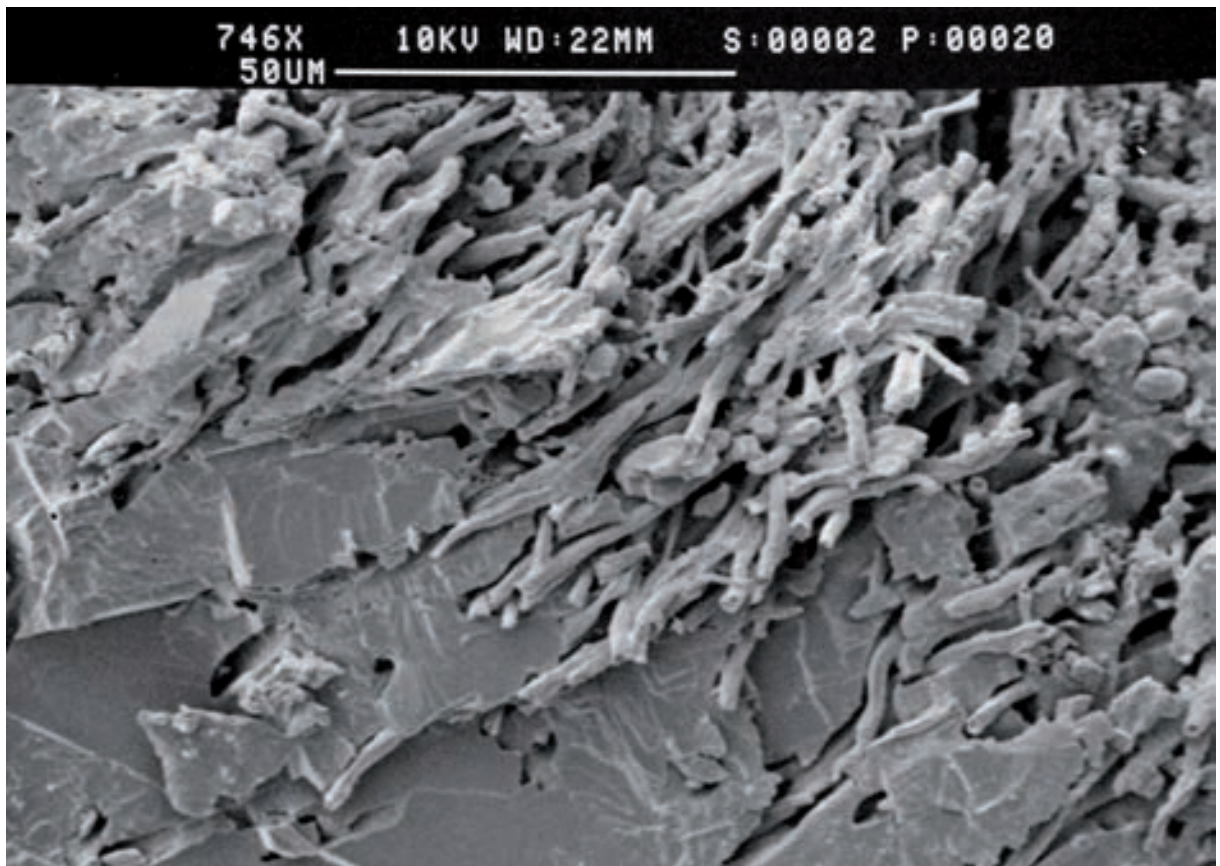


**Figure 4:** Fungal hyphae from crustose lichens boring into marble, central Namib desert. Scale bar = 50 microns.

biochemical and biophysical processes. Pioneering experiments carried out in the 19<sup>th</sup> century by Julius Sachs indicated the efficacy of roots from plants such as *Phaseolus multiflora* (bean) etching into polished marble surfaces. Recent attempts to reproduce such experiments have met with mixed success, however (Mottershead and Viles, 2004). Several studies have shown that plants are capable of taking up calcium and magnesium from limestone and other rock surfaces and soil minerals through biochemical activity in the roots and rhizosphere and thus may play a role in sculpting both bare and subsoil limestone surfaces (Hinsinger et al., 2001).

Animals actively denude limestone surfaces through a range of biochemical and biophysical processes. Many gastropods, for example, can graze effectively on rock surface biofilms and

remove particulate limestone along with the biofilm. Detailed experimental studies by Andrews and Williams (2000) on the chalk shore platforms along the south coast of England found a considerable amount of calcium carbonate within limpet (*Patella vulgata*) faecal pellets, which appeared to have come from limpets grazing on algae. Visible limpet grazing trails were found on the chalk surface, emanating from the “home scar”. The “home scar” also appears to be excavated by a combination of physical and chemical processes by the limpets themselves, perhaps enlarging a pre-existing depression within the chalk surface. Limpets here are thought to be responsible for 12% of downwearing of the platform in areas they frequent, and 35% or more where population densities are very high. Similar processes are carried out by a range of rock-dwelling organisms, largely

on coastal limestone exposures, although Stanton (1984) and others have found distinctive hollows that appear to be produced by terrestrial gastropods.

Biochemical attack on limestone surfaces can occur without direct involvement of organisms. For example, many reports have been made of the chelating and dissolving effect of a range of

organic acids which may be produced in soils and by decaying organic material (see the early work of Murray and Love, 1930). Trudgill (1985), for example, illustrates the highly corrosive nature of water acidified as it flows over tree bark producing characteristically polished and weathered limestone surfaces under trees. Animal urine may also dissolve calcite, producing runnels. It



**Figure 5:** The impacts of rock wallaby urine on limestone surface biofilms, Napier Range, NW Australia. Width of view is 7 m, on the upper edge.

can also have an indirect effect on the weathering of limestone surfaces, as evidenced in Figure 5 which shows the defoliating impact of rock wallaby urine on limestone surface biofilms from the Napier Range in NW Australia.

Although a wide range of biochemical and biophysical processes capable of effecting weathering and erosion can be identified, it must also be remembered that organisms can protect limestone from other agents of denudation as has been found for other rocks (e.g. Kurtz and Netoff, 2001; Mikulas, 1999). Biofilms, for example, act to bind surfaces together and absorb incoming rainfall and runoff thereby reducing the inorganic dissolution. Until the community decays and dies the underlying surface is protected. Lichens act in a similar fashion, acting as a net agent of protection even whilst producing fungal boreholes at the base of the thallus, but contributing to dramatic episodic surface removal as they decay. Some lichen species decay from the centre, with large sections of the thallus peeling away bringing with it portions of the underlying rock. Recent studies by Carter and Viles (2003) indicate the general protective role played by black lichen-dominated biofilms on limestone used as a building material. In field and laboratory experiments a cover of epilithic lichens (*Verrucaria nigrescens*) was found to retain moisture and dampen thermal stresses at the limestone surface thus reducing the potential for weathering. Rock surface dwelling biofilms may also contribute to surface protection through biomineralization processes, as found by Rodríguez-Navarro et al. (2003) in an experimental study. The bacteria *Myxococcus xanthus* was found to be able to produce a protective and consolidating carbonate matrix on stone samples under laboratory conditions.

## Biokarst and karren

*Biokarst* refers to karst landforms created, or influenced to a significant degree, by biological processes. In turn, the processes involved in the forma-

tion of such landforms are often called biokarstic. Biokarst features can be erosional or depositional, or involve a combination of the two processes, and are commonly found on exposed limestone surfaces in a range of environmental settings (Viles, 1984). An early paper by Jones (1965) describes many of the erosional features found on limestone pavements as being at least partly biokarstic in origin. Organic-rich soils cause accelerated dissolution here, and endolithic lichens on clint surfaces produce roughened surfaces from dissolution. More recent work has identified suites of small-scale karren along coastal areas as being biokarst (e.g. Schneider and Torunski, 1983).

If organisms commonly inhabit limestone surfaces on which karren features are developed, can an explicit link be made between some of the biochemical and biophysical processes reviewed in the previous section and the production of karren? If so, then karren may be at least partly biokarstic in nature. At the simplest level, the near ubiquity of biofilms on limestone surfaces (in non-soil covered terrain) and the importance of organic acids in most soils suggest that both bare and soil-covered karren are influenced by organic processes. However, it has so far been found to be difficult to prove a strong link between organic processes and the development of karren features. Some progress has been made with experimental studies, for example the work of Fiol et al. (1996) on the influence of rock surface microorganism communities in *rillenkarren* development. Their investigations showed that mechanical detachment of small particles is a key process in the development of rillenkarren, caused by raindrop impact which is enhanced in areas where endolithic cyanobacteria have previously corroded the surface.

In some cases highly unusual karren features have been identified which appear to owe their origin dominantly to biological processes, such as *phytokarst*. The classic phytokarst landscape is that described by Folk et al. (1973) at Hell, Grand Cayman island. Here, a series of limestone pinnacles in a low-lying swampy environment have been



Figure 6: Phytokarst pinnacle from Aldabra Atoll.

blackened and dissected in a random spongework pattern which Folk et al. ascribe to the action of cyanobacteria (blue-green algae). Figure 6 shows similar randomly sculpted forms from Aldabra Atoll. Jones (1989) has provided further detailed microscopic observations of this phytokarst and illustrated the variety of weathering roles played by the cyanobacteria and fungi dominated biofilms. On hard dolostones, epilithic microflora dominates, whereas on softer limestones a diverse endolithic flora is found. Another commonly iden-

tified type of phytokarst are the light-orientated erosional pinnacles found in the lit zone of many cave entrances (as reported by Bull and Laverty in 1982 in Mulu, Borneo, for example, and sometimes given the alternative name of *photokarren*). However, making a convincing process/form link between biofilm processes and phytokarst has proved to be difficult and there may be a range of controls operating at different scales (Viles, 2001). Indeed, Taboroši et al. (2004) propose that much karren on young island karst is better called “eo-

*genetic karren*” rather than “phytokarst” as it is probably polygenetic in origin and the heterogeneous nature of the young limestones exerts a major control on the resulting karren forms.

In other cases, process/form links may be easier to prove. Some interesting work has been done by Simms (1990) on coastal phytokarst or photokarren in Ireland. He finds ample evidence of light orientated pinnacles adjacent in ancient cave passages. The photokarren develop near unroofed sections where light can enter. Simms notes that scallops, formed when the caves were active, are well preserved in other parts of the caves despite the ingress of seawater today. This implies that seawater is not having a direct dissolutional effect, and thus the creation of the photokarren is the only form of weathering occurring today.

### Issues for further work

Most surfaces on which karren features are developed are exposed to biological influences. However, it is difficult to prove whether such biological influences are a necessary part of karren formation, or whether they have little real impact. Indeed, some authors have argued in the past that biological processes act to degrade karren features produced by inorganic dissolution processes. Further information on rates of biological weathering may help resolve some of the questions about the role of biokarstic processes. It is difficult to assess the speed at which biological weathering

and bioerosion occur, especially as they are often highly spatially and temporally patchy. Danin (1983), however, used information on the depth of pits occupied by cyanobacteria on dated walls in Jerusalem to estimate an annual biological weathering rate of 0.005 mm per year, which probably exceeds the rate of dissolution in this semi-arid area. More recent work in Jerusalem and Rome indicates pitting of marble by cyanobacteria from the genus *Myxosarcina* to be occurring at the rate of 0.025 mm per year (Danin and Caneva, 1990).

One key issue in assessing the role of organisms in karren formation is that of temporal scale. Are organisms permanent enough features of the rock surface environment over the timescales of karren formation? Another issue is spatial scale. Many of the biological processes take place at the sub-millimetre scale, whereas karren features develop over the centimetre to metre scale. Even if biological processes play a role in karren development, other factors undoubtedly exert larger scale controls (such as jointing). Thus, it is probably more accurate to say that biological processes contribute to the formation of many karren and other karst landforms. Whether they can be seen to play the dominant or decisive role is perhaps much less important.

The debate over biokarst draws attention to the many, diverse ways in which biological processes influence karst features and furthermore the large role that organisms play in the global carbonate cycle (Schneider and Le Campion Alsumard, 1999).



# KARREN SIMULATION WITH PLASTER OF PARIS MODELS

Tadej SLABE

The experimental modelling of rock features in plaster helps reveal the manner of their formation, the development of individual rock features in nature, and their connections in rock relief. It also helps us distinguish the proportion and significance of the legacy of various factors that participated in the formation of rock relief and indirectly therefore the various periods of its development.

Limitations do exist regarding either the size of the models or the more rapid solubility of plaster compared to carbonate rock. Primarily, we can follow the manner of the shaping of soluble stone in various conditions and the development of the rock relief on it; however, the direct comparison of individual rock features on plaster and on rock is more difficult, especially due to their size. As a rule, features on plaster are smaller (Slabe, 1995b). The rapid solubility of plaster influences their frequently jagged form and rough surface. Experiments on the formation of subsoil rock features must be interrupted and models must be taken apart since this is the only way to observe their continuous development. However, the experiments continue to confirm that their use is helpful.

Industrial plaster ( $\text{CaSO}_4 \cdot x \text{ water}$ ) is used in the experiments. In one litre of water, 2.5 grams of gypsum are dissolved at 20°C (Klimchouk, 2000a).

The chapter presents the latest findings of experiments in the formation of subsoil rock relief and plaster blocks exposed to rain.

## Previous experiments described in the literature

Pluhar and Ford (1970) studied the formation of flutes (rillenkarren) using hydrochloric acid on a dolomite block. However, when they covered the dolomite with a layer of quartz sand, only micro pits developed.

Glew (1976) and Glew and Ford (1980) studied flutes with experiments exposing plaster surfaces inclined from 22.5° to 60° to artificial rain. They determined that flutes develop where the layer of water flowing off an inclined surface is thin and does not prevent the direct impact of raindrops on the rock. Under a thicker layer of water, however, a smooth rock surface develops. The length of the flutes is related to the inclination of the rock surface and their cross-sections have a parabola shape, the shape that most efficiently directs the erosive action of raindrops along the axis of the flute.

Dzulynski et al. (1988) used modeling to study the formation of karren, exposing a fissured piece of plaster to artificial rain. They studied karren shaped by rainwater as well as subsoil karren.



They were interested in the dissection of the plaster into channels that developed along the fissures, the formation of the protuberances between them, and the influence of the level of water surrounding them on their development. Thicker columns formed when the plaster was crisscrossed by only a few fissures, and when the network of fissures was dense, the columns were thinner. They determined that the amount of rain influences the speed of the dissolution of the plaster but not the form of the artificial karren. Karren that developed on plaster covered with sand was similar to that which developed on bare plaster, and only the columns were less sharply dissected. On the walls of a small model of uncovered karren, it was possible to discern vertical channels at the end of lapies wells (karrenröhren) and funnel-shaped recesses on their tops with channels underneath them.

Experiments with plaster have been employed in researching cave rock features as well. Scallops were studied by Rudnicki (1960), Curl (1966), Goodchild and Ford (1971), and Allen (1972). Such experiments helped Quinif (1973) explain the formation of ceiling pockets, Ewers (1966, 1972, 1982) study the development of the network of original watercourses through rock, and Lauritzen (1981) study above-sediment channels. Tučan (1911) exposed limestone and dolomite to hydrochloric and nitric acid and established that their surfaces were similar as on the karst surface, of course with characteristic differences between limestone and dolomite. Trudgill (1985) describes the smoothing of rock surfaces due to exposure to acidic waters. He proved his findings through laboratory experiments using acids and scanning rock surfaces with an electron microscope.

Experimental research (Slabe, 1995a, b) on cave above-sediment ceiling channels and anastomoses, below-sediment flutes, various types of scallops and the influence of rock and hydraulic conditions on their size and shape, and ceiling pockets that occurred due to the percolation of water through fissures helped a great deal in conceptualizing their development and the diverse formation of karst caves.

## Recent experiments

### Experimental formation of subsoil karren

Some of the findings from the experiments described below are presented in detail in *Zeitschrift für Geomorphologie* (Slabe, 2005).

I attempted to verify the descriptions of various subsoil features (see chapter 11) with experiments on the formation of *subsoil karren*.

We sliced a plaster cube into small columns with six-centimetre square cross-sections and heights of 30 centimetres (Figure 1). The separated columns were placed tightly side by side in a large bucket and covered with soil. We drilled small holes in the bottom of the bucket and then filled it with water. We provided a continuous supply of water to keep the surface of water five centimetres above the surface of the soil. Slowly, the water started to percolate through the soil and then flow through the holes in the bottom of the bucket. After the experiment, which with breaks lasted almost 400 hours, the columns were eighteen to twenty-seven centimetres tall (Figure 2).

The upper two thirds of the walls of the columns are eroded with tiny features, the traces of the percolation of water through the alluvium and its flow along the contact point between plaster and alluvium.

The entire surface of the peak section of columns is minutely eroded with *micro recesses* (Figure 3a). The micro recesses are up to two centimetres in diameter, although the majority is smaller. It appears they are the consequence of the constant percolating of water through the most permeable layer of soil. As a rule, epikarst rock features (see chapter 11) have this sort of roughness on rock covered with soil where the contact with the rock is loose.

The larger *recesses* found as a rule in the middle of columns (Figure 3b) have relatively smooth surfaces. I called recesses of this type - incomparably larger, of course - subsoil scallops (Slabe, 1998).

Along fissures or other weak spots in the rock, individual deeper semicircular or channel-shaped

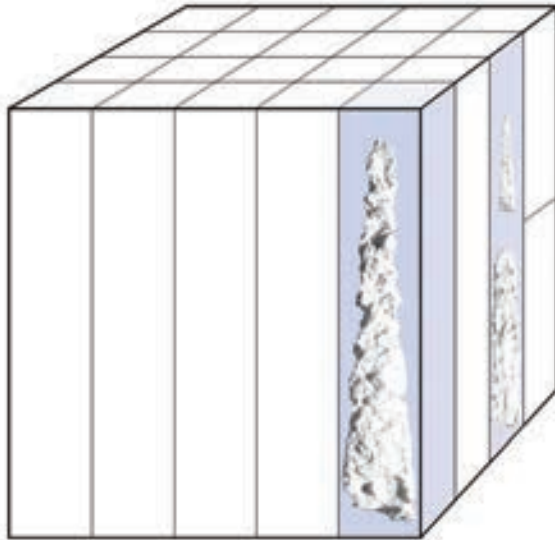


Figure 1: Plaster block from which stone forest developed.

recesses often occur in many cases that can in time grow into *subsoil tubes*.

*Channels* (see chapter 11) whose diameters

ranged from one to three centimetres formed on the walls of the lower sections of the columns (Figure 3c). The locally flooded zone, which developed because the quantity of water flowing along the contact was greater than the quantity that could flow out of the perforated bottom of the bucket, reached the upper level of the channels. This margin is often marked by *notches* (see chapter 11). This subsoil formation of karren is characteristic of the alluvium-covered and periodically flooded valley systems of the lower karst regions in southern Slovenia and the estavelle mouths on Cerknjško polje.

On the lower surfaces of the columns (Figure 3c), including those cut in half horizontally, there are distinctive networks of *above-sediment anastomoses* (Slabe, 1995a). The channels composing them have omega-shaped cross-sections with diameters measuring up to three centimetres. The networks have several stories.

Angular and square cross-sections were only



Figure 2: Subsoil stone forest in plaster.

preserved in the lower sections of the columns. The characteristically pointed shape of the upper



**Figure 3:** Column with characteristic rock relief: a. recesses and protuberances; b. recesses; c. channels and anastomoses.

sections of the columns is the consequence of the dispersed percolation of water through the soil that covered the plaster.

In the final experiment (Figure 4) of this series, we covered larger plaster pillars (the cross-section of the larger pillars was 20 centimetres, and they were 25 centimetres tall) with fine-grained clay, which is poorly permeable to water as therefore was the contact between the clay and the pillars. Subsoil shafts were the first feature to develop between the columns. On the upper sections of the columns (Figure 4, left), vertical subsoil channels formed as parts of the shafts with funnel-shaped mouths at the top. Their cross-sections reached 3 centimetres. It appears that water finds the most conductive path along the poorly permeable contact between plaster and clay and forms streams. This hypothesis was confirmed by the bubbles that appeared on the water surface, which revealed numerous distinctive ponors. Special channels formed in the locally flooded zone, like those described in the previous experiment, developed in the lower section of the columns. Anastomoses developed on the lower planes of the columns.

The peaks of the columns gradually sharpened, nearing a pointed shape. We interrupted the experiment several times to observe all the stages of development of subsoil karren.

After 800 hours, when the experiment was concluded, the two taller columns were 20 centimetres high, and the width of the thicker column was 20 centimetres. From the smaller columns remained two 5-centimetres tall and up to 1.5 centimetres thick pieces of plaster.

The columns are quite pointed (Figure 4, right), which is most evident in the two larger columns, especially the thickest. The sharp side edges were preserved.

Over time, the rock relief became increasingly similar to that in the first experiment, especially on individual faces although as a rule the surface of the columns was flatter. New characteristics are preserved, such as dissection with more or less vertical and, depending on the varying degrees of permeability at the contact between the plaster

**Figure 4:** Development of gypsum subsoil pillar; left: early stage, right: final stage of experiment.



and clay, more or less meandering subsoil channels. Higher on the walls of the columns than in the first experiments, horizontal or variously inclined notches are preserved, reflecting the more completely filled cracks and tighter contact between the plaster and clay and consequentially the lower permeability of the model. The surface of the plaster was weathered in more places, meaning the solution was not carried away everywhere at the same time.

#### Experimental modeling of “rock peaks” in plaster exposed to rain

In studying the rock relief of karren and stone forests, questions arose regarding the development of

rock peaks exposed to rain and their rock relief, which often formed on top of the legacy of older, especially subsoil relief. I therefore decided to expose small plaster blocks with sides measuring forty centimetres square to rain.

I exposed three blocks of various shapes to natural and artificial rain. I leaned an uncut cube at a  $27^\circ$  angle and cut a second cube diagonally into two halves. I placed the first resulting prism on a shorter face and wedged it so its longest face had a  $36^\circ$  incline. I placed the second one on an edge so that one of its smaller square faces was horizontal, the second was vertical like the triangular side faces, and the longest face was overhanging with a  $45^\circ$  incline. I thus obtained flat faces inclined at  $27^\circ$ ,  $36^\circ$ ,  $63^\circ$ , and  $90^\circ$ , overhanging faces with inclination of  $9^\circ$ ,  $27^\circ$ , and  $45^\circ$ , and edges of various

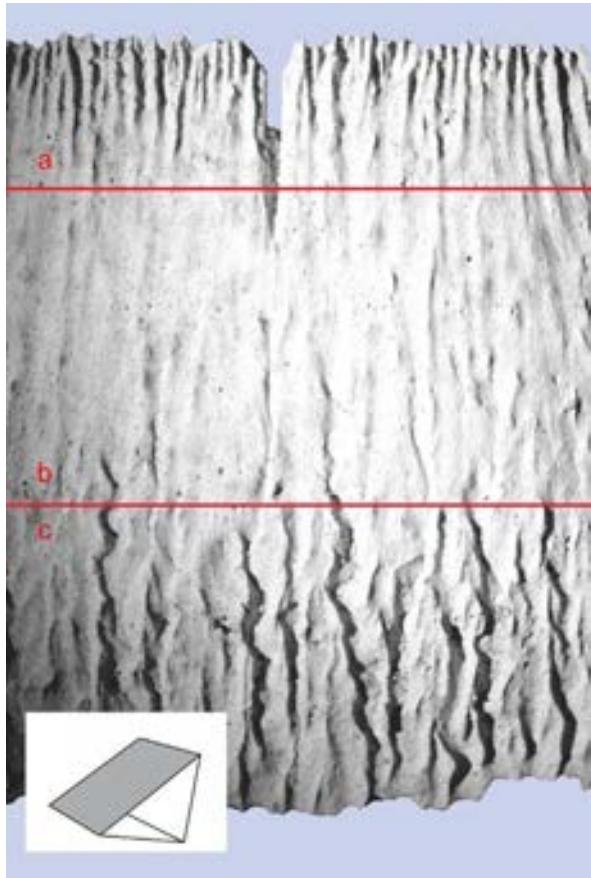


**Figure 5:** Surface of plaster exposed to rain with characteristic rock relief: a. flutes; b. smooth surface; c. channels.

lengths along them. I cut a channel similar to a subsoil channel, one centimetre in diameter, into the face with an inclination of 63°. The surface of the faces with different inclinations was smooth.

We can distinguish two kinds of development on the plaster blocks. The variously inclined faces exposed directly to rain and the vertical faces were formed in a characteristic way. The overhanging faces, however, were formed uniquely in both cases.

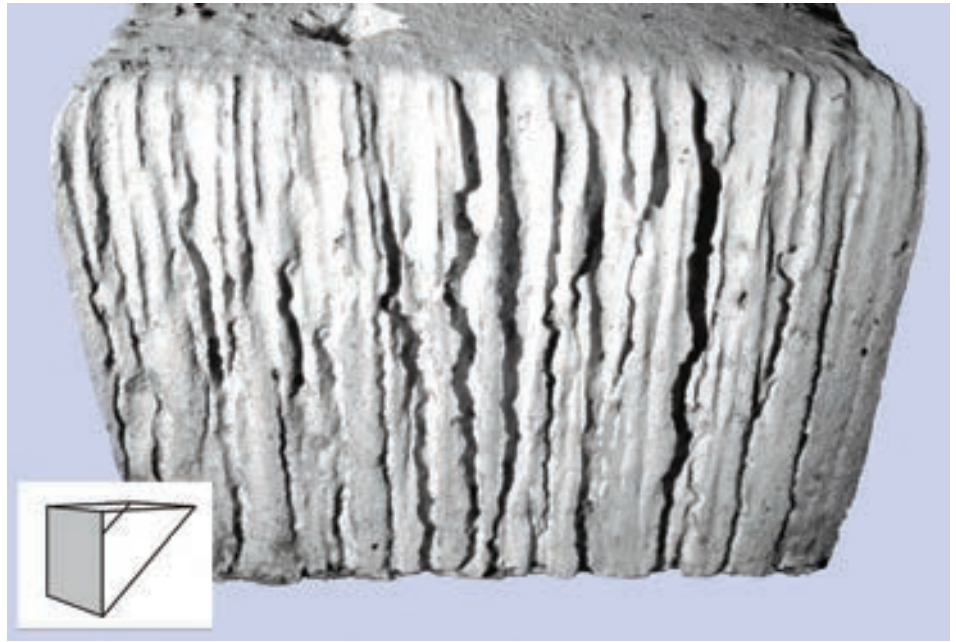
After ten hours, straight, narrow, long, and shallow scallop-like recesses first appeared in the middle of the face with a 36° inclination, and narrow channels appeared on their lower sections. The upper edges were dissected into semicircular notches, below which *flutes* began to appear. Gradually, three distinct sections of the faces were

created (Figure 5). The upper sections were covered by flutes (Figure 5a), the central sections were relatively smooth, and channels developed on the bottom sections. This characteristic shaping of the faces is also shown in a drawing in a book by Ford and Williams (1989). The flutes grew slowly from the upper edge downwards and deepened. At first, their form was indistinct and it was impossible to measure their size in detail because the ridges between them were rounded. However, I believe that their width did not differ substantially from the size of “mature” flutes. On the face inclined at 27°, the flutes average 3.6 centimetres long, 0.7 centimetres wide, and 0.5 centimetres deep in the upper part; lower down they are more shallow and end in a wedge-shape. On the face inclined at 36° they average 4 centimetres long, 0.8 centimetres wide, and 0.5 centimetres deep in the upper part. On the steepest surface (63°), their most distinct parts average 7 centimetres long, 0.5 centimetres wide, and 0.3 centimetres deep in the upper section. In the last case, it is difficult to determine the length because individual flutes extend all the way to the channels in the bottom section of the face. On the steepest surface, the flutes are therefore longer and also somewhat narrower. They also appeared on the overhanging surface inclined at 9°.

Individual *channels* (Hortonian-type runnels; Ford and Williams, 1989) formed on the bottom section of the inclined faces (27°, 36°, 63°). At first, they were relatively straight, 0.5 centimetres wide and 10 centimetres long. Between them were larger areas without channels. Initially, the channels mainly deepened. Their cross-sections took the shape of the letter omega turned upside down. The ridges between them were gradually sharpened by rainwater. The channels widened to 2 centimetres. In the bottom section thus forms a web of channels that initially develop as collectors of water from the upper section of the inclined face and when they become deeper, rainwater starts to shape them as well as carving flutes on areas between the channels (Figure 5c).

A special type of *channel*, which Ford and Williams (1989) call a “Hortonian-type dissolution

**Figure 6:** Channels on a vertical wall.



channel”, forms on vertical faces on which water flows from the horizontal top (Figure 6). At first, channels with three-millimetre diameters formed that meandered slightly. They were most distinct on the upper section of the faces, below edges that were jagged with semicircular notches. These channels extended to the bottom of the vertical faces. Initially they deepened and their cross-sections acquired the form of the Greek letter omega. Between the channels were larger undissected areas, but channels later covered the majority of the face. The channels gradually begin to merge and the largest reach 3 centimetres in diameter with smaller channels remaining on the ridges between them. The rock relief of the pillars in Spain’s El Torcal stone forest was formed in this fashion. The upper sections of the vertical faces of the plaster blocks that are directly exposed to rain gradually become less steep; so far, they have diverged by three centimetres from the vertical. The edges between the upper parts of channels, which are increasingly exposed directly to rain, therefore become sharp and the channels open semicircularly. Slowly they transform into flutes (Figure 7).

I carved two channels with diameters of one centimetre into the surfaces inclined at  $63^\circ$  and  $36^\circ$  to represent *subsoil channels*. Their diameters

grew by one centimetre, and a smaller meandering channel cut into the bottom, particularly distinct in their lower part. The mouths of the channels became funnel-shaped, 3.5 centimetres wide, and at first dissected by flutes. This is a frequent and characteristic form for the peaks of the Lunan stone forests (Knez and Slabe, 2002).

The entire plaster blocks are shaped in a characteristic way. The exposed edges remain flat and sharp but become jagged in accordance with their dissection by flutes. The outer corners of the horizontal and vertical faces are dissected by notches that are the mouths of vertical channels into which water flows from the upper face. All the plaster blocks get sharper, and the upper sections of originally vertical faces incline inwards and are increasingly exposed to the direct action of the rain. On the plaster block with a flat upper face, the vertical side faces bow concavely and the corners project outward three or four centimetres.

## Conclusion

In spite of the limitations of experiments of this type described in the introduction, particularly the rapid solubility of plaster due to which the



**Figure 7:** Development of rain flutes on channels.

surface is often more minutely dissected and the limited possibilities for monitoring its formation, these experiments offer numerous advantages. They complement the knowledge acquired in nature and frequently open new directions for further thought and research. Often the forms that develop during the shaping of models are un-

known at first and are only later discovered in nature with the help of or because of our previously acquired knowledge. In any case, these experiments should continue, supported of course with a comprehensive and interdisciplinary foundation and upgraded knowledge.

# THE PROBLEM OF RILLENKARREN DEVELOPMENT: A MODELLING PERSPECTIVE

Matija PERNE and Franci GABROVŠEK

A few chapters discuss morphological aspects of rillenkarrren and observation of their formation. However, a satisfactory model of rillenkarrren formation based on the first principles has not been presented so far. For the time being, it would be of a benefit if we could prove or disprove some assumptions used for the rillenkarrren development.

Experimental and field evidences lead to the following conclusions for the rillenkarrren development:

- rillenkarrren form on initially flat inclined surfaces of soluble rock under constant rain;
- they form on all soluble surfaces provided that these are exposed to the rain long enough;
- the formation of rillenkarrren is dissolutional; they form if dissolution rates are different on different positions on the rock surface.

To convert these observations into a mathematical model, we assume a flow of thin water film with uniform (continuous) recharge over an inclined surface of soluble rock. The question which we want to answer is whether such film alone is sufficient for the rillenkarrren development. Our model includes some other assumptions which are making the calculations easier:

- concentration of dissolved rock is small enough that it does not influence hydrodynamics, i.e. the flow is calculated in advance;
- the flow is calculated in a steady-state approxi-

mation. The rain is continuously distributed to the surface of the water film. Consequences of raindrop impacts are not investigated;

- we use thin film approximation for the Navier-Stokes equation. Additionally we neglect surface tension;
- the development of rillenkarrren has to go through a stage in which the surface is only gently undulated, covered with shallow rills which are becoming deeper.

A satisfactory model of rillenkarrren formation thus has to predict that a rill which is not as deep as mature rills will deepen.

## Methods and results

### Protorrill

All the models are tested on the same rock surface form, dubbed protorrill. It has parabolic shape because every gentle curve is parabolic in the first approximation. Its slope is  $40^\circ$  and it is 2 cm wide, which are typical values for rillenkarrren, while it is only 0.5 mm deep, much less than real rillenkarrren. The upper 16 cm of such a rill were studied. The density of water is taken to be  $10^3 \text{ kg/m}^3$  and its viscosity  $10^{-3} \text{ Pas}$  (Figure 1).



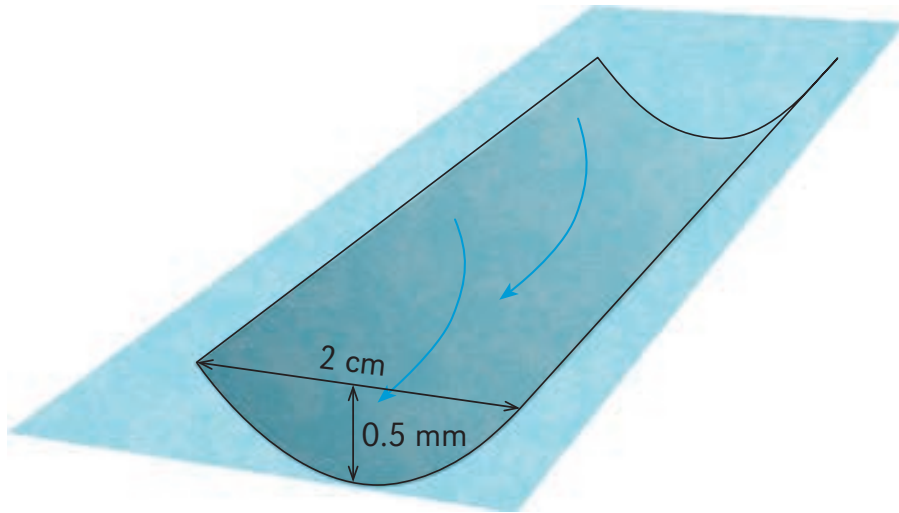


**Figure 1:** The protorill. Rain is uniformly distributed over the whole surface. Blue arrows indicate flow lines.

### The flow

Fluid flow is described by Navier-Stokes equation which is generally difficult to solve. Because of that some reasonable approximations are used in order to simplify it.

For our needs water can be considered incompressible. In this case the Navier-Stokes equation becomes

$$\rho \left[ \frac{\partial \mathbf{v}}{\partial t} + (\mathbf{v} \cdot \nabla) \mathbf{v} \right] = \mathbf{f}_b - \nabla p + \eta \nabla^2 \mathbf{v}, \quad (1)$$

where  $\rho$  is density,  $\mathbf{v}$  is velocity,  $t$  is time,  $\mathbf{f}_b$  are body forces per unit volume,  $p$  is pressure and  $\eta$  is viscosity.

We neglect inertial forces to get the so-called lubrication approximation (Kondic, 2003). In other words, we neglect the whole left side of equation 1, and second derivatives of velocity in direction parallel to the surface. Additionally we neglect surface tension.

A local Cartesian coordinate system in which the rock surface lies in  $xy$  plane is introduced (Figure 2). Here  $\alpha$  is the surface slope,  $h$  is thickness of the water film,  $m = h / \cos \alpha$  is water depth and  $z_0$  is elevation of rock surface above a reference level. Within the mentioned approximations the density of water flow  $\mathbf{j}$  is proportional to the third power of the water film thickness and to the surface slope.  $\mathbf{j}$  is proportional to the third power of

the water film thickness and to the surface slope. That is

$$\mathbf{j} = -\frac{\rho g}{\eta} \frac{h^3}{3} \nabla (z_0 + m), \quad (2)$$

where  $g$  is acceleration of gravity and  $\nabla$  stands for derivation in  $x$  and  $y$  directions only. Conservation of water gives another equation:

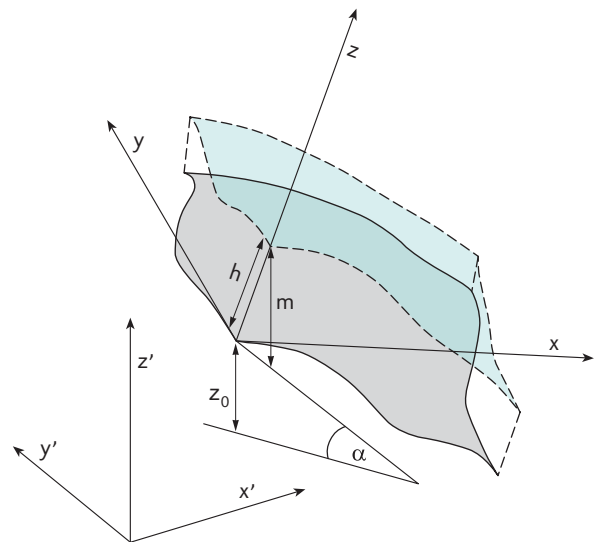


**Figure 2:** Coordinate systems. The local coordinates are introduced, so that the rock surface lies in  $xy$  plane. See the text for notations.

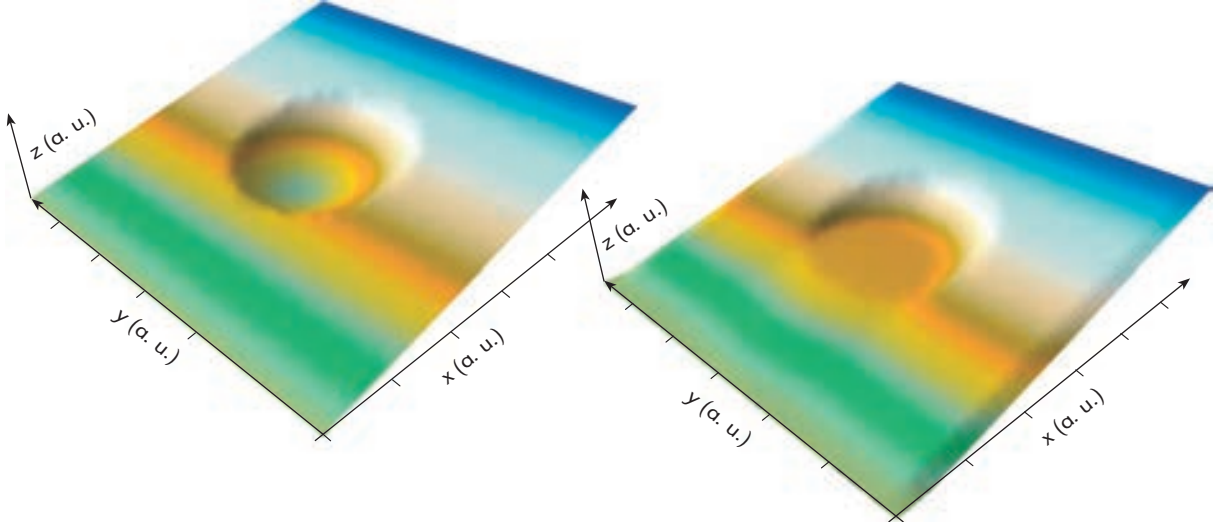


**Figure 3:** The left graph shows the rock surface and the right one the steady-state water surface when the rock is exposed to rain.

$$\nabla \cdot \mathbf{j} = \tilde{v}_r - \frac{\partial h}{\partial t}, \quad (3)$$

where  $\tilde{v}_r$  is rain intensity in the  $z$  direction.

The equations 2 and 3 can be solved numerically for arbitrary surface shape. We applied the method of time propagation which is efficient enough to find an approximate steady-state solution. The algorithm flows as follows: an initial approximation for  $m$  is taken,  $\mathbf{j}$  is calculated from equation 2 and the new  $m$  after a short time step is calculated from equation 3. The procedure is then repeated with the new  $m$  as initial approximation until  $m$  converges to a steady state and does not change anymore.

Figure 3 shows a test result of the algorithm on a slope with a depression. A pool of water fills the depression the same way as in reality. The method performs as good as expected, or even better. It should be noted that in this case an assumption of lubrication approximation that water and rock surfaces are nearly parallel is not fulfilled but the result is realistic anyway.

To test the numerical solution, which is inherently only approximate, the water flow over the protorrill can be calculated analytically. The steady-state form of the equation 3 is

$$\nabla \cdot \mathbf{j} = \tilde{v}_d \quad (4)$$

where  $\tilde{v}_d$  is time average of rain intensity. The flow density  $\mathbf{j}$  is parallel to the water surface slope. The equation is nonlinear because  $\mathbf{j}$  depends both on the third power of water film thickness, or  $m$ , and on gradient of  $m$  itself. But if the local water depth is much smaller than typical height differences between points on the rock surface, the rock surface slope is approximately equal to the water surface slope and can be used in its place. Thus the equation becomes linear and easy to solve analytically. We used the method of characteristics to solve it.

Results of numerical and analytical solutions are shown on Figure 4. The results are almost identical for the upper part of the rill. On its lower part the numerical solution becomes smoother while the analytical one stays sharp. The numerical algorithm suffers from numerical diffusion which smoothnes the solution. Differences could also result from the additional approximation used in analytical calculation. It turns out that the difference between both solutions is important only when the water is deep in comparison to the rill and the presumptions of the analytical method are no longer fulfilled. Thus, both solutions are in

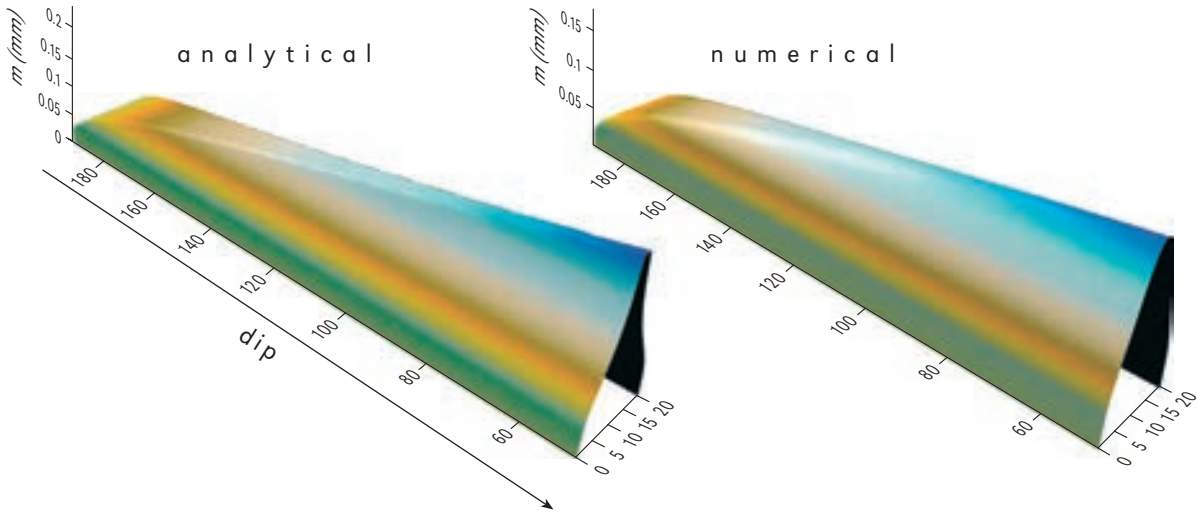


**Figure 4:** The depth of water film as a function of position on the protorill. Left graph presents the results of analytical calculation and the right graph the numerical one. The rill dips from left to right. The results are for rain intensity of 10 mm/h. All coordinates are in mm.

agreement when the analytical one is correct. That means the difference results from the additional approximation in analytical method, so the numerical solution was used in further calculations. Results are also in good agreement with experimental data given by Pettersson (2001).

### Dissolution kinetics

The dissolution rates of calcite are determined by three rate-controlling processes (Kaufman and Dreybrodt, 2007):

- the kinetics of dissolution at the mineral surface, which depends on the chemical composition of the solution at the mineral surface;
- the diffusion of ionic species and  $\text{CO}_2$  towards and away from the calcite surface;
- the conversion of  $\text{CO}_2$  into  $\text{H}^+$  and  $\text{HCO}_3^-$ .

Depending on particular conditions any process can be rate limiting (see Kaufman and Dreybrodt, 2007). In the case of a few tenths of a millimetre thick water film, molecular diffusion and  $\text{CO}_2$  conversion are rate limiting. It turns out that the dissolution rate is only weakly dependent on

the film thickness (Dreybrodt, 1988; Kaufmann and Dreybrodt, 2007). Therefore, we use equation

$$\frac{\partial \rho_s}{\partial t} = \beta(c_{eq} - c) \quad (5)$$

to describe the dissolution rates.  $\beta$  is a rate constant,  $\rho_s$  is surface density of dissolved matter, and  $c_{eq}$  is the equilibrium concentration of calcium with respect to calcite and  $c$  the concentration of calcium in the solution.

In the cases of gypsum or salt  $\text{CO}_2$  conversion plays no role in dissolution. Even more, we assume that the surface reaction is fast and only diffusion is rate limiting. For more details on gypsum dissolution a reader is referred to Jeschke et al. (2001).

Diffusion is described by diffusion equation

$$\frac{Dc}{Dt} = D\nabla^2 c, \quad (6)$$

where  $D$  is diffusion coefficient and  $Dc/Dt$  denotes substantive (or material) derivative of concentration. The dissolution rate at the rock surface becomes:

$$\frac{\partial \rho_s}{\partial t} = D \left. \frac{\partial c}{\partial z} \right|_{z=0}, \quad (7)$$

where  $z$  is the coordinate normal to the rock surface.

### Models of rillenkarren formation

Both modes of dissolution, for limestone and for gypsum and salt, are first applied on inclined flat surface and then on the protorrill. For limestone, the equation 5 is used. Therefore dependence of concentration on  $z$  is not taken into account.

For gypsum and salt, equation 7 is used with the value of  $D = 10^{-9} \frac{\text{m}^2}{\text{s}}$  which is close to real diffusion constants for these substances at normal temperatures.

#### LIMESTONE, FLAT SURFACE

The surface is oriented so that its upper edge is horizontal. Rainwater then flows in the direction of the slope. It turns out that the dissolution rate is the same everywhere on the surface (Kaufmann and Dreybrodt, 2007; see chapter 2).

On a steeper surface, the dissolution rate is

slower; as rain is falling vertically, there is less rain for a given surface on steeper slopes so concentration of dissolved limestone is higher and dissolution rate is slower according to equation 5.

On the other hand, for a given vertically projected surface there is more rock surface if the slope is steeper. Therefore, steeper surfaces lower faster than gentler ones.

#### LIMESTONE, PROTORILL

Water flow is always parallel to the slope direction of local water surface. The shape of the water surface is calculated as described in section before. We use it to calculate flow lines, paths along which water flows downward. The protorrill is uniformly covered with flow lines such as schematically shown on Figure 1 and dissolution rates are calculated along every one of them. Each flow line can be treated independently, because water in the film neither enters nor leaves it. The lateral gradients of concentration are assumed to be small enough to neglect the diffusion of solutes into or out of the flow line. Dissolution rates on the points

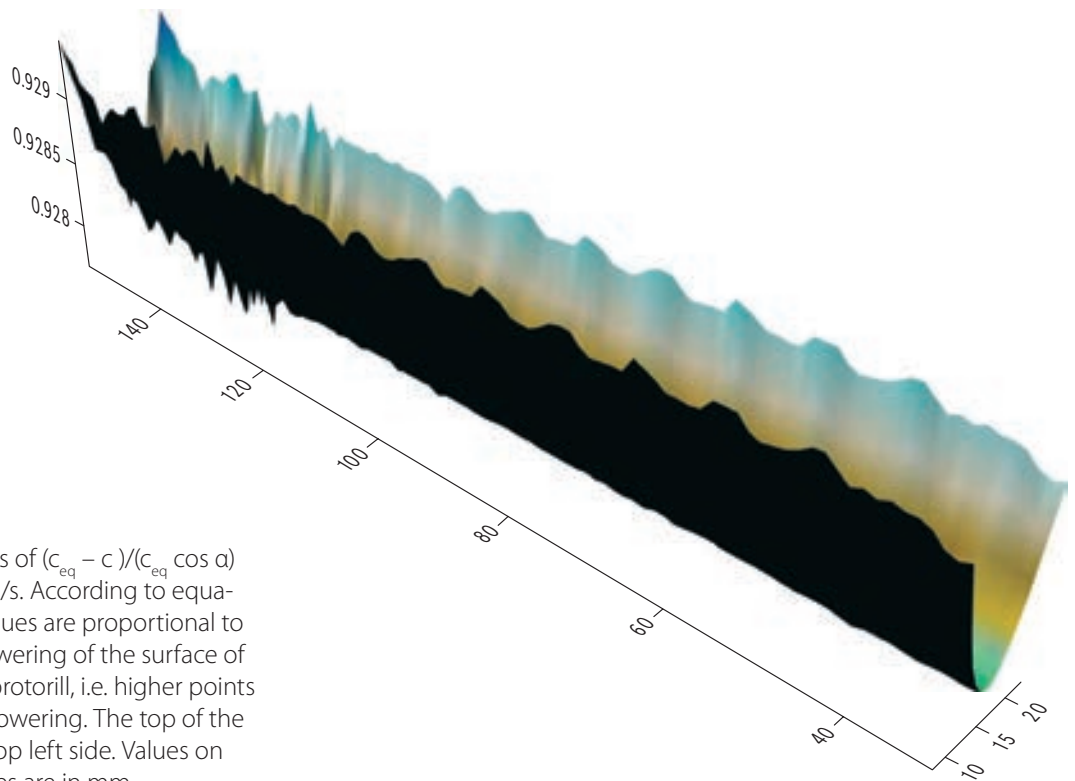


**Figure 5:** Values of  $(c_{\text{eq}} - c) / (c_{\text{eq}} \cos \alpha)$  for  $\beta = 10^{-7} \text{ m/s}$ . According to equation 5, the values are proportional to the rate of lowering of the surface of a limestone protorrill, i.e. higher points mean faster lowering. The top of the rill is on the top left side. Values on horizontal axes are in mm.

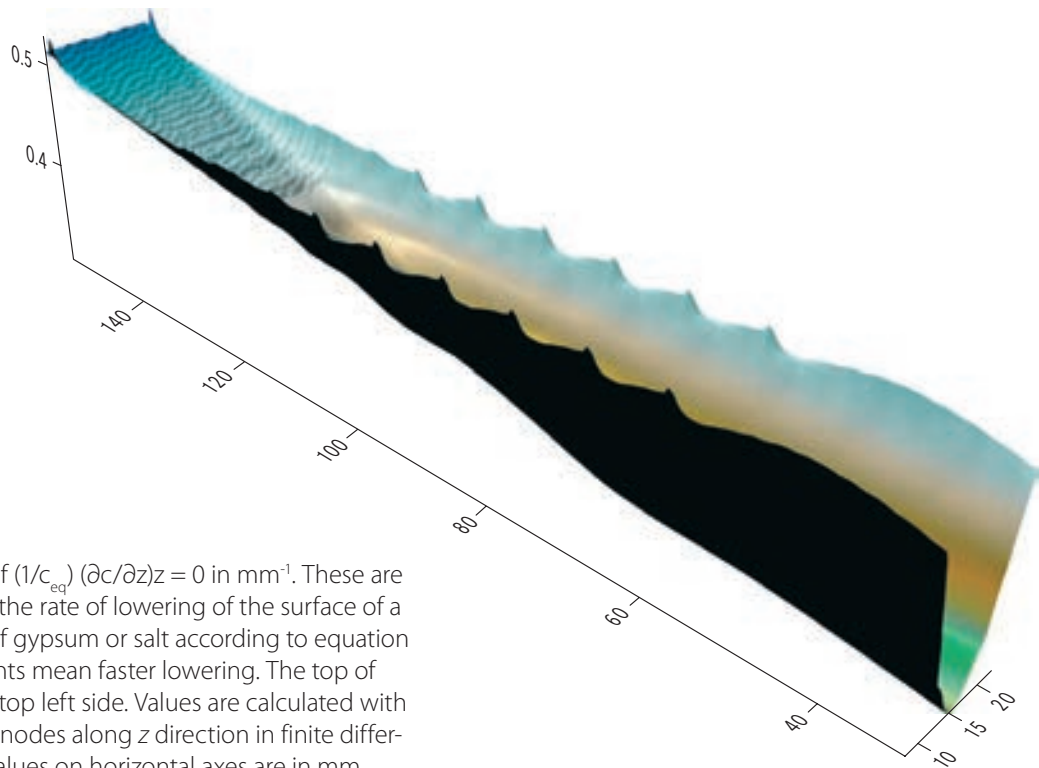


**Figure 6:** Values of  $(1/c_{eq}) (\partial c/\partial z)z = 0$  in  $\text{mm}^{-1}$ . These are proportional to the rate of lowering of the surface of a prorill made of gypsum or salt according to equation 7, i.e. higher points mean faster lowering. The top of the rill is on the top left side. Values are calculated with resolution of 51 nodes along  $z$  direction in finite difference scheme. Values on horizontal axes are in mm.

of rock surface that do not lie directly on a calculated flow line are obtained by interpolating. The results are shown on Figure 5.

#### GYPSUM OR SALT, FLAT SURFACE

On these rocks, the concentration of dissolved rock is dependent on  $z$  while at the rock surface it is assumed to be at  $c_{eq}$  (see previous section), so mass transport in both  $x$  and  $z$  direction is taken into account. From the lubrication approximation water velocity field is calculated and advection in both  $x$  and  $z$  directions is accounted for. Diffusion in  $x$  direction is neglected because of small concentration gradients while in  $z$  it is the main force driving the mass transport and so has to be taken into account. We end with advection diffusion problem, which can be solved with finite difference scheme applying suitable coordinate transformation. Dissolution rates directly follow from the resulting concentration field. In this case, dissolution rates on different points on the flat surface are different.

#### GYPSUM OR SALT, PROTORILL

The model for the flat surface has to be only slightly modified to handle dissolution on a flow line along a curved surface. The same flow lines as for the limestone prorill are used, dissolution rates all over the rill are calculated and are presented on Figure 6.

## Discussion and conclusion

The presented models do not predict rillenkarren formation although it is known from nature and experiments that they do form under the modelled circumstances. This means that something crucial for rillenkarren formation was not accounted for correctly.

Some of the approximations, simplifications and inaccuracies common to all models are:

- instead of Navier-Stokes equation an approximation is used as described before. The ap-

proximation works well on average but on the upper edge of the rock it does not;

- steady-state approximation of the water flow is used;
- the phenomena at raindrop impacts are not accounted for. Fresh water is added only at the water surface, eventual penetration of drops into the film is neglected.

Conditions during rillenkarren formation are certainly not steady-state. The steady-state shape of water film on 2 cm by 16 cm is calculated using time propagation. It turns out that after three seconds of simulated water flow the film shape is very near the steady state, even if initial state is far from the steady one. We assume that state in reality is nearly steady if a lot of drops fall on the rill in less than 3 s. If we take  $1 \text{ mm}^3$  as an average raindrop volume (Elert, 2001), in the simulated rainfall rate of 10 mm/h only 27 drops impact the rill in three seconds.

The raindrop does not stay at the surface of the water film, as presumed for the calculations, but pushes off some of the old film. It is also possible that it does not stay at the site of impact, maybe it bounces toward the centre of the rill, effectively increasing rainfall rate at the centre. This effect is not taken into account either. So it would make sense to include raindrop impact and non-steady state situation into future models of rillenkarren formation.

Experiments have shown that the size of droplets is not crucial for rillenkarren formation (see chapter 4) but we know of no experiments on rillenkarren formation without drops, that is under fog or condensation. The importance of raindrop impacts and non-steady-state effects might even be easier to check experimentally than numerically.



# SOME METHODOLOGIES ON KARREN RESEARCH

Gábor TÓTH

The recognition of karren forms and research on them commenced at the end of the 19<sup>th</sup> century when karren did not represent an independent group among the karst landforms. A. Favre was the first to mention the karren forms, calling them *lapiés* (Favre, 1867). This term became naturalized in many languages and is still used as the German expression *Karren*. A few years before Favre, Sachs made experiments to produce karren forms in laboratory conditions by root corrosion, although he did not nominate them yet (Sachs, 1865). At the end of the century Eckert investigated the evolution of karren forms and the effect of vegetation (Eckert, 1898). For a long period classification of karren forms accounts for the mainstream of researches, an outstanding researcher being J. Cvijić (Cvijić, 1924). The most comprehensive and recently used system classifying karren forms was established by Bögli, who is considered to be the most significant authority on karren researches (Bögli, 1951, 1960a, 1976, 1980). His studies on karren morphology are the most cited and his terminology was adopted in several languages.

Two conference volumes are significant in the present morphological literature: those edited by K. Paterson and M. M. Sweeting (1986), and by J. Fornós and A. Ginés (1996), which contains the newest and most modern methods and information about karren forms. It is worth mentioning five other studies dealing with the total process

of karstification, but which also depict the karren forms in detail (Bögli, 1980; Trudgill, 1985; Jennings, 1985; White, 1988; Ford and Williams, 1989).

## Mapping methods

As the karren forms are so extremely complex and such small-sized features, the traditional mapping methods could not be adopted for their documentation.

The first problem is to determine the best scale ratios, because scales used on geomorphologic maps are not suitable for the correct delineation of karren forms. When measuring the single forms, maps at the scale 1:5 and 1:10 can be chosen in order to make a correct record, but in the case of larger *karren surfaces maps* at scales 1:20, 1:50, and 1:100 values are preferred. These scales refer to the karren features of the temperate climate zone; for tropical karren forms different scales may be appropriate.

Another important problem is the application of traditional map-making instruments. Regarding the tiny features, the method of contour line mapping can only be utilized with good results in very special situations. The extensively applied “grid method” is outlined in detail later in this study. These difficulties mean that mapping of



karren forms cannot be done on traditional geomorphologic maps that depict larger geomorphologic areas. Certainly, these maps are suitable for the location of karren forms, e.g. the morphological map of Lapiés de Tsanfleuron, which depicts the location of the karrenfields (Schoeneich et al., 1998).

Only the larger forms are suitable for marking on contour maps, so the application of the method is very limited. Veress and Barna tried to survey several well developed features when they were mapping *solution runnels* (rinnenkarren) in the Totes Gebirge in Austria (Veress et al., 1995). These features are 10-15 metres long and their widths are 0.5-1 metre. Using this method in the delineation, the terrace grooves and microforms in the karren forms were shown precisely.

It seems more useful to choose mapping methods that adapt better to the sizes of karren forms, so making measure as precise as possible.

One of these methods is square-grid mapping, which gives suitable recording for middle-sized (2 x 2 metres) and larger (20 x 25 metres) karren surfaces. The basic principle of this method is to cover the chosen area with a horizontal, suitably meshed net, and then to determine the distance of points of the forms in relation to the points of the net (Figure 1). In the field these data are drawn on

squared paper which is calibrated in advance. By linking up the resulting points the karren features of the surface become easy to sketch. The distance of the net grid is basically determined by the size of the mapped area as well as by the election of a useful scale.

By using this procedure, maps on the scales of 1:10, 1:20 and 1:100 can be made applying 10, 20 and 50 centimetre-distanced nets. These methods were applied by Szunyogh, Veress and Tóth especially in order to study the mountain karren features (Szunyogh et al., 1998; Veress et al., 1995). The largest area mapped (20 x 25 metres) was surveyed near the Widerkar peak of Totes Gebirge (Figure 2).

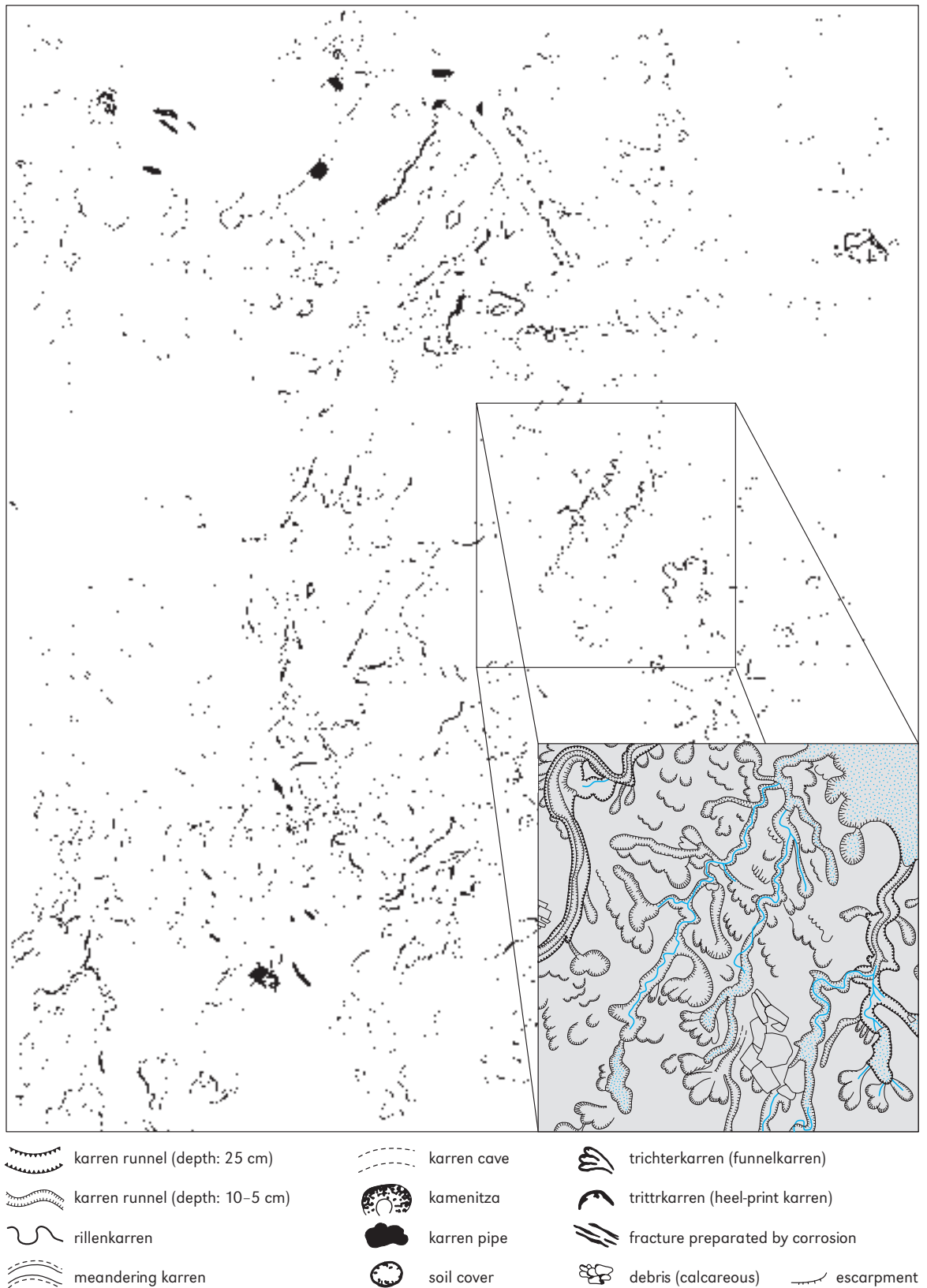
Karren morphological maps can be drawn by square-net mapping of smaller surfaces, and the history of dissolution of the area can be deduced from these maps (Veress and Tóth, 2001).

## Morphometrical methods

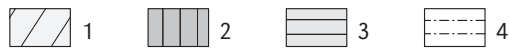
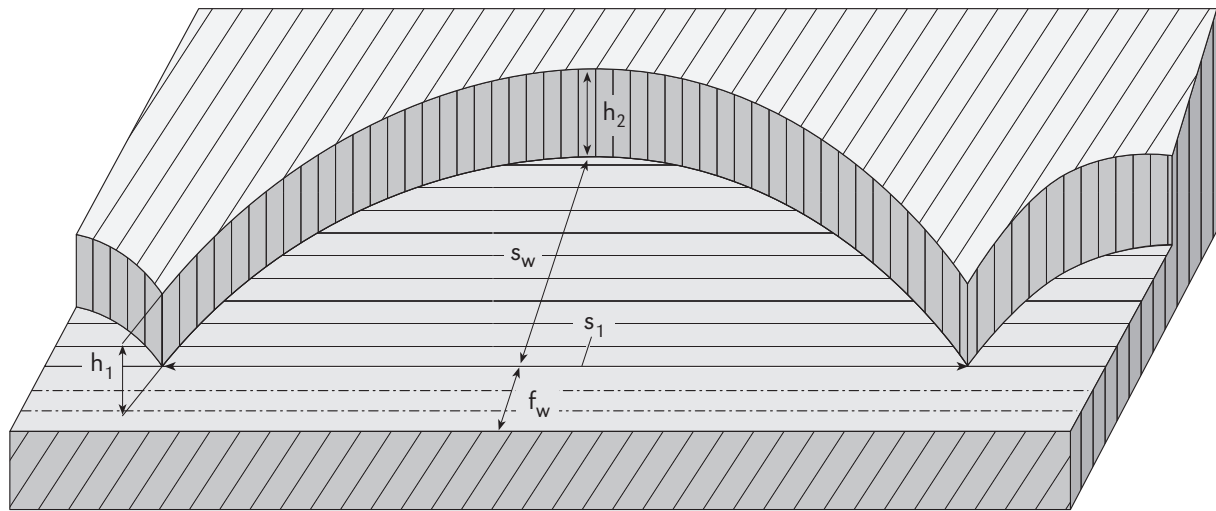
Morphometry is widely used being easily adaptable to particular circumstances and conditions, and suitable for the examination both of single forms and karren terrains. A further advantage of morphometrical methods is that they can be used



Figure 1: Grid mapping in the Julian Alps.



**Figure 2:** The largest mapped karrenfield area in Totes Gebirge.



**Figure 3:** Parts of a heel-print karren (trittkarren). 1. slope; 2. riser; 3. tread; 4. foreground;  $h_1$ : smallest height of riser;  $h_2$ : greatest height of riser;  $s_w$ : greatest width of tread;  $s_1$ : greatest length of tread;  $f_w$ : width of foreground.

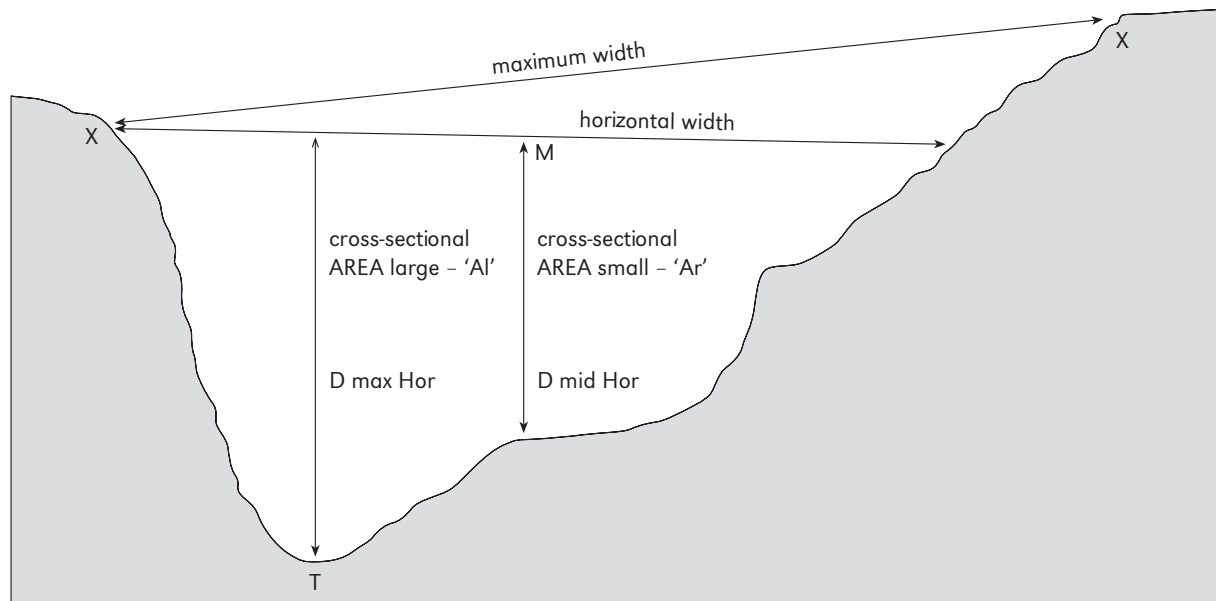


**Figure 4:** Different parameters for meandering karren morphometry (after Hutchinson, 1996). X: field identified channel rims; D mid Hor: horizontal mid-depth; Shape:  $A_l/A_r$ ; M: mid-point of channel width; D max Hor: horizontal maximum depth; form ratio: width/depth; T: channel lowest point/thalweg.

in places which are difficult to approach, since it requires only easily movable equipment. For data collection it can be used for manual or instrumental measures, which then are analysed by statistical methods.

P. J. Vincent investigated the different parameters of *heel-print karren* (trittkarren) and researched how they were interlinked. He discovered that the relationship between the characteristic parameters of heel-print karren (e.g. the heel

height, the bottom, etc.) was not accidental (Vincent, 1983a).

Z. Balogh also studied trittkarren with a similar method and measured several parameters (the height of the riser, the angle of the tread, the length of the tread, the width of the riser, the length of the arch of the riser and the width of the foreground (Figure 3) on slopes with different angles (10°, 20°, 25°, and 40°). Analysing the data he revealed that different sized trittkarren represented the different phases of an evolution process (Balogh, 1998).

L. Rose and P. J. Vincent measured the widths of *grikes* (kluftkarren) in three different areas, and then they depicted the results on bar charts based on frequency. They found that grikes of the three areas had evolved in two different periods, before and after the period of ice cover (Rose and Vincent, 1986a).

Also in *rillenkarrren* morphometry, it is feasible to collect data to define the diagnostic width for such a microform (Ginés, 1996b). Measurements of the length of longer rillenkarrren and altitude above sea level correlate negatively at sites receiving more than 800 mm of rainfall in Mediterranean-climate karrenfields (A. Ginés, 1990).

In the case of meandering karren some parameters originating from the meandering of the groove are worth defining, because they provide the most important information for the classification and make possible the comparison of these microforms with other types of meanders. J. Zeller was the first to measure the sinuosity of meandering karren, the lengths of inflexed arches and the width of the belt. Comparing these data with other data of fluvial meanders and glaciers he found out that the sinuosity of meandering karren is the largest. Analysing the results he also demonstrated that the wider the groove is, the larger the size of the belt results (Zeller, 1967).

D. W. Hutchinson emphasized the shape of the *meandering grooves* in his research and chose the parameters to be measured for this purpose (Hutchinson, 1996). His survey criteria are shown in Figure 4.

M. Veress and G. Tóth also examined the *me-*

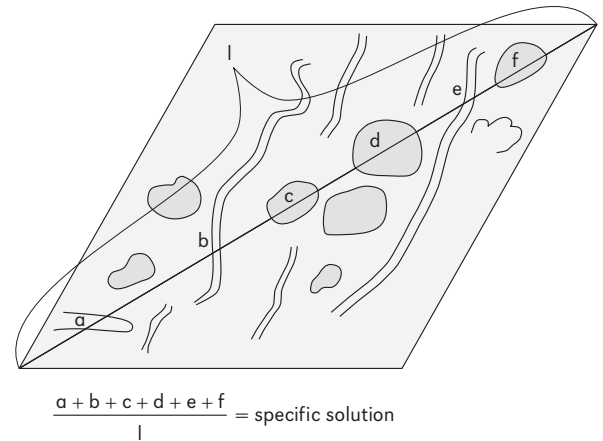


**Figure 5:** Estimation of specific karren-solution: it expresses how many centimetres of karren landform are present on 1 metre of exposure of karrenfield.

*andering karren*, applying morphometric methods; they differentiated the types of meanders by detailed measuring of both sides of the bend (Veress and Tóth, 2004).

Another basic investigation method for the morphogenetics of karren landforms is to make a transect on significant *karren outcrops* (Veress et al., 2001a). The type and occurrence of the forms placed along a spread band-chain is determined, measuring its width, depth and direction and the slope angle and direction of the terrain. The lengths of transects are 15–25 metres, depending on the size of the karren outcrop. By analysing the resulting data several specific and global parameters can be estimated. In this manner the value of specific karren solution can be determined by adding the width of the karren forms occurring along the section and dividing this total karren width by the length of the whole transect. So the specific karren solution shows how many centimetres of forms have significantly dissolved in 1 metre (Figures 5, 6). This value characterizes the grade of development of the karrenfield. This calculation can be applied to each distinct karren form. An additional characteristic value is the density of landforms. The density of forms can be counted by dividing the number of occurrences

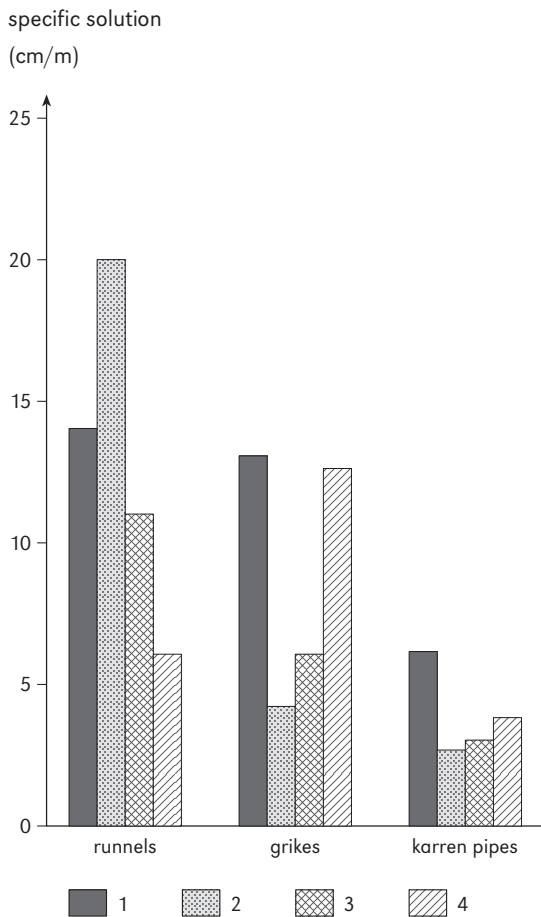


**Figure 6:** Specific karren-solution in the various vegetation zones per karren features. Showing the specific solutions, one close to each other, and measuring specific solutions in different vegetation zones, the relationship between the vegetation and karren forms can be deduced. 1. pine zone; 2. mountain pine zone; 3. without vegetation (1–3 Julian Alps, Totes Gebirge and Dachstein); 4. mountain pine zone (Asiago plateau).

of each karren feature by the length of the whole transect (Table 1). In this way we will see how many individuals of the different forms are found in 1 metre. From this data we can conclude the frequency in which forms are increased by certain factors (slope angle, precipitation, vegetation, exposure). For instance, the increase of slope angle is favourable for the development of wall karren.

The directions of karren features can be de-

scribed in a circular diagram divided into 20° spacing with weighted average (Figure 7). The radius of the sector shows the occurrence of each form. For a better depiction of the data sets, the forms are grouped by their genetics. The first group is constituted by the runnels or grooves with different genetics, which evolved along the slope direction. The grikes were put into the second group, because they occur perpendicular to slope direction and are formed by the coalescence of vertical *karren hollows* or are preformed by the direction of fissures. The third group contains the heel-print karren (*trittkarren*), *solution pans* (*kamenitzas*) and *karren wells* (*Karrenröhren*), which are basically *circular forms*. Their evolution is strongly influenced by the slope angle.

By applying the data of different transects some conclusions can be drawn regarding how the topographic and stratigraphic position of the karst terrain (mainly the slope angle and the direction) influences the evolution of forms and which types of forms are preferred.

Another widespread and successfully applied method is the comparison of different parameters of the same form. The basic principle of the method is to choose one or more characteristic parameters (width, depth, length) and to analyse their measurements under different circumstances (slope angle, exposure, precipitation). It is worth using this method to differentiate a karren form into subtypes. In this case parameters must be chosen according to the characteristics of the forms, and the proportions are used to draw conclusions.

## Examination of dissolution process

These methods refer to the process of dissolution, the rate of dissolution and the denudation of the surface caused by the development of karren forms. The methods are classified into three groups:

The first group determines the beginning of the forms evolution and evaluates the rate of solution

**Table 1:** Specific karren-solution and density of karren forms. The table contains the data of four different terrains and gives the values of specific solution and density of each karren landform. S. s.: specific solution, total width of the karren forms on 1 metre; density: occurrences of each karren feature on 1 metre; Hi: Julian Alps; T: Totes Gebirge; D: Dachstein; A: Asiago plateau.

Number of the transect	Surface			Grikes (Kluftkarren)		Network karren		Karren wells and karren pipes		Runnels and flutes (Rillen- and Rinnenkarren)		Kamenitzas		Heel-print karren (Trittkarren)		Total	
	altitude (m)	slope angle	no. of the forms	s.s. (cm/m)	density (no/m)	s.s. (cm/m)	density (no/m)	s.s. (cm/m)	density (no/m)	s.s. (cm/m)	density (no/m)	s.s. (cm/m)	density (no/m)	s.s. (cm/m)	density (no/m)	s.s. (cm/m)	density (no/m)
HI/2	1695	24°	41	29.76	0.84	-	-	6.88	0.36	5.32	0.44	-	-	-	-	43.28	1.64
HI/1	1715	26°	36	9.72	0.52	-	-	8.88	0.4	5.4	0.4	3.56	0.12	-	-	27.56	1.48
HI/3	1695		34	21.94	0.87	-	-	4.5	0.25	11.44	0.25	4.5	0.25	-	-	40.56	2.19
HI/1	1776	28°	44	6.00	0.56	-	-	6.00	0.32	25.52	2.4	-	-	-	-	37.52	3.28
HI/2	1776	28°	32	4.07	0.33	-	-	10.13	0.47	16.47	0.86	0.73	0.07	-	-	32.93	2.27
T/4	1800-1900*	10°	27	2.45	0.16	-	-	2.78	0.08	25.47	1.55	8.00	0.12	5.27	0.29	43.96	2.20
T5	1800-1900*	15°	44	-	-	-	-	0.8	0.04	31.64	1.64	-	-	27.0	0.08	33.52	1.76
T3	1900-2000*	20°	15	13.89	1.67	-	-	-	-	13.22	0.67	-	-	-	-	27.11	1.78
T2	1900-2000*	30°	39	2.08	0.19	-	-	5.33	0.24	15.47	1.04	-	-	3.68	0.38	26.56	1.84
T1	1900-2000*	31°	27	4.93	0.64	-	-	5.0	0.29	15.64	1.0	-	-	-	-	25.57	1.93
D/1	1630		35	5.81	0.13	0.81	0.18	0.68	0.04	21.5	1.09	-	-	0.81	0.18	29.63	1.59
D/1	1820	17°	31	1.85	0.2	-	-	2.75	0.2	20.75	1.15	-	-	-	-	25.35	1.55
D/III/1	2051	21°	35	4.44	0.4	-	-	-	-	15.85	0.77	1.29	0.11	-	-	21.58	1.3
HI/2	2090	4°	16	19.67	0.83	-	-	7.22	0.06	-	-	-	-	-	-	26.89	0.89
HI/1	2098	8°	20	-	-	-	-	-	-	14.90	0.97	-	-	6.62	0.41	21.52	1.38
HI/1	1900-2100*	25°	32	-	-	-	-	4.35	0.15	13.50	1.4	-	-	1.0	0.05	18.85	1.6
A/1/6	2055	0°	37	3.16	0.2	11	1	0.8	0.04	1.88	0.08	2.4	0.16	-	-	19.24	1.48
A/1/2	2055	4°	45	9.48	0.28	10.52	0.72	4.44	0.36	5.2	0.4	0.32	0.04	-	-	37.96	1.8
A/1/7	2055	4°	37	15.56	0.2	13.12	0.64	2.67	0.2	1.8	0.08	1	0.04	-	-	34.24	1.48
A/1/1	2055	5°	37	7.3	0.22	20.18	1.04	3.18	0.31	2.77	0.22	0.86	0.09	-	-	34.36	1.9
A/1/3	2055	6°	66	15.08	0.68	30.6	1.56	2.12	0.24	3.12	0.12	3.2	0.04	-	-	54.12	2.64
A/1/5	2055	10°	37	8.36	0.28	14.36	0.68	0.8	0.04	5.96	0.48	-	-	-	-	29.48	1.48
A/1/4	2055	15°	37	13.04	0.29	-	-	0.37	0.04	16.25	1	11.16	0.25	-	-	40.83	1.58
A/II/2	2061	0°	63	42.16	2.08	1.4	0.08	1.48	0.16	2.24	0.2	-	-	-	-	47.28	2.52
A/II/3	2061	0°	48	18	0.72	3.96	0.28	6.8	0.28	9.32	0.4	4.64	0.24	-	-	42.84	1.92
A/II/4	2061	0°	34	19	0.76	-	-	12.6	0.36	-	-	5.12	0.24	-	-	36.72	1.36
A/II/1	2061	4°	43	14.24	0.4	4.28	0.4	1.08	0.08	15.32	0.72	7.4	0.12	-	-	42.32	1.72

\*altitude on map

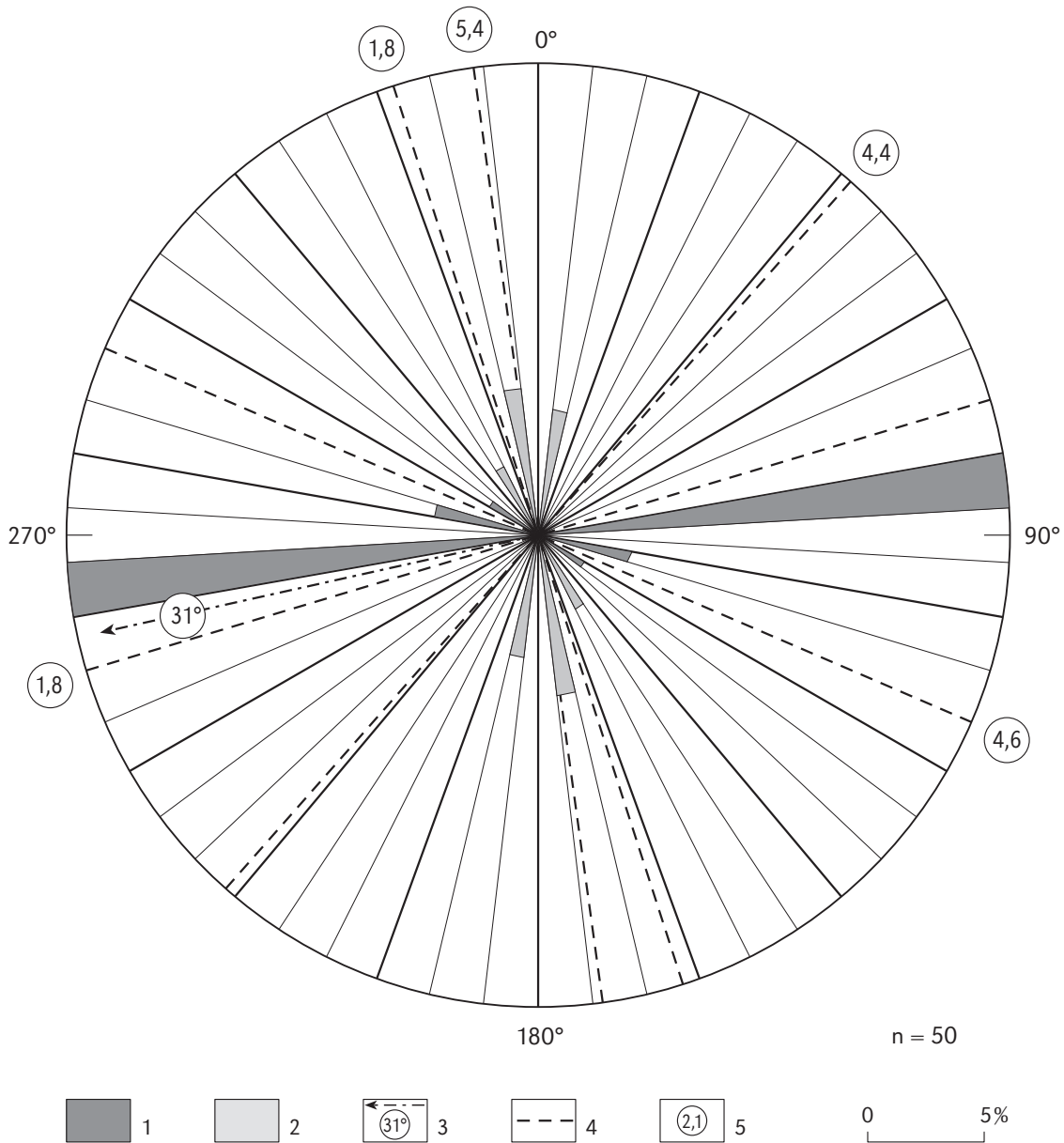


**Figure 7:** Directional dispersion of the karren features along T 1 section (mountain pine zone, Totes Gebirge). The circular diagram shows the relationship between the formation of karren features, the slope angle and the strike directions. 1. runnels; 2. grikes (kluftkarren); 3. slope direction with angle of gradient; 4. strike direction; 5. density of fractures (occurrences/10 centimetres).

by measuring the sizes of the forms. This process gives average values, and does not take into consideration that intensity of dissolution might have changed. In the case of alpine karrenfields most

researchers consider the beginning of evolution of forms started at the regression of the ice cover, supposing that evolution began immediately. The first researcher to be mentioned is A. Bögli, who

determined the rate of solutional erosion by measuring the heights of *karren tables* (Karrentische; Bögli, 1961). The heights of karren tables were 10-15 centimetres, so - if the recession of the ice cover is considered to have happened ten thousand years ago - the velocity of erosion was 10-15 millimetres per one thousand years.

D. Sellier used a similar method on granite surfaces measuring the sizes of forms evolved on the megaliths in Brittany supposing that the megaliths had been erected 5,000 years ago (Sellier, 1997).

The second group is the collection of applications which measures directly the velocity of solution and erosion by measuring the speed of erosion compared to a fixed height given in a certain point of time. F. Cucchi put metallic points in the rock and measured the extent of the surface's degradation compared to the original surface (Cucchi et al., 1996). The same method was applied by a French expedition on the island of Diego de Almagro in Chile. They had painted signs using waterproof painting 50 years before and the surface protected with the painting proved to be 3 millimetres higher than the surrounding surface (Hobléa et al., 2001).

The third group represents other chemical methods for investigations on dissolution processes. Several scientists have tried to determine the solute content of karstwater at different locations for measuring of the erosion (Sweeting, 1966; Newson, 1970; Thomas, 1970). In order to apply this method it is essential that the catchment area of a certain spring should be correctly delimited. F. Hobléa et al. measured the solute content of solution pans on the island of Diego de Almagro and determined the beginning of dissolution process at ten thousand years BP which was the time of the ice regression. In this way the rate of erosion was measured as 95 millimetres per thousand years (Hobléa et al., 2001). Considering the precipitation of 8,000 millimetres per year on the island, the survey data are in good agreement with the dissolution of the temperate climate zone.

Examinations of solutional erosion are often applied on covered surfaces to analyse the influ-

ence of the soil on the processes of karstification. Many researchers examine the chemical composition of the soil. In the case of a karstic surface covered by soil the most frequent method is to put limestone tablets of known masses into the soil; then after a period of time their masses are again measured. The reduction of the tablet mass shows the measure of dissolution (Gams, 1985; Trudgill, 1975, 1985; Kashima and Urushibara-Yoshino, 1996). Trudgill found out that in case of high content of heavy metals and small value of limestone content the intensity of solution is larger.

To summarize the researches, the most doubtful fields of karren research are the velocity of solution and the growth rate of karren features. The main reason for this is that the process of solution and its velocity are influenced by several environmental conditions. The amount of precipitation, the quality of rock, the vegetation, the soil and the temperature could strongly modify the value of local velocity of the dissolution process. After a survey on the available data, most of the values are 0.4-10 millimetres per a thousand years, with 1,500-2,500 millimetres of annual precipitation.

## **Examination of topographic and lithological conditions**

As several features of limestone rocks could influence the process of dissolution, examination of lithological condition is widely represented in the literature. This brief summary describes the methods linked directly to karst morphology.

Roughness is a factor which can strongly influence the spatial expansion of solution process, and it has been investigated by several scientists. J. Moses et al. applied the electron microscope to examine roughness (Moses and Viles, 1996). J. Crowther applied a manual method: he put a carpenter gauge vertically on the surface of the rock, then took photos of the profiles obtained; the photos were then digitalized and the height difference between consecutive points was applied to determine the measure of roughness (Crowther, 1996).



The relation between the development of karren forms and the slope angle is essential as longitudinal forms evolve down slope; the slope angle of the karren outcrops determines the drift speed of the solvent. One of these investigations have been done by J. R. Glew and D. C. Ford, who dripped solvent on gypsum surfaces with different angles of slope (35°, 45°, 55°) and found that the increase of slope angle increased the lengths of rillenkarren. Then they dripped solvent on different rock surfaces and realized that wider rillenkarren had evolved on limestone surfaces rather than on *salt* or *gypsum surfaces* (Glew and Ford, 1980). D. N. Mottershead divided the slope into 10° intervals and measured the frequency of rillenkarren. His results show that their number is the largest on the slope of 60-70° (Mottershead, 1996b).

The types, sizes and frequency of karren features are greatly influenced by the quality of the rock. On porous or large grained limestone the dissolution is less. The evolution of *kluftkarren* is enhanced by a strong network of fissures on the rock. P. Vincent examined the calcite content and

grain size of the rock substrate by analysing the evolution of *rillenkarren* and found that high calcite concentration and fine granulation helped to evolve the rillenkarren (Vincent, 1996).

## Theoretical method of karren development

A theoretical-physical study of the process of karren development has been developed recently. It is based on the equation system of the karstification of a sloping limestone terrain, considering the hydrodynamic, chemical and morphological rules of the karstification processes (Szunyogh, 2000a). The main magnitude was a three-variable function, which can describe the form of rock surface in time. The determination of this form also postulates the calculation of the speed of flowing water over limestone surfaces, the concentration of solution  $\text{CaCO}_3$  in water and the thickness of liquid film. It is done as a computer algorithm for the solution of equations (Szunyogh, 2000b).

Lluís GÓMEZ-PUJOL and Joan J. FORNÓS

*Microrills* are the smallest form of the exokarstic linear features on limestone and gypsum rocks. They are typically described as about one millimetre wide rills, round bottomed and packed together with characteristic tightly sinuous to anastomosing plan view patterns on gentle slopes, becoming more parallel and straighter with increasing slope (Ford and Lundberg, 1987).

They appear widespread, from mountain to supralittoral domain in rock coasts, and from arid to temperate environments; and rarely in cold environments (Davis, 1957). Microrills are found in coastal environments, both macro- and microtidal, such as Vancouver island, Canada, or the Welsh coast, Great Britain (Ford and Lundberg, 1987), on the northern Palawan coast, Philippines (Longman and Brownlee, 1980), Dalmatian coast, Croatia (Perica et al., 2004), Sicilia (Macaluso and Sauro, 1996a), and also at the Balearic islands (Ginés, 1993; Gómez-Pujol and Fornós, 2001, 2004a). They also have been reported in arid and semi-arid continental environments such as the Chillagoe and Gregory karsts, Australia (Jennings, 1981; Dunkerley, 1983; see chapter 31, Tropical monsoon karren in Australia), the Mohave and Colorado deserts, southern California (Laudermilk and Woodford, 1932), Pakistan (Cilek, 1989), and from southeast Morocco (Smith, 1986, 1988). These micromorphological features are believed to be representative of arid or semi-arid environ-

ments (Ginés, 1999a), although they are present on localities with rain precipitation greater than 800 mm per year (Ford and Lundberg, 1987). The microrills distribution could be broadly related to lithological control and to genetic agents such as dew and sea spray water inputs. Capillary flow is believed to explain much of their characteristic sinuosity (Ford and Williams, 2007).

The aim of the present paper is to contribute to the understanding of the origin and evolution of microrills through an examination and description of the form of features, rock texture and lithology properties from samples collected in Balearic islands both in coastal and mountain sites.

### Study sites and methods

The island of Menorca together with Mallorca (the greatest of the Balearic Archipelago) are characterized by diversified and abundant karstic geomorphology. The karstic features, both the subterranean (Ginés J., 1995; Ginés and Fornós, 2004) and the surficial ones (Ginés and Ginés, 1995), constitute one of the most characteristic aspects of these island's geographical context. In particular, extensive areas of Mallorca, especially in the main range (Serra de Tramuntana), and of both, Mallorca and Menorca coastal sites, present an exceptional range of exokarstic morphologies. *Kar-*

renfields cover large expanses of limestone exposures lacking a soil covering. In the case of mountain environments the microrills analysed in this paper appear in combination with *rillenkarren* forms that evolve to meandering decantation flutes, as well as with *kluftkarren* and some characteristic smooth surfaces. At coastal sites microrills appear between a complex assemblage of mesokarren formed by the combination of pinnacles and basin pools. The rocks involved in these karrenfields are mainly formed of Lower Liassic massive limestones and breccias, as well as conglomerates and calcareous breccias from the Burdigalian. Reefal limestones, calcarenites and associated sediments, Tortonian and Messinian in age, are the characteristic rocks in both Mallorca and Menorca coastal sites.

Samples of limestone with well-developed microrills were hand-cut using a chisel at different coastal environments of Mallorca and Menorca as well as in mountain landscapes of the Mallorca northern range (Table 1). From each limestone rock, fragments have been prepared for thin section study, optical microscope observation and SEM exploration. Thin sections allowed analysis of rock texture properties, sorting and grain-size mean diameter. Photos of optical microscope samples were used to assess microrill width and geometry. Microrill width was obtained by means of a digital image processing standard software measuring the distance between the crests that delimits laterally the microrill. Several measures

along each microrill-path were obtained when the feature limits were clear enough. Results of the measurements are presented as mean width values for microrills in each study location; the mean width of the thinnest individual microrill and the mean width of the widest microrill were also reported. A qualitative SEM and resin cast study (Moses et al., 1995; Taylor and Viles, 2000; Viles, 2001) was done on pieces of 10×10×10 mm in order to, first, identify the abundance of *nanomorphologies* (Viles and Moses, 1998), secondly to conclude which kind of processes (chemical, physical or biological) are operating on microrill formation, and thirdly, to elucidate the relation of the microrill plan view orientation pattern with the joint and rock structure alignments.

### Microrills rock type, plan view and morphometry

Systematic data on microrill width, length and plan view pattern are scarce in literature. Since Lauder milk and Woodford (1932) there is an agreement in distinguishing four types of microrills according to plan view and cross section. This classification (see discussion in Grimes, 2007) separates four main types that range from parallel and moderately sinuous and rather shallow rills, to less tightly packed and shallower rills with smooth crests and a polished appearance. Ford and Lundberg (1987) suggest that the develop-

**Table 1:** Sampling sites and main environmental parameters (climate data from Guijarro, 1986). Ma. Mallorca; Me. Menorca.

Island	Locations	Altitude (m)	Precipitation (mm)	Temperature (°C)	Environment	Rock type
Ma	Puig Major (PM)	1,300 m	1,246.6	9.1	mountain	Lower Jurassic massive limestone
Ma	Cala Sant Vicenç (CB)	> 2 m	731.1	16.5	coastal	Lower Miocene carbonate breccia
Ma	Punta de Tàcàritx (PT)	> 2 m	580.8	16.2	coastal	Quaternary carbonate breccia
Ma	Cala Màrmols (CM)	> 3 m	321.3	17.6	coastal	Upper Miocene biocalcarenite
Me	Punta Prima (PP)	>2 m	444.9	17.1	coastal	Upper Miocene biocalcarenite
Me	Cap d'en Font (CF)	> 4 m	545.4	16.6	coastal	Upper Miocene biocalcarenite

ment and the plan pattern of microrills are consequences of rock type and texture and the differing amount of effective liquid.

In the Balearic islands microrills appear patchily on mountain and coastal limestone outcrops. On the mountains, where the Jurassic material forms most of the structured terrains, microrills are related to Lower Jurassic massive micrite limestones with stratified levels with bioclastic and oolites components (Fornós and Gelabert, 1995). At coastal sites microrills sculpture a widespread variety of rock exposures that comprise from Neogene to Quaternary limestones and calcarenites. This kind of feature has also been identified in Lower Miocene conglomerates, namely in the Sant Elm fm (Rodríguez-Perea, 1984). Most of the pebbles which compose these carbonate Miocene conglomerates are Lower Jurassic. Microrills also appear at coastal sites in Upper Miocene rocks. The Upper Miocene is composed by massive reefal limestones, calcarenites and calcisiltites that form respectively, the Reefal Unit and the Terminal Complex (Fornós and Pomar, 1983). Finally, microrills also are developed on Quaternary breccias. These Quaternary deposits correspond to aeolianite matrix-supported clasts related to the mixing of dune episodes with alluvial and colluvial events. The clasts resulted from Jurassic, Cretaceous and Lower Miocene denudation materials and are composed of micritic limestones. All the

rock types described, where microrills have been identified at Balearic islands, are fine-grained and homogenous in grain size. Texture control on microrill development is shown by their different presence according to textural variation between conglomerate clasts and matrix. In thin section analysis and SEM observations the grain size ranges from maximum mean diameters of 8.65  $\mu\text{m}$  to minimum mean diameters of 3.23  $\mu\text{m}$  and all the samples are well sorted. The absolute values of grain size ranges from 2.305  $\mu\text{m}$  to 17.43  $\mu\text{m}$ . This fact shows that microrills are developed only on a mudstone texture.

Microrills appear on rock surfaces where vegetation and *biofilm* colonization are not present and on rocks cropping out with ancient rounded *subsoil karren*, which have been recently exposed. The orientation of these surfaces is generally horizontal or near horizontal. Although some of the rocks are rough in a mm or lower scale, at cm-scale microrills do not develop on vertical or rough surfaces.

There are no differences in microrills plan view pattern between mountain and coastal study sites despite the differences in rain supply and lithology. Straight and sinuous or meander-like rills can be seen on different rocks (Figure 1). At Cala Sant Vicenç (Figure 1g, h) microrills appear developed on Miocene breccia with Miocene and Jurassic matrix-supported clasts. These fine-grained rocks

**Table 2:** Microrills morphometrical assessment.

Sample	Site	Mean width (mm)	SD	Min (mm)	Max (mm)	N
CM a	Cala Màrmols, Ma	0.869	0.267	0.453	1.375	57
CM b	Cala Màrmols, Ma	0.728	0.207	0.412	1.050	59
CM c	Cala Màrmols, Ma	0.758	0.181	0.509	1.163	63
CB a	Cala Sant Vicenç, Ma	0.747	0.138	0.547	1.016	55
CB b	Cala Sant Vicenç, Ma	0.539	0.115	0.269	0.781	48
CB c	Cala Sant Vicenç, Ma	0.760	0.198	0.514	1.128	49
PT a	Punta de Tacàritx, Ma	0.440	0.106	0.256	0.606	61
PT b	Punta de Tacàritx, Ma	0.611	0.141	0.446	0.926	52
PT c	Punta de Tacàritx, Ma	0.997	0.233	0.632	1.434	46
PM a	Puig Major, Ma	0.648	0.112	0.391	0.918	32
PP a	Punta Prima, Me	0.662	0.152	0.503	1.033	48
CF a	Cap d'en Font, Me	0.470	0.096	0.307	0.644	57

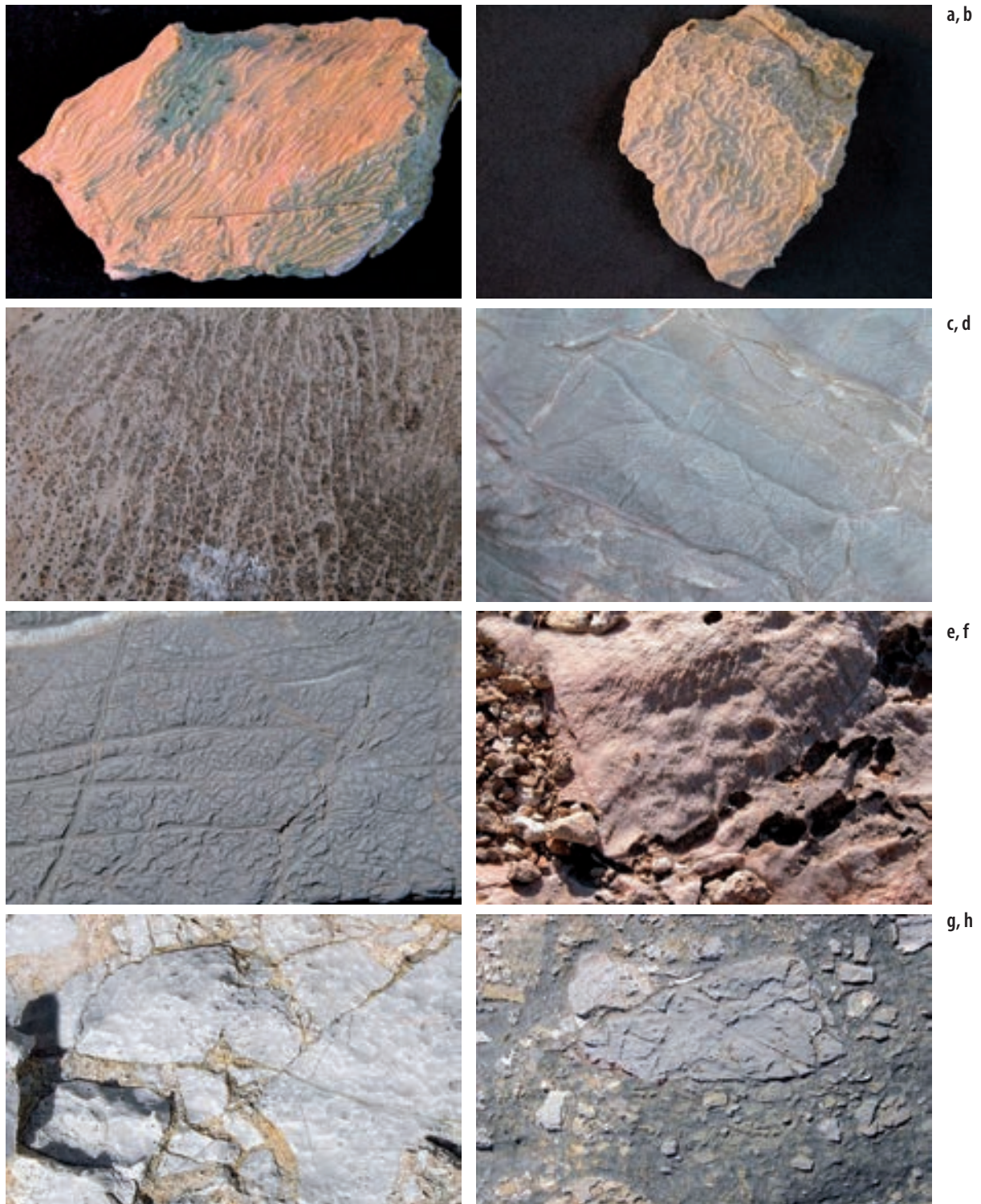


**Figure 1:** Microrill photographs from mountain and coastal sites at Balearic islands study sites: a. microrill linear-like forms on Lower Miocene limestones at Cala Sant Vicenç, NE-Mallorca; b. plan view of microrill features showing meandering-like forms on Lower Miocene limestones at Cala Sant Vicenç, NE-Mallorca; c. Cap d'en Font, Menorca. Note the blue-green algae and fungi colonization at microrill bottoms; d. microrills developed on micritic Jurassic limestones at Puig Major, Mallorca. The microrills, path is normal to the main microfractures and →

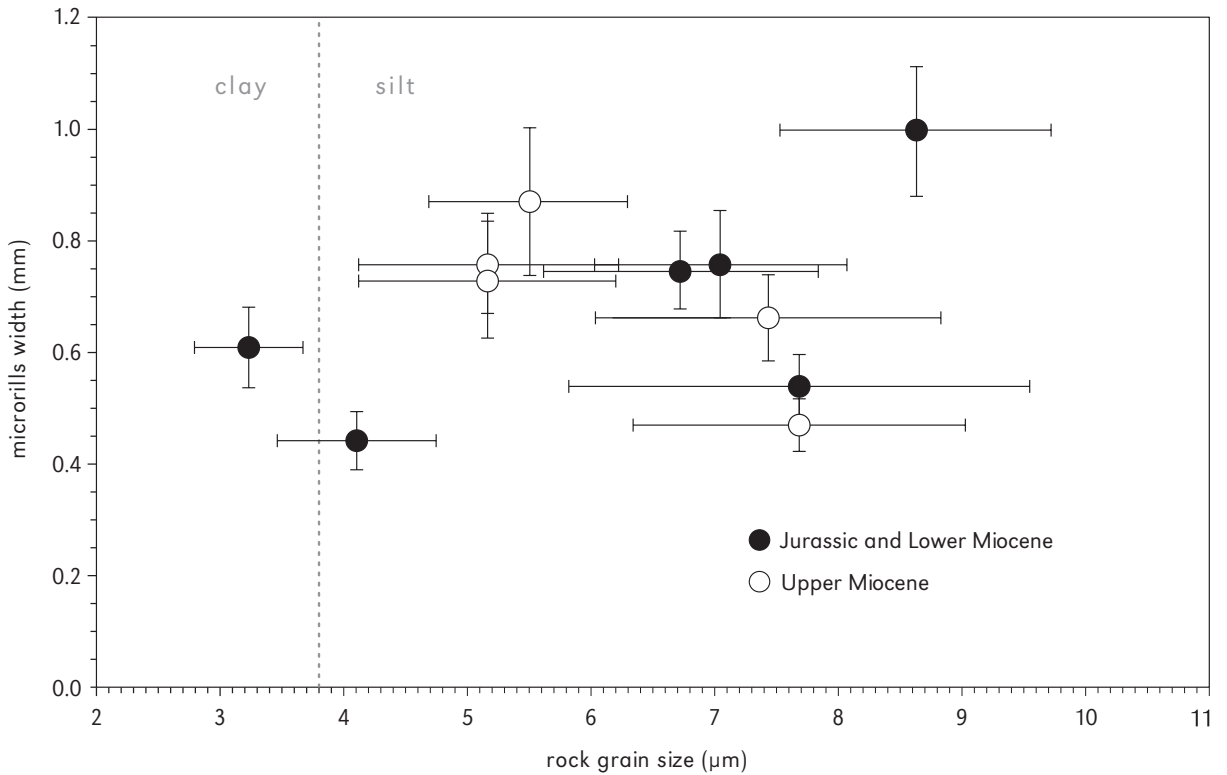


**Figure 2a:** Microrill textural and morphological properties. Relationship between microrill width and rock grain size.

present a wide array of orientations, outcrop exposition surfaces and slopes and do not show a clear relation with the plan pattern or the length of the microrills. The same type of clast can have meandering microrills and straight microrills in several cases. The same situation can be identified at the Punta de Tacàritx (northern Mallorca) coastal site, where rock outcrop is built up by Quaternary carbonate aeolianites that support Jurassic limestone clasts. There are many cases where on the same clast microrills follow both meander and straight paths (Figure 1e). In the case of the Lower and Upper Miocene limestone outcrops (Figure 1a, b, c, f) and also in Lower Jurassic massive limestone

outcrops (Figure 1d) it seems that meandering forms correspond to fine-grained textures and straight forms to coarser textures. Nevertheless, there are many cases where sinuous and straight microrills share wall partitions or where the same microrills follow both configurations changing from sinuous to straight path. The plan view of microrills uses to be parallel or moderately sinuous but there is not any evidence at any study locality of a dendritic or truly branched organization of the microrills.

The dimensions of the microrills are quite variable in length and more or less regular in width. It has not been possible to measure accurately mi-

→ joint directions in the rock; e. meandering and sinuous microrills, plan view on a Jurassic clast at Punta de Tacàritx, Mallorca; f. microrills developed in a rough surface at Cala Màrmols, Mallorca; g. sinuous and rectilinear microrills at Cala Sant Vicenç developed on clasts from a carbonate matrix supported breccia Lower Miocene in age. Note that there are some pits that begin to modify the microrills plan view; h. detail of microrill distribution at Cala Sant Vicenç rock outcrops where, differences in breccia clast and matrix texture, demonstrate the textural control on microrill development.

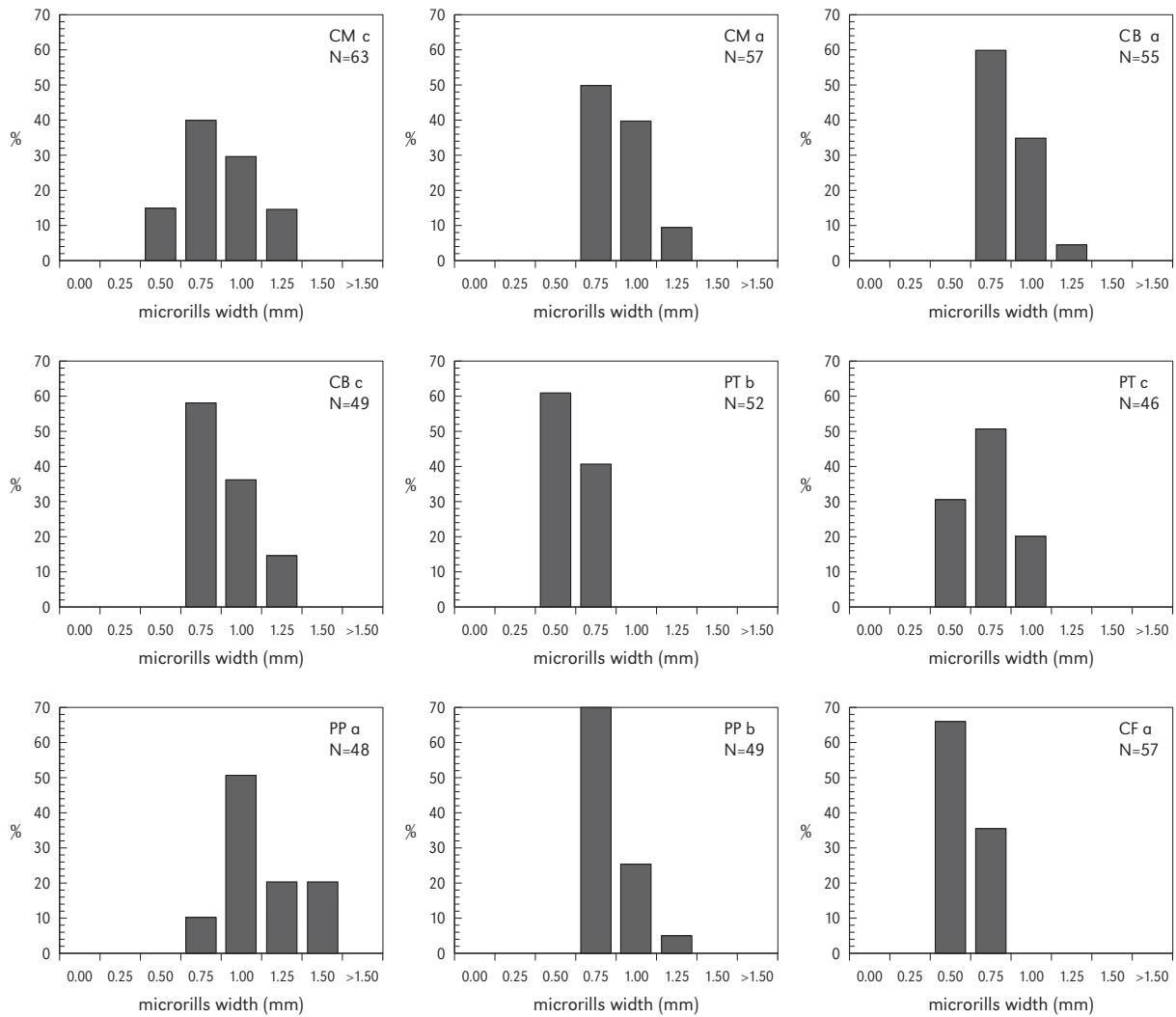
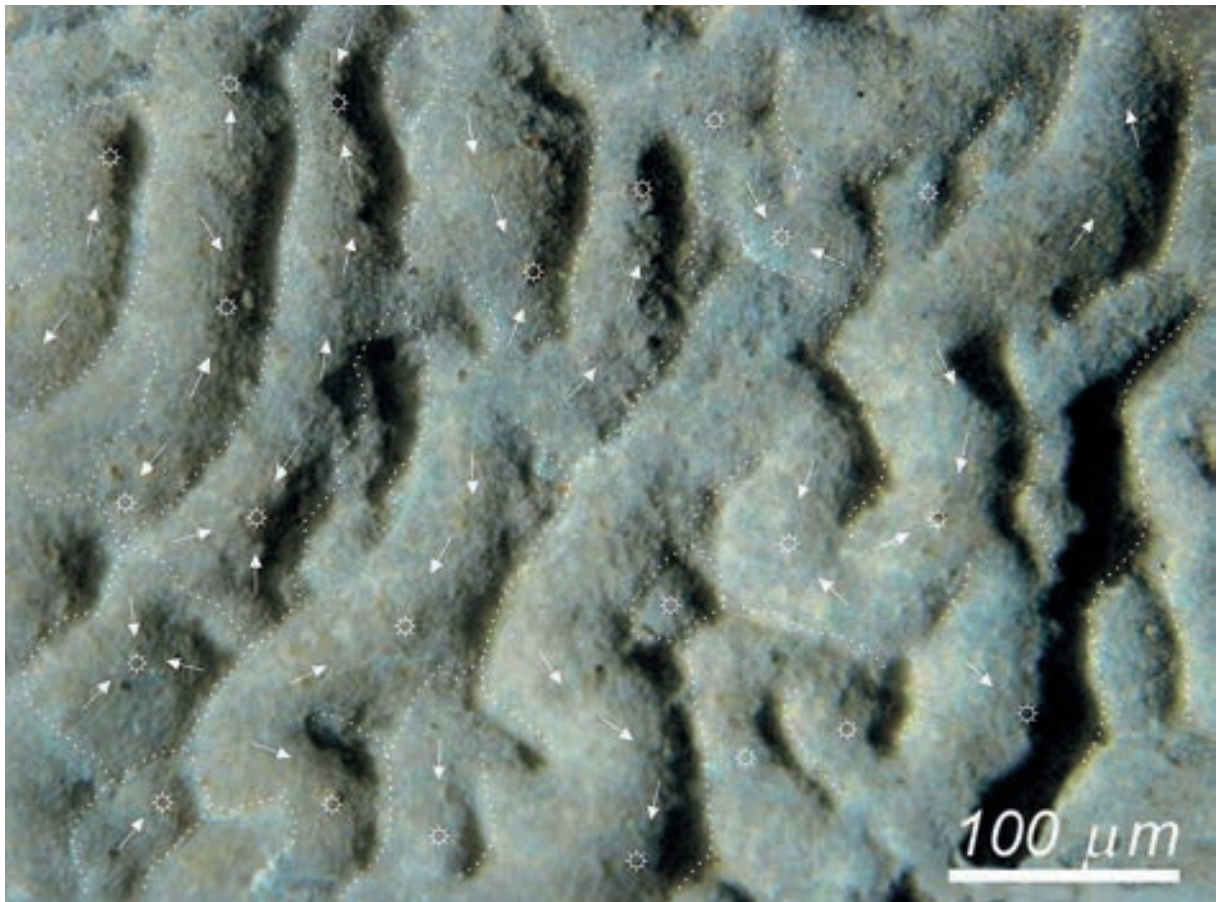


Figure 2b: Histograms of microrill width.

crorill depth, although this seems to be close to the width values or slightly lower. Microrill width measured on different rock textures in mountain and coastal environments from Mallorca and Menorca ranges from a minimum width of 0.26 to a maximum of 1.43 mm (Table 2). The mean width value for the whole microrills present at the different sampled surfaces ranges from 0.44 to 1.00 mm. It is important to note that the mean width standard deviation is not bigger than 0.10 to 0.27 mm, which shows that the homogeneity in width is the essential parameter of this feature regardless of environments and rock types. There is not a

clear relationship between the age of rocks and the microrills width. Figure 2 illustrates the microrills mean width values and width distribution against the mean rock grain size. The characteristic microrill width frequency distribution shows a slightly skewed typical peak-pointed shape (Figure 2b). The scatter graph (Figure 2a) points up two main relationships. The first one is that microrills are developed only on mudstones or fine-grained rocks. The second is that microrill width is not dependent on the rock grain size ( $r^2 < 0.01$ ;  $p < 0.001$ ). If the data on microrills developed on Upper Miocene rock outcrops are assessed alone, then there



**Figure 3:** Microrills plan view. They are not true linear forms and can be considered as an alignment of micro depressions. The graph shows the ridge crests (dotted), the direction of slopes (arrows) and the concave bottoms (circles).

is a weak negative correlation between microrills width and rock grain size ( $r^2 = 0.62$ ;  $p < 0.001$ ).

### Optical microscope and SEM observations

Binocular microscope observations show that conventional features that we use to describe microrills are not real lineal elements (Figure 3). Slope orientations are not organized as a logical or classical flow feature. Microrills that to the naked eye seem one individual lineal feature are, in fact, an array of elongated or near circular depressions that share wall partitions. They can be compared, just from a morphological point of view, to an elongated polygonal karst (Ford and Williams,

2007). Sample observations show that there are many features closed by well-defined partitions, and other ones that connect with neighbouring features although there are secondary wall partitions, or soft chains that separate opposite slopes. SEM observations contribute to previous information. Microrills are not true channels but a set of micro depressions joined or sharing walls aligned according to a rock texture pattern. Thus, in some cases chains and depression walls correspond to coarser grains whereas microrills bottoms overlie finer grains (Figure 4). SEM micrographs and resin casts reveal that microrills are not aligned according to joints and micro fractures present in the rock, some of them clearly cross or have their



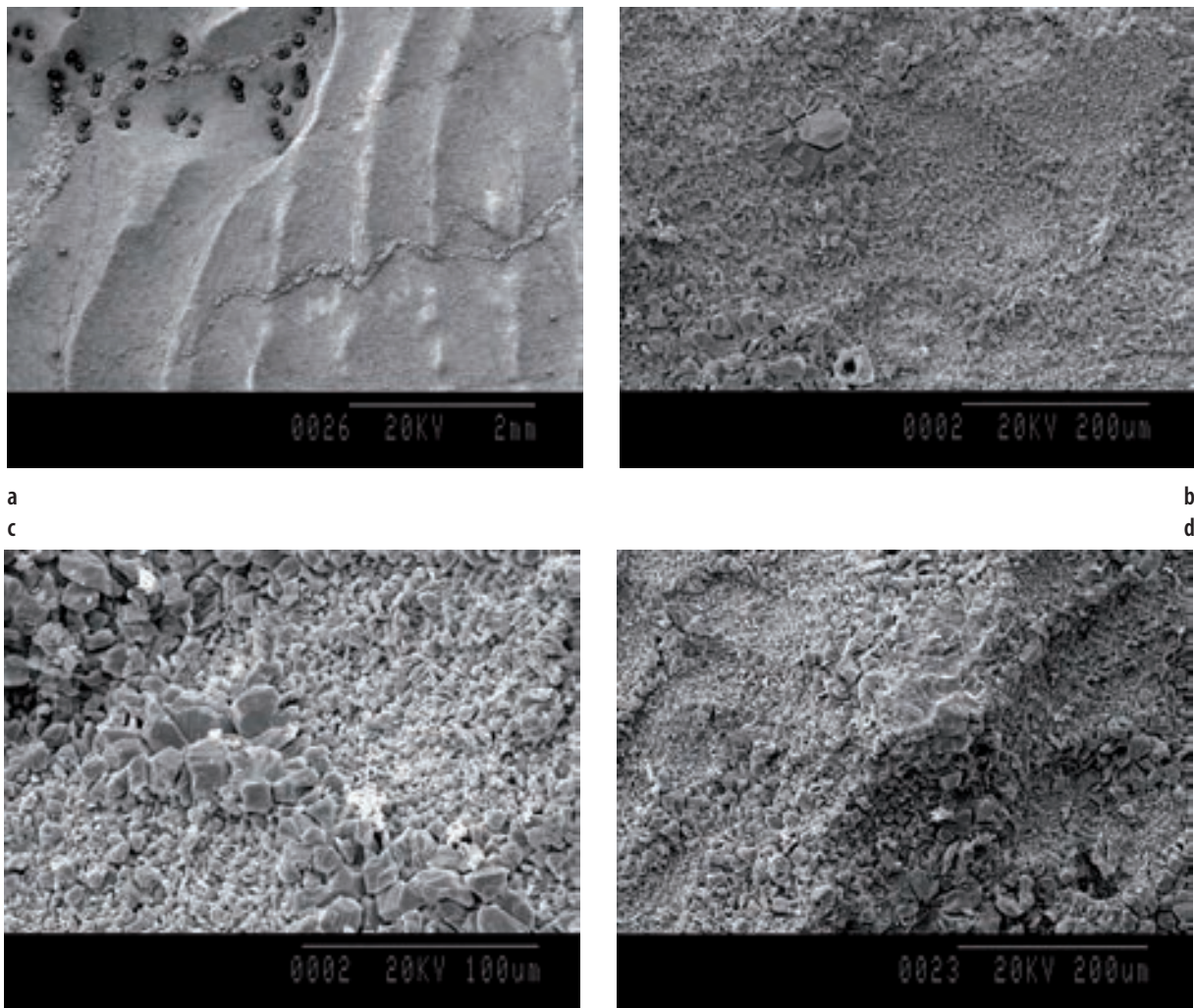


**Figure 4:** Microrills SEM photographs: a. general overview of microrills and fungal biopitting. Note the microrills crossing the joints filled by calcite crystals; b. detail of the array of elongated or near circular depressions that share walls inside the gross morphology of microrills; c. and d. in some cases microrills chains and depressions walls correspond to coarser rock grains.

major axis orientation perpendicular to structural alignments (Figures 4, 7a, b).

Scanning electron micrographs also show that grain *boundary widening*, *V-in-V etching* and *blocky etching* are very abundant nanomorphologies. All these nanomorphologies, according to Viles and Moses (1998), are thought to be related to dissolution and crystallographic control on dissolution in its morphological expression. In this way, the general overview is that rock grains, because of solutional attack, seem to be floating (Fig-

ure 5). There are few samples in which evidences of *biological weathering* nanomorphologies such as *circular etched pits*, *etched tunnels* and *filament shaped trenches* are present, and these are mainly at microrill bottoms. Nevertheless, lichen fructiferous bodies, fungi and blue-green algae pits appear in those samples that have been exposed for longer times and in more humid locations (Figure 6); although they have no relation with the development of the microrills. All these features are clearly superimposed over the solution and crys-

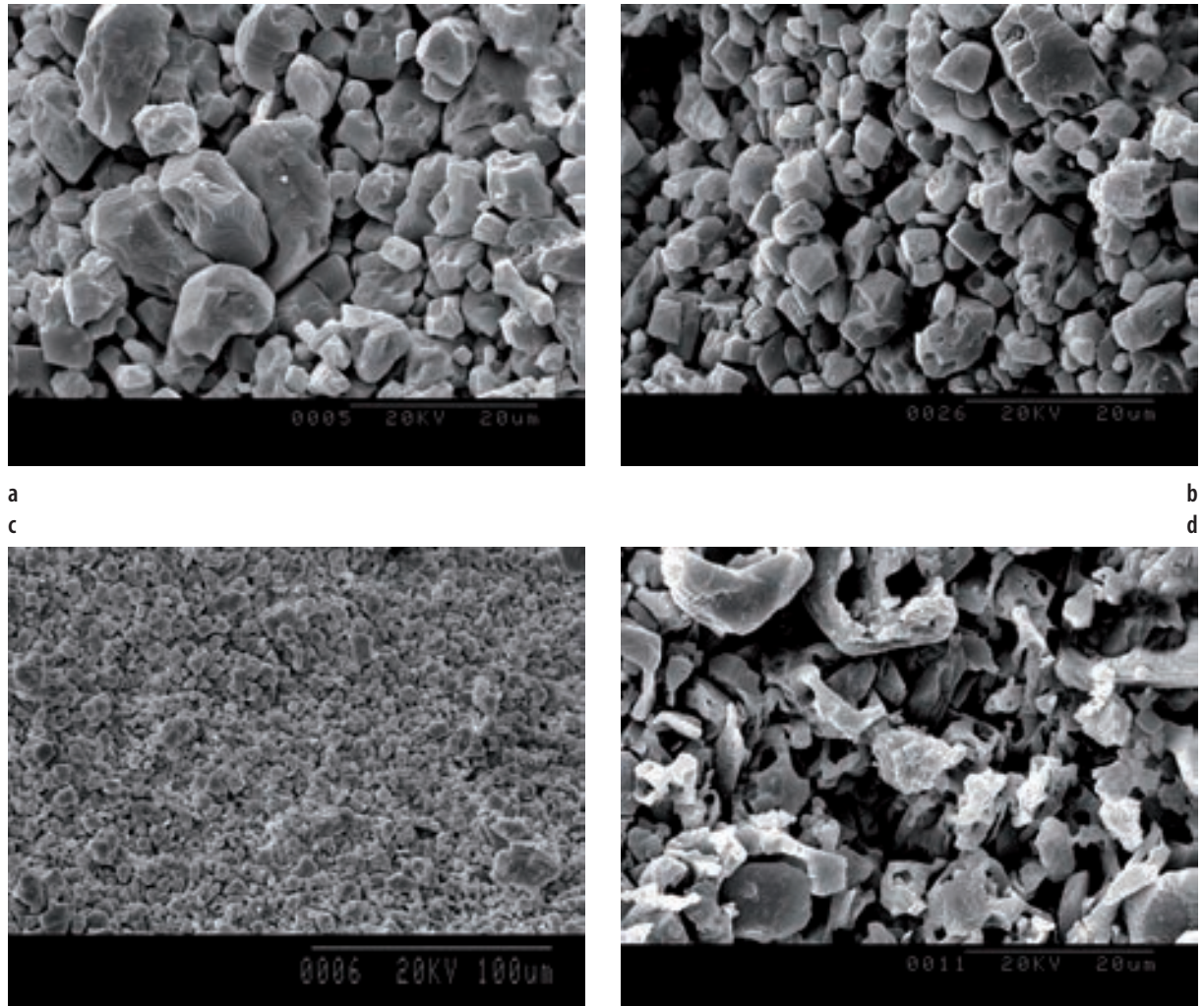


**Figure 5:** SEM micrographs showing the grain size and good sorting at different rock exposures where microrills are developed. Note that rock grains seem to be floating, they are poorly cemented.

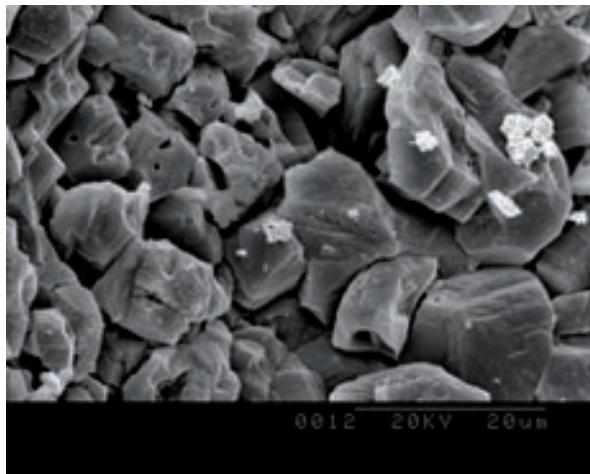
tallographic controlled nanomorphologies, and the gross morphology of the microrills.

Resin cast observations support the information from the previous techniques. Similarities are found from different samples and study locations. In the inverse resin cast image of microrills the walls appear as a set of depressions and they resemble the geometry of intestines (Figure 7) in which bottom surfaces are smooth and crests slightly sharp. The plan view of resin casts reinforces the SEM observations of the non-linear nature of microrills. It could be seen how depressions are attached one to the other, although there

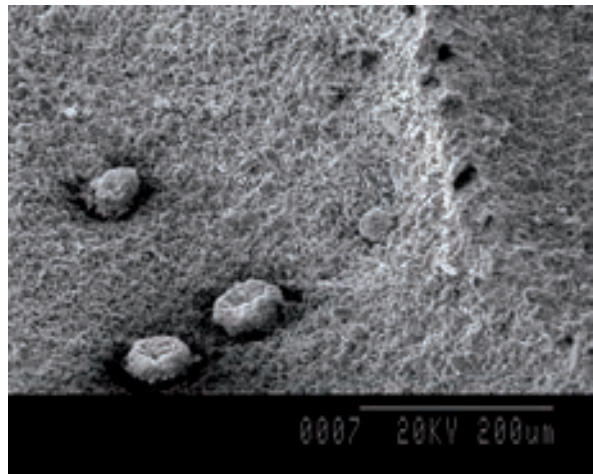
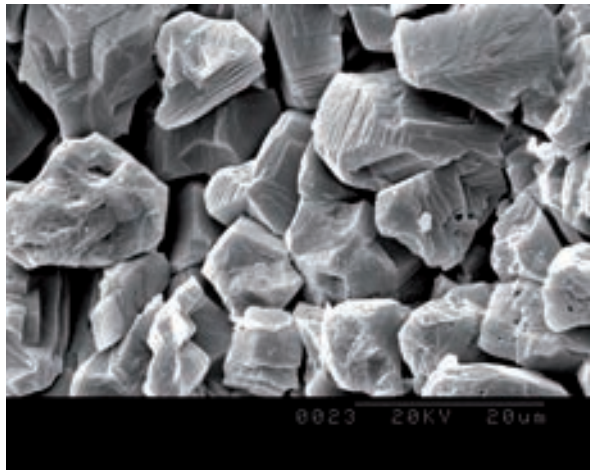
are cases in which depressions are isolated. In some cases a second order of small pits appears in the bottom of microrills and those relates to incipient colonization of fungi or blue-green algae superimposed on the gross morphology of microrills (Figure 7a, c).

### Some genetic considerations

From our observations in the Balearic islands, it would seem that microrills do not show truly linear *microkarren* morphologies. Among other



a  
c



b  
d

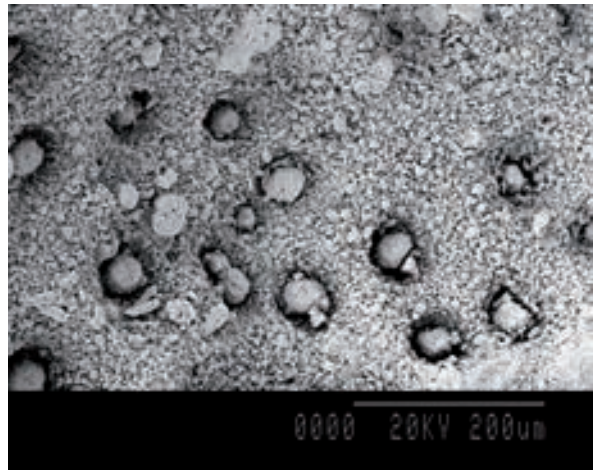


**Figure 6:** Nanomorphologies identified in microrill walls and bottoms: a. and c. detailed observations of rock grains where V in V and crystal limits widening a crystal growth controlled nanomorphologies are the most abundant features. It can be appreciated a second set of nanomorphologies, although less important, as micropits and circular etchings related to blue-green or fungal biological action; b. and d. lichen and fungi fructiferous bodies and associated pits appear in those samples related to longer time exposed surfaces and more humid positions.

factors, rock texture is the key element for their development. Rock texture must be fine enough (mudstone) to develop microrills. The mean grain size that we have measured ranges from 3.23  $\mu\text{m}$  to 8.65  $\mu\text{m}$  (Figure 2a). The fact that the set of aligned or joined depressions do not follow fractures and joint directions enhances the idea that microrill genesis is related to the textural nature of the rock rather than its structure (Vacher and Mylroie, 2002; Taboroši et al., 2004). All these

variables can better explain the disposition and organization of microrills. Detailed observations show that the channels are not simple channels, but rather chains of depressions, and that meander-like forms are related to the size of rock grains and to the plan view arrangement of depressions.

Microrills appear in a wide set of environments, with mean annual precipitation ranging from greater than 800 mm down to less than 400 mm. Nevertheless, solution, according to SEM observa-

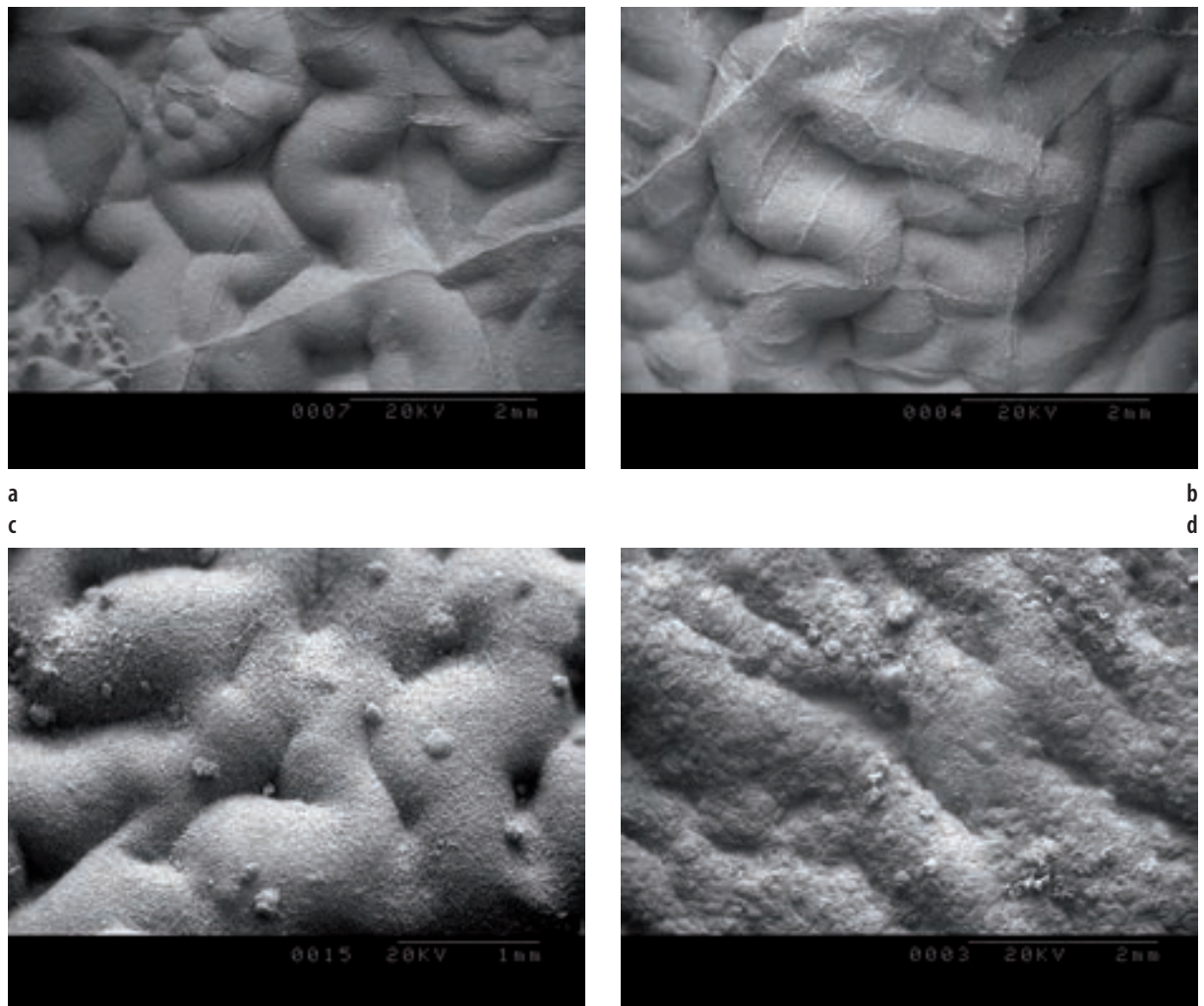


**Figure 7:** Resin cast observations show that microrills do not follow the microstructural and joint alignments of rock (a and b) and that the gross morphology of microrills is of rounded bottoms (a and c) and sharp walls (b and d), as well as the different depressions that appear inside a microrill (d). In some cases it can be appreciated small depressions superimposed to microrill paths that seem related to biological weathering agents (a and c).

tions, is the key process operating on the development of this feature. The absence of real channel forms exclude runoff as the gross agent for microrill enlargement. For this reason thin water films derived from dew or sea spray and driven by capillary forces seem to be the mechanism by which microrills are formed and then enlarged. Grains detached by solution are pushed out of the depressions in a mechanical way by runoff and rain, and this fact is enhanced by the shallow nature of

these features. In some way the evolution in two stages of this micromorphology has resemblances to those described for rillenkarren by Fiol et al. (1996). The first mechanism by which the rock grains are weakened corresponds to dew solution, and in a second stage rain or water film runoff detaches the grain and mechanically enhances the morphology. The biological contribution is a secondary agent that can affect the microrill development, helping us to understand the temporal

framework of the microrill's genetic model. Microrills never appear on highly-dissected relief zones (i.e. pinnacle zone at coastal karren, or well developed rillenkarrren surfaces). However, it is easy to find them landward from coastal sites and on round surfaces recently exposed in mountain or inland environments. According to observation from longer exposed samples, as biological action increases then microrill formations disappear and evolve to *biokarstic* features. Thus, according to the model presented by A. Ginés (1995, 1996a), karren assemblages can be understood or observed from an ecological point of view in which they are interpreted as a succession of morphologies. In this way, microrills would be the first step in this karren forms colonization or development of recent exposed limestone rocks to the weathering agents.

The literature on microrills is scarce, and most of the works are concerned with descriptive approaches. There is not much work that links quantitative data on microrills dimensions and observations at different scales to rock properties and the active weathering processes. From data

addressed on the Balearic islands microrill characterization it is highlighted that microrills are a more complex form than was initially thought. A worldwide field study exploring all the features described would be advisable to get a better knowledge of the specific role of rock texture and nature, as well as how dew or water films are operating jointly with runoff in the shaping of microrills.

## Acknowledgements

The authors are indebted to staff of the Electron Microscope Unit and to the laboratory staff of the Department of Earth Sciences at Balearic islands University. We are grateful to Dr. Angel Ginés and Dr. Ken G. Grimes for their helpful comments and suggestions. This study is a contribution to the investigation project CGL2006-11242-C03-01 BTE from the Ministerio de Educación y Ciencia-FEDER. LGP is indebted to the “Consejo Superior de Investigaciones Científicas” (CSIC) for the funding provided in the JAE-Doc Program.

Andrew S. GOUDIE

In common with sandstones, granites and many other rock types, the surfaces of limestones and dolomites may frequently be pitted with a range of *cavernous weathering* forms of different sizes. The smaller features (a few cm in size) are commonly called *alveoles* or *honeycombs*, whereas the larger features (which may be some metres in size) tend to be known as *tafoni*. Both *alveoles* and *tafoni* are common in coastal environments, and *tafoni* appear to be especially common in drylands. *Tafoni* developed on limestones have been described from Malta (Hunt, 1996), Bahrain (Doornkamp et al., 1980), and north Africa (Smith, 1978, 1986), and are widely developed on the limestones of the Oman mountains. They are also reported on limestone buildings. However, most detailed studies of cavernous weathering forms and the processes that form them, have been conducted on non-carbonate rocks (Goudie and Viles, 1997).

The apparent preferential development of *tafoni* and *alveoles* in coastal and dryland environments gives some *prima facie* support to the idea that salt and/or wind abrasion may be involved in their development. Indeed, salt weathering has often been seen as associated with the development of cavernous weathering forms (Martini, 1978) and experimental simulations have shown that limestones are very susceptible to salt attack (Goudie, 1974, 1999) or to attack by a combination of salt and wind (Rodríguez-Navarro et al., 1999). How-

ever, as Smith and McAlister (1986) have rightly pointed out:

“There has been a tendency in field studies of salt weathering for either dangerous circular arguments or a form of ‘guilt by association’. In the first case, the presence of certain landforms in an area is used to infer the activity of salt weathering mechanisms, without incontrovertible evidence that the landforms derive solely from these mechanisms. In particular, *tafoni*, which are commonly attributed to salt weathering, may...be convergent forms produced by different mechanisms, of which salt weathering is only one possibility. Whereas, in the second case it is assumed that because certain salts are abundant in an area, and because rocks are being weathered, then those salts must be responsible for the weathering.”

The role of salt may cause chemical weathering (Young, 1987), volume changes in clay minerals (Pye and Mottershead, 1995) as well as the physical mechanisms of crystal growth, crystal hydration and volumetric expansion. A wide range of salt minerals have been found associated with *tafoni*, including halite, gypsum and various forms of magnesium sulphate (Rögner, 1986; Mustoe, 1983; Bradley et al., 1978).

Preferential development of *alveoles* has been noted in windy situations (Cardell et al., 2003), and the simulation study of Rodríguez-Navarro et al. (1999) suggested that wind and salt could

work in tandem to produce honeycomb weathering forms. As they wrote: “Incipient honeycomb weathering in a homogeneous limestone has been experimentally reproduced by wind exposure and salt crystallisation. Our experiments show that heterogeneous wind flow over a stone surface is important in the development of small, randomly distributed cavities. A reduction in air pressure within the cavities results in increased wind speed and rapid evaporation. A high evaporation rate and evaporative cooling of the saline solution in the cavity leads to more rapid and greater granular disintegration than in the surrounding areas. It seems that this local supersaturation and subsequent build-up of salt crystallisation pressure ultimately result in the formation of honeycomb features.”

Some cavernous weathering forms may be the result of seepage erosion and arise from concentrated weathering related to greater moisture availability at ground level (Smith, 1978). Hunt

(1996) has argued that Maltese tafoni are dissolution phenomena that were initiated underground (e.g. under a mantle of soil), subsequently exhumed, and then enlarged by subaerial weathering processes.

Some scientists have argued that the development of cavernous weathering forms requires the presence of rocks with *case-hardened* exteriors and weakened interiors. Once the outer skin is breached, it is argued, weathering and erosive mechanisms can then hollow out the rock’s interior (Winkler, 1979). However, whether case-hardening is a requisite has been challenged by Bradley et al. (1978), Conca and Rossman (1985) and Smith and McAlister (1986). On the other hand it is remarkable how many tafoni do appear to occur in rocks that have been case-hardened (Goudie et al., 2002).

Another possible reason, apart from breaching of a case-hardened carapace, why cavernous forms may develop, is a positive feedback effect (Smith and McAlister, 1986): “... once a hollow is initiated it creates an environment in which weathering is favoured, weathering in turn extends the hollow to produce an optimum form in which weathering is further enhanced, and so on. Such re-enforcement cannot continue indefinitely and a condition must eventually be reached where the weathering rate is reduced. This could occur, for example, where a cavern becomes so deep that it either prevents the ingress of moist air, or rock temperature variations are reduced to the point where precipitation and evaporation no longer occur.”

They argue that on exposed cliff faces salts would be deposited by the outward migration of salts derived from within the rock, but that they would be removed by subsequent rainwash, whereas salts precipitated in hollows would be protected from such leaching and so could cause salt weathering to occur, which would progressively expand the hollow.

It is probable that cavernous weathering forms such as tafoni are the result of a combination of

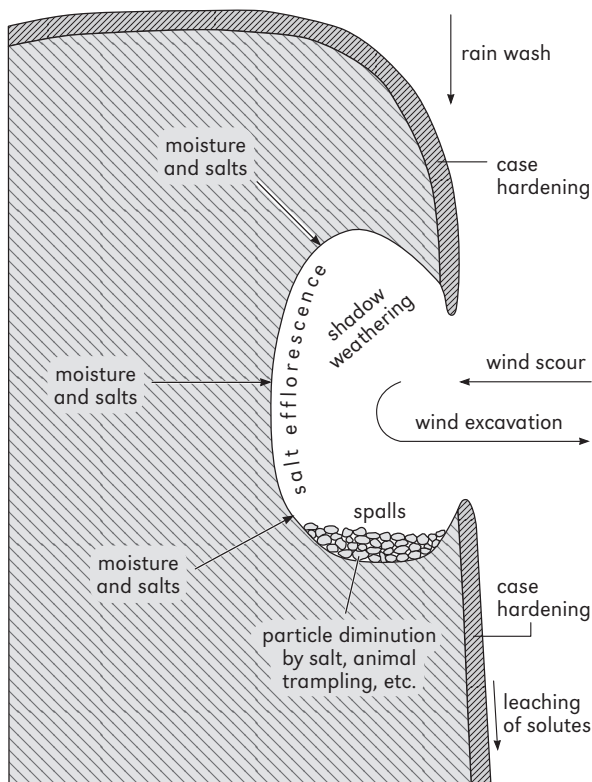


Figure 1: Tafoni.

processes, as indicated in the model presented (Goudie and Viles, 1997), Figure 1.

There is very little hard and fast data on the rates at which tafoni may develop in limestones. An experiment undertaken in Bahrain in a siltstone member of the Al Buhayr carbonate formation indicated that back wall retreat and rock flour production were rapid (Goudie and Viles, 1997).

Larger cavernous weathering forms are more than just morphological curiosities. In time they lead to the undercutting of slopes, so that slope failure occurs. Hume (1925) argued that the limestone cliffs of the Eocene Ma'aza limestone plateau in Upper Egypt has been so oversteepened by extreme cavernous weathering that they had become "absolutely unscaleable".





# KLUFTKARREN OR GRIKES AS FUNDAMENTAL KARSTIC PHENOMENA

Helen S. GOLDIE

Kluftkarren are fissures in karstifiable rocks, especially limestone or dolomite, that have been widened by weathering and erosion processes, largely corrosional. They are fundamental to karst, as a limestone without fissures of some sort is karstifiable to only a limited extent. Definitions of karst testify to and support this notion. For example, a glacially scoured limestone surface without any remaining fissures has essentially had all of its karstic characteristics removed. Limestones that are unfissured may develop surface solution pools for example, but without openings into the rock there will be no notion of drainage going underground, so the fundamentally important third dimension of karst will not develop.

## Literature: definitions, dimensions and distribution

Kluftkarren can be discussed in various terms including scale, degree of development, and their relationships to other karst features, including other karren (*lapiés*) features, particularly *clints*, or *Flachkarren*. Development can be examined from both ends of the spectrum, that is, from where the features begin, to where they are evolving. There has been much work on karren definition and description (Fornós and Ginés, 1996) and an important point as regards *kluftkarren*, *grikes*, or *cutters*,

as they are also known, is their distinction from many, solutional etching, karren features since they are linear features determined by rock structures such as joints and veins. Kluftkarren are thus not so exclusively a solutional feature as are some karren types, and fissure formation can indeed produce a visible topographic feature without any solution having yet taken place, for example, where pressure release caused by quarrying has occurred.

Ford and Williams (2007) define kluftkarren as “the master karren features in most karren assemblages. They are the principal drains, either to the deeper epikarst, or to dolines or to surface discharge such as river channels.” They identify their relationships to major joint sets or systems and to bedding planes. Some kluftkarren or grikes cut through only one rock layer, others may extend through two or more. These latter will receive drainage from shallower fissures and therefore develop dominance of the drainage systems. Goldie (1976) defined grikes as features cutting through at least one bed of rock.

It can be seen that grikes are absolutely fundamental to karst landform and landscape development, and without them karst would be restricted. Indeed, karstifiable rocks must be mechanically competent and not with too few fissures, nor too many, nor a dominance of high porosity, since these properties prevent true karstic landform

suites from developing. The *chalk* of southern England is one limestone where the nature of the fissures and the porosity restrict karstification, unlike in the harder, more mechanically competent and less-fissured limestones of the Carboniferous in northern England and elsewhere in the British Isles, or the Cretaceous limestones of the Alps, for example. Some of the difference in karstifiability is because the joint or fissure spacing in the chalk is quite small, reflecting bed thickness. Bed thicknesses of 10 to 30 cm are typical in chalk and joint spacing is similar (Ameen, 1995; Gunn, 2004).

Making comparison with other karren features, White (1988) describes *kluftkarren* thus: “In the middle of the size scale, and perhaps most widely distributed, are the linear slots cut in the bedrock along a guiding structural element.” In reality the size range is from incipient cracks only millimetres wide to several metres in width and depth and tens of metres length. Some sources define these features as beginning with larger lower width dimensions, but in a theoretical sense it is important to consider absolutely minimal dimensions and a scarcely visible hairline crack in the rock is the beginning of the feature. As soon as such a crack exists solution processes can begin to operate on the opening, there is thus a grike or cleft from mm widths. Since grikes are the features that cut up the landscape, and along which processes operate, White referred to their identification as one of the three principal landforms of karst along with sinkholes and caves. In fact, as already implied, it can be argued that their presence is even more fundamental, that the existence of fissures is a necessary condition for the development of karst, along with a strong and soluble rock, and the presence of water. Sinkholes develop in association with fissures and so do caves. So fissures are a condition for the development of these fundamental forms. *Kluftkarren* or grikes are merely the visible surface expression of the fissures of a karstifiable rock. As such, they are a significant component of the *epikarst*, or the outer skin of the whole karst system. The variation in their scale and form is enormous and relates in partnership

with the form of the intervening rock, composing *flachkarren*, clints, *pinnacles* or other remnant solid forms.

Much research has material on or reference to grikes (the term to be used here), and it would be impossible to summarize all but the main ideas that more specifically focus on these features. Factors affecting grike development must be outlined and it is worth commenting on their distribution, which is world wide in any fissured strong limestone exposed at the surface. Although grikes are most clearly seen in plan on glacially scoured surfaces with some time to solutionally open, and have been thought therefore to be best displayed in glaciated upland karsts, the fissures along which solution has dissected mature karsts such as pinnacled karst, even the Stone Forest of China (Gunn, 2004), are essentially the same basic feature, however hard they might be to observe in plan view. Indeed, definitions and discussion of grikes in the literature often move on to consider enlarged features and complex areas. This is not the place for an extended description of such features but it is relevant to remark on various mature griked landscapes in different environments to set the grike networks of the British Isles in a wider context. Feeney (Fornós and Ginés, 1996) compared *limestone pavement* in New York State with the Nahanni karst, noting similarities independent of their very different scales. However, his diagrams do not incorporate the type of mature surface roundedness which is observable in mature sites in the British Isles, southern Spain, or the *Giant Grikeland* of Australia (Gale et al., 1997). The Giant Grikeland is an established example of a mature griked area (Jennings and Sweeting, 1963), now with a semiarid climate, although not always, the Chillagoe area is another example (Marker, 1976b). The more maturely weathered areas of northern England that are thought to have survived the Devensian glaciation have in common with these other maturely griked areas very massive limestones and considerable time for the landforms to evolve without the radical hiatus of erosional stripping of the well-weathered upper

blocks by, for example, glacial scour or other process. There are more similarities than differences between the basic forms of many of these different landscapes around the globe and an apparent difference can often be ascribed to scale.

## **Factors affecting grikes**

Factors affecting grike characteristics can be grouped as geological, process and time-related. Of necessity, some detailed description of grike characteristics and examples must be incorporated into this discussion. Rock characteristics influence development of structural lines that are the starting point for grikes. Processes produce the features, still constrained by the material properties of the rock, and perform their action over varying time periods. Historical considerations, involving sequences of development, and possibly changes in conditions, are also very important. Grikes can be examined from two main aspects: from the plan view or map of their spacing and pattern which is clearly important for its influence on the pattern development of landforms; and from the cross-sectional view, that is their side-ways shaping and their depth.

## **Geological factors affecting grike development**

It is clear that the existence of fissures in a rock mass is the prior condition for grike development. The prior condition producing the fissures are the tectonic forces that put strain on these rock masses, the release of which results in brittle fracture. Influences on fissure patterns and density thus ultimately explain the potential for grike development. Basic geological characteristics include bed thickness, macroflaws within the rock material and tectonic forces affecting the rock mass. The fissures that develop from fracture patterns resulting from stress fields in the rock masses, namely the regional joint systems, tend to produce inter-

section angles of 60, 90 and 120 degrees in plan view. Ford (Gunn, 2004) refers to jointing density being inversely proportional to bed thickness and its considerable variation between carbonate formations. Thin to medium beds, < 10 to ca 30 cm, are regarded as unfavourable to good karst development due to the wide dispersal of solution. Thicker beds, > 30 cm, even > 100 cm, with joint spacing of 100 cm or more, are the most favourable for karstification, allowing as they do some focussing of solution processes. Explanation of variations from this generalization has been discussed by geologists (e.g. Narr and Suppe, 1991; Gross et al., 1995), with considerable emphasis on the role of macroflaws in the rock material in influencing joint occurrence and pattern.

The distribution of fissures in depth through rock layers influences how extensive and large grikes can become, and the propagation of joints across beds is of considerable importance here (Helgeson and Aydin, 1991). An important characteristic influencing grike depth development are the presence, scale and pattern of veins, which may or may not be contained in joints. Gillespie et al. (2001) demonstrate that veins have different influences on the grike network from jointing, in particular the greater likelihood of persistence by veins through a greater number of rock beds than the joints (Figure 1). This can be affected by the presence or thickness of shale layers, or by other changing lithologies. This has material impact in explaining varying plan patterns of grikes and also influences development in the vertical plane. Maturely griked areas which have not been scoured by glaciation, for example El Torcal de Antequera, Spain (Figure 2), show grikes extending through several beds of rock to attain great depths and leaving tower-like features between. Limited examples of grike persistence through more than about 2 or 3 beds do exist in northern England, in spite of glacial erosion. They are best observed on the edges of outcrops or cliffs, in sheltered, higher altitude locations, such as High Sleets, above Littondale in Yorkshire, or by the Monk's Path (Figure 3) above Cowside Beck (Goldie, 2006).

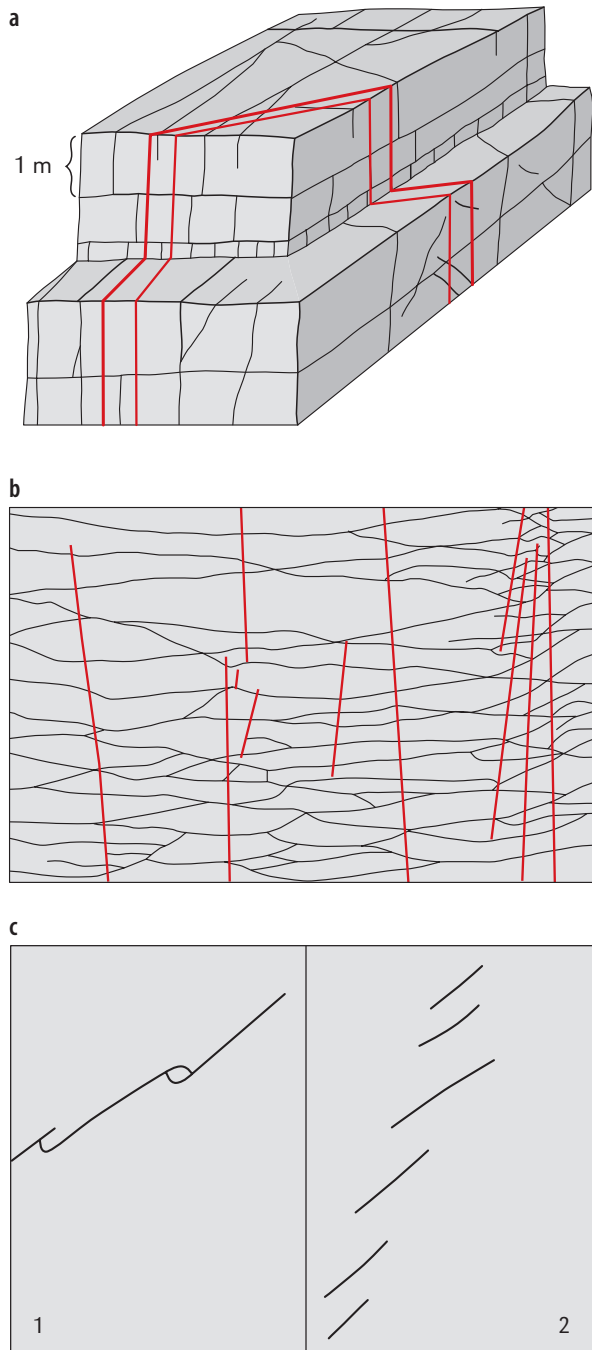


**Figure 1:** a. Block diagram, demonstrating possible relationships between bed thickness, joint spacings and veins (red lines) based on Gillespie et al. (2001); b. grike pattern, derived from photograph of pavement at Sheshymore, Burren (Gillespie et al., 2001), with one main joint set, and veins crossing (red lines). Notional scale: diagram is 30 m across; c. hooks and “en echelon” features, plans of minor surface fracture and veining features (after Ameen, 1995). Notional scale: diagrams are each 1 m across.

Angles of jointing in the vertical direction can significantly influence a grike. Most joints are approximately perpendicular to bedding planes, but some are at lower angles, and very massive beds may have curiously curved grikes running at quite low angles across outcrops. Bedding planes in such rocks may also be uneven or curved (Figure 4). Angled joints produce sloping grikes, affecting grike wall solutional features. In plan most joints are also more or less straight with some minor irregularities, but curved joints are not unknown, for instance on limestone pavement on the west coast of the Burren near Murrough, Ireland (Figure 5), where the beds are the favourable massive type.

Gillespie et al.’s work on the Burren distinguishes vein networks from joint networks, an idea applicable elsewhere. Veins run north-south in the area of Sheshymore on the Burren and the joint patterns run east-west with enough joining up to produce a grike network with plenty of low angles (Figure 1). This low angled joining produces long and narrow clints, not a rectangular pattern. A separate set of cross joints, or veins, is needed for rectangularity. It is suggested that other areas of long narrow clints, identified by morphometric work (Goldie and Cox, 2000), reflect the same influences but at different scales according to local tectonic stresses. The similarity between the patterns displayed at The Clouds (Figure 6) and Sheshymore (joints only, not veins) is interesting although the clints at The Clouds are smaller; whereas at Scar Close in Yorkshire there are similarities with the total overall pattern at Sheshymore (with veins) with both strong veining and cross jointing, which is seen particularly in the maturely developed area (Figure 7) of Scar Close.

One fascinating pavement site on Arainn, County Galway, Ireland, has very straight joints at almost perfect right angles with virtually no oblique angles (Figure 8). This is in a narrow tectonically stressed zone (Langridge, 1971) and its simple network contrasts with complex patterns involving several joint sets and minor plan fea-



**Figure 2:** El Torcal de Antequera, Spain. General view showing varied massive beds surviving to form towers, well-rounded upper edges and good runnelling (photo by L. Hook).



**Figure 3:** High Sleets, Littondale, UK. Tower-like outcrop, with grikes through several beds.

tures stemming from the joint formation process. In plan view these latter include hooking patterns and *en echelon* features (Figure 1); and, on the face of joints and therefore on the sides of grikes, many small surface markings, such as hackles, steps and ridges (Ameen, 1995). These small marks may influence how these surfaces erode by solution; certainly hooking and *en echelon* features are seen on less-dissected pavement areas such as Gaitbarrows, Cumbria. Grike patterns may also be affected by rotation of joint directions across areas, reflecting changes in stress fields (Gillespie et al., 2001).

Further generalizations about grikes need comment and amplification. For example, White (1988) refers to their orientation in folded areas as along the strike. This is not exclusively so, however. Grikes may favourably



**Figure 4:** Dowkabottom, Littondale, UK. Massive limestone outcrops with curved grikes.

develop along this strongly stressed direction but there may still be a rectilinear pattern if cross joints or veins are involved. An example is at Hutton Roof Crags in NW England where strongly dipping limestones have two equally strong grike directions. What is most striking here is that relations between topographic slope, dip alignment and grike orientations produce diamond patterns (Figure 1). At The Clouds, strike direction appears to have the stronger influence. On the other hand a difference in strength between one joint set and

another is not exclusive to folded limestones, it is observable in many horizontal pavements, the Burren, Ireland (Figure 9), for example. Effects of stretch and compression in folded terrain can be important, for example it is very relevant to understanding gently folded outcrops at Great Asby scar, as well as more pronounced folding such as at The Clouds (Fornós and Ginés, 1996).

Ford and Williams (2007) observed that grike length is inversely proportional to the density of major joints. This is an understandable observa-



**Figure 5:** Murroogh, west coast of the Burren, Ireland. Curved grikes in very massive limestones.



**Figure 6:** The Clouds, Cumbria, UK. Lower limestone beds at centre of denuded anticline with joint set parallel to strike of fold with similar pattern to that from one set of joints at Sheshymore on the Burren (Gillespie et al., 2001).



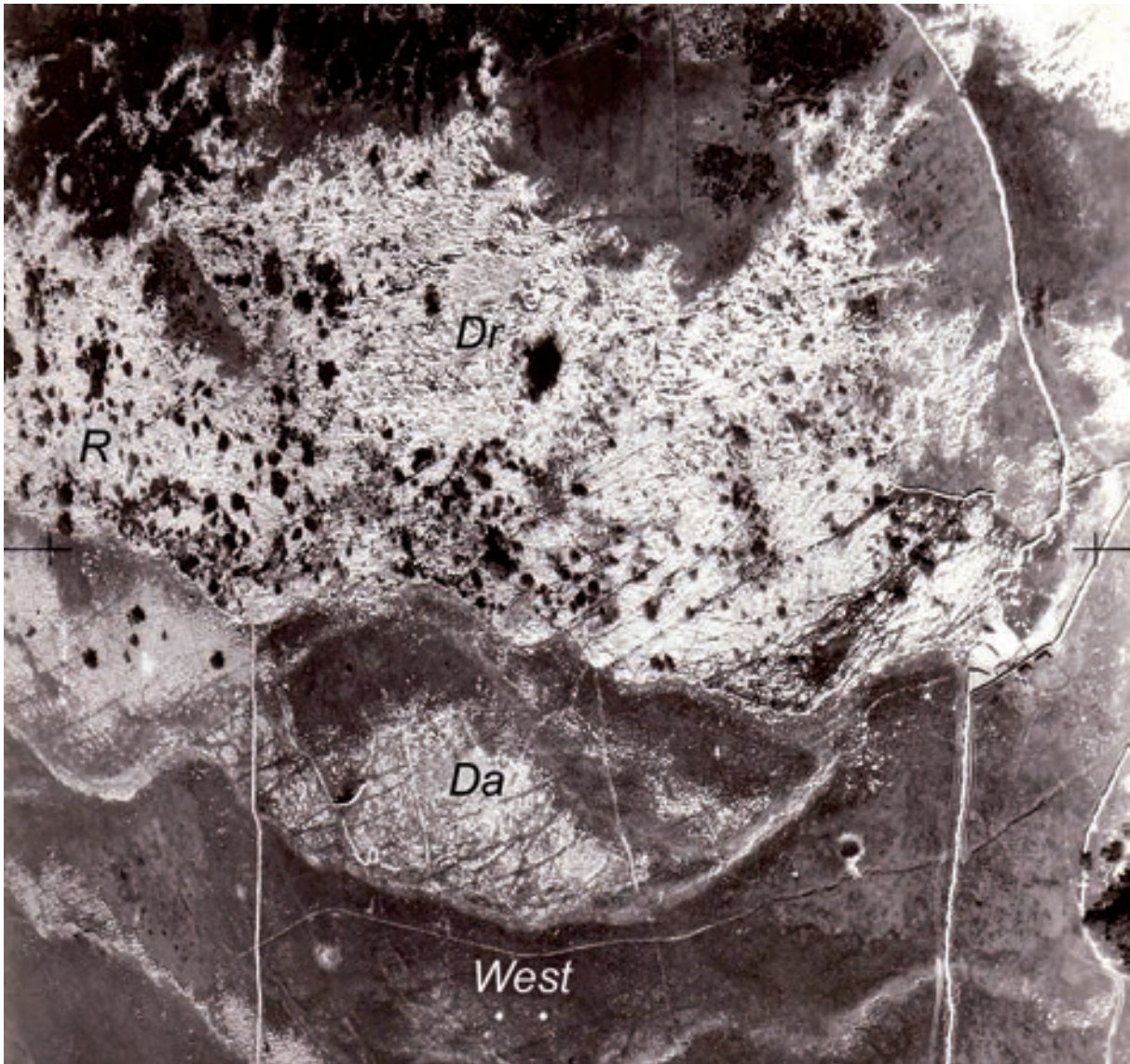


**Figure 7:** Scar Close, Yorkshire, UK. Aerial photograph of Scar Close demonstrating different grike networks, dendritic (Dr) networks seen to the east where acidic waters come off drift and peat, rectilinear (R) on older, longer-exposed surfaces at outer, west edge of outcrop, and in the foreground between modern walls (long and straight) are signs of old settlement/walls and damaged surfaces where grikes are less clearly visible (Da). Long wide griked lines pocked with large holes cross from northwest to southeast.

tion in some ways, implying that a major joint will persist for great distances, but not all major joints will do this. Such a pattern may partly depend on the degree of joint opening; if this is well developed it may be virtually impossible to determine individual grike length on the ground, although aerial photography may resolve the question and

identify the most important grikes. Scar Close has major grikes spaced tens of metres apart, although in between there are many other grikes, some of which are as wide as the very long features (Figure 7). The major wide grikes persist across country both in the well-evolved rectangular area, and in less continuous lines they visibly influence the

dendritic patterned less evolved area. Sites with closely spaced fractures still have the grikes proceeding over long distances, for example in the Burren, Ireland (Figure 9). The effect is reflected in clint-grike dimensional work which finds that square clints are very rare (Goldie and Cox, 2000), with the ratio of clint width to clint length generally being well below 1 (indicating squareness). There are many complex patterns with different levels of development, so a tight relationship between grike length and joint spacing is unlikely. Length also depends on time available for fissure widening and linking up of small features to form true grikes.

The influence on joint spacing by bed thickness (Ford and Williams, 1989; Gross et al., 1995) needs further discussion. Widely spaced grikes in thick strata may be able to become deep, long and possibly very wide too, although this depends on propagation of joints between beds. El Torcal de Antequera in southern Spain well illustrates (Figure 2) a site with plenty of time for grikes to develop through several beds, including some very massive ones nearly two metres thick, not having been interrupted by glacial scour in the Quaternary. Wider spaced joints in thick beds usually link across well-bedded limestones into further thick beds permitting grike depths to become many metres deep. In other sites stronger beds beneath weak ones may restrict grike depth. This appears to be the case in parts of Great Asby scars (see chapter 22). Plan patterns of grikes at any locality certainly need very careful analysis to be fully understood. High Alpine sites such as at Sanetsch, Glattalp, and the Julian Alps, are useful due to their scanty vegetation allowing features to be seen clearly in both plan and section views (Figure 10).

### Process influences on grike development

Processes affecting grike evolution are wider ranging than may seem obvious in a karstic context. In

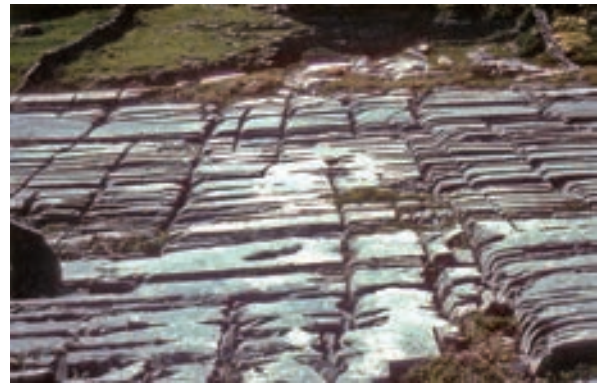


Figure 8: Arainn, Ireland. South of Cill Ronain with very straight, rectangular patterned closely spaced grikes.



Figure 9: Burren, Ireland. Pavement showing differences between strength of two joint sets.

particular it must be remembered that the many possible solutional processes are not the only erosional processes affecting grikes. The other main processes are mechanical. In numerous circum-



**Figure 10:** Triglav, Slovenia. Stepped limestone with grike persistence through several beds.

stances mechanical processes may completely overshadow solutional action. There are two main situations where this occurs: firstly where the limestone involved is well fractured, in the horizontal or vertical plane or both, and secondly where some major mechanical process is able to remove blocks of limestone. In the latter case human activities must not be forgotten for their ability to have major landform effects (Goldie, 1986), although cliffs clearly provide a location where natural large-scale mechanical effects are likely.

To understand how grikes develop it is useful to consider a clear, ungriked surface, after varying lengths of time and in differing solution conditions. Small slits or kamenitzas develop into larger and more complex features, which merge at varying size stages. Long grikes are invariably associated with many minor features along their line linking up over time (Figure 10) which occurs on different scales. In plan a simple grike at Gaitbarrows looks

very like a long, wide grike of 10-fold size across Scar Close, both have plan variation in their line pattern due to this linking up of many features.

Although solution processes will not be discussed in detail here, being adequately treated elsewhere, it must be emphasized that the solutional environment of grikes includes infiltration, direct rainfall, stream flow, and soil percolation water. Biological influences are very important, as the many initial small features preparatory to fully developed grikes are the pans, and slits in which vegetation can grow for as long as moisture is available. These small features initiate in dips and flaws in the rock surface. Some may develop in plan form until moisture drains out as the slit opens up to drain under the relevant bed (Figure 11). Grikes covered in acid soil will develop rounded smooth features on their sides and be protected from mechanical processes until soil erosion exposes them.



**Figure 11:** Gaitbarrows, Lancashire, UK. Complex area of radiating runnels and grikes around what was originally a *kamenitza*.

Physical influences have already been implied in discussion of geological factors. Erosion of karstic features itself influences the geological properties, i.e. the fissures, by pressure release for instance. Pressure release cracks can be generated, or existing cracks widen, due to removal of lateral confining material from human quarrying, glaciation, or long-term geomorphic processes. Glaciation as a specific influence has already been referred to concerning mature grike development. Also grikes cannot be dissociated from what is affecting the solid forms of their sides, the clints, *flachkarren*, pinnacles and so on, which includes the formation of other karren features such as *riilenkarren* and *rundkarren*. Differences between vertical or horizontal attack affect grikes. Overall, processes affecting grikes and their patterns will be strongly guided by the geological factors already outlined. However, there are situations where the solutional environment may initially

impose a pattern due to its own properties. Such may be the case where the rock surface is very immaturely karstified, possibly even devoid of pre-existing widened fissures, and there is a strongly acidic source of water directed across that surface. Dendritic solutional runnels result that will gradually cut through the rock, and become grikes. With time the rock properties influence locations for solution and the rectilinear pattern reflecting these rock characteristics develops after the dendritic one. Scar Close in Yorkshire, UK, shows this sequence (Figure 7).

#### Time

The whole issue of time is embedded in the discussions of geological and process influences on grike development. If the grike evolution process involves the total breakdown of the intervening



**Figure 12:** Trowbarrow Quarry, Arnside-Silverdale, UK. Interstratal palaeokarst from Late Carboniferous showing grike and kamenitza-like features on what is now a vertical quarry face, exposed in 20<sup>th</sup> century by quarrying.

clints, involving mechanical as well as solutional processes, then it permits much erosion and the development of very deep and wide, open gaps through the limestone. Widened features are given various local terms, including *bogaz* and *strugas*. Giant grikeland has already been considered. As time progresses what may be regarded as a perfect or typical karst landscape will decay due to a combination of processes. The question of when a particular landscape type is perfect or best expressed is a very challenging one. ‘Decay’

by mechanical processes of clear simple grike features is inevitable in well-fractured and well-bedded rocks. In less-fissured thick beds mechanical processes may also eventually become more important as solution dissects the rock. In many places however, the decay of one type of feature simply produces another feature, perhaps at a scale order larger.

The model from Goldie and Cox (2000) (see chapter 22) (Figure 13) summarizes many possibilities in the field of grike development. An im-

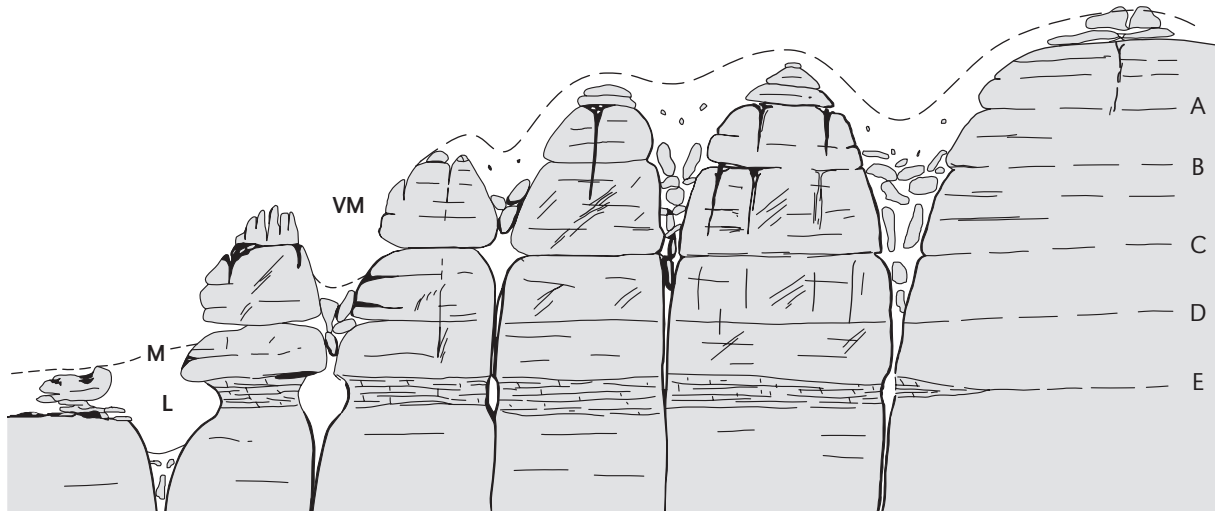


**Figure 13:** Goldie-Cox model. Sketch showing pavement-scar sequence indicating topography before glaciation. Factors affecting variety of topography after glaciation include depth of glacial scour and plucking, lithological variation including palaeokarst bedding plane features, interacting with the pre-glacial topography. Notional clint size ~1 m in columns. VM. very massive; M. massive; L. laminated; A-E. limestone bedding planes.

portant further point is the possibility that grikes and related features are not merely mature but relict from earlier periods altogether and re-activated at the present day. A palaeokarstic explanation of the large grike holes at Great Asby Scar, for instance, dated at the Late Carboniferous, is given by Vincent (1995). These palaeokarstic explanations accord with and relate to survival from glacial scour that must help account for some of the better-developed grikes in northern England. This is especially so since it is now thought that limestone solution rates in the Holocene in many parts of northern England have been much lower than assumed until very recently (Goldie, 2005). Thus many wide and deep grikes and related features could be Pre-Devensian, possibly much earlier, in origin. An example of probable Late-Carboniferous features is supplied by vertically bedded limestones at Trowbarrow Quarry, Arncliffe-Silverdale, UK. Here grikes and other karstic features are perpendicular to bedding (Figure 12) demonstrating that they must have been formed before tilting to their present position, which occurred in the Late Carboniferous.

## Morphometric work

It is valuable to discuss general morphometric work as it establishes a basis, or structure on which to fit specific cases. Goldie and Cox (2000) present data on clint width and length, and grike width and depth (Table 1). Clint width to clint length ratios have already been referred to regarding grike patterns (Figure 14). Only a moderate correlation between grike widths and depths was found, suggesting that vertical and horizontal developments of these features are not yoked. Variations between and within field sites were related to depth and date of glacial scour, rates of post-glacial solution, tectonic disturbance, and lithology, not necessarily in that order of importance. Human impact was identified as influencing present landforms both directly and indirectly. Surveyed grike widths vary over two orders of magnitude, from 1 cm to over 1 m. Outcrops sampled in Switzerland (Glattalp and Sanetsch) and NW England (Cumbria and Ingleborough) had relatively wide grikes, in spite of some of these areas being the most recently or severely ice-scoured. It is suggested that

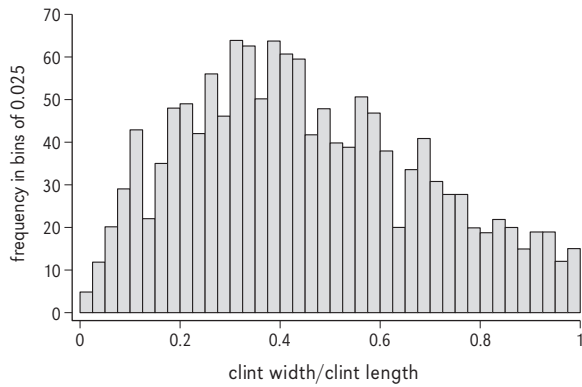


**Figure 14:** Frequency distribution of clint width/clint length for all areas.

wider grikes could have existed before glacial erosion and survived to develop greater width in the Holocene (Figure 13). The data for the whole population of over 1,400 showed 95 % of grike widths are below 30 cm, whilst the median is 13 cm. Grike depth data also showed a great range, varying 70-fold from 4 cm to 274 cm, with a median of 74 cm. These grike measures can be ambiguous. The four areas of the largest clints, Glattalp, Burren, Sanetsch, and Arainn, have very varied grike characteristics. Bed thickness needs examination, as an important factor influencing joint spacing and, if linked to strength, possible survival from glacial scour. Clint morphometry helps in understanding grike patterns, particularly the ratio of clint width to length which varies from just above 0 to exactly 1, which would be square. Photogenic clints that are squarish are often depicted in texts as typical and these would have a ratio close to 1. The data in Goldie and Cox actually indicates that this pattern is fairly uncommon, and that ratios of about 0.4 are the most frequent (Figure 14) although the least common clints are the extremely elongated, with ratios approaching zero. The dis-

**Table 1:** Grike widths and depths: summary statistics for each sample area (from Goldie and Cox, 2000). Measurements rounded to nearest cm. Columns show: n (sample size); p 25 (lower quartile); med: median; p 75 (upper quartile); max: maximum; range = max–min; iqr = p 75–p 25.

Grike widths	n	min	p 25	med	p 75	max	range	iqr
Sanetsch	100	5	12	15	20	140	135	9
Glattalp	29	10	20	28	30	80	70	10
Ingleborough	138	1	13	18	25	56	55	12
Malham	35	2	8	13	23	61	59	15
Wharfedale	70	1	10	15	23	76	75	13
Cumbria	250	2	10	16	20	140	138	10
Wales	85	1	7	10	17	46	45	10
Burren	510	1	10	13	17	71	70	7
Arainn	200	1	6	9	11	100	99	5
Grike depths								
Sanetsch	100	20	43	55	73	150	130	31
Glattalp	29	50	60	73	100	140	90	40
Ingleborough	138	5	71	99	132	244	239	61
Malham	35	38	66	84	96	244	206	30
Wharfedale	70	15	53	71	91	168	153	38
Cumbria	250	12	54	83	116	274	262	62
Wales	85	4	27	42	56	95	91	29
Burren	510	8	57	84	114	260	252	57
Arainn	200	9	38	58	81	157	148	43

ussion on geological influences earlier suggested that even where there is only one major joint direction there is meandering and oblique joining which limits clint elongation (e.g. The Clouds).

It is concluded that any discussion of grikes can extend very widely, involving many global karstlands, and a continuum with smaller and larger karst features. So definitions and dimensions are crucial. Grikes really are truly fundamental karst landscape features, a pre-condition for karst. Illustrative examples in the case study chapter (see chapter 22) more fully demonstrate some of the generalizations here.

Anikó ZSENI

The first classification of karren forms, which served as a basis for most of the later researchers and which discussed subsoil karren, was by Bögli. Bögli (1960a) classified karren types according to their genesis: *free karren* develop where the rock is bare, *half free karren* where the rock is partly covered and *covered karren* where the rock is covered by soil or dense vegetation. According to his scheme, free-karren are *Rillen-*, *Tritt-*, *Rinnen-*, *Mäander-*, *Wand-* and *Kluftkarren*, half-free karren are *Kamenitzas*, *Korrosionskehlen* and *Hohlkarren*, while covered karren are *kavernösen Karren*, *geologische Orgeln* and *Rundkarren*. Bögli (1951) had previously debated the genesis of *Rundkarren*. Bögli's classification and the German names he gave them have been adopted by most of the later researchers. Unfortunately, many additional terms have been added by other authors and some authors have used or translated Bögli's terms in a different sense to the original.

Bauer (1962) gave a detailed explanation of how the forms under soil develop. He claimed that the water penetrating through soil produces a basically different form than subaerial outflow does. He named forms under soil cover *soil-karren* (*Bodenkarren*).

Jennings (1971, 1985) also differentiated between partly or totally soil-covered conditions. He translated Bögli's terms as follows. Partly-covered karren include: *solution pans* (*Kamenitzas*),

*undercut solution runnels* (*Hohlkarren*), *solution notches* (*Korrosionskehlen*), and he also described *swamp slots* (an extreme form of *Korrosionskehlen*). Covered karren include: *rounded solution runnels* (*Rundkarren*), *cavernous subsoil weathering* (*kavernöse Karren*) and *solution pipes* (*geologische Orgeln*).

Gams (1976) classified subsoil karren as follows: 1. *subsoil rundkarren*, 2. *subsoil niches*, 3. *covered bogaz* (*subsoil bogaz*), 4. *subsoil cavernous karren or subsoil tubes* (*rock holes*), 5. *covered solution pans* (*subsoil kamenitzas*, *covered kamenitzas*), 6. *subsoil (covered) wells*, 7. *covered dolines* and 8. *filled pits*. He used the term subcutaneous karst as the synonym of subsoil karst. The term *subkutane Karren* was used in the speleological dictionary edited by Trimmel (1965) and means karren which develop or are being transformed under soil or vegetation layer. See also Williams (1983).

Sweeting (1972) describes the chief types of karren. Covered karren comprise *rundkarren*, karren formed by roots and soil (which she incorrectly termed *Deckenkarren*) and *hohlkarren*, while *solution basins* (*kamenitzas*) and *kluftkarren* (*grikes*) can be both free and covered.

Ford, Lundberg and Williams reviewed the nature and genesis of karren developed under soil cover and in open-air conditions (Ford and Lundberg, 1987; Ford and Williams, 1989). The



karren classification of Ford and Williams (1989) is based on morphology with subdivisions that incorporate genetic factors. Their main groups are circular plan forms, fracture controlled linear forms, hydrodynamically controlled linear forms and polygenetic forms. In some cases they gave the same name for the similar forms which can be found or can be developed both beneath soil and on bare rock (e.g.: solution pits, karren shafts or wells). In those cases I put a “subsoil” attribute before the name that they gave. Thus, they recognized the following subsoil forms: *subsoil pits*, *subsoil karren shafts or wells*, *cutters (subsoil grikes)*, *subsoil pinnacles*, *rundkarren (subsoil solution runnels)*, *pinnacle karst*, *ruiniform*. Soil also has an important effect in the genesis and formation of decantation or overspill forms: these are *decantation runnels* (“Wandkarren”; Bögli, 1960a) and *decantation flutings*.

A. Ginés (1995, 1996a) named karren features that developed on the bedrock surface beneath soil cover *subcutaneous karren* or *cryptolapiaz*. He listed *smooth and rounded rock surfaces*, *hollows*, *pits*, *tubes* and *pinnacles*.

Slabe (1999) distinguished rock forms (which are due to various factors acting on the surface of the rock) from karst forms (which are due to water percolation through fissured or porous rock). For rock forms that developed on karst surfaces covered by soil or sediment he used the term *subcutaneous*. According to their origin, *subcutaneous* rock forms are grouped as follows (Slabe, 1999): 1. a consequence of water flowing along the contact between rock and soil, in the form of *subcutaneous small and large channels* (*rundkarren*), *subcutaneous scallops*; 2. a consequence of the percolation of water through the soil, in the form of *subcutaneous small and large channels* (*rundkarren* and *kavernösen karren*), *subcutaneous small and large recesses*; 3. a consequence of an inflow of water to the surface of the soil surrounding the rock, in the form of *subcutaneous half-bells* and *subcutaneous notches*. Forms in group 1 and 2 develop under soil; forms in group 3 develop at and just below the ground surface.

## The role of soil cover in the evolution of karren features

There has been a lot of research in the international literature not only on the classification of subsoil forms but also on the soils on karst. Much of this deals with the role of soil cover in the evolution of limestone forms. Sweeting (1966, 1972) in her study about the solution process of limestone, assigned a great role to the soils and plants in the development and evolution of limestone pavements. Pigott (1962, 1970) also studied the connection between soil and evolution of forms occurring on limestone. Trudgill (1975, 1985) described the connection between morphology of karren and the different dissolution processes of subaerial and subsoil conditions. He emphasized the importance of soil reaction in the subsoil solution processes: cusped, arcuate and runnelled forms are only found under acid soils and if these forms are observed on bare rocks then soil loss has occurred (Trudgill, 1975, 1985, 1986; Trudgill and Inkpen, 1993). Experiments by Urushibara-Yoshino et al. (1999a) proved that the solution rates of limestone tablets in soils are several times higher than those in the air.

Jakucs P. (1956) considered the biogenic effects very important in the development of surface karst forms. He thought that the acid-secretion of plants and microorganisms in soil was the primary factor in the development of karren. Jakucs L. (1977) emphasized the common role of soil, climate and vegetation in the evolution of karst features. He proved that the rate of limestone solution mainly depends on the biological aggressivity of soil covering the limestone. So karst-corrosion is determined by the physical and chemical properties of soils, closely connected with microclimate (Jakucs, 1977).

Soil has an important role in the evolution of different karst features, such as types of karren (Figure 1). Briefly, the difference between forms which occur under a soil and those which developed in open-air conditions is that angular forms are produced directly by dissolution by rain and

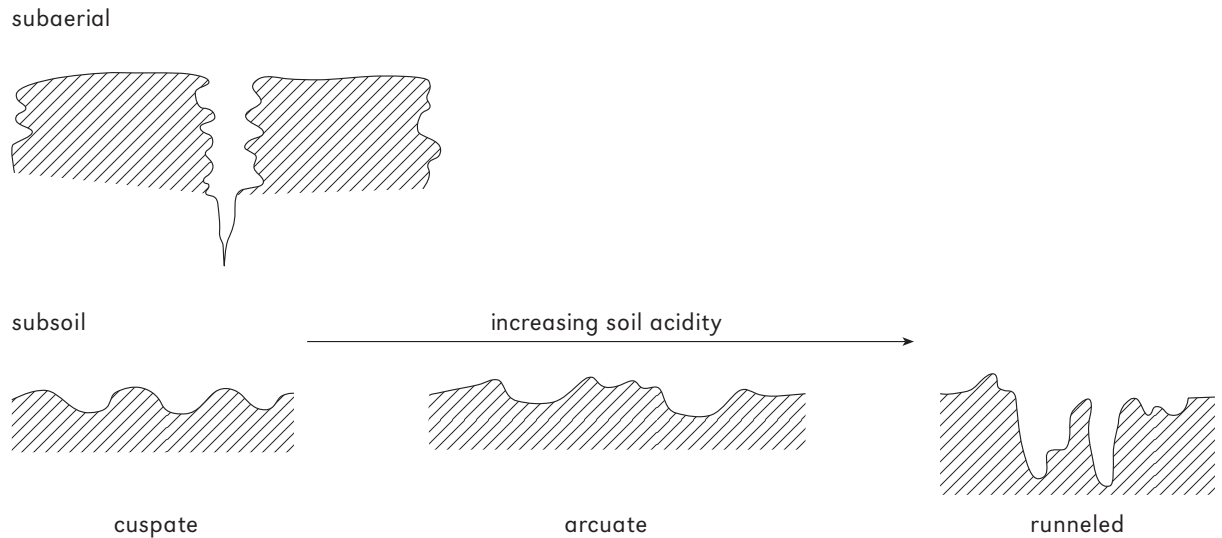


**Figure 1:** Subaerial and subsoil bedrock forms (after Trudgill, 1986, modified).

surface runoff, while rounded forms have formed under a soil or peat cover (Bögli, 1960a; Jennings, 1971; Sweeting, 1972; Trudgill, 1986).

Karren which develop in open-air conditions are fretted and sharp, having been subjected to much more selective corrosion. On bare rock surfaces rapid runoff occurs on sloping surfaces, whereas on flat surfaces or in basins water will be resident on the surface much longer. It can be said that a soil-free surface suffers only episodic dissolution by rainwater. However, in addition, rainwater has considerably less dissolution potential than acid soil water. Thus, under conditions of rapid, transient flow, where water depths are limited, only the rapidly soluble constituents of the rock will be removed. Forms will be related to dissolution kinetics and the overall chemical reactions will be rate limited (Trudgill, 1985; Ford and Lundberg, 1987). The main types of karren that form on bare surfaces are discussed in other chapters of this book. In addition, selective solution produces deep grikes and runnels and a rough pitted surface.

Due to the higher  $\text{CO}_2$  concentration and the longer time period of direct water-rock contact, the solution of limestone is more intense under

soil and the denudation rate of limestone is higher in the case of subsoil/subcutaneous karren than of subaerial, bare karren. In the case of subsoil solution, the  $\text{CO}_2$  dissolved by rainwater from the air is not the only factor. Billions of microorganisms live in the soils which cover the limestone. These microorganisms break down the organic matter (decomposition of organic waste, fallen foliage, animal remains, etc.) and produce  $\text{CO}_2$  and other acids from it. The macroflora produces  $\text{CO}_2$  directly through respiration of roots. The regularly renewed  $\text{CO}_2$  produced by micro- and macroflora changes the composition of soil-air, so the flora becomes, indirectly, the main factor of karst corrosion. In the case of temperate, mediterranean and tropical karst corrosion the most crucial source of the dissolving power of water is the  $\text{CO}_2$  originated from biogenic process in the soil (Jakucs, 1977). Although the main role is played by  $\text{CO}_2$ , various organic acids (fulvic, humic acids, formic acid, acetic acid, oxalic acid, lactic acid, propionic acid, humus, etc.) – originating from the bioactivity of soils – also take part in the dissolution of limestone. Jakucs (1977) declared that the dissolution of limestone or karstification is essentially a response by the bedrock to the phe-

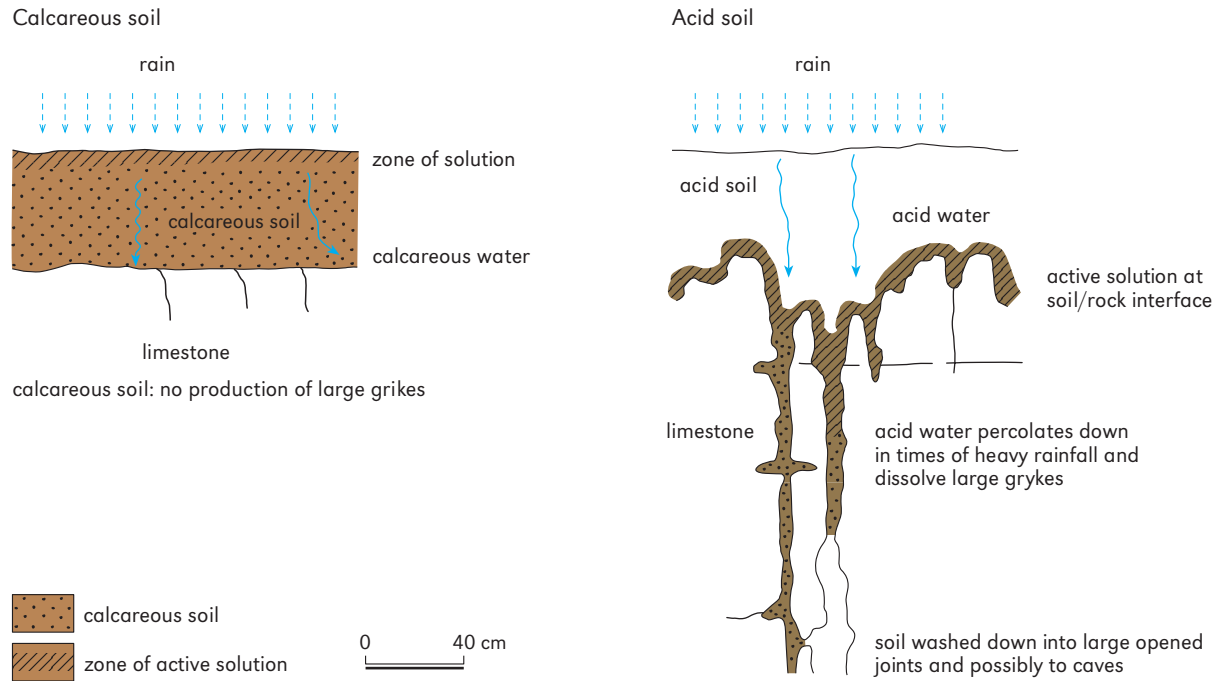


Figure 2: Weathering under acid and calcareous soils (after Trudgill, 1985, modified).

nomena of biological and chemical development of the paedosphere covering the rock.

The chemical production of acids in the soil is extremely climate-sensitive, as the biological activity of soil microorganisms is very sensitive to variations in temperature, soil-moisture, etc. So, in the case of soil-covered karst areas the intensity of limestone corrosion is determined indirectly by the climatic conditions of the area, through its effect on the paedo- and biosphere. That is why striking differences (in the order of a magnitude) and the very characteristic regional morphologic differences of the karst forms can be seen in different climate zones of the Earth. In the tropics, where both the rich vegetation cover and the microorganisms in the soil exhibit much more vigorous activity, the effect of the biogenic, subsoil formation is much higher (Jakucs, 1977).

So the surface karstic phenomenon and forms are mostly the results of processes initiated by subsoil biogenic corrosion and only in a smaller part by processes initiated by tectonics or erosion (Jakucs et al., 1983). And as almost every karst is

or has been a covered karst, we can assume that the bulk of karren was originally generated, developed and shaped when the bedrock was still buried below soil cover (A. Ginés, 1995) (see later section in this chapter on “Remnant subsoil forms inherited and transformed after soil removal”).

Under drift and soils, rock surfaces can be attacked from many directions, so smooth, rounded, rannelled and pinnaced forms may be found frequently with etched surfaces and comparatively shallow incision of the bedrock. Subsoil attack on tabular blocks from three sides may give rise to a pinnacle form. Arcuate and cusped forms also occur under acid soils.

According to Trudgill (1985), the role of a soil cover in karst evolution depends on the pH of soil. In general, calcareous soils with high pH (pH of 7 to 9, where calcium carbonate content is higher than 10%) protect the underlying limestone almost completely from erosion, because water becomes saturated with bicarbonate on passing through the soil profile. So the soil water arriving at soil-bedrock interface is incapable of dissolving



**Figure 3:** Tafoni-like features promoted under soil covering at the foot of a karren pinnacle. Llac karrenfield, Mallorca, Spain (photo by A. Ginés).

the bedrock (Williams, 1966; Trudgill, 1985). The existence of preserved glacial surfaces under drift and soils must be related to the calcareous cover. So there is a relationship between soil characteristics, especially pH and calcium carbonate content and the rate of bedrock erosion (Sweeting, 1966; Trudgill, 1986).

If the percolating water is not saturated, then solution will take place. Under acid soil limestone is extensively weathered. Erosion of limestone is most severe beneath deposits supporting an acid vegetation and with a pH between 4 and 7 and a calcium carbonate content less than 1% (Trudgill, 1985). The extensive weathering under acid soils leads to the formation of solutionally opened joints (grikes), and soil is often washed down into the larger grikes (Figure 2). This can result in the

lowering of the soil surface down the developing cleft, possibly also with soil loss into near surface cave systems. But surface wash induced by the felling of trees also causes erosion. So, for example, many *limestone pavements* could have been post-glacially covered more extensively with drifts and soils (Trudgill, 1985). The presence of smoothly eroded surfaces in many pavement areas supports this hypothesis (see chapter 9).

Soil moisture distribution, drainage rates, soil texture, soil depth, water-flow rates, slope, vegetation, and the nature of the limestone will all have a strong influence on the distribution of subsoil solutional erosion and resulting landforms.

The degree of erosion is commonly greater under deeper soils, which may reflect the increase in soil air carbon dioxide values with greater



**Figure 4:** Irregular subsoil sculpturing on exposed rundkarren. Hutton Roof Crag limestone pavement area, England, UK (photo by H. S. Goldie).

depth. There seems to be less erosion beneath soils on steep slopes than under those on flat or gently sloping ground. Soils on the steeper upslope sites tend to be thinner than those on flat ground; the top of the soil profile is often truncated and there is a higher rate of downslope removal of material. Hypothetically, a light textured soil should enhance leaching with a concomitant decrease in pH and increase in erosion, but this effect is masked by other factors (Trudgill, 1985). The nature of the limestone is important in determining the rate of its erosion beneath a soil. Hard, massive limestones do not break down easily and the soils above them tend to be easily leached. More friable rocks fragment more easily and become

incorporated in the soil, making it less acid. Softer rocks typically support a calcareous flora, while hard limestones may support a calcifuge vegetation, which has the effect of increasing the erosion rate (Trudgill, 1985).

Time is a factor that has great importance in determining whether or not soil characteristics will tend to encourage weathering or protect the rock beneath it (Trudgill, 1985).

### Subsoil forms

Grouping of subsoil karren forms is not easy, as similar forms have been given different names by



**Figure 5:** Cavernous zone at the foot of a karren pinnacle, Australia (photo by K. G. Grimes). Width of view is 5 m.

different people. As we can see at the beginning of this chapter, the researchers' approach to classification is also different. Some authors have used a variety of genetic classifications (e.g. Bögli, 1960a, 1978) while others have used descriptive or mixed classifications, and this has influenced their terminology. There is a tendency for gradations to occur both in the nature of the forms and in their sizes and orientations. Different people have put the boundaries at different points along those continua.

Also, it has not helped that the original terminology evolved in Europe before the tropical karren were well described. The different languages (and translations) also increase the confusion. Despite the above mentioned difficulties, a classification of subsoil karren has been created. Table 1 gives us an overview of the different subsoil karren forms, including the mostly used synonyms as well.

### Irregular subsoil sculpturing – the kavernösen Karren of Bögli

#### CAVERNOUS KARREN

Cavernous features are openings generally of a small size bored into the rocks. They are complex of irregular, randomly shaped, inter-connecting cavities intricately perforating the rock (look like a “spongework”) (Bögli, 1960a, 1978). The size of the cavities is from a few centimetres to more than a metre across. Cavernous weathering is not always the result of subsoil corrosion, but frequently some tafoni-like features are clearly promoted under soil covering (Figure 3).

There is a lot of overlap in the usage, by different authors, of the terms *honeycomb*, *boneyard*, *cavernous weathering*, *cavernous karren* and *root-karren*. They are all deep, irregular sculpturing of the rock (Figure 4), caused by a soggy material in

**Table 1:** Classification of subsoil karren.

1. Irregular subsoil sculpturing (the kavernoösen Karren of Bögli)	2. Horizontal notches at or just below the ground surface	3. Pits and vertical pipes/shafts (the geologischen Orgeln of Bögli)	4. Linear subsoil channels (the Rundkarren and Hohlkarren of Bögli)	5. Pinnacles and cutters, covered bogaz
<p><b>1.1. Cavernous karren</b> variations/synonyms: honeycomb, boneyard, cavernous weathering, subsoil cavernous karren, rock holes, subsoil hollows, subsoil tubes, root-karren</p> <p><b>1.2. Subsoil scallops</b> variations/synonyms: subcutaneous scallops, smooth undulating surfaces</p>	<p><b>2.1. Subsoil notches</b> variations/synonyms: small subsoil notches, smaller subcutaneous notches (= subsoil niches), large subsoil notches, larger sub-cutaneous notches</p> <p><b>2.2. Subsoil half-bells</b> subcutaneous half-bells</p>	<p><b>3.1. Solution pits</b> variations/synonyms: subsoil pits, subcutaneous recesses, tapering hollows, covered solution pans</p> <p><b>3.2. Karren wells</b> synonym: subsoil (= covered) wells</p> <p><b>3.3. Karren shafts and solution pipes</b> synonyms: filled pits, deep subcutaneous recesses</p>	<p><b>4.1. Rundkarren</b> variations/synonyms: rounded runnels, Hohlkarren (= undercut solution runnels), large subcutaneous channels, small subcutaneous channels</p> <p><b>4.2. Decantation or overspill forms</b> decantation runnels variations: soil-fed wandkarren, soil-fed meanderkarren</p>	<p>variations: cutters, subsoil pinnacles, covered bogaz, ruiniforms</p>

contact with limestone, with irregular concentrations of activity related to roots, or other localized flow and owing to its biological or chemical effects upon the rock surfaces.

On a scale greater than the tiny cavernous weathering, subsoil cavernous karren (subsoil tubes and rock holes included) have round cross-sections (Gams, 1976) and they run in all directions (Figure 5). Their development usually follows a joint or fissure.

Slabe (1999) used the name *subcutaneous tubes* for small irregular karst cavities, which appear filled with sediment or soil. They develop mainly in distinctly fissured rock: the initially small tubes filled with soil are widened by dissolution. The vegetation often has an important effect in their formation. Smaller ones are 1-10 cm in diameter, larger ones can be up to 1 m.

Root-karren (*root grooves*) in the strict sense of etchings that show the shape of the causative root are not often recognizable as such (e.g. see plate 3.4 of Bögli, 1978). These are formed under compact soil where roots etch into the limestone surface, or penetrate along joints (Jakucs, 1977). The evolution of these subsoil corrosion channels is helped by the root-acids of greater plants and the intense CO<sub>2</sub> production of microorganisms surrounding the root system. The roots penetrating

into the initially fine cracks in the rock eventually enlarge these into a spongework of wider, meandering and branching dissolution channels, which are usually round or oval in cross section. These grade to cavernous karren, and the term “*root lapies*” has been used in a broader sense to include those forms (Jakucs, 1977).

**SUBSOIL SCALLOPS**

*Subsoil scallops* (subcutaneous scallops, after Slabe, 1999) are scallop- or ripple-like forms, 15-50 cm in wavelength and shallow, but mostly deeper on the upper side (Figure 6). Because of subsoil origin they have smooth walls. They are found on steep to overhanging rock surfaces surrounded by soil or sediment and observed following distinct fissures along which soil-filled cracks develop. They are usually linked in a network. According to Slabe (1999) subcutaneous scallops develop on a relatively permeable contact between the rock and the sediment when there is simultaneous water flow along both the contact and through the soil and sediment.

*Smooth undulating surfaces* are also common features under soil, showing a larger and irregular wavelength than subcutaneous scallops and giving a characteristic rounded pattern to the walls of clefts, cutters and solution pipes.

## Horizontal notches at or just below the ground surface – the Korrosionskehlen of Bögli

### SUBSOIL NOTCHES

*Small subsoil notches* (smaller subcutaneous notches, after Slabe, 1999) are shaped as semicircular horizontal channels. They are 10–20 cm in diameter and their upper edge is sharper while the lower is rounded. *Large subsoil notches* (larger subcutaneous notches, after Slabe, 1999) are indented 1 m or more into the limestone and can be up to 1 m high. They develop due to the corrosion of limestone in contact with the soil at or near a stable ground surface (Figure 7). Smaller semicircular notches appear first and then they grow larger with the slow lowering of the level of soil or sediment. They occur when more water flows to the soil-limestone contact area than can immediately be conducted away and therefore the solution of limestone is more rapid and stronger in this area.

The lower part of subsoil notches is undercut, smooth and rounded because here the solution is stronger and lasts longer. The bottom of the notch is horizontal. The upper part descends toward the

bottom in a semicircular fashion and usually is reshaped by the dissolving effect of rainwater.

The term “subsoil niche” (Gams, 1971, 1976) may refer to Slabe’s small subcutaneous notches. A subsoil niche is a horizontal recess, which is usually many times wider than deep and its depth into the rock face is usually less than 10 cm. They can be found in unbedded or thick bedded limestone. Their cross section is irregular. On vertical rock walls they are more open and semicylindrical, while on inclined wall they are rather like a furrow. Similar forms can be found in caves filled or formerly filled with loam or clay.

Note that the forms described here are quite distinct from notches that form by the preferential solution of rock along horizontal bedding planes: these latter are narrower and relatively deep in relation to their height.

### SUBSOIL HALF-BELLS

*Subsoil half-bells* (subcutaneous half-bells, after Slabe, 1999) develop under vertical subaerial channels from which large amounts of water enter the sediments or soils at a localized point (Figure 8). Just as in the case of subsoil notches, subsoil half-bells occur when more water flows into



**Figure 6:** Subsoil scallops exposed in an excavation. Chillagoe, northeast Queensland, Australia (photo by K. G. Grimes). Width of view is 100 cm.



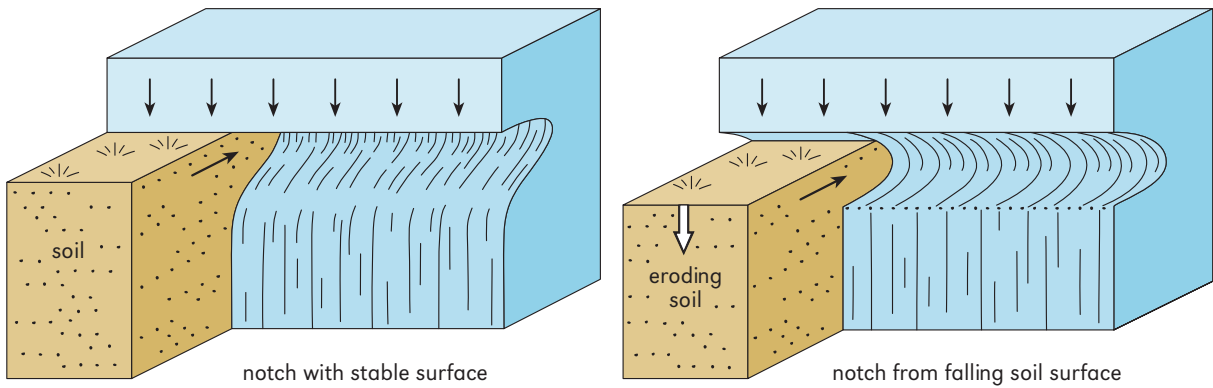


**Figure 7:** Subsoil notches. Solid arrows indicate water flow, open arrow indicates a dropping soil surface (drawing by K. G. Grimes).

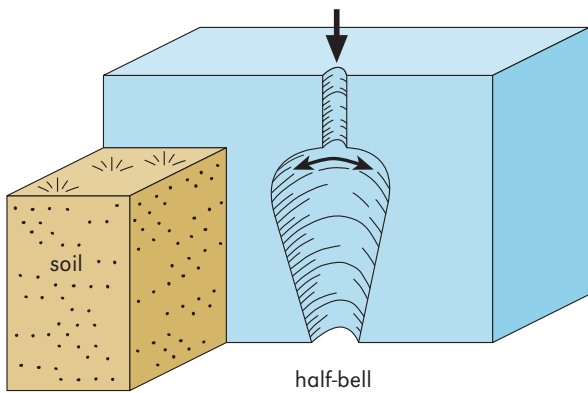


**Figure 8:** Subsoil half-bell (drawing by K. G. Grimes).

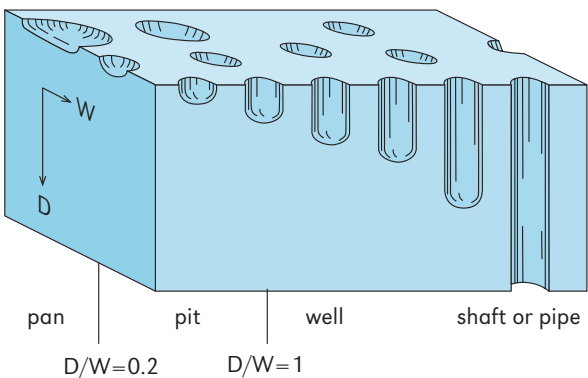


**Figure 9:** Distinction between pan, pit, well and shaft or pipe, based on depth to width ratio (drawing by K. G. Grimes).

the limestone contact zone than can be conducted away, therefore intensive solution can take place. Their shape and size is controlled by the amount and solution power of the water that reaches the soil, the permeability of the soil-limestone contact zone and the rate of the soil lowering.

The walls of the subsoil half-bells from which soil has recently removed can be criss-crossed by subsoil recesses (i.e. small rundkarren).

### Pits and vertical wells, shafts and pipes – the geologischen Orgeln of Bögli

To make a distinction between pits, wells, pipes and shafts we use the ratio of depth to width ( $D/W$ ) rather than the absolute depth (Figure 9). “Pits” are shallow holes with a  $D/W \leq 1$  (they are wider than their depth). “Wells” are vertical holes with a  $D/W$  between 1 and 2. “Shafts” or “pipes” (we use them as synonyms) are deeper vertical holes with a  $D/W > 2$ . In that  $D/W$  scheme a pan has very low  $D/W (< 0.2)$ . For inclined and horizontal pipes we suggest using “tube”.

#### SOLUTION PITS

*Subsoil solution pits* are shallow circular, semicircular, oval, rectangular or irregular plan forms with rounded edges and rounded or tapering floors (in contrast to *solution pans* – which are sub-

aerial forms and have a flat bottom). Smaller ones are 1–5 cm in diameter, larger ones are up to 1 m (with a  $D/W \leq 1$ ). According to Ford and Williams (1989) they occur both on bare rocks and under soil cover (see chapter 15). Slabe (1999) included solution pits in his “subcutaneous recesses”, along with deeper solution pipes. He suggested that they developed under a thin soil layer due to the percolation of water through the soil to the rock.

Their formation begins on little spots on the rock under soil and the solution power of the water percolating through the soil enlarges them. A lot of them, located along small joints, taper down into them; others have developed at a cluster of primary pores or a vug. They are often side by side or already connected.

Rundkarren (subcutaneous channels) often lead from the larger solution pits. Many subcutaneous forms can develop from the initial pits. On flat surfaces solution pans can develop from the more rounded pits when the rock is denuded, so there are several intermediate stages of forms. Gams (1976) described covered solution pans (subsoil pans, subsoil kamenitzas, covered kamenitzas), which hold stagnant water after the soil has been stripped off. Subsoil pans have more oval and elongated form than surface kamenitzas and lack the flat bottom.

Wider solution pits can also evolve into either vertical soil-filled wells, shafts or into an irregular spongework (cavernous karren).

#### KARREN WELLS

*Karren wells* (Ford and Williams, 1989) are short (usually few centimetres to 2–3 m) vertical or inclined caves draining into the epikarst, with a  $D/W = 1-2$ . Longer versions are called solution pipes or shafts. Their cross section is often circular, elliptical or funnel-shaped. Their formation is initiated by joints, calcite veins, fissures or bedding planes: they can develop from proto-caves or from pits and pans where the floor of the former features intersects bedding planes. They can be very complex and variable if developed under deep, periodically saturated soil cover where dis-



**Figure 10:** Sections of karren shafts, tubes and solution pipes exposed in a marble quarry at Wombeyan, New South Wales, Australia (photo by K. G. Grimes). Width of view is 5 m.

solution is intense, because the dominant condition is epikarstic. They can grade to a “boneyard” or “spongework” morphology. Gams (1976) called them subsoil (covered) wells.

#### KARREN SHAFTS AND/OR SOLUTION PIPES

*Karren shafts* are vertical, cylindrical holes developed by vertical dissolution processes (they are similar to karren wells, but karren shafts and solution pipes are deeper, with a  $D/W > 2$ ). Downward water flow can occur along the intersection of joints or where the bedding plane is dipping steeply, or water moving vertically down through porous limestone can be concentrated into localised paths that form a field of solution pipes (Lundberg and Taggart, 1995). They can be as much as 20 m



**Figure 11:** Exposed rundkarren. Great Asby Scar limestone pavement area, England, UK (photo by H. S. Goldie).

in depth, filled with soil, loam, clay, sand, gravel, rubble, etc. Where open pipes are seen, this represents loss of an earlier fill. They are often excavated on walls of quarries (Figure 10). If the filling is allochthonous, the pipe (as a rocky form) seems to be fossil. They are most common in porous limestone (see chapter 42). Gams (1976) called them filled pits. Slabe (1999) called them deep subcutaneous recesses. These features constitute the transition between the deeper karren and the epikarst.

### Linear subsoil channels – the Rundkarren and Hohlkarren of Bögli

#### RUNDKARREN

Rundkarren are solution runnels which are formed under soil or acid till, moss, vegetation, humus or litter cover (Sweeting, 1972; Ford and

Lundberg, 1987; Ford and Williams, 1989). They have rounded cross sections and smooth surfaces (Figure 11). They are similar to rinnenkarren (see chapter 17), as both are Hortonian channels, heading where sheetflow or wash on a slope breaks down into linear threads and, as they gain discharge downstream, they normally widen and deepen downstream. Both of them develop on most carbonate rocks, but are best formed on homogeneous and medium- to fine-grained carbonate rocks. They also develop well on gypsum, basalt, granite and sandstones but are not known on salt. The main difference is that rinnenkarren develop on bare slopes and have sharp rims and flat or rounded bottoms.

The width of rundkarren can vary from 2-50 cm, their depth is up to 50 cm or more and their length is from a few centimetres to over 10 m. The size of rundkarren is usually related to time: the

longer the period of soil-covering the deeper the runnel. But it also depends on the power of solution processes under the soil.

They are basically drainage features and are related to the slope and dip of the rock. On steeper slopes they tend to run parallel (Slabe, 1999). On gentle slopes or flat surfaces their development is usually orientated towards pre-existing solutional openings along major joints: they often have dendritic confluence or centripetal orientation into a karren shaft or grike (Figure 12).

Slabe (1999) used the term “subcutaneous channels” for vertical (or sometimes horizontal or inclined) channels of various sizes, usually with semicircular cross-section, which develop where water flow is concentrated along the contact between the wall and the sediment that covers the rock and fills the cracks along vertical fissures. The size and shape of the channels are dictated primarily by the permeability of the contact with

the soil and the quantity of water flowing over the contact, along with the composition of the rock.

Slabe (1999) distinguished between large and small subcutaneous channels. Large channels develop when larger quantities of water flow continuously along the permeable contact with the rock. They have diameters from 20-100 cm or more. Their width can fluctuate along their length.

Small channels are 5-20 cm in diameter and they are equally wide along the entire length or wider at the contact with other channels. These are the more typical rundkarren. They criss-cross the vertical or sloping wall at various angles, can be linked in a network and can have winding shapes. Less permeable the contact is the more winding channels develop. The most windings channels are 1-5 cm in diameter. Small channels can occur on the walls of larger channels. Vertical subcutaneous channels are common in stone forests.

Hohlkarren furrows are an accentuated vari-



**Figure 12:** Subsoil rundkarren exposed by soil stripping adjacent to a cliff. Border Rivers karst region, southeast Queensland, Australia (photo by K. G. Grimes). Width of view is 1 m.

ety of rundkarren formed under an acidic peat or humus cover (Bögli, 1960a; Sweeting, 1972). They are rounded and smooth – similar to rundkarren – but tend to have broader troughs and more undercut sides. They are 0.6-1 m in depth, about 50 cm wide and can be several metres long. Jennings (1985) called them “undercut solution runnels”.

#### DECANTATION OR OVERSPILL FORMS

Decantation or overspill forms are classes proposed by Ford and Lundberg (1987) and include “halbfrei” or “partly covered” karren of previous classifications (Bögli, 1960a; Sweeting, 1972; Jennings, 1971).

Mostly they occur upon bare and partly covered surfaces but can also form beneath soil. The common feature of these forms is that the solvent is supplied as an overspill from an upslope store. This store can be soil, moss, humus, snow bank, etc., retained in a depression and overflowing to form decantation runnels on the adjoining bare surface (wandkarren on steep slopes, meanderkar-

ren on gentle slopes) (Ford and Williams, 1989). Because they do not collect additional acidic water downslope, away from the source, the size of the channels reduce downslope. Decantation runnels occur where overspill is at a point.

The dimensions of runnels are in proportion to the volume and acidity of water. Generally runnels have 1-10 cm in widths and depths and up to 10 m in length. They are usually sharp-edged as they form subaerially.

#### Pinnacles and cutters, covered bogaz and ruiniforms

Pinnacles are residual forms. Dissolution beneath deep and acid soil, or over a long time enlarges grikes (kluftkarren; see chapter 9). These become much widened at the top and taper with depth to form *cutters* (a North American term) (Figure 13). Simultaneously, intervening clint tops are cut back by subsoil runnels to form subsoil pinnacles:



**Figure 13:** Cutters (subsoil kluftkarren) exposed in a quarry. Wombeyan, New South Wales, Australia (photo by K. G. Grimes). Width of view is 7 m.

peaks with rounded runnel incuts (Ford and Lundberg, 1987; Ford and Williams, 1989) (Figures 14, 15). They appear to form best in very thick bedded to massive strata with well-spaced joints. The pyramidal forms cannot easily retain soil and because of soil erosion their tops often become exposed. Then they become sharpened by subaerial karren forms (see next section on “Remnant subsoil forms inherited and transformed after soil removal”). Pinnacles can be several metres in height. As their development needs a long time they are common in the humid tropics and rare in recently glaciated areas. The best known pinnacle karst is the “Stone Forest” in Yunnan, China (see chapters 35, 36).

Bogaz are also a type of kluftkarren: a more complex and larger scale corridor landform than grikes. Covered bogaz (or subsoil bogaz) (Gams, 1976) are corridor-like features, which can develop by widening of joints, fissures, fault zones and zones of fractured limestone. They are 2–4 m in width and up to 5 m or more in depth. They are more frequent in thick bedded or massive limestone. After soil erosion, covered bogaz can be transformed into surface bogaz. Most surface bogaz occur on inclined slopes where soil erosion is faster.

Ruiniforms were first described by Perna and Sauro (1978). They are terrains where soil has been removed from very deep and wide grikes but

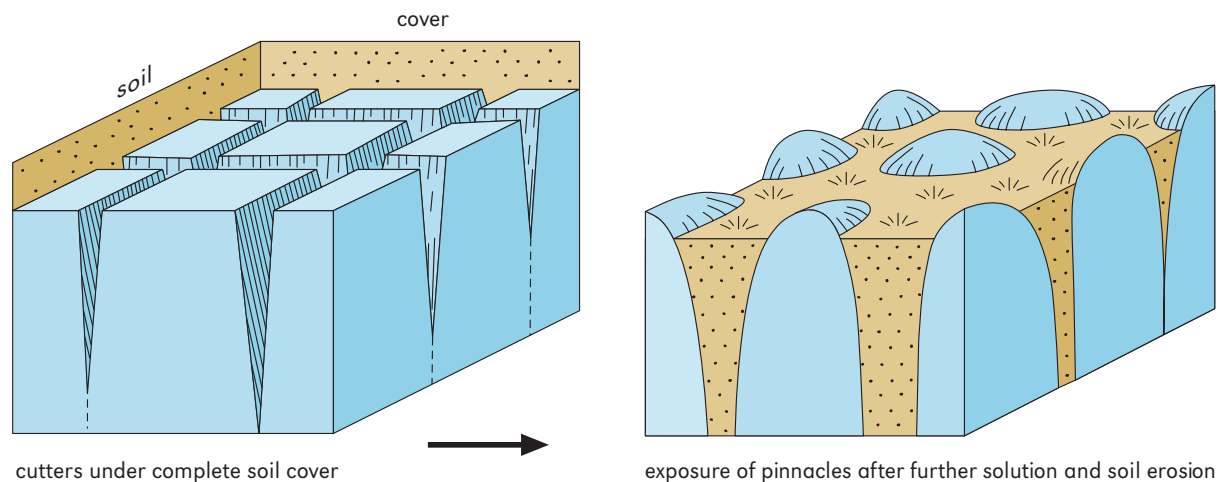


**Figure 14:** Cutters and pinnacles form by progressive subsoil enlargement of vertical joints (drawing by K. G. Grimes).



**Figure 15:** Subsoil pinnacles being exposed by soil erosion at the edge of an old quarry. Face is about 5 m high. Quarry north of Railton, Tasmania, Australia (photo by K. G. Grimes).



**Figure 16:** Rillenkarrren growing over subsoil-inherited forms. Rillenkarrren with steps and horizontal solution ripples exposed by soil erosion. Border Rivers karst region, southeast Queensland, Australia (photo by K. G. Grimes).

where the clints are not sharpened into pinnacles but stand out like miniature city blocks in a ruined townscape (see chapter 38).

### **Remnant subsoil forms inherited and transformed after soil removal**

As we see, subsoil forms are characterized by smooth and rounded surfaces. After soil removal they are exposed to subaerial solution and mechanical and biological weathering (rain-water, algae, fungi, etc.), which reshapes their forms (Figure 16). The originally smooth surface be-

comes sharper, rough and serrated (Figure 17). Many karst sites of the world have gone through removal or qualitative/quantitative changes of soil cover and vegetation. Deforestation also enhances soil erosion. Conversely, bare surfaces can be colonized by vegetation and covered by soil or till deposits in glaciated areas. The alternation of buried and bare stages during their life causes the mixed origin of many karren forms. Sometimes a clear distinction between bare and covered karst forms is very difficult to make or even impossible.

A. Ginés (1995) in his two-stages-model of karren development assumed that beneath natural vegetation and soil cover an intense growth of



**Figure 17:** Sharp break between smooth subsoil surface and sharp rillenkarren above. Molong, New South Wales, Australia (photo by K. G. Grimes).

subsoil karren is produced. His model, based in Jakucs (1977), attributes great importance to the loss of soil. After soil removal the former subsoil forms begin to be reshaped and transformed under subaerial conditions (rainfall, rapid runoff water, etc.). The soil loss usually results from ecological crisis (e.g. climate change) and anthropogenic effects: deforestation, change in cultivation, etc. A. Ginés' (1995) two-stages-model can be applied to most karren landscapes in warm and temperate climate.

If a limestone was covered by a calcareous soil and the dissolution power of the percolating water was weak, then after soil removal the remaining surface is smooth, plain with no or only a few subsoil karren forms (Figure 18). On the bare surfaces microkarren, rillenkarren, solution pans, trittkar-

ren and other subaerial karren forms appear. Morphometric analyses (e.g. width, depth, length of rillenkarren) can be used for dating the age of soil erosion or deforestation and for reconstruction of a palaeoenvironment (Ginés, 1996b).

If a limestone was covered by acid soil then more and many kinds of subsoil forms are exposed by soil removal. These begin to reshape. As an example, according to Sweeting (1972), the runnels of Hutton Roof limestone pavement in Britain, which are narrow, have rounded edges and deepen downslope just like a closely spaced, overdeepened rinnenkarren, were originally rundkarren which have been modified after soil removal.

Another good and spectacular example are the high columns (pinnacles) of stone forests. On the





**Figure 18:** Soil cover protects underlying limestone from solution at Great Asby Scar limestone pavement area, England, UK (photo by H. S. Goldie).

lower part of the columns, rounded subsoil surfaces and formations are predominant and these grade up to the more strongly reshaped, rougher and sharper upper part of the columns, which have been corroded by rainwater for a longer time (see chapters 35, 11).

### **Recent soil studies in England and Hungary**

To understand the evolution of different karstic features, especially types of karren, the investigation of soils on karst landforms is very impor-

tant. There are some interesting questions, e.g.: are there any connections between solutional power of soil (e.g. pH and carbonate content) and the depth, smoothness, and roundness of limestone forms? To answer this question soil samples were collected from limestone pavement areas of north England and on karrenfields of Aggtelek Karst and Villányi Mountain, Hungary (Zseni, 1999, 2002a, b; Zseni and Keveiné-Bárány, 2000; Zseni et al., 2003). Samples were from rundkarren, grikes and cavernous karren, representing different solutional and tectonic features of limestone. During the examination, the pH and carbonate content of the soils were determined and the connection between the soil characteristics and features of limestone was examined. Various solutional conditions, which result from soil variations, have produced a variety of forms.

Human influences have played an important role in the evolution of both Hungarian karrenfields. Previously the slopes were covered by sediment but intensive cultivation (viticulture) caused soil erosion, and increasing exposure of the limestone blocks. On the bare and thin-covered surfaces of limestone different solutional forms can be seen.

The comparison of the Hungarian and English soils results in the following:

- great differences can be found in soil pH associated with the different karst features in the English samples. However, in the Hungarian karrenfields, in spite of the similarly rich vari-

ety of karst features within short distances, the results show only minor differences in soil pH. Soils on both the Hungarian karrenfields seem to be rather homogeneous, while on the English limestone pavements not only the appearance of the limestone surface but even the soil pH can vary considerably within short distances;

- the results of the English measurements verify that the soils with lower pH are associated with deeper solution features, not surprisingly as their solvent power is greater than that of the soils with higher pH;
- the neutral and weakly basic pH-values of Hungarian soil samples came from deep and well-developed solutional forms. This suggests the almost complete protection of the underlying limestone from dissolution (although the carbonate contents are low). By reason of the present soil pH, these solutional forms in the Hungarian karrenfields either had to develop formerly (during the period of dense vegetation cover and more acid soil) or there are processes which can lower the pH occasionally or seasonally, so that solution can take place.

## Acknowledgements

The author thanks Helen S. Goldie and Ken G. Grimes for the photos and Ken G. Grimes for his very valuable suggestions and for making improvements to the English text.



Tadej SLABE and Hong LIU

Shapes created on karst surfaces covered by soil or sediment are called *subsoil rock forms*.

Soil or various types of sediment that completely or partially cover carbonate rock influence the shaping of the rock. Water flowing along the contact between the cover and the rock creates subsoil channels (Table 1) and subsoil scallops. We can distinguish tiny forms at the most permeable contact between rock and soil. These include finely dissected channels, small cups, steps, and small pendants. Water that percolates through the soil forms subsoil cups and solution pipes. When so much water flows down the rock to the soil or sediment that it can not all flow away rapidly between the rock face and the soil or sediment, it carves out half-bells and notches. Unique rock forms also occur due to the oscillation of the level of the water table.

In this chapter we distinguish the *subsoil dissection* of the rock that is mostly the consequence of the rock structure and its fissuring and stratification, that is, spots of weakness in the rock, from the subsoil rock forms created by the factors mentioned above.

Due to the relatively even dissolving of rock under soil and sediment, the *rock is rounded* as are the subsoil rock forms, and the *surface of the rock* is relatively smooth to the naked eye or characteristically rough on diversely-structured or recrystallized carbonate rock. Only the smallest

subsoil rock forms deviate from these characteristics. Under great magnification, the subsoil rock surface as a rule is distinctly finely rough due to the even corrosion of the grained rock (Slabe, 1994).

Subsoil rock forms were described by Bögli (1960a) as part of karren. Subsoil channels were introduced by Williams (1966). The importance and development of this type of shaping of rock was presented by Gams (1971) and Sweeting (1972). Jennings (1973) divides subsoil rock forms into those formed by the dissolving of partly covered or completely covered limestone. In the first group, he includes solution notches, and in the second, deep subsoil solution pipes. Nicod (1976) presents the subsoil shaping of rock in the Mediterranean. Subsoil scallops are described by Sauro (1976b). Subsoil rock forms, mostly channels, are graphically presented in the atlas of rock forms prepared by Perna and Sauro (1978). Bögli (1981) describes rock forms that occurred under the ground and calls them *rundkarren*. Fabre and Nicod (1982) amalgamate the knowledge on the subsoil shaping of rock. The importance of the shaping of rock under soil is defined by Trudgill (1985), who also describes subsoil cups (Trudgill, 1986). In his classification of karren, White (1988) singles out those which were covered by soil. Ford and Williams (1989) also describe *karren shafts* and *wells*, *solution pits*, and channels that occur

**Table 1:** Subsoil rock forms.

Subsoil rock forms			
Under soil and sediment			At the level of soil
Due to the percolation of water through soil	Due to the flowing of water along the contact	Due to the periodically flooded rock	Due to the water flow to the contact between rock and soil
	channels		
cups	flutes	notches	half-bells
	scallops		
	minute subsoil dissections of the rock		

under weathered debris. Karren formed by water flowing through the soil is also described by A. Ginés (1990). He names the karren formed under the ground *subsoil karren* (Ginés, 1996a) and also specifies some subsoil forms: tubes and cups. The importance of the subsoil shaping of rock is also emphasized by those studying the Lunan stone forest, who describe it as a form of covered karst: *sub-jacent* after Chen et al. (1986), *crypto karst* after Maire et al. (1991) and Sweeting (1995) and *subcutaneous* after Slabe (1999) and Knez and Slabe (2001a, b, 2002). The rock is often overgrown or criss-crossed by roots (Jakucs, 1977; Ollier, 1984). Traces of this kind are not directly classified as subsoil rock forms, but of course vegetation influences the formation of the described subsoil rock relief.

## Rock forms occurring due to the percolation of water through soil and sediment

### Subsoil cups

Under a thinner layer of porous soil that partly or entirely covers the rock, smaller and larger subsoil cups form on horizontal surfaces (Figure 1). The former are one to five centimetres in diameter and the latter are larger. They occur due to the percolation of water through the soil to the rock. As a rule, they form on weak spots in the rock. The water saturates the soil in the cups, as

a rule enlarging them outwards when the rock is covered by fine-grained sediment or soil. Their cross-sections are therefore circular or elliptical along fissures. Subsoil cups are often found side-by-side or already connected. Subsoil tubes can develop from subsoil cups, especially on fissured or porous rock.

If the rock becomes exposed, solution pans can also develop from subsoil cups found on horizontal surfaces. This development is illustrated by Gams (1971), who calls subsoil cups of this kind *covered kamenitzas*.

Special subsoil cups form under newly occurring weathered debris. As the exposed surface becomes overgrown, disintegrating vegetation piles up on the rock, retaining moisture and accelerating the corrosion of the rock. The cups are initially shallow and have gently sloping walls. Their diameters measure from a few centimetres up to many decimetres. Some have channels through which excess water drains away. On inclined surfaces, their upper parts are semicircular and wide, and they taper downwards. The cups also form under moss, lichen, or algae that cover the rock in places.

This section could also include subsoil channels formed due to the converging and flowing of the water that percolates through the soil. However, due to their characteristic formation, their description matches that of subsoil channels occurring due to the flowing of water at the contact of the rock and the soil.



**Figure 1:** Above subsoil cups in Lunan stone forest, and below a subsoil cup in south Atlas (Morocco), width of view is 4 m.

## Subsoil rock forms occurring due to the flowing of water along the contact between rock and soil or sediment

### Subsoil channels

Subsoil channels form due to the concentrated flow of water along the contact with the soil. As a rule, the largest channels form when the water runs down vertical or steep contact points. These large (Figure 2), usually vertical and separate channels have diameters from twenty centimetres to one metre and more. Along fissures, where the channels are most frequent, they are also deeper, and along the most pronounced, a *subsoil shaft* (well) can develop. The diameter of a channel can vary along its length. Deeper under soil and sediment, large channels frequently narrow. The rock therefore dissolves most rapidly in the upper sec-

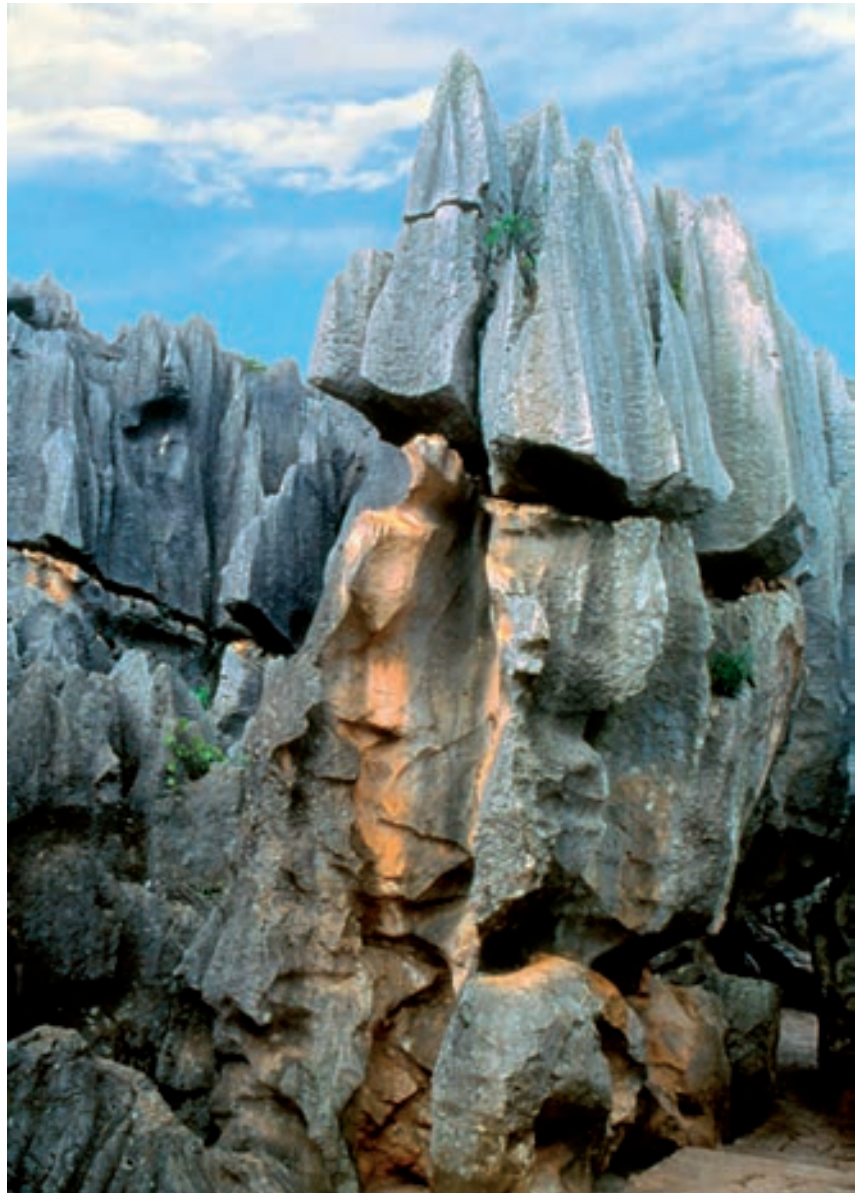
tion of soil and sediment. Distinctive and diverse channels are found in the Lunan stone forest. Song (1986) attributes the widening of subsoil channels to the mixing of water sliding along the contact and water penetrating through the soil. Smaller subsoil channels with diameters of five to twenty centimetres criss-cross the wall at various angles and are often sinuous. They are equally wide over their entire length or wider where they intersect other channels. They can be joined in a network. As a rule, the smallest channels, whose diameters reach only five centimetres, are the most sinuous. Their occurrence is most distinctly influenced as well by the structure and fissuring of the rock on which they form.

Subsoil channels form primarily through the moistening of the soil and sediment at a permeable contact with the rock and less often by distinctive smaller flows. This is indicated by their shape



Figure 2: Subsoil channels.

Figure 3: Subsoil channels.



and frequent dissection by horizontal notches. Smaller tubes with a diameter of up to one centimetre through which water flows often form at the bottom of channels between rock and clay. Along the contact with moist soil, the dissolving of rock is more distinct and of longer duration. Along with the composition and disintegration of the rock, the permeability of the contact with the soil and the quantity of water flowing along the contact largely dictate the size and shape of the channels. It appears that smaller and more meandering channels form along less permeable contacts.

The type of contact between the wall and the soil can differ in places or can change. Meandering small channels can therefore occur on the walls of larger channels (Figure 3). Along less permeable contacts, subsoil channels are larger at the level of the sediment and soil, while below it they quickly narrow. Gams (1997) identifies the link between the growth of subsoil hollows and the permeability of their filling. In the upper part immediately below the surface, such channels most often have funnel-shaped mouths whose diameter can exceed one metre.





Figure 4: Subsoil channels.

Subsoil channels also occur on limestone when the latter is in contact with flysch and on the walls of old roofless caves filled with sediment. When water runs on the contact through a narrow crack in the rock, the channel widens several dozen centimetres below the surface. Here and there, subsoil scallops also occur below narrow mouths.

On more or less gently sloping rock covered by soil, channels (Figure 4) with semicircular bottoms develop, being frequently described in the literature as *rundkarren* (Sweeting, 1972; Perna and Sauro, 1978) and *subsoil runnels* (Trudgill, 1985). These are the consequence of the joining of water percolating through the soil. On steep surfaces, they can be parallel (Williams, 1966), and we can talk about subsoil flutes since the water percolating through the soil flows evenly over the entire surface. On gently sloping rock surfaces,

they are joined in a branched network. Deeper channels can have smaller subsoil flutes on their walls. In the Lunan stone forest, unique channels with semicircular or upside-down omega-shaped cross-sections form at the bottom of cracks between rock pillars or teeth where fissures wedge out (Figure 5).

Special channels (Figure 6), called *hohlkarren* by Sweeting (1972), form when they are filled with soil or when their bottoms are covered and the rock around them is bare. In most cases, they have the characteristic shape of an upside-down Greek letter omega. They can have several stories. As the level of the soil dropped, it remained only on the bottom of the channels and thus deepened and widened them. Channels also lead from subsoil cups formed where water streams flow together. They often developed from subsoil tubes that were

**Figure 5:** Subsoil channels. Width of view is 1.5 m.



uncovered when the upper strata of rock disintegrated. These become subsoil channels from the moment the level of the soil surrounding the pillars drops lower than the channels. We can often trace the transition from channels formed on rock completely covered with soil to those where only the channels are covered. After uncovering, when they contain no more soil, they are transformed by rainwater. Subsoil channels start to reshape the rock, including the rain-created rock forms, when

formerly uncovered karst becomes overgrown again (Jennings, 1973). This is also characteristic of the Classic Karst region of Slovenia where weathered debris or a thick layer of moss is ever more distinctly covering the rock.

In the areas of locally flooded zones, above-sediment channels and anastomoses (Slabe, 1992) can occur. These are also characteristic of the lower planes of the basal, carbonate conglomerates in flysch (Figure 7).



**Figure 6:** Subsoil channels. Width of view is 3 m, in the middle.



**Figure 7:** Subsoil anastomoses. Width of view is 1.5 m.



Figure 8: Subsoil scallops.

### Subsoil scallops

Subsoil scallops (Figure 8) occur due to the flow of water along the entire-permeable contact of the rock with the soil. These are subsoil cups with diameters between fifteen and fifty centimetres connected in a network. They are shallow and most often a little deeper in their upper part. As a rule, they are found on overhanging rock surfaces. On distinctly overhanging surfaces, they can be arranged one above the other like fish scales (Figure 9). Their narrower lower parts protrude from the rock wall.

Subsoil scallops can be observed along distinct fissures where cracks filled with soil occur. They are also characteristic of overhanging walls of pillars in the stone forests. The circumference of subsoil notches is often dissected below the ground by subsoil scallops. In places, channels lead to the higher subsoil scallops that are larger in size.

As a rule, subsoil scallops do not form along distinct fissures that criss-cross walls or along bedding planes where semicircular channels develop instead.

Along-sediment cups are also frequent on the walls of caves filled with fine-grain sediment.

### Rock relief of subsoil karren that is periodically flooded

The peaks of subsoil karren (Figure 10) that are periodically reached by the water table and are entirely formed below the ground are sharp. Relatively smooth rock characteristic of formation beneath soil and fine-grained sediment dominates the upper part. Subsoil notches are most pronounced in the lower part of the karren. Larger horizontal notches reach up to one metre in diameter, and smaller ones are found one above the



**Figure 9:** Subsoil scallops. Width of view is 2.5 m.

other. Semi-panned notches are the conclusions of vertical subsoil channels that formed along the most conductive paths. The individual peaks of subsoil teeth above the most distinct notches are spongy. Subsoil channels on this karren can be divided into vertical and horizontal. The former are conductors of the oscillating water table along the most conductive paths. The latter, which criss-cross more sloping rock and larger rock surfaces, are further formed by the moisture that remains in them the longest after the lowering of the level of the water table. Similarly, along weaknesses in

the rock, most often minute fissures, subsoil cups form that in time can grow into tubes. Between the cups and channels, there are subsoil tubes criss-crossing the rock at various angles.

This type of formation of subsoil karren is illustrated by an experiment using plaster pillars that we covered with soil and then exposed to artificial rain. The water drained from the model at the bottom. The upper section of the pillars was shaped by the water that percolated through the soil in a dispersed fashion, while the lower part was shaped in a locally flooded zone. The outflow



Figure 10: Subsoil karren occasionally flooded.

of the water was too slow and the water therefore accumulated at the bottom part of the model.

To sum up, two dominant processes for the formation of this type of subsoil karren can be deduced from the shape of the karren and its rock relief. The rock forms that are the traces of frequent oscillation of the level of the water table that floods the karren from below give it a special stamp. When the water table is low, the karren is shaped by the water that periodically and dispersedly percolates from the surface through the soil and slides evenly down the rock. It remains longer in the subsoil cups and gently sloping channels and along the less permeable contact between the rock and the sediment surrounding it.

#### Minute subsoil dissection of rock

The walls of cracks through which water carries

soil but does not fill completely and dolines that are thinly covered with soil are often dissected by unique subsoil cups, while overhangs are dissected with ceiling pendants. On gently sloping sections in such conditions, the rock is dissected by steps. Subsoil cups (Figure 11) are semi-circular or oblong and arranged in steps. Their diameters measure between 0.5 and two centimetres. The largest are combinations of smaller ones. In all cases, the rock forms are connected in a network. Their formation and shape are primarily the consequence of the characteristics of the structure of the grained rock and the inclination of the wall along which the water slides. In such conditions even the less distinct channels that often form in cracks are minutely dissected with subsoil cups. It appears that the water sliding down the rock carries soil and deposits it at individual points in subsoil cups on vertical surfaces, on steps on gently sloping surfaces, and on pendants on over-



**Figure 11:** Subsoil cups. Width of view is 0.5 m.

hangs. Moist sediment in subsoil cups can corrode the rock more effectively since the water accumulates in the sediment and remains in it for a longer period. On inclined surfaces, the water deposits sediment on the most gently sloping sections. Old sediment protects them from corrosion, while the rock lying next to them corrodes more quickly and is therefore dissected into steps. On overhanging surfaces, the sediment collects on the pendants and protects them from dissolving.

### Subsoil tubes

The rock below the ground is often criss-crossed by tubes of various sizes, karst hollows that during their formation are filled with sediment or soil. They are of various size and shape. The larger ones

are dissected in the rock relief by above-sediment (Slabe, 1995a) and under-sediment channels.

Smaller tubes with diameters between one centimetre and one decimetre pierce the rock in various directions and are often connected into a system. Most form on distinctly fissured or porous rock, and vegetation often plays an important role in their formation.

### Rock forms that occur at the level of the soil or sediment

#### Subsoil notches

Subsoil notches form due to the corrosion of the rock along a long-lasting level of sediment or soil surrounding it. The water flows to the contact over



Figure 12: Subsoil notch.

a larger surface, more or less distinctly corrodes it, and then flows away between the rock and the soil. Smaller subsoil notches with diameters between ten and twenty centimetres have the shape of semi-circular horizontal channels, only with their upper edges most often being sharper and the lower edges more rounded. Larger (Figure 12) subsoil notches: *undercut notches* (Waltham, 1984; Ford et al. 1997), *solution notches* (Jennings, 1973), *swamp undercut* (Ollier, 1984) are corroded one metre or more into the rock, and in the Lunan stone forest they are frequently up to one metre high. The lower part of the notches is undercut. The rock was subject to faster, long-term dissolving below the moist ground and is therefore rounded and smooth. The lower section of the notch is horizontal, while the upper tapers out toward the lower in a semicircu-

lar fashion. The upper part of the notch is reshaped due to water sliding down the rock. Smaller semi-circular notches develop first and can then grow increasingly larger with the slow lowering of the level of sediment. The notches can be seen at various heights on rock that was rapidly and sporadically exposed. Smaller exposed notches are more reshaped by rainwater, and larger ones less distinctly so. The water that shapes them often flows between the rock and soil below them and creates subsoil channels or scallops.

The forms described above are distinguished from notches formed due to the often more rapid dissolving of rock along horizontal bedding planes. As a rule, the latter are narrower and very frequently relatively deep relative to the diameter of the opening.





**Figure 13:** Subsoil half-bell. Width of view is 5 m.

### Subsoil half-bells

Half-bells (Figure 13) form below channels that continuously bring larger quantities of water to the sediment or soil surrounding the rock. The contact is not conducive enough for all of the water that reaches it. There are large and distinct half-bells in the Lunan stone forests. Above the soil or sediment there are characteristic bell or

half-bell shapes whose shape and size are related to the quantity of water flowing to the soil, the permeability of the contact between the rock and soil, and the speed at which the level of the soil or sediment lowered. The upper part of a channel can also be a tube where it formed along a distinct fissure, while the wall is only corroded along the widenings. Immediately below the ground, the walls of large bells can be dissected by oblong sub-

soil scallops that reach up to one metre in diameter. Deeper under the ground, bell-like widenings often narrow gradually into subsoil channels.

## **Surface of subsoil rock forms**

If the rock is relatively evenly structured, the surface of subsoil rock forms is usually smooth. With the great magnification of a scanning electronic microscope, however, we can see that it is minutely dissected, the consequence of the faster dissolving of the rock at weak spots, that is, at the contact between the various particles that compose it. The smoothness or roughness of the rock is of course influenced by its composition and fracturedness. Slowly dissolving particles, which can protrude distinctly from the rock surface, remain on it (Slabe, 1994) even though they are subject to faster dissolving due to their larger exposed surfaces. Trudgill (1985) measured the roughness of rock

surfaces and on the basis of their porosity and the height of fossils and chert protruding from them determined the degree of the corrosion of the rock.

## **Conclusion**

The sediments and soils covering rock in layers of varying thickness have different structures. This influences their permeability and the permeability of the contact between them and the rock and the manner in which water flows through them and along the contact. The rock and its composition, stratification, and fracturedness determine the development of subsoil rock forms and their appearance and surface.

Subsoil rock forms are a distinct and indicative sign of the formation of rock sculpturing under the ground and often an important trace of the development of the karst surface and its use.



Franco CUCCHI

Kamenitzas are closed depressions that develop on karst surfaces exposed to the atmosphere. The presence of static water produces small, round, closed pans (Figure 1) that are shallow as compared with their depth.

Kamenitzas form on horizontal, or slightly inclined, undulating surfaces where water does not flow but collects into the small depressions. Their genesis is usually more controlled by micro-relief patterns rather than by discontinuity of surfaces.

The floors of kamenitzas are usually planar and horizontal but sometimes show minute irregularities and rough protuberances. Their walls are sub-vertical or slightly inward leaning and their

depth is always a fraction of their width. They are usually rounded in shape, with decimetre-scale plan dimension and centimetre-scale depth. Most have a diameter ranging between 4-5 cm and 1-2 m, even though some up to 6 m have been documented (Bryan, 1920). In a *palaeokarst* surface in the Upper Pennington formation limestone (Mississippian-latest Chesterian), Humbert and Driese (2001) found a “flat-floored kamenitza with a width of 7 m and a depth of only 0.5 m”. In other palaeokarst deposits, the Aran limestones in Scotland, Vincent found some “palaeopits”, remains of karst depressions (personal communication).

Their genesis has been widely discussed. Ac-



**Figure 1:** Perfectly round-shaped kamenitzas in Cretaceous micrites of the Classical Karst (left), width of view is 85 cm, and (right), width of view is 50 cm, in Cretaceous breccia of Kornat island (Croatia). In one of them the overflow channel favours the formation of notches.

According to the major theories, they could be either essentially chemical (Gavrilović, 1968; Forti, 1972) or essentially biochemical, and thus linked to the action of endolithic algae (Perna and Sauro, 1978). Some researchers are in favour of an exclusively corrosive origin and therefore take into consideration increases in growth or changes in shape, which are linked to *phytokarst* phenomena (Belloni, 1969; Belloni and Orombelli, 1970) or to the presence of dissolved deposits (Bögli, 1960a). Other researchers (Gams, 1974) differentiate two types of *kamenitzas*: those formed by means of subcutaneous corrosion on primary depressions, and those formed on bare carbonate surface, which might be related or not related to pre-existing subcutaneous depressions.

Some consider them semi-covered landforms, assuming their formation has already started while they are still covered by clods of earth or rock fragments. *Kamenitzas*, in fact, are often present on fairly smooth surfaces, whose present-day undulations are likely to have been inherited from covered karst conditions. Soil erosion and exhumation then leads to the development of *kamenitzas* and landforms of dynamic corrosion origin such as *rinnenkarren* and *rillenkarren*.

Even though the term *kamenitza* or (plural) *kamenitzas* – *kamenica*, *kamenice* and also *kaminitza* (the term seems to come from the wrong hypothesis according to which a small pebble – *kamen* in Serbo-Croat – left on a limestone surface led to the formation of a depression. Cvijić, 1924; Gavrilović, 1968) is now widely accepted, below are some corresponding terms used in different countries and languages (Rose and Vincent, 1986b):

- Brazilian, Portuguese: *marmite*;
- Czech and Slovak: *kamenice*;
- English: *solution cup* or *solution pan* (Zotov, 1941), *rock tank* (Bryan, 1920), *lapiés pot-hole*, *etched pothole* (Udden, 1925), *solution pit* (Wentworth, 1944), *solution pan* (Fry and Swineford, 1947), *corrosion basin*, *clint pool* (Sweeting, 1966), *rock pool* (Williams, 1966), *corrosion cup* and *solution basins* (Sweeting,

- 1972), *true solution pan* (Gams, 1974), *solution pan* (Ford and Williams, 1989);
- French: *lapiés à nid de poules* (Gèze, 1973);
- German: *Napfkarren* (Bögli, 1960a);
- Italian: *vaschette di corrosione*;
- Polish: *miseczka krasowa* or *kamenica*;
- Slovene: *škavnica* (also *kamenica*);
- Croatian term see Cvijić, 1924;
- Spanish (also Caribbean): *tinajitas* (Udden, 1925).

## Evolution, lithological and structural control

When the surface depression fills up during periods of rain, the rainwater lasts there until total evaporation occurs. The dimension of the pans (probably also linked to climatic conditions and to rainfall regime) almost always allows for their nearly total filling and sometimes for marginal overflow that form *effluent runnels* (Figure 2). In time, the water collecting inside the pan, becomes more aggressive on the pan walls rather than on its floor. The solute, in fact, accumulates on the pan floor due to its density and insoluble impurities and other material (mainly silt) caught in the depression “protect” the floor, thus decelerating the solution process. Moreover, carbon dioxide diffusion from the atmosphere rapidly decreases with depth, thus leading quickly to over-saturation. The depression walls are more subject to the water action because superficial water, still interacting with the atmosphere, replaces over-saturated and dense water, which seeps downwards, mixing with silt on the floor of the pan. This explains why *kamenitzas* tend to widen rather than to deepen (Figure 3).

Organic material or fine sediments that either float on the water or are transported by the wind can accumulate in the depression, inducing prolonged humidity and therefore corrosion on the bottom thus explaining the evolution of the typical undulating floor and other minute concave-cup depressions.



**Figure 2:** A kamenitza and pits of Gait Barrow, UK (photo P. Vincent).

The same result, often accompanied by limited furrows of parietal corrosion origin, can be linked to the phytokarst, and the biological activity of fungi, lichens, algae, etc. Crowther (1997) shows that individual *karren* possess distinctive roughness characteristics that seem to be attributable to differences in the (assumed) nature of water flow, i.e. greater turbulence inflow along rillenkarren and unstepped rinnenkarren produces rougher surfaces than those found on steps and stepped flats, and to the presence or absence of litter/humic soil fill within kamenitzas.

In this respect, it ought to be noted that kamenitzas act as “traps”, which can accumulate sediments either transported by the wind, or runoff water “captured” by the depression (Figures 4, 5, 6). The sediments can vary in origin, ranging

from rock fragments to twigs, from seeds and pollen, to decaying birds and small mammals.

The presence of such material on a damp surface can favour the formation of a kamenitza. Clayey deposits and organic accumulations (such as leaves and twigs, for instance) restrain water and induce some prolonged humidity in contact with the rock, thus leading to static corrosion phenomena.

Spillage water usually overflows and creates a *solution runnel* – also decantation runnel or overflow channel. At the outlet point, karst phenomena become dynamic, thus forming a furrow that, often, lowers rapidly, to the extent that it reaches the level of the kamenitza bottom. In this case, kamenitzas do not widen any longer, thus becoming accumulation cups, which feed karst furrows. As

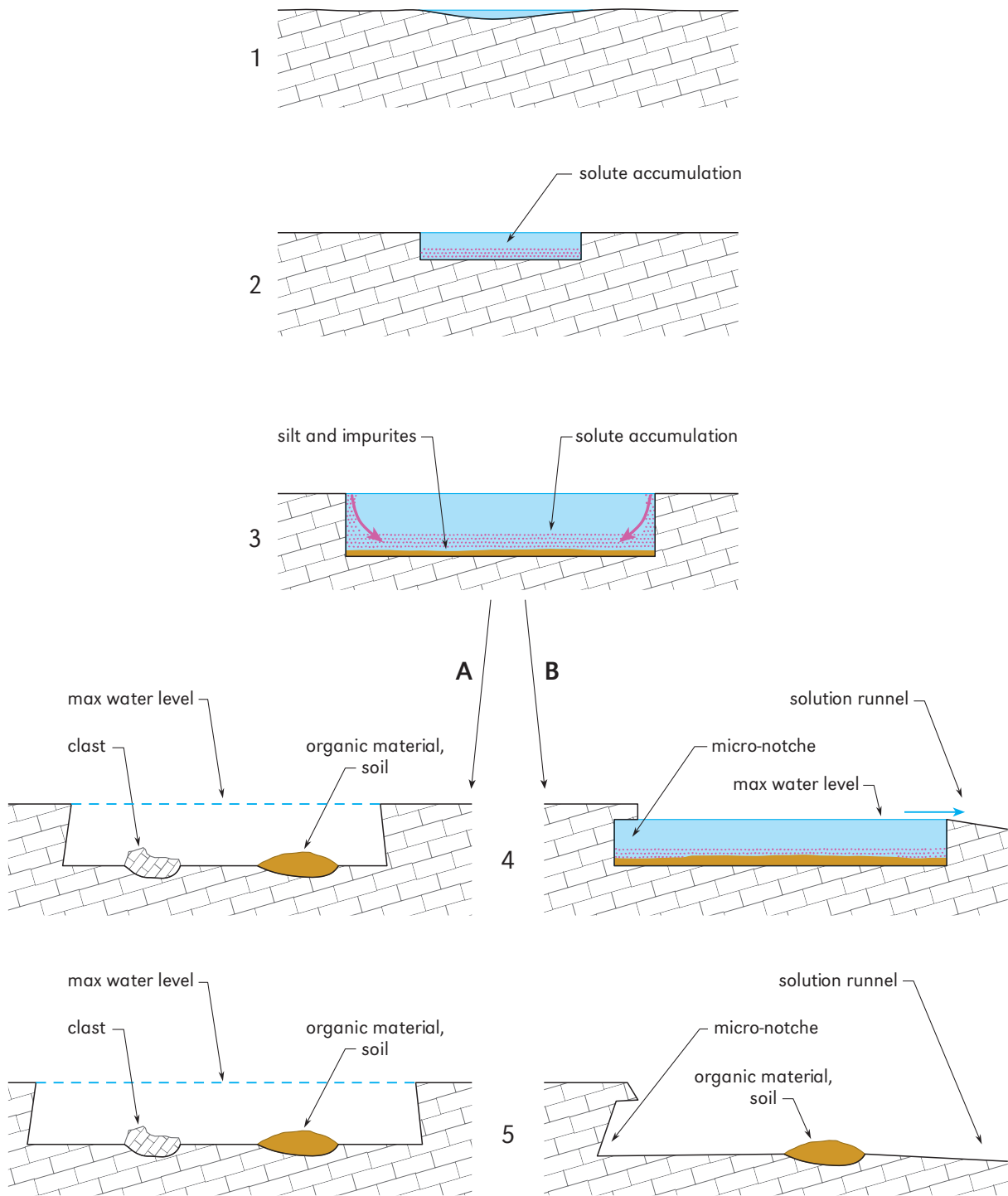


**Figure 3:** In the kamenitza the walls evolve more than the bottom because of solute and other materials accumulate on the floor. A. organic material, soil, clasts and biological activity induce a sort of subcutaneous corrosion on the bottom and cause undulating or minute depressions; B. micro-notches along the pan walls form when the solution runnel – the over flow channel – progressively deepens.



a



b



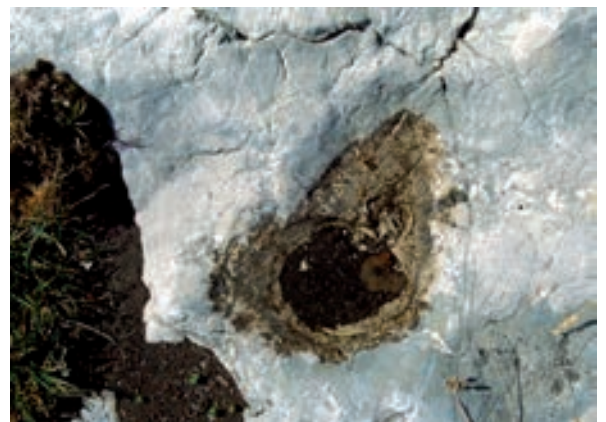
c



d



e



f

**Figure 4:** Kamenitzas of Classical Karst: a. filled by debris and soil; b. by "terra rossa"; c. by a small *Juniperus* plant; d. by foliage; e. by mosses (width of view is 65 cm); f. kamenitza of Fanes Natural Park (Dolomites, Italy) at 2,288 m a.s.l. partially filled by soil and polished by snow during winter (width of view is 70 cm).



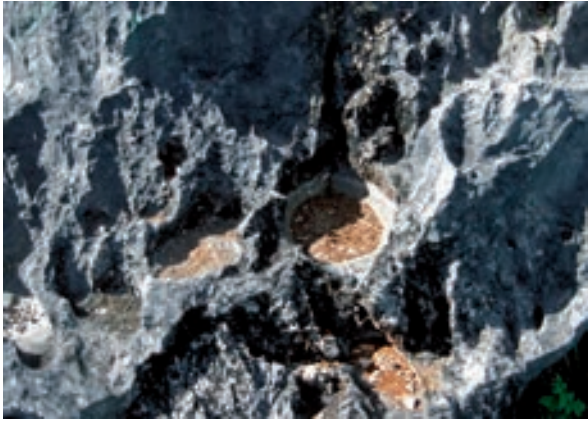


Figure 5: Kamenitzas of Viñales Park, Cuba.



Figure 6: Misczka krasowa filled by ice during winter occurred in Upper Jurassic limestone of Cracow-Czestochowa Upland, south Poland (photo A. Tyc).

the solution runnel deepens, the level of the water present in the depression progressively decreases and the walls tend therefore to overhang, because

the corrosion processes no longer affect the whole wall but only its wet parts. Sometimes real *micro-notches* form (Figures 2, 4b). This term is borrowed from a term used to describe the peculiar landforms that originate along the coast, at the sea level, due to bio-corrosion or bio-alteration of rocky walls.

A particular development characterizes the kamenitzas resting along the shoreline (Figure 7) as, beyond the “standard” ones, there are other factors coming into play, such as those linked to water swash, spray zone, mixing corrosion, the mix of salted waters, endo- or exolithic organisms and the intense biological activity (Perica et al., 2004). They may also be remarkable in size and are characterized by irregular and indented floors and rims, due to corrosion (dynamic, static and point corrosion) caused by water mixing, bio-karst phenomena and erosion caused by wave motion.

It is possible to recognize several phases in the development of kamenitzas: formation, development, degradation and disappearance (Figure 8).

The first phase consists in the corrosion caused by waters in the depressions following denudation. Corrosion continues and, during the second phase, lateral widening occurs, sometimes accompanied by outflow and/or runnel channels at the same level as the bottom of kamenitzas (Figures 3, 4a, 8). Therefore degradation occurs due to the widening of the outflow groove, and the kamenitza margin gradually lowers, thus becoming rounded. Finally, the kamenitza disappears due to the progressive overhanging of the walls and to the widening of the outflow channel (Figure 3). The development of kamenitzas can also stop when an open fracture is encountered during the development phase. The water, in fact, can widen it and then disappear in the infiltration point (Figure 2).

Experimental studies on the evolution rate of kamenitzas are scarce. Sweeting (1966) observed on an experimental site in northern England an increase in depth up to 3–5 cm within less than ten years. It should be noted that such rates are exceptional. Zotov (1941) hypothesized that solution



**Figure 7:** Kamenitzas along the shorelines of the La Habana, Cuba, harbour (left) and of the Mali Lošinj island, Croatia (right).



**Figure 8:** Elongated kamenitza characterized by complex evolution. The original elongated form first evolved into a form with a drainage channel that originated lateral notches and karren runnels. It deepened afterwards at its centre. At present, it also features two round sub-depressions (similar to corrosion cups) favoured by sediments and organic material.

cups would be completely destroyed in a few thousand years. Rose and Vincent (1986b) estimated that the time required by a kamenitza to form and reach a depth of 10 cm and a radius of 20 cm was approximately 3,260 years.

Measurements in the Classical Karst (Cucchi et al., 1987, 1990) proved that the floor of a kamenitza has a lowering rate of approximately 0.02–0.03 mm/year: a 4–5 cm deep kamenitza would need at least 2,500 years to be completely formed.



**Figure 9:** Kamenitzas conditioned by discontinuity of the Classical Karst. Note the secondary central depressions corroded by sediments accumulation. Width of view is 55 cm.

Ready-formed kamenitzas can be found on surfaces that are currently exposed to weathering: they may belong to two or even three periods of formation because of their size range. One might think that they form and evolve rapidly until they reach a “standard” size determined by climatic and geographic conditions, and develop more slowly afterwards. In this sense, they are equilibrium landforms.

As with all landforms linked to chemical dissolution (but also for those stemming from erosion), the morphology of kamenitzas is conditioned by the lithological and structural characteristics of the host rock, i.e. by that complex set of factors



**Figure 10:** Elongated kamenitzas reaching a depth of up to 1.5 m on the limestone pavements near Borgo Grotta Gigante (Classical Karst) partly conditioned by discontinuity planes perpendicular to sub-horizontal stratification.

that leads to the so-called selective corrosion (Figures 4e, 8).

In case of fine-grained homogeneous rocks (such as micritic limestone), landforms are smooth, regular and symmetrical; if the rock is coarse-grained and heterogeneous (as in the case of breccias), the forms originated by selective corrosion are less regular (Figure 1). Also the presence of organic residues within the rock may cause roughness and irregularities (Figure 8). It is in fact known that the dissolution also depends on the  $\text{CaCO}_3$  crystal size, as its rate inversely proportional to grain size. Experiments with micro-erosion meter on Classical Karst have been made since 1970, showing lowering rates ranging between 0.04 and 0.01 mm/year, with annual rainfall amounting to approximately 1,350 mm/year in Mediterranean climate (Cucchi et al., 1987, 1996). The lowering rate can vary: it is higher in case of micritic limestone (mudstones), lower in case of sparitic limestone (rudstones or grainstones) and even lower in case of dolomitic limestone and limestone dolomite. Selective corrosion phenomena that highlight the petrography and structure of affected limestones can therefore manifest.

The shape, or plan, of kamenitzas is also conditioned by the discontinuities present in the rock mass. If fractures lead to higher porosity and permeability along a plan intersecting a kamenitza, the intersection becomes the preferential direction of development, thus originating elongated forms, also called linear or elongated kamenitzas (Figures 9, 10). Joints can simply condition the alignment of a kamenitza when it forms on them. If this happens, the fracture is persistent and involves the whole stratum. When fractures are less persistent, they can either condition only one of the kamenitza sides, or originate complex-plan kamenitzas if two or more fractures families are present. Fracture sets can therefore differently affect the size and morphology of kamenitzas; only non-persistent fractures cannot lead to the evolution of karst *grikes* or *holes*. Rose and Vincent (1986b) describe active and fossil kamenitzas strongly controlled by the presence of calcite veins



**Figure 11:** A “corrosion cup” of Perolas cave (Iporanga, São Paulo, Brazil), with diameter amounting to approximately 30 cm and depth to nearly 20 cm (photo P. Forti).

which traverse the pavements in low-altitude limestone pavements in the British Isles of Gait Barrows National Nature Reserve. Dissolution and fracture of the calcite veins at the bases of a kamenitza eventually leads to water leakage and the termination of kamenitza development.

## Other similar forms

*Corrosion cups* are peculiar formations, similar to kamenitzas, recently described in Slovenian (Mihevc, 2001: *korozijske kotlice*) and Brazilian (Forti et al., 2001: *marmitta da corrosione*) caves. They are similar in geometry to some peculiar “pot-hole-like” forms (Figure 11), described in non-carbonate rocks (White, 1988; *Opferkessel* or *solution basins in granites*). In the depressions formed on microcrystalline lightly dolomitic limestone, sand deposits with silt, essentially composed of quartz or silicates saturated with water rich in organic substances, favour static corrosion processes that preferentially affect the bottom: the dissolved calcite diffuses in the solution (Figure 12). Depressions whose shape evolution is heavily conditioned by the sediment accumulations on their

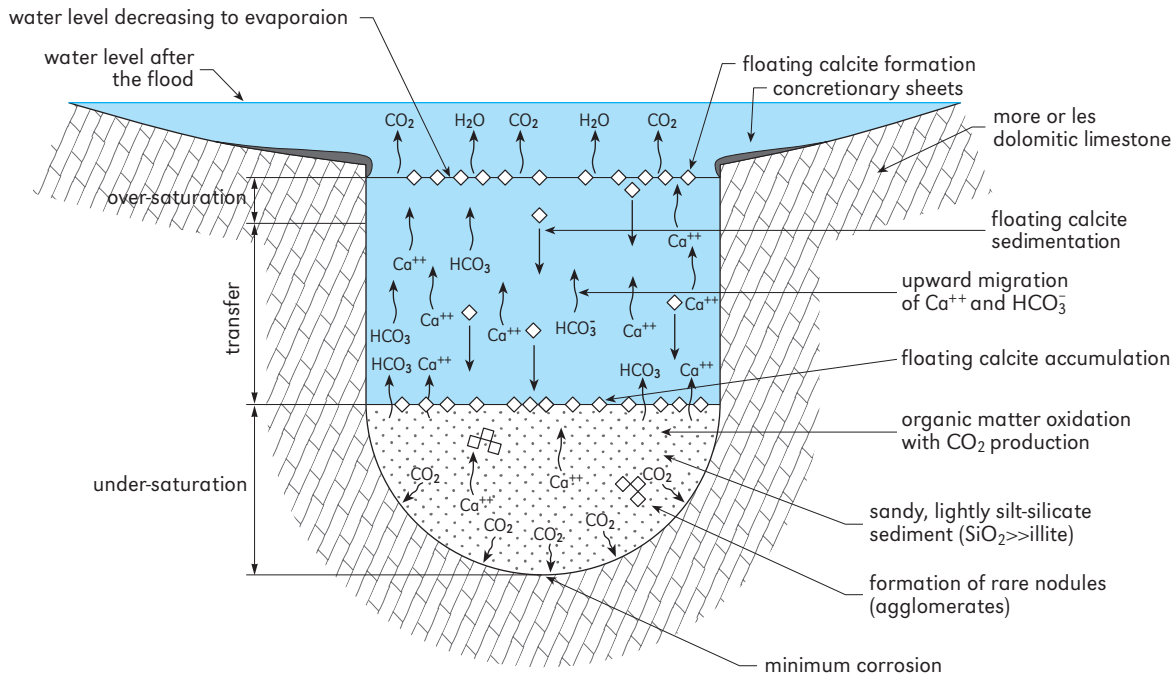


**Figure 12:** The genetic model of a “corrosion cup” according to Forti et al. (2001). Solution cup evolution is controlled both by the degree of under-saturation and the time during which the corrosion process is active. If these parameters remain constant in time, the process leads to a progressive tapering of the equilibrium cup floor with the evolution of a cylindrical section. If the degree of super-saturation and/or the time of activity increase, the equilibrium diameter of the cup is forced to increase and, consequently, the cup starts evolving into a cone shaped depression. During a flood, part or whole of the sediment filling the depression is washed away. At the end of the flood, sand and organic material are deposited on the bottom of the depression (pre-existing rill flutes, scallops and the already developed corrosion cups), which is filled with water. The oxidation process of the organic material releases carbon dioxide, which in turn causes the dissolution of the limestone located at the bottom of the depression. This process lasts until water floods the depression again. The dissolved calcite migrates through diffusion layer and at the end of the process, accumulates on top of the sandy sediment. Genetically, corrosion cups may be subdivided into three zones: in the lower one, corrosion is induced by the oxidation of the organic material; in the intermediate section, the transfer of  $\text{CO}_2$  and  $\text{Ca}^{2+}$  towards the air-water interface and the sinking of calcite rafts towards the top of the sand fillings are dominant; in the upper zone,  $\text{CO}_2$  diffusion in the atmosphere, and evaporation lead calcium carbonate to deposit mainly as calcite rafts but sometimes also as thin calcite crusts.

floors and by environmental characteristics are, in fact, not uncommon. This is basically the case in tropical and sub-tropical environments, where organic substances and  $\text{CO}_2$  are particularly important for the evolution of karst phenomena.

Landforms similar to those typical of carbonate rocks (White, 1988) have been observed on non-carbonate rocks: in granites (Isola d’Elba, Italy, and Antarctic), in basalts, quartz-feldspar sandstones with calcite or quartzite cement (Tepuys,

Venezuela, and Ethiopia), and in metamorphic rocks.

On granites, for instance, flat-bottomed, sub-circular depressions similar in genesis (but not in shape) to the so-called “tafoni”, can originate on the rocky walls, owing to attack by solution weathering. Sub-horizontal landforms comparable to kamenitzas could be the result of a concomitance of factors, such as selective corrosion in femic differentiates (involving the contact with the host



**Figure 13:** A cup in the pink granite of Capo d'Orso, Sardinia, Italy.



**Figure 14:** Femic nodules in riolite, Atacama desert, Chile, because alteration generate cups: pseudo-kamenitzas?

granites), in areas with different crystallization (both regarding crystal size and regarding adherence and cohesion). Furthermore, they can be induced by progressive alteration and disintegration due to temperature fragmenting, to the swelling of hydro-sensitive crystals, to silicate feldspar argillification, as well as to bio- and phyto-alteration (Figure 13). Interesting pseudo kamenitzas originate from feric nodules alteration in riolites or in ignimbrites (Figure 14).

To conclude, it is undeniable that, the aggression mechanisms can vary and interact in various ways with the different rocks involved, nevertheless they can generate very similar landforms. Gustavson et al. (1995), recognizing tens of thou-

sands “playa basins” (small, roughly circular to oval, internally drained depressions), whose genesis is conditioned by a concurrence of geomorphic, pedogenic, hydro-chemical and biological processes, state that they are economically “important because they collect runoff and recharge the aquifer”.

## **Acknowledgements**

I would like to thank Paolo Forti, Ugo Sauro and Peter Vincent for having critically and constructively contributed to the drawing up of my paper, and Silvia Mancaloni for the English translation.

Márton VERESS

*Trittkarren* are steps that develop on bare slopes (Figure 1). This karren form is also called *step karren* (Werner, 1975) and *heelprint karren* (Bögli, 1980). Trittkarren can be from 2 cm to 25 cm wide. According to Sweeting (1973), the *riser* may be



**Figure 1:** Trittkarren and rinnenkarren on bedding plane surface (Dachstein).

from about 3 cm to 5 cm high, while the *tread* may be from about 20 cm to 100 cm wide. According to Haserodt (1965), tritikarren occur at altitudes between 1,900 and 2,200 metres in the Alps. Trittkarren occur mostly on surfaces with a small dip angle. According to Sweeting (1973), they can develop in the initial phases of surface karren formation. Trittkarren occur on marble (Vincent, 1983a), on gypsum (Calaforra, 1996; Macaluso and Sauro, 1996a), and on sandstone (Veress, 2003). Trittkarren have a riser, a tread, and a *foreground* (Vincent, 1983a; Veress and Lakotár, 1995). The riser is usually curved and surrounds the tread. The tread is the flat, more or less horizontal section, the riser is the vertical surface at the back, and the foreground is the sloping section at the front of the tread that is not surrounded by a riser.

We can distinguish the following tritikarren types:

- *embrionic tritikarren* differ from developed tritikarren. Their shape is varied, they are only partly like developed tritikarren, and they are smaller (Figure 2);
- *nischenkarren* (Figure 3) are a type of tritikarren whose wide tread is surrounded by a small riser-system that is interconnected (Haserodt, 1965);
- *trichterkarren* (Figure 4) are a type of tritikarren whose tread is missing (Bögli, 1951);
- *uvala tritikarren* (Figure 5) are a type of



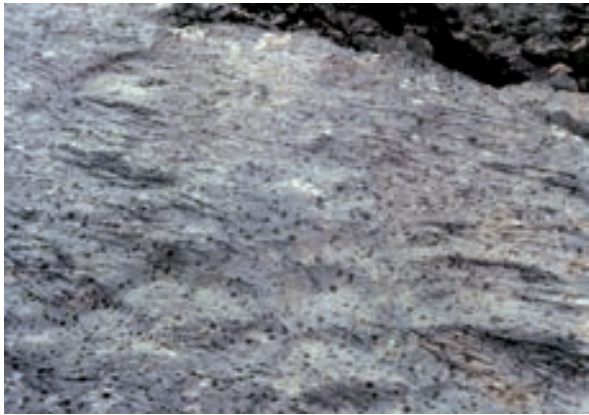


**Figure 2:** Embryonic trittkarren; the risers of several are more arched and their treads wider; below a grike on “Ausgleichsfläche” (Totes Gebirge). Width of view is 2.5 m.



**Figure 3:** Almost closed “Nischenkarren” (Totes Gebirge).

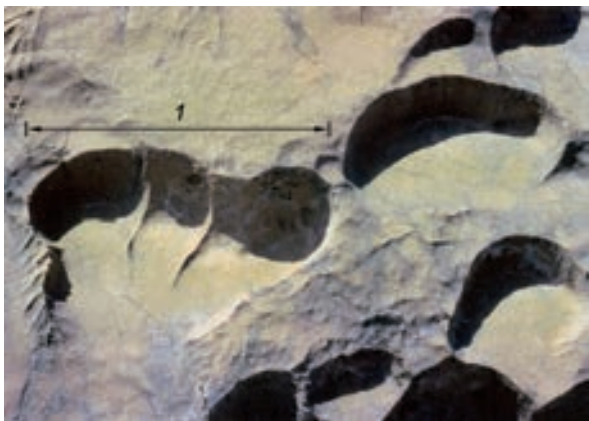


**Figure 5:** Uvala trittkarren (Dachstein). Width of view is 0.5 m. 1. uvala trittkarren.



**Figure 4:** Trichterkarren (Dachstein). Width of view is 0.5 m. 1. trichterkarren.

trittkarren whose risers are coalescing (Veress, 2000a);

- Veress et al. (2006) described *ripplekarren* on marble (from Diego de Almagro island). The risers of this type are straight and are not curved. Although the risers of this form are straight and not curved, these forms are indeed small steps and “ripplekarren” can therefore be considered as trittkarren;
- *step-trittkarren* develop around or on the margins of grikes and shafts. Their form is semi-circular. The treads and risers occur in a series, and the risers of separate “step-trittkarren” can develop parallel to each other (Figure 6);
- there are karren forms that have treads but do not have risers (Figure 7). They occur on very

**Figure 6:** "Step-trittkarren" with narrow steps (Totes Gebirge).



**Figure 7:** Trittkarren-like forms (Dachstein). Width of view is 0.5 m. 1. trittkarren like forms; 2. wandkarren.



steep slopes. These forms are like trittkarren but they may also be a special variety of *Spitzkarren*. Choppy (1996) calls these forms *tetrahedron karren*.

Trittkarren occur in rinnenkarren, in kamenitzas, on *Ausgleichsfläche*, and on ridges between *rinnenkarren*. They occur on bare rock as well.

## Methods of trittkarren research

Near the Svartisen glacier, Vincent (1983a) investigated the relationships between the values of various parameters of trittkarren (Figure 8), analyzing the distribution frequency of six parameters (Figure 9). He grouped the data into inter-

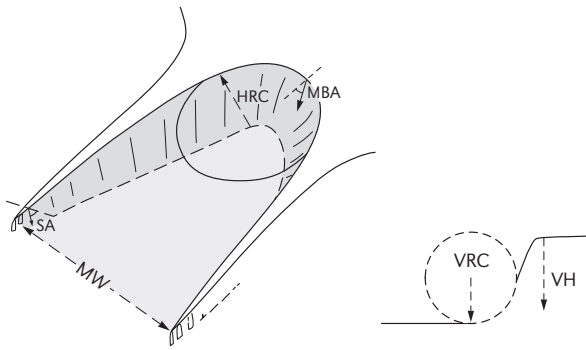


**Figure 8:** Morphological parameters describing the shape of trittkarren (according to Vincent, 1983a). MBA. maximum angle of riser; SA. average angle of side walls; VRC. radius of curvature of riser tread junction at center; HRC. maximum horizontal radius of curvature of riser; MW. maximum horizontal width; VH. vertical height of riser.

vals. The maximum values are the following with the boundary of the interval shown in parenthesis: VH 5–6 cm (2–10 cm), VRC 2–8 cm (2–18 cm), HRC 8–10 cm (4–18 cm), MW 12.5–15 cm (4–21 cm), MBA 50°–60° (30°–80°), and SA 40°–50° (10°–80°). The meanings of the abbreviations are shown in Figure 8. Vincent was able to show a linear function relationship using regression calculation. For example, the form of the function between the MW and the VH parameters is  $VH = -2.27 + 0.53 MW$ , where  $r = 0.575$  is the value of the correlation coefficient. He created a matrix by using the correlation coefficients, and we present the components of the matrix in Table 1. The asterisk beside a number indicates a 95% reliability level of the correlated components in the matrix.

Working in the Totes Gebirge mountain range, Balogh (1998) measured the following parameters of 240 trittkarren occurring on 10°–20°, 25°, and

40° slopes: the height of the riser, the angle of the tread, the length of the tread, the width of the riser, the length of the arch of the riser, and the width of the foreground. Assuming that trittkarren of different sizes in the same place represent different phases of development, Balogh (1998) describes the development of trittkarren as follows: the riser of the trittkarren develops evenly on slopes with a small inclination and the tread of the trittkarren lowers evenly as well. The treads of the trittkarren do not lower on slopes with a medium inclination. The riser develops mainly in its central section. The lower part of the riser dissolves more, and therefore the riser becomes steeper during its development. The upper part of the riser dissolves if the angle of the slope is about 40°. The riser becomes gently sloped during its development.

### Morphology of trittkarren

Trittkarren occur in groups. According to Bögli (1951) and Haserodt (1965), the tread of a trittkarren is an “Ausgleichsfläche”. According to Bauer (1962), there is a close relationship between the angle of the bearing slope and the morphology of trittkarren. If the angle of the slope is small (less than 10°), the height of the riser will be one or two centimetres, and the width of the tread a few decimetres (Figure 3). If the angle of the slope is between 10° and 30°, the riser and the tread will be larger (the height of the riser will be several centimetres, and the width of the tread one or two decimetres, Figure 5). If the inclination of the slope is large (above 30°), the height of the riser will be several decimetres while the width of the tread will be one or two centimetres. The riser can be gently sloping (Figure 10a) or steep (Figure 10b). Viewed from above, the curve of the riser can be short (Figures 4, 10a) or long (Figures 5, 10f). In the first case, the length of the riser is smaller than a semi-circle; in the latter case, its length is longer than a semi-circle. The riser may also be almost closed (Figure 10c). The curve of the riser can be almost straight (Figure 10d) or angular like a

**Table 1:** Matrix of correlation coefficients (Vincent, 1983a).

VH	–				
MBA	.50*	–			
VRC	.71*	.17	–		
MW	.58	.41*	.50*	–	
HRC	.32*	.26*	.33*	.46*	–
SA	.24	.30*	.06	.01	–.24
	VH	MBA	VRC	MW	HRC

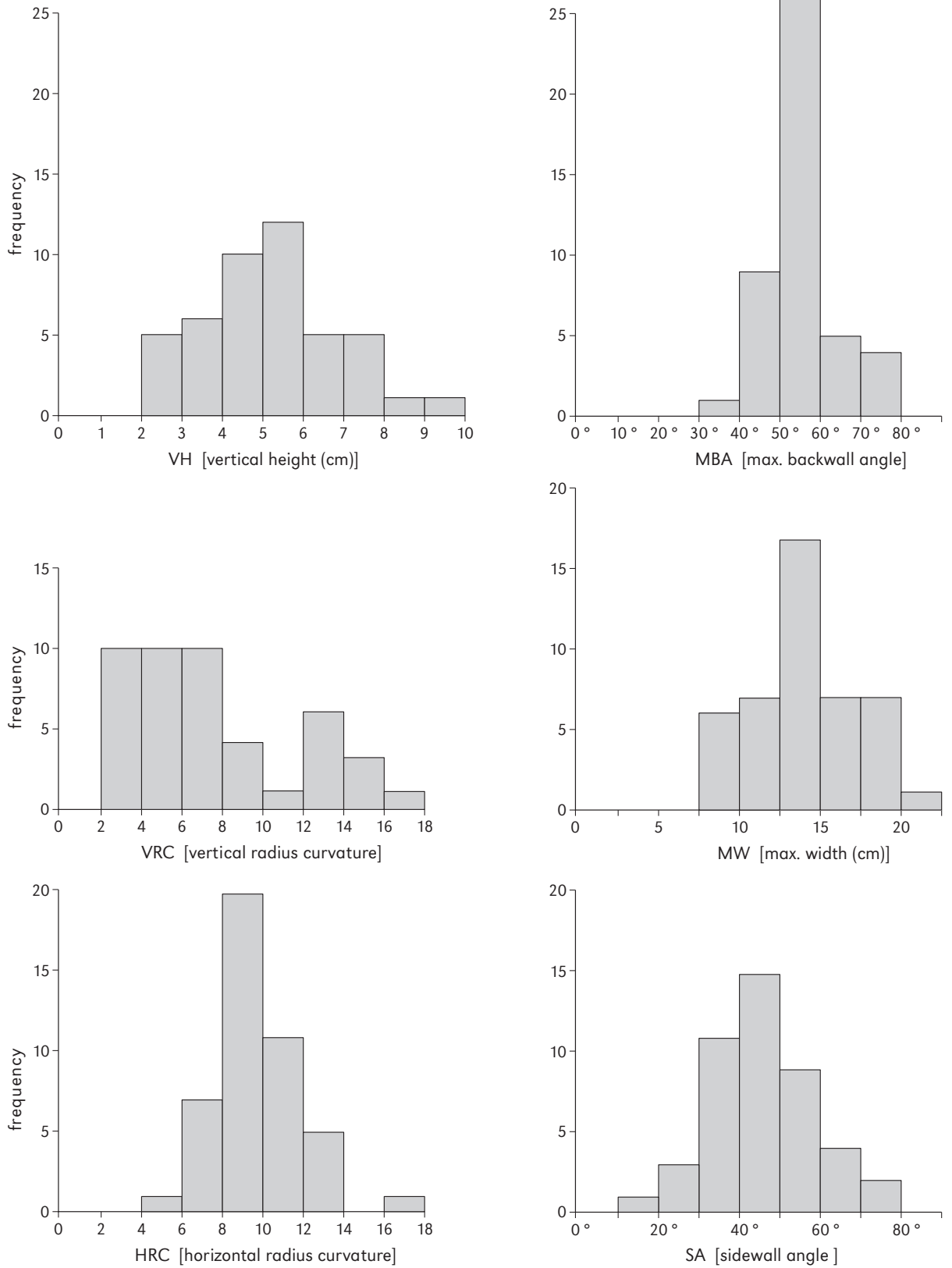
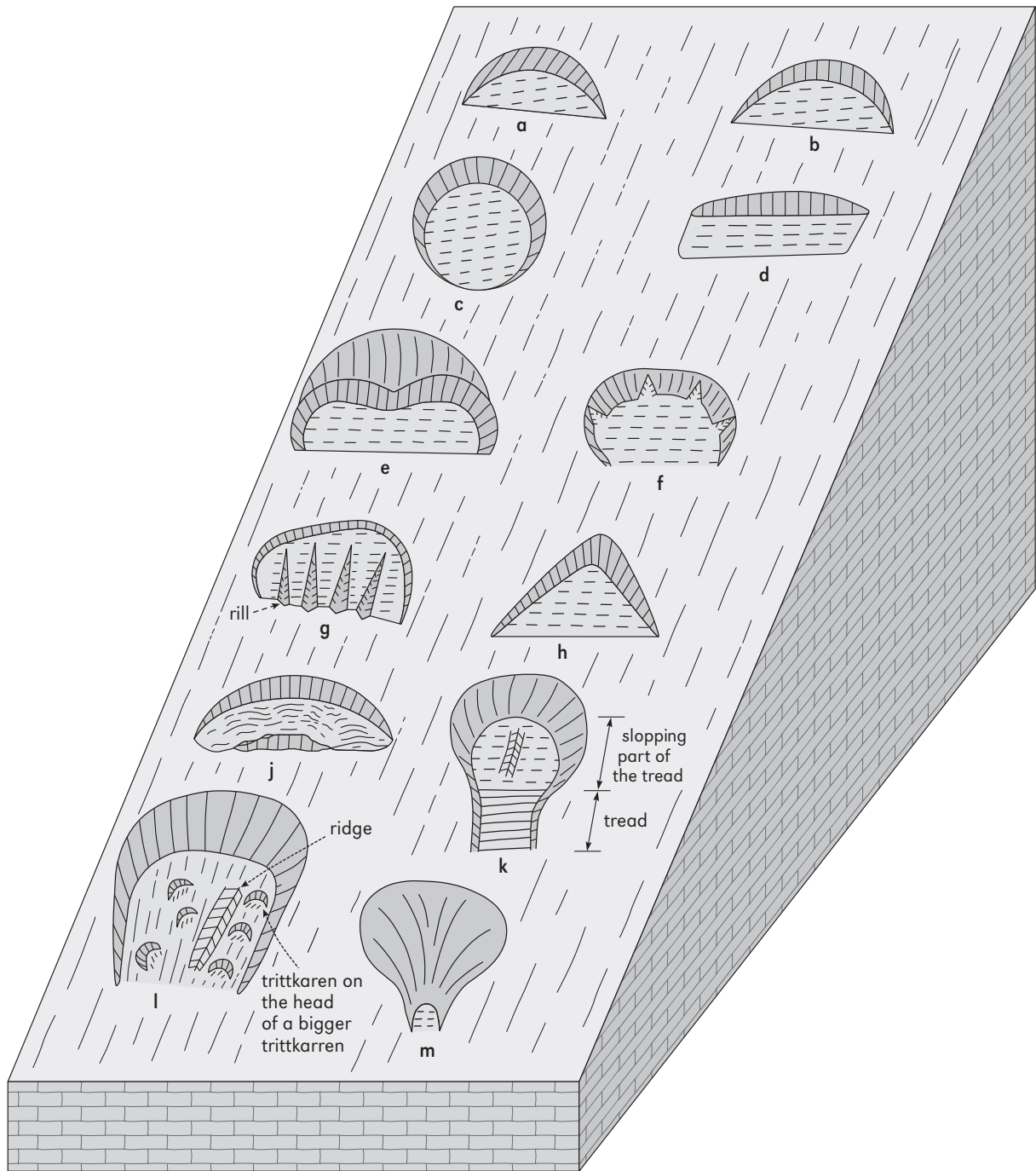


Figure 9: Histograms of the six morphological variables, n = 45 (from Vincent, 1983a).



**Figure 10:** Model trittkarren (from Veress and Tóth, 2002). a. trittkarren with gentle riser; b. trittkarren with steep riser; c. trittkarren with almost circular riser arch; d. trittkarren with straight riser; e. trittkarren without tread with uvala trittkarren below it; f. trittkarren with rills on riser; g. trittkarren with rills on tread; h. trittkarren with sharply angled riser and gentle tread; j. trittkarren with undulating tread; k. trittkarren with elongated tread; l. trittkarren with ridge and trittkarren on its tread; m. trichterkarren.

**Figure 11:** Trittkarren with riser similar to a right angle; below it are trittkarren with peaks on their treads (Dachstein). Width of view is 0.5 m. 1. trittkarren similar to a right angle.



right angle (Figures 10h, 11). *Rillenkarren* (Figure 10f) or secondary (small sized) trittkarren can occur on a riser. The tread may be horizontal and planar, or complex. It can be composed of surfaces with various slope angles. Smaller forms can occur on the surface of a tread, for example, *waves* (Figure 10j), *steps* (Figure 11), *ridges* (Figures 10k, l), *peaks*, *secondary trittkarren* (Figure 10l), *rillenkarren* (Figure 10g), and *kamenitzas*.

Trittkarren and rinnenkarren can occur on the tread of “Nischenkarren” (Figure 12). A small rinnenkarren can occur on the interior of trichterkarren.

The characteristics of trichterkarren are the following:

- they are large;
- their morphology is not varied;
- they do not occur in groups;
- they develop together with other karren forms (such as trittkarren);
- mostly they can develop together with rinnenkarren;
- small rinnenkarren can occur inside them.

## Development of trittkarren

According to Bögli (1960a), trittkarren develop where the intensity of the dissolution is great. This phenomenon occurs where the flow of water is thin. In one of his later papers, Bögli (1976) claimed that these forms developed by dissolution under snow when small drops of melting snow fall into already existing depressions on the limestone surface. Haserodt (1965) thought that trittkarren occur under micro snowdrifts. According to Haserodt (1965), the development of trittkarren occurs due to the melting of snow patches. The melting dissolves limestone through surface corrosion. This process needs the presence of snow patches for a long time, a characteristic of northern slopes. The amount of the dissolution (and thus the size of the forms) depends on the value of the saturation. According to Sweeting (1973), trittkarren develop due to large rain drops (during intense rainfall). She thinks there is horizontal dissolution on their areas primarily because two water layers merge on the surface. According to Ford and Williams (1989), trittkarren develop on homogenous



**Figure 12:** An area of “Nischenkarren” treads (Dachstein). 1. “Ausgleichsfläche”; 2. rinnenkarren that developed on the “Ausgleichsfläche”; 3. remnant surface (“peak”) of the “Ausgleichsfläche” with rillenkarren; 4. “Nischenkarren” treads; 5. young trittkarren on “Ausgleichsfläche”.

fine-grained rock if micro-steps developed earlier on its surface. These micro-steps could develop, for example, by erosion. According to Ford and Williams (1989), these forms can develop from kamenitzas. According to several other authors (Vincent, 1983a; Trudgill, 1985; Veress and Lakotár, 1995), the development of trittkarren can be caused by turbulent flooding. Carbon dioxide enters the water due to the turbulence. As the turbulence grows, the surface of the rock becomes uneven, which further increases the turbulence of the flow. According to Jennings (1985), the development of rillenkarren is rapid. The surface of the “Ausgleichsfläche” contributes to the development of trittkarren.

The morphology of trittkarren suggests they develop through surface dissolution under sheet

water fed by snow. The following facts prove this process:

- trittkarren develop under rillenkarren on a slope. The “Ausgleichsfläche” often develop below the trittkarren down the slope. Therefore, the water saturation belt does not occur at the trittkarren but on the “Ausgleichsfläche”;
- there are trittkarren that occur on ridges between rinnenkarren that can only develop under snow. If they are not covered with snow, they can only get water from the rain that falls on their surface, but this water drains quickly into the adjacent troughs. If the adjacent rinnenkarren are filled with snow, the melt water can flow along the ridges;
- sheet water develops on areas of trittkarren. The presence of rillenkarren on the riser and on the

tread proves the presence of sheet water. The presence of rillkarren also proves that sheet water dissolution can occur without snow;

- secondary trittkarren can develop on the perpendicular riser of the *primary trittkarren*.

Secondary trittkarren cannot be created by dropping rainwater since the drops can not touch the surface of the riser:

- the density of trittkarren is great;
- the width of the tread of “Nischenkarren” proves the large surface extent of dissolution;
- secondary trittkarren develop on the tread of uvala trittkarren.

Dissolution occurs on the tread. The following facts prove this process:

- the rills of a riser can continue on the tread;
- the uneven surface of a tread including “peaks” and ridges is a sign of dissolution on the tread;
- *young trittkarren* exist on the ice-free bottom of the valley of the Hallstatt glacier because the environment of the trittkarren was covered with ice only a few decades ago. The risers of the trittkarren are short and the dip of their tread is large. The dip of the tread of older trittkarren is small since the inclination of the tread decreases during its development. This can only be explained by the dissolution of the tread.

Trittkarren often occur below one another along a slope. This fact shows that dissolution happens repeatedly down a slope. Given the presence of the tread, the dissolution must be local. We think that trittkarren develop on slopes where the stream of sheet water is turbulent, and at such places the local dissolution is significant. That local turbulence develops under snow, is proven by the fact that trittkarren occur on ridges between rillkarren. Furthermore, there are no rillkarren on most trittkarren and therefore the turbulent sheet water cannot be caused by rain. According to Glew and Ford (1980), raindrops must strike

sheet water so it can become turbulent and help the development of rillkarren. We think that trittkarren can develop if the dissolution happens locally and periodically, which is possible if sheet water flows under snow.

The development of trittkarren can happen in three phases:

- in the first phase, a planar surface develops on a slope. This surface part becomes the tread of the trittkarren;
- if the inclination of the slope is small, in the second phase the tread and the riser form simultaneously, probably because there is no or little turbulence on the slope. Because of the laminar flow, the dissolution is similar over a larger area. These trittkarren are stable forms, and the tread increases more and more. On a slope with a medium inclination, the dissolution is greatest at the junction of the riser and the tread. The dip of the tread decreases while the riser becomes steeper. On slopes with a steeper inclination, the riser subsequently becomes less steep because dissolution is more rapid. As a result, trittkarren cannot exist on such slopes for a long time; however, we think that trittkarren can redevelop since their density is also high on such slopes;
- in the third phase, the intensity of the dissolution can vary along the length of the riser when the curve of the riser is longer. The shape of the riser does not change if the dissolution is similar all along the riser, and the riser becomes longer as it develops. The development of trittkarren with small risers is rapid, which is why the width of the tread is great. When the risers coalesce, the trittkarren change into “Nischenkarren.” In the case of trittkarren with higher risers (if the riser is not destroyed), the speed of the development is slower. Uvala trittkarren (with small width of tread) develop if the trittkarren are close to each other.





# CORROSION TERRACES, A MEGAAUSGLEICHSFLÄCHE OR A SPECIFIC LANDFORM OF BARE GLACIOKARST

Jurij KUNAVER

The article deals with corrosion terraces, a specific landform of bare glaciokarst. They are a secondary stage of development of different corrosion landforms located on limestone rock surface. They resemble to *Ausgleichsflächen* from Bögli (1960a), but they are of greater dimensions and more complex development. Furthermore they are also geocologically important.

Until recently the term *corrosion terraces* has not been used for the surface landforms of bare karst. They are delimited by a few tens of centimetres high walls cut into bedrock and have been linked so far with *ausgleichsflächen* and described as a subclass of them in the case of Kanin Mts, Slovenia (Kunaver, 1983). The basic characteristic of these surface landforms is the minimum of 10 cm high wall dividing two flat surfaces levelled by corrosion. Figure 1 shows, that in some cases deep *kluftkarren* or even minor *Schachtdolinen* or *kotlich* (*kotlič* in Slovene; *snow kettle* in English; *puit à neige* in French) can be cut into these flat surfaces; however, they can be claimed to be of younger origin. In other places walls, measuring up to 30 cm or even more, seem to be remnants of some extremely large *ausgleichsfläche* surface which mainly do not develop nowadays any more. They are supposed to be remnants of certain forms which occurred and developed in the past.

A question about these forms arose when similar ones were also discovered in other parts

of Kanin Mts, i.e. on the northern (Italian) side (Figure 2), and especially when similar forms were also discovered elsewhere. The same landform was found in the Dinaric mountains as well: i.e. in the south Velebit, in the central part of Prokletije Mts, and in the North Limestone Alps of Austria, e.g. in Steinernes Meer. So we have come to the conclusion that these cases are not isolated, but that they represent relatively infrequent surface forms of the bare mountains or high mountain karst which are regularly more or less associated to these forms. Just were in particular the corrosion terraces found in the Prokletije Mts (Caf Bor area at the altitude of 1,800 m a.s.l.) that raised some basic questions about their origin and development. Owing to their particular position and geological characteristics of the area, as well as because of the proximity of vegetation and its possible intense change in the past, the question was also raised, especially about the impact of vegetation and soil cover on the development of corrosion terraces; and thus also the question about direct and indirect impact of man.

## Morphological characteristics of corrosion terraces and terminology

At first we linked the terraces, as far as their morphology and origin are concerned, with aus-



**Figure 1:** Remains of an older corrosion terrace below Veliki Babanski Skedenj, 2,000 m a.s.l., western Kaninski podi plateau.



**Figure 2:** Corrosion terraces below Col delle Erbe, 2,100 m a.s.l., northern Kanin mountains, Italy.

**Figure 3:** Shallow ausgleichsfläche on Bjelić, 2,000 m a.s.l., Caf Bor, Prokletije mountains, Montenegro. Width of view is 2 m, in the middle.



**Figure 4:** A great kamenitza on Kačarjeva glava, 2,000 m a.s.l., southern Kaninski podi plateau.



gleichsflächen forms, i.e. regarding the process of their genesis (Figure 3). But after similar forms have also been found in considerably diverse environments and at different altitudes, the question about their origin claims to be solved in another way. Considerations about the Holocene climatic and vegetational fluctuations and the impact of man have also must be included here. At the same time, the need for giving to the phenomenon an adequate name is becoming evident: to differentiate between ausgleichsfläche, which have much lower walls and are of recent origin, and such much bigger terraces we suggest to introduce a new technical term. They could be called corro-

sion terraces, since several cases have been found where at least two or three flat shelves are laid one above the other and separated by a steep or vertical slope or wall.

Let us look now at some concrete examples. Formerly described corrossion terraces (Kunaver, 1983, 1991) on the Kaninski podi plateau under Veliki Babanski Skedenj occur at the altitude of 2,000 m a.s.l. They represent a first type of corrosion terraces (Figure 1). The height of wall is about 30 cm. The characteristics of the shelves consist in only slightly dissected rock surfaces, the lowest one of them, surrounded by the wall on three sides, resembles a large ausgleichsfläche. Its

bottom is perforated by a widened corrosion fissure caused by the progressive corrosion process. Above this, the next rock shelf follows being very poorly dissected and ends again into a steep wall, of approximately equal height as the lower one. But this one is flat on the one part and inclined on the other.

An alternative way of explanation for the development of some corrosion terraces is offered by the unique case of a great kamenitza on the lower edge of Kaninski podi plateau, 2,000 m a.s.l. (Figure 4). With exceptionally big dimensions, 5 x 2 meters, this kamenitza seems to be a quite old surface karst feature. Exceptional is also its location near the top of extreme *roches moutonnées*, which prove the connection of this and similar landforms on limestone rock, at least in its early development. This kamenitza is now not more active because its bottom is perforated by a karren well and filled with turf. Although it would be quite interesting to establish the time of the start and the end of its development, it is at this moment difficult to say anything about this. But it is evident, that the original kamenitza form, with the undercutting walls and flat rock bottom, will be preserved still for a long time.

On the northern Italian side of Kanin Mts, there is an area of distinctive corrosion terraces, which lie in a smooth, glacially eroded karst pla-

teau at the altitude ca. 2,100 m a.s.l., under Col delle Erbe. Such corrosion terraces fully resemble the above described ones, and thus they belong to the first described type (Figure 2).

Another type of *ausgleichsfläche* has been found in the central part of the Kaninski podi at the altitude of 2,100 m a.s.l., as well as on Steinernes Meer in the North Austrian Limestone Alps. The latter location lies on a limestone pavement, appr. 850 m north of Riemannhaus, in close vicinity of a location of *trittkarren*. In both cases, these are a kind of more or less distinct linear bends in otherwise evenly inclined surface of limestone pavement.

The next area to be mentioned in this context is Caf Bor (1,810 m a.s.l.) which belongs to the glaciokarst of Bjelić in the central Prokletije (Plav, Montenegro). It is a location of corrosion terraces developed on the *roches moutonnées*, near the alpine pasture of Caf Bor below the saddle of the same name, representing a border line between Montenegro and Albania. This region of typical high mountain glaciokarst has been poorly known and described so far. By now, it has been studied by J. Cvijić and recently by S. Belij. These corrosion terraces have a slightly lower position when compared with the above mentioned ones, and they also differ from them by their typical location. In this area the vast limestone region of Bjelić tectonically meets with non carbonate



**Figure 5:** Successive corrosion terraces at Caf Bor, possibly originating from subcutaneous corrosion, 1,800 m a.s.l., Prokletije mountains, Montenegro.

flysch-like region located to the north. From the latter, superficial denudation and erosion brought vast deposition of fans of glacial and periglacial origin which accumulated on the contact with limestone and on the limestone itself (Figure 5).

Glacial reshaping of *roches moutonnées* is in the same area also proved by certain *karrentische* which have a maximum of 10 cm pedestal. The prolonged *roches moutonnées*, running parallel to the valley, have well preserved forms of glacial erosion, to which the positioning of rock bedding has contributed in the first place. But intense alteration of the surface caused by Holocene corrosion activity of soil and vegetation is also evident. There are also some deep schachtdoline-like depressions on the ridge, most probably of older origin. Thus, traces of Würm glacial erosion can be observed on schachtdoline-like depressions and corrosion terraces. Close proximity of these phenomena, which might genetically even exclude one another, raises some questions about the development of this bare karst surface in Holocene. Here, corrosion terraces mostly occur in the form of narrow rounded shelves, located for the most part on the top of the ridge. They can follow one another or they can occur as independent formations. The height of the slope above the shelf

amounts to the average of 15–20 cm. In their close vicinity there are certain shelves which are partly filled with turf, but such cases only occur sporadically. There is an open question about this turf, whether it is of primary or secondary origin (Figure 5).

Corrosion terraces of Caf Bor reveal closer genetic and formal connection with the subterranean karst forms. There might have been some more vegetation and soil in the past on this bare ridge, but probably they disappeared due to the impact of man. Namely, this is a pasture area of the nearby alpine pasture of Caf Bor and because of the vicinity of a *karrentische* it is difficult to claim that vegetation and soil had substantially changed the surface of the former glacially rounded ridge.

Let us mention in the end, as an illustration and comparison, the extraordinary large *ausgleichsfläche* and *kamenitzas* of recent origin in the region of Bojin Kuk (1,100 m a.s.l.) at Veliko Rujno in the southern Velebit. Bojin Kuk is known by its steep towers, mainly formed by exfoliation in the Jelar-Promina limestones of Eocene age. The walls of the shelves are up to 15 cm high, but the walls of old abandoned shelves are even up to 40 cm high, or even more (Figures 6, 7, 8).



**Figure 6:** A great kamenitza and corrosion terrace in development. Bojinac, 1,100 m a.s.l., southern Velebit, Croatia. Width of view is 10 m, in the middle.



**Figure 7:** Fresh corrosion terrace. Bojinac, 1,100 m a.s.l., southern Velebit, Croatia.



**Figure 8:** Two phases and levels in the development of corrosion terraces: the higher and older, and the lower and younger. Bojinac, 1,100 m a.s.l., southern Velebit, Croatia.

## Problems of development and conclusions

Because of morphological characteristics and similarities of locations, we assume that the above described examples are also genetically alike. The differences occur, above all, in the dimensions and directions of corrosion terraces, which can be the result of local conditions and/or the result of unequal durations of development. We can undoubtedly state the following facts:

- locations of these forms at the above described sites are not isolated or casual but can most

probably be also found in other places. The above mentioned examples prove the regularity of occurrence of such forms in the regions of bare, non-dissected rock, glaciokarstic surfaces. A great majority of the examples come from the altitudes between 2,000 m and 2,100 m a.s.l., one comes from 1,800 m a.s.l., and another from 1,100 m a.s.l. Except for the lowest location, all corrosion terraces belong to areas of typical glaciokarst;

- morphologically these forms are, to the great extent, independent formations, which can be proved by the following:

- it is the cross-section of the terrace which is important for the morphological identification;
- transition from a more or less flat surface into wall is sharp. It is usually composed of two parts: the upper, vertical one, which passes into its lower evenly formed concave end. This transition into flat surface is not in the form of corrosion notch as in the case of *kamenitzas* and very often also in the case of *ausgleichsflächen*;
- the surface of the vertical wall and its concave end is not all evenly smooth but can be composed of individual more or less shelved segments sculptured by *rillenkarrren*;
- somehow the profile of the wall resembles the wall of *trittkarren*;
- the next element is the levelling, which is usually slightly wavy, non-dissected and not very wide shelf that can pass at its bottom side into the next terrace;
- water is drained in the form of film and rarely accumulates;
- the above described characteristics point to differences between these forms and the typical *ausgleichsflächen* which are still being formed;
- as for terminology (Sweeting, 1973; Gams et al., 1973; Kunaver, 1973a; Perna and Sauro, 1978; Trudgill, 1985; Ford and Williams, 1989), the above described terraces can be called *corrosion terraces* or *megalausgleichsfläche*. Since the main accent of this form is its wall, where the morphology and the dimensions of the upper and the lower levelled parts are less important, although still being its components, this form might be terminologically defined as corrosion terrace;
- as for genesis, it might be said that *ausgleichsfläche* as well as corrosion terrace, are both the result of a similar or even the same process, i.e. horizontal levelling of a bare limestone surface which also comprises formation and regression of walls. Although the formative features are similar to those of *trittkarren* (and, to a lesser extent, to *kamenitzas*), it is necessary to distinguish between them because of the differences in dimensions;
- corrosion terraces are the result of development in longer periods of Holocene. In interpreting terraces geomorphologically, it is necessary to take into account the climatic, vegetational and soil changes for each individual region. The fundamental question is whether the corrosion terraces have developed independently or are they a successive formation, originating formerly in some other way. Judging from our observations, we incline to support the second



**Figure 9:** An example of *ausgleichsfläche* on Velika vrata, 1,900 m a.s.l., Komna, Julian Alps. Width of view is 10 m, in the middle.





**Figure 10:** Even in a dolomitic limestone rock of Altipiano di San Martino, Dolomites, Italia, 2,300 m a.s.l., a kind of large *ausgleichsfläche* could develop. Width of view is 4.5 m, in the middle.

possibility. In fact, it is a matter of development of a corrosion terrace which had formerly been smaller.

We assume that the initial corrosion wall, out of which a larger one developed later, had been a form of an *ausgleichsfläche* or some other horizontal landform of the bare karst (e.g. a depression, excavated either by the subcutaneous corrosion or by the glacial erosion). Therefore not only is the original form important, but also the fact, that the bedrock and, in proper climatic conditions, rock surface can be sculptured and developed, for a longer period, under special circumstances which result in special forms. This is the process of levelling of a rock surface (Figures 9, 10). Corrosion terraces could be therefore defined as zonally reformed older climozonal karst forms;

- a tendency of augmenting the height of walls is evident as a result of their retreat. A conclusion about their age can also be made from this fact. According to this thesis, lower terraces are of younger date, and vice versa – the higher ones are of older date, i.e. their genesis was longer.

Another indicator of their age is also the fact that some terraces have remained untouched by vertical karst dissecting, while in other cases this process has already begun and can completely ruin them. Eventually, karst terraces are not forms to be searched for in strongly dissected *kluftkarren* surfaces.

If a supposition is made that corrosion terraces originate from depressions in rock surfaces generated by continuous or discontinuous vegetation and soil cover (which is very likely at these altitudes in the past), then it can be concluded that at some time in the past vegetation limit was at higher altitude and that the arrangement of altitude belts in high mountain regions was different from the present one. This fact is more or less proved by means of the presence of *hohlkarren* features, the frequency of which is higher at the altitude between 1,900 m and 2,000 m a.s.l. in our regions. There can be no doubt today about shifting of altitudes of climatic and vegetational zones in the past, caused both by climatic oscillation and the impact of man.

# RAINPITS: AN OUTLINE OF THEIR CHARACTERISTICS AND GENESIS

Angel GINÉS and Joyce LUNDBERG

Rainpits are small karren depressions not greater than a few centimetres in size, circular in plan view, semi-spherical to parabolic in cross section, with very sharp edges and very regular morphologies. They typically occur in suites on the flat tops of rock bosses, packing all the available space so that the sides of neighbouring pits meet to form a knife-edge, with no inter-pit flat surfaces (Figure 1). They develop on any soluble rock but are most often reported on carbonates. They have rarely been studied in detail. In this chapter we

explore the rather limited literature, present some of our unpublished field studies, attempt to outline their defining characteristics, and speculate on their genesis.

## Terminology and classification

Because these features are not often reported in the literature, there is no clear consensus on terminology. Some authors use the general term *pitting*,



**Figure 1:** Closely packed rainpits in an extremely rough and jagged limestone surface from El Colomer (Serra de Tramuntana mountain range, Mallorca). Width of view is 40 cm.

but this designation is more frequently utilized (together with *boring*) for nano- to small-scale karren-forms that lack any clear size limitations and morphologies. In his detailed “Lexique des termes français de Spéléologie physique et de Karstologie”, Gèze (1973) lists the following synonyms for rainpits: *lapiés à cupules* in French and *Grübchenkarren* or *Napfkarren* in German. In some publications, mainly in those devoted to the early discussion on rillenkarren genesis (e.g. Dunkerley, 1979, 1983), they are called solution pits. In their papers on gypsum karren, Macaluso and Sauro (1996a) suggest the neologism *minute craters*, changing to *mini-rain craters* in a publication issued a few months later (Macaluso and Sauro, 1996b). None of these alternative terms have achieved widespread use in the literature.

Taking into account the bulk of the short and scattered publications on this type of karren, especially those associated with semi-arid karst environments, it seems that the best option is to assume the term introduced in the international literature by the Australian researcher, Jennings (1971). Thus we suggest that *rainpit* be the preferred term. Note that some authors, for example White (1988), separate it into two words, as in *rain pit*.

Rainpits are not always included in classification schemes, perhaps because they do not occur in all environments. They are quite common in environments characterized by semi-arid and even arid climates. However, they seem to be rather infrequent in alpine karrenfields. It is probably because of this that no specific mention of this feature appears in the well-known karren classifications developed by Bögli (1960a, 1980), although they would fit into his “free karren” category because they usually form on bare rock surfaces. The small size of these karren features may account for the disregard perceived by Jennings (1983) with respect to the scant knowledge on arid and semiarid karst landforms in specialized literature. White (1988) classifies rainpits under “etched forms” (the etching being of massive bedrock rather than of structural weaknesses). Ford and Williams

(1989) include them under the group of “circular plan forms”. They fit into “small dissolutional forms” as defined by Macaluso and Sauro (1996a). Ginés (2004) places them in the “free karren, single” forms developed in a solutional environment of storm showers and within a scale limit of 1 to 10 cm. Although White (1988) classifies rainpits separately from rillenkarren under “etched forms” rather than “hydraulic forms”, we believe that the rainpits and rillenkarren are genetically related (see discussion below).

We define them here as small-scale, free, single, circular, hydrodynamically-controlled by droplet impact, produced in a solutional environment of direct rainfall and within a scale limit of 1 to 4 cm.

## Description of rainpits and rainpit-related features

### Description

In spite of being very distinctive and recognizable features, a review of the literature reveals that there is little consensus on what constitutes a rainpit. Jennings and Sweeting (1963) describe rainpits as “tiny hemispherical hollows, about 5 mm to 20 mm deep”. In the definitive citation of Jennings (1971), rainpits are merely described as “being usually less than 3 cm across and 2 cm deep” and are considered to be “the simplest effect of rain falling on bare rock”. No other description is included regarding the shape or profile of the pits.

White (1988) offers a broad description of rainpits as “the smallest of the features resulting from etching of the bedrock” and indicates that they are “few millimetres to a few centimetres in diameter, roughly circular, symmetrical pits etched into the bare limestone surface”. In their classification of small scale solution sculpturing, Ford and Williams (1989) describe rainpits as “circular, oval or irregular forms in plan view, with rounded or tapering floors and greater than 1.0 cm in diameter”. According to Macaluso and Sauro (1996a, b), rainpits “are crater-like depressions; ...their

borders are nearly elliptical or polygonal, with a diameter of 12–30 mm and a depth of 1–30 mm, and their cross profiles are parabolic, with rounded bottoms, steep sides and sharp crests”. Smith et al. (1996) speak about “rounded solution pits with V-shaped cross profiles”. Ginés (1996a, 2004) defines rainpits as “small hollowed cup-like karren features, sub-circular in plan, nearly parabolic in cross section, whose diameter ranges from 0.5 cm to 5 cm, and exceptionally exceeding 2 cm in depth; frequently they appear clustered in groups”.

The most common properties appear to be that they form on bare rock, have roughly circular plans and parabolic profiles, and are approximately 1–3 cm in diameter and depth. However, in view of the variety of descriptions and definitions quoted above, some obvious needs arise. The first is to choose size limits for rainpits, in order to permit a useful distinction from the larger pits (e.g. some kamenitzas or solution basins) as well as from the smaller ones (e.g. some biokarst borings or solutional micropits). A second need is to define the shape of the bottom or the cross section, in order to differentiate rainpits from the characteristic flat bottom of many kamenitzas and also from the irregular profiles that are typical of solutional etching and biokarstic boring pits. A third need is to document the pattern in space in order to distinguish rainpits (that invariably occur in suites and frequently in non-random patterns) from isolated solutional or biokarstic pits and also from randomly-spaced or structurally-governed etchings.

## Distribution

As a general rule, in many descriptions about the karren assemblages in which rainpits occur, it is stated that they develop mainly on gentle slopes or on the summits of the rocks rather than on their steep flanks. A repeated pattern, observed and described by Dunkerley (1979) from limestone outcrops, is of a well-packed group of nearly circular depressions (i.e. rainpits) that appear on the flat

tops of rock outcrops: on the steeper flanks of the rocks, developing radially outwards from the rainpits, are groups of rills. The same pattern was recognized by Macaluso and Sauro (1996b) on narrow gypsum crests from Verzino (Calabria, Italy). In the karren assemblages where rainpits and rillenkarren coexist, the rills are frequently distributed downslope over the sides of the protruding rocks whilst the tops and upper parts of the ridges are occupied by rainpits (Figure 2). This is an alternative to the common herringbone pattern usually produced where rillenkarren ribs meet back to back at the crests of pinnacles. In some rather exceptional cases rainpits are reported to be aligned, interrupting the flow of small runnels (Figure 3) or even producing distortions inside rillenkarren flutes (Ginés, 1999a). However, special attention is required in order to distinguish rainpit features from other small concave features caused by the



**Figure 2:** Typical pattern of rainpits and rillenkarren on a gently rounded clint in the Gregory Karst, Northern Territory, Australia (photo by K. G. Grimes). Width of view is 55 cm.



**Figure 3:** Sloped limestone surface in El Colomer (Mallorca), showing rainpits in association with rillenkarren and greater rinnenkarren grooves.



**Figure 4:** Rainpits from El Colomer (Mallorca) in a ribbed or lined pattern. According to Dunkerley (1979), the conjunction of rainpit-like depressions like these could be involved in the early stages of rillenkarren formation. Width of view is 50 cm.

action of thin water films, like the so-called *cockling patterns* described by Sweeting (1972).

On bare exposed rock surfaces rainpits usually occur clustered in closely-packed groups (Figure 1) and sometimes coalesced (Figures 4, 5), although they may occur singly (Jennings, 1985). Where

the coalescence of rainpits becomes extensive, the circular or elliptical contour of these small basins is substituted by polygonal shapes, and the sharp rims between them produce a characteristic honeycombed pattern over the surface of the rocks (Figures 1, 5). Macaluso and Sauro (1996b) com-

**Figure 5:** Zenithal view of clustered rainpits on a 40° sloping rock in El Colomer (Mallorca). Note the conspicuous biokarstic overdeepenings on the bottoms of many rainpits. Width of view is 55 cm.



pare the micro-topography resulting from extensive rainpit coalescence with “miniature versions of a polygonal doline karst”. The whole surface then shows a chaotic appearance divided into irregular and often jagged micro-watersheds.

## Hydrology

Rainpits form from the direct impact of raindrops onto bare rock surfaces but only at the crests or summits where deep water films do not occur. The mechanism for drainage of rainpits is not obvious. They are clearly associated with surface roughness which hinders the formation of contin-

uous thin water sheets over the rock. In normal rainpits suites, as well as coalesced pits, drainage patterns can not be recognized; no rivulets are seen to form. Splash is obvious and presumably is a major way (along with overspilling or decantation) that water is transferred from pit to pit and then down the slope.

The prevalence of rainpits in arid and semi-arid environments may be a consequence of the scarcity of sheet or channel flow. Limited amounts of rainfall cannot generate enough flow of water over karst surfaces to produce sustained sheet or channel flow. Thus channelled karren forms, apart from rillenkarren, are not common in association with rainpits. In this manner, the group



**Figure 6:** Tiny pitting and rainpits of different sizes in the Gregory Karst, Northern Territory, Australia (photo by K. G. Grimes). Width of view is 35 cm.

of karren features classified by White (1988) as *etched forms* develop from nanoscale weathering and biokarstic processes in the absence of significant flow action. Instead, dissolution occurs in water films and pools that do not readily drain efficiently. Rainpits are one expression of this kind of rough etched surface characterized by tiny irregularities, borings and pittings (Figure 5). In the semi-arid localities of the Mallorcan mountains (Ginés, 1996a), the geographical distribution of rainpits is strongly correlated with that of micro-rills (*rillensteine*), another karren form that seems to be related to limited water supply.

#### Variations in pit form

Wherever water drips onto bare rock, a pit will form, but for many it is apparent that they are not simple rainpits. Simple rainpits form where rainfall hits bare rock of low slope angle. The rain falls with no impedance and no other mechanism for erosion is apparent (at least macroscopically).

Where pits develop from drips that are not simple direct rainfall, the drip size is typically larger than raindrops and the distribution is not necessarily random. In addition, the chemistry is likely to differ from that of simple rainfall. In all these

cases the pits are not the product of simple rainfall and are not part of the genuine *rainpit* category. Instead, they should be called *drip pits*. Examples include pits developed where leaf interception delivers large drops that may have enhanced aggressivity. Decantation drips from overhanging rocks, mats of vegetation, snow melt or drips inside caves also fit into this category of “drip pits”. Some drip pits are distributed in groups but many are single. The size of drip pits will vary with size of drip; they are often larger than rainpits.

Simple rainpits form on low angle surfaces that are approximately normal to the incoming rain. Another distinct type of a pit, of roughly the same dimensions as rainpits but found on steeply dipping, vertical, or even overhanging faces, does not appear to be formed by either flowing or dripping water. These pits are ~1–3 cm both in diameter and depth, bored horizontally into steep faces, very similar to borings by large gastropods such as whelks. While the mechanism of formation of these horizontal pits is not at all obvious (they do occur in supra-littoral coastal locations but they also occur in many inland situations where there has been no possibility of gastropod boring), it is clear that these pits are not caused by direct rainfall and should not be called “rainpits”.

Finally, careful observation of nearly flat limestone surfaces where a thin cover of soil has been removed by recent erosion, demonstrates that extensive pitting can also be produced as a particular case of subsoil karren. Additional research and statistical data are required in this respect, but some examples of subsoil *pitting* from Dragonera islet and Mallorca (Balearic islands) show some significant differences regarding dimensions, distribution and sharpness when compared with genuine rainpits. Subsoil pitting produces pits of very different size (many of them smaller than normal rainpits), that are shallower and smoother, with blunted rims and generally less coalescence. Casual observation suggests that “subsoil pitting” seems to be quickly transformed into true rainpits when it becomes exposed to direct rainfall. An interesting question then arises about the evolution

of subsoil pitting towards polygonal rainpit-fields: is this merely an occasional occurrence or are the majority of well-packed rainpits simply the final result of this process?

## Morphometric data

No protocol has ever been established for the measurement of rainpits. As with the sampling of any population, care must be taken that all samples included are within the population, in this case of simple rainpits. Morphometric study of rainpits is similar to that of rillenkarren (except for length). Width (the distance between edges or cusps) may be measured along the slope and across the slope (as a measure of roundness of plan). Depth (the maximum depth from the cusp-to-cusp line) is measured at the deepest point. Some measures of the nature of the edge (steepness of side slope, asymmetry of sides) should be included. Profiles are recorded by means of a carpenter’s profile gauge (Figure 7). This is not always ideal: unless the pits are arranged in a line, any linear profile that includes several pits may not sample the centre point and thus the deepest part of the profile for each pit. (This proved not to be a problem for Lundberg, in 1976, profiling rainpits in Chillagoe, Australia. The rainpits tended to occur in lines.) Slope angle of the rock face on which the pits are developed may vary across the top of a boss and thus should be recorded for each pit. The spatial distribution patterns might be recorded by overhead photography and perhaps measured by nearest neighbour analysis.

Actual data based on careful observations in the field and real measures of rainpits are very scarce in the literature. Our bibliographical research, presumably representative of the current knowledge on these features, produced only a few references. For instance, Dunkerley (1983) describes the micro-topography of several sampling sites in the Chillagoe karst (Australia) and comments on the presence of “solution pits of normal dimensions (i.e. about 1–2 cm in diameter)”. Smith et



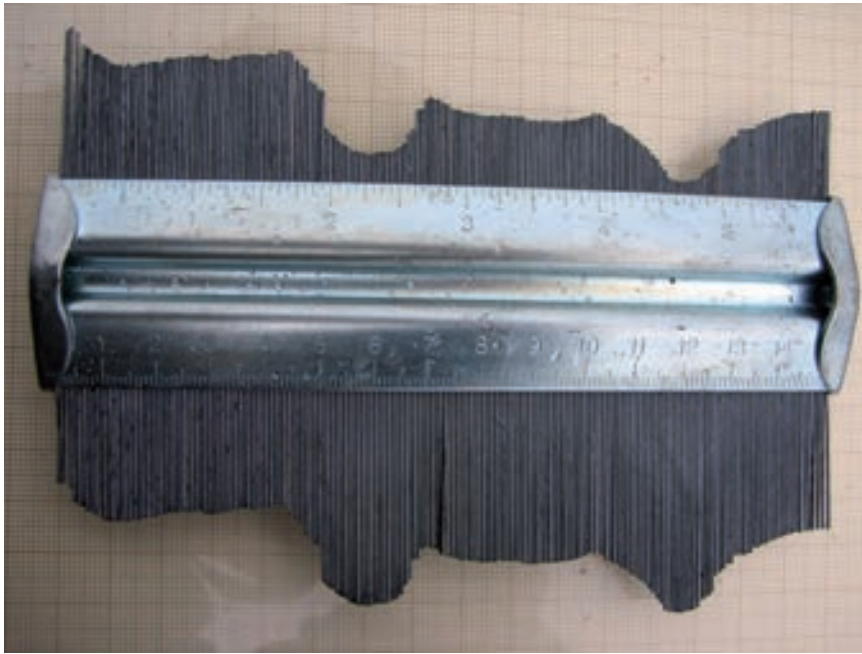


**Figure 7:** Profile of two rainpits recorded by means of a carpenter's profile gauge.

al. (1996), speaking about surface weathering features from Tatahouine (southern Tunisia), found a variety of solutional features, including "...solution pans, extensive pitting (1–3 cm in width and depth) and some poorly developed rillenkarren".

Statistical data based on a significant number of measurements of individual rainpits are scant. One of the few rigorous studies is that by Lundberg (1977a) in Chillagoe (Australia) for two well-differentiated kinds of rocks: namely fossiliferous reefal limestone and coarsely-crystalline marble. The majority of the rainpits are simple in form, occurring in clusters on the tops of rounded bosses. Rainpits occur on slopes from 0° up to 20°, but the majority are in the range 0°–10°. On the steeper slopes pits are noticeably asymmetric where the upslope side is taller. Complex forms observed include rainpits grading into cups, and into rillenkarren. Only the clearest, simple forms were measured. The analyses presented here include some from the 1976 unpublished theses and some additional analyses.

Data on rainpits from Chillagoe (Lundberg, 1977a)

Width, depth, radius of circle that fits into the base (the more parabolic the profile, the smaller the circle) and sharpness (average angle of top 0.5 cm of pit walls to the vertical) were measured on 1,710 rainpit individuals. Results are summarized in Table 1. The pits are on average 1.5–2 cm wide and 0.5–1 cm deep. The pits on reefal limestone are wider, deeper and sharper than those on marble. A pertinent observation is that the rock surfaces on marble are regularly destroyed by exfoliation or disintegration and thus the morphometric indices for the short-lived rainpits on marble may not be of fully mature forms. For this reason, further analysis is confined to pits on the reefal limestone (n = 1,029).

Depth (54% variation) is more variable than width (36% variation). This suggests that the characteristic width is reached while the depth continues to increase. The simplest measure of shape, average width to depth ratio is 2.48 (s = 1.12). Ratio of depth to radius of fitted circle, average 1.60 (s

**Table 1:** Morphometric data from rainpits in Chillagoe, northern Queensland (Lundberg, 1977a).

Lithology	Reef limestone	Marble
Width (SD)	20.9 mm (7.6)	16.3 mm (8.2)
Depth (SD)	9.3 mm (5.0)	5.4 mm (3.2)
Radius	7.8 mm (4.6)	7.9 mm (7.1)
Sharpness	33° (13)	44° (13)
Slope angle of rock	6.6° (6.2)	10.1° (9.5)
N	1,029	681

= 1.30), indicates that the pit profiles are typically shallow parabolas.

Further analysis shows that the profile changes with size. If depth is used as a measure of size, and W/D ratio as a measure of shape, a plot of W/D against D shows that small pits are shallow and, as they enlarge, approach a characteristic W/D ratio of 1.5 (Figure 8, above: exponential relationship,  $R^2 = 0.48$ ,  $p = 5e-108$ ). If depth to radius of fitted circle (D/R) is used as another measure of shape (the more parabolic the profile, the higher the D/R value), a strong relationship is seen between log D/R and log D (Figure 8, below:  $R^2 = 0.53$ ,  $p = 6e-166$ ). This shows that small rainpits are more rounded and larger ones more parabolic. Width, however, does not show a significant correlation. If width reaches equilibrium early on in the development, then the form can get deeper and more parabolic without any change in width.

**Data on rainpits from other sources**

Smith (1986) describing some arid karstic sites from southeast Morocco reports a survey made by Kerr (1983) in Wadi Akerbouss, which identified significant differences between rainpits developed in vertical surfaces (average diameter 14.5 mm and depth 10.9 mm) and rainpits developed on horizontal surfaces (average diameter 9.4 mm and depth 7.2 mm); but no indications about the number of individuals measured is given. It is not clear if the two populations are both simple rainpits.

Zhang (1994) measured rainpits in three karst areas of Tibet characterized by remarkably low

temperatures and precipitation values below 500 mm per year. The number of measurements made on each site varied between 36 and 139. These pits are rather small: the means of the rainpit diameters are 7.5 mm in the mountains of Dingri, 8.1 mm in Amdo and 7.9 mm in Lhasa valley; and the mean depth values are 3.1, 3.0 and 4.2 mm respectively. Even the maximum diameter found in each sampling site appears to be small: between 11 and 12 mm.

The rainpits in Mallorca island appear to be simple in form and origin. Ginés (1996a) measured 50 rainpits from a karren site 200 meters above sea level, in the mountain range called Serra de Tramuntana (Mallorca island). The climate is characterized by an annual precipitation between

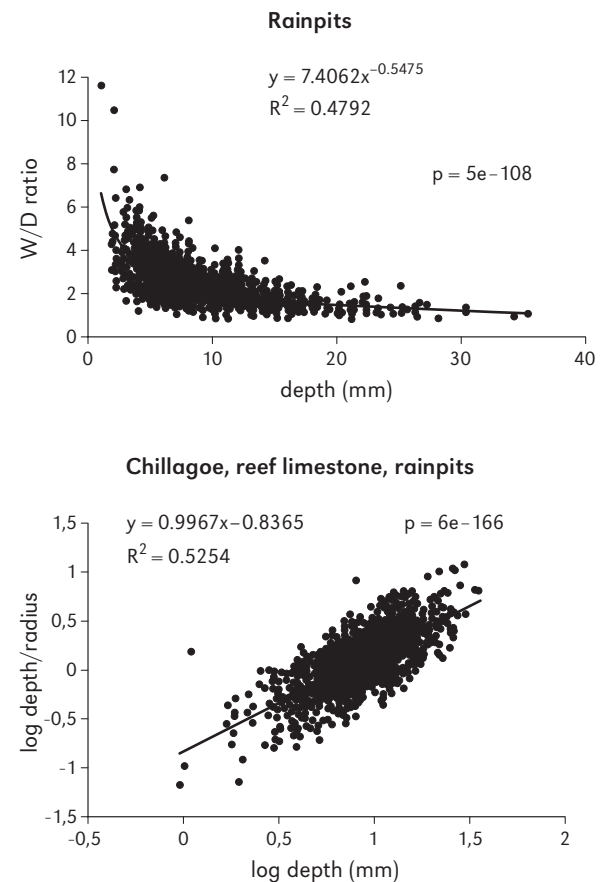


**Figure 8:** Rainpits from Chillagoe, Queensland, Australia: above is relationship between width to depth ratio (W/D) and depth (D), and below relationship between depth to radius ratio (log D/R) and depth (log D).



**Figure 9:** A general view at the meso-scale of the karren assemblages in El Colomer (Mallorca). At this level of observation, rinnenkarren grooves are outstanding as well as the grey biokarstic patina coating all the rock surfaces. Evidence of subsoil karren remnants can also be noticed.

800 and 900 mm that falls in the form of short and intense showers, following the typical Mediterranean pattern of rain distribution that implies a very dry summer. The sampling shows that in this karren outcrop (Figure 9) the mean of the rainpit diameters is 20.1 mm; with a maximum value of 61 mm, a modal value around 14 mm, and a minimum value of 9 mm. Additional measurements obtained in the same karstic area show congruent diameter mean values of 20.5 mm ( $n = 100$ ) and depth mean values 10.4 mm ( $n = 50$ ).

Progress in the understanding of rainpit genesis is hindered by these extremely scarce morphometric data (Table 2), but at least the definition of the feature is becoming substantiated by several sets of measurements. It is very clear that many more studies are required before a definition of rainpits in terms of morphometric criteria and diagnostic shape characteristics can be presented. It is not clear if all these features are in fact simple rainpits: perhaps the very small Tibetan rainpits documented by Zhang (1994) call

**Table 2:** Summary table of morphometric data on rainpits.

Location	Notes	Width (mm)	Depth (mm)	No	Reference
Chillagoe, Australia	reef limestone.	20.9	9.3	1,029	Lundberg, 1977a
Chillagoe, Australia	marble	16.3	5.4	681	Lundberg, 1977a
Tramuntana, Mallorca	200 m a.s.l.	20.1		50	Ginés, 1998
Tramuntana, Mallorca	200 m a.s.l.	20.5	10.4	100 50	Ginés, unpublished data
Dingri, Tibet	low temperature and precipitation	7.5	3.1	36–139	Zhang, 1994
Lhasa, Tibet	low temperature and precipitation	7.9	4.2	36–139	Zhang, 1994
Amdo, Tibet	low temperature and precipitation	8.1	3.0	36–139	Zhang, 1994
Morocco	vertical surfaces	14.5	10.9		Smith, 1987 after Kerr, 1983
Morocco	horizontal surfaces	9.4	7.2		Smith, 1987 after Kerr, 1983

**Table 3:** Comparison of morphometric measures on rainpits and rillenkarren of reefal limestones in Chillagoe, Australia (Lundberg, 1977a). Significant differences are shown by Z-scores of  $> 3.3$  (either positive or negative) and probability values  $< 0.001$ . The morphometric measures are explained in the text.

	Rills (no = 1,174)	Pits (no = 1,029)	Z-score	p
Width,SD	19.47 (7.33)	20.95 (7.64)	-4.4	$< 5e-5$
Depth, SD	8.39 (4.38)	9.34 (5.00)	-4.5	$< 1e-5$
Sharpness, SD	35.49 (13.07)	33.19 (12.94)	4.2	$< 5e-4$
Radius	7.30 (3.84)	7.78 (4.60)	-2.6	0.01
W/D ratio	2.72 (1.30)	2.48 (1.12)	4.3	$< 5e-4$
D/R ratio	1.43 (1.03)	1.60 (1.30)	3.25	0.0015

for a more precise definition of the feature. In the absence of clear diagnostic criteria, some degree of confusion is likely because of the *natural continuum* that can be expected between nanoscale pitting, rainpits and kamenitzas, as suggested implicitly by Ford and Williams (1989). In fact, the minimum diameters of pits reported from Tibet are as small as 5 mm and in the same paper basin-shaped features ranging from 2 cm to 15 cm are classified as *solution pans* (kamenitzas). Macaluso and Sauro (1996a) are probably thinking of this problem when they state that “minute craters [called rainpits in this chapter] must not be mistaken for micro-pits, described by Ford and Williams (1989), which correspond to the micro-honeycombs (or micro-alveoli) of biological corrosion”.

A short note on the effect of lithological variation is relevant here. Factors controlling the presence or absence of rainpits are probably similar to those for rillenkarren (see chapter 16): both need rocks of high purity, high hardness, and low porosity and generally high homogeneity. In Chillagoe (Australia), Lundberg (1977a) found that, apart from radius, all the morphometric measures on rainpits showed a statistically significant difference for two lithologies, the pits on reefal limestone being wider, deeper and sharper than those on the more coarsely crystalline marble (Table 1). Grain size may prove to be an important variable once further studies have been done.

## A preliminary discussion on the genesis of rainpits

### The relationship between rainpits and rillenkarren

Rainpits and rillenkarren have so many resemblances (except for the obvious difference that rillenkarren are elongate down slope) that genetic similarity is suspected. They have a strikingly similar trough-width and cross-sectional profile, both being very close to a parabolic shape. Both develop on bare rock that is open to unmodified raindrop impact. They are often associated in the same karren outcrop as an integrated karren assemblage: the rainpits form on summits of rocky blocks where raindrops impinge directly onto an approximately flat surface while the rillenkarren develop from the crest downwards where rain drops fall directly onto a sloping surface.

Lundberg (1977a) measured both rills and pits on limestones in Chillagoe (Queensland, Australia). Table 3 shows that the distributions have considerable overlap at the 1 standard deviation range. However, there is a consistent slight difference: rainpits are marginally wider and deeper than rillenkarren (by ~7% for width, 10–20% for depth). While the mean values are very close, the Z-test of significance (Dunkerley, 1983) shows that rainpits are significantly wider and deeper than rillenkarren on both rock types at 0.01 probability level. (To

place this in perspective, the significance of the difference between *rock types* is much higher than between rillenkarren and rainpits within one rock type.) In all locations rainpits conformed to the same parabolic profile as rillenkarren (radius of fitted circle showed no significant difference), but W/D ratios and D/R ratios indicate that pits are a slightly deeper form than rills.

Development of profile over time is almost identical for both, rainpits and rillenkarren. For W/D against D, rillenkarren yield  $y = 7.6x^{-0.56}$ ,  $R^2 = 0.40$ ,  $p = 4e-125$ , while rainpits yield  $y = 7.4x^{-0.55}$ ,  $R^2 = 0.44$ ,  $p = 2e-129$ . Both reach a characteristic W/D ratio of  $\sim 1.5$ . Log D/R against log D for rillenkarren yields  $y = 0.95x + 0.8$ ,  $R^2 = 0.53$ , and  $p = 2e-188$ , and for rainpits yields  $y = 0.99x + 0.8$ ,  $R^2 = 0.53$ ,  $p = 6e-166$ . These suggest that both, rainpits and rillenkarren, reach a characteristic width early on in their development, become deeper over time and approximate to an equilibrium parabolic profile.

The morphometric observations made by Ginés (1998b and unpublished data) in El Colomer (Mallorca) are in good agreement with the observations from Chillagoe: cross sections are predominantly parabolic and rainpit diameters appear to be slightly, but significantly, wider than rillenkarren flutes. Distribution frequency of both, rillenkarren and rainpits from El Colomer, is presented in Figure 10, showing a clear skewness in the curve toward greater values, which may suggest an additional solutional enlargement caused by the stagnation of water in the pits after rainfall showers. Many of the wider pits reported in this site show non-parabolic cross sections and probably could be the result of modifications produced by some kind of “kamenitza-effect”. Further studies are obviously needed to address this question.

### Environmental conditions and rainpit occurrence

In spite of the sparse and unevenly-distributed studies on rainpits (especially from the geograph-

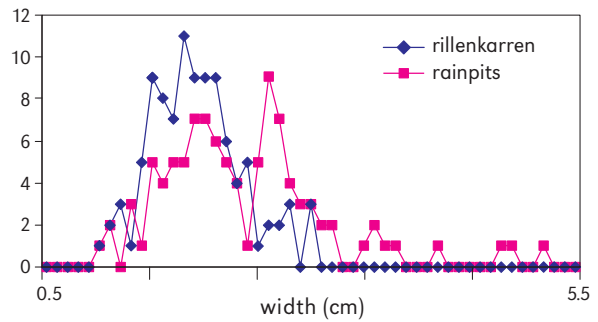


**Figure 10:** Frequency distribution of rainpit widths in El Colomer (Mallorca) compared to rillenkarren widths in the same locality.

ical point of view), the available documentation intimates that environmental conditions may enhance or inhibit the development of rainpits. The majority of occurrences (Smith, 1986; Goudie et al., 1989; Veni, 1994; Zhang, 1994) correspond to karst areas characterized by small amounts of rainfall, such as the Hamada de Meski (southeast Morocco), the Limestone Ranges (western Australia), the Edwards plateau (Texas, USA) or the Lhasa valley (Tibet, China) respectively. The presence of rainpits in places like Chillagoe (Queensland) and Serra de Tramuntana (Mallorca island) extends the distribution to tropical monsoonal and mediterranean climates, but in all the cases receiving less than 900 mm of precipitation per year.

White (1988) argues that rainpits “occur where the bare rock is exposed in climates in which minor etching can be preserved” and indicates that “rainpits are found on many limestones of the American southwest”. Veni (1994) agrees in this respect when he affirms that “...like cleft karren and tinajas (the Texan word for kamenitzas), rainpits are common in arid climates... but are often overlooked as just rough rock”. The presence of rainpits in desert karst terrains is also documented in north Africa (Morocco and Tunisia), with annual precipitation less than 200 mm (Smith, 1986; Smith et al., 1996; Nelhans and Svensson, 1997).

Several references confirm that rainpits are associated, in arid environments, with poorly developed rillenkarrren (Jennings, 1983; Smith, 1986; Smith et al., 1996; Veni, 1994; Nelhans and Svensson, 1997; Ginés, 1999a), but with increasing amounts of precipitation it appears that both kind of karren types are able to grow together in optimum conditions. The coexistence of well-developed rainpits and rillenkarrren was reported early from some well-known Australian locations, such as Napier Range and Chillagoe, as well as more recently from different Mallorcan locations at the periphery of the Serra de Tramuntana limestone range. However, the striking absence of rainpits in many Mediterranean karrenfields where conspicuous rillenkarrren are the dominant feature, as occurs in the main mountains of Mallorca, calls for some additional specific explanation.

Owing to the existence of good karren outcrops in Serra de Tramuntana, Mallorca, that are distributed along the climatic gradient of decreasing temperatures and increasing precipitation, over the whole range of altitudes from 0 to 1,450 metres a.s.l., these mountains can be regarded as an excellent natural laboratory for the study of karren assemblages. For this reason, within the framework of a wider research project, Ginés (1996a) developed a statistical sampling strategy in order to verify the observed extinction of rainpits with increasing altitude and eventually to elucidate the main factors involved in their development or inhibition. The sampling was carried out at 100 sites (each delimited by approximately 50 m<sup>2</sup> of karrenfield surface) where the presence of both, rainpits and rillenkarrren, were recorded using the following semi-quantitative scale: Abundant (10), Common (8), Frequent (6), Occasional (4), Rare (2) and Zero or Absent (0). The data show a clear overlapping of their distribution in the altitude range from 50 to 400 metres a.s.l., as well as extinction of the rainpits above 500 metres a.s.l. where conversely rillenkarrren become dominant. Over this “extinction limit” the rillenkarrren crests exhibit the typical herringbone pattern on the tops of the projecting rocks but rainpits are lacking. In

the case of Mallorca, the altitudinal “extinction limit” observed for rainpits corresponds approximately to the annual rainfall isohyet of 900 mm and mean annual temperatures around 15° to 16°C. These results, especially concerning precipitation amounts, are in good agreement with the data available from the Australian karrenfields of Chillagoe (Queensland) and Napier Range (western Australia), where rainpits and rillenkarrren constitute characteristic karren assemblages.

This study of rainpits exemplifies the usefulness of the environmental approach to the understanding of karren forms (the environmental approach is obviously complementary to the physico-chemical approach). It demonstrates that aridity is an important factor in the development of this specific karren feature. It seems that the recurrence of strong but short showers enhances the development of rainpits but the aridity is just enough to avoid the competitive substitution of the rainpit form by other forms that grow more efficiently with higher rainfall, as seem to be the case of rillenkarrren.

### Some provisional ideas about the genesis of rainpits

As early as 1979 Dunkerley pondered the idea that rillenkarrren develop from conjunction of rainpits into downslope sequences: solutional attack was presumed to begin at scattered points on a rock face, chains of depressions becoming connected and smoothed downslope. Dunkerley (1979) states clearly that in “those sites where solution pits (rainpits) are developed on nearly horizontal surfaces and grade directly into solution flutes (rillenkarrren) as the slope of the rock increases... the diameters of the solution pits are equivalent to the width of the flutes”. Macaluso and Sauro (1996b), again noting the similarities of widths and depths, discuss the possible genetic relationship of rainpits and rillenkarrren. If this is true, then one might expect a good morphological correlation in statistical terms. As discussed above,

the morphometric data from Queensland and Mallorca do lend support to this concept.

Dunkerley (1979) suggests, in the caption of a picture taken from a karren outcrop in Huon peninsula, that solution flutes [or rillenkarren] are “evolving from an irregularly pitted rock face” and remarks, in the text of the paper, on the presence of “lineations”, considered to be “suggestive of incompletely developed solution flutes”. These kinds of supposed early stages of rillenkarren that result from the “conjunction of the depressions giving the appearance of ill-formed flutes” (Dunkerley, 1979) are also a common feature in many sites of Mallorca (Figure 4). The joint occurrence of both karren types, in Chillagoe, Mallorca, and, as recounted by Dunkerley (1983), in Wee Jasper (New South Wales, Australia) and Huon (Papua, New Guinea), lends further support to the proposal of a genetic relationship. However, the work of Ginés (1996a) on the environmental limitations for both forms (above), indicates that they are not inter-dependent: both forms do develop in isolation from one another.

Macaluso and Sauro (1996b) suggest that rain-pit erosion appears to be result of some kind of “splash erosion” focused on the centres of depressions, while rills are also the result of similar “splash erosion” but not point-centered. It seems that the impact of the raindrop forces water out of the pits such that it does not usually flow over the rims. Thus the parabolic shape is maintained, but it requires that the effect of direct interception of raindrops is not significantly overshadowed either by the effects of overspilling flow down the sides of the pit or by the effects of water stagnation on the bottom of the pit. By this reasoning, splashing is probably an even more important factor for rainpits than for rillenkarren, owing to the different mechanisms of removal of spent solvent that are associated with each one. Nevertheless, rainpits can retain water and thus may have increased aggressivity from further dissolution of atmospheric CO<sub>2</sub> or biological action (both biochemical and biophysical).

Assuming that interception of raindrops can

explain the similarities in size and cross section between rillenkarren and rainpits (namely, their parabolic shapes), stagnation of water after rainfall may explain some of the differences observed between them. If pits fill with water, then their form might be more rounded than tapering, and eventually also larger. Rounded or flat bottoms could indicate that water stands temporarily inside the pit producing further dissolution and over-widening of the former hollow. The recurrent presence of small amounts of water and moisture in the hollow can also favour biokarst processes. Different kinds of biokarst borings are able to cause over-deepening of rainpits (Figure 11), as demonstrated in several Mallorcan sites.

### Summary of processes

If we presume that the geneses of rainpits and rillenkarren are related, then the processes of rillenkarren formation can be assumed to operate, at least to some extent, for rainpits (see chapter 16), although rainpits are likely to involve a slightly more complex suite of processes.

The chemistry of dissolution is probably restricted for most of the time during active rainfall to Bögli's (1960a) phase 1 and 2, but after a rainfall event stored water may move into phase 3. Obviously, sampling of karst waters from rainpits is necessary in order to understand the sequence of solutional events that can occur during and after short and recurrent storm showers.

Biological processes similar to those documented for rillenkarren by Fiol et al. (1996) are likely to be important, but have not yet been investigated. SEM studies of nano-scale features of rainpit cusps, walls and bottoms are suggested.

Physical processes are probably similar to rillenkarren but with variations. Mechanical impact of rainbeat is important, probably involving the removal of protrusions produced by preliminary biological weathering. Hydrodynamic controls are expressed through raindrop kinetic energy impinging on the rock surface through a thin film



**Figure 11:** Close-up of several rainpits from El Colomer (Mallorca), showing numerous biokarstic borings over the concave surfaces.

of water. Considerations of critical thickness of water film in relation to raindrop size and energy are presumed to be important. Rainpits form in a solutional environment of direct rainfall. The kinetic energy of raindrops cuts through the thin film of water keeping flow turbulent, causing rapid direct dissolution of the rock surface, rather than delayed dissolution after diffusion through a laminar sublayer. Rain splash, and sometimes also overspilling, continually renews the solvent. The discussion of the boundary layer model for rillenkarren (see chapter 16) is pertinent for rainpits. We feel that much of this is operative for rainpits and that several of the implications for rillenkarren are likely to be true also for rainpits. For example, kinetic energy of raindrops should control the thickness of film that can be penetrated and thus rainpit dimensions should vary with rain-

fall intensity. We also presume that controls on reaction rate such as rock solubility, temperature, turbulence of flow, and thickness of laminar layer should control rainpit dimensions and rate of formation. Rates of formation are likely to be similar to those of rillenkarren – of the order of  $10^3$  years for carbonates (Mottershead and Lucas, 2001).

## Acknowledgements

The authors thank Ken G. Grimes for photos (Figures 2, 6) and Ken G. Grimes and Joaquín Ginés for their very valuable comments and suggestions. This paper is a contribution to the investigation project CGL2006-11242-C03-01/BTE from the Ministerio de Educación y Ciencia-FEDER.





# RILLENKARREN

Joyce LUNDBERG and Angel GINÉS

Rillenkarrren – often referred to by the somewhat ambiguous *solution flutes* (ambiguous because the same term is used for quite different forms akin to *scallops* that develop under stream current activity on cave walls; Curl, 1966) – are small scale, straight, narrow, closely packed, parallel solution channels that head at the crest of a bare rock slope, and are extinguished downslope (Figure 1a, b, c). They develop on any soluble rock but are most commonly documented on carbonates. Their dimensions in limestone outcrops are typically 12–25 mm in width, 2–6 mm in depth and 100–300 mm in length. Individual flutes are parabolic in cross-section and are separated by sharply pronounced cusp lines described by Glew and Ford (1980) as “razor-sharp edges” (Figure 1b).

In plan view, they may form a simple suite of parallel flutes on a planar surface with “remarkable regularity of form and dimension” (Glew and Ford, 1980). Their development to either side of a crest often produces a herringbone pattern, where the original straight crest line is modified to a wiggly line between alternating rills (Figure 1d). On planar slope facets they rarely bifurcate. However, on convex slopes they will diverge, and on concave slopes they converge and are transformed into *runnels* (Figure 2c). Around a summit they may form a complex of rills splaying out in all directions from the crest centred around a suite of *rainpits* on top of the summit. Macaluso and

Sauro (1996b) note that mini-spikes may develop in the nodal points between the borders of contiguous rills or rainpits; these are especially apparent in the deep relief of salt, and where the rilled surface is convex (Figure 2c).

In long profile, rillenkarrren have a relatively constant width and depth for much of their length but decrease in depth before their downslope termination in the smooth planar surface with no channeled erosion, termed the *ausgleichsfläche* (Bögli, 1960a). It is often, but not always, a continuation of the rilled slope profile at the same slope angle. In certain places it appears to develop into a horizontal surface that is not related to bedding planes (Macaluso and Sauro, 1996b). All rillenkarrren, given an adequate expanse of homogeneous rock, will reach a characteristic length and give way to the *ausgleichsfläche*; however, in natural situations it is rare for a rock surface to be uninterrupted by inhomogeneities such as less soluble laminae, sedimentary structures, or fractures. Thus the *ausgleichsfläche* is not always evident in the field (Figure 2a, b). In discussing rills on gypsum, Stenson and Ford (1993) point out that the observed length is dependent on the down-slope extent of exposed bedrock.

In terms of worldwide distribution, rillenkarrren were first reported from alpine environments of Europe where they are widespread (e.g. Glatalp, Switzerland). They have since been reported

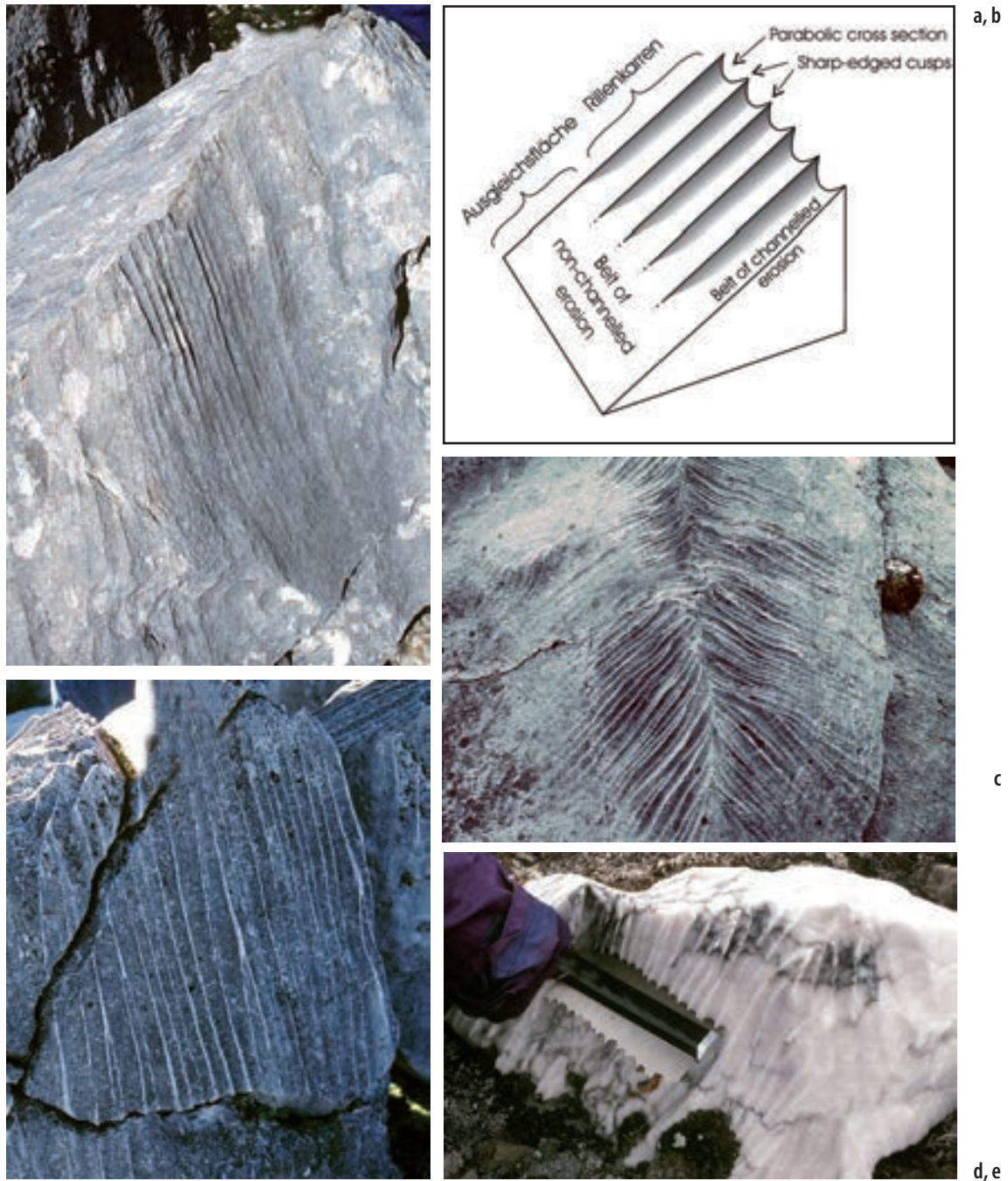


**Figure 1:** Typical simple rillenkarren: a. shallow rillenkarren on dolomitic limestones in Cortina D'Ampezzo, Italian Alps. These show all the typical features: they head at the crest of the block and extinguish downslope at the belt of non-channelled erosion, the *ausgleichsfläche*. The crustose lichens colonizing the rocks have no apparent effect on the rill profile. Width of view is 20 cm; b. diagram of rillenkarren showing typical features; c. sharp, deep rillenkarren on limestone of Wee Jasper, New South Wales, Australia. These do not naturally extinguish in the *ausgleichsfläche*; rather they are terminated by a fracture. Width of view is 45 cm; d. rillenkarren on a landslide block of limestone in Surprise valley, Rocky Mts, Canada. The herringbone pattern is created where rills form to either side of the originally straight crest line. Width of view is 90 cm; e. using the profile gauge to document rills on gypsum in Svalbard. These rills extinguish in the soil and vegetation mat. Width of view is 45 cm.

from many climates ranging from tropical monsoon (e.g. Chillagoe, Australia), to mediterranean (e.g. Mallorca island, Spain), and humid temperate (e.g. Trentino, Italy). Rillenkarren formation is inhibited in situations with cover of sediments or vegetation (e.g. many equatorial regions), where rainfall is limited (e.g. desert regions), where rainfall is of low intensity (e.g. British Isles), where the rate of non-dissolutional weathering or erosion exceeds the rate of rill formation (e.g. arctic regions), and where lithological characteristics of the rock are unsuitable (e.g. highly inhomogeneous texture).

## Classification and terminology

Rillenkarren are “small dissolutional forms” as defined by Macaluso and Sauro (1996b) where at least two of the three dimensions are measured in centimetres, but in general less than one metre long. Bögli (1960a, 1980) classifies them as a type of *free Karren* – they develop only on rock surfaces that are free of soil/vegetation cover. Ford and Lundberg (1987) and Ford and Williams (1989) introduce further constraints on genesis: rillenkarren are sited under “linear forms – *hydrodynamically controlled*”, and *gravitomorphic solution channels*. Ginés (2004) places them with “free karren, single” forms in a solutional environment of direct rainfall and within a scale limit of 1 cm to 1 m.

Rillenkarren forms were depicted in old descriptions of alpine karsts, and Eckert (1902) used the term *Kannelierungen*. In the early German literature they were called *Firstkarren* and more usually “Rillenkarren” (Bögli, 1951, 1960a; Bauer, 1962; Trimmel, 1965). Then, during the 1970s, Monroe (1970), Jennings (1971), Sweeting (1972), and Gèze (1973) spread the term “rillenkarren” into the international literature. In this way rillenkarren become a synonym of *solution flutes* (after the translation suggested by Jennings, 1971) as well as equivalent to the French word *canne-lures*.

## Rillenkarren morphometry

Many morphometric studies of rillenkarren on carbonates have been reported: (e.g. Belloni and Orombelli, 1970; Heinemann et al., 1977; Lundberg, 1977a; Dunkerley, 1979, 1983; Goudie et al., 1989; Bordoy and Ginés, 1990; Zhang, 1994; Vincent, 1996; Mottershead, 1996a; Crowther, 1998; Gil, 1992; A. Ginés, 1990, 1996a, 1998a). Similar studies on other soluble rocks are few (e.g. Stenson and Ford, 1993, measured flutes on gypsum). Mottershead et al. (2000) tried to address this paucity of comparative data on non-carbonates by measuring a small number of rillenkarren on a great variety of sites on limestone, gypsum and salt. Most of the discussion below relates to data from carbonates only.

### Protocol for rill morphometric measurements

Typical measures reported for rillenkarren morphometry are width, depth, length, and slope angle. Often a profile is taken of the rill cross section with a carpenter’s profile gauge whose pins conform to the shape of the rills (Figure 1e). However, the measures are not necessarily taken in the same way.

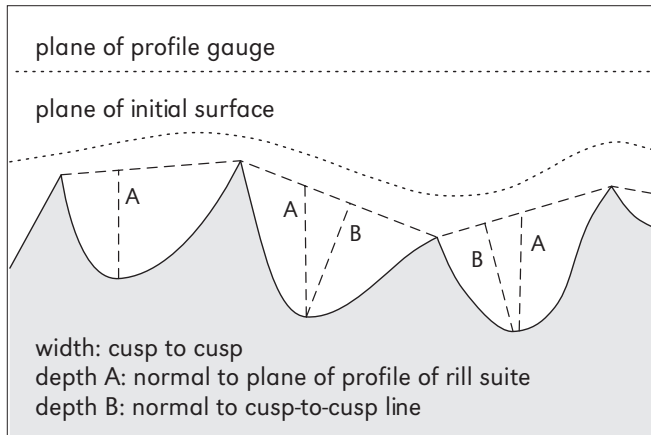
Width is relatively clear cut: it is the distance between cusps. Thus width data in the literature are probably reliable and consistent.

Depth is not as clear. Depth is a measure of surface denudation and thus ought to be from a presumed original surface. In most cases this may be the plane of the profile gauge but this is correct only if this plane conforms to the tops of most of the cusps. If the cusp top is regarded as the original rock surface, then depth has to be measured normal to the cusp-to-cusp line. Figure 2d shows how this may yield a smaller depth. Most publications do not clarify their depth measurement protocol and thus may not be directly comparable.

Length data in the literature are also sometimes problematic. Length is often constrained by rock



a, b



c, d

**Figure 2:** Complex rillenkarren, and some of the difficulties encountered in field documentation: a. rillenkarren developing on the tops of formerly rounded sub-soil pinnacles, Wee Jasper, New South Wales, Australia. This illustrates one of the difficulties in measuring true rillenkarren length – the smooth rock just above the soil may not be the *ausgleichsfläche*; rather it may simply be an indication of recent soil retreat; b. rillenkarren in natural rock salt, Cardona, Spain. The rill form is continually interrupted by detrital bands in the rock; the exact position of the crest of each rill is not clear; and the *ausgleichsfläche* is not clear. The rills in the foreground appear to extinguish, but those in the background do not; c. very sharp, deep rills in rock salt of Cardona, Spain. Width of view is 65 cm. These show the mini-spikes between the borders of contiguous rills mentioned by Macaluso and Sauro (1996b). The forms in the foreground are a mixture of deep, asymmetrical pits, mini-spikes, and rills. This also shows two channels that are not rillenkarren: both are fluvial channels (i.e. *rinnenkarren*) from concentration of drainage in a concavity. The one is the wide channel of rectangular cross section, the second is the wide channel on the left-hand side where the original rill cusps are being destroyed; d. measurement protocol for rillenkarren width and depth.

properties (joints, variations in texture, length of rock face available, and length of rock face available at an appropriate angle; Figure 2a, b) rather than hydrodynamic properties. Mottershead et al. (2000) observe that flute length is defined by the length of the divides, the flute ending where the divides die out downslope. The only measure of true rill length has to be from the crest to the *ausgleichsfläche* (e.g. Ginés, 1996b; Crowther, 1998). If this is not possible, length must be reported as a minimum and not included in the general calculations of averages. Ginés (1996b, 1999a) measured every tenth longest rill in a set on the assumption that the longest rills represent the potential length. For all length measurements, care must be taken to correctly identify any abnormally long rills caused by Glew and Ford's (1980) *edge effect* where water drains over the side edge of the block.

Although rill depth is relatively constant down-rill, a further detail that ought to be specified is the position down-rill at which the profile was measured. Ginés (1996b) took profiles 5 cm below the crest, Mottershead (1996a, b) at 10 cm from the crest, while Lundberg (1977a) and Crowther (1998) chose a distance proportional to the rill set under study, midway down-rill. Mottershead (1996a, b) limited sources of variation by sampling only the straight slope facets; this eliminated the convergent or divergent rills that occur on curved slopes.

Slope angle is unambiguous to measure. Slope of the *ausgleichsfläche* is rarely included, but ought to be.

Several studies have included a measure of the parabolic profile. Dunkerley (1983) and Mottershead (1996b) fitted a parabolic function to the rill profile. Crowther (1998) provided an asymmetry index in addition to fitting a curve to each side of the rill profile. Both Lundberg (1977a) and Crowther (1998) provide a measure of the sharpness of the inter-rill cusp.

The general problems of field sampling apply here. The definition of the population to be sampled is not always clear (see discussion of non-

rillenkarrren rills below). Random sampling is typically assumed (e.g. Lundberg, 1977a; Ginés, 1996b) although rarely specified. Selective sampling may be required in order to limit complexity of controls (e.g. Mottershead, 1996b). In places with few rillenkarrren, sampling strategy may be reduced to taking all samples that can be found.

## Rillenkarrren morphometry on carbonate rocks

### WIDTH, DEPTH AND CROSS-SECTIONAL PROFILE

Table 1 summarizes data for rills in carbonates from many regions of the world. Figure 3 shows width (W) to depth (D) graphs for our data from various parts of the world. Several general patterns emerge from these data. Rills on carbonates have width limits of ~5 to ~50 mm and depth limits of ~0.5 to ~20 mm. All regions show a strong relationship of width and depth (by simple power functions). Both Crowther (1998) and Mottershead (1996a, b) report a significant relationship of width and depth for the rills at Lluc, Mallorca. In general depth is more variable than width, both within rills and between rills. Mottershead (1996b) reports a small increase in rill width downslope, while depth increases from the head to a maximum at 0.25 mm to 0.35 mm of the down-rill length. Flutes are shallower on steeper slopes (Mottershead, 1996b). Ginés (1996b, 1999a) shows a very slight positive skew for rillenkarrren width frequency distributions but mean and modal values are almost the same; the depth frequency distributions do show a distinct positive skew. Because of a moderate positive skew, Mottershead et al. (2000) report only median values but all other publications quote mean values.

Not all these data are equal in reliability. The median values from Mottershead et al. (2000) are included at the end of the table. These data are from a small number of samples over a great variety of climates and some of the individual values are rather strange. For roughly normal distributions, means and medians should be compara-

**Table 1:** Rillenkarren morphometric data for carbonate rocks. Each measure is given (where available) as mean, standard deviation and number of samples. The data from Mottershead et al. (2000) are not quite comparable with all the others since they are given as median rather than as mean values, in acknowledgement of the skew of the distribution.

Location	Lithology	Width (cm)	SD	n	Depth (cm)	SD	n	W/D	Length (cm)	SD	n	Reference
Svalbard island (Norway)	marble	1.37	0.5	60	0.19	0.1	29	6.63	12.7	7.3	8	unpublished data
Surprise Valley, Rockies (Canada)	limestone	1.4	0.3	113	0.35	0.2	113	4.54	18.36	6.7	53	unpublished data
Surprise Valley, Rockies (Canada)*	limestone	1.132	0.2	38								Glew and Ford, 1980
Istria (Croatia)	limestone	1.7							16			Ford and Lundberg, 1987
Istria (Croatia)	limestone	1.54	0.4	72					16.3	4.7	36	unpublished data
Luc, Mallorca island (Spain)	limestone	1.72	0.3	150	0.46	0.1	150	3.93	24.2	14	150	Mottershead, 1996a
Luc, Mallorca island (Spain)	limestone	1.59	0.3	30	0.44	0.1	30	3.82				Mottershead, 1996b
Luc, Mallorca island (Spain)	limestone	1.82	0.6	20	0.42	0.2	108	4.17	19	6.1	20	Crowther, 1998
Ses Parades, Mallorca island (Spain)	limestone	1.76	0.6	100	0.29	0.1	100		19.5	6.9	100	Ginés, 1996b
Vall den Marc, Mallorca island (Spain)**	limestone	1.84	0.5	200	0.49	0.3	200	5.23	22.7	8.3	200	Ginés, 1996b, 1999a
Tramuntana range, Mallorca (Spain)#	limestone	1.64	0.7	2,590	0.5	0.2	1,200		25.3		480	A. Ginés, 1990, 1996b, 1999a; Bordoy and Ginés, 1990
Mortero de Astrana, Cantabria (Spain)	limestone	1.69	0.5	100	0.27	0.2	100		17.9	8.4	100	Ginés, 1996b
La Safor, Valencia (Spain)	limestone	1.8	0.5	49	0.4	0.3	49		12.5	6.1	49	Gil, 1989, 1992
Barx, Valencia (Spain)	limestone	1.43	0.5	100								Ginés, 1999a
La Madalena, Valencia (Spain)	limestone	1.6		300								Pérez-Cueva and Simón, 1979
Grazalema, Andalusia (Spain)	limestone	2.52	0.9	100								Ginés, 1996b
Coolman Plain, New South Wales (Australia)	limestone	1.6	0.5	277					11.6	3.6	277	Dunkerley, 1979
Wee Jasper, New South Wales (Australia)	limestone	1.9	0.6	293					34.8	18	293	Dunkerley, 1979
Chillagoe, Queensland (Australia)	marble	1.52	0.7	680	0.44	0.3	680	3.91				Lundberg, 1977a
Chillagoe, Queensland (Australia)	limestone	1.95	0.7	1,174	0.84	0.4	1,174	2.73				Lundberg, 1977a
Chillagoe, Queensland (Australia)	marble	1.74	0.5	555					22.5	14	555	Dunkerley, 1983
Chillagoe, Queensland (Australia)	limestone	2.08	0.8	428					33.5	21	428	Dunkerley, 1983
Napier Range, Western Australia (Australia)	limestone	1.95	0.8	626								Goudie et al., 1989
Griqualand West, Transvaal (South Africa)	dolomite	1.36										Marker, 1985
Griqualand West, Transvaal (South Africa)	dolomite	1.76										Marker, 1985
Griqualand West, Transvaal (South Africa)	dolomite	1.85										Marker, 1985
Gait Barrows, England (U.K.)	limestone	1.81		50								Vincent, 1996
Amside, England (U.K.) / coastal site##	limestone	1.72		100								Vincent, 1996
Moelfre, Wales (U.K.) / coastal site##	limestone	2.09		32								Vincent, 1996
Black Head, Burren (Ireland) / coastal site##	limestone	1.68		50								Vincent, 1996
Lhasa, Tibet (China)	limestone	1.08		204	0.71		204		11.3		204	Zhang, 1994
Dingri, Tibet (China)	limestone	1.9		74	0.42		74		20.4		74	Zhang, 1994
Amdo, northern Tibet (China) / over 4,500 metres a.s.l.	limestone	1.6		93	0.39		93		19.3		74	Zhang, 1994
Batu Pala, Sarawak (Malaysia)	limestone	1.74	0.6									Osmaston, 1980
Dachstein (Austria)	limestone								12.7	7.2	505	Heinemann et al., 1977

Location	Lithology	Width (cm)	SD	n	Depth (cm)	SD	n	W/D	Length (cm)	SD	n	Reference
Prealpi Veronesi (Italy)	limestone						410		14.0			Henemann et al., 1977
Podcib and Zabaret sites, Carso di Monfalcone (Italy)	limestone	2.0		49	0.7		49	2.63	15.6			Belloni and Orombelli, 1970
Borgo Grotta Gigante, Carso di Trieste (Italy)	limestone	2.4		88	0.8		88	2.94	20.0			Belloni and Orombelli, 1970
Sieben Hengste, Berner Oberlandes (Switzerland)	limestone	1.67	0.4	100								Ginés, 1998a
Bödemern, Schwyz (Switzerland)	limestone	1.5	0.4	200								Ginés, 1998a
Vallon des Morreys, Fribourg (Switzerland)	limestone	1.54	0.4	100								Ginés, 1998a
Lapis de Grand'gouilles, Valais (Switzerland) / 2,475 metres a.s.l.	limestone	1.44	0.3	50								Ginés, 1998a
<b>Mean of all values</b>		1.69			0.44			4.37	19.23			
<b>SD</b>		0.28			0.16			1.15	6.62			
<b>1 SD range: low</b>		1.41			0.26			3.22	12.61			
<b>1 SD range: high</b>		1.97			0.60			5.52	25.85			
		Median		n	Median		n	Median	Median		n	
Wee Jasper, New South Wales (Australia)	limestone	4.09			1.66			2.45	44			Mottershead et al., 2000
Buchan W, Victoria (Australia)	limestone	2.27			1.29			2.33	35			Mottershead et al., 2000
Buchan MR, Victoria (Australia)	limestone	2.25			0.39			4.83	35			Mottershead et al., 2000
Buchan PH, Victoria (Australia)	limestone	1.7			0.25			6.5	20			Mottershead et al., 2000
Lassithi, Crete (Greece)	limestone	2.06			0.72			4.07	32			Mottershead et al., 2000
Lluc, Mallorca island (Spain)	limestone	1.7			0.44			3.63	22			Mottershead et al., 2000
Es Molí, Mallorca island (Spain)	limestone	1.51			0.53			3.55	28			Mottershead et al., 2000
Black Head, Burren (Ireland)	limestone	1.6			0.35			4.99	30			Mottershead et al., 2000
<b>Summary of these 8 sites</b>		1.81		~600	0.47		~600	3.77	30			

\* reconstructed from Glew and Ford, 1980 (Figure 5)

\*\* W/D calculated from Ginés, 1999 (Table XIII)

# data from many altitudes, length is slightly overestimated by selective sampling

## coastal sites not included in means



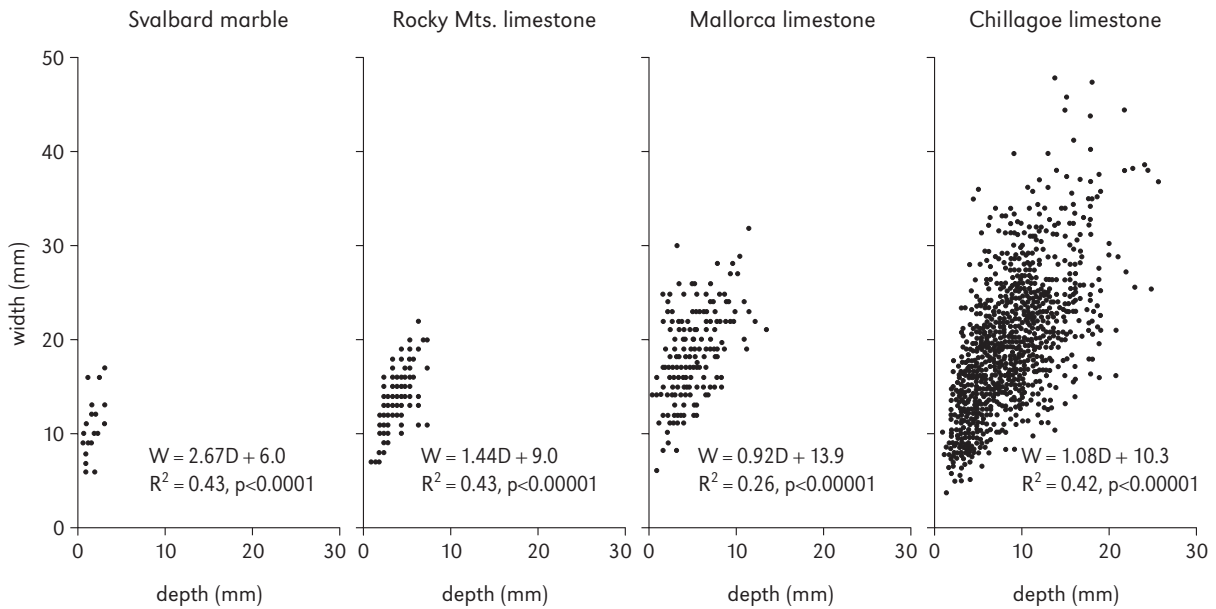


**Figure 3:** Width/depth graphs for rillenkarren: marbles in Svalbard (arctic climate), unpublished data; limestones in Rocky Mts, Canada (continental/mountain climate), unpublished data; limestones in Mallorca, Spain (mediterranean climate), from data in Ginés (1999b); limestones in Chillagoe, Queensland (tropical monsoon climate), from data in Lundberg (1977a). For a parabolic profile,  $W = \sqrt{4D/a}$ , shown by the red line.

ble: although they claim that values of flute size are comparable, the data from Mottershead et al. (2000) for Wee Jasper (median width of 4.09 cm) seems to be very strongly out of keeping with Dunkerley's (1979) data from the same region (mean width of 1.9 cm) and out of line with other rill width measurements.

Most rills are reported as having a parabolic profile (e.g. Glew and Ford, 1980) but it is not often quantified by means of curve fitting. Crowther (1998) reports that 80% of the rills studied in Mallorca are parabolic, but asymmetrical sides are common. He also reports some rectilinear rills considered to be truncated or immature forms. For a simple parabolic function of the form  $y = ax^2$ , lower values for  $a$  indicate a more open parabola, and higher values a more closed parabola. When depth  $D$  and width  $W$  are measured in mm,  $a$  has the unit  $\text{mm}^{-1}$ . Thus  $D = a(W^2/4)$  and  $W = \sqrt{4D/a}$ . Mottershead (1996a, b) reports an  $a$  value of 0.075, and Crowther (1998) 0.073, for Lluc, Mallorca. Figure 3 shows fits of width versus

depth. For our Chillagoe data (fitting a parabolic profile to the width and depth data) the best fit value for the constant is 0.073, so the equation of the relationship is  $W = \sqrt{4D/0.073}$ . However, if the anomalously large, shallow rills are omitted (< 2% of the data), the constant that best fits is  $0.077 \text{ mm}^{-1}$ . The data from the Rockies fit well to a constant of  $0.065 \text{ mm}^{-1}$ , and, less well, Mallorca to  $0.051 \text{ mm}^{-1}$ , and Svalbard to  $0.053 \text{ mm}^{-1}$ .

The profile of the developing rill changes as the forms enlarge: our data indicate that the parabolic profile becomes more closed as the rills are incised until the form reaches equilibrium. If depth is used as an indicator of development, and  $W/D$  ratio as an indicator of profile, a plot of  $W/D$  ratio against  $D$  shows the changes (Figure 4). If all rills from the same population conform to the same parabolic profile, then the relationship is simply  $W/D = \sqrt{4/aD}$  or  $W/D = \text{const} \cdot D^{-0.5}$  and the exponent should be  $-0.5$ . However, as Figure 4 shows, the exponents for our data are slightly higher because the values for  $a$  that best fit the majority of

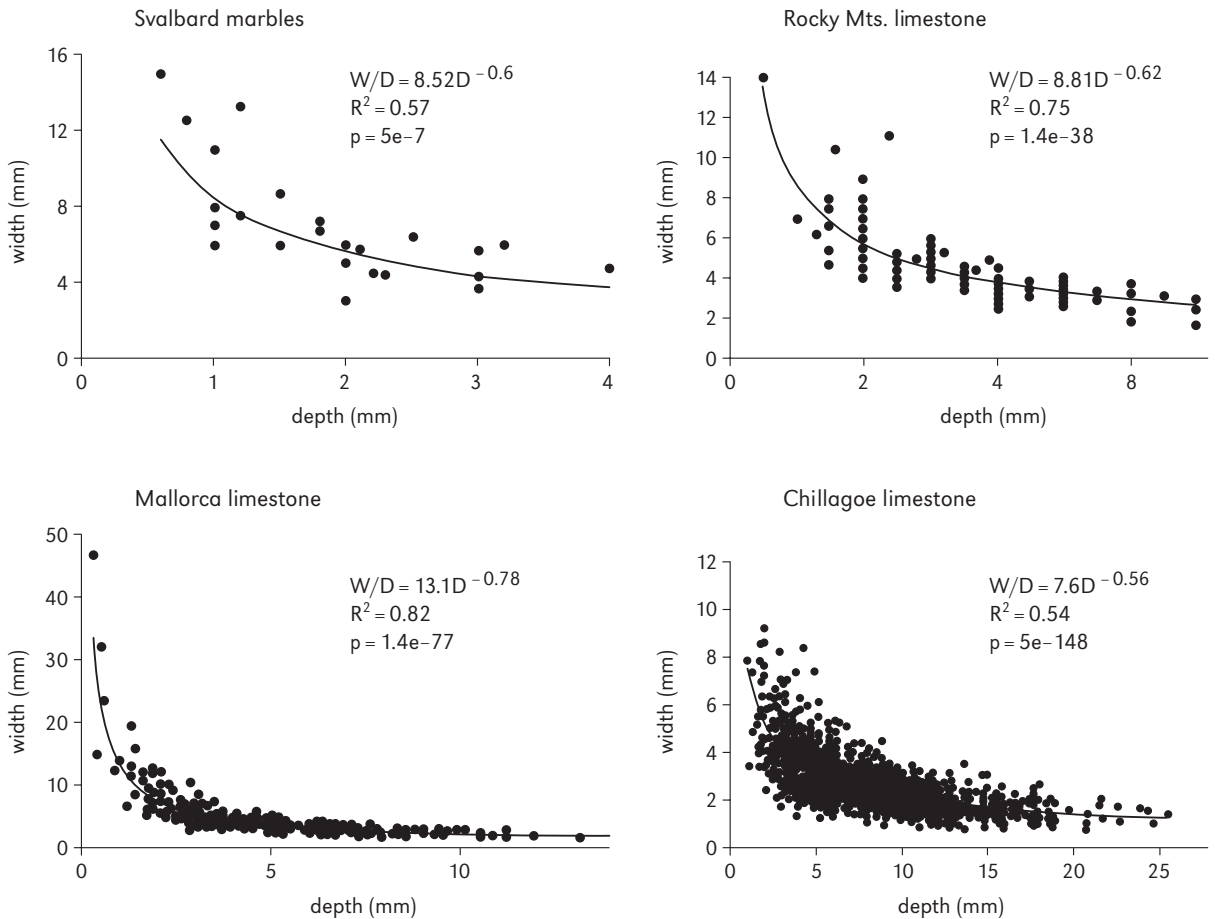


**Figure 4:** Change in width/depth ratios with rillenkarren development: marbles in Svalbard, unpublished data; limestones in Rocky Mts, Canada, unpublished data; limestones in Mallorca, Spain, data from Ginés (1999b); limestones in Chillagoe, Queensland, data from Lundberg (1977a).

the data somewhat underestimate  $W/D$  for the smallest rills. For Rockies rills  $< \sim 3$  mm in depth  $a = 0.04 \text{ mm}^{-1}$ , the value of  $a$  rises to  $0.065 \text{ mm}^{-1}$  for the majority of the population (as shown in Figure 3). For Mallorca rills  $< \sim 3$  mm in depth  $a = 0.03 \text{ mm}^{-1}$ , rising to the standard value of  $0.051 \text{ mm}^{-1}$ . Chillagoe is closest to the ideal parabolic population with  $a = 0.06 \text{ mm}^{-1}$  for the small rills, increasing to  $0.073 \text{ mm}^{-1}$  for the majority of the population. This shift in form with development is also apparent if the relationship between depth and the size of circle that fits into the base of the rill is used as an indicator of profile (e.g. for Chillagoe data; Lundberg, 1976).

#### RELATIONSHIP OF RILLENKARREN WIDTH/DEPTH AND CLIMATE/ALTITUDE

From Figures 3 and 4 it is apparent that all regions have the smallest rills but the cooler the region the smaller the maximum size. Thus rill size appears to be related to climate. However, width is relatively invariant ( $1\delta = 14\%$ ), so the majority of the relationship with climatic variables is of depth ( $1\delta = 37\%$ ). In the absence of climate data for most of the published sites we have estimated mean annual temperature and precipitation values (www.worldclimate.com, means from 1861–1989). Width (linear or log scale) proves to have no significant relationship with precipitation or with temperature.

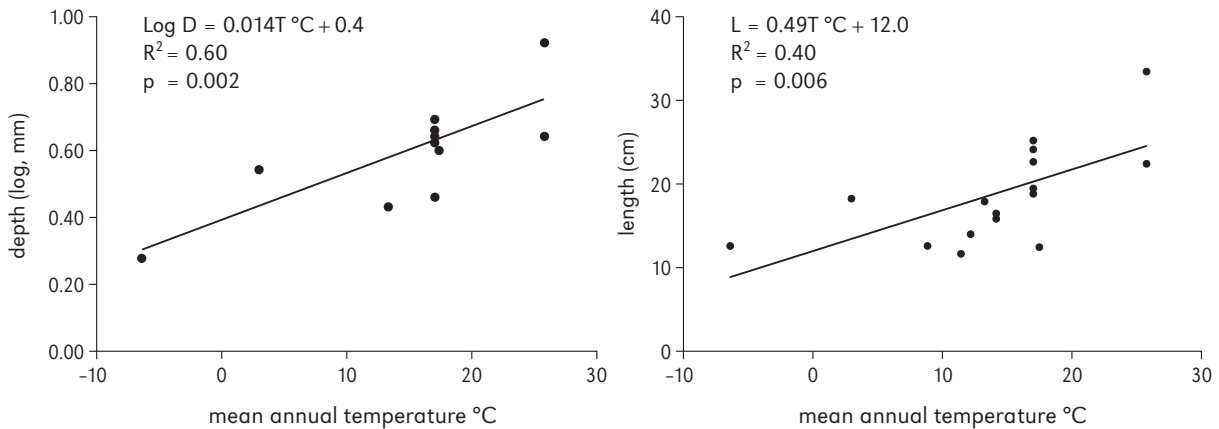


**Figure 5:** Rillenkarren from sites in Table 1: left. relationship of depth (log) with mean annual temperature; right. relationship of length with mean annual temperature. Temperatures are from the nearest climate station, rather than the actual site.

Depth (log scale) shows no relationship with precipitation, but a relatively strong one with temperature:  $R^2 = 0.60$ ,  $p = 0.002$  (Figure 5, left).

Ginés’ (1996b) study of the relationship between rillenkarren and altitude shows very clear results. He measured rillenkarren from nearly 100 sites in Mallorca, at altitudes ranging from ~150 to ~1,150 metres a.s.l. No relationship of width and altitude is apparent but depth (log) shows a very clear negative relationship with altitude (re-plotted in Figure 6, left:  $R^2 = 0.91$ ,  $p = 1.5e-6$ ). Rill depth varies from 0.63 cm down to 0.28 cm over the 1,000 m range (Bordoy and Ginés, 1990; Ginés, 1999a). Temperature decreases and rainfall increases with altitude. Thus the relationship is with climate. So we can say that rill depth is lowest at high rainfall and low temperatures, but, from these data, the two effects can not be separated out.

#### RILLENKARREN LENGTH

Length data are summarized in Table 1. The published values that are only estimates of maximum and minimum sizes, have not been included here. Mean lengths range from ~10 cm to ~35 cm.

#### RELATIONSHIP OF RILLENKARREN LENGTH AND CLIMATE/ALTITUDE

Plotting length against the estimated mean an-

nual temperatures and rainfall for each site yields no relationship with precipitation but a weak one with temperature:  $R^2 = 0.40$ ,  $p = 0.006$  (Figure 5, right – omitting the exceptionally long rills from Wee Jasper – with the Wee Jasper point included  $R^2$  is only 0.30,  $p = 0.02$ ). The relationship is presumably governed by viscosity. Dreybrodt and Kaufmann (see chapter 2) test these data against their theoretical models and find a relatively close relationship. Of course, empirical data include a variety of rainfall intensities and slope angles so the data do not fit perfectly.

Ginés’ (1996b) study of rills in Mallorca shows a much more clear relationship of length with climate using altitude as a proxy for increased rainfall and decreased temperatures (re-plotted in Figure 6, right). Here the  $R^2$  value is a robust 0.75 ( $p = 1e-11$ ). Rather than using the mean length of all rills, Ginés plots the mean of every tenth longest rill in each set (assuming these to represent the “optimal” rill length for each sampled location). This relationship is clearest if the few sites receiving less than 800 mm per annum of precipitation are eliminated (A. Ginés, 1990, 1999a). Rill length varies from ~50 cm at 100 m a.s.l. to ~10 cm at 1,200 m a.s.l. Dreybrodt and Kaufmann (see chapter 2) use these data in their model, assuming that rainfall intensity and water

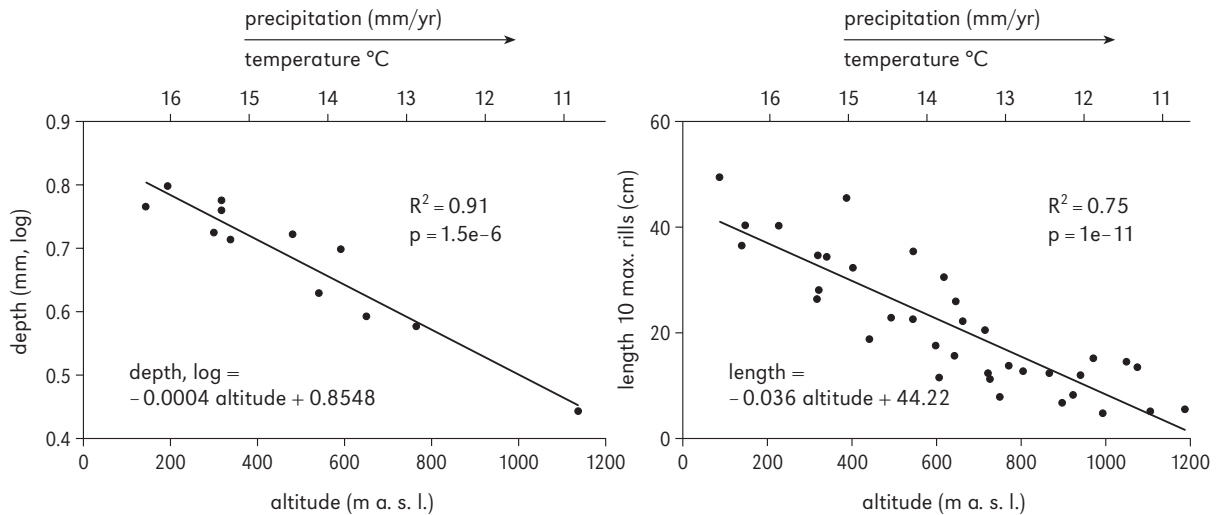


**Figure 6:** Rillenkarrren of Serra de Tramuntana, Mallorca island, Spain: left. relationship of rill depth with altitude; right. relationship of rill length with altitude. Data from Ginés (1996b). Temperature and precipitation values are estimated from Palma de Mallorca mean annual values (17°C, 461mm, 4 m a.s.l.), using the climatic gradients for Serra de Tramuntana of  $-0.65^\circ\text{C}$  per 100 m, and  $+80$  mm of rainfall per 100 m.

viscosity (temperature) vary with altitude (and ignoring other variables such as ranges in slope and rainfall intensities) to calculate the expected lengths. While not mirroring the empirical data precisely, the predicted lengths are relatively close. That empirical data can be approximated by equations based on hydrodynamics alone, is important for consideration of rillenkarrren formation (see discussion below).

#### RELATIONSHIP OF RILL LENGTH AND SLOPE

The simulations of Glew and Ford (1980) yield a very strong direct relationship of rill length and slope ( $R^2 = 0.92$ ). Natural rills are not so simple, but they do seem to show a relationship; e.g. Ford and Lundberg (1987) find a weak relationship for data from various field sites ( $R^2 = 0.31$ ,  $p = 1e-6$ ). It is of interest that Dunkerley (1979), working in NSW (Australia), reports a very weak to non-existent relationship with no significant change in flute length over the  $30-80^\circ$  slope range, although slopes of  $< 30^\circ$  have shorter flutes. Ginés (1999a) also reports no relationship of rill length and slope for several sites in mainland Spain and Mallorca.

Further studies from field sites have partly

clarified the issue. Figure 7 shows rill length in relation to slope for various sites. All regions show optimum development within a slope range of  $\sim 20^\circ$  to  $\sim 80^\circ$ , although there is some indication that the cooler regions have rills on more gentle slopes. Three of them show a positive relationship of length and slope, but the data from Mallorca (Ginés, 1999a) do not clearly show this.

It may be that the data of Ginés (1999a) and those of Dunkerley (1979) include many slope types and complex rills. In order to limit complexity, Mottershead (1996a, b) chose only those rills with unconstrained length on simple planform slopes of constant gradient with no apparent joints and approximately horizontal crest lines. These rills, from Lluc, Mallorca, demonstrate strongly that length does vary with slope: cosine of slope angle and log of flute length show  $R^2$  values of 0.31–0.62,  $p < 0.01$ . Crowther (1998), also working at Lluc, confirms this relationship. Following the theoretical considerations of Dreybrodt and Kaufmann (see chapter 2), it is more correct to consider the relationship of tangent of slope and length (as shown in Figure 7 – the fitted lines are empirical; see chapter 2 for a discussion of the theoretical

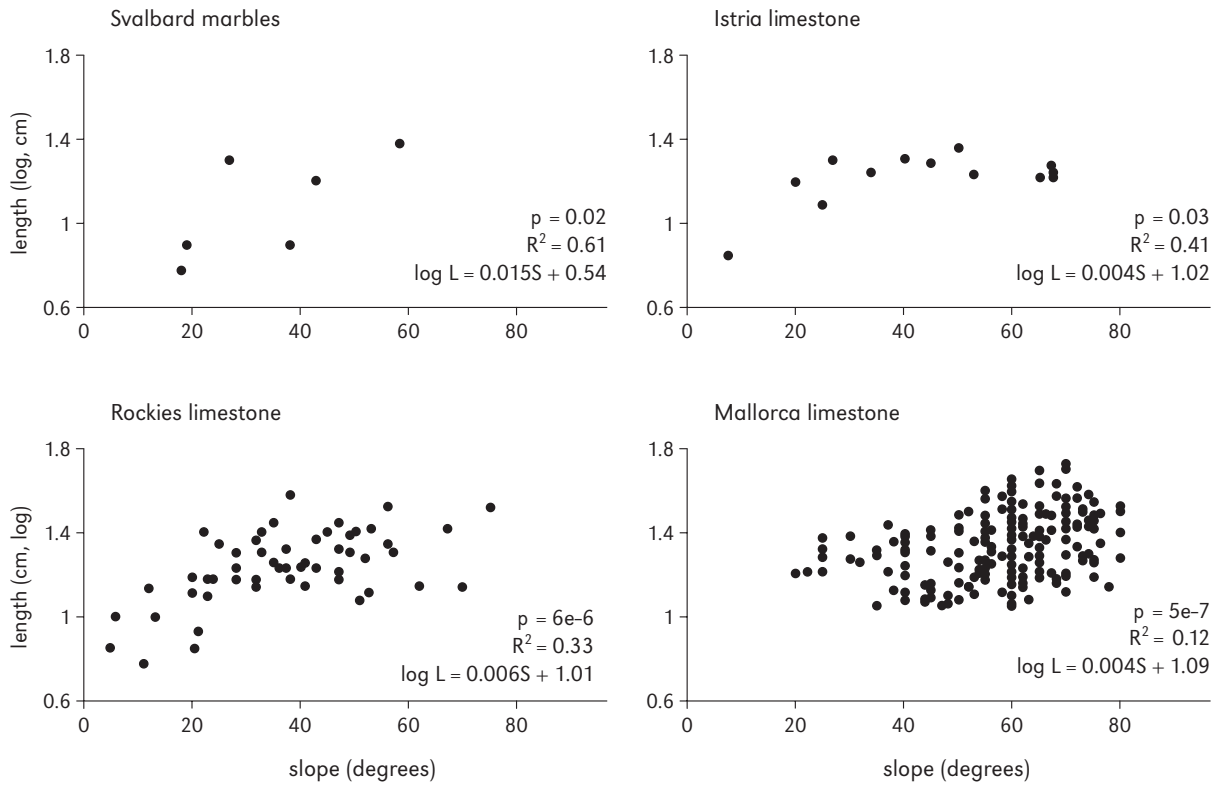


**Figure 7:** Rillenkarrén length in relation to slope for marbles in Svalbard (unpublished data), limestones in Istria, Croatia (unpublished data), limestones in Rocky Mts, Canada (unpublished data), and limestones in Mallorca (data from Ginés, 1999a).

relationships using these data). The relationships displayed by field data are of course complicated by variations in temperature, slope angle, rainfall intensity, and surface roughness. Nevertheless, they conform reasonably well to the model. The implications of this are further discussed below in the section on rillenkarrén formation.

**RELATIONSHIP OF RILL MORPHOMETRY AND LITHOLOGY OF CARBONATES**

The role of lithological variations has been of interest since the earliest morphometric studies on rillenkarrén (e.g. Lundberg, 1977a, b; Dunkerley, 1979, 1983; Marker, 1985; Goudie et al., 1989). The different lithological characteristics that have been examined, include homogeneity, grain size, and surface roughness.

The first question is how lithological variations

affect presence or absence of rillenkarrén. High purity, high hardness, and low porosity seem to be important. Sweeting (1972) observes that rills are best developed on dense, massive, fine-grained, strong/hard rocks. Marker (1985) reports that rillenkarrén on hard Precambrian dolomitic limestones in south Africa are restricted to beds that are dense with regular grain size and low impurities, and that the best rills develop on rocks with closely packed, homogeneous, small crystals. Goudie et al. (1989) note that hardness and low porosity are probably necessary pre-disposing conditions but are not the sole explanation for rill development, at least in western Australia.

Homogeneity is normally required: rillenkarrén are very irregular in form where fossils dominate rock texture. Goudie et al. (1989) report that only the more pure and homogeneous beds in

the limestones of western Australia develop rills. However, Mottershead (1996b) notes that the limestones of the classic karren site at Lluc, Mallorca, are fine-grained, hard, pure, with low dolomite content, but they are not very homogeneous.

Vincent (1996) notes that rillenkarrren-bearing rocks in the British Isles are all very hard, extremely pure and dolomite-poor. Both for his data from UK and for data from western Australia from Goudie et al. (1989), he shows that % calcite in fabric and % calcite in cement is the key to explaining rill presence or absence.

Grain size/shape may be important where it affects friability. Sweeting (1972) indicates that rills do not form where rock disintegrates, such as some marbles and dolomites. Ford (1996) attributes the scarcity of rillenkarrren on dolostones of Canada to the medium- to coarse-grained character of the rock.

The second major question is how lithological variations affect the morphology of rillenkarrren. Again, no clear pattern emerges from the literature. Grain size is generally presumed to be important. Glew and Ford (1980) argue, from evidence of simulations, that flute width increases with increasing grain size. However, this is not true for Chillagoe, Australia. Both Lundberg (1977a, b) and Dunkerley (1983) find significantly larger rills on fine-grained but less homogeneous fossiliferous reef limestone compared to rills on coarsely crystalline marble. Lundberg suggests that the rills on the marbles are destroyed by exfoliation before they reach maximum size. Dunkerley, also finding significant differences between groups within the reef limestones, suggests that grain-size is only one of the variables. Marker (1985) also finds smaller rills on the coarser-grained rocks of Kimberley, south Africa, and larger rills on the dense, fine-grained rocks. However, it is apparent from her data table that several of the dense, fine-grained beds do not show rillenkarrren at all. Mottershead et al. (2000), in a study of “lithological control of solution flute form”, observe significant variations in flute size between limestone sites but fail to give details of lithological variations.

## Rillenkarrren morphometry on evaporite rocks

Rillenkarrren on other soluble rocks have been studied very much less often than on carbonates. Nevertheless there is enough photographic (e.g. Figures 1e, 2b, c) and morphometric data (Table 2) to confirm that rillenkarrren on evaporite rocks are fundamentally similar. Rigorous statistical data have been published for only three locations: Nova Scotia, Canada (Stenson and Ford, 1993), Spain and UK (Mottershead et al., 2000). Unpublished data from Svalbard have been added to Table 2. The rills in Svalbard are forming on anhydrite. The process of hydration is clearly destroying rills, but their size – comparable with those from Nova Scotia and UK – suggests that they have reached maturity. The rills in Spain are slightly larger than the others. Macaluso and Sauro (1996b) give estimates of < 2 cm for rill width and 0.4 to 1.5 cm for depth in gypsum of another Mediterranean region, south-west Sicily. These are considerably higher values than the others, but without a rigorous treatment of data, they have not been included in the table.

These few data do not allow any relationships with slope or climate to be tested. Mottershead et al. (2000) have measured lengths and slope angles but present only the median values for each. Thus we cannot assess the relationship of slope and length. Average length for rills on gypsum in Svalbard are 12.7 cm, in Spain 12.0 cm (median value, Mottershead et al. 2000), and in Glew and Ford’s (1980) simulation, 14.2 cm.

### RELATIONSHIP OF RILL MORPHOMETRY AND LITHOLOGY OF EVAPORITES

The data available do not allow a rigorous assessment of the relationship of rock properties and rill morphology. General observations indicate that lithology is significant, perhaps more to the occurrence of rillenkarrren than to the morphology. For example, Stenson and Ford (1993) note that rills are somewhat more likely to form on anhydrite than on the more friable gypsum. Calaforra

**Table 2:** Rillenkarrren morphometric data for evaporite rocks. Each measure is given (where available) as mean, standard deviation and number of samples. The data from Mottershead et al. (2000) are not quite comparable with all the others since they are given as median rather than as mean values, in acknowledgement of the skew of the distribution.

Location	Lithology	Width (cm)	SD	n	Depth (cm)	SD	n	W/D	Length (cm)	SD	n	Reference
Svalbard	anhydrite	0.92	0.25	114	0.35	0.2	50	2.94	12.68	7.33	8	unpublished data
Nova Scotia, Canada	gypsum	0.8	0.15	226	0.26	0.18	226	4.64				Stenson and Ford, 1993
UK	gypsum	0.89#		~100	0.27#		~100	3.82#	13*		1	Mottershead et al., 2000
6 sites in Spain#	gypsum	1.09#		~750	0.37#		~750	3.64#	10*		3	Mottershead et al., 2000
Mean		0.92	0.12		0.31	0.05		3.76	11.9	1.6		
1 SD range		0.80–1.05			0.25–0.36			3.06–8.22	10.3–13.5			
	gypsum**	0.45 *							14.54	9.13	7	Glew and Ford, 1980
Cardona, Spain	rocksalt	2.16	0.36	96								unpublished data
Cardona, Spain	rocksalt	2.47*		~60	1.39*		~60	1.82*	14.9			Mottershead et al., 2000
5 sites in Cardona, Spain	salt	1.73*		~250	0.86*		~250	2.32*	21			Mottershead et al., 2000
	salt**	1.75*										Glew and Ford, 1980

\* median values

\*\* from simulation

# values averaged from medians for all sites, n estimated from 125 profiles for Spain and 20 profiles for UK

(1996) observes that rillenkarrren are best developed on massive, finely micro-crystalline gypsum (e.g. in Sicily, Italy); they are not found on macro-crystalline gypsum or on selenites (e.g. in Sorbas, Spain). Forti (1996) suggests that crystal size needs to be < 0.5 mm for normal karren to develop on gypsum. However, these observations are entirely contradicted by the findings of Mottershead et al. (2000). They observe that the widest flutes in their gypsum study sites in Spain are from the coarse-grained facies. They give an example of rills at the Sorbas site (0.93 cm wide) that are at a smaller scale than the crystals. They note that particularly deep flutes (0.65 cm deep, 1.07 cm wide) are developed in the macro-crystalline gypsum of crystal size 5 to 10 mm. Smaller flutes (0.42 cm deep, 0.91 cm wide) develop on the microcrystalline gypsum of crystal size 0.1 to 0.5 mm.

Reports of variations in rillenkarrren on salt are even more rare. Mottershead et al. (2000) claim that coarsely granular rock bears larger rills; however, their data from Cardona, Spain, seem to contradict this. The rills on halite, the purest rock, with the biggest crystals up to 30 mm wide, are only 1.33 cm wide and 0.75 cm deep; the rills

on rock salt, with intermediate-sized crystals of 5 to 10 mm, are the largest at 2.5 cm wide and 1.4 cm deep; the rills on carnalite, with the smallest crystals of 1 mm (but the more porous rock), are intermediate in size. Certainly their data indicate that the relationship of rill size and crystal size is not simple.

### Effect of rock type on rillenkarrren, comparing evaporites and carbonates

It has been tacitly assumed since early studies that rock solubility must play a large role in the processes in action and thus be apparent in the morphology. It has seemed intuitively obvious that the greatly enhanced solubility of gypsum and salt compared to limestone would contribute to larger rills that form faster.

Table 3 summarizes the available data on gypsum, on salt, and on limestone. If enough data are assembled for each rock type, then it may be feasible to assess differences in mean values. However, at present a comparison of means and ranges has no real value in view of the complexity represent-

ed by the mean values and the huge differences in rigour of studies. In order to explore effect of rock type alone, sites should be sought where the different rock types co-exist, within the same climatic and altitudinal zone. It may be impossible to isolate chemical variations from physical variations since it is unlikely that any one field site would have several rock types, all of the same texture.

With so very little data for rills on evaporites, it is premature to offer a firm conclusion about differences in width. Glew and Ford (1980) in their simulations report the widest rills on salt, but their comparison is with field data from limestones of Canada, which are amongst the narrowest rills on limestone. Mottershead et al. (2000) find that rills on salt are significantly narrower than those on limestone. However, they acknowledge that their samples on limestone are biased towards the large rills in Australia and their data on salt are from only one location in Spain. Their median value for limestone is rather higher than the mean shown in Table 3, but both, 1.73 cm for salt and 1.81 cm for limestone, are well within the 1 $\delta$  range of values for limestone worldwide. Glew and Ford's (1980) simulated rills on salt are actually very similar in width to the natural rills of Mottershead et al. (2000) and the average rill width on limestone. Viewed in this light, the widths of limestone and salt rills are not significantly different.

We also suggest that the limited data do not yet allow a valid comparison of widths for gypsum rills and limestone rills and that it may be difficult to isolate chemical influences from textural influences. Gypsum rill average widths are clearly outside the 2 $\delta$  range for limestone worldwide. However, the limited data presented above from studies on marbles and gypsum in the same region, Svalbard, show that, while the average width of rills on gypsum (0.92 cm) is lower than for marble (1.37 cm), they overlap at the 1 $\delta$  range and thus cannot be considered to be significantly different. Neither rock has been studied for textural properties.

Differences in average depths from Mottershead et al. (2000) for salt and limestone are more

dramatic with salt rills, ~80% deeper than limestone rills, but, again, with such limited data we cannot offer any generalizations.

The data do not allow a test of the relationship of length to rock type. Few data are available for rill lengths on salt or gypsum because the full length is rarely expressed. Mottershead et al. (2000) note that "the longest flutes are associated with the deepest strata, representing the longest available rock slope" rather than the natural length of the rill.

### Non-rillenkarren or complex rills

It is important that all comparisons are of the same features. Rillenkarren are simple forms from raindrops falling on bare rock where flow is governed by gravity alone. The term cannot necessarily be applied to all suites of small dissolutional channels. Narrow channels often develop in soluble rocks simply as a result of channelled corrosion. These are more correctly termed *rinnenkarren* (Bögli, 1960a) rather than "rillenkarren" and are usually, but not necessarily, at a larger scale. The presence of *scallops* inside a trough is usually a clear indication of current flow and indicative of *rinnenkarren*.

Another mechanism for channel formation is decantation (Ford and Lundberg, 1987). Decantation from a joint or bedding plane, or a vegetation mat, or a bank of snow often produces parallel flutes that extinguish downslope. Although typically larger and shallower, in all other respects they resemble rillenkarren but they are formed by a completely different mechanism. In cases where the origin of the decantation water is no longer apparent (e.g. snow or no-longer-extant vegetation), the flutes may be mis-identified.

It is apparent that some forms described in the literature as 'rillenkarren' may actually be more complex forms. For example, the source of water is not simply rainfall for the features described in Mazari (1988): the caption for Photo 1 – "solution is augmented by soil cap at the top" – suggests



that these are *decantation flutes*. That they are not simple rillenkarren, must also be suspected from the dimensions: at 3–7 cm wide and 3–5 cm deep these are significantly bigger than all rillenkarren reported in the literature.

Another example of a non-rainfall water source are rills in seashore locations that are open to salt spray. This is true for the rills reported by Vincent (1996) for three of the four sites in the British Isles where the rills are affected by wave spray during “most spring tides and storm events”.

Every field situation should be carefully studied. Rills that develop down the sides of *clint* blocks are particularly difficult because they may change function. At the beginning of rainfall they act as simple rillenkarren, but as rainfall continues they often act as decantation routeways for water draining from the clint top.

Simple rillenkarren develop where the water falls from above. Sweeting and Lancaster (1982) describe rills on marbles in the Namib desert that form only on the sides of boulders facing the incoming advection fog. These rill dimensions (2.2–3.0 cm wide, 0.15–0.32 cm deep) are also on the high end of published rillenkarren dimensions. True rillenkarren are purely gravitomorphic features: Sweeting and Lancaster’s (1982) rills are further complicated by the action of wind in controlling flow dynamics, as are the impressive wind-enhanced dissolution rills in Patagonia (Maire et al., 1999).

The rills described by Migon and Dach (1995) on porphyritic granite in Poland have also to be assigned to the non-simple category. These are probably Pliocene in age and relict, with a poorly known history.

It seems that rillenkarren width is invariant enough to be able to offer a definition of true rillenkarren based on their width. Ginés (1996b) demonstrates that width is the most stable characteristic of rillenkarren. Table 1 demonstrates that rills from widely different locations have rather close mean widths: the frequency distribution centres on 1.70 cm, the majority of the population lying between 1.50 cm and 1.95 cm. Ginés (1999a),

from a survey of over 100 sites along the 90 km long Serra de Tramuntana, reports only two instances of rillenkarren wider than 2.1 cm. These are from locations over 800 m a.s.l., which experience snow several times a year, and from locations under a forest cover where rills are presumably affected by tree canopy interception. In both cases the source of water is not simply direct rainfall. Based on the data available at present, we suggest that features in limestone that have a mean width outside of the range ~1.3 to ~2.1 cm should be considered suspect, and the formative mechanisms carefully studied.

## Rillenkarren formation

The features of rillenkarren that must be explained in any model of formation are the separation of foci of erosion into almost evenly spaced components, the parabolic cross profile of each rill, the formation at a crest and extinguishing downstream, and the continuation of erosion in the *ausgleichsfläche* as sheet flow.

Modes of formation may not be apparent from field evidence because of the complexities of nature. Glew and Ford, in 1980, were the first to simulate rillenkarren production in the laboratory and thereby limit the variables. They created rillenkarren on gypsum blocks in the laboratory and documented their development. Rill width emerged early on; the first narrow and variable rills coalesced in stages until the stable, characteristic, and relatively constant width was reached. Width then remained stable as rills deepened and lengthened. They developed at the crest and propagated downslope, lengthening and deepening steadily at the beginning, then at a reduced rate until a stable length was reached. The rill cross section developed into a parabolic form as they deepened. The rill trough and *ausgleichsfläche* surfaces showed parallel retreat.

These observations are confirmed in other plaster simulations by Slabe (2005) and are generally supported by field evidence. Mottershead and

Lucas (2001), examining rill development in natural gypsum on surfaces of known age, confirm that width stabilizes early whereas depth continues to increase. Field evidence that flute length and slope angle is maintained as divides are lowered, suggests that the whole system is in dynamic equilibrium; rills maintain their overall form over time, but change in detail as cusp lines shift because existing flutes are captured and new ones are initiated (Mottershead, 1996a; Crowther, 1998).

Studies of morphometry (both at the macro- and nano-scales) and of chemistry help to elucidate process. Rillenkarrren formation, as with almost every karst feature, appears to be the product of chemical, biological, and physical processes.

### Chemical processes

The chemical processes that produce rillenkarrren must take place in a very thin film of water (see relevant discussion in Dreybrodt and Kaufman, chapter 2) and in the few seconds required for flow from crest to *ausgleichsfläche*. On evaporite rocks, simple dissociation is realistically the only possible chemical process (it is unlikely that biological action will be important). Bögli (1960a) asserts that rills on carbonates must also form by simple, rapid dissolution, and cannot include the long-term and slow complexing of CO<sub>2</sub>. Rillenkarrren must thus be formed from simple dissociation of CaCO<sub>3</sub> in water. This is Bögli's phase 1, yielding water of around 14 ppm CaCO<sub>3</sub> content. Phase 2 of the chemical reaction involves the CO<sub>2</sub> that is chemically dissolved in rain, governed by atmospheric CO<sub>2</sub> (relatively constant worldwide) and temperature (less dissolution of CO<sub>2</sub> at higher temperatures). This yields another ppm or so. These first two phases take only seconds to complete. Further phases of carbonate dissolution require longer time (an order of magnitude longer and much slower than the drainage rate of rills) and are thus not relevant for rillenkarrren formation. Dreybrodt and Kaufmann calculate that 20 seconds would be required for apparent equilibri-

um to be reached in a water film of 0.2 mm thickness for the fast phase of dissolution, but 500 seconds for the slower.

If dissociation is the only process, then karren waters should have very low hardness values. Empirical data for CaCO<sub>3</sub> contents of karren waters on bare rock are few but do indicate very low values. Dunkerley (1983) quotes total hardness values of only 22 to 28 ppm for flow distances of 120 to 170 cm – much longer than typical rillenkarrren. Fiol et al. (1992) report values between 9 and 45 ppm for natural rainfall waters collected at the end of rillenkarrren flutes. Fiol et al. (1996) find values of around 10 ppm, and Mottershead (1996a) around 20 ppm, from rillenkarrren irrigated with distilled water.

### Biological processes

Rillenkarrren are limited to surfaces that are free of macroscopic cover. However, Fiol et al. (1996) convincingly demonstrate that biological action at the microscopic scale is an important part of rillenkarrren erosion in carbonates (although not in gypsum and halite – Mottershead and Lucas, 2004). Fiol et al. show, by scanning electron microscopy (SEM), that colonies of cyanobacterial cells inhabit the rock surfaces, and that bio-erosion weakens the crystalline structure of the limestone. The impact of raindrops is then presumed to cause the detachment of particles contributing to the considerable particulate load in run-off water.

The effect of colonization by lichen is not clear. Macaluso and Sauro (1996b) and Mottershead and Lucas (2000) found that lichen hindered, but did not completely inhibit, dissolution of gypsum surfaces. Yet sharp rills on gypsum in Svalbard show no apparent effect of colonization by crustose lichen (unpublished data). The effect of lichens on carbonates is similarly unclear. Moses and Viles (1996) offer direct SEM evidence of bio-erosion under lichen cover on rillenkarrren from carbonates in eastern Australia: they show that the whole

rill surface, both ridge and base, is dissected with circular etch pits and tunnels and that the lichen thallus colonizes the top 0.1 to 0.15 mm with fungal hyphae penetrating to 1.4 mm. On the other hand, in their experiments of particulate matter removal by raindrop impact on different limestone surfaces, Fiol et al. (1996) found that lichen-covered rock released significantly fewer particles than “bare” rock (which actually is colonized by endolithic cyanobacteria).

### Physical processes

Physical processes may be expressed as the mechanical removal of particles and/or in the influence of hydrodynamic action on the process of dissolution. The two potential sources of physical control in the rill environment are raindrop impact and fluid flow. Raindrop impact is generally considered to be the more significant of the two, but discussion continues.

#### MECHANICAL

Fiol et al. (1996) show that mechanical removal of small limestone protrusions (albeit produced as a direct result of biological activity) is one of the principal processes involved in the growth of rillenkarren in carbonates (accounting for nearly half of the erosion). Mottershead (1996a) suggests that fluid flow down the rill trough may cause mechanical erosion but Fiol et al. (1996) argue that it is caused by raindrop impact. Mottershead and Lucas (2004) offer further evidence of the importance of mechanical removal of particulate matter, this time from gypsum and, to a much lesser extent, salt surfaces. The nano-morphologies indicate delicate promontories and etchings as well as considerable loosened particulate matter (presumably caused by physical or chemical weathering because there is no evidence of any biological action). They suggest that the mechanical force of raindrop impact will detach these and contribute to the sediment load of run-off water from gypsum surfaces in the field.

While the mechanics of removal may not be clear, it is apparent that loss of particulate matter is a significant part of rillenkarren erosion, especially in carbonates.

#### HYDRODYNAMIC

Bögli (1960a), observing that rillenkarren form only where bare rock is exposed to uniform rainfall coverage, suggested the probable importance of physical characteristics of the water-precipitation, mode of flow, thickness of water layer, and predicted that rillenkarren should increase in length with increasing slope and with intensity of rainfall. Since then, discussions about rill formation have focussed mainly on hydrodynamic controls. (Dunkerley, in 1979, finding no evidence in field studies for the predicted increase in length with slope, questioned hydrodynamics as the principal control. However, later field studies did find the predicted increase in length with slope, and thus the focus of studies returned to hydrodynamic controls.)

Glew and Ford, in 1980, postulated that hydrodynamic controls – rain drop kinetic energy and thickness of water film – are dominant. Raindrops, striking randomly over the whole surface, keep the upper layer of water in constant motion, renewing the solvent and creating mixing. Where the water film is thin enough, and raindrop energy great enough, the drops penetrate the laminar sublayer to cause dissolution directly on the surface rather than by diffusion through the laminar sublayer. Rillenkarren are the result of dissolution from direct raindrop impact on the rock surface; the *ausgleichsfläche* is the expression of dissolution under a deeper water film. While new research has highlighted additional processes such as biological and mechanical action, the essence of these interpretations provided the basis of studies for the next 15 years or so.

### Development of the *ausgleichsfläche*

The development of the *ausgleichsfläche* is not

well understood. Field evidence is quite variable; in some cases the *ausgleichsfläche* continues to develop at the same angle of slope as the rilled belt (as happened in Glew and Ford's simulations, 1980). In other cases the rillenkarrren will terminate in an obvious decrease of gradient into the smooth face of a *step karren* (Mottershead, 1996b). Macaluso and Sauro (1996b) suggest that the *ausgleichsfläche* develops where erosion slackens. This is probably not caused by an approach to saturation. Rather it is likely that the dissolution rate will vary for the two regions. It may be that the evidence from Glew and Ford's (1980) simulation of parallel retreat of slope does not necessarily apply to carbonates because of the high solubility of gypsum. For carbonates, where direct raindrop impact is inhibited, and the reaction becomes diffusion-limited, dissolution may be correspondingly reduced. However, velocity of flow also governs dissolution rate. Discharge and velocity increase downslope, so reaction rate may increase down the *ausgleichsfläche*.

If dissolution proceeds at different rates for the rilled section and the *ausgleichsfläche*, then the profile of a single face should thus become modified into a double face, with a break of slope at the junction of rill and *ausgleichsfläche*, a situation that is often observed in the field but not consistently.

### Rates of formation

Rates of formation are estimated from simulation studies (e.g. Glew and Ford, 1980), from water chemistry studies (e.g. Dunkerley, 1983), and from field studies of dated surfaces (e.g. Gams, 1990; Mottershead and Lucas, 2001). Table 4 summarizes these estimates for carbonates, gypsum, and salt. Rates of formation are in the order of  $10^3$  years for carbonates,  $10^2$  years for gypsum, and  $10^1$  years for salt (Mottershead and Lucas, 2001). This information can, in turn, be used as a rough dating tool: e.g. Gams (1990) used depth of rills as measure of time since deforestation.

### The relationship of rillenkarrren and rainpits

Rillenkarrren and rainpits (Jennings, 1985) have so many similarities that a genetic relationship is suspected. This idea is further developed in chapter 15 (Rainpits: an outline of their characteristics and genesis).

### Modelling rillenkarrren formation

Any model for rillenkarrren formation must offer a reasonable explanation for the salient features and embrace all the available evidence of chemical, biological, mechanical and hydrodynamic processes. The simulation studies of Glew and Ford (1980) provide the basis for the theoretical model of rillenkarrren development discussed below, which we have called the "Raindrop impact and boundary layer model".

**RAINDROP IMPACT AND BOUNDARY LAYER MODEL**  
Glew and Ford (1980) offer a hypothesis of rillenkarrren formation. It includes the following concepts:

- rillenkarrren are a rim effect induced by direct rainfall impact on the rock surface;
- dissolution is fast and at the point of impact – no further dissolution occurs from splash or from water draining down the rill;
- the differentiation into two distinct morphological zones (rilled and planar) is a consequence of a critical change in the thickness of the film of water flowing over the surface and the degree of turbulence at the base caused by impacting raindrops;
- raindrop impact produces a constant dissolution rate over the rilled section, where the water film becomes deeper than the critical thickness, a laminar boundary layer protects the surface from direct raindrop impact and the *ausgleichsfläche* continues to dissolve in a planar form (Figure 8, left);
- the troughs erode only, or principally, through direct raindrop impact – channel flow is not

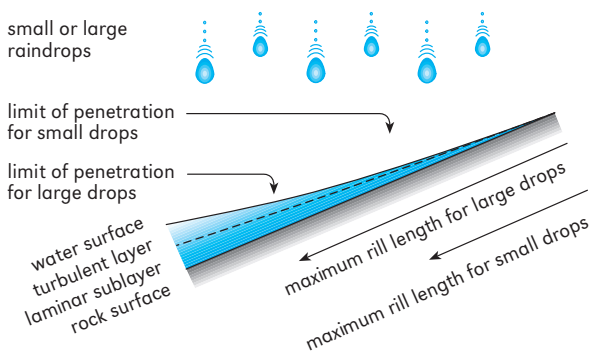
important; thus the rillenkarren channel is radically different from the conventional Hortonian stream channel that propagates downslope of the belt of sheet overland flow where converging flow creates channels.

The implications of this model are: a) that kinetic energy of raindrops should control the thickness of film that can be penetrated and thus rillenkarren length (the relationship should be with rainfall intensity rather than total rainfall, and should relate to water viscosity); b) that controls on depth of flow downstream should control rillenkarren length (discharge, slope angle, surface roughness); and c) that controls on reaction rate should control rillenkarren dimensions (e.g. rock solubility, temperature, turbulence of flow, thickness of laminar layer). Rock solubility will interact with hydrodynamic controls to affect rill depth, width and speed of formation.

a) Effect of raindrop kinetic energy: Raindrop size and energy vary with the type and intensity of rain events and thus will vary geographically. Mean drop diameter relates to rainfall intensity, and terminal fall speed relates to diameter, and

therefore raindrop kinetic energy relates to rainfall intensity, all by power laws (Kinnell, 1987; Uijlenhoet and Stricker, 1999; Salles et al., 2002). For example, light rain, heavy rain, and thunderstorms have a mean droplet diameter and kinetic energy of 1 mm and 1 kJ/(m<sup>2</sup> h), 2.1 mm and 10<sup>3</sup> kJ/(m<sup>2</sup> h), and 3 mm and 10<sup>4</sup> kJ/(m<sup>2</sup> h) respectively (Auerswald, 1998). Obviously, the higher the kinetic energy of the drop the thicker the laminar layer that can be penetrated (Figure 8, left). Rain splash erosion on soils is especially effective where the water film is less than ~0.1 to 0.3 of the drop diameter; and water films thicker than 3 drop diameters protect the surface from raindrop impacts (Auerswald, 1998). In Glew and Ford's (1980) simulations drop size was centred on 1.0 to 1.5 mm. They found experimentally that the limiting film thickness was 0.15 mm on a 45° slope. This is 0.1 of the drop diameter – at the lower end of the effective water film thickness for raindrop erosion of soil. Dreybrodt and Kaufmann (see chapter 2) modelled film thickness using only hydrodynamic controls (density, viscosity, slope angle, rainfall intensity) in the region of 0.075 to 0.1 mm. Petter-

Influence of raindrop size on rill length



Influence of slope on rill length

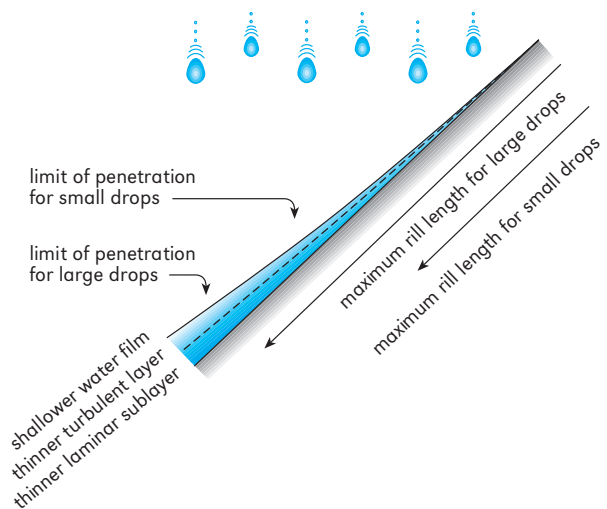


**Figure 8:** Structure of water film and controls on rillenkarren length: left. critical thickness of boundary layer depends on raindrop size/energy level; more intense rainfall should produce longer rills; right. critical thickness of boundary layer relates simply to slope angle; steeper slopes should produce longer rills.

son (2001) measured thicknesses of 0.2 to 0.8 mm on a 30° slope.

Although rillenkarren morphology appears to have no relationship to total (mean annual) precipitation, variations in raindrop properties may explain much of the variation found in rillenkarren properties. Tropical rainfall is typically convective, and characterized by larger raindrops than the lighter rains of temperate regions (Calder, 1996). Raindrops in mediterranean regions are variable but the majority are small (e.g. in Cerdá's 1997 study in the Western Mediterranean, the majority of raindrops were less than 1 mm). Therefore rillenkarren ought to be longer (and presumably wider and deeper) in subtropical regions compared to temperate and Mediterranean regions. The only substantial data sets relevant to this question are from subtropical, monsoonal Chillagoe (Dunkerley, 1983) and Mallorca (Ginés, 1999a). The difference in average rill length for Chillagoe ( $33 \pm 20$  cm,  $n = 428$ , with an average slope of  $65^\circ \pm 12$ ) and for Mallorca ( $23 \pm 8$  cm,  $n = 200$ , with an average slope of  $58^\circ \pm 12$ ) is highly significant (z-score of 9). If we account for the difference in slope by using the relationship of length and slope shown in the data of Mottershead (1996a) from Mallorca to calculate the average length in Mallorca for an average slope of  $65^\circ$ , this would be 26 cm. Testing this against the length for Chillagoe is still highly significant (z-score of 6). Similarly rill width in Chillagoe is significantly larger than in Mallorca (z-score of 4.6) and rill depth (z-score of 14). However, these comparisons are complicated by temperature differences, Chillagoe's mean annual temperature being  $\sim 26^\circ\text{C}$  and Mallorca's  $\sim 17^\circ\text{C}$ .

A survey of a population of rills forming under trees reported in Ginés (1999a) is relevant to this discussion. The mean width, at  $\sim 2.5$  cm, is clearly outside the normal range of rillenkarren widths for all the non-forested regions in the rest of the study. This is explained as the result of interception of rain by the forest canopy and the subsequent formation of larger raindrops (Brandt, 1989, 1990; Hall and Calder, 1993).

The slightly concave long profile of the rill trough observed by Mottershead (1996a, b) can also be explained by raindrop kinetic energy. The position of the critical depth will vary with variation in rainfall intensity. For any region, raindrop energy varies temporally. Thus there will be a constant slight shifting of the position of the critical depth throughout a single storm, throughout the year, and over climatic cycles. The gentle transition from rill to *ausgleichsfläche* is a response to the natural variations in rainfall intensities and the associated variations in the position of critical depth. Flow in the upper part of the rill is always shallower than the critical depth. Flow in the lower part will vary. A region with more constant rainfall intensities should have a sharper transition.

The impact of raindrop kinetic energy should also vary with water viscosity (see chapter 2), which in turn varies inversely with temperature. All other things being equal, rill length should be greater at lower viscosities and higher temperatures, but this effect will be complicated by the impact of temperature on reaction rate (below).

b) Depth of flow controls (discharge, slope angle, surface roughness, porosity): Discharge is directly related to rainfall intensity ( $q$ ). Depth increases downslope with length  $L$  (as  $\sqrt[3]{L/q}$ ). The higher discharge caused by higher rainfall intensity should therefore reduce the length of rillenkarren, but is counteracted to some extent by the higher kinetic energy of the drops.

Increasing slope angle reduces the effective rainfall per unit area, increases the velocity of flow and thus decreases the thickness of the water film (Figure 8, right). The positive relationship of rillenkarren length and slope support this argument. The position downslope at which the critical depth is reached is a function of slope and length. Logically, if hydrodynamic controls are the only or principal control, then the best relationship should be produced by length against  $\tan$  slope (see chapter 2). However, for our empirical data, the relationship is not very strong. For Istria and Rocky Mts data, a slight improvement is

shown when the data are limited to slopes smaller than ~60°: e.g. for Istria limestones data  $L = 1.9 \tan \text{slope} + 14$ ,  $R^2 = 0.16$  for all data, but for slopes less than ~60° the relationship is  $L = 9.4 \tan \text{slope} + 9$ ,  $R^2 = 0.63$ .

Surface roughness provides additional frictional retardation and thus decreases velocity of flow, increasing the depth of the water film and reducing the length of the rillenkarren. If surface roughness causes significant retardation of flow, then the slope of the relationship of length by slope angle would be lower. Data are not yet available to test this effect.

Rock porosity (within limits – very porous rocks will not show any rillenkarren development at all) should also affect flow depth and thus rill length. A slightly porous rock will have a slightly less deep film, so slightly more porous rocks should have longer rills.

c) Reaction rate (rock solubility, temperature, turbulence of flow, thickness of laminar layer): There is a simple positive relationship of rate of dissociation and temperature (reaction rate doubles every 10°C, a logarithmic function). If rillenkarren are produced by simple dissociation of calcite (Bögli, 1960a; also see chapter 2), and if depth is a measure of reaction rate, then depth should show a relationship to temperature. The demonstrated log-normal relationship of depth and altitude in Mallorca (Figure 6, left), combined with the observations of very deep rills on salt (Mottershead et al., 2000) do appear to confirm that depth is strongly controlled by reaction rate (on condition

that the mechanical strength of the rock can support the steep sides; Dunkerley, 1979). However, if it were so simple, then the depths of rillenkarren on gypsum ought to be larger than on limestone and smaller than on salt. This does not appear to be so (Table 3), although the impact of biological erosion on limestone has not been taken into account in this comparison.

There is no logical reason to expect length to vary with reaction rate. It does show a relationship with mean annual temperature (Figure 5, left), and with altitude (Figure 6, right), but this is most probably explained by the effect of temperature on fluid viscosity and thus on the depth of the critical layer. If reaction rate is an important control on rillenkarren length, then length should vary directly with solubility for different rock types in the same field situation. The very limited data from Svalbard show average rill length on marble to be 12.7 cm (n = 8) and on gypsum to be only 9.0 (n = 5). Putting together length data from Spain from various sources, limestone rills are 20 cm (Ginés, 1996b), gypsum rills are 10 cm (the Spanish sites taken from Mottershead et al., 2000), and salt rills are 21 cm (Mottershead et al., 2000). Until further data are collected, it appears that rock type does have a significant effect on rill length, but it is not governed simply by reaction kinetics because length is not in order of reaction rate.

The relationship of rillenkarren width and reaction rate is not so clear. Width shows no relationship to mean annual temperature and Ginés

**Table 3:** Summary of rillenkarren morphometry. Averages and 1 standard deviation ranges for rillenkarren on carbonates, gypsum, and salt from Tables 1 and 2, and median values from Mottershead et al. (2000).

Rock type	Width (cm) ± 1 SD	Depth (cm) ± 1 SD	W/D	Length (cm) ± 1 SD	Source
limestone	1.70 1.43–1.98	0.44 0.26–0.60	4.37 3.22–5.52	19.23 12.61–25.85	Table 1
limestone	1.81*	0.47*	3.77*	30*	Mottershead et al., 2000
gypsum	0.92 0.80–1.05	0.31 0.25–0.36	3.76 3.06–8.22	11.9 10.3–13.5	Table 2
gypsum	1.07*	0.37*	3.27*	12.0*	Mottershead et al., 2000
salt	1.73*	0.86*	2.32*	21.0*	Mottershead et al., 2000

\* median values

**Table 4:** Estimates of rates of formation for rillenkarren.

Rock	Time (yrs)	Place	Method	Reference
limestone	724–1,159	Lluc, Mallorca	chemistry	Mottershead and Lucas (2001); Fiol et al. (1996)
	400–600	Hercegnovi, Montenegro	field	Jakucs (1977)
	2,000–2,500	Lluc, Mallorca	chemistry	Mottershead (1996a)
	2,100	Dinaric karst	field	Gams (1990)
	1,330–2,600	Queensland, Australia	chemistry	Dunkerley (1983); Mottershead and Lucas (2001)
gypsum	< 26–100	United Kingdom	field	Mottershead and Lucas (2001)
	< 20	Mallorca, Spain	field	Mottershead and Lucas (2001)
	4–38	Crete, Greece	field	Zeza (1994); Mottershead and Lucas (2001)
	40–100	Nova Scotia, Canada	field	Stenson and Ford (1993)
salt	8–20	Catalunya, Spain	field	Mottershead and Lucas (2001)

(1996b) demonstrates that width does not vary with altitude in Serra de Tramuntana, Mallorca. As discussed above, width is the most invariant of rillenkarren characteristics, mean widths showing only minor differences for widely differing locations. These observations suggest that rillenkarren width is not controlled by reaction rate.

If the supply of fresh solvent is not inhibited by a laminar layer, then the reactions are reaction-rate limited rather than diffusion-rate limited. Thus, surface roughness should be greater in the belt of rillenkarren compared to the belt of non-channelled erosion of the *ausgleichsfläche* – exactly as Crowther (1997) observes.

Reaction rate should also vary with grain size. While the empirical data are few, there seems to be slightly more evidence that small rills are associated with coarse grain for all three rock types. In summary, the data show smaller rills for coarser grain in carbonates of Chillagoe and south Africa (Lundberg, 1977b; Dunkerley, 1983; Marker, 1985), best developed rills on microcrystalline gypsum of Spain and Italy (Calaforra, 1996), and smaller rills on coarsely crystalline halite of Spain (Mottershead et al., 2000). Publications do not always give quantitative details of grain size, so as yet it is not possible to make a table of grain size against flute dimensions.

Rill cross section is presumably related to both, rain splash and reaction rate. For a constant rain splash, a slower reaction rate would produce smaller rills. Coarse texture is often quoted as less

soluble than fine (as discussed with reference to rillenkarren by Dunkerley, 1983). Ford and Williams (1989) give many examples of finer grained rocks being more soluble. This might explain why rills on coarser texture are smaller than those on finer texture. However, it does not explain why rills on gypsum seem to be so small. We must conclude that at present this question cannot be answered.

Grain size should also affect rill length (again in association with reaction rate). If coarse grain is associated with rougher surface texture (and with reaction-rate-limited dissolution within the rills, that is to be expected), then flow down the rill is inhibited so that length to the critical depth would be shorter. In the absence of adequate data on length we cannot assess this.

#### CHALLENGES TO THIS MODEL

The only real challenges to this model come from Mottershead. In 1996, while claiming that his model is “entirely consistent with the conclusions of Glew and Ford (1980)”, he suggests three fundamentally different processes. Arguing that raindrop impact will lead to divide reduction and thus raindrop action alone would destroy the rills, he suggests that rills can be maintained only because troughs are deepened by channel flow. He further claims that downslope channel deepening becomes limited by decreasing aggressiveness rather than critical depth, and thus the rill gives way to the *ausgleichsfläche* (Mottershead, 1996b).



We offer several counters to these arguments. First, simple modelling of the dissolution from raindrops falling vertically onto a parabolic profile demonstrates that the form is maintained and does not require any additional trough deepening. Second, if the troughs require focussed erosion by channel flow, then they require an upstream area of sheetflow (with no channelled erosion) for collection of discharge, in the standard Hortonian fashion. Yet rillkarren are usually close to their maximum depth right at the crests. Third, Glew and Ford in 1980 had already rejected the arguments of changing aggressivity. For the highly soluble evaporite rocks, water certainly does not approach saturation, yet the rills still naturally extinguish downslope and give way to an *ausgleichsfläche* at the same slope angle.

By 2004 Mottershead has shifted focus, offering instead a kind of omni-inclusive model incorporating raindrop impact and critical depth but with a focus on mechanical stresses (imposed by rain drop impact rather than channel flow) and a focus on the processes on inter-rill divides rather than troughs (Mottershead and Lucas, 2004). The new (rather complex and confusing) model suggests: 1. that rill troughs are “subordinate forms” to rill divides; 2. that rainbeat is a significant force causing mechanical damage on the steep slopes of the rill divides but not on the flatter trough (because the proportion of shear force versus compression will increase with slope); 3. that the steep slope of the rill divide is also the region of maximum chemical action, with the maximum surface exposed to dissolution – the solvent is spread more thinly, bringing more of the solvent into contact with the rock – but they also say that the maximum dissolution is at the point of rainbeat impact (up to a critical depth); 4. that the troughs have the deepest water film, maximizing the solvent volume and increasing the potential for dissolution; 5. that the variation of dissolution kinetics with lithology and the concentration of solvent in channels explains why the “relatively deeper flutes are present on the more soluble rocks” (sic) – but they also say that mechanical strength governs

rill magnitude. Their final point is that the rill long profile is produced by differences in channel downcutting rates (rather than rill divide erosion rate – in apparent contradiction to the designation of channels as subordinate forms): at the top of the rill both, mechanical shear forces and chemical aggressivity, will be most effective; midway down both forces will be balanced; towards the base both will be weakest (because increased depth of flow reduces the chance of direct rainbeat on the rock surface).

Obviously, we have no argument with some parts of the model, but we suggest that the focussing of any process (mechanical or chemical) on the inter-rill divides will necessarily cause them to be lowered while the troughs remain relatively unaffected. The form must therefore lose its integrity over time. Modelling of dissolution at point of raindrop impact (dissolution, related to cosine of slope, occurs by surface reduction normal to slope) shows that the maximum effect is in the troughs and that the form is maintained over time (Figure 9, above). If we add mechanical erosion (shear, related to sine of slope, acts vertically), then the trough-to-divide distance decreases and the rills eventually extinguish (Figure 9, below).

#### LIMITATIONS OF MODELS

It is likely that there is some truth in every model, but at present, the available data offer the most support to the simple rain-drop impact and critical depth model. There certainly are a great many variations in nature, but on the whole, the majority of evidence from rill morphometry studies supports Glew and Ford’s (1980) model. However, Dunkerley’s (1983) arguments, that many observed characteristics of rillkarren are still not explained by this model, should not be forgotten.

While it may be the best explanation we can come up with, there are some problems apparent with the raindrop impact theory. Dreybrodt (personal comment, 2006) has pointed out that raindrop impact on any one point is actually rather rare: for rainfall intensity of 10 mm/hr (heavy rainfall) and drop size of 1 mm radius (volume

0.004 cm<sup>3</sup>), only 4 drops fall onto a 1 cm<sup>2</sup> area every minute. Furthermore, the work of Petterson (2001) indicates that laminar flow is the norm and turbulent flow rare.

Another consideration that is not fully understood is the effect of reaction kinetics on rill formation. Flow velocities are typically ~2 cm per second but it takes about 20–30 seconds to reach apparent equilibrium (see chapter 2). Logically, rills should not reach their maximum size until the flow has reached ~40–60 cm. Thus short rills and rills that head at the crest should not be possible. Enhanced dissolution under raindrop impact, and within only a second of impact, seems to be the only explanation that applies to all situations.

As far as we understand, no model has fully explained why the region of randomly impinging raindrops should develop into such neat parallel channels rather than random surface lowering. Glew and Ford's model explains why the form develops at the crest, why it extinguishes, and how it is maintained. Once a rill has attained the parabolic profile, it is easy to maintain its equilibrium profile solely by raindrop impact. Raindrop impact is delivered uniformly. The surface area over which the impact is dissipated increases with slope angle of each facet. Depth of surface lowering is thus a direct function of surface area exposed to rain. A curved form, once established, is maintained. This simple concept works if dissolution is the only process. It also works for mechanical action if kinetic energy is dissipated according to surface area, ignoring potential differences in shear versus compressional forces. What is difficult to model, is the initial, highly ordered pattern of differential erosion that sets up the profile.

We feel that simple dissolution from raindrop impact explains the basic formation of rillenkarren on all rock types. Rills in carbonates are probably the result of a combination of dissolution, biological, and mechanical action. However, because biological action is not observed on gypsum or halite, and because mechanical action is probably not active on the smooth surfaces of halite, any model of rill formation must focus first on

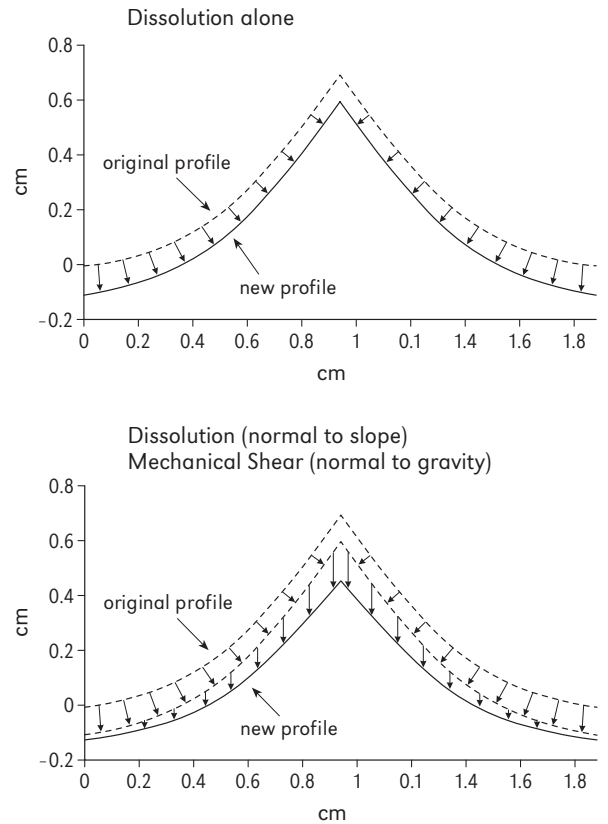


**Figure 9:** Profiles produced by modelling: above. result of dissolution alone, where solvent from vertically falling raindrops is distributed according to surface area and removal of molecules is parallel to slope. The form is maintained over time; below. result of dissolution in combination with mechanical erosion as envisioned by Mottershead and Lucas (2004). The form is destroyed over time.

dissolution alone. Biological and mechanical action may then be added for susceptible lithologies, as modifiers of rill form and dimension.

## Conclusions

Rillenkarren have been reported from a variety of geographic locations worldwide. We have summarized the available data for around 20 locations ranging from arctic to tropical climates. Rillenkarren width is remarkably constant worldwide, while depth and length vary with slope/temperature/altitude. None of the morphometric

properties varies with mean annual precipitation. Because width is so constant, rillenkarren may be defined by their width: any suite of channels of mean width outside the range ~1.3 to ~2.1 cm are probably not simple rillenkarren.

The best explanation of rillenkarren formation is that it is by rapid dissociation where raindrops impact directly onto the rock surface, uninhibited by the laminar boundary layer. The kinetic energy of the raindrop dictates the critical depth of flow that can be penetrated. The belt of non-channelled erosion, the *ausgleichsfläche*, develops where the critical depth is exceeded. Rill dimensions are controlled largely by raindrop kinetic energy and water viscosity. The effect of lithology is not clear but there is a suggestion of smaller rills on coarser-grained rocks.

Future research efforts should focus on the areas of weakness. Morphometric data on rillenkarren are reasonably comprehensive (although length data are not often available). However, data on the *ausgleichsfläche* are rare. We need considerably more data from regions other than the two favourites, Australia and Mallorca. Ideally a search should be made for rillenkarren on limestone, gypsum, and salt within the same

locality. The relationship of altitude and climatic variables needs to be clarified. The complexity of the relationship of slope and rillenkarren length needs further study. While the focus on detail and consistency of studies recommended by Crowther (1998) is important, the value of the research lies mainly in the sampling strategy, which should be clearly stated. Sampling efforts should be organized around ecological principles, to elucidate the impact of environmental variables. Experiments on the chemistry of natural and simulated runoff waters are vital. Future research efforts could also profitably be focussed into more simulations introducing additional controls, such as grain size, raindrop size, temperature, initial slope characteristics.

## Acknowledgements

We thank Wolfgang Dreybrodt for very helpful comments on an earlier version of this chapter. This work was partially supported by the research fund of Ministerio de Educación y Ciencia – FEDER, CGL2006–11242–C03–01/BTE.

# RINNENKARREN

Márton VERESS

*Rinnenkarren* are solution channels (*runnels, flutes*) that occur parallel with each other and whose direction coincides with the line of the dip of the slope. According to Eckert (1898), Bögli (1976), and Ford and Williams (1989), rinnenkarren are several decimeters wide and deep, and they can be several dozen meters long. They are large forms that cover extensive areas and do not taper out at the ends (Figure 1). According to Haserodt (1965), rinnenkarren occur between the altitudes of 480 and 2,300 meters in the Alps, and according to Kunaver (1984), between 1,650 and 1,700 meters in the Julian Alps. They can develop parallelly on steeper slopes (as mentioned above), but they can also be separated as main channels and subsidiary channels on gentler slopes where they create interlocking systems. Large channels can have depths and widths of about one meter (Veress, 1995). According to Wagner (1950), rinnenkarren occur on slopes between 30° and 90°, but we believe rather that *wandkarren* develop on the steeper slopes (ca. 60°–90°).

## The types of rinnenkarren

Rinnenkarren can be divided into several types. According to Bögli (1976), the surface remnant between channels can be flat or round. Bögli (1976) called the latter karren form *Rundkarren* or *roun-*

*ded solution channels*. Several researchers explain the development of this form by dissolution under soil (Eckert, 1902; Bögli, 1976; Jennings, 1985; Sweeting, 1955). Other researchers think that *rundkarren* could have developed when rinnen-



**Figure 1:** Rinnenkarren (Triglav Lakes valley, Slovenia). Width of view is 3.5 m.



**Figure 2:** Semi-exhumated rounded rinnenkarren (Totes Gebirge, Austria).

karren were transformed during their development (Bögli, 1960a; Haserodt, 1965; Louis, 1968; Wagner, 1950). Those surfaces that are covered with soil today were bare during the glacial period, and therefore rinnenkarren could have developed on such surfaces. These rinnenkarren were covered with soil after the retreat of the ice in the Holocene, and due to dissolution under the soil, the ridges between the channels were rounded off. The side walls of the channels dissolved steeply (resulting in a U profile), depressions could develop at the bottom of channels (*Korrosionshohlkehlen*), and the slope angle of the bottom of the channels became smaller (Bögli, 1976; White, 1988). The side walls of the channels can also be overhanging due to dissolution under the soil. Bögli (1976) called this type *Hohlkarren*. The soil can erode and the rounded ridges partly or totally protrude (Figure 2).

According to Jennings (1985), flutes and smaller channels (*rain solution channels*) form on the ridges between channels. We consider the latter to be *rillenkarren*.

Ford and Williams (1989) describe one rinnenkarren type as *Horton-type channels* whose forms become larger and more complex downward

along the slope, taking a branched form. They are fed from the upper part of the slope (for example, from an *Ausgleichsfläche* area), but in our opinion they receive further water from their margins on the lower part of the slope. According to Gladysz (1987), they are complex forms (*complex channels*) from about three to five meters below their upper ends and their development is also complex. There can be *pits* (*karren sinkholes*) and *grikes* on their bottoms. According to Ford and Williams (1989), there are single rinnenkarren that receive their water directly from rain whose width and depth decrease farther down the slope. There are also *decantation channels* fed by *kamenitzas*. The water supply of decantation channels is therefore local, but they can also receive water dropping from leaves and the trunks of trees. According to Sauro (1976b), all rinnenkarren are decantation channels. According to Ford and Williams (1989), “decantation flutes” are forms of large density with narrow combs between them. These forms are fed by sheet water from the upper part of a slope.

Bögli (1960a) described *Regenrinnenkarren*, forms that develop on a steep slope due to rainwater. However, this form type is probably a decantation channel or a special wandkarren. According

to Jennings (1985), this type can develop with the coalescing of neighbouring rills. Crowther (1997) distinguishes different types of rinnenkarren according to their vertical section: those with a flat bottom, with a stepped bottom (*step rinnenkarren*), and with a changing bottom slope angle (*bevel rinnenkarren*).

Rinnenkarren can develop on a variety of rock. For example, they can occur on marble (Veress et al., 2006), on granite (Rassmusson, 1959), on calcareous sandstone, on calcareous conglomerate, on amorphous silica sandstone (Veress and Kocsis, 1996), on gypsum (Calaforra, 1996), on basalt (Bar-

trum and Mason, 1948), on quartzite (White et al., 1966; Marker, 1976a; White, 1988), on halite (Macaluso and Sauro, 1996a), and on calcareous green-schist (Veress and Szabó, 1996; Veress et al., 1996). Large channels can develop in particular on granite and halite. The rinnenkarren on halite (Parajd, Romania) begin on covered sediments, and they can be several meters wide. Rills and channels can develop on their bottoms. Rinnenkarren on marble (Diego de Almagro island, Chile) are also large. Here, the bottoms of the rinnenkarren are stepped and they join dissolution basins.

Combinations of various karren forms occur on

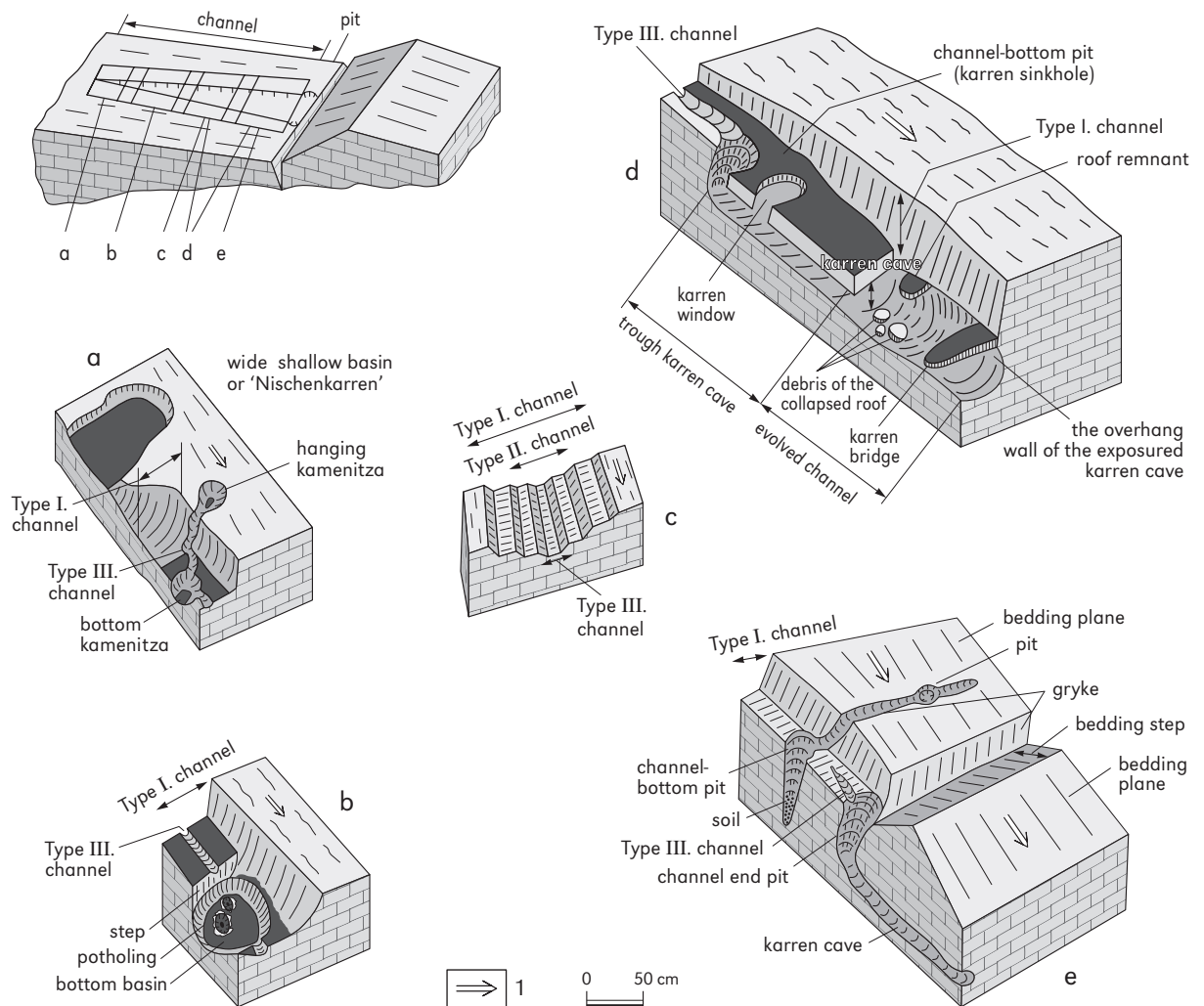


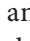

**Figure 3:** The morphological complexes of different parts of a channel. a, b. upper part of the channel; c, d. middle parts of the channel; e. lower part of the channel; 1. dip of the surface.

slopes. The most common combinations of forms are the following: *rillenkarren–Ausgleichsfläche (solution level)–rinnenkarren*; *Ausgleichsfläche–rinnenkarren*; and *rillenkarren–rinnenkarren*. Rillenkarren can develop under sheet water where the current of the water is turbulent from time to time. Dissolution is small and superficial on the *Ausgleichsfläche*. Rinnenkarren develop on the slope if the water separates into streams (Bögli, 1960a, 1976; Trudgill, 1985; Ford and Williams, 1989).

## Morphology of rinnenkarren

To describe rinnenkarren, we must consider their environment and their morphology. *Trittkarren*, *leafkarren* (Szunyogh et al., 1998), and *kamenitzas* can occur near rinnenkarren and feed the rinnenkarren. *Hanging kamenitzas* are often connected to a main channel by a small subsidiary channel.

The morphology of rinnenkarren varies according to sections of the channels (Figure 3). Forms with a water-feeding function such as *kamenitzas* are characteristic of the upper sections of rinnenkarren, while forms created by water flowing on the channel bottoms (steps, bottom basins) characterize the middle section of the channels. Various types of pits increasingly dominate the middle and lower sections of the channels.

The cross-section of a channel can take simple (Figure 4A.a–d) or complex forms (Figures 5, 4A.e). The shape of the ridges between the channels depends on the density and shape of the channels (Figure 4B). The cross-sections of *simple rinnenkarren* can be V, U, , or  (Figure 4A.a–d; Veress, 2000b).

We group simple rinnenkarren according to the size of the cross-section (Veress, 1995, 2000b, 2002). The widths and depths of *Type I rinnenkarren* are several decimeters, while the widths and depths of *Type III rinnenkarren* are only several centimetres. The smaller *Type III rinnenkarren* can develop on surfaces without other karren formations. The widths and depths of *Type II rinnenkarren* lie between the sizes of *Type I* and

*Type III*. *Complex rinnenkarren* have “simple complex” and “manifold complex” forms. In the case of simple complex rinnenkarren, only *Type III rinnenkarren* develop in a *Type I rinnenkarren* (although occasionally two *Type III rinnenkarren* can develop at the bottom of a *Type I rinnenkarren*). *Scallops* can occur at the bottom of *Type III rinnenkarren*. The rate of the size increase of the bearing rinnenkarren and the rate of the size increase of the inner rinnenkarren can be congruent or incongruent. In the case of manifold complex rinnenkarren, *Type II rinnenkarren* occur inside *Type I rinnenkarren*, and *Type III rinnenkarren* inside *Type II rinnenkarren* (Figures 5, 4A.e; Veress, 1995, 2000b, 2002).

*Terraces* can develop at the bottom of the channels (Veress, 1993) in wide complex rinnenkarren. Terraces are the remnants of former rinnenkarren bottoms. The surface of terraces slopes toward the middle of the channels and to the end of the channels. The terraces drop in gently concave stages from the edges of the main *Type I rinnenkarren* but have sharp edges where they meet the steeper walls of a lower channel.

According to Veress (1995, 2000c, 2002), *steps*, *bottom basins* (Figure 6), and *bottom kamenitzas* occur at the bottom of channels. *Potholes*, which can coalesce into one another, occur at the bottoms of the basins.

The pits or karren sinkholes in rinnenkarren are called *bottom channel pits* and there are several types. *Chimney pits* can develop where rinnenkarren are crossed by crevices or grikes (Figures 3e, 7). Soil and plants can accumulate in the pits, and the diameter of occupied pits is greater than those without soil and plants. The so-called *channel-end pits* occur in the lower sections of rinnenkarren (Figures 3e, 7). Their upper edges coincide with the upper edges of the channels.

In general, the development of karren caves is similar to the development of rinnenkarren but occurs below the surface. *Karren caves* develop along joints or bedding planes and can be *sinkhole karren caves*, *spring karren caves*, or *through karren caves* (Figures 3d, 8, 9).

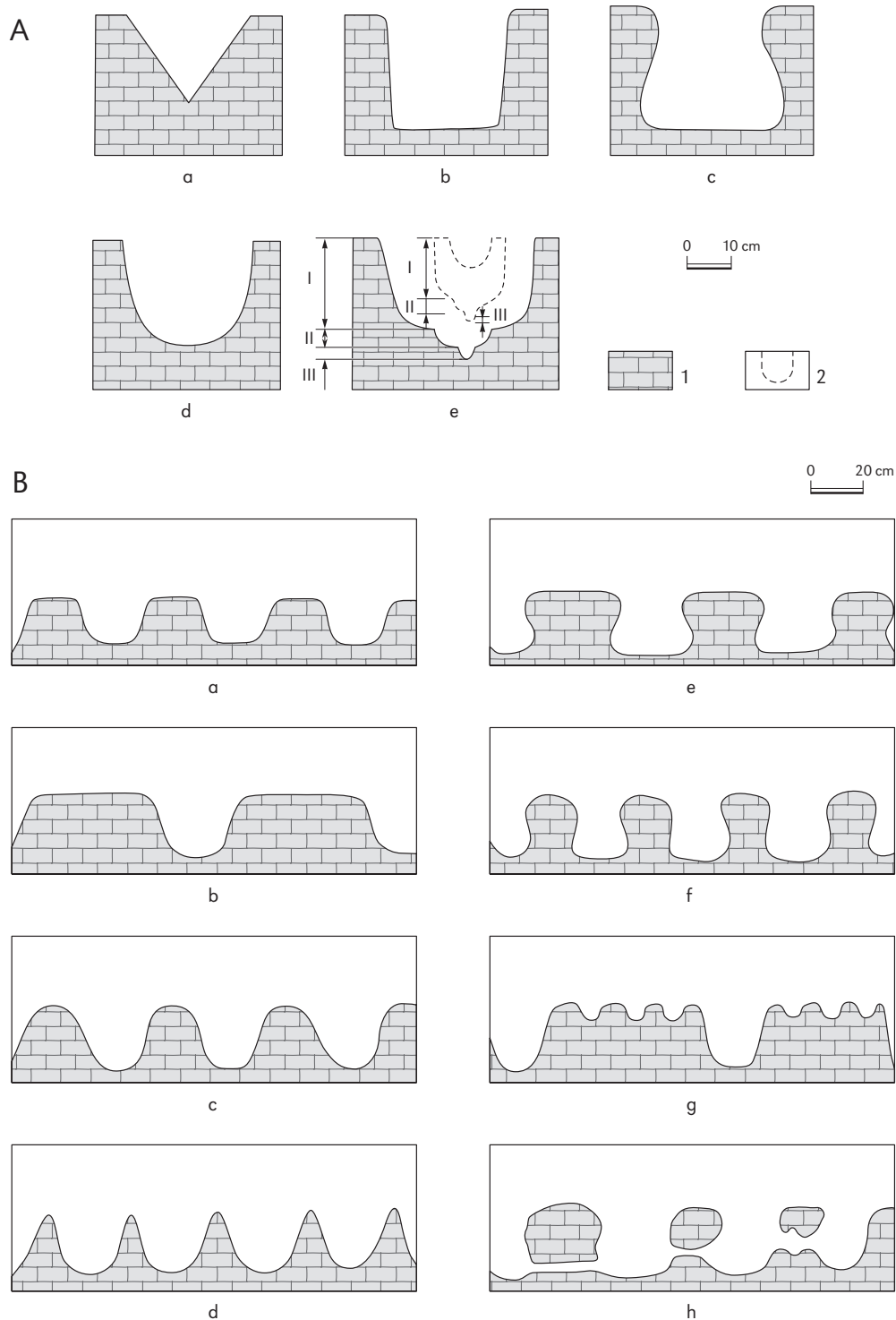


**Figure 4:** Types of channels (A) and ridges between channels (B) in profile. A: a–d. simple channels; e. a complex channel; B: a. flat and narrow ridges between channels; b. flat and wide ridges between channels; c. rounded ridges between channels (round karren); d. ridges between channels that have become sharp; e. flat ridges between channels that become narrow downwards; f. rounded ridges between channels that become narrow downwards; g. wide ridges between channels with small channels; h. windows through ridges between channels; 1. limestone; 2. former channel.



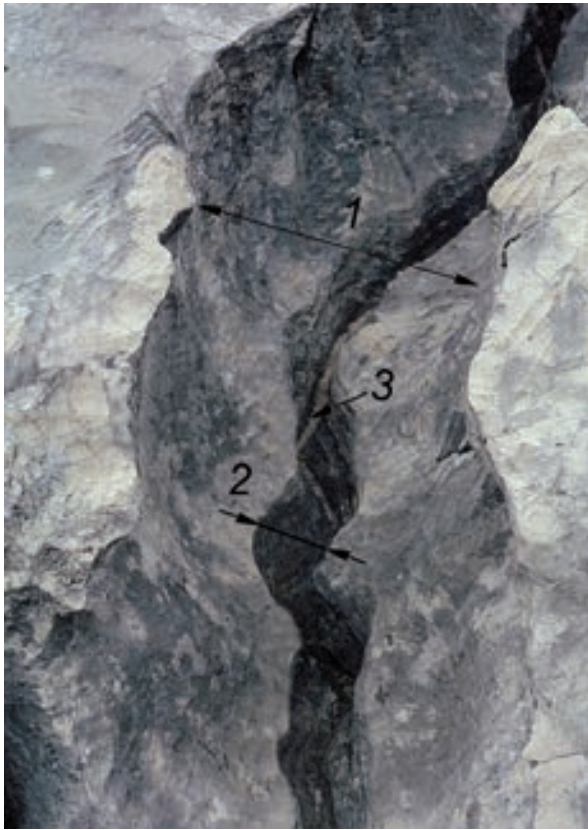


**Figure 5:** A complex channel (Totes Gebirge). Width of view is 50 cm. 1. Type I channel; 2. Type II channel; 3. Type III channel.

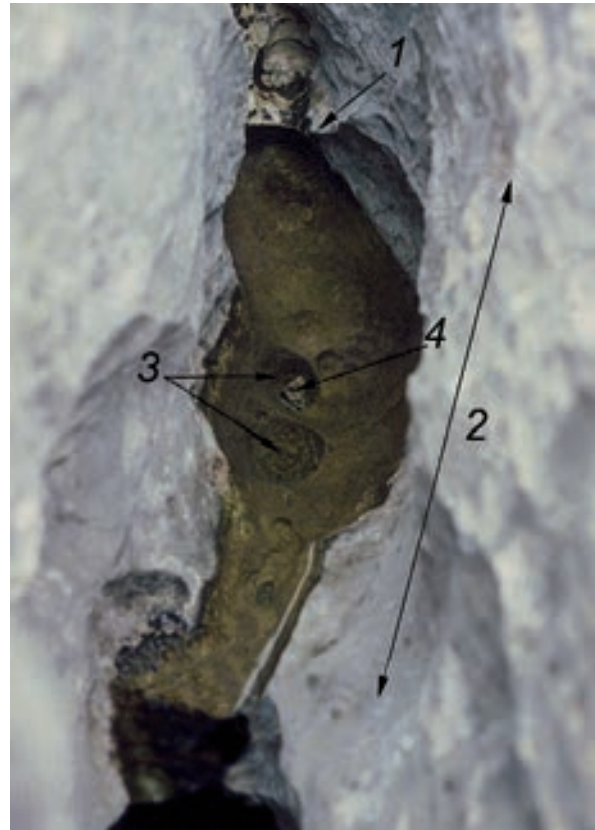


**Figure 6:** A channel bottom with basins and steps (Triglav Lakes valley). Width of view is 35 cm. 1. step; 2. bottom basin; 3. pothole; 4. debris.

## The development of rinnenkarren and their forms

Groups of karren forms such as rillenkarren, rinnenkarren, wandkarren, and *meänderkarren* are created by flowing water on bare slopes (White, 1988; Ford and Williams, 1989). Rinnenkarren can be formed by *rivulets* as the limestone dissolves under them (Ford and Williams, 1989). According to Parry (1960), they could have developed during the ice ages due to abundant melt water. He theorized that the quantity of CO<sub>2</sub> in the atmosphere was higher than it is today, although this theory has not been confirmed by measurements. According to Smith (1969), the quantity of CaCO<sub>3</sub> in the melt water on Somerset island

was only 60 mg/l. According to Trudgill (1986), rinnenkarren can also develop from subsoil dissolutional forms.

We believe the following factors (in combination or separately) cause the development of rinnenkarren:

- the development of rinnenkarren occurs under turbulently flowing rivulets. The laminar flow becomes turbulent if the value of the Reynolds number is higher than 1,500–6,000. The value of the Reynolds number depends on the angle of the slope (and furthermore on the change of the slope angle), on the depth of the flowing water, and on the roughness of the surface (Emmett, 1970). The roughness of the bottoms of the channels is considerable (Crowther, 1997),

and therefore the development and the maintenance of the turbulent flow can be caused by the roughness of the bottom of the channel as well. Because of the turbulent flow, the boundary layer is broken (Curl, 1966; Ford, 1980; Trudgill, 1985). A new boundary layer develops repeatedly and because it is unsaturated,  $\text{Ca}^{2+}$  ions can enter it from the limestone;

- plant and soil patches since they produce more  $\text{CO}_2$  (Jennings, 1985; Ford and Williams, 1989);
- mixing corrosion: Zentai (2000) showed that the area of the diameter of the main channel below two coalesced rinnenkarren is larger than the diameter lengths of the two subsidiary rinnenkarren added together. Therefore the solubility of the water increases where the waters of two subsidiary rinnenkarren join each other;
- the difference in the ion concentration between the boundary layer and flowing water is greater if the velocity of the current is higher; therefore, the quantity of the ion transport increases outside the boundary layer (Dubljanskij, 1987). Therefore, more ions are able to enter the boundary layer from the limestone;
- $\text{CO}_2$  enters the flowing water from the atmosphere (Jennings, 1985);
- according to Mariko et al. (1994) and Körner (1999), the quantity of  $\text{CO}_2$  is high if the plants are covered with snow (and the snow is solid). This phenomena can be explained by the fact that the plants are unable to photosynthesize but are able to dissimilate. For this reason the average diameter of channels found in a meter distance on bare slopes is  $3.65 \text{ dm}^2/\text{m}$ , according to our measurements, while this value is  $9.35 \text{ dm}^2/\text{m}$  on slopes covered with dwarf pine.

We measured the density of karren forms (including rinnenkarren) and their specific dissolution (the overall width of the karren forms to a distance of one meter) in several high mountain areas (Dachstein, Totes Gebirge, Julian Alps). The decreasing of the values of this data is only small in the course of the increase of the altitude. The density of rinnenkarren is 0.87 piece/meter at



**Figure 7:** Pits (Totes Gebirge). Width of view is 3.5 m. 1. bedding plane; 2. head of the bed; 3. channel bottom pit; 4. channel end pit; 5. channel; 6. grike.

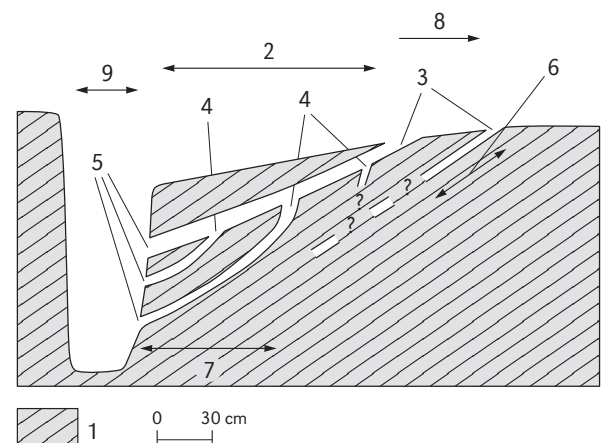


**Figure 8:** Karren channel cave system (observation, from Veress, 1995). 1. bedding plane; 2. through karren channel cave; 3. karren channel swallet; 4. karren cave swallet; 5. debouchure; 6. swallet type karren cave; 7. spring karren channel cave; 8. retreat of bathycapture; 9. grike.



**Figure 9:** Sinkhole karren cave and through karren cave (Totes Gebirge). Width of view is 65 cm. 1. Type II channel; 2. sinkhole karren cave; 3. through karren cave; 4. unroofed karren cave.

1,700 meters (in the pine belt), 1.18 piece/meter at 1,800–2,000 meters (in the *Pinus mugo* belt), and 0.79 piece/meter at 2,100 meters (on bare surface). The specific dissolution of the rinnenkarren is 12.83 cm/m, 20.29 cm/m, and 9.47 cm/m at these altitudes respectively (Veress et al., 2001a).

We can explain this with two factors:

- the quantity of CO<sub>2</sub> can be high in solid snow even on surfaces with no soil cover because the CO<sub>2</sub> cannot escape the snow;
- the higher the altitude, the longer the melting of snow takes. The water is therefore in contact with the rock for a long time.

We distinguish two phases in the development of rinnenkarren:

- the development of channels begins under rivulets (embryonal phase). The origin of the rivu-

lets can be sheet water or local sources. The latter can include soil patches, kamenitzas, leafkarren, trittenkarren, and cave karren;

- the further growth of the channels is due to percolating or flowing water. When the percolating water originates from the snow filling the channel, the dissolution occurs everywhere in the channel and its quantity is the same. However, the amount of dissolution is small since the CO<sub>2</sub> content of snow is also small. In the case of channel development generated by a rivulet, the channel becomes deeper and wider if the rivulet fills the channel completely. If this does not happen and the water flow decreases quickly, dissolution occurs mainly at the bottom of the channel. The growth of the channels on bare slopes is mainly due to percolating water as the water flow and CO<sub>2</sub> content of the rivulets are small. Since the CO<sub>2</sub> content of such snow is small, the growth of the channels is negligible. The growth of the channels is significant on slopes with *Pinus mugo*. The greater growth of the channels is due to flowing water since melt water originating from the snow covering the dwarf pines has a high CO<sub>2</sub> content.

The different channel shapes can develop in two different ways. Either the sheet water originating from the boundary surface or the water (rivulet) flowing in the channel dissolves the side slope of the rinnenkarren. However, sheet water can not dissolve the channels under the following conditions:

- the margins of channels (except of roundkarren) are sharp;
- the side walls of some rinnenkarren are unbroken and free from smaller karren forms (Figure 5). Rillenkarren occur in the neighbourhood of some rinnenkarren. These rillenkarren cannot continue at the margins of the channels. Hence, the water is saturated before it enters the channel;
- the channel wall slopes similarly (except with meanderkarren) along its whole length;
- the line of dip of the bearing surface and the

direction of the channel are equal. Therefore water from the boundary surface cannot flow into the channel. Sometimes we observe that channels can develop on ridges and water can not flow into the channel because of the ridges.

The shape of a channel is determined by the quantity of the water present and its changing quantity over a period of time. These characteristics depend on several factors including: the velocity of the current (which depends, for example, on the angle of the bearing slope) and the quantity of the recharge (which depends, for example, on the thickness of the snow and the intensity of the melting). In an active period, the dissolution works in a narrower width because the quantity of water decreases. In this case, the shape of the rinnenkarren takes a V-form in cross-section. The wall of a channel is perpendicular if the quantity of water does not change over a longer period.

Internal channels develop (Type II or Type III rinnenkarren) in a channel (which could develop earlier) if the quantity of water decreases considerably and subsequently does not change further for a long period.

Karren terraces develop if the older channel can not grow. The internal (younger) and smaller channel can partly consume the bottom of the older channel. Terraces can also develop because of bottom channel pits since internal channels develop by corroding backwards from bottom channel pits.

The deepening of a channel can take the following forms:

- the channel deepens in the direction of the channel head and the channel becomes longer during its development. The head of the channel extends up the slope;
- the depth and length of the channel develop uniformly as the head of the channel extends up the slope;
- the depth of the channel increases uniformly while its length does not change;
- the depth of the channel increases downward along the dip of the slope while its length does not change;

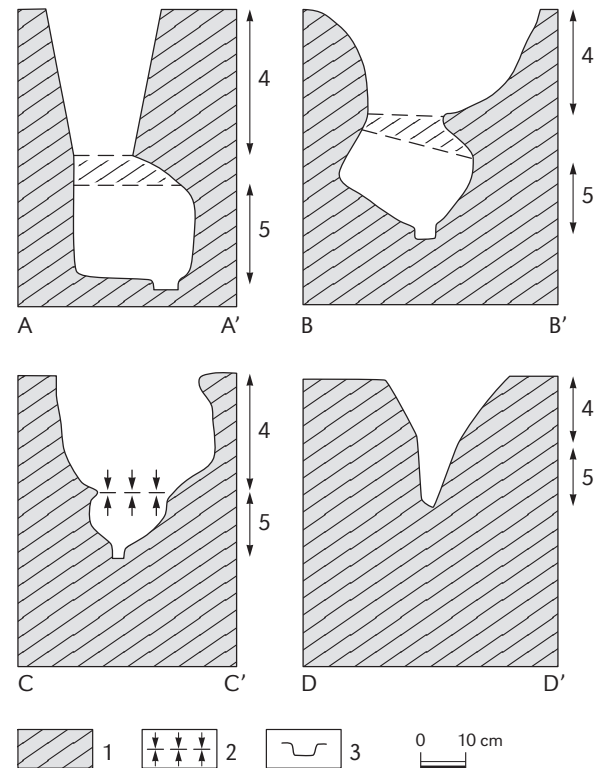


**Figure 10:** Characteristic cross-sections of an evolved channel in various stages of development (Totes Gebirge, from Veress, 2000b). 1. roof destroyed by collapse; 2. roof destroyed by merging of a channel and a karren channel cave; 3. Type III channel; 4. upper channel section developed by surface solution independently from bathycapture; lower channel section intensively developing due to beheading; 5. channel section developed by subsurface solution. In the A-A' and B-B' cross-sections, the evolution occurred with the collapse of the roof of the karren channel cave; in the case of the C-C' cross-section, it occurred through coalescing; bathycapture occurred between the C-C' and D-D' sections.

- the depth of the channel decreases below the lower end of the channel as it extends down the line of dip of the slope;
- some sections of the bottom of the channel are dissolved to varying degrees.

In the first two cases, the development of the channel is regressional. The causes for this phenomena are the following. Rivulets develop along the line of dip of the slope, and such currents have



**Figure 11:** Channel and karren cave which are partly coalescing (Totes Gebirge). Width of view is 80 cm. 1. channel; 2. former karren cave; 3. evolved channel; 4. roof remnant.

the highest velocity. In the first case, the development of the channel is exclusively regressional; in the second case, it can be partly rain-furrowed (regressional rain-furrowed channel development). In the third and fourth cases, the length of the channel does not change and therefore their development is rain-furrowed. The rate of deepening can increase toward the lower section of the channel due to the increase of the current velocity. The deepening of the channel results in a horizontal movement. The dissolving of the bottom of the channel is more significant in the lower parts than in the upper section of the form. In the fifth case, the development is antiregressional, which

is characteristic of decantation channels. “Bevels” develop in the sixth and seventh cases.

We can also distinguish other channel development processes:

- from “leafkarren” (Szunyogh et al., 1998);
- from trittkarren (Veress and Tóth, 2002);
- from scallops (Curl, 1966);
- from *ripple karren* on marble (Diego de Almagro island; Veress et al., 2006);
- from the opening-up of karren caves (Veress, 2000b, 2002).

We observed eddies (Veress, 2000c; Veress et al., 2006) in the bottom basins of rinnenkarren and at the bottom steps of rinnenkarren in the Julian Alps and on Diego de Almagro island. We therefore believe the development of these forms occurs at eddies. Capture pits and channel pits can develop at bathycaptures. The sites of bathycaptures develop back toward the ends of the rinnenkarren.

The development of karren caves can largely be linked to rinnenkarren (Veress, 1995, 2000b, 2002). Karren sinkholes are capture pits and channel pits. It can sometimes happen that a karren cavity swallow develops first through dissolution at a bedding plane, and then a channel develops from the swallow (*blind channel*). Karren caves can develop like deltas if there are bathycaptures at the bottom of a channel. Spring karren caves develop below each other if bathycaptures occur in a karren cave. It is also possible that a karren cave network of several levels develops. An *evolved channel* develops when a channel coalesces with a karren cave under it. This can occur through dissolution and collapse. At the beginning of the process *karren windows* and *karren bridges* develop. These rinnenkarren channels have a double cross-section (Figure 10). These double cross-sections occur at the karren swallow of earlier karren caves. The upper section of the channel grows narrow in its cross-section (a former channel), while the lower section of the channel is basically circular in cross-section (a former karren cave). Roof remnants can remain in the wall.

According to Veress and Tóth (2001), channels can coalesce during regression. The process oc-

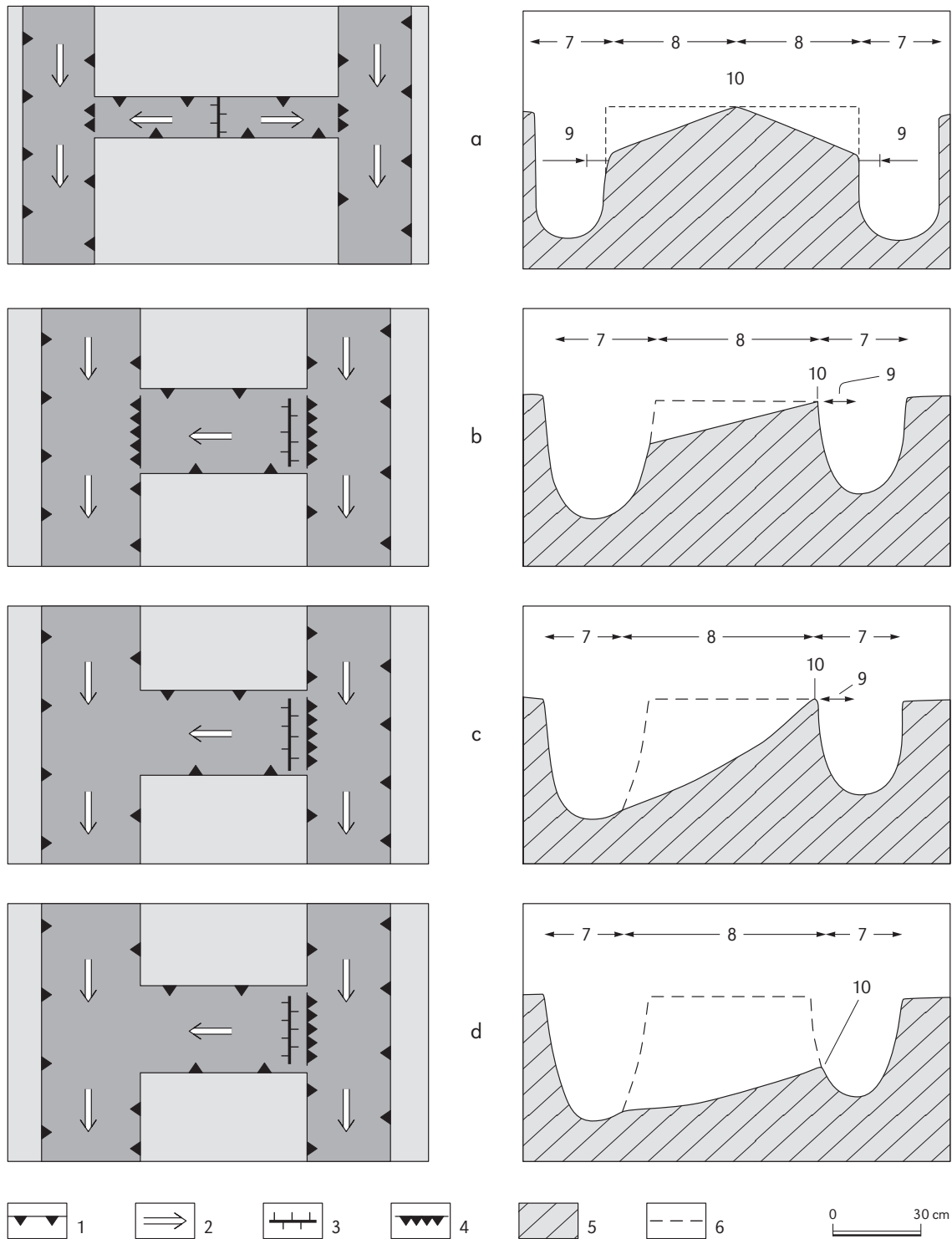


**Figure 12:** Coalescing of channel ends (a) and false beheading (b, c, d) (from Veress and Nacsá, 1998). 1. Type I channel; 2. slope direction of Type I channel bottom; 3. channel bottom watershed divide; 4. step; 5. limestone; 6. ground surface before channel entrenchment; 7. master channel; 8. regressing tributary channel; 9. step; 10. channel bottom watershed divide; left. view from above; right. cross-section; a. the regressing tributary channel heads join; b. the beheading channel deepens constantly; c. the beheading channel retreats; d. the beheading channel entrenches to the bottom of the main channel.

curs when the ends of the channels coalesce into each other (Figure 12a). It can also happen that the end of a regressing channel reaches or cuts through the side wall of another channel. This is called “false beheading”. In the event of false beheading, the original direction of the flow of water along the bottom of the “beheaded” channel does not change (Figure 12b-d). In the case of “real” be-

heading, either a channel end reaches the wall of another channel or several channel ends coalesce into each other and the direction of the flow of water along the bottom of the beheaded channels will change partly or totally. The water of the beheaded channel will run partly or totally into the beheading channel.

Márton VERESS

*Meanderkarren* are described by Bögli (1976) and others (Jennings, 1985; Ford and Williams, 1989) as a special type of *rinnenkarren*. According to Bögli (1960a), the cross-section of meanderkarren decreases along the direction of the slope. We present pictures in this chapter that show the typical asymmetrical cross-section and the under-detailed morphology of meanderkarren.

Small *micro-meanderkarren* (*decantation micro-meander*) are described by Macaluso and Sauro (1996a), who claim these forms are found on halite but not on limestone. However, we discovered micro-meanderkarren on limestone as well, for example, a few on the sides of an abrasional solution *spike karren* on Lokrum island (Croatia). We should also mention that various authors describe the morphology of meanderkarren differently. Sauro (1973a), for example, regards channels that have non-symmetrical cross-sections and changing directions as meanderkarren (for this type we use the term *false meander*). In his later publication, Bögli (1976) describes these forms emphasizing their small size and that they are developed by a solutional flow percolating from the soil. According to Ford and Lundberg (1987), the sinuous *Horton-type rinnenkarren* are associated with meanderkarren, while according to Sweeting (1972) meanderkarren are *internal channels* of larger channels. We have already observed that meanderkarren can develop not only

on limestone but also on other rock, for example, on evaporites (Macaluso and Sauro, 1996a; Calaforra, 1996) and marble (Veress et al., 2006).

Hutchinson (1996) published a new way of classifying meanderkarren as young and mature types. He distinguishes *gutters* that have a V cross-section, *gorges* that have steep sides, and a *meandering type* of the mature type. This latter type is characterized when a smaller *meandering channel* occurs inside a large *straight channel*. According to Hutchinson (1996), meanderkarren have two main characteristics: *sinuosity* and an *asymmetrical cross-section*. According to Hutchinson (1996), meandering occurs when *rinnenkarren* become old and when the inclination of the surface is between 7° and 14°. He notes that *young channels* flatten downwards along the slope while older ones do not and that *older channels* have less sinuosity than young ones.

According to Ford and Williams (1989), meanderkarren develop where the flow of the water is slow, while according to Zeller (1967), they may be formed where the velocity of the water current is high (Froude-number 1.8–20) and the velocity of the water current is higher than the velocity of the currents of river and melt water. Hutchinson (1996) describes the development of meanderkarren as a characteristic process when *rinnenkarren* become older, while according to Davies and Sutherland (1980) they are forms that adapt to the



flow (along the line of least resistance). According to Zeller (1967), meanderkarren develop during turbulent flow, related as well to when the flow changes from turbulent to laminar. However, Zeller (1967) also suggests that secondary currents can cause the development of meanderkarren as well.

## Morphology and development of meanderkarren

Veress (1998, 2000d) distinguishes two groups of meanderkarren: *false* and *true meanderkarren*. False meanderkarren change direction in such a way that the cross-section of the channel is symmetrical when true meanderkarren do not develop during the deepening of the channel (Figures 1a, 2). The cross-sections of the meanders of true meanderkarren become asymmetrical (Figures 1b, 3).

Like other authors, Veress (1998, 2000d) classified the morphometry of meanderkarren using

the parameters applied to rivers. The morphology of the *loops* of the meanderkarren and the meandering rivers may be different, but in both cases the cause of the meandering is the *swinging of the channel line*. The differences are as follows:

- the profile of meanderkarren is asymmetrical. The bed of an alluvial meandering river may be slightly asymmetrical due to lateral erosion. On the concave side of a meanderkarren the bank will be steep but it will never be overhanging. On the convex side of the meanderkarren the bank will be gentle, where shoals can develop. If a valley with V cross-section is created by linear erosion, its cross-section will be symmetrical;
- the morphology of the loops of meanderkarren is largely like that of the valleys of forced meandering rivers. The cross-sections of the loops of forced meandering rivers are also asymmetrical. With this valley type the bank of the river can overhang somewhat over the concave side of the loop if the river bed developed in rock.

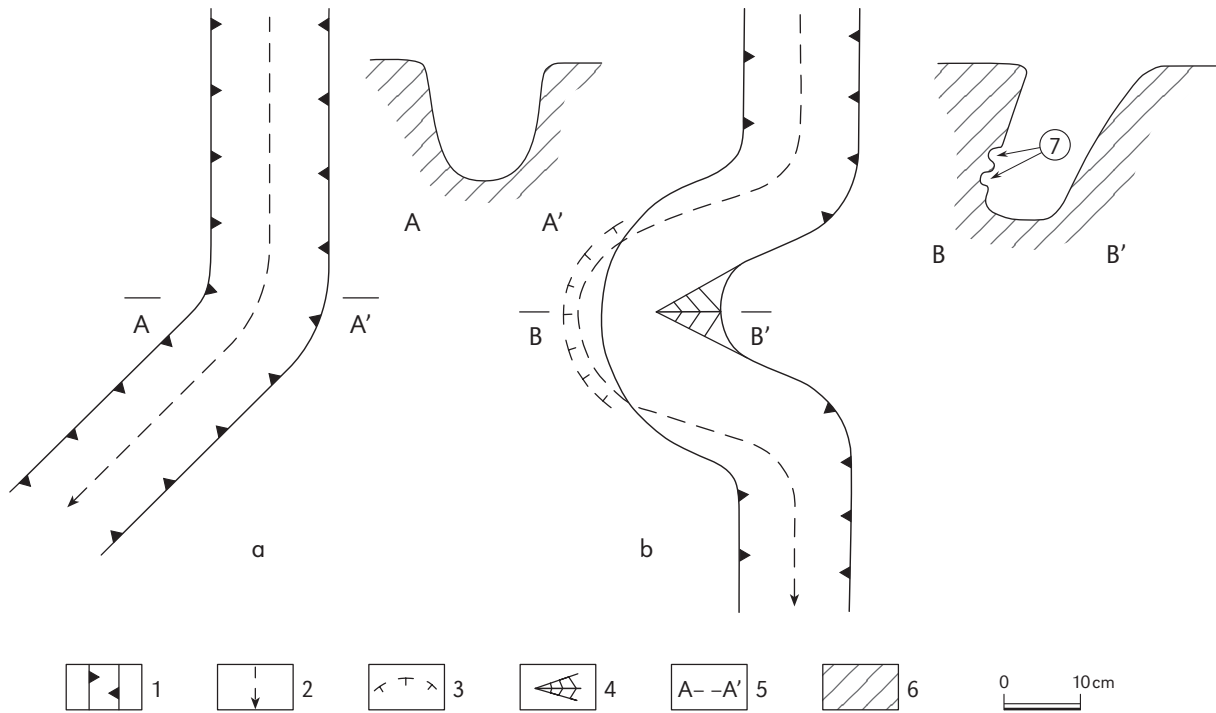


**Figure 1:** False (a) and true meanderkarren (b). 1. vertical channel side; 2. stream line; 3. edge of concave channel side; 4. moderately sloping side of channel (skirt); 5. cross-section; 6. bedrock; 7. meander scour grooves (from Veress, 2000b).

The side wall of a meanderkarren overhangs on the concave side of a meandering channel while the slope of the wall is gentle on the convex side of the meandering channel. Veress calls this gentle side wall a *skirt*. The form of the skirt is very varied both in profile and seen from above. According to the data measured by Veress (1998, 2000d), at the meanderkarren of a channel the degree of inclination of the opposite walls is very different. He established that the size of the overhang is less than the lateral extension of the skirt. Skirts sometimes can extend beyond the edge of the *overhanging wall*. The shape of a skirt is *half-conical* or *half-pyramid*, seen from above (Figure 3). If the meandering is complex, the *skirt* will be *complex* as well. Skirts frequently become detached and form *oxbows* and *islands* (*karren Inselbergs*) for many reasons (Veress, 2000b; Tóth and Balogh, 2000), for example, when the flowing water at the bottom of the channel hits a skirt and dissolves its way through it. The roof of the tunnel that develops this way will eventually collapse. The process can also occur when some of the water flowing at the bottom of the channel overflows at a *karren neck* and dissolves the rock, resulting in a detached form (Figure 4).



Figure 2: False meander (Julian Alps, Slovenia).



Figure 3: True meander (Julian Alps, Slovenia). Width of view is 35 cm. 1. meander scour grooves.



**Figure 4:** Detached loop-neck (Totes Gebirge). Width of view is 1.5m. 1. detached karren oxbow; 2. karren neck; 3. karren recess (karren "inselberg").

*Meanderkarren scour grooves* can develop on the overhanging side walls of meanderkarren. They occur one below another at several levels (Figure 3) and are like small horizontal channels on the side walls. *Meanderkarren terraces* are embayments of the bottom of the channel on the side wall that is below the concave edge. *Hanging terraces* develop when the bottom of the channel is able to deepen more intensively in the middle. Meanderkarren terraces can also develop on parts of the surface of a skirt where the inclination is small.

According to Veress (1998, 2000d), the cross-sections of channels are asymmetrical because the rate of solution is different on opposite sides of the meanderkarren. He explains this by the fact that the velocity of the current is different on the opposite sides of a channel. The difference in the ion concentration between the boundary layer and flowing water is larger if the velocity of the current is higher, and therefore the quantity of the ion transport out of the boundary layer increases (Dubljanskij, 1987). Therefore, more ions pass from the limestone to the boundary layer. A fast current causes turbulence and therefore the boundary layer is broken (Curl, 1966; Ford, 1980; Trudgill, 1985).

A new boundary layer will develop repeatedly and because it will be unsaturated,  $\text{Ca}^{2+}$ -ions can enter it from the limestone. Veress (2000d) therefore explains the development of the asymmetrical cross-sections by the asymmetrical relationships of the currents. The *channel line* will not stay in the middle of the channel (in the middle of the rivulet flowing down the slope); instead, it will move laterally and at some points will even reach the wall of the channel (*oscillation of the channel line*). The dissolving of the channel wall will be more intensive here than on the opposite side of the channel where the velocity of the flowing water is smaller because the channel line has moved away. The development of meanderkarren as well as the development of meanderkarren types may be explained by the oscillation of the channel line (see *Types of meanderkarren* in the following).

According to Veress (1998, 2000d), the oscillation of the channel line can be explained by *external* and *internal causes*. He regards morphology as an external cause. He observed this in several cases, for example, when water from a *tributary channel* flows into the *main channel* (in this case, the main channel meanders locally below the mouth of the tributary channel). Meandering

can also be caused by a false meanderkarren, by a change in the inclination of the bottom of the channel, by calcareous spar lenses, and by an older skirt. The channel line can also often oscillate in a homogeneous environment. In this case, we explain the process by the changing conditions in the current of the water (internal cause). Probably due to the current of the water, a wave motion develops that can change the oscillation of the channel line of the *rivulet* downstream.

## Methods

Meanderkarren were first quantitatively described by Zeller (1967) on Mount Silbern (Switzerland) along with other different types of meandering including beds of alluvial meandering rivers, forced meandering rivers, and channels of meandering melt water from a glacier. He used the following features to describe meandering: sinuosity ( $w$ ), length of curve ( $\lambda$ ), inclination of the bottom of the channel ( $J$ ), and amplitude ( $A$ ). The last equals the width of the meanderkarren zone. The sinuosity is calculated as the ratio of the channel line and the axis length of the meanderkarren zone. He measured the sinuosity of meanderkarren, the length of the meanderkarren curve, the width of the meanderkarren zone, and the inclination of the bottom of the channel. He found the sinuosity of the meanderkarren in the Silbern area to be 2.84, the length of the curve of the meanderkarren 5.8 cm, the inclination of the bottom of the channels 60–500‰, and the amplitude 6.6 cm. He also found that meanderkarren can wander laterally and that their side walls overhang. He describes the length of the meanderkarren curve, the width of the meanderkarren zone which he called amplitude ( $A$ ), and the width of the meanderkarren channels in a function. One linear function can be adapted to the above-mentioned parameters of each of the four different types of meandering. These functions are the following:

$$\lambda = 10.0 \cdot b^{1.025},$$

$$A = 4.5 \cdot b^{1.0},$$

where  $b$  is the width of the channel.

The functions show that the wider the river or meanderkarren is, the bigger the curves and the zone of the meanderkarren are. The above parameters of meandering forms are probably associated with the width of the water flow.

Hutchinson (1996) examined the proportions of the shapes of meanderkarren and their forms on Mallorca. He defined the ratio of the shape (“form ratio”) as the quotient of the width and the depth of the forms, defining width as the distance between identifiable channel rims. He measured two different width data: “Maximum width” and “Horizontal width”. Presumably he calculated the mean of this width data and used it as the width in his calculations. He measured the depth of the forms at two points: “Horizontal mid-Depth” where the depth is measured in the middle of the horizontal width (Dmid Hor), and “Horizontal maximum-Depth” where the maximum depth is measured perpendicularly to the horizontal width (Dmax Hor). We also think he used a mean depth calculated from these two measurements. He could calculate the shape of the forms from the quotient “Al” and “Ar” where “Al” is the cross-sectional “Area large” – calculated using the Dmax Hor data – and “Ar” is the cross-sectional “Area small” – calculated using the Dmid Hor data. He found that the average form ratio is larger for young channels (9.1) than for mature channels (2.54). The change of the shape is probably less significant; however, the asymmetry of mature meanderkarren is greater. Therefore, the maximum depth of a meanderkarren channel shifts away from the middle of the channel in the course of its development. Hutchinson assumed there was a direct relationship between the shape and the ratio of the forms.

Hutchinson (1996) also investigated the slope inclination data relative to the sinuosity of meanderkarren. He measured the sinuosity on the axis of abscissa (x-axis) and the inclination on the axis of ordinate (y-axis) of a coordinate system. However, he did not do a regression analysis but merely used a line to connect the points. He noticed that the amount of sinuosity increases with a decrease of

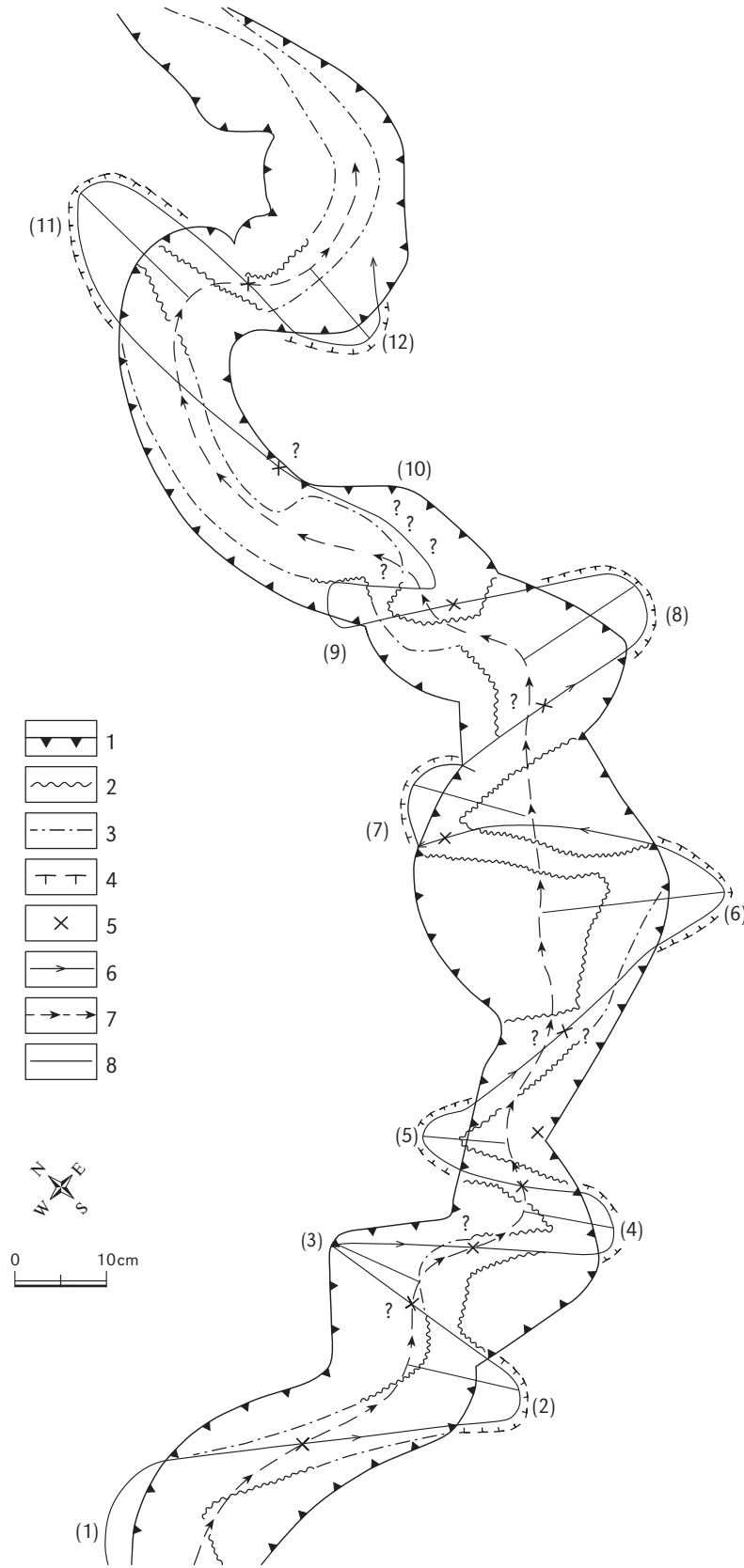


**Figure 5:** Constructed channel lines of channel No. 7 (number in parentheses identifies the loop; Totes Gebirge, Austria, from Veress, 2000d). 1. edge of Type I channel; 2. lower edge of skirt; 3. end of gently sloping channel; 4. bottom of overhanging wall at the plane of the channel bottom; 5. inflection point; 6. present channel line; 7. previous channel line; 8. accessory straight along which the  $SK_k$  and  $SK_k$  values can be measured.

inclination and concluded that sinuosity depends on the degree of inclination. According to Zeller (1967), sinuosity (meandering) develops if the angle of the slope is between 3.44° and 36°, while according to Hutchinson (1996), it occurs if the angle of the slope is between 25° and 40° (although in mature channels it can occur between 7° and 14°).

Veress (1998, 2000d) used different parameters (described below) to construct maps of seven meanderkarren in Totes Gebirge (Austria). The data from four of the meanderkarren appears in Table 2. He wished to identify the factors that can determine the oscillation of the channel line in order to describe typical meanderkarren development. A constructed channel line of a meanderkarren drawn by Veress (2000d) is shown in Figure 5.

Veress used the channel line as the basis for the various parameters of meandering. He defines wave length ( $\lambda$ ) as the smallest distance between adjacent inflection points, which mark where the channel line is in the middle of the channel. The length of the curve ( $m_i$ ) is the distance measured between the neighbouring inflection points along the channel line. The width of the meanderkarren zone is the shortest distance between the boundary lines of the meanderkarren. The boundary lines touch the edges of a channel on its concave sides. Veress (2000d) calculated the development

of the meanderkarren ( $\beta$ ) as follows using Laczay's (1982) method (Table 1):

$$\beta = \frac{m_i}{\lambda}$$

**Table 1:** River bend types specified by their development (Laczay, 1982).

Type of river bend	Value of $\beta$
Undeveloped bend	<1.1
Developed bend	1.1–1.4
Well developed bend	1.4–3.5
Fully developed bend	>3.5

The parameters used by Veress (2000d) to describe meanderkarren are shown in Figure 6: wave length ( $\lambda$ ), the length of the curve ( $m_i$ ), the width of the meanderkarren zone ( $m_{sz}$ ), etc. He acquires these parameters by drawing the oscillating channel line and identifying the inflection points. The channel line moves to the bottoms of the side walls at the concave channel edges, and by connecting these points we can identify the channel line.

The channel line will become lower and lower due to the deepening of the channel. The channel line moves laterally and obliquely downward as well during its deepening. Veress (2000b) called this process the “slippage” of the channel line.

If the slippage of a deepening channel is ex-

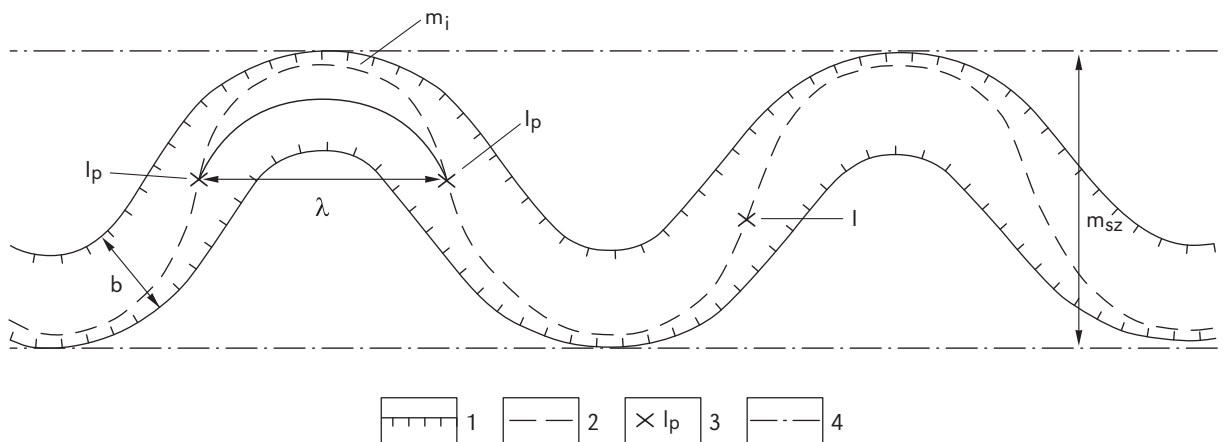


**Figure 6:** Parameters of a meander (from Veress and Tóth, 2004). 1. channel margin; 2. channel line; 3. inflection point; 4. boundary line of meanders;  $\lambda$ . wave length of meander;  $m_i$ . length of arch of meander,  $m_{sz}$ . width of meander zone; b. width of channel.

pressed in units, we can determine the intensity of the slippage of the channel line. The intensity of slippage ( $L_i$ ) can be calculated using the following formula:

$$L_i = \frac{Sk_j - Sk_k}{M}$$

where  $Sk_j$  is the difference between the present and original channel lines measured on the map,  $Sk_k$  is the difference between the initial slippage and the original channel lines measured on the map, and  $M$  is the depth of the channel in the bend.

The slippage of the channel line will be greater where the oscillation of the channel line occurs due to an external cause. According to Veress (2000d), the stream characteristics of the surface water flowing downward have little to do with the oscillation of the channel line.

The loops can not be ranked using the width of the meanderkarren zone alone since their values

also depend on the width of the channel (Zeller 1967). Therefore Veress and Tóth (2004) employed the idea of the width of the specific meanderkarren zone. They could calculate it from the equation as follows:

$$m_f = \frac{m_{sz}}{b}$$

where  $m_f$  is the width of the specific meanderkarren zone,  $m_{sz}$  is the width of the meanderkarren zone, and  $b$  is the width of the channel.

### Types of meanderkarren

Using the morphology and the measured parameters of meanderkarren, Veress (2000b) and Veress and Tóth (2004) classified them into the following types: “looping,” “remnant,” “developing,” and “perishing” (Figure 7).

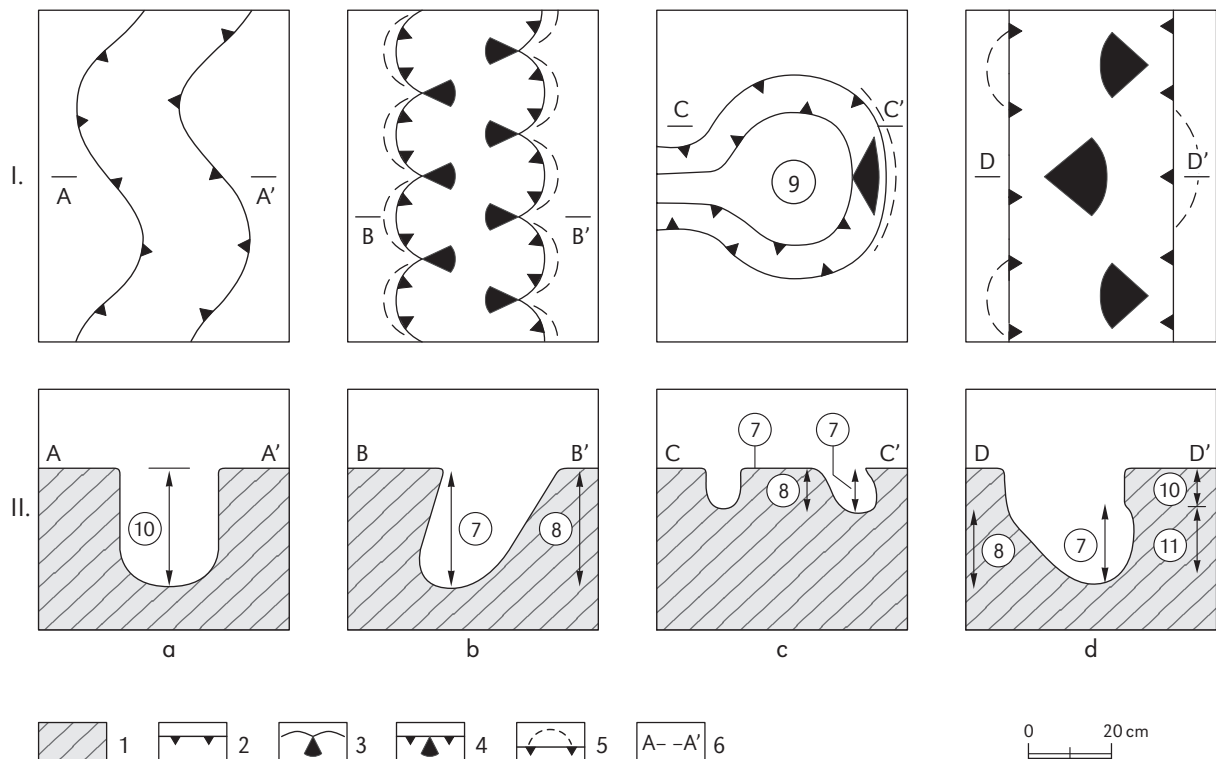


**Figure 7:** Meanderkarren types (from Veress, 2000d). I. planimetric representation: 1. limestone; 2. Type I channel; 3. skirt starting at channel rim; 4. skirt on lower part of channel side; 5. overhanging wall; 6. site of section; II. on cross-section: 7. overhanging side wall; 8. skirt; 9. karren recess; 10. symmetrical cross-section channel and part of channel; 11. asymmetrical cross-section channel; a. false meander; b. “remnant” meander; c. “looping” meander; d. “developing” meander.

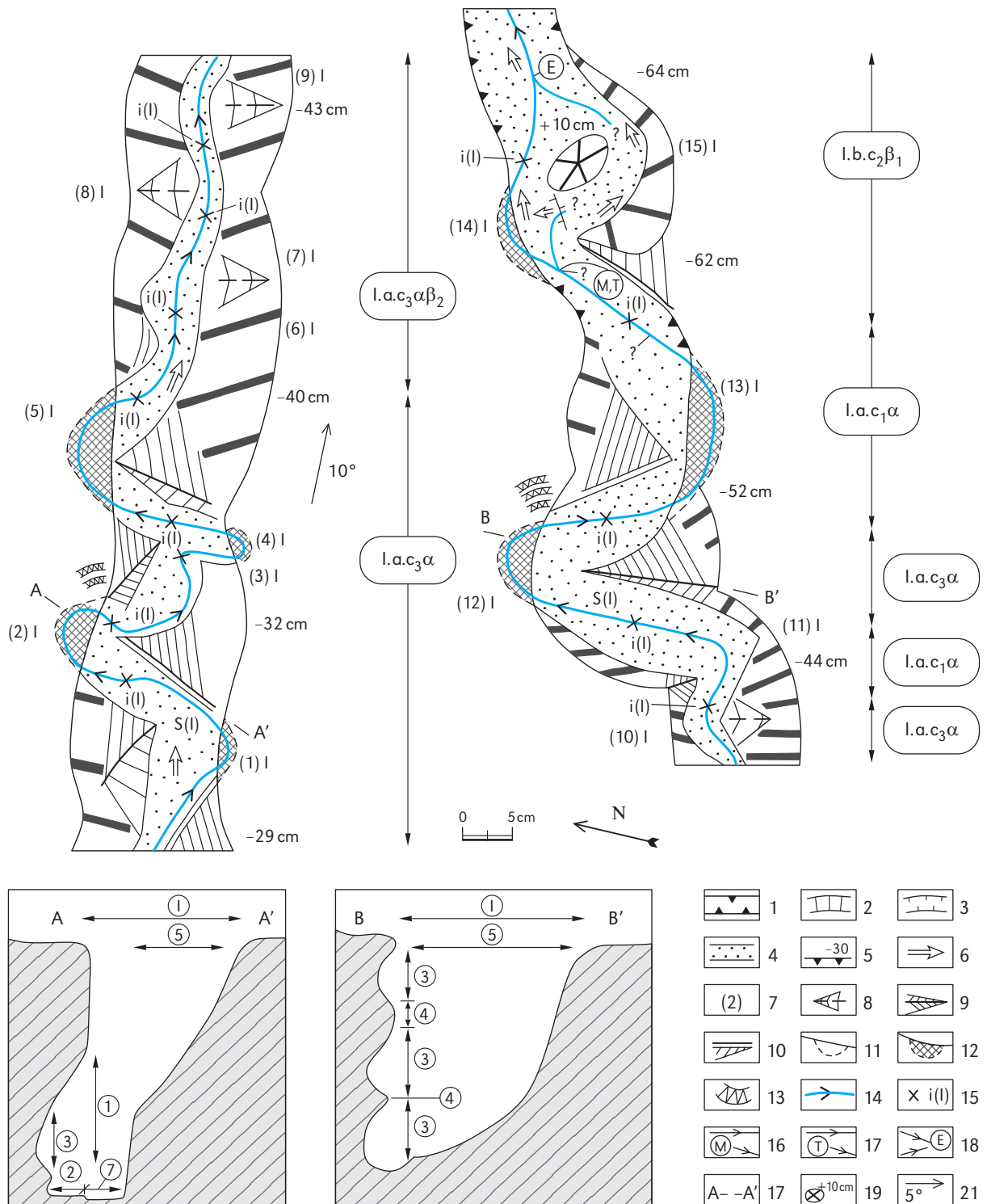


**Figure 8:** Morphological map of channel 4 (Totes Gebirge; from Veress and Barna, 1998). Planimetric representation: 1. vertical side wall of Type I channel; 2. gentle side wall of Type I channel; 3. vertical side wall of Type III channel; 4. plane channel bottom; 5. depth of channel (in centimetres); 6. slope direction of channel bottom; 7. number of meander loop; 8. developing skirt; 9. asymmetrical skirt; 10. half skirt; 11. overhanging wall; 12. meander terrace on overhanging wall; 13. meander scour groove and major meander scour groove (position and size of the small meander scour →



It is clear that *looping meanderkarren* may be distinguished from the other types by using the value of curve-length and the value of the development of the meanderkarren. The average length of the curve of “looping” meanderkarren is 45.75 cm, and the average value for the development of a “looping” meanderkarren is about 3.0. The average length of the curve of “developing” and “remnant meanderkarren” is 21.06 cm and 30.54 cm respectively, and the development value of these meanderkarren is 1.96 and 2.17 respectively (Table 2). When the loops that belong to the different types are compared, the difference is especially great. Thus, for example, in the case of the meanderkarren seen in Figure 4 the development value is 4.27. The value of the development is 2.76 in the case of loop number 11 of the “looping” meanderkarren seen in Figure 5, but this value is only 1.66 in the case of the number 3 “remnant” meanderkarren in the same meanderkarren.

Meanderkarren can be ranked in the “looping” meanderkarren type when the average length of

their curves is over 30 cm and the average of the meanderkarren development value is above 2.5.

According to Veress (2000d), the slippage of the channel line can best characterize the morphology of a meanderkarren because it can explain its asymmetry. The average intensity of slippage of the channel line is 0.33 for “looping” meanderkarren, 0.17 for *developing meanderkarren*, and 0.12 for *remnant meanderkarren*.

The sinuosity and the width of the meanderkarren zone can be different for different meanderkarren types. For example, the sinuosity is 2.1 for the number 11 and 12 loops of the “looping” meanderkarren seen in Figure 5 while this value is 1.7 for “developing” meanderkarren and “remnant” meanderkarren sections (Figure 8, number 11, 12, 13 loops). The sinuosity values calculated by Zeller (1967) are between 1.1 and 1.7. According to Hutchinson (1996), the value of sinuosity is between 1.0 and 1.6 if the slope inclination is between 25° and 40°.

The width of the specific meanderkarren zone is

**Table 2:** Averages of parameters (using data measured in the No. 3, 4, 6, and 7 channels; from Veress, 2000d).

Meandertype	Looping	Developing			Remnant			All types	
		internal n = 3	internal n = 7	external n = 13	all n = 20	internal n = 2	external n = 6	all n = 8	internal n = 10
cause of swinging	external n = 3	internal n = 7	external n = 13	all n = 20	internal n = 2	external n = 6	all n = 8	internal n = 10	external 21
length of bend	45.75	23.5	18.6153	21.0576	27.5 (66.71)*	33.5833	30.54	25.5	32.6495
wave length	15.125	12.0	10.38	11.19	16.0 (16.87)*	13.8333	14.9166	14.0	13.1128
stage of development	3.0233	2.0210	1.8992	1.9601	1.7239 (4.08)*	2.6181	2.171	1.8724	2.5135
intensity of slippage	0.3336	0.1056	0.2300	0.1678	0.08 (-3.32)*	0.1608	0.1204	0.0928	0.2439 0.2966**

\* the number in parenthesis belongs to channel No. 6 (n=7)

\*\* with the data of channel No. 3 (n=3)

→ groove in the bend are not drawn to scale); 14. estimated channel line, with stream direction (number in brackets indicates type of channel in which channel line developed); 15. estimated inflection point; 16. bifurcation of channel line connected to function; 17. bifurcation of channel line connected to slippage; 18. uniting channel lines; 19. site of cross-section; 20. karren “inselberg” at bottom of channel (with altitude data); 21. slope direction and degree of slope of boundary surface; a. straight channel segment; b. false meander channel segment; c. true meander segment ( $c_1$  “remnant” meander,  $c_2$  “looping” meander,  $c_3$  “developing” meander), the swinging of the channel line can occur due to an internal ( $\alpha$ ) or external ( $\beta$ ) cause ( $\beta_1$  false meandering of channel,  $\beta_2$  bend and its skirt). Cross-section: I: Type I channel; 1. overhanging side wall of concave channel margin; 2. meander terrace on side wall of concave channel margin; 3. meander scour groove on side wall of concave channel margin; 4. ridge between meander scour grooves; 5. skirt; 6. vertical wall of skirt that developed due to solution; 7. bottom of channel.



**Figure 9:** "Looping" meander (Julian Alps). Width of view is 55 cm.



**Figure 11:** "Perishing" meander (Julian Alps). Width of view is 2.5 m, in the middle; 1. asymmetrical cross-section, 2. symmetrical cross-section.



**Figure 10:** "Developing" meander (Julian Alps). Width of view is 50 cm. 1. complex skirt; 2. partly detached skirt (karren "inselberg").

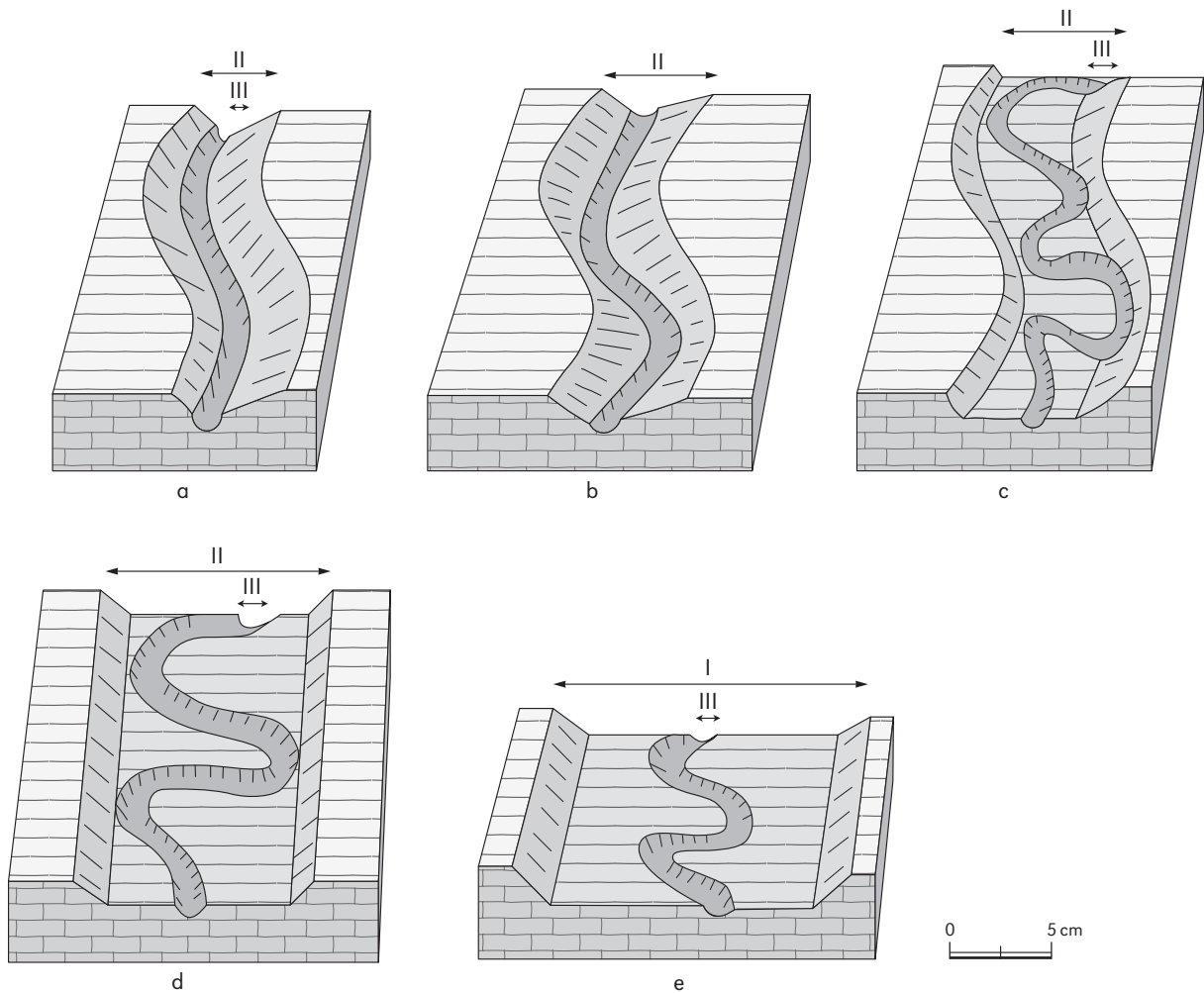


**Figure 12:** Inherited meanders of composite karren channels (from Veress, 1995). I, II, III. channel types; a. from the beginning forced meandering, similar to strained meander; b. from the beginning forced meandering, shifted meander; c-d. strained meander; e. free meander.

2.41 for “looping” meanderkarren (Figure 5, loops 11, 12) while it is 1.56 for “remnant” meanderkarren (loops 2 to 10 in Figure 5). This parameter is considered small for remnant meanderkarren.

“Looping” meanderkarren will develop if the channel line swings due to a direction change in a false meanderkarren at its curvature (Figures 4, 7c, 9). The length of the curve of a “looping” meanderkarren is large as is the width of the meanderkarren zone, the sinuosity of the meanderkarren, and the intensity of slippage. On the other hand, the wave length of “looping” meanderkar-

ren is small. The oscillation of the channel line occurs in part of a false meanderkarren during the deepening of the channel.

“Remnant” meanderkarren may develop in a straight channel as the sides of the channel are dissected by curved sections. The curved sections become the concave sides of the channel, and where the curved sections meet we can see the peaks that become the convex sides of the channels where skirts develop. The peaks and skirts occur opposite the center of the concave sections of “remnant” meanderkarren (Figures 3, 7b, 8). The length of

the curve of “remnant” meanderkarren is small as is the width of the meanderkarren zone, the intensity of slippage, and the development of the meanderkarren. For this type of meanderkarren, the oscillation of the channel line begins in the rivulet on the surface before the development of the channel begins.

“Developing” meanderkarren can originate if the oscillation of the channel line occurs later than when the channel started deepening. These meanderkarren have symmetrical cross-sections in the upper part and asymmetrical cross-sections in the lower part. In this type of meanderkarren, the vertical side walls will start to overhang at a certain depth below the concave channel rim and begin to slope gently at a similar depth below the convex channel rim (Figures 7d, 10).

*Perishing meanderkarren* occur rarely. This type will develop if the oscillation of the channel line ends during the deepening of the channel. Therefore at the lower part of the channel a symmetrical cross-section develops (Figure 11). On the concave side the wall of the channel changes from overhanging to vertical.

Meanderkarren can often be complex. In this case, a smaller younger channel will develop at the bottom of a larger older one. When the meandering of the internal channel is similar to the meandering of the bearing channel, the process is called *forced meandering* because the meandering of the internal channel is “forced” by the bearing channel (Figures 12a, b). It is also possible for the meandering of an internal channel to be independent of the meandering of the bearing channel (it can also be that the bearing channel does not meander, Figure 8d). When the bearing channel is able to limit the meandering of the internal channel, the meandering of the latter channel will be *strained* (Figure 12c, d). One type of complex meanderkarren is the “developing-looping” meanderkarren seen on the marble of Diego de Almagro island. This type develops from “remnant” meanderkarren. The loops border the large skirts that developed from the side walls of the “remnant” meanderkarren of the bearing channels.



# WANDKARREN

Márton VERESS

*Rillenkarr*, *rinnenkarr*, and *wandkarr* (wall karr) are created by water flowing on slopes (Ford and Williams, 1989). Wandkarr develop on vertical slopes (for example on the walls of shafts). They are parallel to each other and have a semi-circular cross section (Bögli, 1960a). According to German researchers, wandkarr can be independent karr forms (Bögli, 1960a) but in the English research literature, these forms are described as a type of *rinnenkarr* (Ford and Wil-

liams, 1989). Jennings (1985), for example, calls wandkarr *wall solutional runnels*.

Wandkarr occur mostly on *cuestas* (Figure 1), in karst forms, on the walls of shafts, on the sides of pits, on the walls of *poljes*, and on the sides of *dolines*. They can also develop on steep coasts, on the sides of boulders, in caves (Choppy, 1996), on slopes shaped by glaciers on *cuestas*, erosion steps on the sides of *roche moutonnée* rocks, on the slopes of *horns*, and on the slopes of glacier val-



**Figure 1:** Wandkarr on *cuesta* (Totes Gebirge, Austria). 1. *schichtfugenkarr*; 2. *wandkarr* that wedges out at *schichtfugenkarr*; 3. *wandkarr* that cross *schichtfugenkarr*; 4. complex *wandkarr*.

leys. Their altitude distribution is varied as they can occur near sea level (Diego de Almagro island) and above the snow line in the Alps. Wandkarren can develop on limestone, on marble (Diego de Almagro), on granite (Corsica, Mongolia), and on halite (Atacama desert).

## Methods

Veress et al. (2003) investigated wandkarren with the following methods. They measured the width, depth, and direction of wandkarren, and the inclination of the bearing slopes along seven lines. Using the measured data, they calculated the specific dissolution of the wandkarren (ratio of the total width of the forms and the length of the line), their density (ratio of the number of forms and the length of the line), their cross-section shapes (ratio of the width and depth), and the differences between the direction of the wandkarren and the direction of the inclination of their bearing slopes (direction differences). This data is presented in Tables 1 and 2 grouped into intervals. The slope angles of the bearing surface along the lines vary (Table 1). We think that wandkarren can also develop on gentler inclinations.

## Size and morphology of wandkarren

The width of wandkarren is between 2.5 and 34 centimetres in Dachstein. Their most common

width is between 4 and 12 centimetres. On Diego de Almagro island (Chile), the size of wandkarren is great, and their width can be several metres. Taking all the studied forms into account, we can establish that the most forms which belong to a certain width interval can be found at lines marked D-5/2000 and D-13/2000. At the line marked D-5/2000, 43.75% of the forms belong to the width interval of 4 to 6 centimetres and in the case of D-13/2000 line 33% of the forms belong to the width interval of 8-10 centimetres. The shape of the wandkarren in Dachstein is between 0.14 and 28. The greatest frequency of the shape is between 2 and 4 (line marked D-13/2000, 71.42%) and 0 and 2 (line marked D-4/1999, 80%). The density of wandkarren can range between 1.49 and 14.55 pieces/meter, while the value of the specific dissolution is 19.37-39.31 cm/m (Table 1).

Wandkarren develop mostly along a down-dip, a characteristic shown for the lines marked D-13/2000 and D-5/2000. 61.98% of the wandkarren of the line marked D-13/2000 differs less than 20° from the slope direction of the bearing slope, while this value for the line marked D-5/2000 is 100%. It can also happen that the difference between the direction of the form and that of the bearing slope is more than 20°. This is the case for 42.3% of the wandkarren of the line marked D-19/2000 and for 47.36% of the wandkarren of the line marked D-16/2000.

The specific dissolution is independent of the altitude or the dip of the bearing surface (Table 1), but connections appear between width, shape, den-

**Table 1:** Characteristics of selected wandkarren. D. Dachstein; Ch. Chile; ö.sz. total of measured widths along a line; f.sz. specific width; s. density; last figure of line name indicates year measurements taken.

Name of a line	Altitude [m]	Length of a line [m]	Angle slope of bearing surface	Characteristics of wandkarren				
				ö.sz. [cm]	number [pc]	f.sz. [cm/m]	s. [pc/m]	
D-4/1999	1700	10.2	51	401	32	39.31	3.14	
D-5/2000	1990	5.5	55	450.5	80	81.91	14.55	
D-13/2000	2180	4.5	75	226	21	50.22	4.67	
D-14/2000	2157	7	48	163	18	23.29	2.57	
D-16/2000	2115	17.5	90	339	26	19.37	1.49	
D-19/2000	2106	9	75	279	17	31.00	1.89	
D-20/2000	2078	12.5	73	371.3	28	29.70	2.24	
average	-	-	-	408	31.71	39.26	4.36	
Ch-2/2002	500*	20	90	804	6	40.2	0.3	

\* estimated

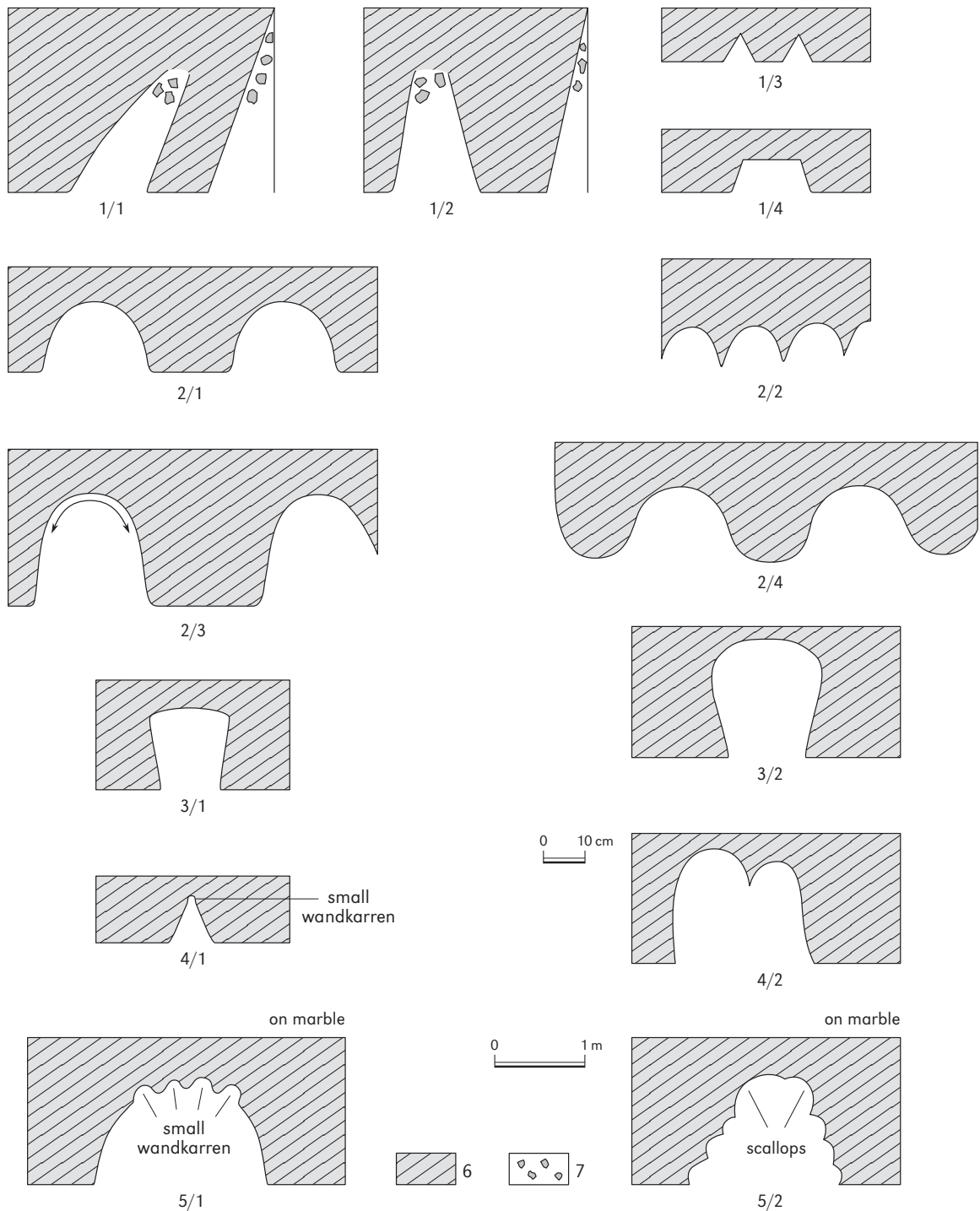


**Figure 2:** Shapes of wandkarren (cross-section). 1. grike-type wandkarren: 1/1 slanting, 1/2 straight, 1/3 wedging-out, 1/4 flat-bottomed; 2. half-pipe wandkarren: 2/1 planar surfaces between wandkarren, 2/2 ridges between wandkarren, 2/3 scallops in wandkarren, 2/4 rounded surfaces between wandkarren; 3. cavernous wandkarren: 3/1 widening with flat bottom, 3/2 widening with curved bottom; 4. complex wandkarren: 4/1 with one internal channel, 4/2 with internal ridge; 5. large wandkarren on marble (Diego de Almagro island): 5/1 with smaller wandkarren, 5/2 with scallops; 6. limestone, marble; 7. debris.



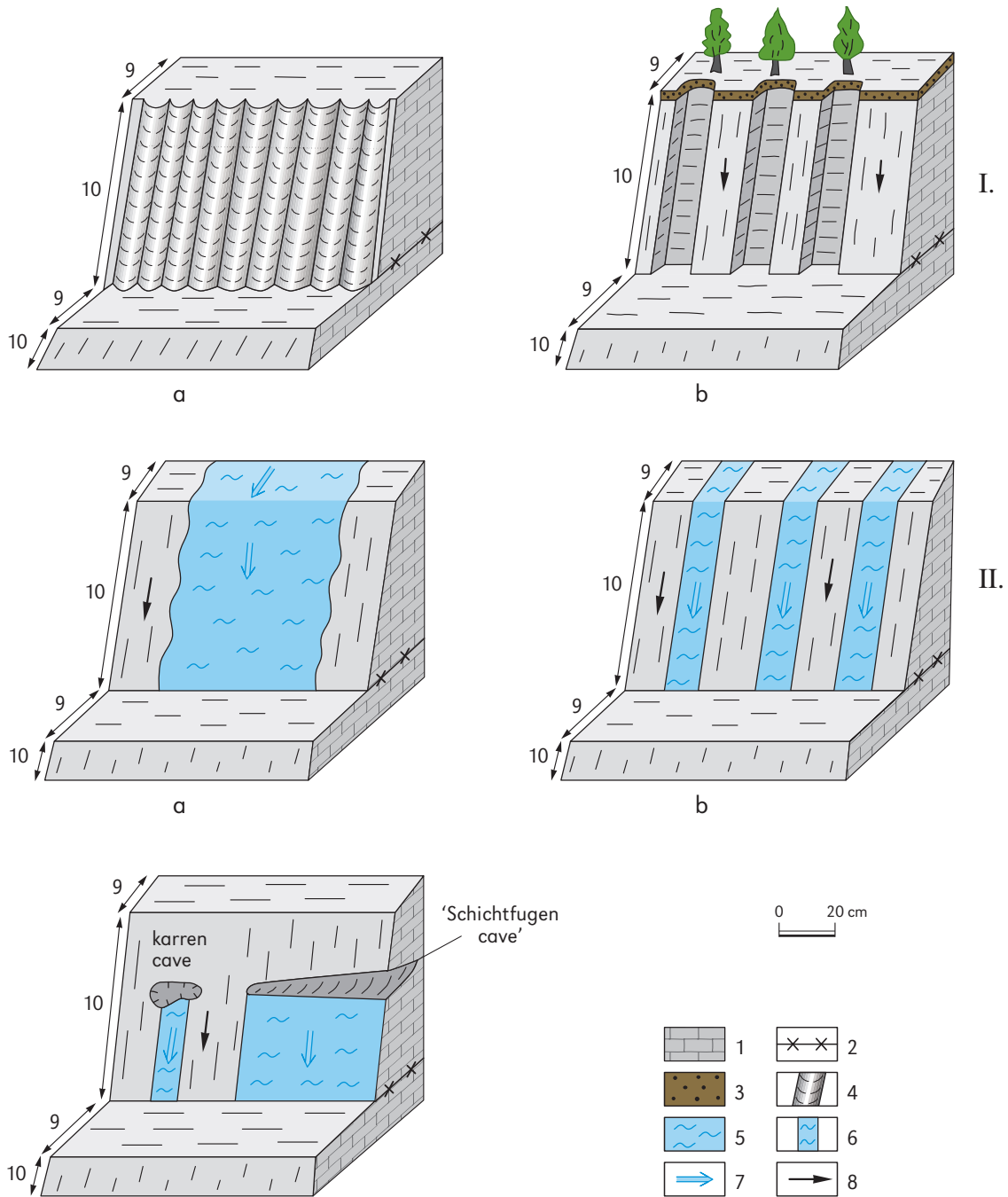


**Figure 3:** Genetic types of wandkarren. I.a. half-pipe wandkarren; I.b. grike-like wandkarren; II.a. wandkarren developing under water sheet originating from surface; II.b. wandkarren developing under rivulets originating from surface; II.c. wandkarren developing under water flowing from hollows in the bed head; 1. limestone; 2. bedding plane in profile; 3. soil; 4. wandkarren; 5. water sheet; 6. rivulet; 7. water current; 8. inclination; 9. bedding plane; 10. head of the bed.

sity, and specific dissolution. For lines where the value of shapes of the wandkarren is high, the density and specific dissolution are large as well. Such wandkarren occur on the lines marked D-5/2000 and D-13/2000. The wandkarren of these lines have a half-pipe shape. On lines where the value of shapes of the wandkarren is small, the density and the specific dissolution are also small. Such wandkarren occur on the lines marked D-16/2000, D-19/2000, D-20/2000, and D-4/1999. Along these lines, grike-like wandkarren developed.

The width of wandkarren varies. According to the data, the width of *half-pipe wandkarren* can spread less, while the width of *grike-like forms* can spread to a greater degree. We hypothesize that where wandkarren occur in great density, the adjacent forms do not let each other widen. Since the grike-like forms are far from each other, they can widen freely and can therefore have great width.

## Types of wandkarren

According to cross-section, wandkarren can be the following (Figure 2):

- *grike-like wandkarren* (Figures 2.1, 3.I.b, 4) have sharp edges and flat side walls. We can distinguish different types as well. Their side walls can take different “V” shapes. If the side slopes do not cross each other, the forms end in a flat surface and the end of the wandkarren can have debris or not. The side wall can be vertical to or slanting relative to the bearing slope. Soil can fill the ends of nearly vertical side-walled forms (Figure 5);
- *half-pipe wandkarren* (Figures 2.2, 3.I.a, 6) have curved side walls. This type also varies. The half-pipe cross-section can be similar to a semicircle or to an ellipse. The bearing slope between these forms is rarely wide (it can be flat or rounded), and its shape is more often ridge-like. *Scallops* can occur on the walls of these forms;
- *cavernous wandkarren* can widen at the bottom of the form (Figure 2.3), and the bottoms can be flat or curved;

- *complex wandkarren* (Figures 1.4, 2.4) can be separated into at least two parts. For example, the form can be the coalescing of two smaller wandkarren. More frequently, however, small wandkarren divide the side walls or the bottom of a larger wandkarren (Figure 2.5/1).

Wandkarren can extend over the complete length or only on a part of the bearing slope. In the first case, wandkarren can have a continuous development or the form can be interrupted by *schichtfugenkarren* or by variously shaped hollows (Figures 7, 8). *Schichtfugenkarren* are grooves with a depth of one or two decimeters that deepen into the rock for several meters along bedding planes. The width of the wandkarren can be unchanged or smaller below the *schichtfugenkarren*, or the wandkarren can also be transformed into several smaller forms below a *schichtfugenkarren*. The upper end of the wandkarren can be at or below the top of the bearing slope. The lower end of the wandkarren can wedge out or end at a *schichtfugenkarren* (Figure 9). When they begin at a *schichtfugenkarren* (Figure 10), they can extend to the lower edge of the bearing slope or to another *schichtfugenkarren*, or they can also wedge out. Wandkarren that end at the lower part of the slope, can wedge out or join a soil-covered surface or another karren form.

## Development of wandkarren

We distinguish two development types of wandkarren according to their characteristics:

- *half-pipe or rill-type wandkarren* (Figure 3.I.a) develop under sheet water that flows down the bearing slope. Their cross-section, the value characterizing their shape, and their great density prove this fact. Sheet water can originate from the bedding plane above the slope (Figure 3.II.a) or from a *schichtfugenkarren* (Figure 3.II.c). When the bedding plane is covered with soil, there is less probability they will develop since soil can retain rainwater. Melt water



**Figure 4:** Grike-like wandkarren (Totes Gebirge). Width of view is 4 m.



**Figure 5:** Wandkarren formed below soil from a distance (Asiago plateau, Italy). Width of view is 2.5 m.

also plays an important role in the development of this type of wandkarren;

- grike-like or *rinnen-type wandkarren* (Figure 3.I.b) develop under *rivulets* (Figure 3.II.b), which their small density proves. Rivulets are fed from bare bedding planes, soil (with nu-

merous source points), or soil patches. Wandkarren can help the development of a soil patch. Rivulets can also flow from a hollow (Figure 3.II.c). Because the distance between rivulets is random, their discharge, the period of their existence, the date of their development, and the

CO<sub>2</sub> saturation level of their water can differ to a great extent. Neighbouring forms can therefore have different sizes. Forms that are close to each other can have different ages and activity levels. We believe, cavernous wandkarren can be included in this type since we believe the cause of their development is an increasing discharge or an increasing dissolution effect.

The directions wandkarren take illustrate that they can be created by two different kinds of water flow. The direction of those forms that develop under sheet water differs less from the dip line of the bearing slope. On one hand, the flow of water can not be diverted by the irregularity of the surface, and on the other, the forms do not have space to develop in different directions. Those forms that develop under rivulets have a different dip direction relative to the bearing slope since the direction of the flow is changed by the irregularity of the slope and the development of wandkarren occurs in various directions;

- complex wandkarren develop if the rivulet cannot fill the form. If there is only one rivulet, we can see only one internal wandkarren while if there are several rivulets we can observe several internal wandkarren;
- *covered wandkarren* develop if soil fills the forms. This type of development occurs where the quantity of plants and soil is significant (for example, the southern slopes of the Alps or on the lower part of a mountain). Because of the soil accumulation, water cannot flow in the forms and dissolution occurs under the soil.

The development of wandkarren is antiregessional, which the following points demonstrate:

- if they do not begin at schichtfugenkarren, their upper end is always at the beginning of the upper margin of a slope;
- their lower ends can wedge out at different altitudes;
- their width usually decreases in the direction of their lower ends;
- there are no rillenkarren and rinnenkarren on slopes with steep inclinations (70°–90°).



Figure 6: Half-pipe wandkarren (Totes Gebirge). Width of view is 25 cm.

Several factors contribute to the antiregessional development of wandkarren, including the following:

- the water flow is faster in already-developed wandkarren and therefore saturation of the water occurs over a longer path;
- because of plants, the CO<sub>2</sub> saturation value of the water increases.

The number of rillenkarren and *channels* decreases as the angle of the slope increases, but as the angle becomes greater wandkarren develop. The development of a turbulent flow, which causes an increase of rock dissolution, depends on the thickness of the water current and its velocity (Emmett, 1970; Trudgill, 1985). The thickness of the water becomes smaller because the velocity of the water increases as the angle of the slope increases and therefore a turbulent flow can not de-

**Table 2:** Distribution of wandkarren along selected lines from Dachstein relative to width.

Name of a line	Width interval [cm]	Most common interval width	Most common width [%]	Shape interval	Greatest frequency of shapes relative to interval [pieces]	Greatest frequency of shapes in interval [%]
D-4/1999	3-50	4-6; 8-10	20; 20	0.14-4	0-2	80
D-5/2000	2.5-11	4-6	43.75	0.75-18	2-4	37.5
D-13/2000	6-16	8-10	33	1.22-5.5	2-4	71.42
D-14/2000	4-16	8-10	29.4	1-10	4-6	35.3
D-16/2000	2-27	8-10	24	0.25-28	0-2	48
D-19/2000	2-61	10-12	31.5	0.19-12	0-2	55.55
D-20/2000	4.3-34	10-12	29.6	0.35-13	0-2	46.42

Notes:

- intervals are in 2 centimetres;
- width interval: the width of the smallest and biggest wandkarren that occur along a line;
- most common width: the width of the wandkarren grouped in an interval (along a line);
- shape: ratio of the width and depth of wandkarren;
- shape interval: ratio of the smallest and greatest width and depth along a line;
- the greatest frequency of shapes: the most common shape along a line from the shapes grouped in an interval;
- last figure of the line name indicates year measurements taken;
- line D-4/1999 is on side of a polje (area 2);
- line D-5/2000 is near Däummel lake on the edge of a doline (area 3);
- line D-13/2000 is on the side of a boulder which is on a moraine;
- the sites of lines D-14/2000, D-16/2000, D-19/2000, and D-20/2000 are on bed-heads of cuestas (area 1).

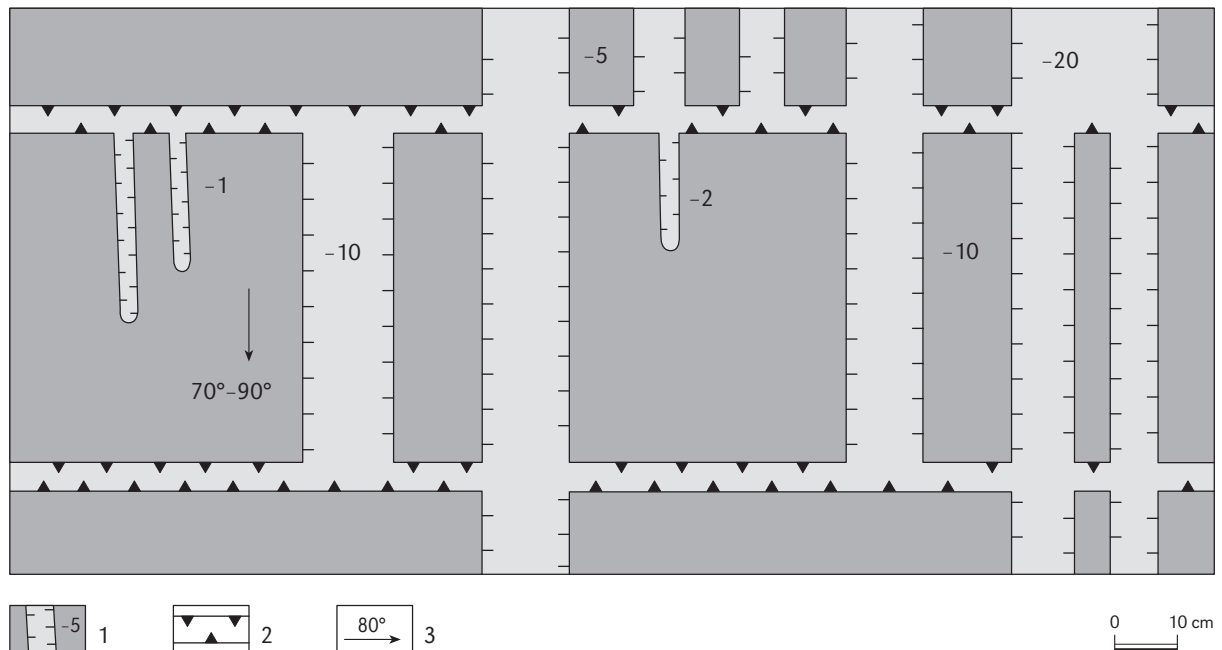


**Figure 7:** Development types of wandkarren where the bearing surface is crossed by schichtfugenkarren. 1. depth of wandkarren (cm); 2. schichtfugenkarren that developed along bedding plane; 3. inclination and angle of bearing surface.



**Figure 8:** Wandkarren that cross schichtfugenkarren (Dachstein). 1. schichtfugenkarren.



**Figure 9:** Wandkarren that end at schichtfugenkarren (Dachstein). 1. schichtfugenkarren.



**Figure 10:** Wandkarren that start from schichtfugenkarren (Totes Gebirge). 1. schichtfugenkarren; 2. wandkarren; 3. karren forms whose direction differs from inclination of a bearing slope.

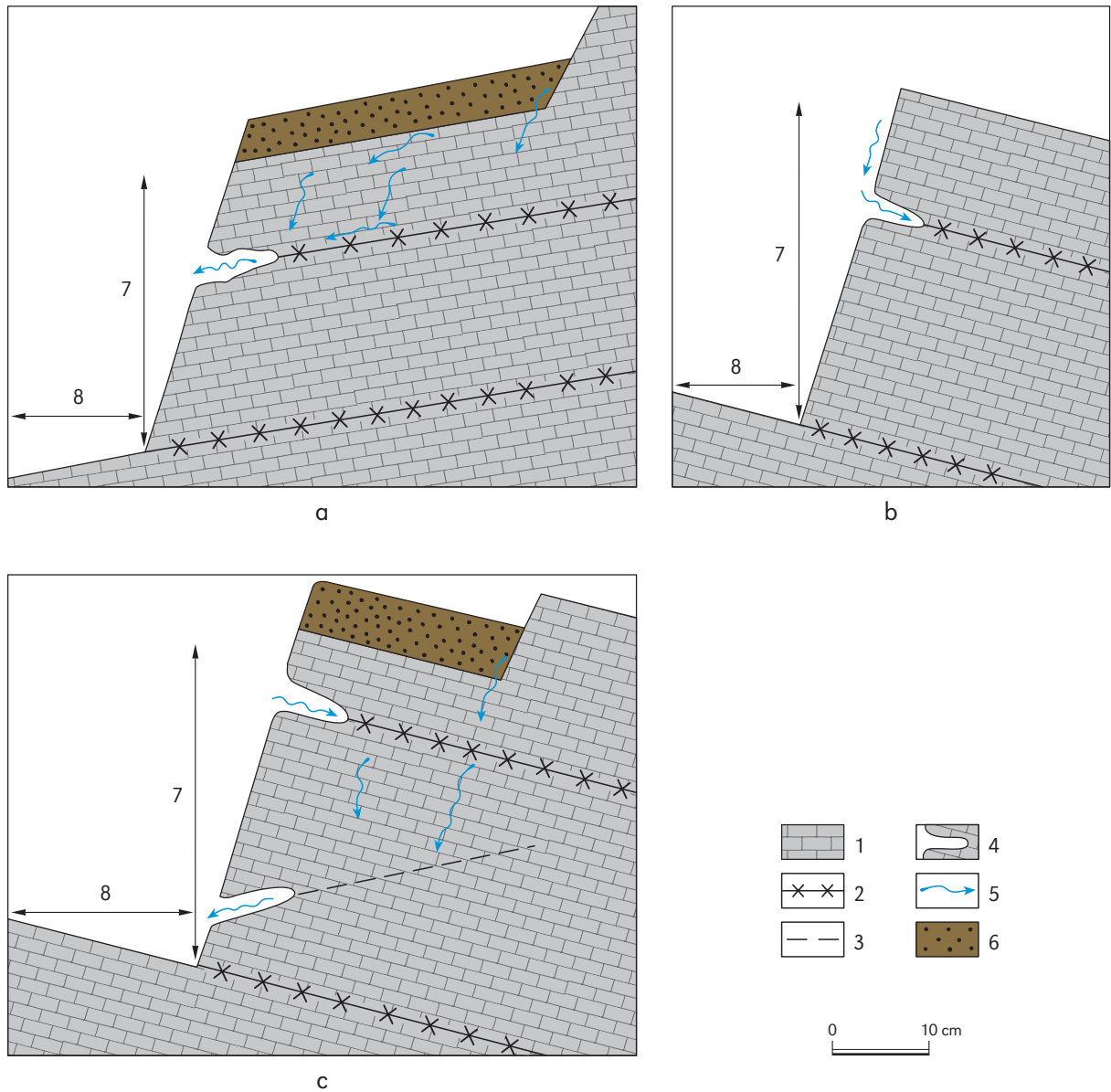
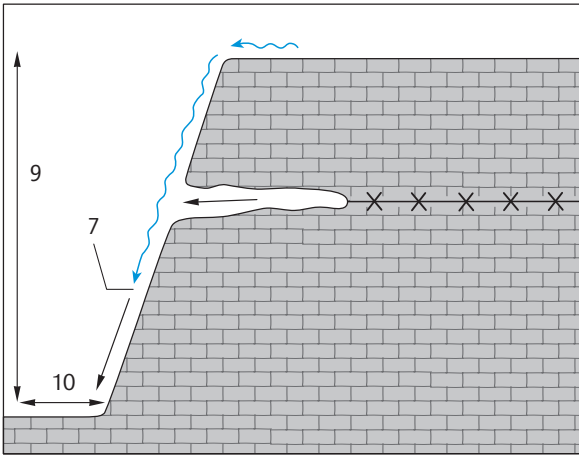
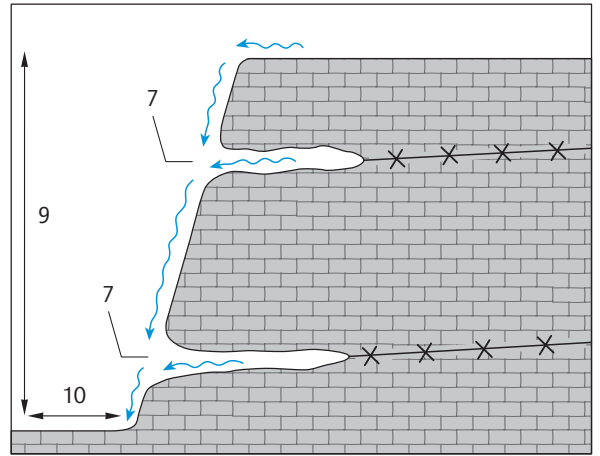


**Figure 11:** Genetic types of schichtfugenkarren developed on heads of beds. a. inclinations of the bedding plane and the head of the bed are similar; b. inclinations of the bedding plane and the head of the bed are opposing; c. inclinations of the joint and the head of the bed can be opposite (see top and bottom parts of the Figure) or similar (see middle of the Figure); 1. limestone; 2. bedding plane; 3. joint; 4. schichtfugenkarren; 5. infiltration of unsaturated water; 6. snow; 7. head of the bed; 8. surface of the bedding plane.

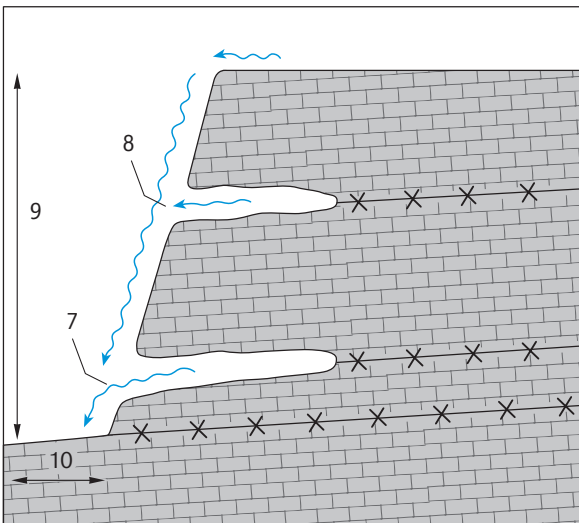
**Figure 12:** Development of wandkarren with different lengths. 1. limestone; 2. bedding plane (in cross-section); 3. joint; 4. schichtfugenkarren; 5. unsaturated water; 6. saturated water; 7. site of complete saturation of water flowing on the head of the bed; 8. dissolution increases because water mixes on the head of the bed with unsaturated water flowing from schichtfugenkarren; 9. head of the bed; 10. bedding plane; a. unsaturated water can dissolve rock anywhere (width of wandkarren is similar above and below schichtfugenkarren); b. water flowing down the head of the bed becomes saturated at the level of the highest schichtfugenkarren, but water flowing from schichtfugenkarren is unsaturated (width of wandkarren is smaller below schichtfugenkarren); c. water from the head of the bed above schichtfugenkarren can no longer dissolve rock but mixes with unsaturated water flowing from schichtfugenkarren (wandkarren crosses several schichtfugenkarren but its width does not change); d. water is saturated (wandkarren can only develop under schichtfugenkarren if unsaturated water flows from schichtfugenkarren); e. water is unsaturated but flows into schichtfugenkarren (wandkarren do not develop between schichtfugenkarren). →



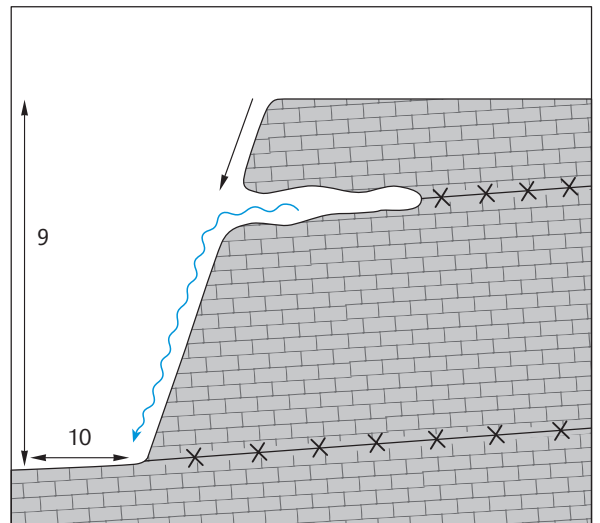
a



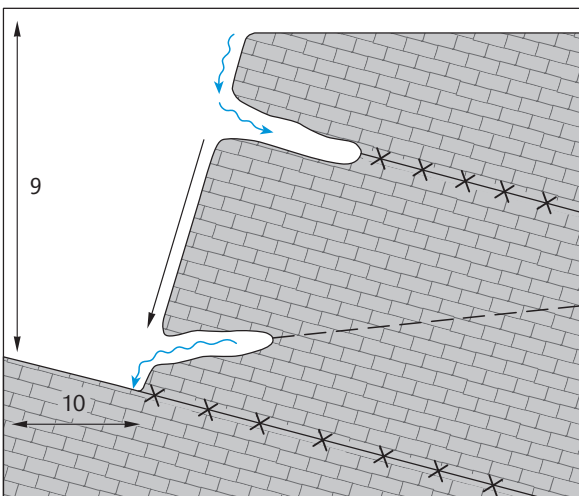
b



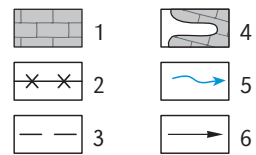
c



d



e





velop. Thus the intensity of dissolution on surfaces with a small dip ( $5^{\circ}$ – $50^{\circ}$ ) decreases as the slope angle increases.

A turbulent flow can develop although the thickness of the sheet water is small if the angle of the bearing slope is large (e.g. greater than  $70^{\circ}$ ). If the velocity of the flow is high on slopes with large inclinations, a turbulent flow develops regardless of the small thickness of the water. Therefore, if the inclination of the slope is great, the intensity of dissolution increases and wandkarren develop.

Grike-like wandkarren generally cut across schichtfugenkarren or develop from the site of the schichtfugenkarren (depending on the time of origin of the forms). According to Weber (1967), schichtfugenkarren develop due to dissolution occurring along bedding planes. Schichtfugenkarren can develop in two ways (Figure 11). They can develop when water percolating through the rock creates caves along the bedding planes in the direction of the face of the bed heads. Schichtfugenkarren can also develop as water flows down the walls and infiltrates the rock along bedding planes to dissolve cavities. However, this latter case happens rarely since usually only a small quantity of the water flowing on the walls of a bed head can infiltrate the rock.

We can formulate a genetic model of wandkarren crossing schichtfugenkarren in the case where the schichtfugenkarren is older than the wandkarren. Such cases have the following characteristics:

- the width of a wandkarren abruptly becomes smaller when the wandkarren crosses a schichtfugenkarren. This can only happen if the schichtfugenkarren developed earlier than the section of wandkarren below it;
- the inner height of schichtfugenkarren does not change. The inner height of schichtfugenkarren can decrease (away from a wandkarren) if the schichtfugenkarren is younger than the wandkarren. In this case, the schichtfugenkarren

will have started at the wandkarren, so its inner height will be the largest there.

Wandkarren with different lengths and widths develop as follows (Figure 12):

- a wandkarren cuts a schichtfugenkarren without changing its width because only saturated water leaves the schichtfugenkarren (Figure 12a);
- we can observe that the width of a wandkarren decreases after it cuts a schichtfugenkarren. In this case, the water flowing down the wall becomes more or less saturated at the height of the schichtfugenkarren, but the water leaving the schichtfugenkarren is unsaturated because there is a wandkarren below it (Figure 12b). The smaller width of the wandkarren below the schichtfugenkarren indicates that while the water that leaves the schichtfugenkarren is unsaturated because the width of the wandkarren is small, the water can only dissolve the wandkarren to a smaller extent;
- wandkarren cut some schichtfugenkarren without a decrease or even an increase in their width. In these cases, the solubility of the water flowing down decreases minimally since the water leaving the schichtfugenkarren is unsaturated and is able to maintain solubility as it mixes with the water flowing down the wall (Figure 12c);
- wandkarren begin at schichtfugenkarren because the water flowing down the bed heads is already saturated. Wandkarren can only develop below schichtfugenkarren when unsaturated water leaves the schichtfugenkarren (Figure 12d);
- wandkarren do not develop between two schichtfugenkarren when the water flowing down the bed head flows into the upper schichtfugenkarren or becomes saturated at this altitude. At the same time, unsaturated water flows out of the lower schichtfugenkarren (Figure 12e).

Joyce LUNDBERG

Coastal karren are the small-scale dissolutional and/or bio-erosional features that develop on rock surfaces in the narrow zone of exposed rock beside a body of water, and within the direct range of the action of that water. The erosional processes are directly related to the water surface and operate in (a) the inundated zone immediately beside the shore, (b) the zone of alternating water levels, (c) the zone of splash, and (d) the zone of spray. The processes are most commonly observed in association with salt water, but they also occur in brackish water and fresh water environments. Unlike most terrestrial settings, tectonic jointing is rarely the focus of activity. The formation is controlled by very small scale, very local hydrology and chemistry of rock surfaces; large-scale environmental settings are less significant than proximity to organisms, to water, and to vegetation or sediment cover. The dominant controls are wetting regime, biological activity, and energy levels. In many settings, bio-erosion dominates. If abrasion overrides, or if cliff retreat rate exceeds that of karren formation, then karren are absent.

A variety of other terms has been used to describe coastal karren, such as *intertidal karren*, *littoral karren*, *biokarst* (Viles, 1984; Schneider and Torunski, 1983), *phytokarren*, *phytokarst* (Folk et al., 1973; Jones, 1989). Some of these obviously include only coastal forms; others, such as *biokarst* or *phyto karst/karren* indicate a general proc-

ess that is not confined to coastal features. Since coastal karren are impacted by a great variety of processes (including abrasion, hydraulic action, wave action, wetting and drying, corrosion, dissolution, bio-erosion, bio-construction and, in cold regions, frost action), it is preferable to avoid genetic terms. Many of the features described below also occur on non-soluble rocks but are usually less clearly developed.

Coastal karren do not include features related to groundwater action in the coastal environment, usually of salt-fresh mixing (e.g. Smart et al., 1988), often described as *coastal karst*. In addition, coastal karren do not strictly include features such as *alveoli*, *tafoni honeycombing*, and certain *shore platforms* that are produced by salt weathering (e.g. Matsukura and Matsuoka, 1991), although these may be associated with dissolutional features.

## Morphology

One of the most striking features of coastal karren is that they can be very delicately etched into surprisingly jagged surfaces. They range in scale from sub-millimetre to several metres. The forms are usually distributed in zones relative to wetting regimes and biological zonation. Zonation is most obvious in meso- to macro-tidal salt-water coasts.

The variety of forms reported in the literature appears to be legion. However, variations can be explained if coastal karren are viewed as a series of modules made up of basic building blocks: the modules are then assembled in different proportions in different geographic settings. This will vary with: (a) organisms present (which may cause, or protect from, erosion); (b) exposure levels (wave energy, wind energy, wave and wind orientation); (c) tidal range and regime; (d) the balance of fresh and salt water; (e) lithological variations (chemistry, crystallography, depositional fabric); (f) structural variations (sedimentary structure, bed thickness, orientation, dip, joint frequency and orientation).

The basic units may develop at different scales (for example, a rounded *basin* may range from a few millimetres to a metre in width). They may also display a pseudo-fractal nature (Torunski, 1979), of forms within forms (so a 30 cm wide basin may enclose a surface made up of 3 cm wide basins, which may in turn enclose a surface of 0.3 cm wide basins).

### Building blocks and modules

The basic building blocks include negative, remnant and (occasionally) positive forms. The negative forms are produced by varying proportions of dissolution through fresh-salt water mixing, dissolution through biogenically-induced aggressiveness, mechanical quarrying by grazing organisms, abrasion, hydraulic action of water, etc. The remnant forms, often the most manifest, are simply the places where erosion has not yet operated; in places this occurs where colonies of organisms provide protection. Positive forms are produced where encrustations build forms up. A common characteristic of karst shorelines is the dynamic interaction of both constructional and destructional processes in the one location (Rust and Kershaw, 2000).

The negative and remnant basic units include: *pans/basins* ( $W/D > 1$ , flat-bottomed/round-bot-

tomed; Figure 1a, b, d), simple/complex *pits* ( $W/D \leq 1$ ), and *pinnacle and basin spitzkarren* (Trudgill, 1979) (Figure 1c, e). All erosional forms show varying degrees of isolation or interconnectedness. Simple pans/basins and simple pits are normally isolated. Pinnacles and basins are usually well inter-connected so that water flows freely between basins. In warm, salt waters of high energy level, bio-constructors such as coralline algae or serpulid worms may protect surfaces from erosion and build up small *ramparts* of encrustations; pans and basins may also become *dammed or rimmed* (Figure 1f, g).

The blocks are assembled into modules. These include: the *erosional ramp*, the *erosional notch*, and the *shore platform*. Some places have all three of these: e.g. a reasonably exposed tropical sea coast will have a notch, a shore platform, and a short erosional ramp. Some places have only one, e.g. a long ramp is characteristic of exposed regions anywhere. The module can further be described by its position in relation to the shore, e.g. a notch may be supra-tidal, inter-tidal, or sub-tidal. In view of the complexity of genesis, and the incidences of convergent evolution, descriptors using genetic terms such as “surf”, “bio-erosional”, etc., should be avoided unless the genesis is evident. These modules are not unique to karst rocks, although the dominance of dissolution, the detailed forms of the units, and the particular assemblage of modules often is.

The erosional ramp, which may stretch from wave base to the supra-littoral spray zone, is the most common form worldwide, ranging from tropical areas, to temperate areas, to cold regions (Figure 2a, b, c), and usually associated with exposed environments. It is an obvious consequence of the diminution of erosion with distance from wave and splash energy. In many tropical regions the deposits from the Last Interglacial high sea level that originally formed a raised platform are now being modified into a ramp (e.g. Moses, 2003).

The erosional ramp comprises zones of pits, pans, basins, and pinnacles, varying with water regime, biological action, and exposure. Typically

the zones furthest from wave action have small pits and flat-bottomed basins (but see discussion of supra-littoral basins below). Biological action is more pronounced closer to the water. The negative forms become bigger closer to the water surface and the pinnacles more pronounced. Basins usually become more rounded, perhaps with overhanging rims, towards the water.

Jaggedness increases with increasing exposure (Figure 1e, f). With strong splash and high energy levels the projections dominate and basins are poorly developed. *Runnels* may appear where gravitational draining dominates (Figure 1d). Mechanical fracture and dissolution are active. Few macroscopic organisms are apparent and direct bio-erosion is minor. *Endoliths* bore into surfaces but *epiliths* are rare. On the reef rock of Bonaire, Netherlands Antilles, the pinnacles are oriented towards the incoming splash.

The forms vary with lithology: e.g. in Puerto Rico reef rock is much more jagged and irregular than beach rock, and more deeply etched but not as sharply fretted as eolianites. Mylroie and Mylroie (see chapter 39) describe karren from San Salvador island, Bahamas, that is very strongly influenced by lithology, developed on eogenetic rocks that show little post-depositional diagenesis.

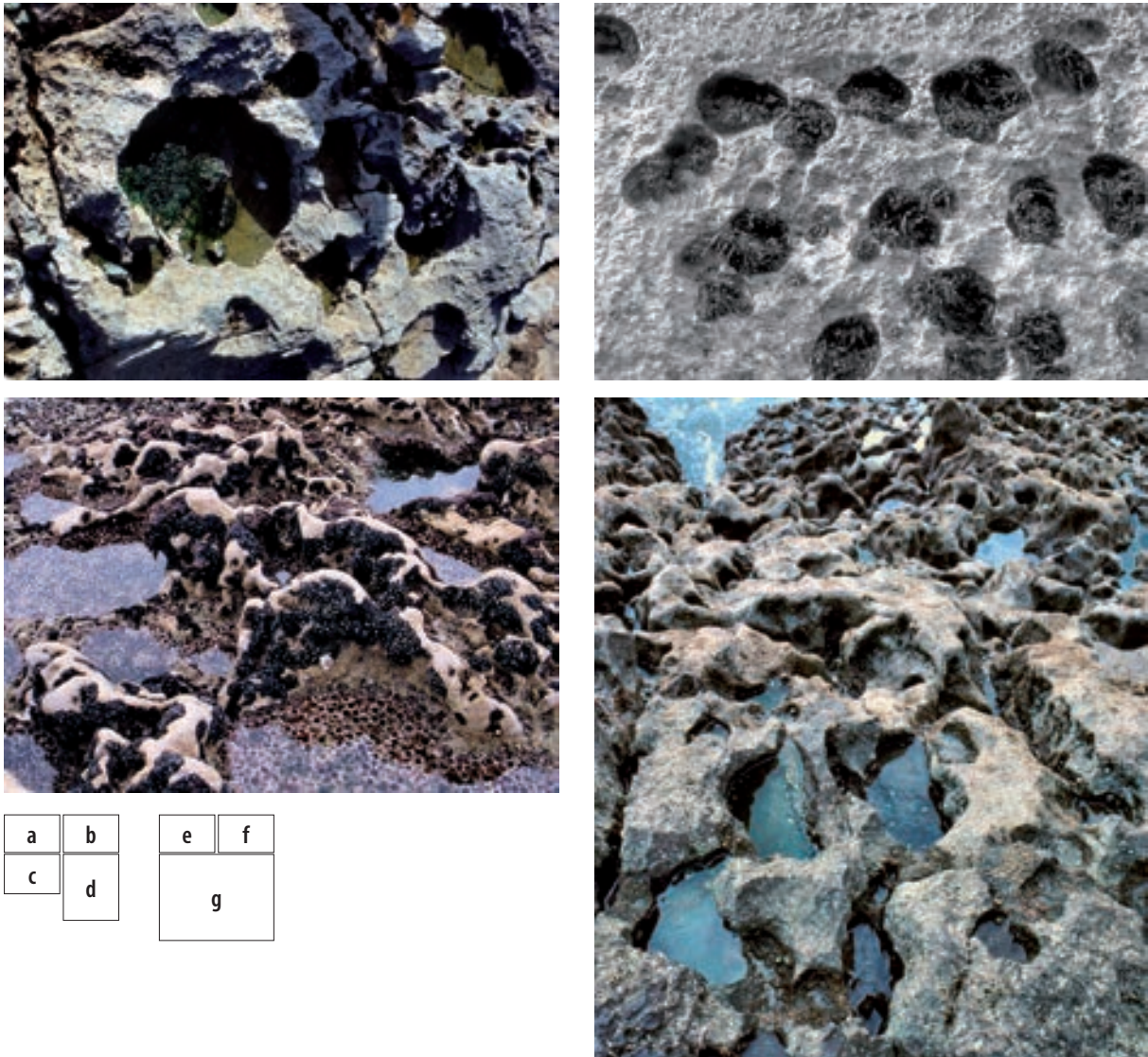
The erosional notch, a horizontal groove parallel to sea level cut into bedrock but not structurally controlled, is the next most common form. It is very well developed in tropical regions where bio-eroders abound, especially in sheltered regions. In temperate regions, with fewer bio-eroders, the notch is not well developed. In addition, most of the temperate regions displaying coastal karren are in exposed settings, so that the erosion ramp dominates over the intertidal notch. A third factor is that tropical coastal karren are almost invariably developed in young carbonates of relatively low diagenetic maturity, whereas temperate coastal karren are in substantially older rocks.

The intertidal zone is the focus of intense biogenic activity, abrasion, hydraulic action, and perhaps dissolutional activity. This produces a notch, incised typically from 1 to 5 m. If the notch inter-

sects a sloped cliff or an erosional ramp, then the top of the notch takes on the form of a *visor*, which in the splash zone bears pinnacles and basins. Thus a commonly-described duo is the *notch and visor* (Figure 2g). Where a stack stands separate from the coast, notching will occur on all sides producing a *mushroom* rock (Figure 2e).

The form and elevation of the notch relates to exposure level, and to tidal range. In sheltered and micro-tidal environments, processes (mainly biological activity) are focused on a small vertical expanse of cliff: the notch digs deeply into the rock at mid tide level but is not very tall (Figure 2d). As tidal range or exposure increase, processes are spread out over a larger expanse of cliff face: the notch will be less incised but taller. Where biogenic activity is dominant then the surface will be inhabited by boring and grazing organisms and may be made up of many sharp-edged pits. Where abrasion and hydraulic action are dominant (only in high energy environments) the notch will be less deeply incised with smooth, rounded surfaces devoid of organisms. The sub-tidal environment below the breaking waves is not subject to much mechanical or dissolutional action, so this part of the notch is probably purely bio-erosional. Clearly, notches may result from a variety of processes: biological (e.g. Abensperg-Traun et al., 1990; Hodgkin, 1970), chemical (e.g. Higgins, 1980; Rust and Kershaw, 2000), and physical (Trudgill, 1976a; Kershaw and Guo, 2001). Convergent evolution may produce similar forms on non-karst rocks: for example, erosional notches just below mid-tide level develop very rapidly in conglomerates of New Brunswick, Canada (Trenhaile et al., 1998). Notch elevation is not always simply and clearly related to sea level: in more turbulent conditions the notch may be as much as 2 m above sea level (Rust and Kershaw, 2000).

Lithology has some impact on notch form. Notches in reef rock are usually more complexly fretted than those on eolianites. It is of interest that Holocene eolianites of San Salvador island (see chapter 39) do not show much notch development, while adjacent Pleistocene eolianites, pre-



a	b	e	f
c	d	g	

**Figure 1:** The basic building blocks: a. basins of the upper littoral of a sheltered bay, north-east Vancouver island. The rock is very hard, fine-grained limestone. The pools are isolated, relatively flat-bottomed, and smooth bottomed. The microscopic green algae lining the pools have been grazed in patches. The inter-basin rock is roughly fretted; b. small basins in the supra-tidal swash/splash zone of Port-au-Port Peninsula, Newfoundland (photo by C. Malis, used with permission), width of view is 1.5 m; c. pinnacles and basins close to low water level on the west coast of Ireland, Burren District. The pinnacles are protected by barnacle colonies (white). Mussels (black) occupy the slightly more protected pinnacle walls. The pinnacle walls and the basin floors are themselves made up of smaller basins, many created by, and occupied by, the spiny sea urchin *Paracentrotus lividus*; d. basins modified by slope in the mid-tide level of Gower Peninsula, south Wales. The basins are cut into a dip slope and all tend towards an elongate form; e. pinnacles modified by high energy splash from Burren District, west coast of Ireland. These pinnacles show a form very similar to the sharp pinnacles of Puerto Rico (right); f. rimmed pools developed in eolianites and exposed at very low tide, Punta Maracayo, Playa de Sardinera, Puerto Rico. In the foreground are the basins and pinnacles of the erosional ramp. Below this the rimmed pools, making up the shore platform, are normally covered with surf; g. constructional rampart exposed at low tide, Boca Kokolishi, northern coast of Bonaire, Netherlands Antilles. Although this is in a small bay it directly faces the dominant wave direction and thus receives high energy. The intertidal shore platform and associated protective rampart are clearly developed. The erosional, rather than constructional nature of the platform is apparent from the remnant isolated sea stacks.



sumably more diagenetically altered, do. Bird et al. (1979) report notches incised 30 m deep into the very easily eroded calcareous marls of Barbados. Dip or slope also relates to notch form: Torunski (1979) observed that steeper slopes result in deeper notches.

The shore platform (Figure 2c) is any horizontal

rock surface at the shore line. It may develop at different elevations in relation to dominant processes such as waves, tides, surf (e.g. sub-tide, mid-tide, high-tide). In general, a shore platform develops wherever differential lateral planation causes cliff retreat above a datum but not below it. The most common shore platforms are simply the wave-cut

platforms that develop at wave base or at the base of subaerial weathering – top of permanent saturation (Trenhaile, 2002). However, in limestones a particular form of shore platform develops in the mid-tide to surf zone where bio-constructors flourish (in warm water regions such as mediterranean and tropical areas). Various terms have been used in the literature such as *tidal platform*, *plate-forme à vasques*, *solution bench*, or *surf platform*.

In warm waters with high energy levels, encrusting organisms abound (e.g. calcareous algae, vermitid gastropods, serpulid worms). These coat the rock surface with carbonate, protecting it from erosion. The crust may be lithified by the pumping action of seawater through the accretions. Many organisms take advantage of the protection offered and hide in crevices between encrustations. The encrusters are not very tolerant of emersion and prefer a continually renewed water supply of high energy level. Thus they concentrate below mean tide level or in the surf zone of very exposed coasts. The rock above (and below to a lesser extent), without this protection, is open to normal notching processes. Thus, over time, the notched part retreats while the encrusted zone remains relatively intact. The remnant form is the shore platform. The outer edge may have an accumulation built up into a *rampart* (the *armoured rim*, or *trottoir*) (see Figure 1g). This can create a landward *moat*, where the rampart bears the brunt of the waves and the water flows downhill towards the land.

Sometimes shore platforms are built entirely of bio-constructors. In less exposed localities (e.g. mediterranean regions) a small and rather delicate bench is built out from a steep rock surface, or from the end of the shore platform, by encrustation alone: this is then called a *corniche* (Trenhaile, 1987). Naylor and Viles' (2002) site in Crete consists of bio-constructural *boiler reefs* (the term boiler referring to the action of the water) on a gently sloping surface. Shore platforms with clear constructional morphology are reported from the Mariana islands (Mylroie, pers. comm. 2004).

The shore platform usually has a gently sloping surface form. The slope is made up of a series

of steps separating wide, shallow, flat-bottomed pans, called *rimmed pools* or *vasques* (Guilcher, 1953). Each riser is a narrow, sinuous, lobed ridge, protected by encrustations. The encrusters thrive on the rim edges because water continually flows over the edge as it drains to lower levels. The form is very similar to that of *tufa dams* or *rimstone pools* and *gours*. This is the classic “plate-forme à vasques” (Figure 1f) of Guilcher (1953).

### Transition between zones

The nature of the transitions varies with tropical and temperate karren. Some of the tropical karren show a distinct division between zones, most obviously in the sheltered regions. The edge of the splash pinnacles and basin zone is clearly demarcated at the edge of the visor giving way to the notch. Similarly the upper and lower edges of the intertidal constructional platform are relatively clear. In more exposed tropical regions and in temperate regions, most zones do not have a definitive edge: all show some degree of gradation between forms. As denudation continues each zone moves landward (even those zones semi-protected by encrustations). Thus denudation in any one spot lowers that area into the influence of the water regime of the next zone. So, each upper zone gets transformed into the zone below it.

## Regional variations

### Salt water coastal karren

Salt-water coastal karren display some or all of the modules described above, depending on conditions. Four general situations are discussed below: tropical, temperate, mediterranean, and cold regions (Figure 3).

#### TROPICAL REGIONS

Tropical coastal karren are widespread because carbonate coasts are so common in the tropics.

These rocks are typically diagenetically immature, rarely of greater age than the Late Pleistocene. The karren are more complex than temperate and cold region forms, and have more often been studied. They have been reported from a variety of locations including Hawaii (Wentworth, 1939; Guilcher, 1953), Florida Keys (Ginsburg, 1953), Bikini (Revelle and Emery, 1957), Puerto Rico (Kaye, 1959), Bahamas (Newell, 1961), Guam (Emery, 1962), Bermuda (Neumann, 1966), Barbados (Tricart, 1972), Aldabra Atoll (Trudgill, 1976b), the Netherlands Antilles (Focke, 1977, 1978a, b), Kenya (Bird and Guilcher, 1982), Madagascar (Battistini, 1981), India (Bedi and Rao, 1984), and the Cayman islands (Woodruffe et al., 1983; Spencer, 1985a, b).

The obvious zones include: splash/spray zone basins and pinnacles on the erosional ramp, visor and notch, inter-tidal to surf zone shore platform, and low tidal or subtidal notch. Not all coasts will have all of these units and the proportions and forms will vary. The model shown in Figure 3 is based on that by Focke (1977, 1978a, b) taking into account observations by Neumann (1966), Safriel (1966), Battistini and Guilcher (1982), Dalongeville and Guilcher (1982), and modified according to field observation.

In this model, form is clearly related to exposure level. The very sheltered areas have only the intertidal notch grading into the subtidal notch without any obvious break in form. Spray zone fretting is usually minor. The more exposed places have a taller, less incised notch and splash will extend beyond the notch to cause splash zone pitting. As conditions become less suitable for borers and more suitable for encrusters, part of the notch becomes protected so that a “double notch” form develops: i.e. the intertidal notch forms above, the tidal platform interrupts it, and the low- or subtidal notch forms below (Figure 2f). Usually such areas are of high enough energy levels to have a well-developed splash zone. In the more exposed areas the platform can be at higher elevation. Where energy levels are very high then coastal retreat is fast and notches are poorly developed. Instead the low tidal terrace gives way upslope to

a ramped platform with rimmed pools, the pools becoming smaller and the rims becoming higher and more irregular upslope. The rims grade into projections and the shallow pools grade into basins. The upper part of the ramp is then of well-developed splash zone basins and pinnacles.

A dynamic equilibrium develops as the cliff edge, notches and platform retreat together. It is of interest that this retreat sometimes exposes flank margin caves that have developed in the landmass. These may then be mistaken for notches.

Variations can be produced through diverse controls. Most of these significantly modify the forms only in moderately exposed situations: very sheltered locations will still show the notch, and very exposed locations will still show the erosional ramp. Tidal range is important in sheltered and moderately exposed locations; at higher exposure levels wave height is more important. The height of the cliff is important (Hodgkin, 1970): for high cliffs, splash energy impinges only on the vertical cliff face producing fretting and fluting on the face, and the splash zone ramp does not develop even in exposed conditions. In contrast, a low cliff will develop a splash zone ramp even in moderate conditions because the thin visor will easily collapse. Very thin beds may be affected by only one part of the shore processes: e.g. *beachrock* often emerges from sandy beaches and is abraded, dissolved and bio-eroded into shallow *grooves* and basins which become more dissected with longer exposure time (Revelle and Emery, 1957; Hopley and Mackay, 1978). Sediment accumulation may prevent the development of notches even in sheltered areas and promote very smooth notch development in more exposed areas (Hodgkin, 1970; Tjia, 1985). *Fossil notches* from former sea levels may complicate the shore profile (e.g. Red Sea; Guilcher, 1952).

Lithology may be significant. Calcareous eolianites usually are of relatively low strength. This contributes to the development of large basins (e.g. the vast rimmed pools in Madagascar up to 500 m long; Battistini, 1981), small but sharp spray zone pinnacles as projections break off easily, and wide shore platforms as visors collapse easily. The me-



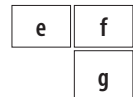
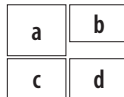


**Figure 2:** The modules: a. erosional ramp in Paleozoic limestones, Gower Peninsula, south Wales, showing zonation in relation to water levels. The basins are cut into a dip slope and all tend towards an elongate form; b. looking from the supra-littoral zone at the erosional ramp developed in marbles, west coast of northern Norway at Gås-bakken. Supra-littoral basins are clear in the foreground; closer to high tide mark the surface is not pitted; the intertidal algal mat providing bio-protection is visible in the background; c. erosional ramp in Pleistocene reef rock, east coast of Bonaire, Netherlands Antilles. The ramp is made up of sharply fretted spitzkarren and basins. It gives way seaward to the shore platform exposed between waves at low tide. Under the platform is a sub-tidal notch (not visible in the photograph); d. a deeply incised intertidal notch developed in Pleistocene limestones at Boca Slagbaai, north western coast of Bonaire, Netherlands Antilles. This notch developed in a very sheltered environment that is now cut off from the sea by a beach barrier. The absence of a pinnacled visor and the slightly pitted nature of the cliff above is further indication of the sheltered conditions; e. notching on all sides of a sea stack in Miocene carbonates from Isla de Mona, Puerto Rico, creates a mushroom rock, which will eventually fall over; f. a fossil intertidal notch from last interglacial high sea level, in Pleistocene reef deposits, north eastern coast, Bonaire, Netherlands Antilles. This shows a small double notch separated by a small intertidal platform, characteristic of a moderately exposed environment. Height of the right edge is 4 m; g. a small visor and intertidal notch cut into Pleistocene reef rock on the south coast of Dominican Republic. The cliff is high enough to avoid splash on its top, so the visor displays only a small erosional ramp of pinnacles and basins. The host rock cannot support a wide visor and collapses easily. The details of form reflect the highly heterogenous nature of the reef rock, which has been minimally diagenetically altered. Height of the right edge is 2 m.



chanically stronger beach and lagoonal calcarenites of Lord Howe island, Australia (Moses, 2003), have a deeply dissected visor in the splash zone cut into highly fretted and jagged pinnacles and basins up to 1 m wide and deep. Rock strength may not always affect form as expected: e.g. soft coral marl in Barbados has not collapsed although an intertidal notch has incised more than 30 m (Tricart, 1972). Lithological differences may not affect gross morphology but may affect details: e.g. in Malaysia both Quaternary reef rock and crystalline Palaeozoic limestones are deeply notched but the reef rock is sharp and jagged while the crystalline rock is smooth (Hodgkin, 1970).

Finally, catastrophic events such as hurricanes or tsunamis may rip up parts of the shore, leaving exposed flat bedding planes (e.g. Grand Cayman; Jones and Hunter, 1992).

#### TEMPERATE REGIONS

There is relatively little literature on coastal karren from temperate areas (see review in Trenhaile, 1987). Essentially temperate region coastal karren are all variations on the erosional ramp (Figure 2a), with some indications of small-scale sub-tidal notches. It is important to note that most of the carbonates from temperate regions are diagenetically mature and thus the karren are not strictly comparable with tropical karren on diagenetically immature rocks.



Guilcher (1953, 1958) shows the littoral zone of cool temperate regions such as the British Isles as pitted to varying depths: the highest zone that gets sea spray has small pits; the upper part of the intertidal zone shows flat-bottomed and larger pools; the lower intertidal is more dissected by sharp pinnacles or *lapiés* between pools. Trudgill (1987) describes the forms as “*scoriaceous*” *cockling* and *fretting* in the spray zone, giving way downslope to a pinnacled zone in mid-tidal region, with pools taking over seaward. The greatest relief is usually in the mid-intertidal zone (Ley, 1979; Lundberg, 1977c), with more subdued relief landward and seaward. The form is related to distribution of bio-erosive organisms, in some cases

the form being directly attributable to particular organisms (Trudgill, 1987). The clearest example of this is the deepening of permanently wet basins (mid-low tide levels) by echinoderms (Figure 1c). Notches do occur in cool temperate regions, e.g. in chalk and limestone in Britain (Trenhaile, 1987), although generally poorly defined. Trudgill (1987) shows many profiles from Ireland with cliffed edges and sometimes slightly overhanging edges at low tide level. Ley (1977, 1979) in a study of coastal karren of south Wales, found that the degree of development of pinnacles increased with the purity of the limestones. Increased porosity and permeability gave increased complexity of microrelief features, caused by rock heterogeneity.

The Burren District, County Clare, Ireland, possibly the best developed temperate coastal karren with clear zonation of forms in relation to organisms (Lundberg, 1974, 1977c, 2004; Trudgill, 1987; Trudgill and Crabtree, 1987; Trudgill et al., 1987), is described in detail by Drew (see chapter 41).

#### MEDITERRANEAN REGIONS

These are essentially intermediate between tropical and temperate forms. The cooler parts show a simple erosional ramp. The warmer parts show variations on the notch and shore platform. Again, exposure, although never so impressive as the more open ocean coasts, plays a part. Trenhaile (1987) notes that the low tidal range of the Mediterranean allows for deep notches and protruding visors.

Guilcher (1953, 1958) observed the warmer parts of the northern Spanish coast showing evidence of a shore platform sloping steeply seaward, ending in a low cliff, but without the classic rimmed pools. Near Marseilles, on the Mediterranean sea coast of France, pinnacles and basins form in the spray zone, sometimes with a high tide notch, and an intertidal constructional cornice (Guilcher, 1953) while nearby, near Nice, there is no cornice. Dalongeville (1977) described from Lebanon a platform a few metres wide with wide, deep basins (i.e. deeper than rimmed pools but not as jagged as the pinnacled pools of the temperate regions) just above mean tide level. The

notches around Sicily are generally shallow with very small constructional rims of coralline algae (Rust and Kershaw, 2000).

Catastrophic events in the form of earthquakes and sea level change are apparent in some regions. Antecedent conditions thus lead to inheritance and modification of forms: e.g. Dalongeville (1977) described a fossil platform above the modern platform in Lebanon where the basins in the fossil platform are being modified into crater-shapes by spray and rain. In Sicily the complicated notch profiles reflecting variations in recent uplift rates are preserved only in the more sheltered locations (Rust and Kershaw, 2000).

The coastal karren of eastern Mallorca is described in detail by Gómez-Pujol and Fornós (see chapter 40).

#### COLD REGIONS

The literature on coastal karren from cold regions is severely restricted. The west coast of Newfoundland (Malis, 1997; Malis and Ford, 1995) is a micro-tidal region with a Late Holocene history of rising sea level (~0.7 mm) where sea ice remains fast to the shore for 5 months of the year. The limited karren that develop are micro-pits and simple basins, generally < 5 cm deep and < 10 cm wide, many with poorly defined edges (Figure 1b). There is little karren development in the intertidal zone proper; basin size then increases with increasing height above mean low water mark to a maximum of ~14 cm wide and ~6 cm deep in the backshore zone. The most abundant karren develop where wave and splash energy, sub-aerial and sub-aqueous exposure are optimally balanced, in the supratidal swash zone (~12 cm wide, ~5 cm deep). Otherwise no obvious zonation of form is apparent. Unlike almost every other region of coastal karren development, bio-erosion is reported to play only a very minor role here. Geological properties and exposure levels are the dominant controls.

Lundberg and Lauritzen (2002) tried to develop a model of karren development on cold coasts from studies in northern Norway and Svalbard. The basic form is an erosional ramp and the kar-

ren are simple basins (Figure 2b). They discovered that the greatest development is in the supra-littoral (see discussion below) because isostatic uplift is the dominant process. The forms are also often an overprint on the legacy of glacial erosional forms, with rudimentary pitting where water pools. Thus the karren displayed today are not in equilibrium with the coastal processes in action.

A rudimentary supra-littoral erosional notch resulting from frost action was observed in some jointed marbles of northern Norway and Svalbard (unpublished field observation).

### Brackish water coastal karren

Brackish water is produced either through mixing of salt and fresh water (e.g. in the zone of sea spray and rainfall) or by evaporation of fresh water. This develops in the supra-littoral zone of seacoasts, or in inland sites with high evaporation. The processes include salt-fresh water mixing dissolution, evaporation, salt weathering (Mottershead and Pye, 1994), and removal of loosened materials by wind. The karren develop into varieties of basin and pits, usually lined by salt encrustations, with some *spallation* and *grusification* caused by salt action. The limit between the upper spray zone of intertidal karren and the lowermost region of terrestrial karren that gets some salt spray is sometimes obscure. In the north east of Bonaire, Netherlands Antilles, the coast facing the prevailing winds grades from the splash zone basins and pinacles characteristic of the tops of the visors up to a complex and very sharp pit karren oriented towards the prevailing wind. Lithology is important in that aphanitic rocks in all climates show micro-rills (rillensteine) in the zone of salt-fresh mixing (Figure 4c).

The supra-littoral seacoasts of tropical regions often simply grade into dense vegetation with no obvious karren features: e.g. Moses (2003) observed a gradual diminution of basin size and rock micro-relief in the transition zone between the supra-tidal splash zone and the vegetation line

in Lord Howe island, Australia. However, where vegetation is absent, the supra-littoral may show surprisingly large isolated basins where water is pooled and aggressivity can be enhanced (Figure 4a): e.g. Kaye (1959) observed spray zone pitting in Puerto Rico eolianites up to 6 m across.

In humid temperate regions such as western Ireland, evaporation is minimal; salt spray and rain water mixing is dominant. The supra-littoral has flat-bottomed isolated pans, with bare intervening rock surfaces. Where a fresh ground water source emerges and mixes with seawater, very big, deep pools (filled with the green alga characteristic of brackish water, *Enteromorpha*) develop.

The supra-littoral of the cold but semi-arid regions of northern Norway shows various bowl-shaped depressions (Moe and Johannessen, 1980; Holbye, 1989; Lundberg and Lauritzen, 2002). These bowls are developed only in exposed situations where basins are typically ~20 cm deep. The bowls are made up of hierarchies of pits; many show considerable salt weathering with large salt crystals in remnant pools (Figure 4b). This results, particularly in the more coarsely-grained marbles, in grusification and the breakdown of the bowl edges.

### Fresh water coastal karren

Fresh water coastal karren are very rarely described in the literature. One example comes from the Silurian dolostones making up the lakeshore of Lake Huron, Bruce Peninsula, Ontario, Canada (Vajoczki and Ford, 2000). Here the form is a subdued erosional ramp with simple to complex pits (Figure 4d). The pits reached up to ~2 cm in width and ~5 cm in depth. Pit depth has a strong positive correlation with water depth. Vajoczki and Ford (2000) consider that dissolution, possibly associated with *biofilms* on the rock surface, is likely to be the dominant control on their formation. The lake has had a complex history of level changes since glacial retreat; the pits are developed in the zone of changing water levels.

A second example comes from the Carboniferous limestones of Ireland. Again, the pits are associated with changing water levels on lakeshores. Here *tubular pits* develop on the underside of boulders and bedding planes and develops upwards. Simms (2002) called them *röhrenkarren* (tube karren). These forms are described in detail by Drew (see chapter 41).

## Rates of development

Rates of erosion are measured directly with micro-erosion meters, and/or relative to some dated event (Trenhaile, 1987). Relatively sheltered areas typically retreat by about 1 mm per year (Hodgkin, 1964; Schneider, 1976). Rates vary with location: e.g. 0.09–2.7 mm per year, Aldabra Atoll (Trudgill, 1976b; Viles and Trudgill, 1984); 0.2–3.8 mm per year, Great Barrier Reef, Australia (Trudgill, 1983); at least 1 mm/yr, Eastern Mediterranean (Kelletat, 1991). Rates from a single location vary with exposure level: e.g. open coasts on Grand Cayman 2.7 mm/yr, reef-protected coasts 0.45 mm/yr, but where bio-construction dominates over bio-erosion only 0.17 mm per year (Spencer, 1985a, b). Surprisingly, erosion rates for calcareous sandstones in Western Australia (Abensperg-Traun et al., 1990) are comparable with those for pure limestones, ranging from 0.2 mm/yr to 0.8 mm/yr.

## Processes

The environment is extremely complex and there remains much controversy about the processes in operation.

### Dissolution

Discussions about the potential for, and possible importance of, dissolution are summarized by Trenhaile (1987). Field evidence indicates efficient

corrosion in intertidal and splash-spray zones but there is a theoretical problem because seawater is normally saturated or supersaturated, especially in the tropics.

Explanations involving the interaction of fresh and salt water can immediately be contradicted by the presence of excellent corrosional forms on small isolated stacks with no fresh water storage, and in the Red Sea where fresh groundwater does not flow (Macfayden, 1930). In a few cases the development of the intertidal notch is clearly enhanced by salt-fresh water mixing corrosion: e.g. Waltham and Hamilton-Smith (2004) note that sea-level notches in the islands of Ha Long Bay, Vietnam, seem to develop only on the larger islands with fresh water catchments.

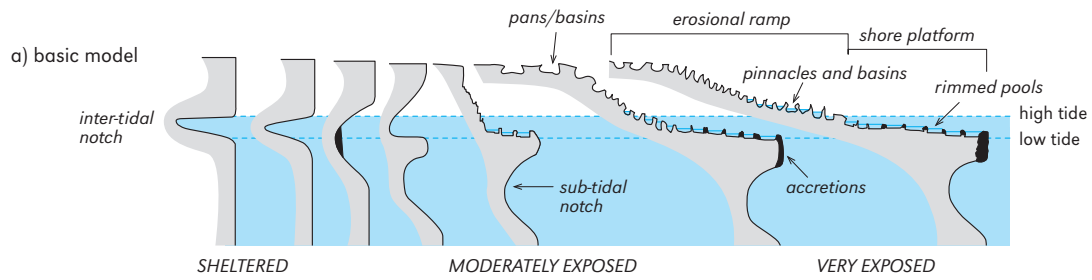
It has been suggested that biochemical processes play an important role by modifying water chemistry. This is probably applicable only where seawater is trapped in enclosed bodies. During the night excess respirational production of CO<sub>2</sub> over photosynthetic removal increases the aggressivity of pool waters (Emery, 1946; Schneider, 1976; Trudgill, 1976a). Obviously such an effect is less in open waters where pH changes of, for example, only 0.15 units can be detected (Schmalz and Swanson, 1969). Indeed, it has been found that biological activity may actually inhibit dissolution in that organic coatings may prevent contact of rock with water (Schneider, 1976).

Many workers have thus concluded that dissolution, even biochemically mediated, can only be of minor importance (Cooke, 1977; Trudgill, 1976b; Torunski, 1979) and probably explains only some smaller forms, although it may be more significant in cooler waters (Alexandersson, 1976). None of the workers has investigated the impact of potential salt-fresh water mixing from meteoric rather than groundwater input.

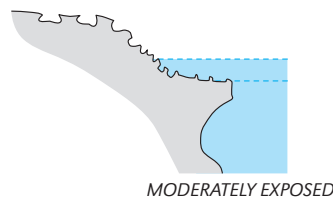
### Biological action

The focus of explanations has moved towards considering effects of direct bio-erosion, of boring in-

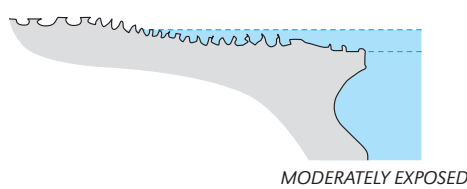
TROPICAL MODEL



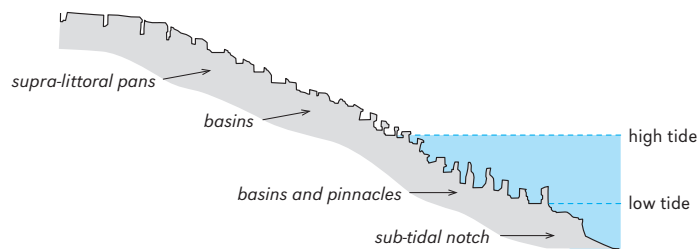
b) impact of high winds, low rock strength, high tidal range



c) impact of low cliffs, thin beds



TEMPERATE MODEL



COLD REGION (northern Norway)

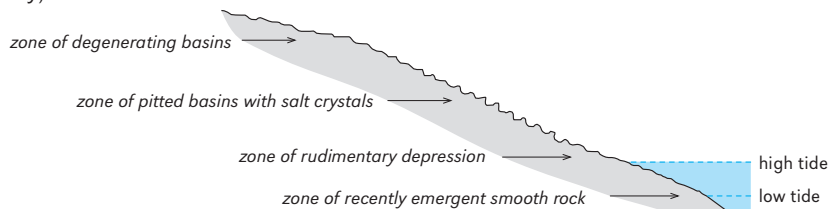


**Figure 3:** Diagrammatic shore profiles to show regional variations. The tropical model shows a clear relationship of form and exposure level (a). Local variations on the basic model (b and c) are usually expressed most clearly in the moderately exposed situation, where variations typically produce an erosional ramp rather than a double notch and tidal shore platform. The temperate model shows a simple erosional ramp with basins and pinnacles. The cold region diagram cannot be called a “model” since it reflects the impact of isostatic uplift more than intertidal erosion.

vertebrates and microflora. Viles (1984) has gone so far as to call coastal karren “biokarst”. There is a very large literature on bio-erosion, not all of it relevant to coastal karren development: Bromley (1978), Viles (1984), Trudgill (1985), Trenhaile (1987), Spencer (1988), and Spencer and Viles (2002) give reviews of this topic.

Bio-erosion is the removal of lithic substrate by direct organic activities (Neumann, 1966). Most exposed rock surfaces both in the marine and terrestrial environment acquire a complex “bio-film” dominated by cyanobacteria, but including algae, fungi and lichens (Viles et al., 2000) and most of these biofilms show a distinct relationship with rock surface weathering. Bio-erosion is particularly important in the tropics because of the richly diverse flora and fauna, susceptible rock, and not very vigorous wave action (Trenhaile, 1987). Duane et al. (2003) found active bio-erosion in the arid coastal terraces of Morocco. Scanning electron microscope studies in Ireland (Trudgill, 1987) showed bio-erosion to be the most important agent of formation of medium-scale and micro-morphology.

Levels of activity and species distribution are controlled mainly by moisture, and therefore tidal regime and wave energy. Generally the wetter the environment the greater the bio-erosion (Schneider, 1976), but it may be reduced where energy levels are too high for organisms to survive or where abrasion or sediments prevent colonization. Rock type is important in that soft, fine-grained rocks are easily bored, especially by mechanical borers such as invertebrates, and the greater the carbonate content the easier it is to chemically bore (e.g. by algae, fungi). Moses (2003) demonstrates that algal boring on calcarenite avoids the grains and operates selectively on the calcite cement.

Bio-erosion is effected by a combination of surface dwellers, direct borers and by grazers. Epiliths, such as algae and cyanobacteria, live on the rock surface and contribute aggressive organic chemicals. Endoliths actively remove rock by boring into it. The depth of penetration depends on light levels: algae and cyanobacteria must stay

within the photic zone. These are probably the most important borers in the spray and intertidal zones (Hodgkin, 1970; Golubić et al., 1975; Schneider, 1976; Dalongeville, 1977), but fungi (probably mainly in bottoms of pools) and lichen (mainly in drier parts of splash zone; see Schneider, 1976) can also bore. Filaments of cyanobacteria may penetrate 500 to 900 microns, and of lichen several millimetres. Up to one third of the rock may be occupied by *borehole* (Schneider and Torunski, 1983).

Boring by invertebrates is also common. Molluscs often carve a *home scar* to shelter in. Gastropods, such as small whelks, are important over most of the coastal karren range, contributing much of the fretted nature of the rock surface (e.g. Hodgkin, 1970). Chitons are also common, and more voracious, inter-tidal eroders (e.g. Abensperg-Traun et al., 1990). Echinoderms colonize close to low tide level and are important in deepening intertidal pools. Boring Clionid sponges are more significant in subtidal locations and are thus important for subtidal notch development (Yonge, 1963).

Both epiliths and endoliths are preyed upon by grazing invertebrates such as chitons, gastropods, echinoids, crabs, parrot fish. Grazers mechanically rasp the rock surfaces, which have been weakened by biochemical weathering or by boring, with some form of hardened teeth or radulae. A large gastropod can carve a *groove* 0.5 mm deep and 1 mm wide in a single traverse (Newell and Imbrie, 1955). The rate of rock removal is determined by a kind of homeostatic balance between the rate of grazing and the rate of boring (Golubić et al., 1975).

The action of microbes is not always simple bio-erosion: in the marine terraces of Morocco, Duane et al. (2003) found a complex suite of organisms responsible for both disintegration of matrix and deposition of *micro-stromatolites* to depths of 50 cm within the limestone.

Biological action often results in protection of the rock surface: this can be effected simply by a covering of organisms resistant to wave energy or by the presence of calcareous encrusting organ-



a  
c



b  
d

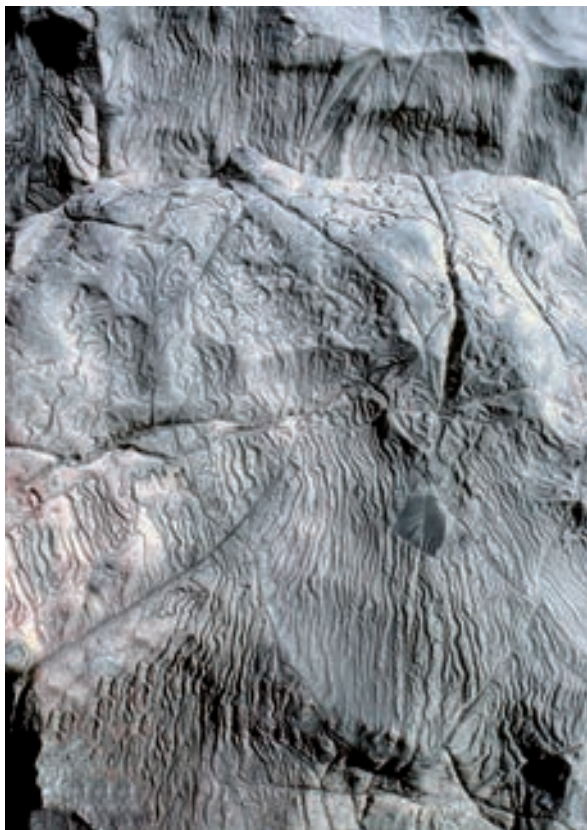


**Figure 4:** Brackish and fresh water forms: a. very wide pans of the supralittoral, north-eastern coast of Bonaire, Netherlands Antilles. This is open to rain water input, salt water input only during storms, and often subject to intense evaporation. Although the pools are occupied by brightly-coloured algae that can tolerate hyper-saline conditions, it is likely that the principal actions are salt-fresh water mixing corrosion and salt weathering; b. supra-littoral basins from the west coast of northern Norway at Gåsbakken. Slope causes the basin asymmetry (shallow lips, deep backwalls). Surfaces within basins have secondary 1–2 cm deep semi-spherical pits. Basin rims are rounded from salt action and grusification. Width of view is 75 cm; c. rillensteine (microrills) developed on aphanitic limestone in the supra-littoral zone of Gower Peninsula, south Wales. Width of view is 7 cm; d. freshwater pitting in dolostones of Bruce Peninsula, around Tobermory, Lake Huron, Canada. This sample is from the splash zone above water level. The below-water level pits are deeper. Width of view is 90 cm.



isms. For example, Naylor and Viles (2002) found that colonizing macro-algae afford bio-protection and that this is most apparent under exposed conditions. The types of organisms performing a protective function vary with temperature. In cool temperate regions barnacles colonize the drier parts of the upper littoral and dense colonies of mussels the upstanding parts of the lower littoral, thus facilitating differential downcutting of the basins. In tropical regions calcareous algae, vermetid gastropods and serpulid worms both protect and encrust.

Biological processes work to varying degrees in all limestone coasts of the world. The resultant karren forms relate to the interplay of environmental factors (such as tidal regimes, water temperature) and inter-specific interactions (such as competition, grazing and predation) (Spencer and Viles, 2002). For example, colonization by echinoderms may have little effect in a sheltered environment such as the Mediterranean (Torunski, 1979) or in the sublittoral because there is no need for a substantial home scar for protection, but in the lower eulittoral echinoderms modify the environment considerably with distinctive semi-spheroidal *cups*. There is a positive feedback effect once the first colony is established and the rock is rapidly removed to create a deep pool (Trudgill, 1987). However, if the water temperature is high then there is greater competition, the lower eulittoral may also be colonized by encrusting organisms which inhibit echinoderm colonization and home scar formation and thus deep pools may not form. A factor that is becoming more apparent is that the biological environment of a rock surface is dynamic and may show considerable temporal/spatial fluctuation (Spencer and Viles, 2002).

## Salt action

As noted above in the introduction, features that are strictly produced by salt action are not consid-

ered to be true coastal karren. However, in reality, processes often are not segregated. The influence of salt action on coastal karren is variously reported. Emery (1946) described karren in calcareous sandstones of southern California as dominated by shallow flat-bottomed tidal pools with raised rims where evaporation has deposited salt. In contrast, medium to coarse-grained limestones in coastal zones often with strong drying winds may erode in the form of tafoni (cavernous weathering forms with spherical elliptical hollows; Trenhaile, 1987; Kelletat, 1991). Moses (2003) found evidence for salt weathering producing *granular disintegration* of calcarenites in the splash zone, but in obvious association with bio-erosion. The supra-littoral bowls in the marbles of Norway (Lundberg and Lauritzen, 2002) clearly show granular disintegration from salt action.

## Abrasion

The presence of tools for abrasion normally results in a less diverse biota and the smoothing of forms, but Trudgill (1979) examined the role of abrasion in relation to other processes in Aldabra Atoll and concluded that even in areas far from beaches abrasion can be important.

## Acknowledgements

Many thanks to John Mylroie and Joan Fornós and Lluís Gómez-Pujol for excellent comments on an earlier version of this manuscript, and to Craig Malis for the photograph in Figure 1b.

# **CASE STUDIES**



Peter VINCENT

*Limestone pavements* are among the most distinctive landforms in the British Isles, and for the purposes of this chapter I have adopted the following definition, slightly modified, from Goudie (1990): “Exposed areas of bare limestone bedding planes, both flat and sloping, which are often, but not always, fretted by microforms produced dominantly by solution activity.”

It is noteworthy that above definition says nothing about the processes which may have eroded the limestone to give rise to the pavement, nor does it indicate that the presence of karren is a necessary condition. As far as the latter point is concerned, there are, for example, several fine examples of pavement in northern England that are almost totally free of karren. And while it is true that much pavement in the British Isles has been produced by glacial abrasion, it is also true that some pavements have been exhumed, mostly by glacial plucking - but not always. To nuance this point further there are magnificent examples on the coasts of western Ireland, north Wales and north-west England of limestone pavements which may have been exhumed by marine action rather than by ice. These are not marine abrasion platforms but demonstrably limestone pavements, as we shall see. Yet a further type of glacially scoured pavement is found in northern England and forms part of a truncated relict palaeokarst landscape.

By now it should be self-evident that conventional definitions of limestone pavement fail to accommodate the polygenetic nature of these surfaces as presently identified in the British karst landscape. If all this is a little disturbing then I will have achieved my purpose. To regard these features as a simple glaciokarst and then place the research emphasis on the presence and measurement of karren is to miss the point entirely. For a proper understanding of the genesis and variety of these intriguing landforms it is necessary to examine denudation process in relation to the detailed geology (Vincent, 1995).

Limestone pavements have attracted the attention of British scientists for more than a century (Sweeting, 1972; Williams, 1966) but somehow developments in karst geomorphology seem not to have engaged much with developments in our understanding of the Lower Carboniferous rock succession. Indeed, as far as the author is aware, there have been no major studies in this regard since the work of Sweeting and Sweeting (1969) who investigated the relationships between lithology and pavement form in north-west Yorkshire (England) and the Burren, County Clare (Irish Republic).

Both the rise of process geomorphology and the quantitative revolution in geomorphology further deflected research away from the geology and two research themes have prevailed for much

of the thirty years or so. Some researchers have investigated the influence of plants and the soil cover on the corrosion of the pavement surfaces, for example Trudgill (1985), while others have investigated karren types and pavement morphometry (Goldie, 1996; Vincent, 1983b; Rose and Vincent, 1986b). The time is now ripe for a paradigm shift back to an examination of the essential relationship between pavement form and genesis in relation to the Lower Carboniferous stratigraphy.

## Pavement distribution

Although the presence of cyclic limestone sequences of Asbian age are the main requirement for the formation of limestone pavements in the British Isles their distribution does not always coincide with a suitable process domain. Thus, for example, there are Asbian stage limestones in the Mendips, in Derbyshire and in south Wales but limestone pavements are for the most part absent. In the case of Derbyshire and the Mendips, pavement-forming ice scour was absent as both areas lie south of the ice limits of the Last Glaciation Maximum (LGM). LGM ice did pass across south Wales but the limestone outcrops are narrow and the bedding planes upturned (Waltham et al., 1997).

The largest area of Asbian stage pavement in the world is found on the Burren, in County Clare, Irish Republic (Figure 1). Here, some 290 km<sup>2</sup> of pavement have been formed as ice passed southwards across Galway Bay from the mountains of Connemarra and the Corrib Basin.

Within mainland Britain there are only 29 km<sup>2</sup> of limestone pavement and as much as 97 percent has been damaged. The most extensive upland pavement occurs in the Ingleborough and Great Asby Scar regions of the northern Pennines (Figure 1). There are also small areas of pavement found on north Wales and in the far north-west of Scotland.

## Geological control

Since the 1970s there have been a number of developments in carbonate and Carboniferous geology that have a direct bearing on the genesis and morphology of British limestone pavements. With the exception of small areas of pavements developed on the Cambro-Silurian Durness limestones in northern Scotland, limestone pavements in the British Isles are developed in Lower Carboniferous (Dinantian) carbonate successions, and in particular the Asbian and early Brigantian stages. These sediments were deposited on extensive shallow-water, flat-topped carbonate platforms (Walkden, 1972) which show marked small-scale rhythmic cyclicity, which is absent from the underlying Holverian and earlier strata. The cyclicity is due to changes in relative sea level but its exact cause is still a matter of debate.

Asbian limestones display a variety of lithologies which are an expression of water depth and environmental energy in which they were laid down. Individual cycles comprise a sequence of carbonate lithofacies arranged in a shallowing upward succession. Each cycle was initiated by a rise in sea level that inundated the carbonate platform. Intervening marine regressions culminated in subaerial exposure and karstification.

The average thickness of the cycles varies from a few metres in the early Asbian to around ten metres in the overlying Brigantian. Some 25 to 35 cycles have now been identified in the Asbian and in the Brigantian there are probably no more than a dozen or so. If it is assumed that the Asbian lasted for about 9 Ma and the Brigantian for 6 Ma (George et al., 1976), individual Asbian cycles lasted between 260,000 and 360,000 years, and Brigantian 500,000. Palaeokarstic surfaces, clay palaeosols, and calcretization of the host rock at the top of each cycle are diagnostic features of the subaerial exposure of Dinantian carbonate platforms during periods of low sea level.

In the Asbian and early Brigantian rocks of the Derbyshire Dome Walkden (1974) showed conclusively that the major bedding planes were

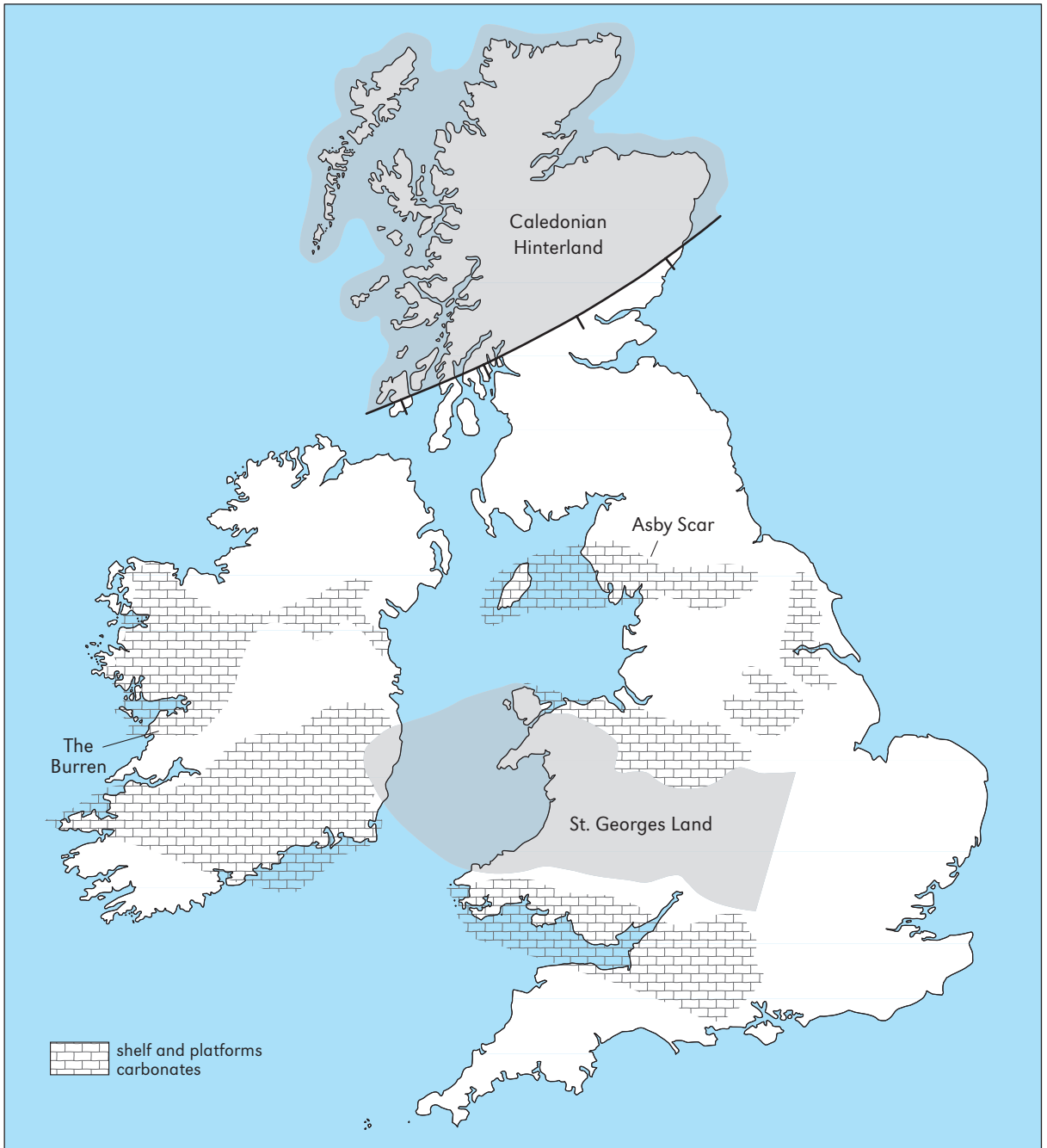


Figure 1: Distribution of Asbian shelf sediments in the British Isles.

produced by contemporaneous Carboniferous subaerial weathering and the formation of karstic surfaces. According to Walkden, the palaeokarstic surfaces underlie thick bentonitic clays which are interpreted by Walkden as subaerial

accumulations of volcanic dust (Walkden, 1972). These clays are often known in the literature as wayboard clays - an old quarrying term. The corroded, karstified surfaces can be shown to have formed before the next deposition of limestone



**Figure 2:** Clay wayboard in Asbian limestone. Crosby Ravensworth, Cumbria, England.



**Figure 3:** Mullach Mór (Burren). Schichttreppenkarst pavement sequence developed on calcreted horizons in the Asbian limestones.

because the lower surface of the overlying limestone is always sub-horizontal and does not follow the irregular palaeokarstic surface (Figure 2). This general model of palaeokarstic development holds for all Asbian shelf limestones in the British Isles and thus includes all the major limestone pavement regions.

Of particular relevance to the development of limestone pavements is the diagenetic alteration of the limestone immediately under the wayboard clay. Horbury (1987) showed that these limestones are mottled with dark-grey circular markings surrounded by pale-grey matrix. The darker patches are interpreted as a diagenetic alteration of the limestone caused by organic acids and associated with vegetation growing in the subaerial wayboard. In addition many palaeosurfaces have crusts of dark grey laminar calcrete. This sub-wayboard diagenesis results in poorly jointed, massive limestones which are relatively resistant to erosion as compared with those limestones above the wayboard. This differential jointing explains the development of the Schichttreppenkarst (Bögli, 1964) by differential glacial erosion, both in the Burren and north-west England (Figure 3). A particularly good exposure of a clay wayboard can be found in Ireland at the entrance of the Ailwee caves (Irish Grid M 23 05) and the associated calcreted limestone bench can be traced all round the Ballyvaughan embayment (Irish Grid M 08 23).

## Post-glacial pavement development

Although there are exceptions, as we shall see later, a general model for post-glacial pavement exposure is as follows. There is now abundant evidence that most limestone pavements in the British Isles were at one time covered by Late Glacial loess (Vincent and Lee, 1981; Vincent, 2004) which, in wetter situations, may have developed a peaty cover. It was under this blanket of loess that widespread rundkarren developed. Much of this loess cover has now been lost partly through disturbance by Mesolithic and Iron Age clearances

and later, by farming activities, and partly as a result of the development of the grike systems which drained the pavement of its silty cover (Raistrick, 1947). Looked at in another light, British limestone pavements are magnificent examples of a soil-eroded landscape.

At Norber Brow, a few miles south of Ingleborough, glacial erratics, eroded from an inlier of Silurian greywacke in the valley bottom, have been lifted by ice onto pavements on the valley sides. These erratics are now perched on limestone pedestals mostly 400-500 mm above the general pavement level, the erratics having protected limestone surface from postglacial solution. There is nothing extreme about the Norber site and it is probably reasonable to assume this figure for pavement lowering in northern England.

The coastal pavements at Fanore (Irish Grid M 13 08), in the south west of the Burren, are interesting since open grikes probably existed before dunes buried the pavements. Erosion of the dunes has now revealed a polished pavement surface with the grikes having been filled by walls of proud beachrock formed from the dissolution of the shells in the dune sand.

## Pavement types

The intersection of geological control and process domains naturally gives rise to five pavement types, namely: glacially plucked joint-dominant pavements; glacially abraided calcrete-dominant pavements without palaeokarst; glacially exhumed calcrete-dominant pavements with palaeokarst; glacially exhumed calcrete-dominant pavements with palaeokarst; glacially truncated palaeokarst; and marine exhumed paleokarst pavements.

### Glacially plucked joint-dominant pavements

This type of pavement is formed where glacial scour coincided with non-calcreted horizons above clay wayboards. These zones have high joint





**Figure 4:** Aerial view of Asby Scar showing a mosaic of glacially truncated palaeokarst, exhumed calcrete-dominated pavement, and glacially eroded joint-dominant pavement.

densities which made them less resistant to glacial plucking processes such as hydraulic jacks and heat pump effects. The net effect has been to produce a pavement with abundant surface clitter and relatively small clints. Many of the pavements on the flanks of Ingleborough are of this type and good examples can be found at the head of Crum-mack Dale.

It is interesting to speculate why glacial scour did not penetrate deeper into the carbonate cyclic succession in these areas. One possibility is that the ice was not particularly erosive and may have been thin and also possibly sluggish due to a cold base. Another possibility is that the ice was erosive but scour was time-limited.

#### Glacially abraided calcrete-dominant pavements without palaeokarst

Where glacial scour coincided with the hardened, joint-poor calcreted horizons beneath the way-board clays the pavements were abraded but not plucked. The net result was to produce a smooth pavement almost a totally without joints. There are excellent examples of such pavements at Great Asby Scar (NY 6409 – NY 6809) – the Shining

Stones pavement north of Castle Folds is but one of many in the area, and at Gait Barrows National Nature Reserve (SD 482 775) – especially the almost grikeless central pavement. In both cases, Schmidt hammer results confirm the high compressive strength brought about by case hardening due to the formation of calcrete.

#### Glacially exhumed calcrete-dominant pavements with palaeokarst

Sub-wayboard surfaces are laterally quite variable (Vanstone, 1998) and where wayboards were thick, karstified, calcreted surfaces developed. In places, these surfaces have been exhumed by glacial action. The evidence for exhumation is unequivocal in that the palaeokarst can be seen passing laterally underneath wayboard clays. This type of pavement is also massive, with few joints, but contains saucer-shaped pits and some runnels and a non-planar topography. Good examples can be seen at Gait Barrows National Nature Reserve in northern England, on the Morecambe Bay coast near Grange-over-Sands and Silverdale, and also at the entrance to the Ailwee caves in the northern Burren.

**Figure 5:** Palaeokarstic pavement exhumed from under wayboard and block beach fall. Inishmore, Aran islands, Ireland.



### Glacially truncated palaeokarst

At Great Asby Scar in Cumbria it is clear that ice moving eastward away from an ice dome over the Lake District was not effective in completely removing a pre-glacial palaeokarst (Figure 4). At this site, a glacially truncated pre-glacial karst is fretted with almost completely circular solution pipes which now form part of the general pavement mosaic. Similar sites can be found on the fells above Appleby in the Eden Valley, and possibly in the Ingleborough region (Jones, 1965).

Excavations of the solution pipes at Asby reveal that they are filled with a dense, mottled, reddish clay. XRD analysis shows the clay to be kaolinite rich and completely unlike a wayboard clay. The pit clays may originally have been a saprolite developed on the Shap granites to the west which was carried onto Great Asby Scar by glaciers and plastered onto the surface of a pre-Quaternary karst.

### Marine exhumed palaeokarst pavements

The definition of limestone pavement suggested at the beginning of this chapter allows for the inclu-

sion of palaeokarstic surfaces exhumed by marine action. These are spectacularly developed at many sites on the Atlantic facing coasts of the Aran islands, western Ireland and on the north coast of Anglesey, north Wales.

At first glance it might seem that these pavements are just marine abrasion platforms with biokarstic pits but this is demonstrably wrong. The evidence is remarkably simple and merely requires the investigator to look cliffward rather than seaward where it will be seen that the karstified surface continues into the cliff section and under well-exposed wayboard clays (Figure 5). Furthermore, it is clear from topographic profiles measured immediately under the wayboards and also out on the exposed pavement that there has been little surface lowering or pit deepening/widening since the pavement was exposed. The exact cause of the exposure has not been examined in detail but one possibility is that these pavements have been exhumed as a result of the development of so-called block beaches. During major storms the heavily jointed limestones on the cliff face become loaded with water, fail and collapse. These fallen blocks are then eventually removed by wave action, and the poorly jointed palaeokarstic pavement is then exposed. An alternative explanation

might relate the exhumation to glacial plucking of the cliff faces as ice passed from Connemarra southward across the islands and on out into the Atlantic.

## **Conclusions**

It now seems clear that the morphology of British and Irish limestone pavements can mostly be accounted for by interaction between erosion/exposure processes and cyclic events in the Asbian

limestones. In general, differential glacial plucking and abrasion seems to have been controlled by the calcretization and consequent joint density variation within each cycle. British limestone pavements are thus in part postglacial, in part exhumed Lower Carboniferous surfaces, and in places part of an older pre-Quaternary, possibly Tertiary, karst. Viewed in this way, these fascinating landforms are clearly important lines of evidence when attempting to decipher the wider geomorphology of the regions in which they are located.

## CASE STUDIES OF GRIKES IN THE BRITISH ISLES

Helen S. GOLDIE

An initial discussion of general morphometry is appropriate to establish a basis on which to fit specific local cases. As Day says (Gunn, 2004): "... quantification of form has made inter-regional comparison more rigorous. It has also helped in the development of meaningful indices of landscape morphology and it has clarified the role of lithological, structural and other factors influencing karst landform development." Reference is made to Goldie and Cox's work on limestone pavement morphometry at British, Irish and Swiss sites, presenting data on *clint* and *grike* measures. Variations between and within field sites relate to depth and timing of glacial scour, rates of post-glacial solution, tectonic disturbance, and lithology, whilst human impact is also identified as influencing present-day landforms directly and indirectly. An important possibility is that some of the wider grikes existed before glacial erosion and survived to be re-activated and to develop greater width and depth during the Holocene. The Irish sites in the Burren and on Arainn are in areas heavily scoured by the Irish midland ice-sheet (McCabe, 1987), and in sympathy with this the data here show relatively narrow grikes (see chapter 9), although it is still theoretically possible for there also to be larger, pre-Devensian survivors. The Arainn *pavements* have the grike population with the lowest median width (9 cm), although this site has maximum width of 1 metre.

The site with the greatest median depth was Ingleborough, 99 cm, and the shallowest was 42 cm in Wales but ambiguity of grike measures has been commented on with great range and local variety. In order to understand the variety of relationships between measures, pre-glacial conditions, as well as depth of glacial scour, must be invoked. Reference can be made to variants of the morphological model, based on the Goldie-Cox model (2000) (see Figure 13 in chapter 9). The bed thickness factor must be carefully examined locally, as an important influence on joint spacing and thus grikes. Bed thickness will also, through being linked to strength, influence survival of glacial scour, since massive beds, with widely spaced joints, produce very large blocks of rock, proportionately harder for ice to remove. Rose and Vincent (1986a), examining grike data at Gaitbarrows, identified a bimodal distribution and considered that this demonstrates two ages of grikes. However, a bimodal distribution is not necessary to support pre-glacial survival. Pre-glacial survival will merely widen population range as surviving scoured fissures will range in size from minimal sizes up to some large survivors, and the minimal ones will merge with the new Holocene grikes.

Varied morphology is consistent with suggestions about ice scour, given varied pre-glacial conditions as well as differing degrees of scour. Arainn's grikes, consistent with deep recent ice

scour, are indicated by level D on the development model (see Figure 13 in chapter 9). The Glattalp (Switzerland) grikes may reflect lesser scour resulting from divergent ice streams on a broad col, a similar situation to Sanetsch (Switzerland). At Sanetsch at present very recently deglaciated limestone surfaces have visible fissures filled with debris now, which will be the wider grikes of the future. Sanetsch's limestone is also strikingly veined, and these veins affect how the grikes develop. Gillespie et al. (2001) discuss both jointing and veining and their separate influences on fissure patterns in the Burren pavements. The Burren's moderately wide and deep grikes include several locations where glacial scour has produced situations B or C in the model. Gait-

barrows (Lancashire, UK) is also an excellent site to examine for the evolution of grikes from immature features with which Perna's 1996 observations of the Trentino area make interesting comparison.

Pavements with smaller clints still show enormous variety in grike data. The Ingleborough and Cumbria sample areas have both deep and wide grikes but high variability particularly over depth. High grike depth variability is also observed in the Yorkshire Dales areas further east, in Malham and Wharfedale. There has also been a complex relationship here between topography and glaciation, with recent field observations supporting the view that features have partly survived glacial scour. Other Dales sites have experienced considerable

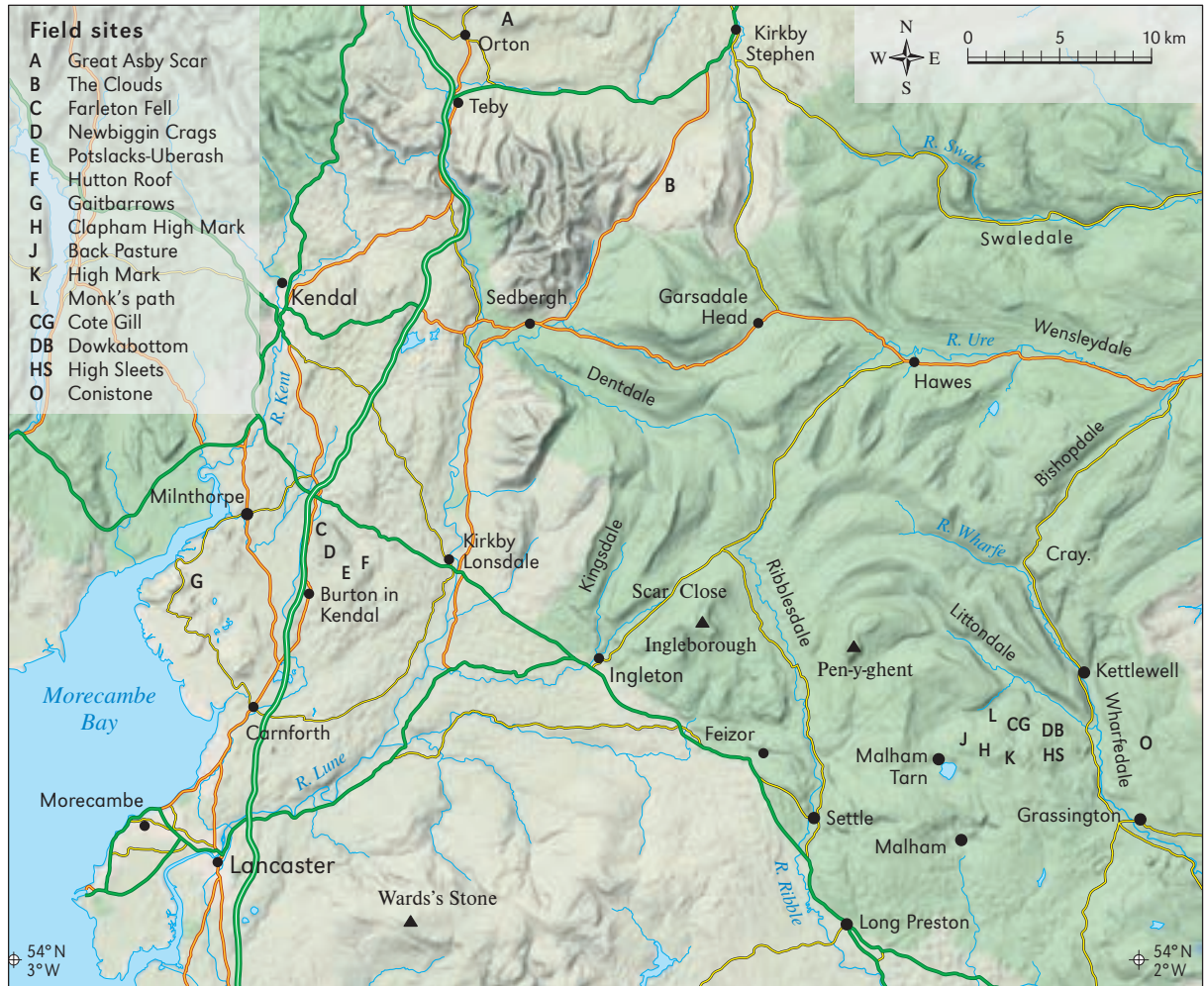


Figure 1: Location map of main field sites in north-west England.

human impact from direct removal of upper clints especially in Wharfedale. Human removal of clints has a significant effect on grike depth, though a somewhat more limited effect on grike width (Goldie, 1986). Clearly grike depth reflects the layers of rock through which fissures exist although fracture propagation from one bed to another must not be assumed. Joints may exist only through one rock layer, whilst others propagate across several thus crucially influencing grike depth. Human removal of clints may thus mean very immediate effects on clint sizing, but not always.

Major factors influencing grike development can best be illustrated with the case studies (Figure 1) which include: Gaitbarrows, The Clouds, Great Asby Scar, Farleton Knott (including Hutton Roof Crag and Farleton Fell), Whernside and Ingleborough, Malham Moor (including Cowside Beck, High Sleets and Dowkabottom), and Wharfedale and Hampsfield Fell, and some comparison with Derbyshire. The sites will be discussed according to locally important characteristics (Waltham et al., 1997; Goldie, 1995, 2006), for example, early stage features, structural influences, stream flow, *palaeokarst* characteristics and evidence of mature development including glacial survival, or human influence.

### **Immature grike features: Gaitbarrows**

Clearly one major influence on grike characteristics is the time available since the grike began to evolve. However, when a feature becomes a grike from an unfissured stripped surface is a question that is hard to answer, as there is no minimal definition. Figure 2 shows early stages of grike formation at this site in NW England, which has been well scoured by ice in the Late Devensian (Rose and Vincent, 1986a) but retains a great variety of features, including probable survivors of ice scour that developed into larger features in the Holocene. The Carboniferous limestone here has calcite veins that influence alignment and features of both in-

dividual grikes and networks (Rose and Vincent, 1986b). Figure 3 shows a short sequence of round holes resulting from boring into the limestone by plants along such a veined 'weakness'. Figure 4 shows a more developed line of small solution features, which will eventually merge and become a true grike. The plan outline of that grike reflects its evolution, and the wavy plan outline of more developed grikes betray similar origins.

A further development of vein influence is that their clustered alignments at staggered angles associated with structural influences (*en echelon*)



**Figure 2:** Line of bio-corrosion holes developing along a vein in well scoured limestone pavement. Gaitbarrows, Lancashire, UK.



**Figure 3:** Kamenitza which has been drained downwards by the development of a slit which breaks through the top bed. Gaitbarrows, Lancashire, UK. Width of view is 1.8 m.



**Figure 4:** View along a prominent vein showing a series of features at different stages of development along this line. Gaitbarrows, Lancashire, UK.

result in linear zones of complex grike patterns. At Gaitbarrows such zones are lower than less griked areas (Figure 5). This may be because greater fracture density here favours increased solutional lowering. Another possibility is that glacial scour gouged down into these zones preferentially due to their vein-related weakening. Thus after glaciation, erosion favoured these areas for more than one reason, the rock weaknesses, and also their lowering by glacial scour, both resulting in drainage waters focussing on these lower zones.

### Structural influences

The importance of folds has been mentioned (see chapter 9). Great Asby Scar in Cumbria demonstrates this with a gently folded structure (Figure 6). The Clouds, Cumbria, are Carboniferous limestone outcrops very close to a major shear stress fault (Dent Fault) that strongly influences the topography (Underhill et al., 1988; Goldie, in Fornós and Ginés, 1996), particularly causing close rock fissuring. Typical clint and grike arrays here have strikingly closely spaced grikes and narrow clints. However, there is also now a greater appreciation of the age of some of these features since, despite the closeness of jointing, it is obvious from Figure 7 that some beds are extremely thick, ca. 1 to 1.5 m, similar to those observed in the Malham area of Yorkshire, and similarly well-rounded in outline. This roundedness does not result from glacial scour as it extends all round the blocks; it is a shaping resulting from pre-glacial karstification (Figure 8). Thus, in spite of glaciation and lengthy periods of periglacial conditions in closely-jointed rock, The Clouds retains remnants of ‘maturely’ weathered karstic features. The usual relationship between bed thickness and joint spacing is overridden where major tectonic stresses have meant joints are closer together than at outcrops of similar thickness but distant from such influences, such as in the Malham area.

## Stream flow influences

Scar Close on Ingleborough has some of the most massive pavements in Yorkshire with a mixture of evolving grike network patterns. The inner edge of the outcrop near peaty glacial deposits (Gosden, 1968) has acidic drainage off these 'islands' and the marginal shale cover (see annotated diagram Figure 9). This drainage has caused *dendritic runneling* patterns, forming grikes when the top limestone layer is cut through. Towards the outer valley side of the outcrop, where the limestone has been longer exposed, more rectilinear patterns reflect increasing influence by rock fractures on grike development rather than the superimposed dendritic patterns. There is also evidence that the outer scar edge has pressure release fissures, since numerous grikes run sub-parallel to it. Lastly, at a scale order higher than individual grikes, large griked areas run across Scar Close from south-east to north-west, which have a varied plan outline comparable to that referred to earlier for Gaitbarrows, but in which the holes are essentially large grike holes or *dolines* often with significant soil and vegetation. The spacing of these wider griked lines is of the order of tens of metres, and a similar scale of fissures is responsible for major indentations in cliff outlines, and for small valleys in this area.

Ingleborough also has sinkholes on its west side, worth discussion here as they are in pavement-like outcrops and are fundamentally widened fissures (Figure 10). These examples are very



**Figure 5:** Linear complex of grikes developed along veins in association with a major fissure, all of which is at a lower level than the general pavement surface. Gaitbarrows, Lancashire, UK.

smooth-sided, about 50 cm to one metre wide, caused by solution from significant streams flow-

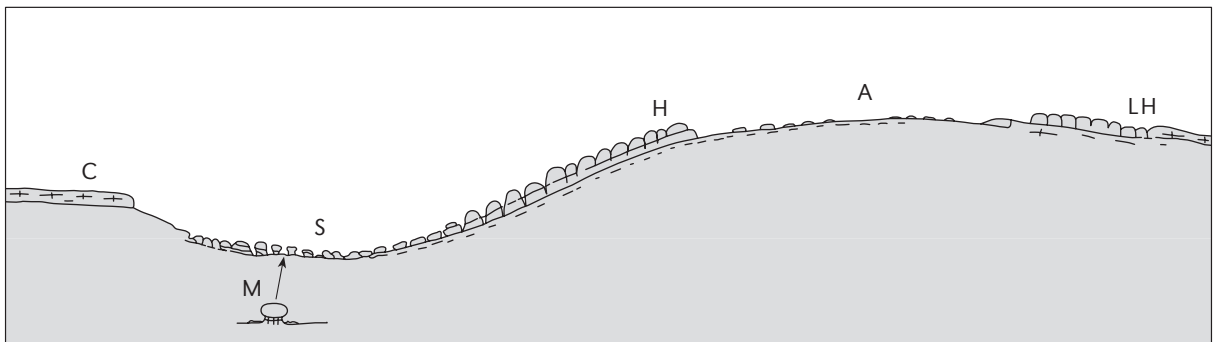


**Figure 6:** Sketch profile across Great Asby Scar, showing relations between geological features and landforms. C. mesa (Castle Folds); S. main syncline; A. denuded anticline; M. mushroom features; H. large holes on steep slope; LH. large holes and extended holes. Not to scale, notional distance across section is ca. 400 m.





**Figure 7:** The Clouds. Massive beds on upper layer at amphitheatre edge (centre of anticline).

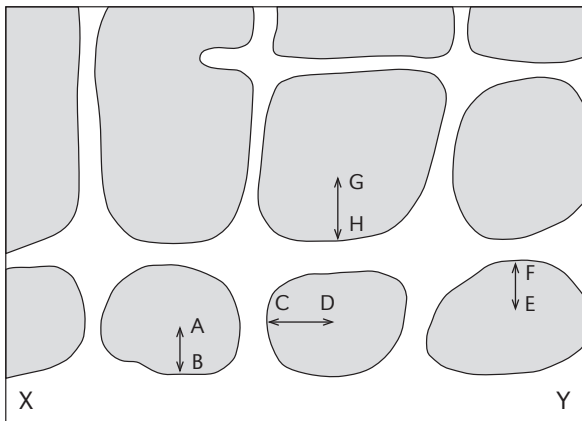


**Figure 8:** Plan diagram (not to scale) of rounding demonstrates that roundedness is found at the sides (C-D) and backs (E-F and G-H) of outcrops edges to the same degree as at the facing edge (A-B). This indicates that the rounding is caused not by glacial scour along the outer edge (X-Y) but is probably the remain of karstic processes.

ing off the Ingleborough massif, which they swallow. Dry versions are found further out on the outcrop, abandoned as streams that formed them disappeared underground down newly opening upstream fissures. Similar exceptional ‘grikes’ involving stream swallowing include Hunt Pot, near Pen-y-ghent. Thus grikes are also features known by other terms; cavities, or major drainage points, also termed *potholes*. On Arainn *runnels* of similar dimensions contain peaty streams. Many such dry features, now on limestone pavement outcrops abandoned from past drainage points, provide puzzles for geomorphologists.

### Palaeokarstic features and mature grikes

Evidence from grike dimensions, shapes, and relationships to other features, helps address the

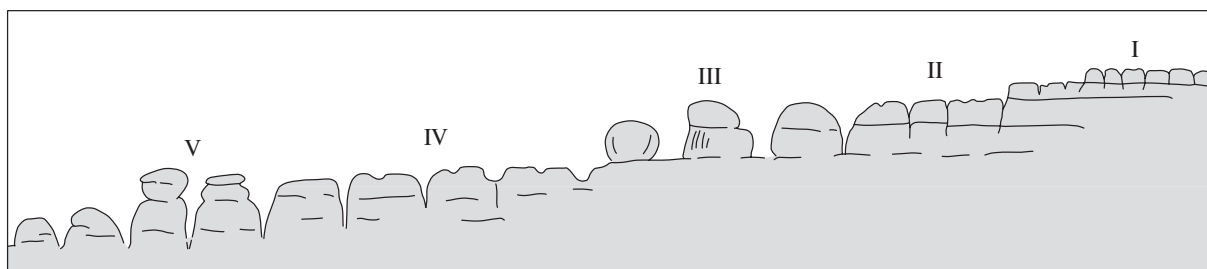


**Figure 9:** Sketch cross section looking east across stepped boulder – pavement sequence, Newbiggin Crag, Farleton Knott, Cumbria, UK, showing sequence of maturely weathered and scoured limestone beds. I. upper pavement layer, well dissected; II. “normal” pavement, merging on into same bed; III. extremely well rounded pavement edge with boulder shapes; IV. “normal” pavement; V. same bed as IV, but with grike holes and well rounded clints and boulders. Not to scale: notional distance across section is ca. 50 m.



**Figure 10:** Ingleborough sink demonstrating stream disappearance down a widened grike.

question of landform age. This can be illustrated at many Carboniferous limestone outcrops in NW England and elsewhere in the British Isles. Rose and Vincent (1986a) discussed the significance of the erratics in grikes at Gaitbarrows concerning grike maturity and similar evidence is observable at Scales Moor, Scar Close and Souther Scales in the Whernside-Ingleborough area of Yorkshire, and at Great Asby Scar, among many examples.

An important grike characteristic is the flared shaping of their upper edges and it is clear that the concept of a grike cannot be separated from clint definition (Figure 11). The diagram summarizes the range of possibilities, demonstrating development of curvature with time. Bed thickness and fracture spacing influence the outcome. The development model (see Figure 13 in chapter 9) expands on the various likely relationships between the main influencing factors. Numerous sites have particular aspects of maturity to exemplify.

Farleton Knott: The area known as Farleton Knott includes the well-known pavement sites, Farleton Fell, Holme Park Fell, Hutton Roof Crags

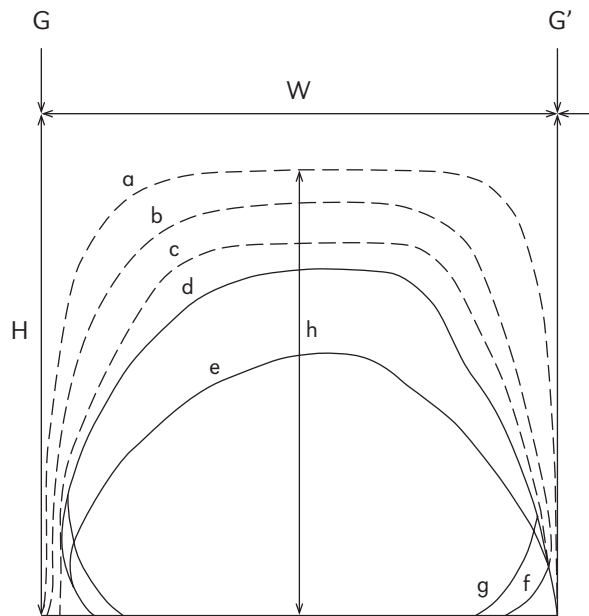


**Figure 11:** Grike evolution, defining and grading roundness. G, G'. original grike centre lines; W. original block top width; H. original block top height; a–e. stages of upper roundedness of the limestone; f–g. stages of under-rounding of the limestone.

and Newbiggin Crags (Figure 12). General grike patterns have been discussed by Moseley (1972). There are many distinctive mature karst features along outcrop edges (Figure 13), including higher beds, and the sides of major geological weaknesses cutting through the area. These weaknesses produce narrow low-lying zones, which must have been sheltered from ice scour in order for the well-

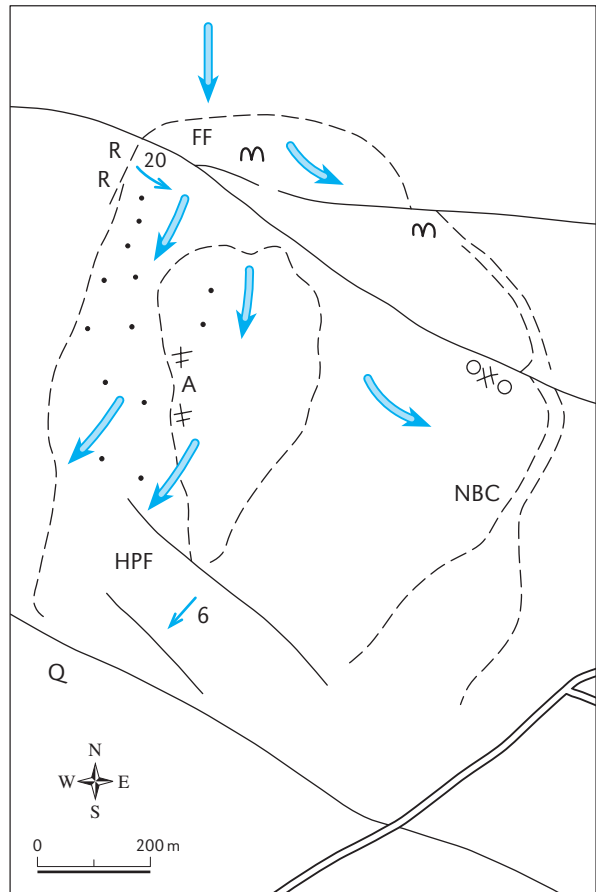


**Figure 12:** Sketch map of Farleton Knott, Cumbria, UK, northern half, to show location of mature karst features cited in text, and relations to direction of Lake District ice flow (double arrow). Solid line. main faults and major fractures; numbered arrows. angles of dip; dashed lines. outline of bedding plane edges; FF. Farleton Fell; NBC. Newbiggin Crags; HPF. Holme Park Fell; R. rounded cliff tops; A. tower-like features and embayments; m. massive rounded edges; OXO. NBC sequence of boulders and pavement; Q. Holme Quarry; dots. glacially-moved boulders—approximate distribution; 1. ice spreading towards sheltered east side; 2. ice diffuence over central 'hump'. Notional distance across map = 1.3 km.



**Figure 13:** Massive rounded bed edge clints at the north end of Farleton Knott (Farleton Fell).

rounded massive features found there now to survive. The Hutton Roof Crag dolines are mostly located along these fissure lines and their edges have rounded boulders and clints, and wide flared grikes that cannot have evolved entirely during the Holocene. The famous sloping diamonds are shown in Figure 14.

The north-east end of Newbiggin Crag on Farleton Knott has some very unusual features not found in the same sequence anywhere else known to the author (Figure 15). In general they are similar to the boulder features along the Hutton Roof dolines and differ slightly from mature features at Great Asby Scar where grike holes dominate. A very massive upper limestone bed at Newbiggin Crag has permitted remnant clints between widening grikes to become boulder-like. Below these features is conventional pavement, and below this is another massive bed with widely flared grike holes, more akin to the Great Asby Scar holes. The relationships between the various layers point strongly to the more rounded features surviving glacial scour, whereas the middle layer must have



**Figure 14:** Diamond-shaped clints on the steep limb of the Hutton Roof Monocline (Hutton Roof Crag).



**Figure 15:** Panorama looking east at the northern end, Newbiggin Crags. To the far left are well rounded clints with flared grike holes leading on to the relatively regular paved clints in the same bed, to the right are very well rounded clints and boulders of the more massive upper limestone layer (Newbiggin Crags).



**Figure 16:** Panorama looking east from the north end of Castle Folds showing varied grike and clint shapes. To the left in the distance are the relatively rectangular shaped clints in the lower massive bed, to the right are the well-rounded clints around the grike hole of the more massive uppermost limestone layer (Great Asby Scar).



**Figure 17:** Bed edge features around the surviving upper limestone layer north of Castle Folds and in its 'shadow' in terms of glacial scour from the south (Great Asby Scar).



**Figure 18:** Close-up of holes to the south end of Castle Folds demonstrating the large number of fissures radiating around them (Great Asby Scar).

had features small enough to have been plucked or scoured away as it now forms a flat runnelled surface. Measurements here suggest ca. 8 cm of solution since bedding plane stripping.

Further variety of grike features on Farleton Knott includes regular rectangular clints, to the south along Newbiggin Crags (NBC), and on the south-east corner the famous diamond-patterned features at Hutton Roof (Figure 14). Grike patterns at both sites suggest that joint sets are very nearly equally strong in two directions at right angles to each other. At Hutton Roof the clints are diamond-shaped because of the relationship between orientation of topographic slope, itself related to inclination of this limb of the Hutton Roof Monocline (Moseley, 1972), and orientations of the joints sets. Squareness as indicated by a clint width to length ratio of 1 (see chapter 9) is not attained, but the ratio at these NBC sites is 0.65, at the higher end of the whole population (see chapter 9) indicating that these clints are squarer than many.

Great Asby Scar is part of the extensive Carboniferous limestone escarpment west of Kirkby Stephen (Figure 1) (Goldie, 1996; Waltham et al., 1997). It has very varied grike patterns, the most rectangular being where upper beds have been stripped away (Figure 16). The upper beds are very massive, often ca. 1 m thick, and where they survive (Figure 17) they are pocked by grike holes of 2–3 m diameter, usually deep and soil-filled (Figure 18). Vincent (1995) has analysed these features and their fill and explained them as dating from the Late Carboniferous, which accords nicely with recent determinations of lower solution rates (Goldie, 2005). Lower solution rates allow for some grikes and grike holes in northern England having developed over a longer time, possibly since well before the Quaternary, not merely in long interglacials before the Devensian glaciation, or in the Holocene. It is probable that rates of surface solution lowering in many dry upland limestone areas are 15 to 20 cm in 15 ka at the most, possibly even lower, for example, 5 to 10 cm, as assessed from pedestal evidence. Thus grike holes of 1 to 2 metres wide or even more, must be palaeofeatures,

and origin in the Late Carboniferous is one possible explanation.

At Great Asby Scar the grike holes also vary considerably. Those in the very thick upper beds have a few joints crossing aiding formation, and are vertically oriented to topography not bedding (Figure 6). Others on horizontal beds areas are smaller and shallower, but in thinner beds and of more complex form having numerous joints and other solutional features draining towards the centre. In a study of 37 holes, an average of 5.6 runnels or grikes focussed towards holes, the average diameter of the top of the flare was 1.45 m and there was a positive relationship between this and the number of features draining towards the hole (Figure 19). When the features formed in their totality is debatable. Greater soil cover in the Holocene is evidenced by smooth surface solutional features and archaeological evidence of human occupation, unlikely without more soil than now (Richmond, 1933). Holocene sub-soil solution would operate at variable rates dependent on conditions of acidity and moisture. Evolution in the Holocene would have occurred, but to what extent this compares with evolution occurring much earlier, including the Late Carboniferous, now needs careful appraisal in view of new

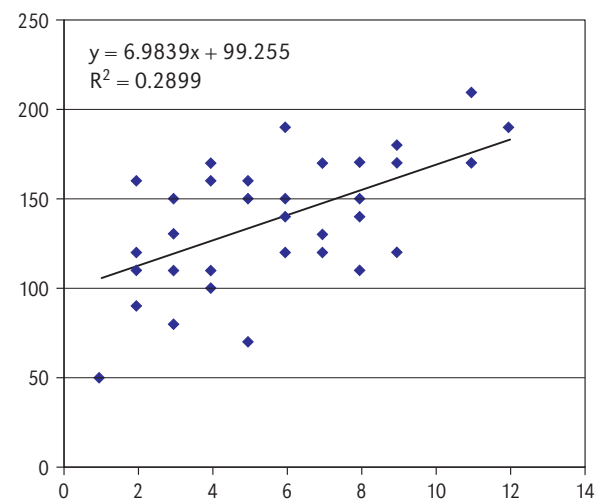


**Figure 19:** Scatter graph of grike hole upper flare diameter (y axis) against number of joints and runnels draining towards each hole (x axis).



**Figure 20:** Monk's Path, above Arncliffe, Littondale; rounded outcrops at ca. 480 m a.s.l.

evidence concerning *palaeokarst* features and solution rates in these upland limestone areas.

Structural influence on the holes is clearest in the upper bed, which persists around parts of the synclinal outcrops (Figure 6), and this may have affected how grikes evolved and whether limestones were removed easily by glacial stripping because of effects involving joint widening over anticlines. Grikes have been strongly influenced by an underlying thinly bedded limestone layer, which will have suffered much mechanical weathering, undercut overlying limestone and hence allowed mechanical erosion of the upper layer. In addition a shadow effect is demonstrated where the mesa (Castle Folds) has sheltered areas in the lee of ice-flow from the south, leaving the upper bed. The edge of this demonstrates many evolutionary features of upper grike edges as the limestone erodes (Figures 16, 17, 18). Few clints at Great Asby Scar have, however, developed as far as those in upper beds at Newbiggin Craggs which are boulder-like, possibly because the limestone bed at Newbiggin is thicker. However, differences between sites could also be due to variations in corrosion conditions or time available. Great Asby



**Figure 21:** Lee Gate High Mark; rounded outcrops at ca. 460 m a.s.l.

**Figure 22:** Scoured pavement at 330 m a.s.l. showing lack of rounded features, but narrow grikes and flat clint tops (Littondale, Yorkshire, UK).



Scar's holes could have been modified to become more vertical by copious melt-water and there is the possibility of biologically enhanced corrosion from vegetation growing in the deep soils in the holes. Some grike holes still retain shrubs. Parts of Great Asby (near Castle Folds) may also have their grike features widened by enhanced corrosion from human and animal occupation, particularly the 'entrance track' to Castle Folds.

Malham-Littondale: North of Malham, many well-rounded limestone outcrops are found at altitudes of about 400 m a.s.l. (Figures 20, 21, 22). There is general agreement that this area is a mature karst with Sweeting (1966) regarding it as the most evolved area of the Yorkshire Dales karst. In addition to being at higher altitudes the most rounded features, with widely flaring grikes are in massive, thick limestones and usually in sheltered locations.

Locations include around edges of large surface karst *depressions* east of Clapham High Mark, near Back Pasture, and around Lea Gate High Mark (Figures 21, 23), a situation similar to Farleton Knott. Many factors favour these forms having survived severe ice scour in the last glaciation. There is also evidence from cave studies in the area

to support this thesis (Murphy and Lord, 2003). Further north and east, towards Cowside Beck, Cote Gill and Littondale, near Dowkabottom and High Sleets, there are many maturely weathered outcrops, including almost pinnacled clints by the Monk's Path (Figure 20) over 2 m in height on their downslope side, and simple tower-like forms. It is suggested that the tower features (2 to 3 m high) at Dowkabottom, at about 380 m a.s.l., are located above the main Littondale ice-flow. Further evidence for this is provided by pavement on the main valley side with narrow, shallow, rubble-filled grikes at a lower level, about 330 m a.s.l., which appears to have been ice-scoured (Figure 22), lacking rounded clints, towers, wide grikes or grike flares. It is worth bearing in mind Linton's views on nearby Pennine tors in gritstone: "... the present landscape still owes not only its main outlines but also much of its small scale relief to processes that were operating before and between the glacial episodes" (Linton, 1964). The observation applies to neighbouring limestone features as well.

Another simple comparison, of NW England and Derbyshire, also highlights the idea that many features in glaciated areas might be pre-Devensian or earlier in origin. Derbyshire was not



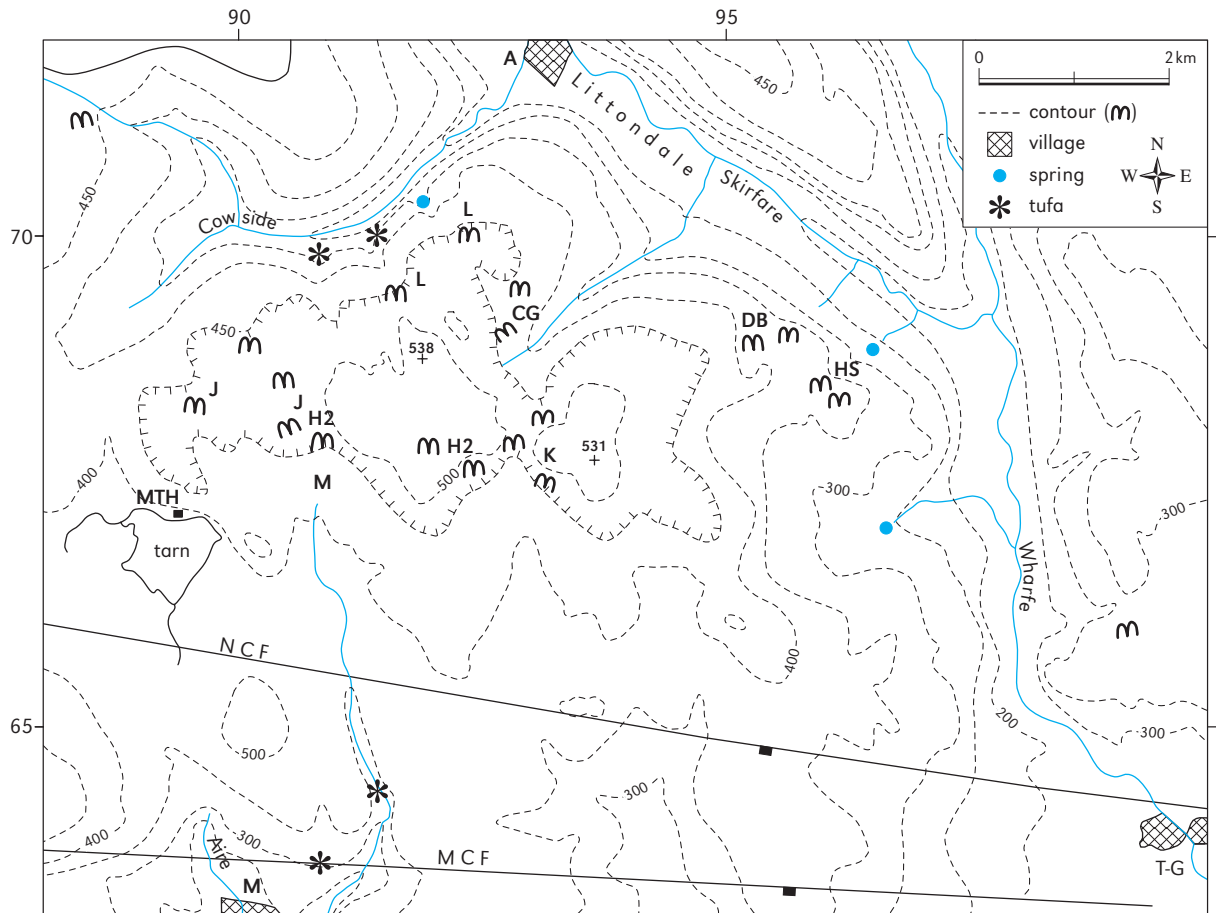


**Figure 23:** Malham-Littondale high country, indicating locations of mature surface outcrops (based on a map by M. E. Marker, 2003). Large, bold m. mature rounded features; CG. Cote Gill; H1. Clapham High Mark; H2. Malham Lea Gate; J. Back Pasture; K. High Mark; L. Monk’s Path; O. Wharfedale; HS. High Sleets; DB. Dowkabottom. Highlighted contour is 450 m; NCF and MCF. North and Mid Craven Faults.

glaciated in the Late Devensian (Waltham et al., 1997), yet outcrops of pavement exist, regarded as palaeokarstic in origin (Walkden, 1972), with characteristics similar to those on outcrops in many glaciated parts of NW England (Figure 24). Their similarity supports the idea that NW England has small glacial survival landforms in limestone outcrops.

### Human activities

Many limestone outcrop areas of the British Isles have suffered direct damage and alteration of

their surface landforms by human activities. This is discussed at length for various sites (Goldie, 1986, 1993), particularly in NW England, but also in Wales, Scotland and Ireland. Two areas considered here demonstrate the effects on grike characteristics and patterns: Wharfedale, Yorkshire, and Hampsfield Fell, Cumbria.

Wharfedale is a well-settled valley, where stone has been taken off the land for building and other purposes for millenia. Limestone has been burnt for lime to add to soil and this process has seen much surface limestone removal in past centuries to be burnt in kilns whose remains dot the landscape. More recently (20<sup>th</sup> century mainly) remov-



**Figure 24:** Rounded pavement edge near Blah (Derbyshire). Width of view is 5.5 m, below.



**Figure 25:** Rounded pavement edge north of Grassington (Wharfedale).

al of solutionally shaped clints for decorative use has had a damaging effect on the appearance of many valley side pavement outcrops. Also, stone removal for walling has occurred, most intensely in the late 18<sup>th</sup> and early 19<sup>th</sup> century Enclosure period. All these activities have left limestone outcrops with various ages of artificially affected forms. The morphometric data for pavements sampled here show moderately shallow grikes, most likely due to these activities (see chapter 9, Table 1). Runnelling also seems immature on apparently suitable outcrops, for example, near Grass Wood, which is consistent with older clint removal. However, there is also very massive mature outcrop that has survived damage (Figure 25) and probably also glacial scour.

placed clints in heaps, much reduced grikes, and larger clints without runnelling are among the effects of relatively recent 20<sup>th</sup> century removal.

## Conclusions

All these cases involve the landform assemblage known as limestone pavement, but their features vary enormously for many reasons. The grikes range from immature slits in surfaces almost as freshly-scoured as those of surfaces near newly-retreated glaciers, to well-rounded limestone blocks left between widening grikes more akin to features observed in semi-arid or mediterranean areas not affected by any Quaternary glacial erosion. The fact that many clints in these areas are so well-eroded that the grike flares merge at the top of the clint begs the question of where the grike finishes. The easy answer is when grikes are truncated by glacial scour or human action, and have an approximately right-angled and or abrupt change of slope at their top, but when there is a gradual grike flare it is not obvious where the turning point between features comes. Degree of roundedness is one measure that could be characterized in this situation to put some sort of quantitative index on the features in order to distinguish them from site to site.

**Table 1:** Clint data at Newbiggin Crags (metres).

	Length	Width	Height/GD
Upper bed (III)	1.6	1.2	1.5
Lower bed (IV)	2.8	1.6	1.5

Hampshire Fell west of Morecambe Bay is distinguished for being subject to the first Limestone Pavement Protection Order (LPO) (Goldie, 1986, 1993) placed on it after extensive removal of clint tops for garden rockery stone. A freshly roughened surface with much small sugary debris, dis-

Obvious visual weathering differences can be

seen between the top limestone layers of different sites. At the Shilin Stone Forest in China these are very sharply runnelled (Waltham, in Gunn, 2004). El Torcal in Spain is moderately runnelled. However, many of the cases here are smooth, rounded and less runnelled than in the aforementioned areas. These different sites have basic features in common in that they have developed their negative landforms, the grikes, along weaknesses in the limestones, and local differences in erosional conditions, both now and in the past, help to ex-

plain detailed differences in the landforms. Lithological variation can bring in the importance of non-solutional processes, and tectonic influences introduce such factors as uplift with some areas experiencing uplift that helps to sustain lengthy periods of karstification by raising base-level. Fundamentally, however, these varied landforms would not exist the way they are without a suitable level of fissuring in the respective limestones, fissuring which is a basic condition for karst development.

# THE KARRENFIELDS OF THE MUOTA VALLEY: TYPE LOCALITIES OF THE MAIN KARREN TYPES AFTER THE NOMENCLATURE BY ALFRED BÖGLI

Michel MONBARON and Andres WILDBERGER

The famous karst specialist Alfred Bögli studied intensively the area of Silberer-Charetalp-Mären (canton of Schwyz, Switzerland) (Figure 1), his favourite terrain for surface geomorphological research. Working on these carbonate rocks of the Helvetic nappes, he classified and defined a nomenclature, still used nowadays (Ginés, 2004), in order to describe the different karrenforms of the “haute montagne calcaire” (a term used by Maire, 1990). Between 1951 and 1987 Bögli published extensively on this topic, with some of his publications still being very influential. We chose to illustrate some of the most characteristic forms of this karstic landscape, paying tribute to Alfred Bögli and remembering his very useful contributions to the field of karst research.

## Geological and climatic introduction

Some of the most extended bare *karrenfields* (“*Karrenfeld*”, a German word meaning ground with karst tracks) of Switzerland (about 50 km<sup>2</sup>) (Bögli, 1987) are located in the southern part of the Muota valley. Within this large surface area several types of karren forms can be found and many of Bögli’s published examples originate from this region (Bögli, 1951-1976).

The whole valley of the Muota river (Figure 2) tectonically belongs to the Helvetic realm (Hantke,

1961). The northern part of the valley consists of the Drusberg nappe (northern Helvetic). The more interesting southern part is shaped within the strata of the Axen nappe s.l. (middle Helvetic). The Jurassic strata of the latter are left in the south, the Cretaceous and Tertiary formations are accumulated by thrusting movements in the northern part of the Axen nappe s.l. In this pile of nappes and slices, the *karstified limestones* of the different nappes are in contact with each other and enlarge the thickness of the karstified series. Therefore, a good prerequisite is given for the existence of long and deep caves (Hölloch: 194.5 km long, 939 m deep; Silberer system: 37.8 km long, 888 m deep; state 2008).

The main karstified limestone formations in the Axen nappe are the Quinten limestone (Malm, Upper Jurassic), the Urgonian limestone (Barmian-Aptian, Lower Cretaceous) and the Seewen limestone (Cenomanian-Coniacian, Upper Cretaceous). In addition, other carbonate formations of lesser importance in the context of karstification occur in this area. The entire stratigraphic column covers strata of Triassic to Palaeogene (besides more or less pure limestones, sandy and siliceous limestones, marls, silty marls, dolo- and sandstones are present).

The mean annual precipitation lies between 2,000 mm in valleys and 3,000 mm on summits (Kirchhofer and Sevruck, 1991). The correspond-

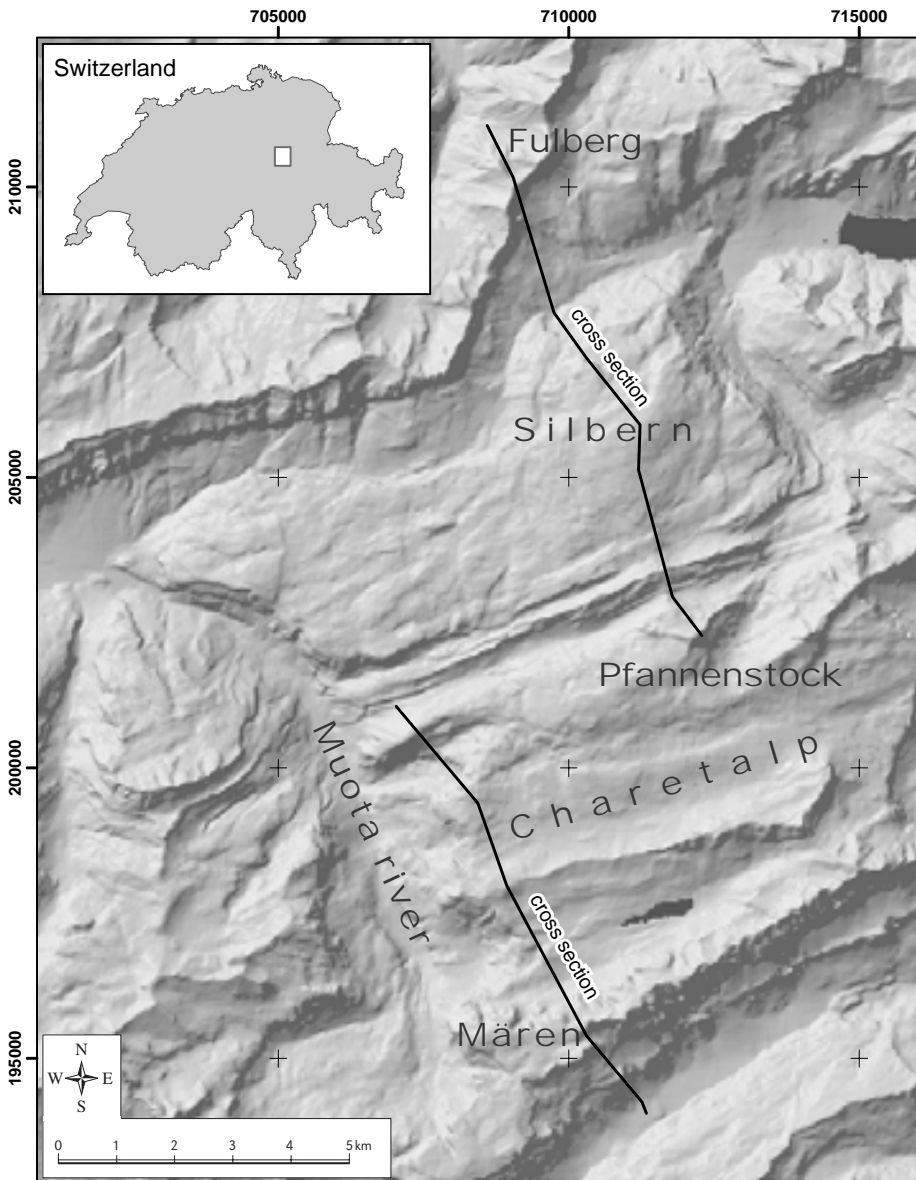


Figure 1: Geographical location of the study area.

ing mean annual temperatures range between 8°C (valley) and -1°C (summits) (Kirchhofer, 1982). A significant part of the precipitations is snow which melts again during spring and summer.

### Nomenclature of the main forms

The karren are the most developed forms of the exokarst in this part of the Helvetic Alps. Table 1 lists the main karrenforms which will be de-

scribed and illustrated in turn below. They are classified by their size and the lithology of the host rock. Most of these forms are contained in the Urgonian limestone formation which is 180 m thick and covers the Silbernen plateau (Figure 3). The Quinten limestone formation (400 m thick) is well represented in the Mären area and has several karstic features, too, which occur less frequently in other carbonate formations. Some of the most spectacular forms of these two areas will be shown below.

## The big karrenfields of the Muotatal area

### Silberer karrenfield

The Silberer (the bare, bright grey rocks give the “silvery mountain” its name) is a flat-topped sum-

mit with an altitude of 2,319 m a.s.l. During the Pleistocene glaciations this top was covered by a glacier which flowed off on all sides of the plateau. The glacier removed loose rock material and left the ground almost bare with a *humocky relief* (in French “*roches moutonnées*”) occurring occasionally. It is now sculpted by Holocene *pavements*.

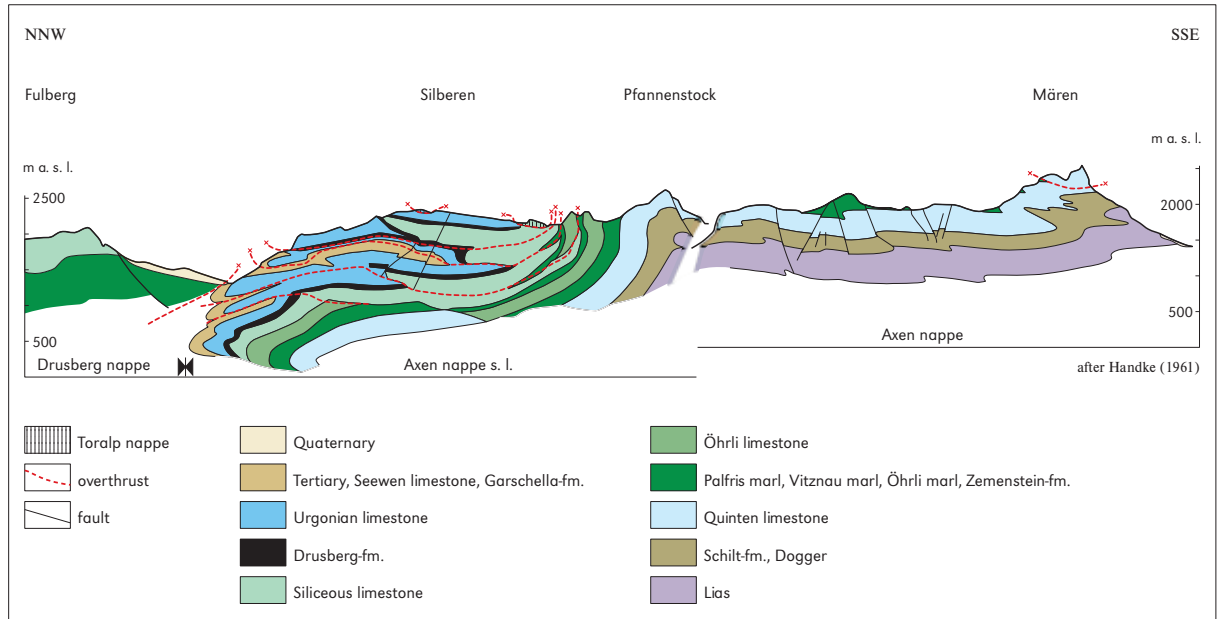


Figure 2: Geological cross-section.

Figure 3: Karrenfield on Urgonian limestone, Silberer plateau. The intensive faulting causes a jig-saw puzzle of karstic (Urgonian and Seewen limestones), semi-karstic (Garschella-fm. p.p.) and non-karstic rocks (Garschella-fm. p.p., Tertiary).



**Table 1:** Different types of exokarst features in the Muotatal area.

Formation	Lithology	Approximative thickness [m]	Macro-scale				Meso- to micro-scale types						
			Schichttreppenkarst / Schichtrippenkarst	Roches moutonnées	Dolines / Uvalas	Karrentische / Karrentables	Rillenkarren / Solution flutes	Kluftkarren / Grikes	Rinnenkarren / Runnels	Mäanderkarren / Meandering runnels	Trittkarren / Heelsteps	Wandkarren / Wall karren	Corrosion pits
Seewen limestone*	Fossiliferous micrite with some argillous flakes, strata often indistinctly developed	50	x	x	x	–	x	•	•	x	x	x	–
Brisi limestone* (Member of the Garschella formation)	Biosparite with quartz–sand (up to 20 %)	5	–	–	x	–	x	•	•	–	–	–	–
Urgonian limestone*	Mainly biosparites and biomicrites, massive limestone or strata often indistinctly developed	180	•	○	x	x	○	○	•	•	•	•	•
Quinten limestone**	Mainly fossiliferous micrite, strata distinctly developed (in the range of decimetres up to 1 metre)	400	○	•	•	•	•	○	•	x	x	x	•

\* Silberer’s karrenfield (1,800 to 2,300 m a.s.l.)

\*\* Mären’s karrenfield (2,200 to 2,400 m a.s.l.)

Relative frequency:

– type not known

• intermediate

x rare / indistinctly developed

○ frequent

The conspicuous *karrenfields* are developed mainly in Urgonian and Seewen limestone at an altitude between 1,800 and 2,300 m a.s.l.

The karren types are determined by the parent



**Figure 4:** Mäanderkarren (meandering karren) on a small slope surface, Urgonian limestone, Silberer plateau. Width of view is 80 cm.

rock material and climate patterns. For the karst of the Muota valley this means, for example, that *rinnenkarren* on Urgonian limestone are rare above 2,000 m a.s.l. but rather widespread below this altitude; just as *rillenkarren* are rare on Seewen limestone but frequent on Urgonian limestone (Table 1).

Below, about 1,800 m a.s.l., rocks are incompletely covered by soil and vegetation, mainly forest. Within this “green karst” the bare limestone is visible only in patches and its karren types are transformed or even absent.

Mäander- and wandkarren are subtypes of rinnenkarren: *mäanderkarren* (Figure 4) are present on flat rocks (slope angles less than about 20°) whereas *wandkarren* can be found on very steep slopes (more than about 70°).

A most typical and frequent microform of this region, the *rillenkarren*, can be observed on the sparitic Urgonian limestones of the Silberer kar-



Figure 5: Small-scale rillenkarren on crests between medium-scale kluftkarren features (Silberer plateau). Width of view is 90 cm, in the middle.

renfield. These karren decorate the crests separating the *grikes* and *solution runnels* (Figure 5). The rillenkarren are more or less perpendicular to the runnels.

*Corrosion pits* are small features spreading on Urgonian limestone of the Silberer region, and although not mentioned by Bögli, they are presented here due to their rather frequent occurrence. The process causing these pits is the oxidation of pyrite in contact with air and water from precipitation. This chemical reaction results in sulphuric acid and minerals like limonite, goethite and haematite. The acid dissolves the limestone locally and leaves behind a hemispherical pit with a diameter of several centimetres. The pits are filled with iron oxides or stay empty if washed out (Figure 6). In cave environments a reaction between sulphuric acid and limestone acts as the source for gypsum crystals (Bögli, 1972).

### The Mären karrenfield

The karren of the Mären plateau are located between 2,200 m and 2,400 m a.s.l.

Essentially, *karren landforms* are developed in the Quinten limestone formation (Malm). As in the Silberer plateau, the area was once covered by

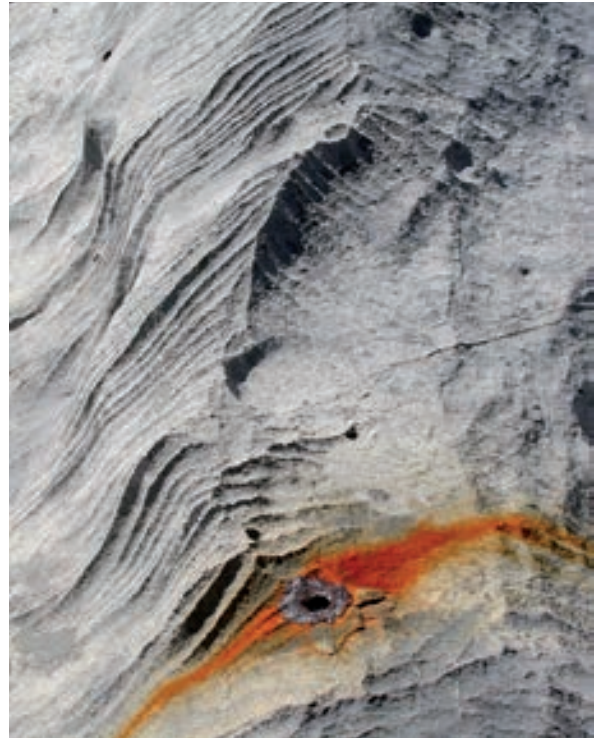


Figure 6: Corrosion pits and rillenkarren on Urgonian limestone, Silberer. In some pits the red-brown minerals limonite / goethite / haematite are still present; in other pits they are removed by rain water (compare empty pits in the right side of the crest). Width of view is 35 cm, below.

Pleistocene glaciers. The polished glacial marks (Figure 7) of the last glaciation (Würm) are still recognizable and soil formations are thin and patchy. Various forms of karren which have been influenced by the main tectonic structures, banking of rocks and the distinct ruggedness of the massif can be found on the Mären plateau. Two typical examples are described below.

The frontal backward erosion of limestone layers due to frost attack (Aubert, 1969) or glacier erosion have resulted in a staircase-like arrangement (*schichttreppenkarst*) (Figures 7 and 8). The Mären plateau is mainly characterized by this particular karstic morphology. A similar form defined by Bögli (1964), the *schichtrippenkarst*, is less frequent.

Smaller typical forms common in the Mären area illustrate the powerful dissolution of the





Figure 7: Witnesses of glacier-polished rocks in the Mären area.



Figure 8: Schichttreppekarst near the small valley of Bockalpele, at the western border of the Mären plateau.

run-off water on the pure micritic limestones of Quinten.

Tectonic fractures can be well observed on the strata surfaces and, due to the present network of these fractures, conclusions about the tectonic stress directions can be made. The cracks are

constantly being enlarged by solution processes resulting in *kluftkarren* or *grikes* which underline even more the diversity of different fracture families (Figure 9).

The second most frequent forms are the *rinnenkarren*, created by runoff on the top and slopes of the



Figure 9: Kluftkarren on Quinten limestone, Mären plateau.



Figure 10: Rinnenkarren features, at the northern border of the Mären plateau.

limestone beds (Figure 10). The result is a network of channels running parallel at the steepest slope.

Both solution forms kluftkarren and rinnenkarren are very common and occur at different spatial scales, that is approximately  $10^{-1}$  to 30 metres.

By means of analysing the *karren tables* (*Karrentische*) (Figure 11) it is possible to determine the dissolution rates of the carbonates during the whole post-glacial period since the last re-

treat of the local glacier – the Tardiglacial, which happened nearly 12,000 years BP. Boulders, left behind over the limestone layers during the last glacial retreat, have preserved the rock surface against solution by rain and snow melt water since then. The height of the limestone pedestal under the boulders represents the average thickness of the dissolved limestone removed during the last twelve thousand years.



Figure 11: Karren tables or Karrentische with pedestal, Mären plateau. Width of view is 15 m in the middle.



Figure 12: Boulder chaos resulting from the dislocation of the staircase front.

Finally, effects of cryoclasty on the limestone could be observed on the bare plateau. Gelifraction has dislocated the blocks, which are piled up in a rocky chaos (Figure 12).

*Dolines* and *uvalas* are less frequent in the Muota region but occur mainly in zones with loose material on the top of karstified rocks (suffosion dolines).

## Conclusions

Alfred Bögli studied and defined typical and widespread *karren forms* of the alpine karst between the upper forest line and the periglacial zone. He tried to explain the different karren types as the result of the different stages of the corrosion strength of water. This attempt, although not fully successful,

can serve as an indicator for unresolved problems as well as a driver for future researches.

Bögli's natural laboratory was situated not far from his home, near Lucerne in Central Switzerland. He was also interested in the phenomenon of endokarst, and hence it is not surprising that he was also engaged in the exploration of the Hölloch Cave in near Silberen, one of the longest cave systems in the world (Bögli, 1970, 1980).

## Acknowledgements

We would like to thank Beat Niederberger for contributing to the overview map and geological cross-section, and Ingo Heinrich for translating the manuscript.

# THE NATURE OF LIMESTONE PAVEMENTS IN THE CENTRAL PART OF THE SOUTHERN KANIN PLATEAU (KANINSKI PODI), WESTERN JULIAN ALPS

Jurij KUNAVER

The aim of this paper is to introduce one of the most significant characteristics of the Kanin Mountains, the *limestone pavements*, found in a variety of forms, according to their origin and evolution. They reflect the relations between the geological structures and the surface as well as the evolution of the mountain karst surface in late Pleistocene and Holocene epoch. Strong traces of glaciation can be found there, as well as an abundance of corrosional forms as the consequences of large amounts of rain and snow (3,400 mm per year); not to speak of Holocene evolution of vegetation and soil that also influenced the development of pavements, at least in lower altitudes. The pavement character of the Kanin plateau and the very common *kotlich* (*kotlič* in Slovene, *snow*

*kettle*, *Schacht-doline*, *Kessel-*, *Karrendoline*, *puit à neige*), normally associated with them, belong therefore to the most important characteristics of the mountain karst surface (Haserodt, 1965; Maire, 1990; Ford and Williams, 1989). For this reason this phenomenon seems to be interesting and justified.

The wider area was partly affected by human impact, e.g. by grazing on the mountain pastures, which is now in strong decline. A great number of human traces date from World War I because of the Austro-Italian front (1916–1918) and, from 1975 on, due to the development of alpine skiing. Human impacts may have also caused the lowering of the forest line in last centuries.

The Kanin Mountains in NW Slovenia (Figure



Figure 1: Geographical location of the Kanin Mts.

1) have become one of the karstologically most investigated high karst mountain range of the Julian Alps in the last ten to fifteen years, not only because of a rich variety of surface karst phenomena but also because of 12 deep shafts with depths from 500 to over 1,500 m and about 100 km of underground channels explored so far. One of the shafts, Vrtiglavica (–643 m), has the world record of a continuous vertical shaft. The investigations of karst geomorphology and hydrology of the mountains are in full progress (Audra, 2000; Kunaver, 1998; Komac, 2001).

Strong karst springs at the foot of the mountain range are the result of abundant precipitation and asymmetry in the underground water discharge between the northern and southern sides of the range. The hypothesis that this mountain range is one of the most characteristic areas of high mountain karst in the Southern Limestone Alps with extremely interesting surface and subterranean karst phenomena was verified by geomorphological and speleological research results (Kunaver, 1973a, b, 1983, 1984, 1991; Pirnat, 2002).

## General geology and geomorphology of the area

The area is extremely rich in pavement surfaces also, compared to some other areas of mountain karst in the Alps, due to the congruence of the bedding planes and the inclination of the surface (a dip slope), both facing south or south-east. This is the basic, distinctive characteristic of the Kanin Mts. The southern slopes of the Kanin Mts are therefore one of the best examples of relief conformity and of structural landforms on a large scale in the Julian Alps. The central part of the mountains of Dachstein in the Northern Austrian limestone Alps, for example, is for the most part completely different due to the total discrepancy between the surface, that slopes towards the north, and the prevailing incidence of strata that is facing south.

According to Buser (1976, 1986a, b), the south-

ern slopes of the Kanin Mts have had a normal stratigraphic evolution from the Upper Trias to the Cretaceous period, following the former view of Kossmat. The bedrock of the mountain range is composed of massive dolomite (Hauptdolomit) of light grey to white colour, which changes upwards into a stratified coarse-grained to micrite dolomite. Such dolomite is found at the bottom of the Možnica and the Krnica valleys. The visible thickness of the dolomite in the Možnica valley is 400 m, and the thickness of Dachstein limestone 1,000–1,200 m, 200 metres of which are made of massive limestone (Buser, 1976). Some areas along the fault lines, in a width of some metres, are dolomitized too.

The dolomite gradually changes upwards into Dachstein limestone. The limestone is stratified and has a typical Loferitic development with a layer's width of 0.2–2 m, rarely up to 10 m. The higher lying strata of Dachstein limestone are formed largely of micrite limestone, while the highest parts of this sequence are composed of massive micrite limestone. Characteristic of this limestone are very clearly visible stromatolitic layers on the contacts of strata, which contain a high proportion of dolomite, being the result of an early diagenetic dolomitization (Ogorelec, 1996). Stromatolitic layers contribute a lot to the strong mechanical disintegration and development of undercuttings and half caves in the subnival zone in the Kanin Mts. The area of dipped slopes in the southern side of the border ridge between Prestreljenik and Visoki Kanin, just along the mountain path, is typical for excellent examples of this sort of mechanical disintegration along the stromatolitic layers.

An important characteristic of Dachstein limestone is also the infillings of syngenetic corrosion hollows and joints with younger, presumably Jurassic material, which additionally makes this limestone similar to that in the Northern Austrian Limestone Alps. In the southern slopes of the Kanin Mts, Buser confirmed and determined the extent of Jurassic and Cretaceous limestones and of other rocks of that age, that are of consider-

able importance for the verification of a synclinal structure of this area. The evolution of these layers varies highly, but they are not very extensive if compared with the Upper Triassic strata (Buser, 1976). In Buser's view, the Bovec basin is the bottom of a large syncline, filled with Cretaceous flysch and hence the Kanin Mts are the northern limb of it. The dip of strata is south-westwards in the western part of the range, eastwards in the eastern part and southwards on Mt. Rombon. This is linked with a bowl-like shape of the syncline. The anticline was later often discontinued as a result of subsequent faulting and thus its axis (east-west) was horizontally shifted.

Besides lithology, fault lines, running either parallel or transversal to the range, also affected the evolution and the present-day shape of landforms and are therefore of great importance. Most often they run in the north, northeast and north-west direction.

To the south of the main W-E ridge with the highest peak of High Kanin (2,585 metres a.s.l.), which divides the northern Italian side from the southern, Slovenian side, there is the main part of the plateau of Kaninski podi, lying about 200-300 m below the ridge, with an area of nearly 10 km<sup>2</sup> that represents the most massive part of the mountain range. From here the plateau sweeps down in steps from the more gentle upper parts below the ridge (between about 2,300 and 2,000 m a.s.l.) to the lower edge of the plateau (between 2,000 and 1,800 m a.s.l.). From there downwards, the inclination of slopes increases to about 22°. The slopes are discontinued by smaller structural or erosional scarps, about six in all. On some of them glacial till was deposited and preserved as patches, which influenced the distribution of surface karst forms (Figure 2).

The slopes are enclosed by narrow side ridges, called *skedenj* (*sing.*), *skednji* (*plur.*) (a local Slovene term for the barn or better, for the hay-rack), extending far down the slopes. According to our investigations, these distinct and slim ridges, resembling giant rock walls, with up to 300 m of relative height and often less than 100 m wide, do not

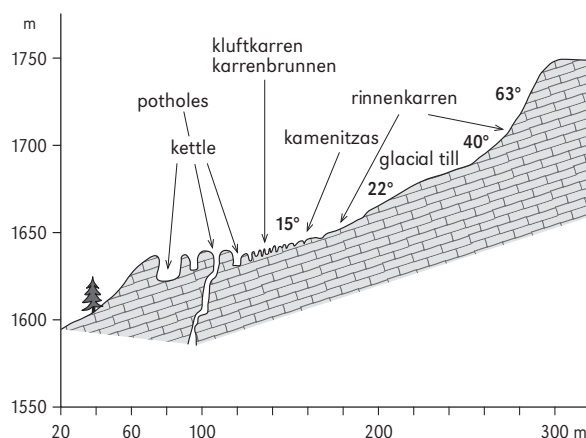


Figure 2: Vertical distribution of karst landforms on inclined glacially abraded limestone pavement on a lower edge of the plateau of Kanin, according to the recession of glacial till in the upper part and concentration of the precipitation water and snow in the lower part, 1,800 metres a.s.l. (after J. Kunaver, 1983).

depend on the fault line system, but are connected with dipped slope strata and are of erosional origin, like other similar features. Their orientation is largely in agreement with the dip of Dachstein limestone strata on the slopes. Evidently the flow of ice had the greatest modifying effect on slopes, especially in their upper parts, also because of reduced space in comparison with a broad accumulation area on the plateau. Thus we can support Linton's claim that the present-day land surface was reduced to a lower elevation than that of the former weathered surface owing to preglacial weathering of bedrock during the ice ages (Linton, 1963). *Skednji* could also be called divides, which corresponds with the term, invented by the same author (Figure 3).

The extensive central part of the southern Kanin high karst plateau or *Kaninski podi* (in Slovene) is not only characterized by extremely well developed limestone pavements with many high alpine glaciokarst landforms, but also with many caves and shafts. The plateau Kaninski podi is characterized also by some long dry valleys of polygenetic origin, which start on the highest part of the plateau and end at an altitude of about



Figure 3: Mali Skedenj, the erosional remnant on the southern Kanin dip slopes of presumably preglacial relief (1,999 m a.s.l.).

1,800 m a.s.l., being more modified by glacial erosion in the lower than in the higher parts. In the central part of the plateau they are over-deepened by greater karst depressions like Veliki Dol, which exceed 700 x 450 m in size and is up to 80 m deep. The original valley depressions could have developed as a result of the older fluvial processes but their present feature is more likely to be only a morphological inheritance, as they were influenced by many phases of non-fluvial development in Quaternary.

### **The Kanin pattern of limestone pavement areas – the interrelation of limestone beds, topographic surface and glacial abrasion**

As pointed out earlier, the geological strata of the Kanin Mts are not only more or less steeply inclined towards the Bovec basin but also all over

the higher places, and so are limestone pavements that occur in different combinations (Figure 4), one above the other like roofing tiles or fish scales. The dip of strata of the plateau Kaninski podi is mostly between 15° and 22°. In some places the dip increases up to 28° or even 30°. The lowest dips were measured in the western part of the plateau, between Mali Skedenj and Veliki Skedenj, particularly below Veliki Skedenj, where the dip was as low as 10°, and in some places even lower. It appears that the strata inclination slowly decreases in the direction towards the border ridge because of the vicinity of an anticline crest. Horizontal strata and corresponding limestone pavements are rarely to be found in the area, except on the plateau Goričica.

In the Julian Alps, the structural relief of limestone pavements primarily occurs in bedrock made up of Dachstein limestone. Evidence of this claim is provided by place names that contain the word “*lašt*” in different combinations, the Slovene

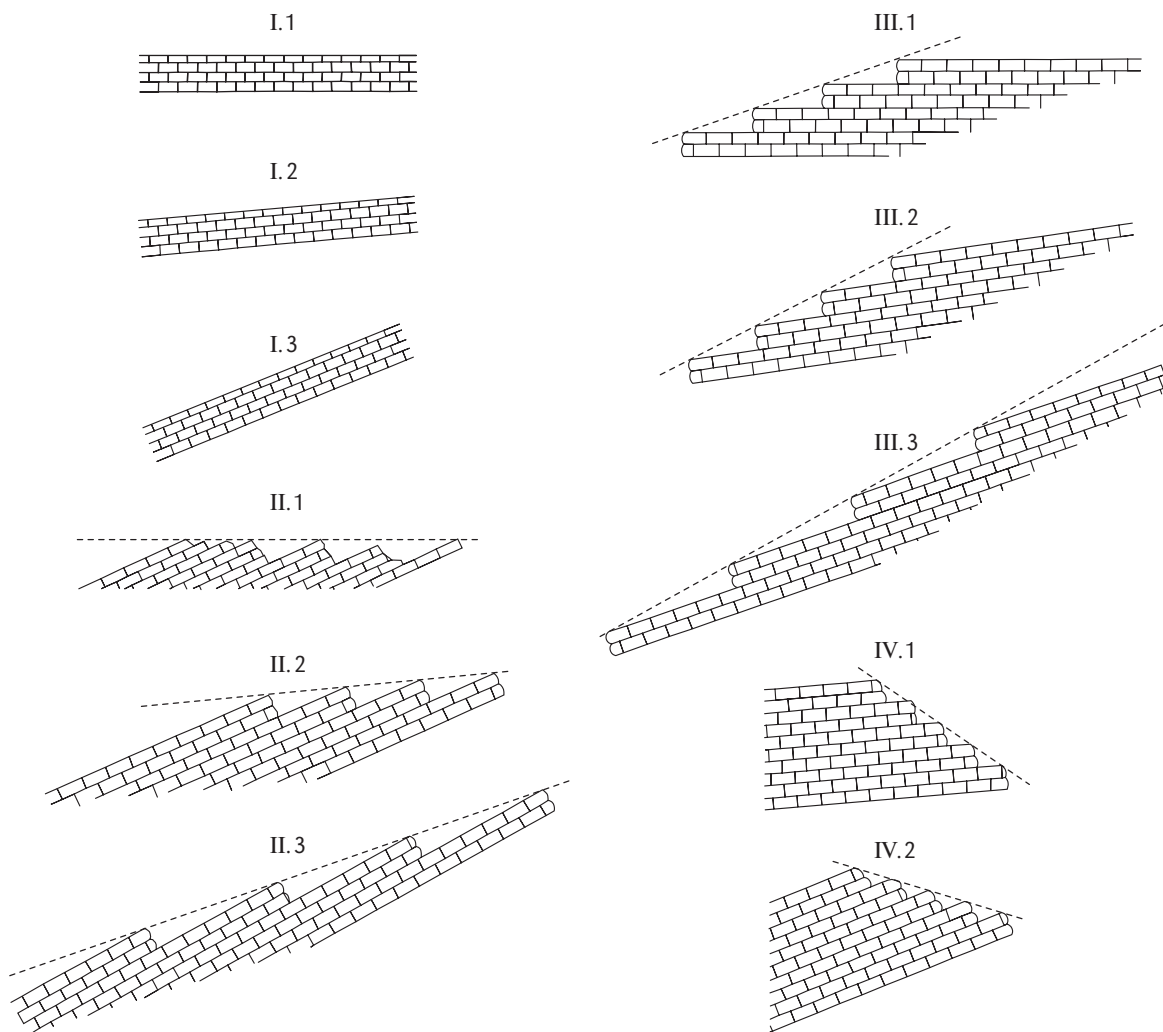


**Figure 4:** The system of limestone pavements of Kaninski podi: I. the even flat and sloping limestone pavements; II. the flat and sloping cuesta-like limestone pavements; III. the flat and sloping stepped limestone pavements; IV. the flat and sloping inverse limestone pavements.

term for limestone pavement (Gams et al., 1973). It is too early to say anything about the resemblance between the Slovene “*lašt, lašti*” (lasht, plur. lash-ti) and “*lastra*”, a name used for the limestone pavements in the area of Dolomites in north Italy.

### The location and the system of limestone pavements

In the central area of the Kanin plateau the pave-

ments are found both at the bottom of dry valleys and some larger depressions, and at the top of rising ground. The first outcrop from the top is the upper plateau just below the main mountain crest, or the highest peak Visoki Kanin, 2,587 m a.s.l. It is followed by the ridge between Visoki and Nizki Talir and both shallow valley depressions Zadnji Dol and Dol Za Mostmi. Extreme pavement areas are Zgornja and Spodnja Osojnica near the mountain hut. South from Veliki Dol there is the next vast area between Gnila Glava and Mali Dol on





Figure 5: The even sloping pavements in the upper part of Kaninski podi (2,300 m a.s.l.).



Figure 6: The even sloping pavements in the central part of Kaninski podi with *kotliči* (2,050 m a.s.l.).

one side, and the ridge Konjc on the other. Smaller and secluded areas of sloping or inclined pavements are situated to the east of the ridge Veliki and Mali Babanski Skedenj, for instance Hudi Lašt, in the upper part of Razor and in the area of Skripi under the upper station of the Kanin cable railway. There are relatively few pavements in the west of Veliki and Mali Babanski Skedenj. Prestreljenik plateau has a fairly pavement-like surface, but it is anthropogenically quite changed. There are pavements in the pass side of Prestreljenik saddle. Pavements on Goričica are not mentioned in this paper, although they also express a very good development. In general, it may be claimed that such a landform characterizes more than half of the plateau area.

The pavements on the Kanin plateau and in the Kanin Mountains in general differ according to: 1) different relation between the incidence of the layers and the inclination of the surface, 2) different assemblages of surface karst forms, 3) different height of pavements above sea level, and 4) different size of the pavements. The height above sea level has been crucial for the intensity of appearing of karst phenomena. The tendency towards the formation of limestone pavements is found in all places where the strata are orientated more or less in the same way as the movement of glacial masses. The strata in the Kanin Mts, however, only rarely lie in the opposite direction, as do those on the lower sides of larger depressions.

## Basic classification of pavements

The starting point for a limestone pavement system in the Kanin Mts was provided by Bögli (1964) and Williams (1966). The latter distinguished between the three most frequent kinds of pavement, the idealized or *flat even pavement*, the *inclined pavement* and the *stepped pavement* (after Sweeting, 1973). At the same time, A. Bögli distinguished only between *Schichttreppen-* and *Schichtrippenkarst*, which means stepped and *cuesta-like pavements* (Bögli, 1978). Both con-

tributions have become a good starting point for further classifications of pavements. Taking the Kanin Mts as an example, we have defined eleven kinds of pavements, divided into four, respectively in two groups, the ones predominantly found on flat surfaces and those found on sloping or inclined surfaces (Kunaver, 1983).

For better differentiation of pavements we suggest the following classification, which uses the degree of congruence between the inclination of the surface and the position of the layers as a criterion. The first group includes pavements with the highest degree of congruence between the surface and geological structure or flat layers of limestone, among others *flat even pavements*, which could also be called stratified plates, and have the simplest form, like Williams' idealized pavements. They can be either entirely flat or more or less inclined (Figure 4.I.1, I.2, I.3). It is difficult to define the border between the more and less inclined pavements, but it has been decided that the boundary-line should be the inclination lower or higher than 10°. Williams believes that the upper limit to find pavements is 45°, but it is hard to agree with the idea that plates with steeper inclination are not possible or they are not considered pavements any more. It is true, however, that there are fewer corrosion forms if the inclination of the surface is steeper (Figures 5, 6).

Another form is the so-called *cuesta-like pavement* (*Schichtrippenkarst*, according to Bögli), which appeared as a result of discordance between the inclinations of the surface and the layers. An average flat surface can be very configured with inclined conformable pavements of different length and shorter unconformable surface, if the layers are inclined for over 10° and more (Figure 4.II.1). *Kotliči* or *Schachtdolines* are very common phenomena on such a surface that can be often found in the area of the upper Kanin plateau. They can be found almost under every short inclined pavement, since there is usually plenty of snow that stays on the surface, while snow-water flows towards the foot of the pavement. Theoretically both surfaces become the same if the inclination



Figure 7: Short cuesta-like pavements on the flat surface of uppermost Kaninski podi plateau with the entrances of *kotliči* and shafts (2,250 m a.s.l.).

of the layer is below 45°, which usually does not happen on Kanin (Figures 7, 8).

The cuesta-like pavements are very common on slopes, normally when the inclination of the surface is smaller than the inclination of the layers. This is typical of the lower and middle parts of the Kanin plateau. Pavements of this kind can also be found on steeper slopes, but only in case of the above-mentioned relation between the surface and the layers. Beside the cuesta-like pavements on flat areas we distinguish more gently sloping and steeper cuesta-like pavements (Figure 4.II.2, II.3). A very strong and clear glacial grinding is typical of the cuesta-like pavements with the front

side of the layer inverted upwards. Holocene corrosion has already lowered the original surface, but the glacial round shaping is still clearly visible (Figure 9).

The third form of pavements is the *stepped pavement*, found in places where the surface is steeper than the inclination of the layers. The first example is a combination of more or less flat layers and an inclined surface, which is relatively rare in the Kanin Mts (Figure 4.III.1). More frequent forms are the stepped pavements on steeper bends and lower steeper parts of the plateaus, where the surface is steeper than the layers. Beside the above-mentioned stepped pavements we know some



**Figure 8:** The irregularly shaped cuesta-like pavements in the central part of Kaninski podi plateau (2,000 m a.s.l.).



**Figure 9:** Glacially abraded upper scarp edge on a limestone pavement (2,300 m a.s.l.). Width of view is 6 m, in the middle.



Figure 10: The stepped limestone pavement on Gorenja Osojnica (2,250 m a.s.l.).



Figure 11: The bottom of initial valley depression of rectangular shape with pavements and kluftkarren, Veliki Graben (2,000 m a.s.l.).

gentle as well as steep stepped pavements (Figures 4.III.2, III.3; 10, 11).

Special attention should be paid to cases, which are quite common, where the orientation of prevalent gradient of relief and that of the dip of strata differs up to 90°. The maximum difference of up to 180° leads to the formation of limestone pavements which are inclined towards the slope or are unconformable. This fourth form is the *inverse or unconformable pavement*, which are not so frequent on the Kanin plateau (Figure 4.IV.1, IV.2). Its presence depends on local topography.

### Dimensions and character of the pavements

The height and frequency of the steps of strata and the size of limestone pavements are an external sign of the extent of relief and structure conformity. On the flat land surface ice moved along the strike, plucking away less resistant upper strata from the surface and the cuesta-like limestone pavements were formed. The direction and the dip of strata in relationship to the direction of ice movement and to the general tendency of relief inclination determine whether limestone pavements are less extensive and steep with high steps of strata or they are wider and longer and steps of the strata between them are lower or even smooth and flat.

The relationship between local relief, surface inclination, and strata orientation is shown by the shape of limestone pavements. Quite common are those with a straight line on the lower side, i.e. along the step of strata, while the upper or exterior side is due to glacial scour of irregular shape. Limestone pavements are often wider and glaciated particularly on the upper side, while they narrow downwards in the shape of a triangle (Figure 8).

The surface corrosion forms on pavements does not differ much from the cases described in the literature. They are mostly of younger, Holocene age. The *napfkarren* or *karrenfussnäpfe* are a common



Figure 12: The lower part of a limestone pavement with Trümmerkarren (2,100 m a.s.l.).



Figure 13: The lower part of a limestone pavement with Hohlkarren (the northern Italian side of Kanin Mts, 1,850 m a.s.l.). Width of view is 1.5 m, below.

phenomenon. The nature of karren depends most often either on the nature of the rock or on the altitude of the location (i.e. the influence of vegetation and soil) (Figures 12, 13). Also older landforms are present, e.g. the *rounded karren* and *tu-*



Figure 14: Rounded opening of a glacially eroded karren; central Kaninski podi plateau (2,050 m a.s.l.). Width of view is 75 cm.

*bular pipes*, which could only be interpreted as the deeper parts of former karren which were eroded by ice (Figure 14).

Also many *kotličiči*, one of predominant surface karst forms of medium size, are mostly of younger origin, although their development (of the biggest ones) has presumably begun even earlier. In particular the *fossil kotličiči*, which are not so rare especially in the area of limestone pavements in consideration, and which contain morainic material, can be reliably claimed as older than the last ice age. The morphogenetic independence and fundamental characteristics of the process and conditions in which *kotličiči* are formed were reported by previous studies of this karst form. Their link with thickly stratified Triassic limestones and with weak lines in rocks (Kunaver, 1976) is their most typical feature (Figure 15).

In terms of intensity of glacial erosion it is possible to recognize a rather strong influence on the surface morphology of the Kanin Mts, as already mentioned. In general, the smaller abrasion landforms were denuded a great deal by the Holocene karst erosion lowering. Therefore the bare rock surface, which clearly looks glacially abraded, e.g. on the scarp edges of limestone strata, looking towards the direction of glacial flow, was in fact



Figure 15: View along the even sloping pavements in the central part of Kaninski podi plateau, with entrances of *kotličiči* (2,050 m a.s.l.). Width of view is 7 m, in the middle.

**Figure 16:** The fossil erosional groove or notch as the effect of the former subglacial water erosion. Lower part of the Kaninski podi plateau (1,900 m a.s.l.).



**Figure 17:** Karrenfield in the northern upper part of Kaninski podi plateau, presumably the remainder of an older karstification because of a weaker glacial erosion in that part (2,250 m a.s.l.). Width of view is 15 m, in the middle.



intensively lowered (at least 20–30 cm), but still shows a typical glacial morphology (Figure 9).

The lowest south-eastern parts of the plateau Kaninski podi are noticeably glacially abraded, especially their lower margin with many *rock drumlins* and steep rock bars or steps, which widen in some places into a smaller rock amphitheatres. They are accompanied by some typical glacial grooves, a sort of shorter rounded furrows, situ-

ated mostly on the edges between less and more steep slopes. Here the frequency of limestone pavements is much smaller.

Smaller forms of subglacial abrasion like grooves, with overhanging lips, too, which have different gradients, even opposite gradients, are often found at the bottom and also on the steep sides of some dry valleys, along with some typical *roches moutonnées* areas. The formation of these



*erosional grooves* or *notches* can be attributed to the subglacial erosion action of glacial water. In many places these subglacial forms remained completely unaffected by corrosion under moraine cover (Figure 16). On such a bedrock surface there shows striation in many places, which has disappeared from the surface exposed to corrosion for a longer time. Glacial mills, which were also searched for by Desio, when he commented on the report by Brazzo about such phenomena north of the border ridge, were not to be found anywhere (Kunaver, 1983). On the other hand, some of the uppermost areas of Kaninski podi plateau are less affected by the glaciation (Figure 17).

## Conclusion

In those sections of land surface that were most affected by glacial erosion, the process would start nearly from a virgin ice scoured surface, while in others the process would be resumed, though under slightly altered conditions. In addition, the till immediately after the last ice age covered a much larger area of the bare rock surface, compared to the present situation, with varying thickness and to an unknown extent. But even larger sections of the plateau remained more or less bare. Thus the rock surface was affected by a process of corrosion gradually and in different periods of the Holocene. This process may be referred to as a phenomenon of successive inclusion of rock surface into the karstification process, which is to be considered for pavements of all sorts.

# KARREN FEATURES IN THE DACHSTEIN MOUNTAIN

Gábor TÓTH

We have carried out annual karren morphological research Austria since 1995. The main purpose of investigations in Dachstein was the study of karren landform assemblages and *karrenfields*. Considering the many factors influencing karren development (slope angle, exposition, vegetation and soil cover, flow characteristics, solvent quantity, precipitation), it is easy to understand that the landforms of karren terrains show several idiosyncrasies in various locations. Accordingly, we examined forms as follow: surfaces of the same slope as well as surfaces characterized by a different kind of exposure, namely, small dipping surfaces bordered by cracks, steep wall karren outcrops, surfaces water-supplied from vegetation, covered terrains, and karren forms near a glacier.

Another part of our measurements comprised the analysis of single forms. We especially emphasized *meandering karren*, *trittkarren* (heel-print karren) and the different types of *rillenkarren* (solution flutes) and *rinnenkarren* (solution runnels).

## Geological survey

The Northern Calcareous Alps consist of Triassic, Jurassic and Cretaceous limestones, Upper Triassic Dachstein limestone being the most remarkable rock regarding karren landforms. The Middle Triassic dolomite appears in the southern wall of

Dachstein mountain only. The most extensive of these formations is the Upper Triassic Dachstein limestone that achieves 1,500 m thickness in the Dachstein mountains. It is made up of two types: the bedded Dachstein limestone and the unbedded fracture-traversed limestone.

The Triassic rocks are covered partially only by small-thickness Jurassic limestone, the age of which is Upper Malm. Small amounts of Cretaceous rocks are also present, while Lower Cretaceous is totally absent. From the Upper Cretaceous are found sandstone, conglomerate and marls.

According to tectonical history, several main units can be distinguished: the Dachstein massif which bends the Hallstatt nappe, and the thrust sheet bordering the Dachstein mountain from the south. The karstic forms are mainly represented by the Dachstein massif, which is broken up along fractures. The dislocated blocks induce significant relief energy.

## Typical karren terrains in the Northern Calcareous Alps

Karren morphological research was accomplished in several terrains of the Dachstein and Totes Gebirge mountains.

Complex examinations were performed with morphometrical methods on the Dachstein pla-

teau near the Krippenstein peak at the intersection of 661 and 662 pathways (Figure 1). The range of altitude on the adjacent peaks (about 2,000 m in height) encloses the main karstified internal terrains of the plateau. In the surrounding environment four kinds of forms can be recognized:

- older and large-sized *paleodolines* that are considerably transformed by the ice and in which lakes also may occur (Lake Däumel);
- the whole area is characterized by young shafts produced by active karstification;

- the most high altitude forms are the elevations at the edge of the plateau (Krippenstein);
- the fourth outstanding forms are the bedding-plane terrains of various size.

Young karren landforms can be found in the vicinity of the Hallstatt-glacier where the exact date of the ice recession is known. Not far from this place, under the Simony house, we measured the different intensity of karren denudation on the bed-escarpments (cuesta) of several *stepped pavement karst* (schichttreppenkarst) locations.

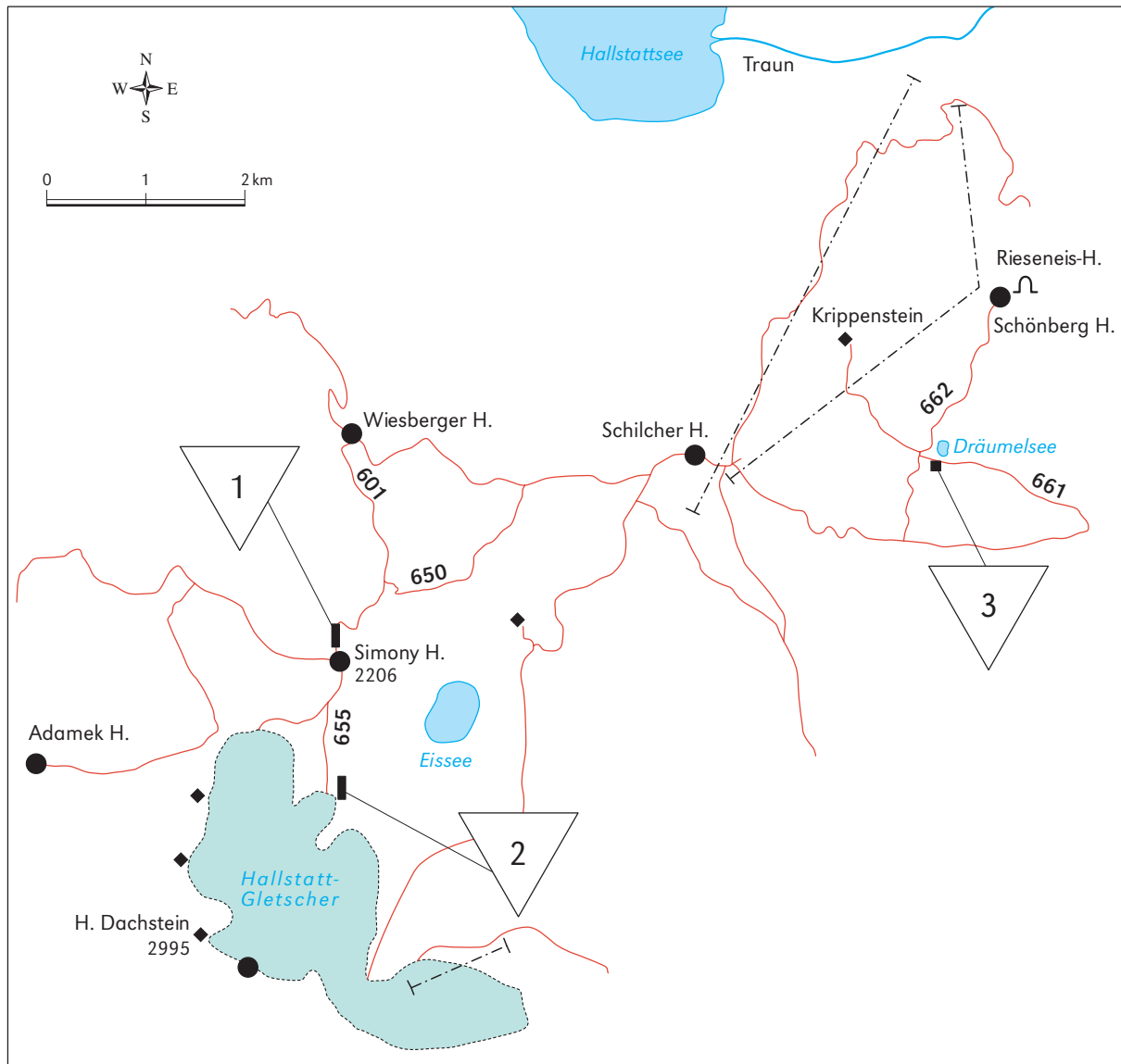


Figure 1: Research areas in Dachstein. 1. schichttreppenkarst under the Simony house; 2. foreground of the Hallstatt-glacier; 3. zonal and local karren assemblages near Krippenstein peak.

The terrains selected for the mapping in Totes Gebirge are aligned near the Scheibling peak along the 230 Path. Here the chosen sites have karren developed on bedding-plane surfaces corresponding to former cirques or slightly dipping terrace plateaus in the side of glacial valleys. Their surfaces are almost impassable due to vertical karst forms and appear dissected into smaller parts by *grikes* (kluftkarren).

Several microforms of a karren location similar to the above mentioned area were examined. The researched area can be found under Widerkar peak, at an altitude of 1,800 metres, on the incline of a glacier valley, which is without any outlet, draining as an independent karstic entity, and separated into smaller parts along fissures and cracks (Veress and Tóth, 2001).

## Research methods

A useful method was mapping through a square grid, which provides suitable documentation for middle-sized and larger karren surfaces. The basic principle of this method is to cover the chosen area with a horizontal, suitably meshed net, and then determine the distance of points of forms compared to the points of the net. By using this procedure, maps on the scales of 1:10, 1:20 and 1:100 have been made, applying 10, 20 and 50 centimetre-distanced nets. The largest mapped area (20 x 25 metres = 500 m<sup>2</sup>) was surveyed next to the Widerkar peak of Totes Gebirge in Austria.

Using surveying instruments, contoured topographical maps of larger karren forms have also been made (Veress et al., 1995). This method seems to be the most suitable for mapping single, several metres long and wide troughs.

The basic investigation method referring to the morphogenetics of karren landforms was to make a transect on selected profiles (Veress et al., 2001a). We determined on the transects the type of each karren form occurring along a spread band-chain, measuring its width, depth and direction and the slope angle and direction of the terrain.

Table 1: Specific solution and density of karren forms. \*altitude on map; S. s. specific solution, total width of the karren forms on 1 metre; density, occurrences of each karren feature on 1 metre; T: Totes-Gebirge; D: Dachstein.

Site code	Surface		Grikes		Network karren		Karren wells and karren pipes		Runnels		Kamenitzas		Trittkarren		Total	
	Height	Slope angle	No.	S.s. (cm/m)	Density (No/m)	S.s. (cm/m)	Density (No/m)	S.s. (cm/m)	Density (No/m)	S.s. (cm/m)	Density (No/m)	S.s. (cm/m)	Density (No/m)	S.s. (cm/m)	Density (No/m)	S.s. (cm/m)
T4	1800–1900*	10°	27	2.45	0.16	–	2.78	0.08	25.47	1.55	0.12	8.00	5.27	0.29	43.96	2.20
T5	1800–1900*	15°	44	–	–	–	0.80	0.04	31.64	1.64	–	–	27.0	0.08	33.52	1.76
T3	1900–2000*	20°	15	13.89	1.67	–	–	–	13.22	0.67	–	–	–	–	27.11	1.78
T2	1900–2000*	30°	39	2.08	0.19	–	5.33	0.24	15.47	1.04	–	–	3.68	0.38	26.56	1.84
T1	1900–2000*	31°	27	4.93	0.64	–	5.00	0.29	15.64	1.00	–	–	–	–	25.57	1.93
D1/1	1630		35	5.81	0.13	0.81	0.68	0.04	21.50	1.09	–	–	0.81	0.18	29.63	1.59
D11/1	1820	17°	31	1.85	0.20	–	2.75	0.20	20.75	1.15	–	–	–	–	25.35	1.55
D111/1	2051	21°	35	4.44	0.40	–	–	–	15.85	0.77	0.11	1.29	–	–	21.58	1.30

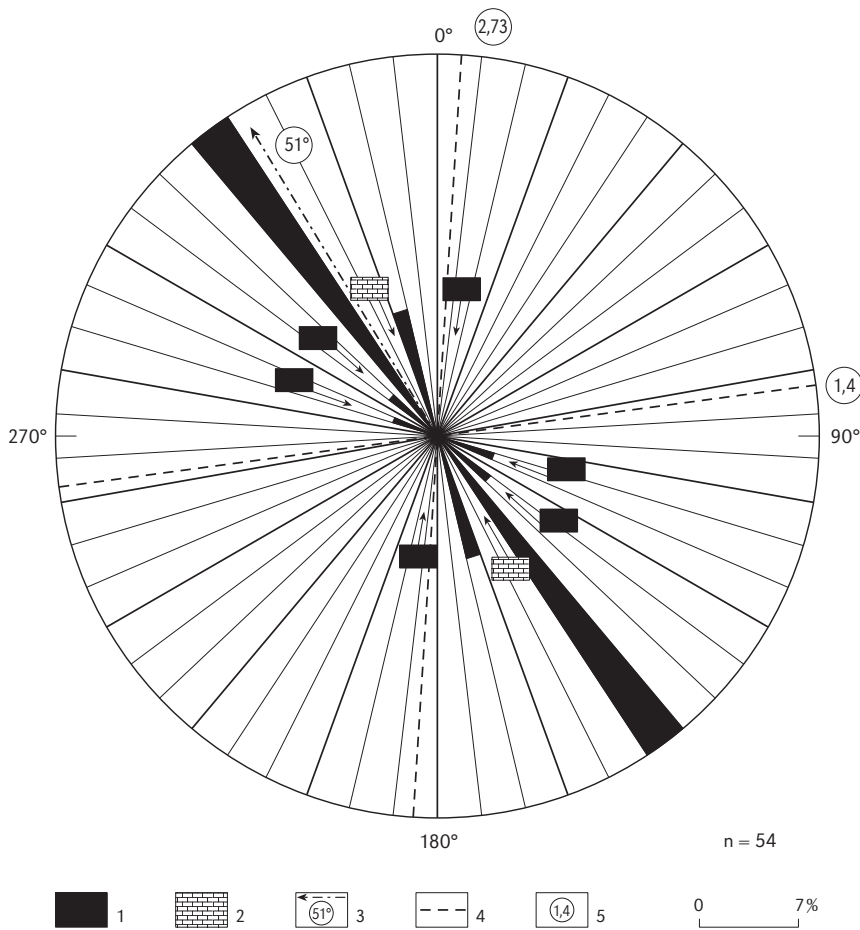


**Figure 2:** Directional dispersion of the karren features along D IV/1 transect (mountain pine zone, Dachstein). 1. wall karren; 2. karren wells and karren pipes; 3. slope direction with the angle of gradient; 4. strike direction; 5. density of fractures (occurrence per 10 centimetres).

The lengths of each transect were 15–25 metres, depending on the size of the measured outcrop. Analysing the data, several specific and global parameters can be determined. In this manner the value of specific karren dissolution can be estimated by dividing the whole widths of the karren features along the section by the length of the section (Table 1, Figures 2, 3).

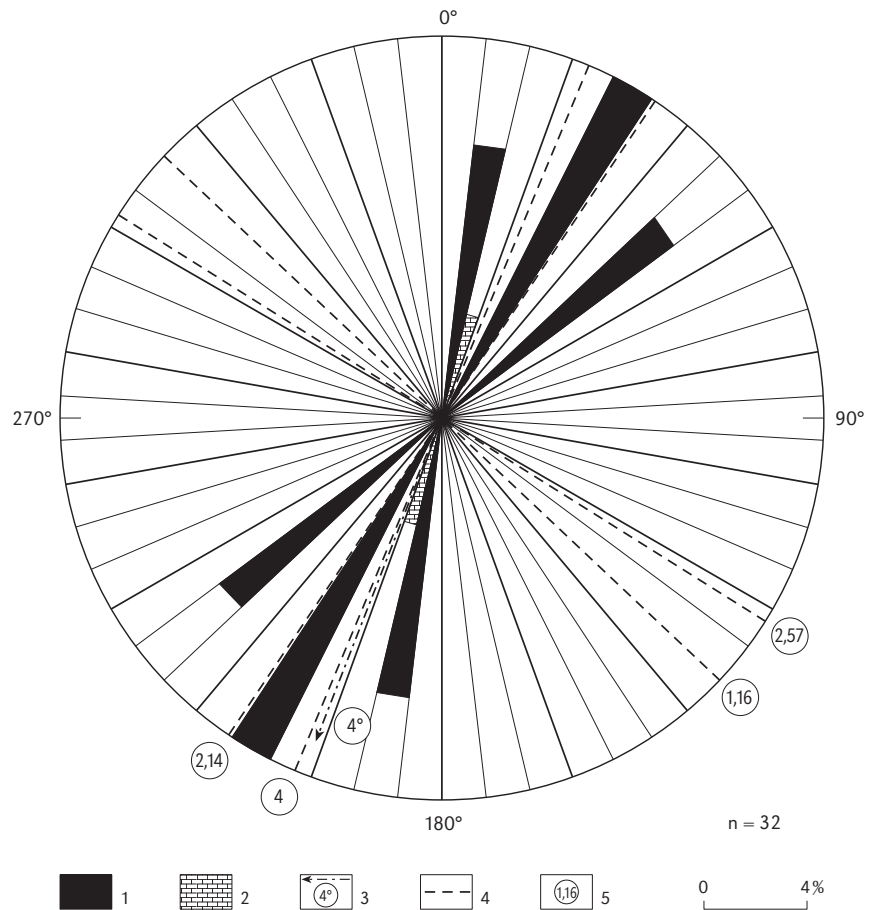
### Morphologic outline

The karren landforms of Dachstein are surveyed principally from the view point of karren landform assemblages.

Glacial influence and intensive karstification determine the actual landforms of Dachstein. After M. Hartlieb the karstic phenomena fall

into two levels. At the lower level between 1,400 and 1,800 metres a.s.l. cavernous forms are typical, whereas at the upper level between 1,800 and 2,000 metres a.s.l. karrenfields are dominant (Hartlieb, 1999). According to our own examinations, the different types of karren forms occur in a wider altitude interval, modifying the two karren zones mentioned above. As the formations of the two zones extend beyond their limits, it is more useful to classify the forms by their genetics. The whole karstic landforms of Dachstein can be gathered into three general groups: subsurface forms, large superficial karst landforms and smaller karstic forms, namely the karren features. As our examinations have been focussed on the small-scale morphology of the mountain, hence the karren landforms of the mountain are being presented (Figure 4).

**Figure 3:** Directional dispersion of the karren features along H III/2 transect (mountain pine zone, Dachstein). 1. grikes (kluftkarren); 2. karren wells and karren pipes; 3. slope direction with the angle of gradient; 4. strike direction; 5. density of fractures (occurrence per 10 centimetres).



Karren features are basically divided into three groups, especially in the case of gentle dip and suitable slope length. In the upper zone of the karrenfields the elementary, embryonic stage is shown, represented by variable sized microforms. Solution flutes (rillenkarren) start at the upper edge of the slope and are characterized by U-shaped cross sections. Below this area *solution levels* (ausgleichsflächen) can be found, which serve as the feeding area for the rinnenkarren (solution runnels) located in the middle zone. The most general forms of the middle zone are single solution runnels, as well as meandering karren, *kamenitzas* and heel-print karren. On the lower part of the slope *karren wells* (karrenröhren), karren shafts and fissures drain off the solvent water. In this way, it can be demonstrated that the typical high mountain karren in the Dachstein outcrops

is characterized by a bedding-plane catchment at the top, a water transmission in the middle and a water drainage towards the bottom.

Karren forms - integrated as *karren assemblages* - are classified into two separable groups based on the stratigraphic position of the surfaces. The first group consists of the less steeply dipping bedding planes and is characterized by longitudinal and circular forms. The second group contains the *wall karren* (only longitudinal forms) developed on the steeply dipping beds. If structural benches (cuestas) have been created by glacial erosion, the whole landform complex of the area is called stepped (or staircase) pavement karst (schichttreppenkarst).

By investigating the surfaces near the peak of Krippenstein we found out coalescent circular forms could develop into longitudinal ones. On the other hand, the different karren features (run-



Figure 4: Karrenfields in Dachstein.

nels, trittkarren, grikes and karren wells) strongly influence each other's evolution. Several trittkarren (heel-print karren), being placed above each other, could frequently develop into downward runnels and could serve as their catchment area. Similarly, circular forms may change into longitudinal forms when small karren wells and pipes join to develop grikes.

Investigations performed at several levels show that the degree of the surface dissolution depends on the altitude and slope angle of the terrain. The amount of dissolution is strikingly high on the gently dipping terrains with southern exposure and on the karren surfaces above 2,000 metres a.s.l. In the latter case one possible reason for intensive corrosion is the thickly accumulated melting snow, which guarantees long-lasting dissolution.

## Juvenile karrenfields in Dachstein

Juvenile karren development is characteristic of the areas where the ice receded not long ago. In the glacier foregrounds *elementary karren* forms appear, most of them being preformed by glacial striae. The first forms to appear are rillenkarren

and trittkarren. Trittkarren evolve on the opposite sides of the roches moutonnées, where glacial striae do not influence the water flow.

The measurements at the ice-free base of the Hallstatt-glacier produced surprising results. Knowing the recession rate of ice cover it was possible to define the speed of evolution of the karren. Our examinations considered the elementary karren forms evolved during the recess of ice cover (Figure 5). The common characteristic feature of these forms is that their sizes and frequencies gradually increase with increasing distance from the glacier (Veress et al., 2001b).

According to the dates marked at the valley bottom, some small-sized solution runnels (Figure 6) evolve after some years, because their evolution process is strongly promoted by the glacier striae. The evolution period of primitive, extremely shallow kamenitzas is seven years, the first trittkarren can be established after 23 years.

## Schichttreppenkarst in Dachstein

Stepped pavement karsts (schichttreppenkarst) stand out among the most spectacular terrains

**Figure 5:** Juvenile karren-fields surrounding the ice-free bottom of the Hallstatt-glacier.



**Figure 6:** Juvenile karren forms at the ice-free bottom of the Hallstatt-glacier. Width of view is 2 m, below.



with karren surfaces; their characteristics were described first by Bögli (1964). This kind of glaciokarstic complex form evolves on horizontal or gently inclined well-bedded limestone during glacial and later solutional denudation. The two parts of the schichttreppenkarst are the ice-rounded scarp (the more abrupt and tilted side of the bed) and the horizontal bedding plane. After

the shrinking of the ice, began the formation of karren features on the ice-prepared gently inclined bedding planes and vertical scarps promoted by glacial striae and fissures beneath the glacier. Such schichttreppenkarst terrain can be found in Dachstein near Moderstein and under the Simony house. It is worth mentioning that the temporal relationship between the dissolution and the gla-





Figure 7: Local form complex with a small karren pipe.



Figure 8: Local form complex with trittkarren (heel-print karren). Width of view is 50 cm, in the middle.

cial erosion is not yet explained. It is well known that dissolution may occur also on ice-covered terrain where the ice does not continuously touch the surface of the rock (the air renders the water aggressive). However, these are isolated terrains, some parts of which are denuded by glacial erosion in their early stage. The wall karren are the main forms over the scarps. The diameter of their U-shaped cross-section is 1–5 cm and their length ranges from 1 to 5 m. Advanced forms can be found densely packed within some centimetre distance in the foreground of the Simony house.

The 5°–15° slope angle makes various landforms of bedding planes possible, the most characteristic of which are trittkarren, kamenitzas and meandering karren. The important peculiarity of the bedding planes is that they are frequently separat-

ed into independent karren surfaces (*units*) along grikes which are not interconnected hydrologically. Also snow plays an important role in the development of the schichttreppenkarst. The snow accumulates at the vertical and horizontal adjustments of the structural bench (*cuesta*) causing a slow and long-lasting dissolution, especially when the flat surface under the structural bench dips towards the wall above it. In this case a zone will develop at the border of the horizontal and vertical part characterized with karren wells or *shafts*.

### Karren complex forms in Dachstein

The karren landscapes constitute *karren complex* forms (or karren assemblages) that one can clas-

sify by several aspects (lithological, biogeographical, climatical). By our investigations, in the Dachstein we established three morphogenetic types of terrains: moderately dipping karren areas, karren zones found on terrains of steeper dipping and karren complex forms developed on structural bench terrains. Each of them is associated to a well-distinguishable kind of surface development.

### Gently dipping local complex forms

These karren complex forms usually develop on inclines of less than  $10^\circ$  and vary morphologically and hydrologically.

Other important phenomenon is that their water-course does not cross over their margins. The water is drained into the depth by shafts and karren wells while their boundaries are ridges and grikes. Their size is fairly variable, ranging from a few  $m^2$  to  $50\text{--}60 m^2$ .

The most frequent features of these local karren assemblages are rillenkarrren, rinnenkarrren, *karren pipes* (Figure 7), karren wells and trittkarrren (Figures 8, 9). In the course of their development, the karren areas may merge into each other and expand, respectively (Tóth, 2003).

### Zonal karren complex forms

These result from normal karren evolution on inclines of  $10^\circ\text{--}60^\circ$  dipping. Their size ranges between  $50$  and  $300\text{--}400 m^2$  (Figure 10). The localization of the several karren forms on the incline varies with the flow features. The rillenkarrren are located at the top and their evolution downwards is related to sheet water flow when the solution level (*ausgleichsfläche*) appears at their bottom, the solutional development of which is not yet clarified. By one of the theories, the solvent is saturated here and no more solvent action is possible. In contrast, however, the solution level is degraded with the surface. By another hypothesis, the degrading of the terrains takes place resulting



Figure 9: Local form complex with concave trittkarrren (heel-print karren).

in the formation of flat surfaces (Ford and Williams, 1989). The solution of small quantities is explained by the falling precipitation and the laminar flow. The formation of the flat surface is also caused by the long-lasting solvent process of small extent because of the thaw of the accumulated snow. The water arriving from the solution level feeds the zone characterized by solution runnels (rinnenkarrren), meandering karren and trittkarrren underneath. Here the flow divides into water branches and is always turbulent.

The zone located at the lower part of the slope has the most varied and well developed form complexes. Mixture corrosion may result in intensive dissolution at the confluence of the water branches, explaining the frequent gradual change of the



Figure 10: Zonal karren surface near the Krippenstein peak.

forms into each other. The main forms of this are the mature rinnenkarren (solution runnels).

Finally, the infiltration zone close to the surface consists of grikes, frequently composed by alignments of small pipes, karren wells and shafts. The water flow is strongly delimited by the rinnenkarren systems placed above this zone. The solution shafts and karren wells drain the water away at the terminations of the runnels, while their accretion results in the formation of grikes perpendicular to the slope direction.

#### Different dipping non-local complex forms

These arise in karren terrains consisting of steeper scarps and gently sloping bedding planes. These karren structural bench terrains correspond to the before-mentioned stepped pavement karst (schichttreppenkarst).

# GLACIOKARST LANDFORMS OF THE LOWER ADIGE AND SARCA VALLEYS

Ugo SAURO

In the lower Adige valley and in the area of the Garda Lake (Italian Southern Alps) many typical glaciokarst landscapes are recognisable. The finest is probably that of Canale, where a rock bench, abraded during the late Pleistocene by the glacial

tongue of Adige, has complex assemblages of karren (Figure 1). Among the most common forms are *kamenitzas*, distinguishable in three main subtypes: *solution cups*, *solution pans*, and *solution pans nested inside runnels*. The karren devel-



Figure 1: Detail of the glaciokarst rocky landscape of Canale in the southern Adige valley.



**Figure 2:** A relatively deep solution cup that holds water almost permanently. There are two outlets: the one to the left is fed by the overflowing water, while that to the right is more recent and is fed by water through a fissure.



**Figure 3:** A solution pan with a well developed outlet with small meanders nested inside.



**Figure 4:** A large runnel with solution pans nested inside. The sides of the pans are characterized by different degrees of edge overhang.

oped inside the rocky mass like the *minute-shafts* and the *grikes* seem to evolve by a speleogenetical process from an inner network of cavities towards outside.

## Description of the karren features

In the lower Adige valley and Sarca valley of Italian Southern Alps, some typical glaciokarst terrains are recognisable. They are worthy of note both for their geographical position and for the variety of karren landforms developed during the late Pleistocene and Holocene. These landforms are situated at very low altitudes (between 100 and 300 m above sea level) and relatively low latitudes (between 45°30' and 46°00'N), and are characterized by a sub-mediterranean vegetation that is influenced by the extensive rock outcrops exposed to solar radiation.

Probably the finest karst landscape is that situated on the northern side of the village of Canale in the lower right slope of the Adige valley, about 150–200 m a.s.l., developed on a massive lens of an oolitic limestone of Lower Jurassic age, and shaped by the glacial tongue to form a rock bench (Corrà, 1972; Sauro, 1973a; Perna and Sauro, 1978). Abrasion by the glacial tongue, and in particular by the lodgement debris at the base of the glacier, shaped the bedrock into rounded knobs elongated in the direction of ice flow (*Rundhöckerkarst*, in the German literature). Into these glacially moulded surfaces, solution has sculptured a large variety of karren, which are expressions of the different microenvironments and hydrological processes.

Analysis of these landforms reveals the style and the progression of karst morphogenesis in a massive limestone. Kamenitzas (solution basins) are very well developed. These basins were the first karst features to develop after the retreat of the glacier. Most of the basins are cut into the higher parts of elongated rock ridges. The variability of these features is substantial: diameters range from a few centimetres to some metres, and

depths between a few millimetres and some decimetres. It is possible to distinguish at least three main morphological types: solution cups, single solution pans, and chains of solution pans nested inside large runnels.

Solution cups (Figure 2) are basins with surface openings smaller than their floors, therefore having overhanging sides; their depths are relatively large, and their floors are flat and horizontal.

Solution pans (Figure 3) are shallower kamenitzas, with greater width/depth ratios; the larger forms are also more elongated. Each solution cup and solution pan has a *solution runnel* as its outlet.

The solution pans organised in chains and nested inside large runnels are deeper forms, with varying degrees of overhanging rims (Figure 4) within their profiles that are an expression of cyclic evolution (Sauro, 1973b).

The evolution of each different type of kamenitza is probably controlled by the relative size of the hydrographic basin that feeds the hollow. The cups have very small basins, while the solution pans have relatively larger basins. Evaporation of accumulated rainwater run-off may cause the deposition of thin layers of silt on the floors of the hollows. If the catchment is small, the layer of silt is very thin, and probably does not match the solutional deepening of the kamenitza, which therefore evolves into a deep cup profile. If the catchment is larger, the layer of silt becomes thicker and the solutional effort develops lateral widening rather than deepening. Within the solution pans that are nested as chains inside a large runnel, the turbulence of the run-off flow during rainstorms is able to remove the silt layer, and therefore the landform may deepen.

Water is present for most of the time in the solution cups, while the solution pans are normally empty of water except during and immediately after rainfall events. So the environment in the two types of solution basins also evolves differently with respect to biological colonization of the rock surface.

After periods of rain, some circular patches of the bare rock surface remain wet for longer pe-



**Figure 5:** A large, inactive kamenitza developed before the last episode of glacial abrasion when the original form was partly eroded, especially on its right side.

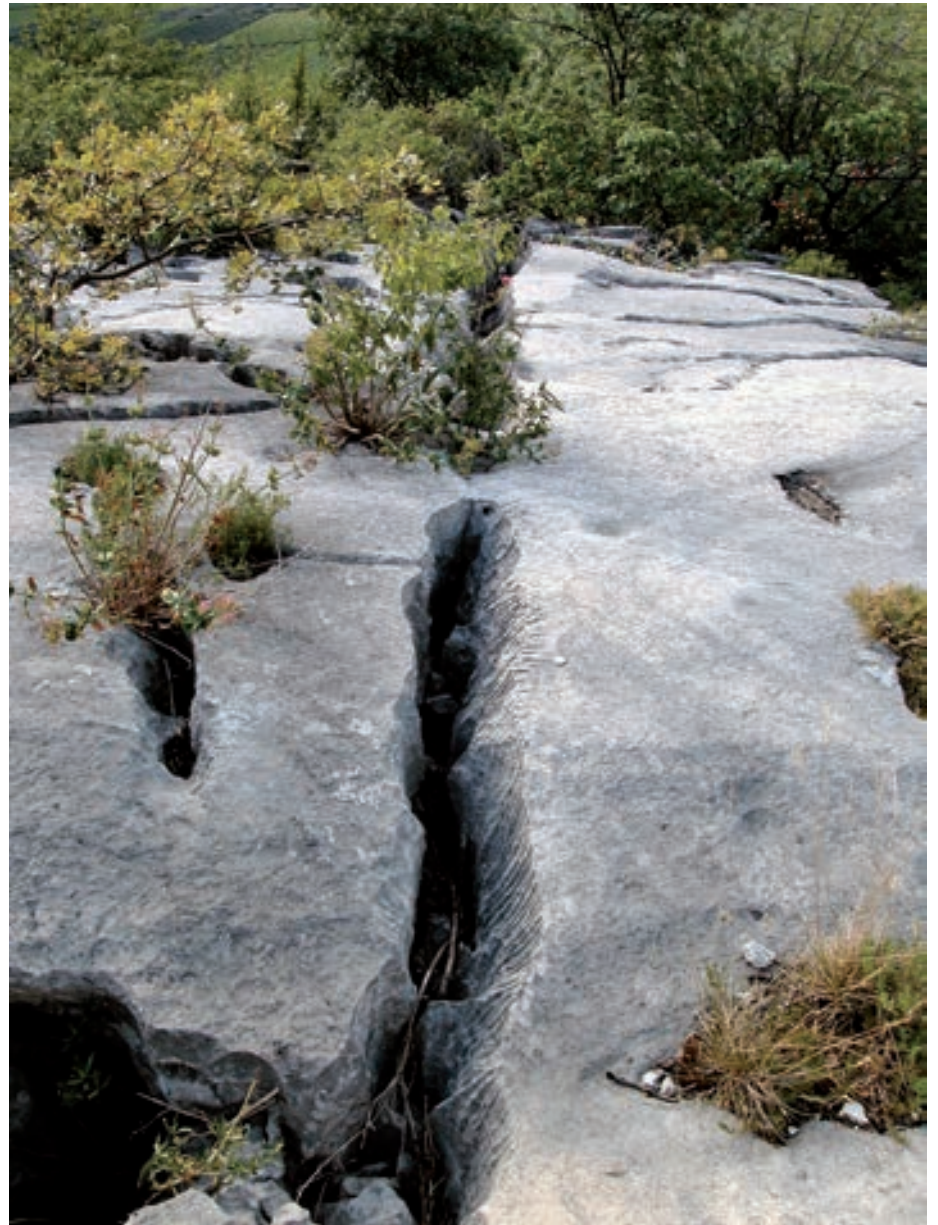
roids than do the surrounding surfaces. These patches appear to be on rock of a higher porosity, probably a consequence of some type of biological colonization. This biological invasion predisposes the rock to the development of kamenitzas, which seem to begin to develop like virtual forms within the rock before becoming real depressions.

Some of the largest solution pans (the largest is 4.5 m long), which are now completely inactive (Figure 5), seem to have evolved in two phases of karstic dissolution separated by a glacier ad-

vance into the Adige valley. They have been partly abraded by glacial erosion.

Many of the solution runnels, that originated as outlets from the solution cups and pans, are characterized by sequences of small depressions similar to heelprint karren; these forms are also similar to the runnels starting from soil patches (Humusrinnenkarren, in the German literature). On the relatively smoothed and gently rounded glaciokarst knobs, rillenkarren or solution rills are not well developed. In particular, they are

**Figure 6:** Grikes and minute-shafts that are progressively subdividing the rock surface into isolated blocks.



absent or scarce where extensive and continuous, gently sloping surfaces exist. On the contrary, they are abundant where the rock surface is partially dissected by grikes (*kluftkarren*), where extensive sheet flow of water cannot develop during rainstorms.

Minute-shafts, *kluftkarren* grikes and *bedding plane fissures* are structurally controlled features that have developed within the rock mass. In some areas, they are noticeably abundant and subdivide the rock into isolated blocks, creating distinctive,

bare, fissured limestone pavements within the karst terrains (Figure 6). In the Canale area, the oolitic limestone is massive and lacks visible bedding planes and fracture discontinuities. However, discontinuities do exist, and are revealed by development of the structurally controlled karren. These karren forms develop in the more porous parts of the rock, and not as a consequence of rainfall run-off flowing directly into holes. It is evident that most of these cavities are not open from the outer surface towards the inside, but from an



internal network of cavities towards outside. An important role in their development is probably played by the air circulation inside the cavities that is induced by the diurnal cycle of solar radiation acting as a heat pump, and by the water condensation associated with this circulation.

In areas near the Canale karst, there are many

other interesting glaciokarst landscapes. Of particular note, for both their karren assemblages and their scenic positions, are those situated north of the Garda lake, including the limestone pavements developed on a flatiron of Eocene limestone near the village of Nago, and the Calodri ridge north of the town of Arco.

# KARREN IN PATAGONIA, A NATURAL LABORATORY FOR HYDROAEOLIAN DISSOLUTION

Richard MAIRE, Stéphane JAILLET and Fabien HOBLÉA

The unusually well developed *hydroaeolian karren* landforms of the Chilean Patagonia archipelago are a paramount natural heritage which we have begun to study recently (Maire, 1999; Jaillet et al., 2000; Hobléa et al., 2001; Maire, 2004).

These karst areas are located between 50 and 52°S in Madre de Dios and Diego de Almagro islands, in the province of Última Esperanza (XII<sup>th</sup> region of Chile: Magallanes y Antártica Chilena) (Figure 1). They are the most southerly and the most in-

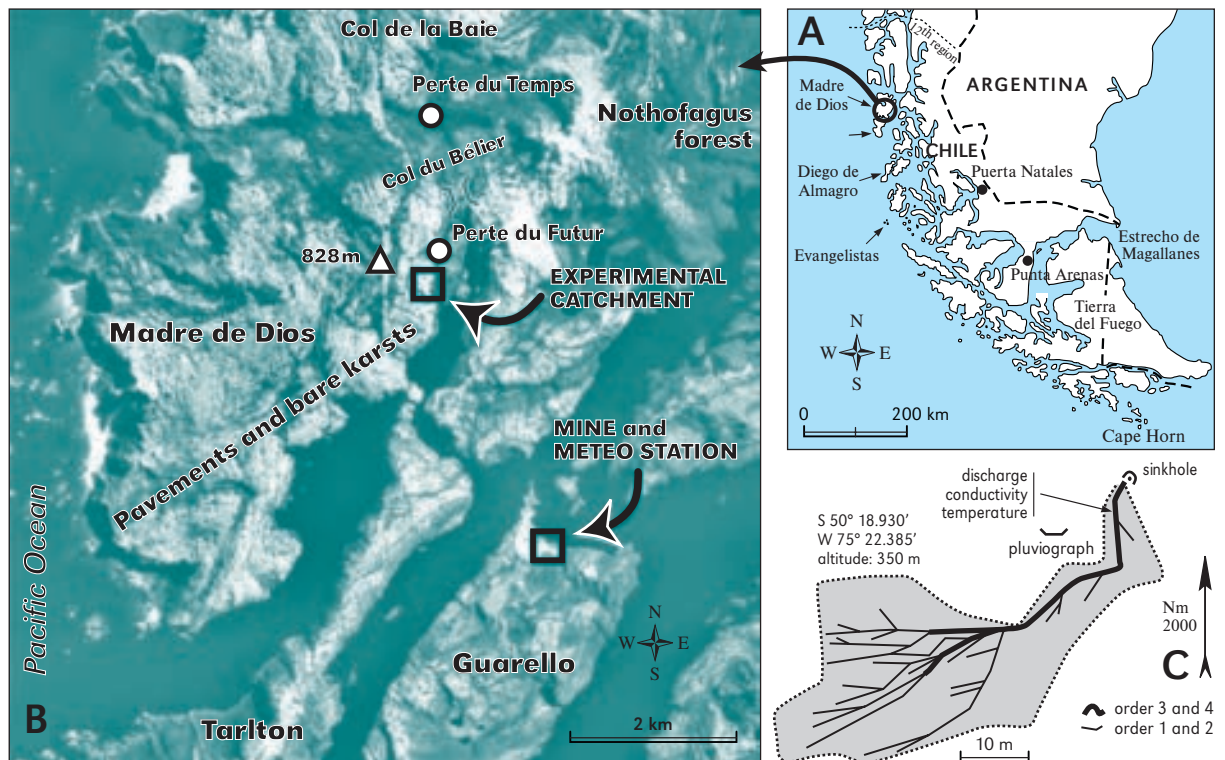


Figure 1: A. Location map of Madre de Dios and Diego de Almagro islands; B. detail of the studied area in Madre de Dios (after an aerial photograph, Servicio Geographico Militar del Chile); C. map of the studied experimental catchment constituted by step-like karren.

hospitable on Earth due to the *subpolar climate* characterized by the extreme rainfall and strong winds (“roaring fifties”). The hydroaeolian karren are a specificity of Patagonian karsts and several forms have never been described before. Because pure limestones are rare in Chile, these islands were recognized in 1930–1950 as within an inventory of mineral resources (Biese, 1956, 1957; Cecioni, 1982).

## The geoclimatic context

### Litho-stratigraphy

The carbonate terrains of the archipelagos form part of the pre-Jurassic basement of the Andean Cordillera which was the former Pacific margin of Gondwana. Limestone and marble outcrops constitute a band a few kilometres wide bounded to the west by the Pacific Ocean and to the east by the Patagonian granodiorite batholiths dating from the early Cretaceous (Halpern, 1973; Forsythe, 1981; Forsythe and Mpodozis, 1983). They are interbedded with volcano-sedimentary rocks and dikes. In Madre de Dios, Forsythe and Mpodozis (1983) distinguish three sedimentary formations. The *Tarlton limestones* are massive limestones and marbles more than 500 m thick and date from the Upper Carboniferous and Lower Permian. The Denaro formation is a sequence showing from bottom to top thick submarine basalts (pillow lavas), a level of biogenic cherts and red shale (30–60 m), grey calcarenites (50 m) interbedded with argillite and siliceous nodules. The Duc d’York formation is a very thick volcano-sedimentary sequence of flysch type.

In Diego de Almagro, situated 150 km south of Madre de Dios, the geological formations are similar (Escobar, 1980; Cecioni, 1982; Forsythe and Mpodozis, 1983; Maire, 1999). The Ploma formation correlates with Tarlton limestones. It is formed by massive and sparitic white marbles and sometimes grey dolomites. These carbonate terrains of several hundreds metres thick are thrust-

ed and layers are subvertical (Avenir peak, 815 m a.s.l.). The Huemul formation which combines the Duc d’York and Denaro formations is constituted by dark bands of volcanic sandstones and grauwackes intruded by dikes of lamprophyre. The metamorphic complex, located in all the SW half, is formed by a thick sequence of pelitic schists, green shales and amphibolites (Escobar, 1980). This folded metamorphic formation does not exist in Madre de Dios; it represents a deeper structural level of the same accretion prism according Forsythe and Mpodozis (1983).

During Upper Carboniferous and Lower Permian, coral reefs formed on underwater volcanic intraoceanic mounts, forming atolls surrounded by bioclastic limestone formations which have been locally dolomitized (Cerro Pelantaro in Diego de Almagro). Between Upper Paleozoic and Lower Mesozoic, this ancient active margin was a accretionary prism, that is to say a thrust sedimentary arc with a Pacific vergence built from the subduction zone. The metamorphism of limestones into marbles is extensive for the Ploma formation and variable for Tarlton limestones. In the two islands, limestones and marbles show numerous dikes of plutonic and subvolcanic rocks. A contact metamorphism is visible on the edge of the largest dikes: brecciation of limestone, recrystallization and fragilization of limestone (“sugar” cryptocrystalline facies), limestone fragments included into subvolcanic rocks. By differential dissolution, these dikes and veins can be used as a tool to measure postglacial surficial dissolution of limestone and marble.

### A hyperhumid subpolar climate

The cold oceanic climate of Patagonia is related to the interaction between the tropical anticyclones (subtropical convergence of South Pacific) and the southern low pressures (polar front) which accounts for the climate of the “*roaring fifties*”. These rotational cells coming from west generate huge precipitation at the contact of the first mountains

and very strong winds (NW, SW, W). Below 50°S, Última Esperanza archipelago has an isothermic subpolar climate called Tundra Isotérmico (Zamora and Santana, 1979). To have a subpolar climate, the temperature of the warmest month must not be greater than +10°C; this temperature is normally the thermic limit for trees. Nevertheless, the ex-

istence of the *magellanic forest of Nothofagus*, one of the last primary forests in the world, is a specificity of Chilean Patagonia and Tierra del Fuego. Even if the climate is subpolar, this forest can be developed in the shelter of rock dolines and at the bottom of cliffs up to an altitude of 400 m. Because of a strong wind, the very low growth of some Not-



**Figure 2:** Giant rinnenkarren and canyon-like wandkarren in Madre de Dios in the Carboniferous and Permian limestones (Tarlton limestones). Width of view is 10 m, below.



**Figure 3:** The floor of a large flachkarren showing the laminar flow by wind deflection during a shower, Madre de Dios (scale = 0.8 m in the foreground), photo Ultima Patagonia.

hofagus gives birth to bonsai with sometimes horizontal trunks of 5 to 10 m long.

Precipitation reaches 7,330 mm per year (80% rain, 20% snow) at the Guarello station (Madre de Dios) for the 1950-1970 period (Zamora and Santana, 1979). The whole of the external archipelagos of Última Esperanza between 49 and 52°S are included into the isohyet 6,000 mm per year as the Patagonia precipitation map (Toledo and Zapater, 1991) shows. This very rainy climate is different from the humid alpine climate which has a snow precipitation of more than 65 to 70% (Maire, 1990). The subpolar climate of Patagonia shows a regularity of precipitation with an average of 611 mm per month and 802 mm for the wettest month (November) and 441 mm for the driest month (June). The wettest year (1960) reached 8,495 mm (Zamora and Santana, 1979). But recently, February 2008 recorded almost 1000 mm

in Guarello station. The mean speed of wind is 70 km/h at Guarello station with a north-west dominant direction. The absolute maximum at Madre de Dios is unknown, but in February 2001 (Diego de Almagro) we have measured frequent speeds between 120 and 140 km/h. In Evangelistas station situated 52°30'S, south of Diego de Almagro (Figure 1.A), the absolute maximum is 183 km per hour in July (NW).

### **Types of karren and hydroaeolian karren**

The karren of Patagonia show remarkable and huge solution features due to the extreme rainfall and strong winds upon ice-smoothed rock karst (Figure 2). The laminar flow, the concentrated flow and the strong wind are three parameters

which combine more or less in relation with slope, topography, fracturation and exposure.

### Karren due to a mixing of a laminar flow and microturbulent flow

There are three types of karren due to a mixing of a *laminar flow* and microturbulence flow related to wind deflection (frictional effect and gravity).

*Aeolian flachkarren* (Figure 3): The flachkarren are known in the alpine karsts (Maire, 1990), but in Patagonia they are remarkably well formed on null or very weak slope ( $< 5^\circ$ ). Here the horizontal dissolution by the wind deflection is due to a quick laminar flow pushed and spread by strong winds in a dominant direction. The laminar flow can reach a high velocity despite the frictional effect on the rock. The streamlines probably divide into two layers: a water film with microturbulence at the rock surface and, just above, a layer of few millimetres with the laminar flow. The water film responsible for the corrosion action is renewed continuously. This very specific process generates flat and very smooth surfaces reaching more than 1,000–2,000 m<sup>2</sup> never observed before at this scale.

*Wave-like ripples* (Figure 4): These are a typical deflection and solutional form. They have been described in New Zealand (Owen Range), in an alpine and windy context, by J. Jennings (1985). In Patagonia, they are widespread all over the karst when the slope is steep ( $30\text{--}70^\circ$ ), on walls and on the edge of solution runnels and karren shafts. These small ripples constitute a dense network of semi-circular microstairs, each measuring 1 to 3 cm long, 0.5 to 1 cm wide and 1 cm high. On vertical walls, step-like rims become small rounded scallops like on a wall of a cave tube. So these micro-karren give a regular micro-crenellated surface. The genetic process of the *regressive dissolution* by small steps is connected with micro-turbulences flow (water film) generated by the gravity (slope), the frictional effect at the contact of the micro-irregularities of rock and above all the rhythmic renewing by the pulsed flow (unsteady



Figure 4: Wave-like ripples on a limestone scarpment in Madre de Dios formed by a laminar flow and wind deflection.

flow) due to the wind shocks. The process goes on by positive retroaction.

*Trittkarren* (terrace-like ripples) (Figure 5): In Madre de Dios, trittkarren cover large surfaces of roches moutonnées and are different enough from the classic heel-print karren described by Bögli (1960a, 1980). When the slope is above  $25\text{--}30^\circ$  we have wave-like ripples, below  $20\text{--}25^\circ$  the step process by laminar flow and regressive dissolution form small staged terraces of 2 to 10 cm wide and several tens of centimetres long. These terraces follow the topographic contours and evoke perfectly at a small scale the terraced cultivation of south-east Asia. In a small “talweg”, the terrace-like ripples transform in large concave steps called step-like karren (infra). As in the Burren (Ireland), trittkarren are also due to heavy rain in an oceanic context (Sweeting, 1973).

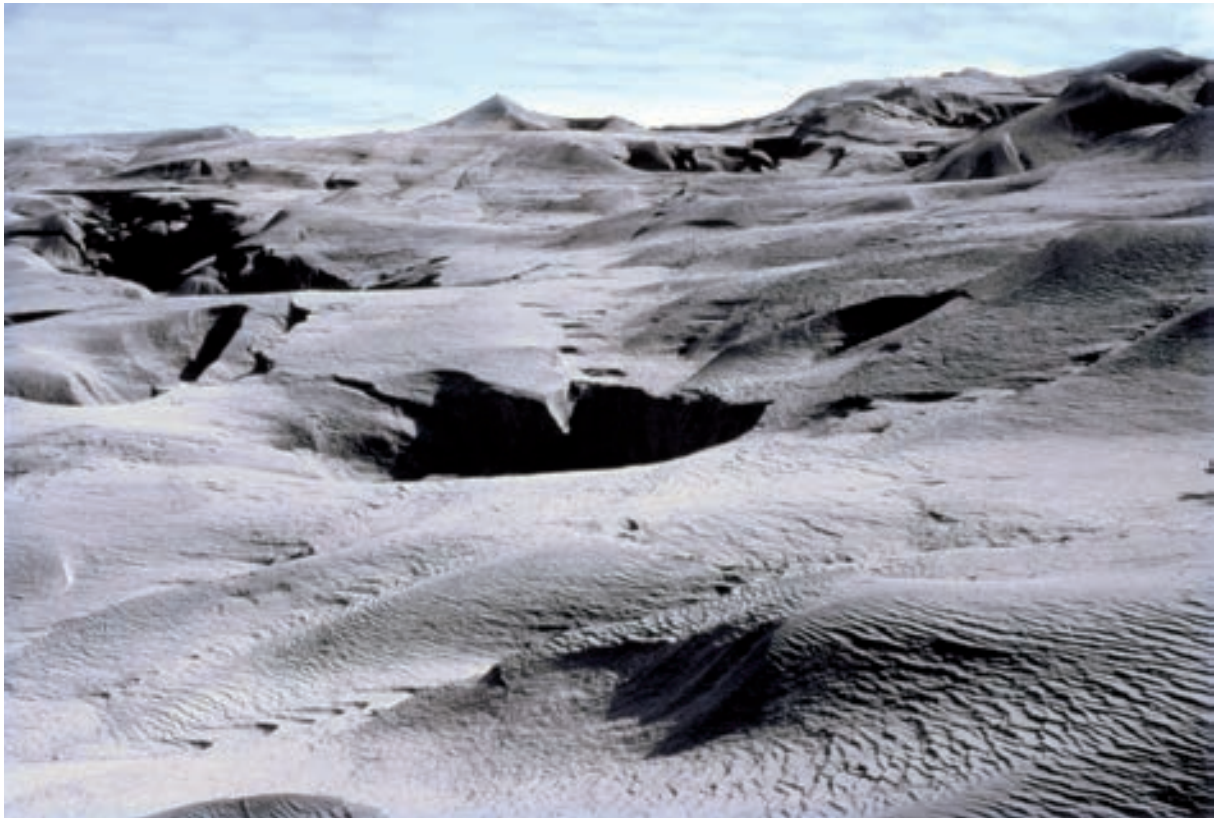


Figure 5: Trittkarren (terrace-like ripples) covering the roches moutonnées karst in Madre de Dios, altitude 450 m (photo Ultima Patagonia).

### Step-like karren: a mixing form of laminar, microturbulent and turbulent flows

The step-like karren constitute a specific and widespread form which combine steps and runnels due to a laminar flow in upstream and a turbulent flow in downstream because of an increase of water concentration (Figure 6). The process of step-like karren occurs especially on col and rounded eminences due to original glacial topography in the vicinity of the flachkarren. As for the terrace-like ripples, the step regressive dissolution occurs when there is a beginning of water concentration. First concave steps of 0.3 to 0.6 m wide and 1 to 3 cm high occur in small “talwegs” (5-25°), often over a distance of several tens of metres. The bottom of each step shows a corrosion depression which fills with water during the flow. The recurrent interruption of water flow at the ex-

trinity of steps because of a strong wind (water seems to go up) is a specific process for which an unsteady flow is responsible. If the distance is only a few metres between a flachkarren and a karren shaft, there is a succession of steps more and more high, a few cm to 0.5-1 m high, on the convex wall of the karren shaft. During a rainfall the laminar flow concentrates and begins to become turbulent in the axis of the upper “talweg”. At the end of the rainfall, the laminar flow disappears completely and a small concentrated flow continues to run in the axis of the step-like karren.

Depending on the topography and slope, step-like karren can continue by steps, 20 to 40 cm wide and 5 to 25 cm high, in the bottom of rinnenkarren 0.5 to 1.5 m deep with a slope between 25° to more than 40°. The height of steps increases with the slope. When the slope is steep, between 40° and 90°, the steps are more numer-

**Figure 6:** Step-like karren above “Col du Bélier”, altitude 400 m, in Madre de Dios. Width of view is 5 m, in the middle.



ous and higher, up to several metres, before disappearing.

#### Rinnenkarren, canyon-like wandkarren and meanderkarren

The large marble and limestone cliffs and glacial valley sides are striated by huge rinnenkarren and wandkarren reaching sometimes 100 to 300 m

high, like on the western flank of Cerro Pelantaro (Diego de Almagro) or in the west part of Madre de Dios (Figure 2). At the base of cliffs, each solution runnel reaches several metres wide and deep as parallel small canyons (Figure 2). Rinnenkaren and canyon-like wandkarren with steps generate *small gorges* reaching until 4 to 8 m deep and 1 m wide in the bottom. These young canyons are generally 10 to 30 m long and show steps reaching sometimes several metres high just before the





Figure 7: Giant meanderkarren on the marble dome, altitude 650 m, in Diego de Almagro. Width of view is 15 m, in the middle.

swallow hole. They occur by symmetric lowering dissolution of each step. This morphology is a good model to study the process of the regressive erosion.

Meanderkarren can reach exceptional dimensions even in catchments of only 1,000 to 1,500 m<sup>2</sup>. A remarkable example has been observed on the top of a marble dome, at 600 m high, in Diego de Almagro, south-west of Avenir peak. During a rainfall the water in a flachkarren basin of about 1,500 m<sup>2</sup> moves NNE down a gentle slope, on which forms a series of meanders with an amplitude of several metres (Figure 7). With the slope increase, the meander deepening can reach several metres deep near the edge of the valley side and 0.6 m wide at the bottom. This type of meander canyon is also a *natural model* at the middle scale



Figure 8: Circular karren shafts with step-like karren. All the limestone surface is covered by wave-like ripples (photo Ultima Patagonia). Width of view is 8 m, in the middle.

for the process of the meander deepening related to the slope in a massive soluble rock as marble.

### Pinnacles, kluftkarren and karren shafts

Pinnacles of 10 to 15 m height can exist on the edge of rock dolines where a magellanic forest grows. These forms join by thin and sharp arêtes which exhibit wave-like ripples and sometimes rillenkarren. Klufkarren occur especially in the fractured Tarlton limestones of Madre de Dios on cols and domes. They are 2 to 5 m wide and 10 to 50 m long. We often observe an asymmetry of the edges related to the influence of the wind direction (W to NW). The side exposed to wind forms a sharp angle less than 90°. The opposite side shows

**Figure 9:** A new family of karren, “the rock comets”, hydroaeolian wedges formed behind erratic rocks (“Col du Bélier”, Madre de Dios). Width of view is 9 m, in the middle.



**Figure 10:** An asymmetrical shaft in Madre de Dios caused by wind deflection. Width of view is 10 m, in the middle.



a convex edge often corroded by step-like karren (Figure 10). Circular karren shafts of 10 to 20 m wide are formed by centripetal sinks of several rinnenkarren and step-like karren from an initial klufkarren (Figure 8). This is a typical post-glacial morphology. But other karren shafts are larger and seem older, for example, the upper entrance 100 m karren shaft of “Perte du Temps” (2.6 km long) and the upper entrance swallow hole of “Perte du Futur” (–385 m deep), the two most im-

portant caves of Patagonia, which are former glacial sinkholes (location in Figure 1.B). In Diego de Almagro, the Avenir swallow hole, a 50 m waterfall at the contact of marble and volcanic sandstones, is a typical Holocene glacial lake sinkhole (Maire, 1999, 2004).

Located downstream of runnels, the karren shafts are young solution swallow holes mainly of postglacial age. They play a main role for quick absorption of water into the endokarst. For ex-



Figure 11: Other hydroaeolian wedges showing the residual and horizontal form by differential dissolution (“Col du Bélier”, Madre de Dios). Width of view is 5 m, in the middle.

ample, on the side of the Abraham fjord, in Diego de Almagro, an active shaft with small horizontal passages is directly fed by a large wandkarren. During a rainfall, a flood of 5 litres per second has been observed at 20 m deep. This example shows that one large solution runnel (or a small group) can provoke a sudden flood in the entrance of the karren shafts a few minutes after the beginning of the rain. By comparison, an instantaneous 100 l/s flood has been observed at 150 m deep in an inclined tube of “Perte du Temps” cave (Madre de Dios) 15 minutes after the beginning of the rain. Several floods can occur in the cave every day. This is a main problem for cave exploration in Patagonia.

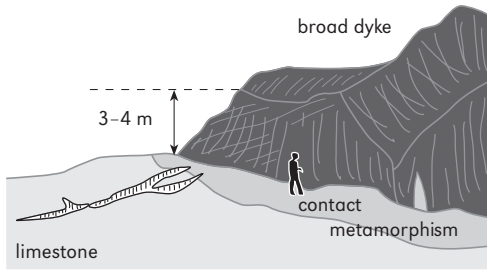
### Hydroaeolian wedges (“rock comets”) and the role of horizontal solution by deflection

The strong and permanent winds facilitate the horizontal laminar flow as for the flachkarren (supra). Also they generate specific hydroaeolian karren as wedges behind erratic blocks and residual small dikes of lamprophyre and subvolcanic rocks. These aeolian ridges are elongated forms due to a differential dissolution, located in the op-

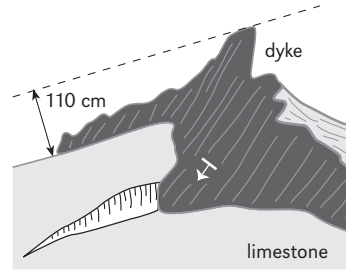
posite direction of the dominant wind. One can observe several remarkable types never described before: the hydroaeolian wedges behind erratic blocks, the hydroaeolian triangles and oblique pillars behind dikes and the keel-shaped wedges (without a shield).

Hydroaeolian wedges or “rock comets” (behind erratic blocks): These exceptional residual forms are easy to interpret. The reference site is the “Col du Bélier” near altitude 400 m (Seno Soplador, Madre de Dios, Figure 1.B). A group of two dozen erratic blocks of plutonic rocks exhibit horizontal and parallel aeolian wedges located on the leeward sides of each glacial block with NW–SE direction (Figure 9). The length of the ridges is 0.5 to 2.5 m and the height is 10 to 25 cm behind the block (Figure 11). Elsewhere, for bigger blocks, they can reach 40 to 60 cm high and 3 to 4 m long (“Col de la Baie”) (Figure 12a.h). The transverse sec-

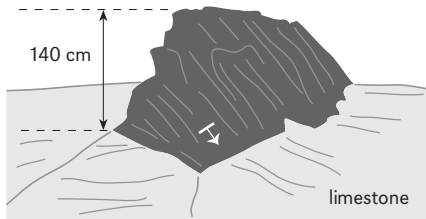
Figure 12a: Morphological indicators of postglacial and actual differential dissolution in Madre de Dios and Diego de Almagro. Mean postglacial dissolution is about 1,000 mm in Madre de Dios (limestones) and 750 mm in Diego de Almagro. →



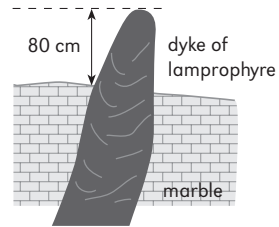
a) Raised dyke (3-4 m) because of weakened limestone by contact metamorphism, front-view



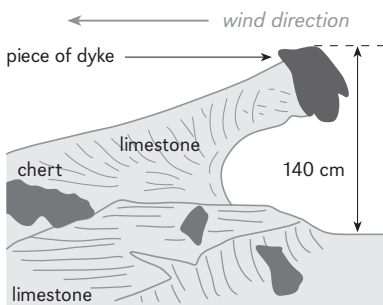
b) Raised inclined dyke (Madre de Dios), front-view



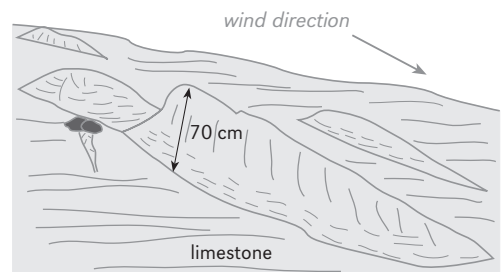
c) Other raised dyke (Madre de Dios), front-view



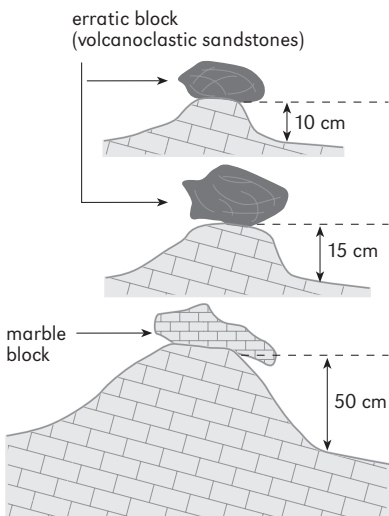
d) Raised dyke near Perte de l'Avenir (Diego de Almagro), profile



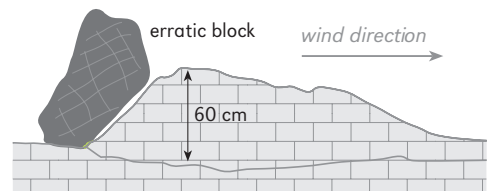
e) Residual oblique pillar near col du Béliér (Madre de Dios), front-view



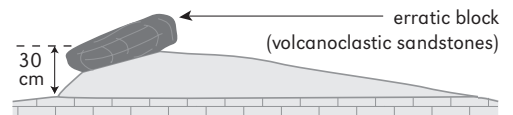
f) Ship bottomlike wedge (Madre de Dios), front-view



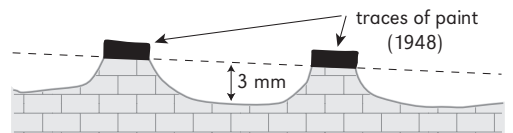
g) Marble pedestals in Cerro Pelantaro (Diego de Almagro), profile



h) Hydroeolian wedge behind an erratic block (Madre de Dios), profile



i) Other eolian wedge (Madre de Dios), profile



j) Traces of paint (Quarry of Guarello) dating from 1948. Dissolved slice measured in 1997, profile



Figure 12b: A pedestal of 170 cm on Monte Roberto near altitude 400 m, Madre de Dios. Width of view is 6 m.

tion is triangular. During the rainfall, the strong wind spreads the water horizontally and obliquely. Upon a flachkarren, each erratic block constitutes a shield which protects against dissolution a limestone elongated surface. There is a differential dissolution between the non-protected flachkarren and the protected part. Aeolian wedges behind blocks are the horizontal equivalent of vertical pedestals situated under an erratic block called *karrentische* or tables of the corrosion (Bögli, 1961). These last residual forms are frequent in the alpine karst where the wind influence is not dominant. But in Madre de Dios, in some protected places, the *highest pedestals* measure between 80 to 170 cm like west of Monte Roberto near altitude 400 m (Figure 12b).

*Hydroaeolian triangles* and pillars (behind dikes): These residual solution forms are similar to horizontal wedges. Here the erratic block is

replaced by a fragment of a small dike which is raised by the differential dissolution. The reference site is also the “Col du Bélier”. We can observe some large triangular aeolian ridges behind small dikes of lamprophyres protected by the wind. They can be generally 0.6 m to 1.1 m high, 1 m wide and 1 to 2 m long. There exists also a unique dramatic example looking like a battering-ram (*bélier*). This is an oblique pedestal inclined to 35° protected behind a thin fragment of the dike which is now isolated from the bedrock surface because of the erosion (Figures 12a.e, 13). This inclined pedestal is 3 m long, 0.5 m wide and 1.4 m in its highest point and indicates a huge surficial corrosion.

*Hydroaeolian ship’s bottom-like wedges*: These remarkable karren are also a positive form of differential dissolution but without a protection block or a dike. The reference sites are all in Madre



Figure 13: A hydroaeolian oblique pillar formed behind a small dyke of lamprophyre (Col du Bélier, Madre de Dios). Width of view is 4 m, in the middle.

de Dios: above Seno Soplador and also the “Col du Bélier” (Figures 1.B, 14). These ridges can reach 5 m in length and 70 cm in height. The upstream side, facing the wind, is steep and the downstream part finishes as a sharp triangle or can be digitated. The whole shape looks like a reversed ship bottom. The arête is more or less crenellated and the sides show step-like ripples. A statistical study of 129 aeolian ridges indicates they are 0.2 to 5.3 m long (mean 1.25 m) (Jaillet et al., 2000). The direction is between N 123° and N 180°, with a dominant direction NNW-SSE (330–345°/150–165°). The wedges are grouped and occur preferentially on cols and eminences showing a former glacial morphology in roches moutonnées. Every group of aeolian ridges has a similar direction and length of the same order. The morphogenesis is controlled by the exposure to wind, especially in the glacial valleys which channel and accelerate the wind by

the Venturi effect. In comparison to hydroaeolian wedges situated behind erratic blocks, these residual forms are poorly understood. They are probably due to an original process of *differential evaporation*. After each shower, we observe the ridges dry more quickly than flachkarren because of the wind. This process repeats several hundred times per year and accounts for why the ridges corrode more slowly than flachkarren. Once the process has begun, there is a positive retroaction effect as for the wave-like ripples.

#### Sword-shaped karren and asymmetrical entrance karren shafts

The wind influence also explains a lot of residual sharp forms such as knife-shaped limestone edges and asymmetrical blocks. The most spec-



**Figure 14:** Hydroaeolian wedges like the bottoms of ships, without a shield. We explain this new kind of karren by a differential evaporation because of the wind after every shower. Width of view is 7 m, in the middle.

tacular is a sword-shaped karren. This extraordinary morphology has been observed on Cerro Pelantaro in Diego de Almagro. This karren is a marble sword, 0.80 m long, 5 cm wide, 2 to 3 cm thick, with very sharp arêtes. Precipitation, wind, purity of the sparitic marble and a specific site effect (exposure) explain this residual karren. Another typical morphology are asymmetrical entrances of the karren shafts. We have already seen the asymmetrical klufkarren in Madre de Dios (Figure 10). In Diego de Almagro, on the top of the marble dome (alt. 600–700 m), between the Huemul fjord and Abraham fjord, entrance oblique karren shafts and klufkarren are eroded by the strong wind with asymmetrical holes and sharp edges (Maire, 1999).

### Coastal karren and coastal erosion notches

Coastal karren show large and sharp solution forms on the margin uplift during postglacial times because of the *glacio-isostatic response*, especially between 0 and +6 m. The intertidal zone is only 1 to 1.5 m high and exhibits solution pans and pools several metres wide as in the north of Guarello island. Between +1,5 m and +6 m, some

thin separation walls are perforated by circular holes. This sharp coastal morphology inherited by the uplift of intertidal pools is accentuated by a strong mixing with heavy rain and spume spread by wind.

In the carbonate islands of Patagonia, the coastal staged notches of corrosion are amongst the most remarkable tide-mark in the world (Figure 15). The reference site is in the Abraham fjord (Diego de Almagro), at the bottom of the marble dome crossed by the “Perte de l’Avenir” cave. Five notches are located at elevations up to 10.5 m (0 = high water). From bottom to top, we observe a notch 1 situated at high water level (0) where there is a mixing corrosion between marine water and overland flow from rain coming from the wall. The notches 2 and 3 are located at +4.5 m and 5 m. The notches 4 and 5 are located at +7 m and +8 m. There is a sharp contact at +10.5 m between the inclined karren wall and the top of the step 5 of 2.5 m high. This remarkable step, 12 m high in the low water, 10.5 m in the high water, indicates a *strong uplift* of more than 10 m since the end of the last glaciation. In Madre de Dios (Guarello, Seno Soplador), marine notches are also well formed, between 0 and +6 m.

Figure 15: Marine staged notches, 10.5 m high, in Abraham fjord (Diego de Almagro) because of the glacio-isostatic response during the Holocene.



### A study of an experimental catchment with step-like karren

The conditions of surficial flow have been studied in a small *experimental basin* situated in Madre de Dios. It measures 972 m<sup>2</sup> (perimeter 185 m, height 26 m) and drains a sinkhole. The catchment area of the drainage network is constituted by 310 m of step-like karren (Figure 1.C).

pools located at the foot of each step into the step-like karren. These small basins form a water reserve on the catchment. Between two showers, the water accumulated in pools dissolves more CaCO<sub>3</sub> than the running water and contributes to enlarging the depression. At the beginning of the rainfall, this water is pushed downstream by the piston-flow.

### A study of a flood series

At the top of the sinkhole we have studied, over a period of 3.5 hours each, two floods caused by two rainfalls. Precipitations, discharges, conductivities and temperatures were measured between every 1 and 10 minutes according to the flow intensity. The short response time, from 5 to 10 minutes, is related to the small size of the catchment. The longest flow distance is 75 m. For each increase of a discharge, there is a small peak of conductivity of 10 μS/cm which is interpreted as a piston-flow (Figures 16, 17). It is followed by a decrease of conductivity related to the dilution of water during the flood peak. The process of a piston-flow is probably due to the existence of small

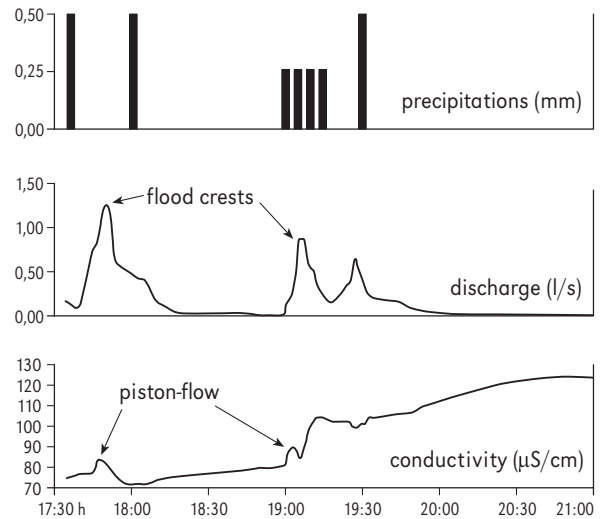


Figure 16: Precipitations, discharges and measurements of conductivity on the experimental catchment in Madre de Dios (cf. Figures 1.A, B).



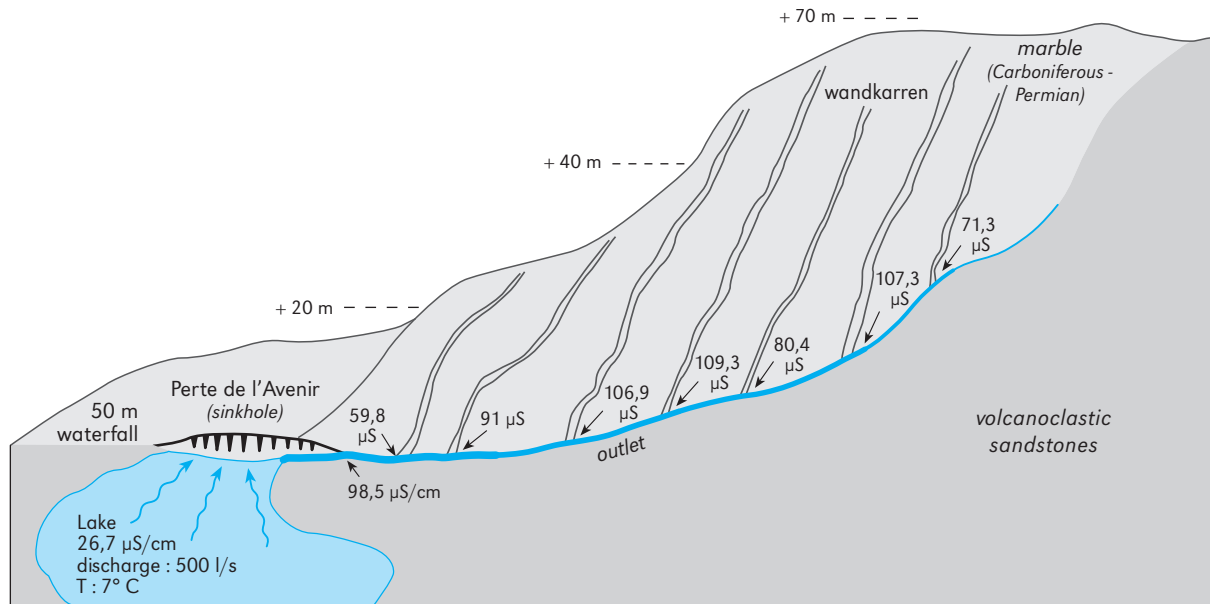


Figure 17: Measures of conductivity during the rainfall (12/02/2001) in wandkarren and in the outlet situated at the base of the marble cliff. “Perte de l’Avenir”, Diego de Almagro.

### The volume and the role of step pools

To understand the hydrologic regime of a flood, we have measured the length, the width and the depth of the 124 *pools* situated along the axis of the main step-like karren drain. The multiplication of the three values divided by two gives a good approximation of the volume. The curve of the pool volume from upstream to downstream shows an acute limit at the level of the step n 39. On the two sides of this limit, the curves are relatively right and it is possible to determine a mean unit volume per step which can be extrapolated for the other step-like karren. To characterize the different drainage parts, we apply the *Horton classification*. The pools of drains of the orders 1 and 2 have a unit volume of 0.14 litres (Table 1). The pools of drains of the orders 3 and 4 have a unit volume of 3.96 litres. In the parts of the orders 1 and 2, the steps have a mean length of 0.25 m. Downstream, in the parts of the orders 3 and 4 the steps are 1 m long. Moreover, downstream of the main drain (orders 3 and 4) nearly all the pools have been measured, so the result is relative-

ly good. With 1,250 steps, the total volume of the pools is about 410 litres (= 0.4 mm).

The combined volume of the two rainfalls is 2,430 litres (2.5 mm) on the experimental catchment. The flow is 2,220 litres (2.3 mm), with a rate flow of 90 % and an evaporation of 10 %, on the same order as the rate calculated by the equations of Turc and Thornwhaite. The volume of the pools (410 litres = 0.4 mm) has no influence in the hydrologic regime because the pools are full at the beginning and at the end of the experiment. During the 3.5 hour experiment, the water volume in

Table 1: Step-like karren; evaluation of the volume of water in the step pools by the method of mean volume extrapolated on two areas of the experimental catchment.

Horton classification	Orders 1–2 (upstream)	Orders 3–4 (downstream)	Total
Length of drains (karren)	253 m	57 m	310 m
Number of steps	1187	63	1250
Number of steps per metre	4.7	1.1	4.0
Volume of basin per step (main drain)	0.14l	3.96l	-
Total volume of basins	161l	250l	410l

the pools has been renewed five times. In one year, for a mean annual precipitation of 8,000 mm, the water of the pools is regenerated fifty times per day according our experience. Despite the renewing of the water in the pools, the *electrical conductivity* increases except during flood peaks, when there is a slight decrease. The two showers studied were not able to dilute strongly the water storage inside the pools. This is due to the persistence of a water film on the limestone surface between the two rainfalls. The carbonate concentration of this film grows and contributes to the surficial dissolution.

### Relations between a surficial flow and underground floods

The transit time of the floods in the caves is related to the transit time of a concentration surficial flow. The *response time* for a small catchment (1,000 m<sup>2</sup>) is quick, between 5 and 10 minutes. But this response can be reached in less than 5 minutes if the rainfall intensity increases. Several transit times in the endokarst have been measured at different depths. The first example is related to a flood generated by a few wandkarren and observed in a young cave of Diego de Almagro (Abraham fjord). The flood of about 5 litres per second occurs at 15 m deep 5 minutes after the beginning of the rainfall. Another underground flood, which was more severe, has been observed in an inclined tube of the “Perte du Temps” (Madre de Dios) at 150 m deep. The rainfall began at 12 o'clock and the flood wave of 100 litres per second occurs at 12<sup>h</sup>15'. This short transit time supposes a surficial concentration of 5 to 10 minutes and an underground transit time also of 5 to 10 minutes. These *instantaneous subterranean floods* are connected directly with the rainfall intensity and the rapidity of flow concentration on karren. For the “Perte du Temps”, we distinguish two kind of underground drains: 1) temporary drain with a great discharge variability (500 to 0.1 l/s in 24 hours) connected with karren sinkholes; 2) perennial drain with a middle discharge variability (1,000 to 100 l/s in 24

hours) due to a permanent sinkhole which drains an impervious catchment in volcanic sandstones with lakes and peat-bogs.

## Quantification of surficial dissolution

### Present and sub-present surficial dissolution

Present surficial dissolution: The *conductivity* of the karren water varies from 52 to 107 µS/cm and the total hardness (TH) from 14 to 35 mg/l of equivalent CaCO<sub>3</sub>. These variations are related to the flow distance (about 20 to 60 m) and the contact time with the rock. The karren water with mosses and small epikarstic springs reaches 135 to 161 µS/cm and 57 to 80 mg/l (pH = 7.30 to 7.65). Measurements of conductivity have been collected during a rainfall at the bottom of a 60° cliff dug by wandkarren 40 to 80 m long and 0.4 to 0.7 m wide near the “Perte de l’Avenir” (Diego de Almagro) (Figure 17). The discharge varies from 0.1 to 0.3 litre per second and the conductivity is 59.8 to 106.9 µS/cm connected with the karren length. At the level of the outlet which sinks in the “Perte de l’Avenir” the mean conductivity is 98.5 µS/cm.

Present specific dissolution: The conductivity and the total hardness have been measured on the experimental catchment in several samples. A linear relationship (R = 0,99) allows the conductivity to be converted to dissolved CaCO<sub>3</sub>. It shows that 100 grams of dissolved CaCO<sub>3</sub> have been exported during the experience and represent a limestone volume of 37,037 mm<sup>3</sup>. For a catchment of 972 m<sup>2</sup>, this dissolved volume is similar to a limestone slice of 3.81.10<sup>-5</sup> millimetre thick. The high purity of Tarlton limestone permits to neglect the weak rate of insoluble minerals. Despite its punctual character, this dissolved surficial slice can be extrapolated if we compare it with other indicators. For the postglacial time estimated to 10,000 years, the surficial ablation would be 0.95 m. This extrapolated value is of the same order as the postglacial dissolution measured with morphological indicators (infra, Figure 12a).

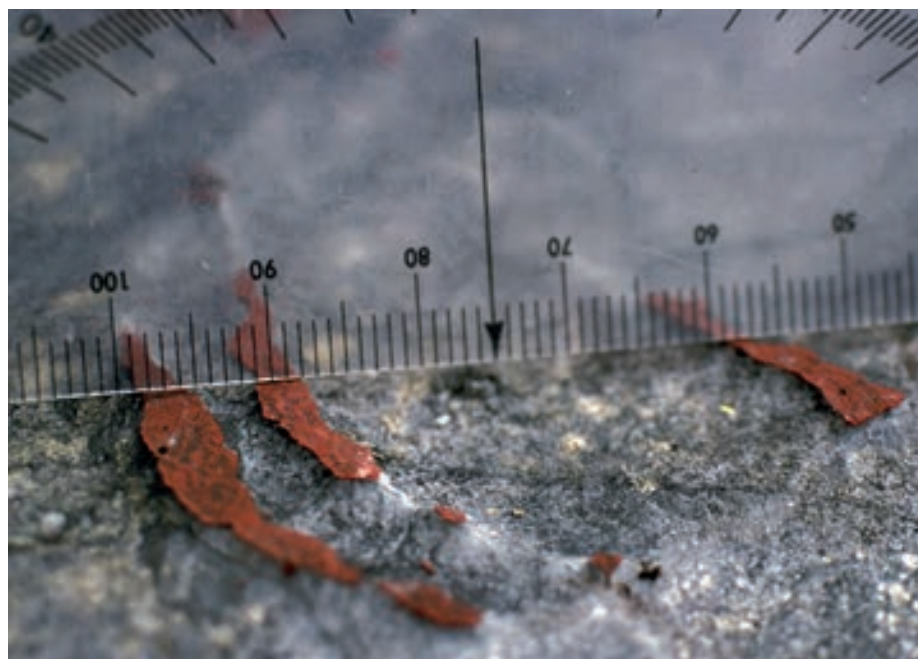


**Figure 18:** Traces of paint around the Quarry of Guarello (concession limits) dating back to 1948 showing a raised relief of 3 mm in about 50 years.

Surficial dissolution in 50 years: A precise morphological indicator was measured in 1997 near the quarry of Guarello exploited for lime. *Traces of paint* for limits of concession dating back to 1948 show a raised relief of 3 mm (Figures 18, 12 a.j). So the rate of surface dissolution is 3 mm in 50 years, that is to say a specific dissolution of  $60 \text{ m}^3\text{km}^{-2}\text{a}^{-1}$ . For 10,000 years, the surficial ablation would be 0.60 m.

### Estimate of postglacial surficial dissolution by morphological indicators

The best morphological indicators are small dikes of basalt and lamprophyre and aeolian wedges protected by erratic blocks highlighted by differential dissolution (Figure 12a, Table 2). They stand proud by 600–1,400 mm with a mean value of 1,000 mm in Madre de Dios. Amongst the highest values, we have measured 1,100 mm for a dike (Figures 19, 12a) and 1,400 mm for the inclined limestone pillar near the “Col du Béli-er” (Figures 20, 12a.e). In Diego de Almagro, the *postglacial dissolution* is 600 to 900 mm (mean 750 mm) probably because of the more resistant

**Table 2:** Evaluation of the surface dissolution in 50 years and during postglacial times according to the paint traces of Guarello and the small dikes, cherts and pedestals highlighted by differential dissolution.

Value of dissolution Morphometric indicators	Dissolution in 50 years	Postglacial dissolution in 10,000 years
Experimental basin (Madre de Dios)	4.5 mm (extrapolated)	950 mm (extrapolated)
Anthropic indicator (paint traces, 1948)	3 mm (measured)	600 mm (extrapolated)
Morphological indicators (Diego de Almagro)	3 to 4.5 mm (extrapolated)	600–900 mm (measured)
Morphological indicators (Madre de Dios)	3 to 7 mm (extrapolated)	600–1,400 mm (measured)

macrosparticle marble (Figure 12a.d). These differences are related with altitude, exposure to wind and petrographic facies. These values are the highest known in the world of the surficial dissolution on naked karren and are four to six times more important than in classic alpine and pyrenean karst (Maire, 1990). In Madre de Dios, a broad dike projected by 3 to 4 m, is due to the differential dissolution of the surrounding limestone which was weakened by the contact metamorphism (Figures 20, 12a). Nevertheless, this exceptional dissolution cannot be extrapolated for the hard limestone and marble.

**Figure 19:** A raised dyke of subvolcanic rock with a differential dissolution of about 1.10 m (cf. Figure 12a.b). Width of view is 5 m, in the middle.



## Conclusion

The subpolar Patagonian karst is unique on Earth and potentially merits the distinction of a *World Heritage site* to allow it to be protected and studied in the near future (Peter, 2001). They constitute a natural laboratory showing in real time

certain fundamental morphogenetic processes in the karstology and general geomorphology. The high speed of a surface dissolution, about 1,000 mm for Holocene period, permits direct analysis of the relation between morphology (effect) and process (cause) which is normally difficult in earth sciences because of inherited phenomena.



Figure 20: A broad dike with a differential dissolution of 3–4 m because of the limestone contact metamorphism. Width of view is 16 m, in the middle.

Heavy rain and strong wind are responsible for a quick laminar flow which generates hydroaeolian karren as flachkarren, wave-like ripples, trittkarren (steplike ripples) and wedges behind erratic blocks. The small catchments represented by the karren arborescence are functional models which follow the laws of the flow and regressive erosion-dissolution in the connection with specific criteria (Veress and Tóth, 2001). The rhythmic forms as wave-like ripples, trittkarren and meanderkarren have a fractal dimension that can be studied, as in subterranean scallops, by the small *wavelet method* (Horoi, 2001). Now the biggest problem to

continue the research is the very inhospitable environment and the financing of the speleo-karstological expeditions.

## Acknowledgements

We thank the French Federation of Speleology and the members of the speleological expeditions in Patagonia. We hereby express our thanks to Guilaine Reaud-Thomas for drawing the Figures and Arthur Palmer for editorial suggestions.

# CUTTERS AND PINNACLES IN THE SALEM LIMESTONE OF INDIANA

Arthur N. PALMER

The Salem limestone of Indiana, USA, of Mississippian (early Carboniferous) age, is well known as a source of building-stone (Figures 1, 2, 3). Many architectural landmarks, such as the Empire State Building in New York City, are faced with this

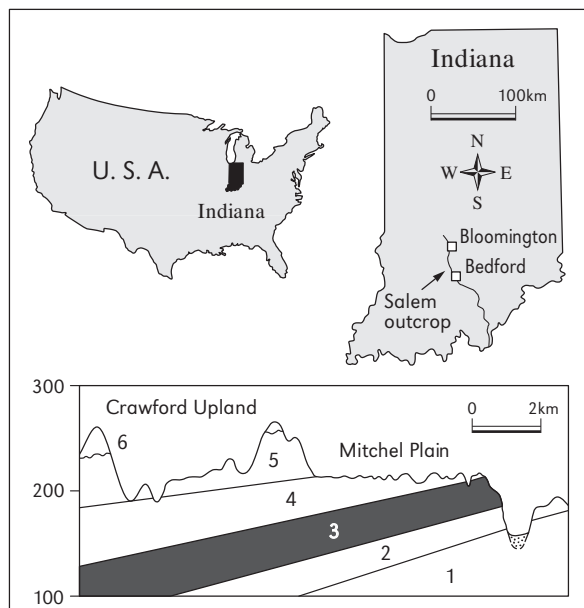


**Figure 1:** Location map and cross section showing the distribution of the Salem limestone in southern Indiana. Cross section is drawn east–west at a location between Bloomington and Bedford. 1. Borden Group (siltstone); 2. Harrodsburg limestone; 3. Salem limestone; 4. St. Louis limestone; 5. Ste. Genevieve and Paoli limestones; 6. younger strata, mainly quartz sandstones and shales. All strata shown are of Lower Carboniferous age.

stone. From the standpoint of karst, the Salem is noted for its well-developed *epikarst* exposed in the sawed faces of quarries and in roadcuts. As shown in Figures 2 and 3, the epikarst consists mainly of high-relief *joint-guided fissures* (*cutters*) with intervening fin-shaped *pinnacles*. These features are generally covered by soil and represent a subsoil version of *kluftkarren*. The quarry faces provide excellent cross sections of the epikarst, and where solutional features or insoluble content have interfered with the economic quality of the rock, numerous abandoned blocks provide multi-dimensional views.

Previous reports give general descriptions of the cutters and pinnacles in the Salem limestone, but with few details (e.g. Malott, 1945; Powell, 1961). Although this present paper expands on these early papers, it is based on limited field work and many questions remain for future detailed study. Regrettably, access to quarries is increasingly difficult because of liability concerns, and abandoned quarries are becoming overgrown with vegetation.

## Geologic setting

The Salem consists mainly of a massive, granular limestone (skeletal grainstone) deposited in shoals and inter-shoal environments (Brown,



**Figure 2:** Cutters and pinnacles exposed in the sawed face of a dimension-stone quarry in the Salem limestone, Lawrence County, Indiana. This is part of face 3 used in the data analysis. The measured sample includes all visible cutters in this photo, plus their downward extensions. The sample includes what appear to be isolated pockets, because they connect with cutters at higher elevations.

1990). Its total thickness averages 20–30 m, although the building-stone facies rarely includes more than half of this thickness. The building-stone facies contains less than 1% insoluble material. It is traditionally considered oolitic, but in fact it is composed almost entirely of fossil fragments dominated by foraminifera. The Salem has gradational contacts with the underlying Harrodsburg limestone, a massive bryozoan-rich limestone, and with the overlying St. Louis limestone, a thin-bedded limestone containing interbedded dolomite, shale, and chert. The building-stone facies is best developed between the cities of Bloomington and Bedford (Figure 1). To the north the Salem is covered by Pleistocene glacial deposits, and to the south it becomes thinner bedded and impure.

Temporary pauses in Salem deposition allowed the development of lithified surfaces known as *hardgrounds*. They provide the only significant

breaks in the building-stone facies, even though they involve little or no change in depositional texture. The conspicuous ledges in the quarry faces are determined mainly by successive stages of quarry deepening, rather than by stratification.

The Salem, along with its underlying and overlying carbonate strata, is exposed in the low-relief karst surface known locally as the *Mitchell Plain* (Figure 1). This is correlative with the more extensive Pennyroyal plateau of Kentucky. The local structural dip is very gentle and averages 0.25–0.5° to the west-southwest. The Salem contains prominent vertical joints that form two major sets, with spacings of about 2–10 m. The strike directions of the dominant joint sets are nearly perpendicular to each other, at 70–95° and 170–185°. The former set, which is dominant, is nearly parallel to the dip. Joints in both sets have been enlarged by epikarst dissolution, and they also determine the trends of many underlying caves.

**Figure 3:** Parts of faces 1 (top) and 2 (bottom) used in the data analysis. Cutters are narrower and more closely spaced than in Figure 2. In face 1 (top), the measured sample includes the six main cutters but excludes the thin fissure at right. Width of view is 9 m. In face 2 (bottom), the sample includes only the two largest cutters. The narrow fissures are simply sawed grooves.





## Field and laboratory observations

Cutters in the Salem limestone are solutionally widened fissures that decrease in width downward. Some have smaller fissures extending outward from them at various dip angles, and in local areas some cutters are surrounded by zones of *solutionally enlarged primary pores* that diminish in size away from the cutters. The *networks of subsidiary fissures* and enlarged pores are apparently formed by periodic flooding of epikarst fissures during high flow (Figure 4). This tendency is enhanced where shrinkage of drying soil produces a

gap between the soil plug and the bedrock walls. Genetically, these networks and enlarged pores resemble *maze caves* formed by floodwater (Palmer, 1975).

One might expect the cutters to be best developed beneath topographic lows, where infiltration can concentrate. But this seems not to be the case, because exposures show no consistent relation to the configuration of the land surface. Some of the most conspicuous cutters are located beneath convex topography. This suggests that cutter growth depends mainly on local infiltration through the overlying soil.



Figure 4: Enlarged pores in the bedrock walls of a cutter, the result of periodic floodwater recharge. Width of view is 1.2 m.

Many cutters have an erratic variation in width with depth (Figure 2). Lithologic control is very small in the massive Salem because of the nearly uniform texture and low insoluble content, and most of the width variations are caused instead by perching of vadose water on poorly permeable soil plugs. However, in the relatively impure transition beds at and around the St. Louis contact, petrographic analysis shows that cutters are conspicuously narrower where the rock is dolomitic or has a high insoluble content. In places the basal St. Louis is both dolomitic and high in insoluble content (up to 60%). Epikarst is greatly subdued in these beds. Instead the rock tends to weather into small fragments, whose combined surface areas are large enough to consume nearly all the aggressiveness of infiltrating water within short flow distances. Where the impure St. Louis cap approaches a thickness of roughly one metre, fissures in the underlying Salem diminish greatly in number and width (Figure 5). Where the St. Louis exceeds 2 m, fissures in the Salem are virtually absent.

conduits perched on sparse bedding-plane partings and relict hardgrounds. Soil in the cutters varies from yellow quartz silt to red, blocky clay composed of illite, kaolinite, quartz, and goethite. The red clay appears to be residual from carbonate weathering, because it has the most intimate contact with the rock surfaces. In composition the red clay is typical of insoluble materials from the St. Louis. The residuum cannot come exclusively from the relatively pure Salem, because too little of that rock has been dissolved in the epikarst to supply more than a tiny percentage of the soil. Furthermore, the insoluble content of the Salem is limited almost entirely to quartz silt. There were probably several sources for the yellow silt fill, because the Mitchell Plain was once covered by more than 10 m of Pliocene alluvial, lacustrine, colluvial, and residual deposits (Powell, 1964; Palmer and Palmer, 1975; Granger et al., 2001). Quaternary loess was later added to the mix.

The effect of these varied soil materials on infiltration has not been quantified, but comparison with similar materials suggests that the blocky clay



Figure 5: Variation in cutter development in the Salem limestone vs. thickness of overlying impure St. Louis limestone.

Widely spaced cutters, such as those in Figure 2, tend to be wide and very irregular in their upper sections. In comparison, closely spaced fissures, as well as the lower sections of widely spaced ones, taper downward in a more uniform manner (Figure 3). A few fissures lead downward to sinuous

has an inherent hydraulic conductivity less than about  $10^{-8}$  cm/sec. The conductivity of the sandier soil is orders of magnitude greater. However, determining the effective hydraulic conductivity of the epikarst soil is greatly complicated by macropores and shrinkage cracks, especially within the

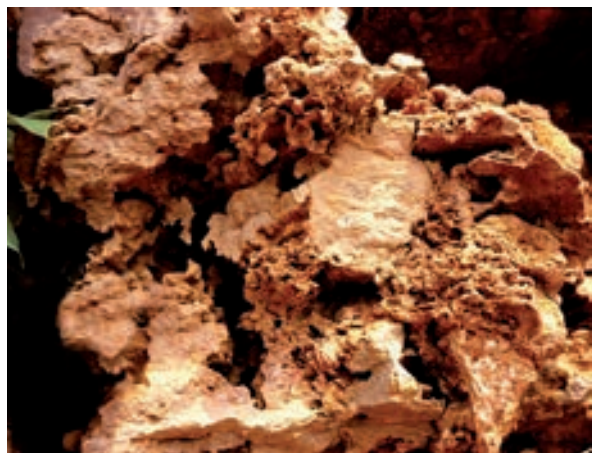


Figure 6: Irregular porosity in the walls of a cutter along a former sulphate zone. Width of view is 70 cm.

clay. The conductivity is also a function of soil moisture content, which varies with time. Macropores transmit water readily if there is ample supply from the surface, but they serve as flow barriers during slow, diffuse infiltration, because their capillary potential is much higher than that of the surrounding silt and clay. Water is drawn to areas of low capillary potential (small pores, low moisture content), while the larger pores conduct water only during the wettest of conditions.

In places the Salem epikarst contains irregular porosity and textures that are clearly related to now-vanished sulphates (Figure 6). *Calcite and quartz pseudomorphs* of evaporites are common, as are  *moldic pores*  from sulphate dissolution. Gypsum is common in these beds farther down-dip, where they are protected by thick overlying rocks. Local acid sources, such as pyrite oxidation, are demonstrated by abundant iron oxides, many of which are pseudomorphic after pyrite. The deep red and yellow colouring of the soil (terra rossa) is derived from the pyrite oxidation. The pyrite was almost certainly produced by reduction of the original sulphates. Thus these colours, so typical of the karst of the east-central U.S., may be derived in part from now-vanished sulphates by way of intermediate iron sulphides.

As viewed in vertical exposures, cutters in the

Salem epikarst become narrower downward at a roughly exponential rate, which is in accord with the diminishing dissolution rate as infiltrating water approaches saturation. Also, the overall development of epikarst diminishes sharply with depth, partly because of the decreasing width and spatial frequency of initial fractures and partings in response to erosional unloading (Williams, 1983; Klimchouk, 2000b). At shallow depths, dissolution is fairly uniform along many alternate flow paths, regardless of their discharge, so a network of widened fissures and pores is typical. The origin of epikarst resembles that of maze caves, where aggressive water follows short paths through carbonate rock (Palmer, 1991). Farther below the surface, as water approaches calcite saturation, the enlargement is highly selective because the most rapid dissolution takes place along paths of greatest discharge. Thus, below the epikarst, only the most favourable paths are enlarged significantly. During much of the year there is no net infiltration, owing to evapotranspiration of soil moisture. However, capillary moisture can still continue to dissolve the bedrock at these times.

### Geochemical modelling of cutters

A finite-difference model was devised to simulate cutter growth. The real system is highly complex, with large temporal and spatial variations in recharge, soil character, moisture content, CO<sub>2</sub> production, capillary potential, etc. A model that includes this degree of complexity would be difficult to interpret and would lead to questions as to whether the proper boundary conditions had been chosen. For this reason, the simplest possible model was used, so that discrepancies between it and real fissures could be interpreted in a broad qualitative manner.

The chosen computerized model is similar to that used to simulate the enlargement of water-filled fissures (see Dreybrodt, 1990; Palmer, 1991; Gabrovšek, 2000; and relevant chapters in Klim-

chouk et al., 2000), except that the epikarst system is open, rather than closed to  $\text{CO}_2$  exchange, because its water is in continuous contact with soil  $\text{CO}_2$ . An idealized vertical fissure 20 m from top to bottom was divided into 0.1 cm depth increments. A uniform amount of vertical flow was introduced at the upper end. In each depth increment, the rate of solutional widening and resulting percentage of calcite saturation were calculated. The resulting water chemistry was passed from each increment to the underlying one, and the calculations were repeated until the bottom of the fissure was reached. The entire sequence was repeated in one-year time steps for a total of 1,000 years of simulated time. It was assumed that mass transfer was rapid enough through the soil that dissolved species were uniform across the entire fissure width at any given elevation. This is highly unlikely, but it provides a standard to which the actual conditions can be compared.

The kinetic variables of Plummer et al. (1978) were used, because their measurements provide the maximum dissolution rates typical of open systems. They used turbulent flow in their experiments, which is not appropriate for infiltration through soil. But according to Plummer and Wigley (1976), turbulence has little effect on dissolution rate as pH rises above about 7, a value that is rapidly reached by seepage water in karst.

As water approaches equilibrium with dissolved calcite, the reaction order changes from about 1-2 to about 4, at roughly 70% saturation (Plummer et al., 1978; see Palmer, 1991, for a summary of their experimental results, and Dreybrodt, 1990, 1996, for an alternative approach). At low-order kinetics (saturation ratio less than about 70%), the dissolution rate is relatively rapid. The onset of high-order kinetics farther downflow sharply reduces the dissolution rate, because the base number ( $1 - C/C_s$ , where  $C/C_s$  = saturation ratio) is less than 1.0. Dissolutional enlargement of openings is fairly uniform at low saturation ratios, because it is not so dependent on discharge rates. At high saturation ratios the enlargement rate varies much more between alternate flow paths because it depends

more directly on discharge, which differs greatly among the various flow paths.

One of the major factors governing the dissolution of limestone is the specific discharge ( $q$ ) through the fissure. This is equivalent to volumetric discharge (volume/time) per unit fissure width. It is also equivalent to velocity  $\times$  soil porosity  $\times$  fissure width. In the model,  $p\text{CO}_2 = 0.03$  atm and temperature =  $15^\circ\text{C}$ , both of which are typical of soils in the Mitchell Plain (Miotke, 1974). Specific discharges ( $q$ ) were varied between 0.1 and  $10 \text{ cm}^2/\text{sec}$  but were held constant during each simulation. Model results are shown in Figure 7 for several values of specific discharge. On the semi-log plot, the slope of fissure depth in relation to log of fissure width should remain roughly constant as the fissure enlarges, as long as  $q$  remains constant. There is little tendency for  $q$  to increase as the fissures widen, because their catchment areas remain nearly constant.

Several quarry faces of Salem limestone were chosen for analysis on the basis of accessibility

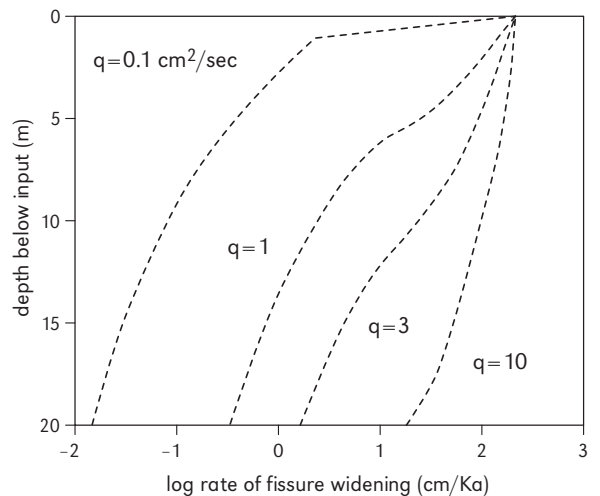


Figure 7: Idealized curves of fissure enlargement from finite-difference modelling, showing rate of solutional widening of epikarst fissures vs. depth and specific discharge.  $p\text{CO}_2 = 0.03$  atm,  $T = 15^\circ\text{C}$ , and saturation concentration =  $290 \text{ mg/litre CaCO}_3$  equivalents. The inflection points in the curves indicate the transition from low-order to high-order kinetics with depth (high and low dissolution rates respectively). In this over-simplified model the profiles are the same, regardless of whether the fissures are soil-filled or open.

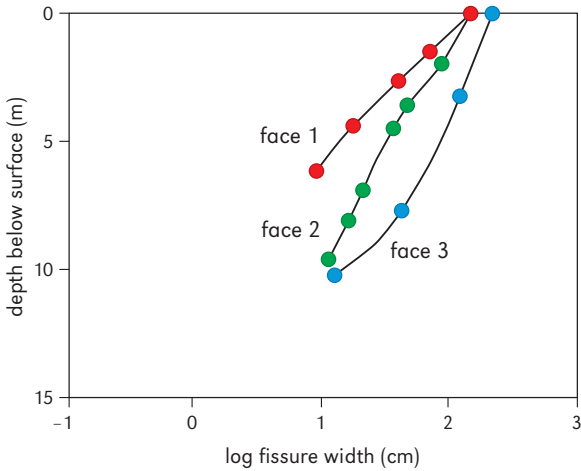


Figure 8: Cumulative data for epikarst fissures in three quarry faces (shown partly in Figures 2 and 3).

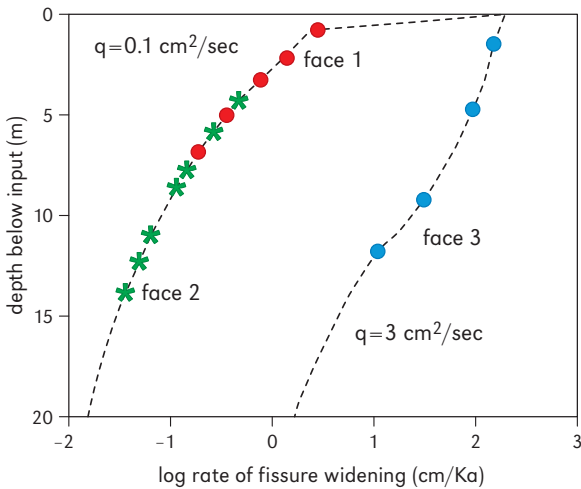


Figure 9: Matches between field data and model curves. Note the lateral and vertical shifts in data from their original positions in Figure 8, which were required to fit the ideal graphs.

and quality of cutter-and-pinnacle development. Others were disqualified because their cutter profiles were distorted by differential dissolution in the vicinity of local dolomites and shaly beds. To smooth out non-systematic irregularities, the mean width of all fissures exposed in each face was calculated as a function of depth below the surface (Figure 8). The resulting composite pro-

files were then compared with the idealized patterns predicted by the model.

### Model interpretation

The model shows the shapes of ideal cutters after 1,000 years of continuous development (Figure 7). These were compared to the actual cutter cross sections viewed in the quarry walls (Figure 8). Because the actual cutters are of unknown age, their proper positions on the graph are uncertain. Furthermore, the water that enters the cutters has already acquired a certain dissolved load before it starts its downward journey. On the semi-log plots, the curves for real cutter geometries retain their shape when they are shifted vertically. In addition, they retain their relative sizes if they are shifted horizontally (i.e. if a fissure is 10 times wider at one elevation than at another, this ratio does not change). The best fit was obtained when the field data were shifted downward and to the left, to match the modelled curves of depth vs. enlargement rate. Data for the cutters in quarry faces 1 and 2 fit the curve for the modelled plot for  $q = 0.1 \text{ cm}^2/\text{sec}$ . Those for face 3 fit best to the plot for  $q = 3 \text{ cm}^2/\text{sec}$ . This seems appropriate, because the fissures in face 3 are wider than those in faces 1 and 2, and they are also more widely spaced, so they accommodate a greater amount of recharge than those in faces 1 and 2. The measured profiles represent the actual shape after an unknown time of development. The amount of horizontal shift should be a crude indicator of their age (relative to the 1,000-year standard). The amount of downward shift should be proportional to the amount of dissolution that has taken place before the water enters the fissures. The 4 m downward shift required for the cutters in face 2 may reflect the fact that the uppermost bed (about 3 m thick) has been stripped away by quarrying.

The resulting fits, shown in Figure 9, are surprisingly good. This is unexpected, because the idealized model is obviously wrong. As expected, the mean *taper of the cutters* is strongly controlled

by dissolution kinetics. But the attempt to understand the nature of cutter growth by contrasting the field data to a purposely over-simplified model seems to have failed.

There are some obvious differences in behaviour between the model and the field conditions that are not illustrated in the graphs. In the field, aggressive water is able to penetrate more deeply than in the model, because water in contact with the real limestone walls does not efficiently transfer its dissolved load to the interior of the soil plugs. The apparent close fit to the model may indicate that much of the infiltrating water moves along the walls of the fissures along the soil/bedrock contact. This topic needs further investigation.

It appears from Figure 9 that the taper of the cutters depends partly on whether the solvent water experiences low- or high-order kinetics. The data from face 3 fits best to the low-order upper part of the graph, whereas the other faces fit a higher-order dissolution graph (i.e. slower dissolution rates). At high recharge rates (wide cutters) the water enters the cutters while it still retains much of its aggressiveness. Where the reaction order increases, the cutters become narrower. The result is a bulbous upper part leading downward to a narrower and more evenly tapered fissure (Figure 2). In narrow cutters, by contrast, the recharge rates are low, and by the time the water enters the cutters most of the dissolutional capacity has already been consumed in lowering the soil/bedrock surface. Therefore, in the narrow cutters the water follows high-order dissolution kinetics over their entire length. Still it is unlikely that cutter shape is an accurate indicator of low-order vs. high-order kinetics, because the depth of the transition varies with the  $q$  value, which in turn varies greatly with time.

Although the quantitative details of the model are not realistic, the general relationships seem valid. Wider *cutter spacing* provides greater discharge rates because the catchment areas are larger. The upper parts of widely spaced cutters enlarge rapidly by low-order kinetics, while the lower parts are enlarged more gradually, with a

gentler taper, by high-order kinetics. Where cutters are closely spaced, each receives less recharge, and most of their water has reached high-order kinetics by the time it enters them, owing to dissolution at the soil/bedrock contact and with carbonate fragments within the soil. The fact that the data for the narrow cutters needed to be shifted downward to fit the ideal curves of the model demonstrates that the water has lost much of its aggressiveness before it enters the narrow cutters.

## Age of cutters and pinnacles

In Figure 9 the amount of lateral shift required to fit the field data to the modelled curves should be proportional to the *age of the cutters*. This is only a crude approximation. The amount of lateral shift suggests that the cutters in faces 1 and 2 required between 75,000 and 500,000 years of cumulative infiltration at small  $q$  values and with slow (high-order) reaction kinetics. The data for face 3 required little horizontal shift, which suggests that its cutters are younger than those in faces 1 and 2, but with greater  $q$  and rapid (low-order) kinetics. These assumptions need closer scrutiny before they can be taken seriously.

The low-relief Mitchell Plain surface, in which the Salem epikarst is developed, dates mainly from the late Tertiary period (Powell, 1964; Palmer and Palmer, 1975). In Kentucky, passage levels in Mammoth Cave that correlate with the Pennyroyal plateau (a continuation of the Mitchell Plain) contain quartz-rich sediments that show cosmogenic radionuclide ages of several million years (Granger et al., 2001). These passages were filled during a major period of aggradation about 2.6 million years ago (estimate revised from Granger et al., 2001). Sediments accumulated to thicknesses of at least 10 m, both in the cave and on the karst surface. These sediments are well preserved in many upper-level cave passages, and in-place remnants of the sediments can still be identified at the surface (Ray, 1996).

Where does the Salem epikarst fit into the

picture? Because of the low structural dip of the Salem limestone in Indiana, small amounts of denudation can cause great lateral displacements of geologic contacts. As shown in Figure 5, the St. Louis limestone had to be removed by erosion before the Salem epikarst could begin to develop. And yet, where local land surfaces cut discordantly across both the Salem and St. Louis, cutters in the Salem extend very close to the St. Louis contact. This shows either that the contact has not shifted greatly since the epikarst began to form, or that the cutters develop quite rapidly. A maximum age of half a million years for the cutters and pinnacles (suggested by the model) is consistent with the antiquity of the overall Mitchell Plain surface as determined from cave-sediment dating.

## Conclusions

Cutters and pinnacles in the Salem limestone shed light on the evolution of the entire Mitchell Plain. The simplified modelling approach used here has shown that cutter morphology is closely tied to

dissolution kinetics. Because of the small size of the sample and the idealized nature of the model, the quantitative results must be considered tentative. Force-fitting of data to idealized curves does not prove a functional relationship. Nevertheless, this study opens a line of inquiry that may help to explain cutter development and shapes. Future field work should include measurements of soil character and infiltration patterns. The role of now-vanished sulphates should also be considered.

## Acknowledgements

Many thanks to Margaret Palmer, Oneonta, NY, for performing the petrographic and X-ray diffraction analyses, and for help with the field work. She tallied the cutter cross sections in the quarry faces independently, to avoid personal bias in obtaining fits to the finite-difference model. Richard Powell and Todd Thompson of the Indiana Geological Survey, Andrew Cheney of C & H Corporation, and Daniel Chase of Indianapolis were especially helpful in directing us to field sites.

# TYPES OF KARREN AND THEIR GENESIS ON THE VELEBIT MOUNTAIN

Dražen PERICA and Tihomir MARJANAC

Numerous karst forms are found on carbonate rocks of the Velebit mountain ridge. There occur numerous varieties of karren (“grizine” in Croatian), whose genesis and number are conditioned by interaction of geology, climate, soils, flora and geomorphology, as well as by anthropogenic influences. The term grizine encompasses various types of small-scale corrosional forms such as various types of karren, grikes, solution pans – kamenitzas (“kamenice” in Croatian), root karren, karren wells, karst tables, pot-like karren, and the karren locally referred to as “sige” (tufa-like karren). Several types of karren display differences as a consequence of their genesis; directly under the atmospheric water, or owing to subcutaneous corrosion by the water which was secondary enriched by soil-derived biogenic CO<sub>2</sub>.

## Previous research

The first true naturalist to study the Velebit Mt karst was apparently Hacquet (1785). Frasn (1835) provided first descriptions of some speleological features on the Velebit Mt, and the first geological research were conducted by Vienna Geological Institute in 1862. The first compilation of geological data was prepared by Hauer (1867-1871) who published a geological map of Austro-Hungarian Monarchy at a scale of 1:576,000. Ever since, the

Velebit Mt has attracted geologists and geographers to study its karst features.

Karren grikes of the Velebit Mt were studied by Simeonović (1921), Cvijić (1926, 1927), Poljak (1929a, b), Rogić (1958), and more recently Bogner and Blazek (1986), Perica (1998), and Perica et al. (1995, 1999).

## Geology of the Velebit Mt

The Velebit Mt is a part of the extensive Dinaric karst region. It consists of a wide variety of stratigraphic units, ranging in age from Carboniferous to Quaternary (Sokač, 1973). The oldest stratigraphic unit is Middle Permian, which is exposed only in the central mountain area, and forms a tectonically reduced anticline core. The units of Paleozoic age are conformably overlain by Mesozoic units. Triassic deposits are predominantly represented by dolomites, whereas the Jurassic deposits comprise various types of shallow marine limestones. The deposits of Cretaceous age are represented by carbonate platform carbonates. These units are transgressively overlain by Tertiary shallow marine carbonates and deep marine clastics. The youngest Tertiary unit, though of controversial age and origin, are the so-called Jelar-beds, commonly referred to also as the Jelar-breccia. The youngest deposits of the Velebit Mt



are Pleistocene glacial and glacio-fluvial deposits, preserved on the mountain's highest parts.

The Jelar-breccia (first described by Bahun, 1974) is the lithostratigraphic unit bearing the best developed karst features. The Jelar-breccia is a massive, or thick-bedded carbonate rock, and comprises predominantly angular, poorly sorted debris. It is commonly grain-supported, although matrix-supported varieties occur locally. The breccia has a carbonate matrix, which is gray to reddish coloured. The stratigraphic composition of debris is varied. Clasts of Cretaceous limestones and dolomites are the most common, and subordinately there occur Triassic carbonates and Paleogene limestones. The debris grain sizes are very variable, and clasts range from a few mm up to several decimetres in size, but also up to several metres or more across.

The area covered by Jelar-beds (breccia) reaches ca. 690 km<sup>2</sup> (Figure 1), but its thickness is poorly known. The only available direct account on its thickness was acquired by drill-holes during construction of the St. Rok road tunnel (Matičec et al., 1999) on the southern part of the Velebit Mt, which documented the thickness of Jelar breccia of 300 m. Not only is the thickness of Jelar-breccia poorly known, but also its age remains a controversy. It was treated as an Eocene-Oligocene unit by authors of the General Geological Maps of Croatia (Ivanović et al., 1973; Mamužić et al., 1969; Šušnjar et al., 1970), which means that it represents a post-Eocene flysch sedimentary unit. However, Tari Kovačić and Mrinjek (1994) interpreted the breccia as a post-Cretaceous but pre-flysch sedimentary unit of the Early Eocene age. The youngest debris found in Jelar-breccia are clasts of Early Eocene *Alveolina* limestones, which constrain its age to Upper Lutetian-Bartonian span (Sakač et al., 1993; Vlahović et al., 1999).

## Superficial corrosion features and karren of Velebit Mt

The development of karst relief has been condi-

tioned by prevalence of carbonate rocks on the Velebit Mt, namely by the high CaCO<sub>3</sub> content. The size of exokarstic and endokarstic features indicates that they were most commonly formed in rock successions dominated by limestones, such as the Middle and Upper Jurassic limestones with a high percentage of pure CaCO<sub>3</sub>.

Structural predisposition implies abundance of primary and secondary fissures and voids, as well as inclination of beds. "Classical" carbonates (primarily Jelar-beds) are characterized by numerous primary fissures. Bedding commonly affects the size and shape of karst features in layered rocks (e.g. asymmetrical dolines), where steepened bedding promoted more intensive corrosion primarily along diastromes. Tectonics created fault planes, fractures and fissures, which initiated formation of numerous karst features. One of the prominent characteristics of these karst features (created along secondary fissures) is their elongation along the strike of the fissure.

Formation of karst features and their frequency also depend on slope inclination. The karst features are more varied and larger on horizontal and gently inclined slopes (up to 12°). On steeper slopes, karst features are much rarer, primarily because of faster superficial drainage, and consequently decreased corrosion intensity.

## Climatic conditions

Climatic factors (rainfall and temperature) are important because of their influence on duration and intensity of corrosion. Rainfall increases with altitude, but it is unevenly distributed. The whole Velebit Mt is characterised by a mediterranean pluviometric regime, with more abundant rainfall in the cold than in the warm season. The lowest rainfall is in the coastal part of SW mountain slope (ca. 1,200 mm annually). The rainfall non-proportionally increases with altitude. The rainfall increase is lowest on the north Velebit Mt where the 2,000 mm isohyet attains altitude of about 1,400 m. Gradually, the 2,000 mm iso-

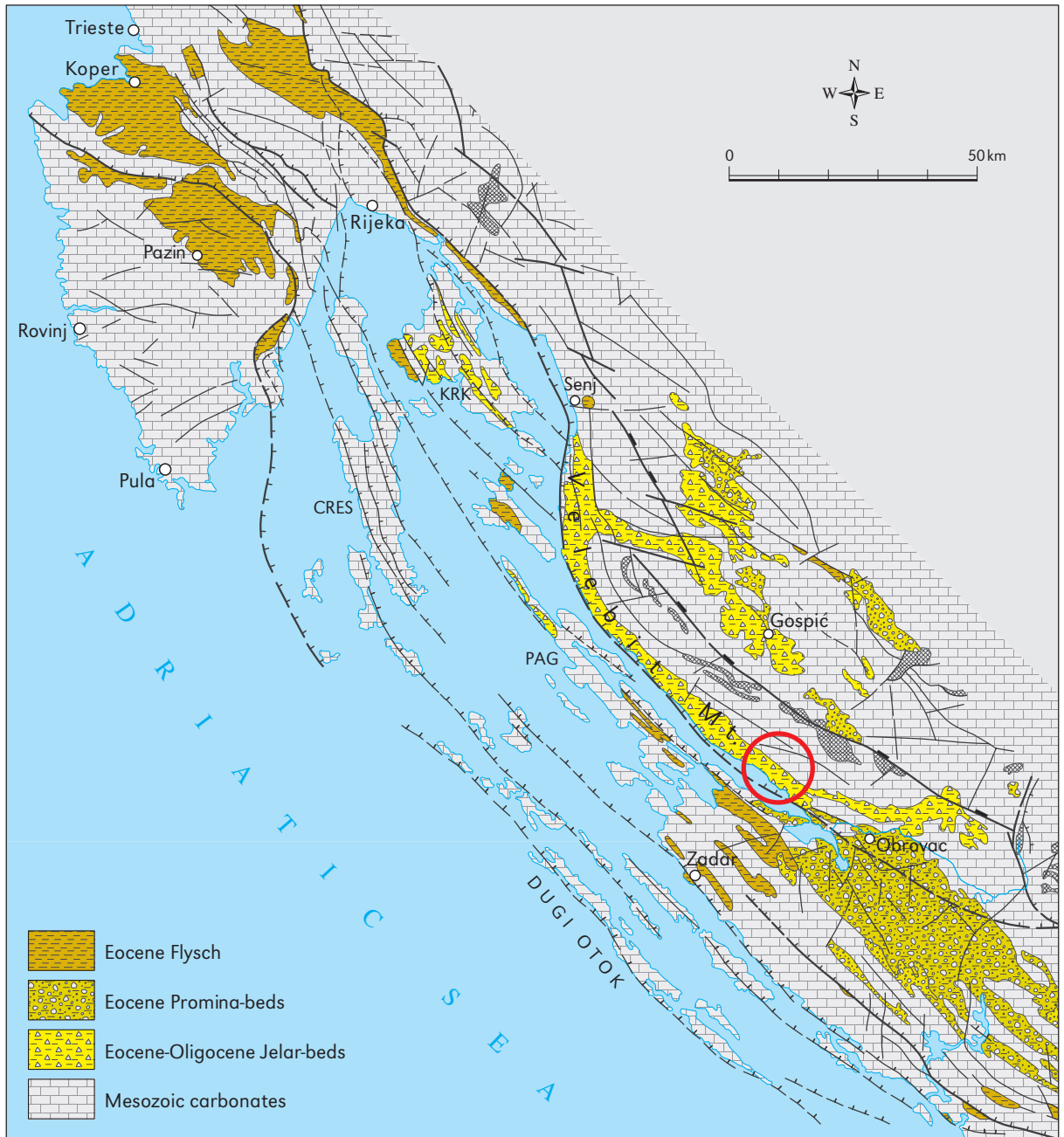


Figure 1: Simplified geological map of the Velebit Mt and neighbouring areas, after Olučić et al. (1972). Circle marks the Paklenica National Park.

hyet lowers to an altitude of 900 m on the south Velebit Mt, where rainfall reaches ca. 3,500 mm at the mountain crest (Bunovac at the leeward side of the mountain crest: 3,419 mm, Perica and Orešić, 1997). However, the intensity of corrosion is significantly affected by additional precipitation

(from mist, fog and clouds) in the crestral part of the mountain, which accumulates orographically. The contribution of this additional precipitation on Zavižan meteorological post (1,594 m a.s.l.) in period 1955–1965 was 249% (Kirigin, 1967), with significant differences between winter (343%) and

summer (171%) seasons. On the NE flank (Lika side) of the mountain rainfall gradually falls below the isohyet of 2,000 mm.

The thermal effect of the sea is restricted to the coastal zone and the lower SW mountain slopes, but it is also weakened by the presence of islands and the Ravni Kotari plateau which stretch parallel to the coast-line. The average annual air temperature on the lowest part of the SW mountain flank reaches about 15°C (Senj 14.5°C, Karlobag 15.6°C), and about 3°C in the crestal part (Zavižan at 1,594 m a.s.l., 3.5°C) of the Velebit mountain. With an increase in altitude, the air temperature rapidly, but unevenly, decreases. The annual vertical gradient between Karlobag (30 m a.s.l.) and Baške Oštarije (924 m a.s.l.) is 0.93°C, and between Baške Oštarije and Zavižan (1,594 m a.s.l.) it is 0.57°C. According to Rogić (1958), heating of carbonate rocks on the lower part of the SW mountain flank (Karlobag has 109.6 warm and 39.7 hot days annually) significantly promotes thermomechanical weathering of the rocks, and exceptionally strong evapotranspiration which causes their marked dryness. The intensity of corrosion and biocorrosion is lowered in these conditions, and it completely stops in thin soils during the prolonged droughts. This assumption was confirmed by the study of the intensity of corrosion at the surface by using limestone tablets (Perica, 1998). The corrosion intensity on the SW Velebit Mt slope is highest in its middle part; it decreases insignificantly downslope, but significantly upslope. The lower and middle part of the SW slope is characterized by significantly stronger corrosion in the soil than at the surface. Thus, the corrosion intensity at the surface and in the soil in Velika Paklenica (560 m a.s.l.) reaches 1:2.55, and on Babrovača (920 m a.s.l.) 1:3.49. This increase in corrosion intensity can be explained by increase in biocorrosion which stems from a prolonged vegetative period.

The crestal part of the Velebit Mt is characterized by large number of cold (160.9), icy (74.9) and freezing (26.3) days which favour the freezing of water in fissures, so that cryogenic processes play

a major role in shaping of the relief. A short vegetative period and a large number of cold, icy and freezing days, favour soil dryness and conditions curtailing the corrosion (Perica, 1998).

The formation of the karst relief was significantly affected by the climate of the last Ice Age. On the one hand karren were destroyed by erosion, or reshaped, and on the other the melting of snow and ice formed new karst features such as speleological features having drainage function.

Finally, the anthropogenic influence in the past was related to deforestation, when enhanced denudation and soil erosion exposed rock at the surface. This is particularly well seen on the Velebit Mt crest and its SW slopes. In the long term, ever since prehistory, bad agricultural practices on this part of the Velebit Mt caused its deforestation. Thus, today, on the SW slope and the mountain crest, bare and semicovered karst prevails, which commonly passes into exposed karst. At the same time, the NW mountain slope is largely forested, and the karst covered (Rogić, 1958).

### Types and formation of karren

The Velebit Mt karst contains all types of karren, but here we will deal only with *solution runnels* developed on Jelar-breccia.

*Karren* formed by water corrosion represent the most widespread karst forms on the Velebit Mt, and their various types occur from the sea-level up to the highest parts of the mountain crest. However, they are most frequently and best developed on the lower and middle, bare parts of the SW (coastal) part of the mountain slope, whereas their development in higher parts is restricted by thermal conditions.

The formation of various types of *karren* results from interaction of: a) slope inclination, b) lithology, and c) rock fracturing. Their shape is preconditioned by the relationship of slope vs. bedding inclination, and degree of carbonate exposure under vegetative and soil cover. These factors controlled the corrosion, which could have acted: a) directly

by corrosion of meteoric waters, b) by corrosion of waters which percolated through the soil, and c) by corrosion of ground water. Lithology also plays a major role in the formation of karren. They are absent or small in thin-bedded carbonates, but varied and very abundant in thick-bedded varieties. Thus, the Jelar-breccia is characterised by extensive development of karren, essentially due to its lithological characteristics.

On the Velebit mountain there occur several types of karren; *furrow-like karren* (locally called *žlibe*), *fissure karren* (locally called *škrape*), *kamenitzas* (solution pans) and *biocorrosion pits*.

Ford and Williams (1989) differentiate microkarren (smaller than 1 cm), karren (1 cm–10 m large), and bogaz or corridor (larger than 10 m). Microkarren are developed in homogeneous fine-grained rocks by corrosion of water under capillary pressure. Biocorrosion due to endolithic bacteria, lichens and mosses, also plays a major role in formation of microkarren. Cyanobacteria form small 1 mm deep hollows, which are later invaded by other organisms (Verges, 1985) that promote corrosion by production of organic acids and emission of CO<sub>2</sub>.

*Rinnenkarren* or runnels (*solution grooves*) (Figure 2) occur at a wide range of altitudes, from the Adriatic coast up to the Velebit Mt summit. Two genetic types of rinnenkarren can be differentiated; a) the variety formed by corrosion of atmospheric water, and b) those formed by corrosion of water enriched with biogenic CO<sub>2</sub>.

The first karren variety (a) is characteristic of steeper (> 20°) slopes on denuded Velebit Mt carbonates. This karren type occurs on small limestone blocks, sometimes not more than a few tens of sq. decimetres in area, but the maximal development is on the Jelar-breccia at the Velebit Mt SW slope 500–1,200 m a.s.l. as well as on Upper Jurassic limestones in Paklenica National Park (Perica et al., 1995) where bedding and slope inclination nearly coincide. The water strongly corrodes bare carbonates, and flows down the rock-face. This type of karren is most frequent on rock faces inclined at 30°–70°. Although the water is



Figure 2: Typical large rinnenkarren (solution runnels) in Jelar-breccia. Paklenica National Park, south Velebit mountain. Width of view is 5.5 m.

eventually enriched in carbonate, it is still corrosive due to inflow of rain water. Thus, the grooves are wider and deeper downslope, whereas the ridges get narrower and sharper. Slope inclination also controls their shape, so they are narrower and deeper on steeper rock faces, a consequence of restricted lateral and enhanced regressive water action, due to accelerated run-off and water inflow in the groove. Gentler slopes are characterised by slower run-off and thus enhanced lateral corrosion, so that the furrows are wider and shallower, and often gently curved.

The furrows commonly attain 50 cm in width, and 1 m in depth, but those developed on the Jelar-breccia and Upper Jurassic limestones in the Paklenica National Park can be much larger (Fig-



Figure 3: Steep runnels with well developed serrated ridges showing solution flutes of the second order. Width of view is 3.5 m.

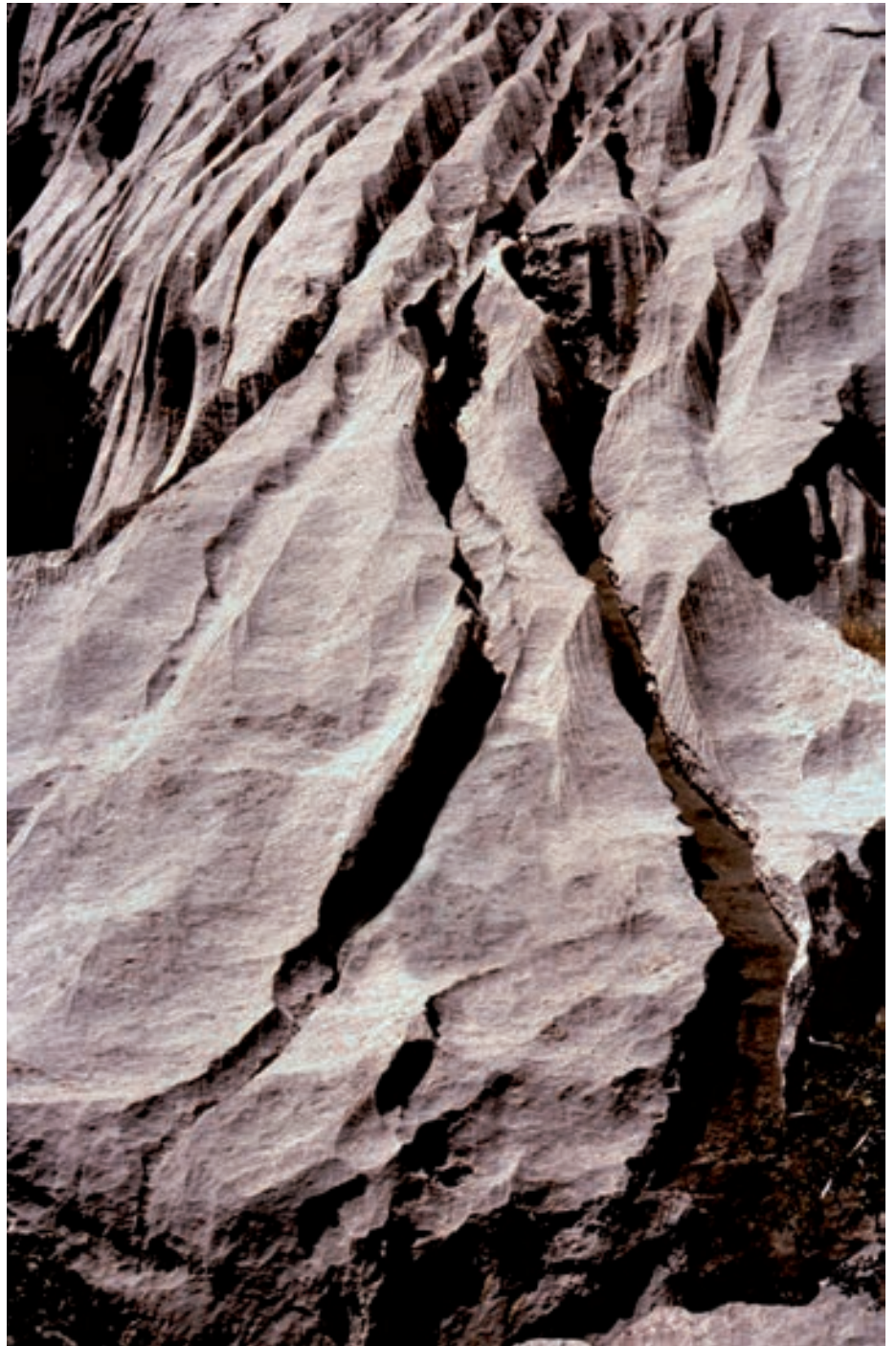
ures 2, 3). These grooves attain a few tens of metres in length, but in the Paklenica National Park they exceed 100 m in length and 1 m in depth. The formation of these large grooves is also controlled by additional water supply by condensation of atmospheric water on the carbonate substrate (Perica and Orešić, 1999). Lateral corrosion narrows the karren ridges, which become very sharp, frequently ornamented by development of solution flutes of the second order (after Bögli, 1980). As they grow, these secondary grooves are progressively shallower and wider, compared to the primary groove which becomes steeper-sided. This is a result of decreased water supply per unit of surface, and its quicker neutralization (and increase in carbonate concentration; Perica and Kukić,

1992). The end result is a decreased ratio between groove width and length, compared to the primary furrow. The incision of the solution flutes of the second order provides a dog-tooth shape to the ridges. Furrows become irregular on the Jelarbrecia, as a result of differential corrosion due to clast inhomogeneity and clayey-limonitic matrix. Depressions are formed in places of corrosion-prone clasts, whereas harder clast lithologies remain as elevated remnants.

The second runnel variety (b) is formed by corrosion of water which is enriched in biogenic  $\text{CO}_2$ . This karren type is much rarer than the first type, described above. On the Velebit Mt we can differentiate two sub-types. The first sub-type is covered karren, which was formed by subcutaneous corrosion under the soil cover. It is well exposed in Hajdučki Kukovi area, where vegetative cover was destroyed. The covered karren occurs individually, rarely in groups, and also occurs on gentler slopes. This type of karren (*rundkarren*) is characterised by a gentle half-rounded shape, which is shallow and wide. It does not widen downslope as does the first karren type. When they occur in groups, they are separated by wide ridges. This shape is a result of slow and long-lasting water percolation in soil, which causes even wetting, and corrosion of the rocks. However, even here the water is concentrated by channelized flow, although to a lesser extent than on the bare rock faces. This karren type occurs on gentle slopes inclined just a few degrees, but its width/depth ratio at the change of slope inclination has identical characteristics as do the grooves formed by direct corrosion by the atmospheric water.

The second karren sub-type is the humus-water-groove (*hohlkarren*), which commonly occurs singly. This type of groove is formed by corrosion of water which percolates from pedogenic cover, and is enriched with biogenic  $\text{CO}_2$ . Their size is smaller than the size of atmospheric water-generated grooves, primarily because of restricted amount of  $\text{CO}_2$  in the water. Locally, in canyons of Velika and Mala Paklenica it is possible to see that for several metres there is precipitation of  $\text{CaCO}_3$ , indicating

**Figure 4:** Lateral biocorrosion caused by mosses forms overhung karren edges. Note residual clays filling the bottom. Bojinac, south Velebit mountain. Width of view is 3 m.



carbonate-saturated water. Slow running of subsurface water is favourable for growth of lichens and mosses which contribute to biocorrosion that widens groove sides which become overhung, whereas the bottom fills with residual clay which insulates it from further corrosion (Figure 4).

A common characteristic of all these karren types is that at steep slopes (inclined  $80^\circ$  or more) they become shallower and narrower, as well as semicircular in cross-section. This is due to accelerated run-off, increased rainfall on the surface unit, and water neutralization with consequence

of decelerated corrosion. However, this karren type is quite rare, and ridges are commonly lacking. If the rock face reaches 90°, or overhangs, groove incision ceases. This wall-karren can be seen on steep rock faces, pillars and cliffs, which are particularly impressive in Varnjača doline on Hajdučki Kukovi, Bojinac, and Velika and Mala Paklenica canyons.

On very gentle surfaces *rinnenkarren* are wider or completely disappear. However, locally they develop as meandering grooves (meandering karren) which can be best seen on Bojinac, Hajdučki Kukovi, Kiza and Alaginac on the Velebit mountain. Karren meanders are typically asymmetric in cross-section, seldom wider and deeper than 10 cm, and the length can exceed 10 and more metres.

Karren features are particularly common on gentler slopes (< 12°). By their shape, fissure and network, karren types can be differentiated. By their genesis we can differentiate karren formed on bare rocks by corrosion of atmospheric water, and karren formed under pedologic and vegetative cover by subcutaneous corrosion. The shape of karren is also controlled by the lithology of the host rocks. *Fissure karren* (*kluftkarren*) are more frequently formed in medium- and thick-bedded Cretaceous and Upper- and Lower Jurassic carbonates, whereas *network karren* almost always predominate in the Jelar-breccia. Formation of *fissure karren* in bedded carbonates is primarily associated with diastromes and diaclases. The formation of network karren is primarily controlled by brachyclases and leptoclases which directed corrosion (Bognar and Blazek, 1986). The formation of network karren in areas built of Cretaceous breccias and Jelar-breccias is controlled by extensive fracturing of unbedded carbonates, various grain sizes and hardness of cemented debris, and particularly better solubility of carbonate cement. The result are large surfaces covered by irregular-shaped network karren (Figure 5). Network karren formed on bedded rocks have more regular shapes (Perica, 1998). Their development is preferred on steeply inclined rocks, where corrosion acts along the diastromes and secondary fissures.

Karren channels formed along diastromes are significantly longer, and commonly deeper than other, primarily vertical channels.

Exhumed karren formed under pedologic cover are characterised by numerous elliptical or rounded hollows. Subsoil channel widths exceed 30 cm, rounded margins are common, bottoms are trough-shaped and channel sides smooth. Formation of this type of subsoil channel is a consequence of corrosion by water enriched with humus-generated biogenic CO<sub>2</sub>. This water acts corrosively in all directions, which affects simultaneous lateral expansion and deepening of the hollows. However, when the bottom of the channel is covered by residual clay, the corrosion is suppressed, as well as deepening of the channel.

Destruction of the woods by burning, sometimes for expansion of cultivated areas, as well as the dip of the slopes, caused strong soil removal (during abundant rainfall) and deflation (bora wind action) which eventually resulted in bare mountain slopes (Simeonović, 1921; Cvijić, 1927; Poljak, 1929a, b; Salopek, 1952; Rogić, 1958). Bögli (1980) states that exhumed karren, exposed for 100–200 years, are hardly recognizable due to corrosion by meteoric waters. The corrosion has been augmented also by strong heating of the rocks at the surface by forest fires (Perica, 1998).

Unlike the karren formed by the subcutaneous corrosion, the ones formed by direct corrosion by atmospheric water have significantly narrower sharp channels (*kluftkarren* and furrows) and crests (pinnacles). The atmospheric water corroding the carbonate substrate, quickly runs through the fissures, so their width/depth ratio is much larger than of other karren formed by the subcutaneous corrosion. Although the *grikes* depth usually exceeds 1 m, that is difficult to estimate due to their small width.

Formation of transitional karren types is related to carbonate substrate which is partly soil-covered, as on the SW slope of Veliki Golić (1,265 m a.s.l.) in the Paklenica National Park. Soil-filled *grikes* are developed along subvertical diastromes, and covered with vegetation, whereas the beds



Figure 5: Network karren (largely developed into debris-karren) developed in Cretaceous limestones, south Velebit mountain.

are bare and fractured. Pedologic cover is locally thick enough to support growth of big trees (Perica et al., 1995).

Particularly large grikes, which exceed 10 m in length, and attain depths of more than several metres are locally called “škarovi” and “škripovi”.

Karren have developed their ultimate stage on the central and lower SW Velebit Mt slope, where they form *debris karren* (locally called *grohot*). On slopes dominated by karren developed on gently inclined limestone beds, the formation of debris karren is promoted by lateral corrosion which prograded along diastromes. On steeper slopes gravitational processes have formed colluvial aprons made of debris karren.

“Sige”-karren (Figure 6) represent a particular type of network karren, and are in Paklenica National Park known also as “vuggy rock”. They are formed predominantly on gentler slopes ( $< 12^\circ$ ) of

glacio-fluvial fans which comprise predominantly small (up to a few cm) debris of Jurassic limestones and dolomites, and only locally on vegetated and stabilized colluvial fans. The bizarre shape of the vuggy rocks are a result of selective biocorrosion of glacio-fluvial breccias, as well as washing of the fine-grained debris and cement. The cavernous karren of this type are characterized by numerous shallow depressions and fenestrae (commonly akin to honeycomb) which have been formed by corrosion of more soluble debris (Perica et al., 1995).

Solution pans (*kamenitzas*) are developed on areas with bare Velebit Mt karst. They are several centimetres up to several decimetres deep, and the width and length span from several centimetres up to several metres. In exceptional cases their depth reaches more than 1 m, and the width can exceed 10 m. Gams (1974) differentiated *kamenitzas* which were formed under the pedologic cover



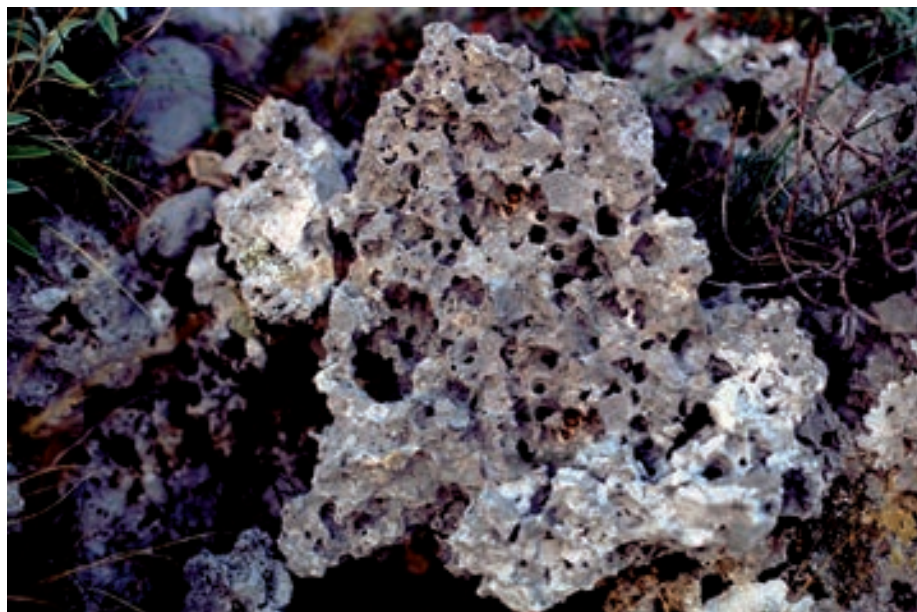


Figure 6: Tufa-like “sige”-karren (“vuggy rock”) is a particular type of karren formed in glacio-fluvial breccia in the Paklenica National Park.

by subcutaneous corrosion, and those formed on bare carbonate surfaces. The former are formed by biocorrosional deepening of primary hollows, and are characterised by a hemispherical cross-section, and lack overhung margins which is otherwise a characteristic feature. Formation of the second type of kamenitzas, or true kamenitzas sensu Gams (1974) is related to hollows on flat or gently inclined surfaces which were formed under the pedological cover by subcutaneous corrosion. These hollows Sweeting (1966) and Ford and Williams (1989) attribute to karren as “solution pans”. One of their characteristics is their more frequent occurrence on inhomogeneous rocks, which is the cause of their irregular shape (Ford and Williams, 1989). Sweeting (1966) holds that in just 10 years they can reach depth of 3-5 cm.

Development of the second kamenitza type (true kamenitzas; Gams, 1974) can be attributed to four phases, the first two being constructional and the second two degradational. The size, primarily the diameter, of this kamenitza type is controlled by the dip of rock face on which the karren is formed. They are significantly larger on flat or gently inclined surfaces, unlike on steeper slopes. Gavrilović (1964) reported their occurrence even on slopes steeper than 35°.

The first phase in the growth of kamenitzas is characterised by prolonged wetting by atmospheric water and its corrosive action in hollows without pedological cover. The width of these hollows is just several centimetres, and the depth only a few millimetres. Gradual lowering of the water level by desiccation, commonly enhanced biocorrosion which comes from decay of drifted organic matter (leaves, grass, algae, lichens and mosses) and promote corrosion which progrades towards the central and lower parts of the hollows by gradual steepening of their margins. As the water gradually becomes more saturated by dissolved carbonate in its lower part, and the uppermost part absorbs atmospheric CO<sub>2</sub>, the kamenitza is widest in its central part. Gradual lowering of the water level, and increase in saturation by dissolved carbonates towards the kamenitza bottom, decrease the intensity of corrosion, so near the bottom kamenitzas are again narrower. Simultaneously with kamenitza formation, there forms its outlet groove, which is in this first phase almost negligible. The groove is formed only during short periods of water run-off from a kamenitza, during and shortly after the rainfall, and occurs in the lowest marginal part of a kamenitza.

The second phase in the formation of kameni-



**Figure 7:** Kamenitza "Jezerce", Bojinac, south Velebit mountain. Note remnants of old kamenitza margins above the water level. Width of view is 7 m, in the middle.

tzas is characterised by increasingly stronger lateral widening, caused by corrosion. Its vertical development is negligible or stagnant because of accumulation of residual clays and decayed organic matter at the bottom. Simultaneously, groove incision becomes increasingly stronger. Although the incision of grooves starts more slowly than the incision of kamenitzas, it gradually becomes quicker than the incision of kamenitza bottoms. At the end of this phase, the run-off through the

groove becomes more pronounced, the water level in the kamenitza progressively falls due to combined run-off and evaporation, and the water becomes increasingly more saturated with dissolved carbonate. The size (diameter) of kamenitzas is controlled by the rate of groove incision, because when the bottom of a kamenitza levels with the groove, it stops growing and starts degrading.

The third phase in the formation of kamenitzas is characterised by the onset of their destruc-



Figure 8: Water-filled kamenitza "Samogred", south Velebit mountain, is 1 m deep and 8 m long. Width of view is 6 m.

tion. This is caused by progressive widening of the groove by lateral corrosion, and by destruction of the overhung part of kamenitza margin by regressive corrosion of the meteoric water. The kamenitza margin gradually loses its overhung shape and becomes rounded, whereas the groove becomes wider and trough-shaped.

The last, fourth phase in kamenitza development, is characterised by complete destruction of its overhung margin and widening of the groove, which commonly reaches (sometimes even exceeds) the kamenitza width. In this way kamenitzas become shelf-like or amphitheatre shaped. The once overhung margin becomes a place of

Figure 9: Pot-like karren.  
See lens cap for scale.



groove incision, which itself becomes meandering due to decreased slope inclination. This type of reshaping of kamenitzas is found on Bojinac in the Velika Paklenica National Park.

If a kamenitza reaches a fracture during its growth, it stops developing prematurely, because the water widens the fracture and creates a tube-shaped channel which eventually drains the water away. In this way, a kamenitza stops developing, but Gavrilović (1964) holds they may still form *karst wells*.

Kamenitzas developed on Jelar-breccias on the Velebit Mt are commonly irregular-shaped and characterised by uneven floors, as a result of clast as well as matrix/cement inhomogeneities.

The largest kamenitzas are developed on southern Velebit Mt on Jagin Kuk and Prosenjak localities. Here they reach diameters of several metres and depths of more than one metre. The kamenitza “Jezerce” (a pond in Croatian) is of particular

interest (Figures 7, 8). The remnants of overhung rims show that it was formed by merging of 5 kamenitzas in various stages of development, which formed one within the other. The oldest seems to be 14 m long, 7 m wide, and about 1 m deep. The fourth kamenitza, which is at the transition between the second and third development phase, is 7 m long, 4.5 m wide and 30 cm deep. The fifth kamenitza is the youngest, at the first phase of development, and is smaller than the previous ones.

The frequency and size of kamenitzas is controlled, in addition to lithology, also by the climate. Kamenitzas are relatively rare on the lower parts of the SW slope of the Velebit mountain and its summit, because the lower slope is characterized by strong evaporation (1,000 mm) and relatively low rainfall (1,200 mm) (Perica and Orešić, 1999) which has a negative influence on corrosion development. On the Velebit Mt summit, the low temperature (average annual temperature reaches



Figure 10: Karren well "Čelinka", Paklenica National Park. Width of view is 2.5 m.

3.5°C) presents a factor which limits development of kamenitzas because at these temperatures cryogenic processes are dominant. Kamenitzas are most frequent, and largest, on the middle part of the Velebit Mt SW slope (400–1,100 m a.s.l.) where mild temperatures prevail (average annual temperature of 10°C), with relatively high rainfall (1,500–2,000 mm) and lower evaporation.

Locally, there occur small depressions with diameters of a few millimetres up to several centimetres which were formed by biogenic corrosion – *root karren*. Two types of biokarst features can be differentiated: a) formed under the pedologic cover by corrosive action of plant roots, and b) formed on bare rocks by corrosion created by bacteria, lichens and mosses. The first type of root karren formed by humic acids is quite rare. They are rapidly destroyed during denudation of mountain slopes even by corrosion of atmospheric water. Bögli (1980) states that this type of karren will not be recognizable after a century of exposure. This is particularly true in the case of small depressions, whereas those larger forms will

trap atmospheric water and will be subjected to extended corrosion and gradually transform into other types of karren (e.g. kamenitzas). The second type of biokarst features is morphologically identical to the first type, but is formed by biocorrosion of bare rock faces by lower plants. Algae receive moisture from the air and, in addition to biogenic CO<sub>2</sub>, they also receive atmospheric CO<sub>2</sub> from meteoric water (Ford and Williams, 1989). However, deepening of this type of karren is commonly obstructed by residual clay at their bottom.

The lower parts of the SW Velebit Mt slope which are predominantly built of the Jelar-breccia, are characterized by occurrence of *pot-like karren* (Poljak, 1929a). The primary feature of this karren type is the occurrence of chains of small pots (Figure 9). The pots are rarely wider than 5 cm, and 2–3 cm deep. They occur most often on rock faces inclined 20–50°, which were previously exposed to corrosion. The pot-like karren are being formed on rotated blocks where water remained trapped in small depressions, and induced development of small kamenitzas. Their development was also

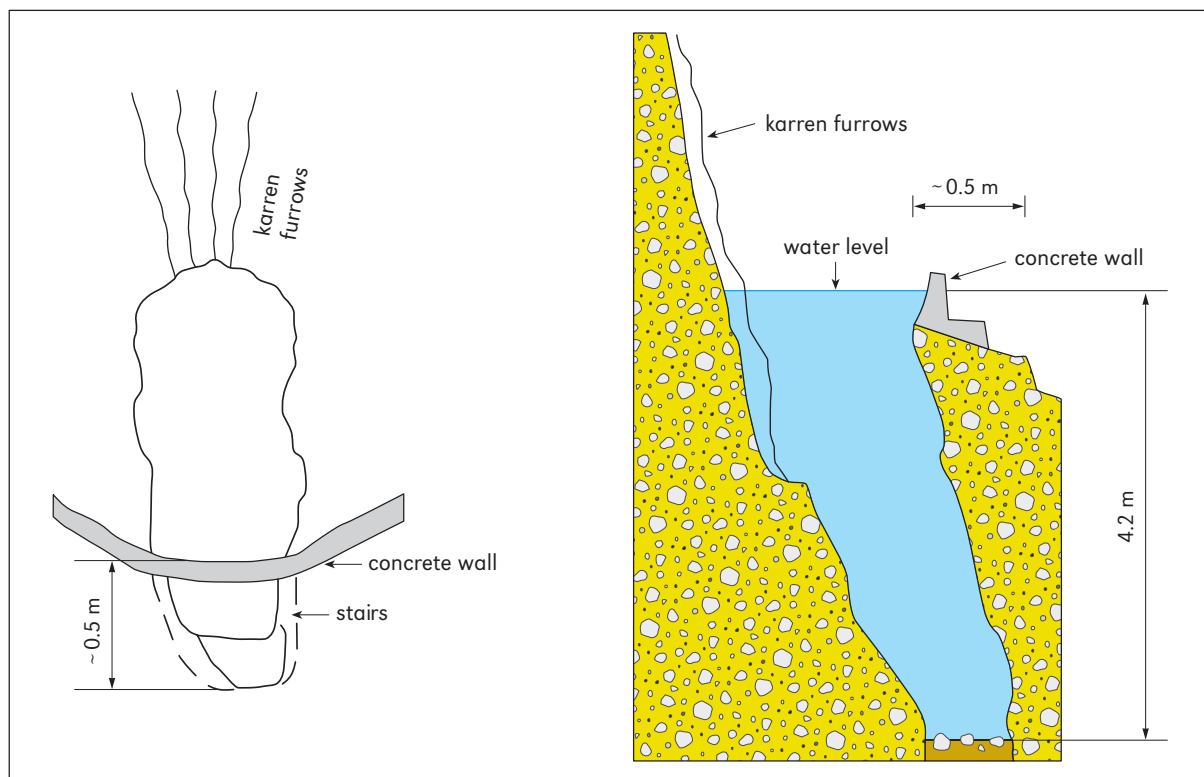


Figure 11: Karren well "Čelinka", diving revealed water depth of 4.2 m in early June.

promoted by differential resistance of various clasts to erosion. Individual pots are later connected by small grooves. Pots may be sometimes connected by lateral biocorrosion. When two pots connect they are known as doublets or twins, and if three pots occur connected they are triplets. In a case when more pots connect, they are called platters or saucers (Rubić, 1936). Prolonged development of grooves due to regressive and lateral corrosion destroys the platters which remain only in form of smaller flatter widenings.

Specific karst features which were formed by the sinking of larger quantities of water are *karren wells* (Figures 10, 11). They most often form in places where *rinnenkarren* furrows develop along a fissure in a semi-circular manner. Because the water flows down these gutters, it concentrates in a small area at the bottom, which promotes stronger corrosion and, consequently, its deepen-

ing. The karren well bottoms are filled with residual clays and silts, which completely seal fissures in some of the wells, making them impermeable. In this way some of the karren-wells permanently or semi-permanently hold water. The Čelinka *karren well* which occurs at 755 m a.s.l. near Vidakov Kuk, is 1.5 m long, 0.7 m wide and 4.5 m deep, and holds water throughout the year which seldom lowers below a water mark at 4 m. The walls of the Čelinka well are fluted down to the depth of 2.2 m, and smooth below. Its bottom is covered by residual fine mud and clay with scattered small rock debris, which makes a layer locally more than 50 cm thick. The analysis of water from this karren well (Perica, 1998) showed (at the time of sampling in the dry season) pH 8.48, which does not explain uniform corrosion of the well walls, and smoothing of the edges of submerged flutes.

## Conclusion

Although the formation of karren is characteristic of parts of the Velebit Mt which are of carbonate rocks, they are best exposed on its SW slope. This is primarily a result of anthropogenic deforestation. Denudation of the mountain slope exposed numerous types of *subcutaneous karren*. Their development is still intensive below the pedologic cover on other parts of the Velebit Mt, as shown by karren which become exposed on recently denuded surfaces.

The size of rinnenkarren features is larger on the middle and lower parts of the SW Velebit Mt slope, than on its higher parts, which confirms Bögli's (1980) hypothesis that their development continued also during the last Ice-Age. This is also confirmed by the development of furrow-like karren in the Julian Alps at altitudes up to 2,500 m a.s.l. (Kunaver, 1985), at an average annual air temperature of  $-1.8^{\circ}\text{C}$  (Bernot, 1985). It has been inferred that the Velebit Mt slopes at 500 m a.s.l. had same average annual temperature during the

Würm period, and that it locally reached even higher values due to south-western slope exposure. Fissured carbonates prevented accumulation of water, which would freeze at low temperatures, and surely cause mechanical destruction of the fissure- and network-type of karren.

During the Pleistocene glaciation, the high parts of the Velebit mountain were affected by periglacial, and the summit parts by glacial processes which destroyed older fissure- and network-type karren. Destruction of fissure- and network-type karren by periglacial processes was interpreted as a major contributory to formation of a pediment during the Quaternary on the SW Velebit Mt slope (Bognar, 1992).

The intensity of postglacial corrosion is demonstrated by the development of large furrows in the highest parts of the Velebit mountain, which confirms observations from the Orjen Mt high parts (Riđanović, 1964, 1966). Development of the large furrows on the Velebit Mt high parts can be explained by significantly stronger corrosion of water in cold mountain climates (Corbel, 1959).

# MID-MOUNTAIN KARRENFIELDS AT SERRA DE TRAMUNTANA IN MALLORCA ISLAND

Joaquín GINÉS and Angel GINÉS

Mallorca island is located roughly at the middle of the Western Mediterranean basin (39°N latitude and 3°E of Greenwich) being a fully representative territory of this particular geographical macro-unit. The geological setting of the island, largely formed of limestone rocks, and its typical mediterranean bioclimatic conditions produce several distinctive karst landscapes, the most outstanding being the Serra de Tramuntana range. This region is the main mountain area in Mallorca, having a surface of approximately 1,000 km<sup>2</sup>, about 65% of that being limestone outcrops.

Karren landforms of Serra de Tramuntana gained the early interest of naturalists (Lozano, 1884). In the second half of the 20<sup>th</sup> century, some researchers from central Europe (Mensching, 1955; Bögli, 1976; Bär et al., 1986) pointed out the spectacular nature and geomorphological richness of the exokarst in the Mallorcan mountains. More recently, from the nineties, a lot of literature has been devoted to surface solutional features in Serra de Tramuntana, ranging from morphological and morphometrical aspects to genetic or evolutive ones; an exhaustive bibliography is given in Ginés (1999a).

The exokarst in the studied area is characterized by a remarkable variety of solutional forms. These are the result of a wide diversity of environmental situations, basically controlled by climatic gradients linked to the altitude (ranging from sea

level to above 1,400 m). The impact of human activity over the last 5 millennia, together with other mechanisms of natural deforestation, have produced a complex evolutive history of the existing karrenfields within a mid-mountain bioclimatic and geomorphological framework.

## Geological and bioclimatic setting

The Serra de Tramuntana lies at the north of Mallorca island forming an abrupt mountain chain, 90 km long and 15 km wide, elongated NE–SW (Figure 1a). Their highest altitude is at Puig Major (1,445 m) with over fourteen other peaks higher than 1,000 m. It is composed of a complex system of folds and thrust sheets, formed by compressive stresses pushing from the SE to the NW. These structures resulted from an alpine tectonic event that took place between the Late Oligocene and Middle Miocene, involving rocks that range from Upper Palaeozoic to Lower Miocene (Gelabert, 1998). In broad terms the structure of the Serra is an assemblage of imbricated sheets piled up towards the NW and aligned NE–SW, integrating the emerged area of the so-called Balearic Promontory that is in fact a prolongation of the Betic chains. The compressional alpine features are capped by Upper Miocene to Quaternary post-orogenic sediments (Figure 1a).



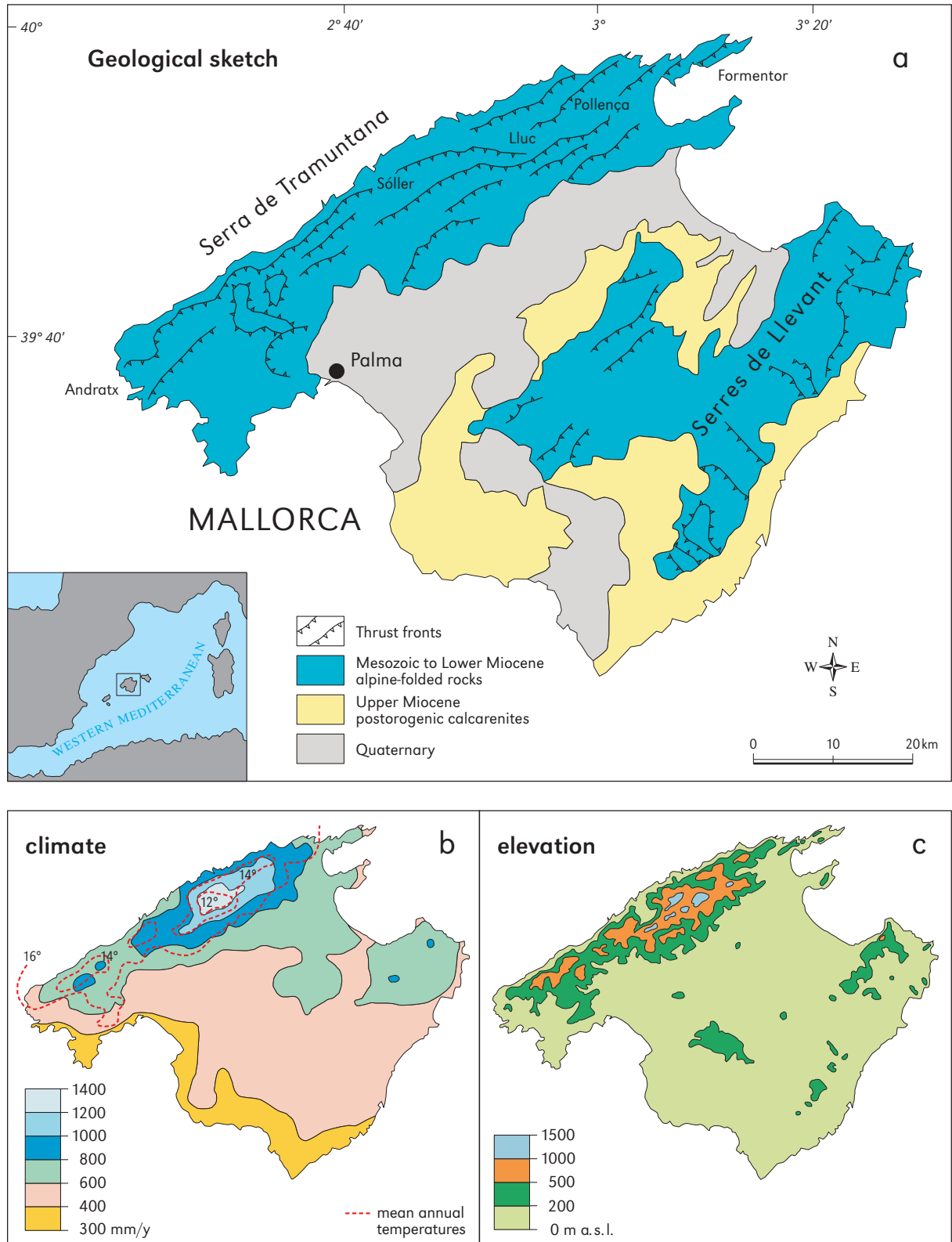


Figure 1: Geographical information on Mallorca island: a. main Mallorcan litho-structural units and situation of sites referred to in the text; b. distribution of the average annual rainfall and temperature values; c. simplified altimetry map.

The geologic structure briefly described above has formed a succession of high energy relief mountain alignments, that have steeper cliffs in the northern side and relatively gentler slopes to the south determined by the general dip of the limestone beds towards the SE. The repetitive alternation of limestones and marly or shale materials due to the sheet imbrications, contributes to the characteristic sawtooth profile that is seen in a transverse NW–SE section of this range.

The lithologies are diverse (marls, shales, sandstones, gypsum, volcanic rocks, etc.) but the limestones are by far the dominant ones (Fornós and Gelabert, 1995). Specifically, karst landscapes are developed on Jurassic (Lower Lias) micritic limestones and Lower Miocene (Burdigalian) calcareous conglomerates and calcarenites. The rocks from both stages are lithologically quite similar and notably pure: insoluble residue ranges between 1 and 10% and Mg content is always < 4%. The only differences between them are textural; the Lower Miocene deposits are very coarse – but supported by a micritic matrix – in comparison with the fine-grained Jurassic limestones. The karstifiable rocks in Serra de Tramuntana are mechanically hard, giving Schmidt hammer values between 40 and 52.

An important role in karst development is played by the Triassic (Keuper) marly deposits. Firstly, these rocks have a relevant hydrogeological function acting as impervious substratum for the underground circulations, in addition to their above-mentioned contribution to the structural and topographical configuration of the Serra. Secondly, these marls supply abundant loose material that contribute significantly to the subsoil shaping of many karrenfields.

Climate in the area is typically mediterranean (Guijarro, 1995), characterized by an important summer drought from June to September. Rainfall reaches up to 1,400 mm/yr in the central, highest, portion of the range, decreasing strongly towards the lower periphery of the mountain chain (< 500 mm/yr, in the SW and NE ends); thus, the rainfall pattern follows that of the elevation (Figure 1b, c).

Snowfalls are scarce and now limited to the highest elevations during a few winter days. Intense stormy rain events (over 250 mm in 24 hours) are not exceptional, particularly in autumn months, due to sudden cold air irruptions – in the middle and upper parts of the troposphere – over a very hot Mediterranean Sea water mass.

Mean annual temperatures range from 12°C in the central highest part of the mountain range, to 17°C in the outermost Formentor and Andratx ends. Seasonal variability is noticeable, with winter mean temperatures below 10°C and summer ones close to 25°C. In general terms, climate in Serra de Tramuntana is that of mid latitudes but modified by the azonal anomaly provided by the Mediterranean Sea. Within this general context, great differences in rainfall and temperature values, linked to altitude, determine local microclimatic conditions ranging from humid to semiarid.

Vegetational stages found in the region are related to this environmental variability imposed by macro- and micro-climatic controls. Dense woods of holm oak (*Quercus ilex*) are the community best adapted to the relatively humid, but seasonally dry conditions which dominate most of this mountain range. Forests of Aleppo pines (*Pinus halepensis*) are well developed in the drier environments, corresponding to the lower altitudes and the outermost ends of the area. Finally, the tree line lies at about 800 metres a.s.l., forests being replaced at the karstified summits by shrub formations very rich in endemic species: the so-called “balearic stage”.

Cultivable lands are restricted to non-karstifiable rock outcrops (mainly Triassic and Cretaceous marls), although a lot of stone wall terracing was made in some limestone slopes for olive tree cultivation. Due to the presence of extensive karrenfields in Serra de Tramuntana range, the agricultural exploitation of these karstic landscapes is minimized by the lack of arable lands. For this reason, the major primary human activities were historically extensive grazing (sheep and goats) together with periodic burning of brushwood in order to renew the grazing cover (Ginés, 1999b).

## Elementary karren features represented in the area

Karren are the most striking and widespread karstic landforms in Serra de Tramuntana region (Ginés and Ginés, 1995). Particularly, the limestones outcropping in the north-eastern half of the area (between Sóller and Pollença villages) constitute great expanses of bare rocks (Figure 2) on which spectacular *karrenfields* extend continuously for several km<sup>2</sup>. These karren areas show their best examples at moderate altitudes (from 200 to 600 metres a.s.l.), frequently forming al-

most impassable terrains jagged with sharp ridges and pinnacles separated by deep grikes. The range of micro- and meso-forms is remarkable (Bär et al., 1986; A. Ginés, 1990, 1998b), many of them having attracted the attention of researchers in the last decades, as shall be discussed below.

### Solution flutes and related features

Starting with the most simple and elementary solution feature, *rillenkarren* are undoubtedly the most investigated microforms in the Mallorcan



Figure 2: Typical appearance of extensive karrenfields in the heart of Serra de Tramuntana. The doline at the bottom of the image is named Clot de l'Infern, being located near Torrent de Pareis, at Escorca municipality.

mountains, being practically ubiquitous over the whole area (Figure 3). Nevertheless, it is clear that this karren feature – as has been defined by Ginés (1996b) – has in Serra de Tramuntana an altitudinal limit at around 800 metres a.s.l. A lot of work has been done on the morphometry of rillenkarrén in this region (Bordoy and Ginés, 1990; Crowther, 1998; A. Ginés, 1990, 1996b, 1999a; Mottershead, 1996a) which provides some data that set the size limits for this form. Morphometric parameters established by those authors are as follows: width from 1.4 to 2.1 cm, length between 12 and 50 cm and depth ranging from 2.8 to 6.3 mm.

Several of the above-mentioned parameters are strongly dependent on a very simple variable: the altitude and the corresponding climatic gradation. Thus, both rillenkarrén length and depth show a clear negative correlation with altitude (Figure 4), the rills becoming shorter and shallower as they approach or surpass the tree line. However, width is the most stable parameter (Ginés, 1996b), showing no dependence on elevation. It is worth mentioning, however, the existence of solutional flutes wider than typical rillenkarrén (from 2.5 to 4.0 cm) restricted to the highest summits of the range,

always at elevations greater than 800 metres. These forms are interpreted as decantation flutes related to snow (Ginés, 1996b), which obviously was more frequent during Pleistocene cold events. That author also refers to wide flutes (mean widths close to 2.5 cm) in particular environmental conditions, corresponding to a cleared forest which keeps up a partial cover of holm oak (*Quercus ilex*). In this last case, a greater water drop size caused by the forest canopy could be responsible for the anomalous width of flutes.

Some other morphological and evolutive properties of rillenkarrén have been investigated, mainly in the renowned site of Lluc, at the heart of Serra de Tramuntana (520 metres in altitude; mean annual precipitation > 1,000 mm). Mottershead (1996a) studied variations in rillenkarrén cross-sections along their longitudinal profile, noting a negative correlation between rill depth and slope angle of the rock surface. At the same time it was observed that depth increases rapidly downwards from the rock crests – mainly along the upper third part of the flute – decreasing afterwards more gently, whereas width remains constant over the whole longitudinal profile; this fact



Figure 3: Well developed rillenkarrén features in Lower Miocene rocks at the mid-mountain site of Mortitx (Escorca).

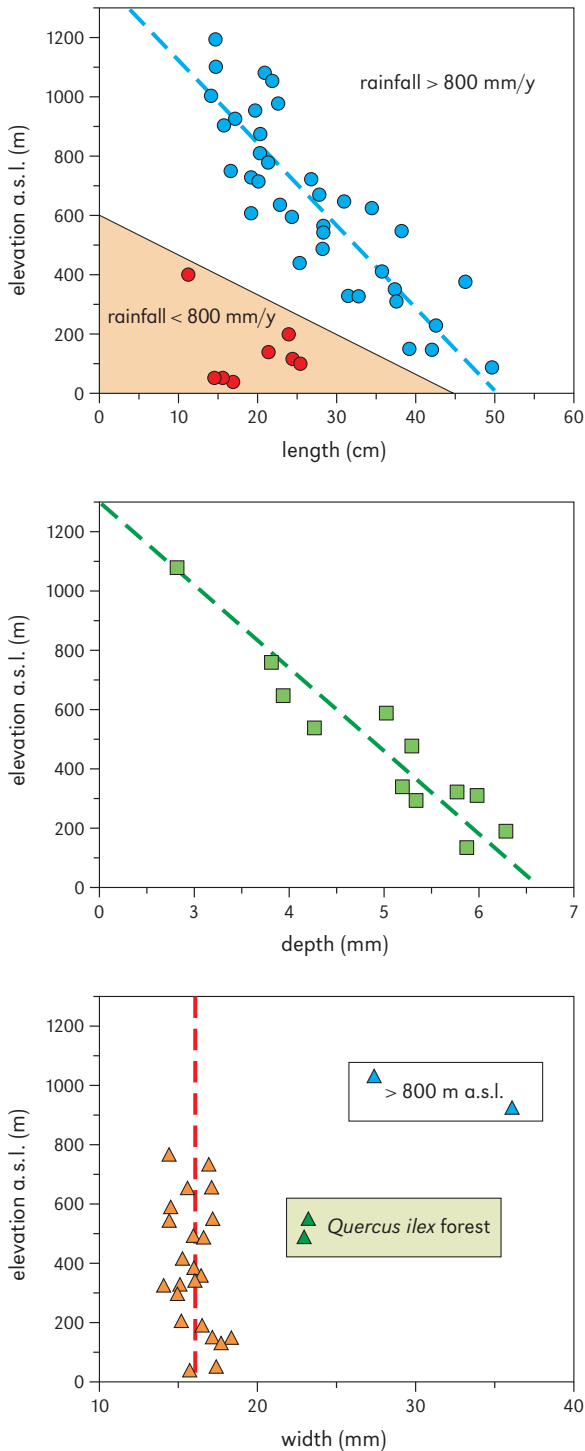


**Figure 4:** Morphometric parameters of rillenkarrren in Serra de Tramuntana plotted against elevation of the sampled localities. Length: average values of the 10 longest flutes in 45 measured sites; depth: average values from 14 different localities (n = 100 flutes/site); width: average values from 26 different localities (n = 100 flutes/site).

suggests a higher rate of flute channel lowering in its upper part. Moreover, Crowther (1998) reported a noteworthy asymmetry of rillenkarrren cross-sections, which are composed of two independent parabolic half-sections. The observed asymmetry could cause a lateral migration of rillenkarrren sets, maintaining still their form and size due to a kind of dynamic equilibrium.

The current knowledge of Mallorcan rillenkarrren shows that their morphometry is a very effective environmental indicator, reflecting altitude-controlled climatic gradients: rainfall increasing and, particularly, temperature decreasing with elevation (A. Ginés, 1990, 1996b, 1999a).

An additional interesting aspect of rillenkarrren is the participation of *biokarstic processes* in shaping these elementary forms. Fiol et al. (1992, 1996) demonstrate that the mechanical removal of small limestone particles, detached by the impact of raindrops, is an efficient process affecting rillenkarrren growth. This detachment is greatly favoured by the presence of algae that have previously corroded the rock surface, with the subsequent weakening of its crystalline structure.

### Runnels and associated forms

Solution channels of various types – generated by water runoff on limestones and decimetric to metric in size – are common where bare karren areas form the landscape. Their morphology is strongly controlled by some medium scale topographic effects, such as the slope of rock surfaces. Most common are the funnel cross-section *runnels* (a sort of *rinnenkarren* feature) more or less incised into the flanks of major karren macroforms such as pinnacles (Figure 5).

Runnels with an overall long profile gradient greater than 35° are the most common in the Serra, usually reaching several metres in length and up to 1 metre in depth. Rinnenkarren of those characteristics have their longitudinal profile interrupted by gentle-sloped segments (from 5° to 20°) that can extend up to as much as 1 m<sup>2</sup>, whereas their

**Figure 5:** Typical karst landscape in Serra de Tramuntana (Muntanya, Escorca). This characteristic karren assemblage is a combination of rillenkarren, trittkarren, rinnenkarren and regenrinnenkarren features, sculpturing the ridges of pinnacles (spitzkarren) which emerge over a cleared holm-oak forest. Elevation of this site is 550 m a.s.l., and rainfall values surpass 1,000 mm/yr.



plan development is rather straight. These flatter areas along the runnel's profile faithfully resemble *trittkarren* features as defined in the German literature (Bär et al., 1986); however, some authors prefer to simply refer to them as *steps* or *stepped flats* spaced along the rinnenkarren long profile (Crowther, 1997). In this last paper it is suggested that small bevels or steps randomly evolve from minor irregularities, due to the slower dissolution occurring in horizontal segments compared with the greater lowering of steeper slopes. This behaviour is attributed to the thicker boundary layer of flow on the horizontal steps, that makes them slower developing forms in comparison with the enclosing subvertical backwalls of the runnels.

Where the slopes of the rock surface are lower than 30° rinnenkarren are also present, but associated with increased sinuosity of the runnels. In this sense, Hutchinson (1996) observed increases of 0.3 in the sinuosity index with every 5° decrease in the runnel slope; so, sinuosity values near 1.0 correspond to high gradient runnels (> 35°) but reach up to 1.5 in more gentle (25°) rinnenkarren. In still flatter areas, Hutchinson (1996) reports real *mäanderkarren* on rock slopes between 7° and 14°.

In the vast majority of cases, these present-day rinnenkarren features derive from prior forms initiated and partially evolved under soil cover. This fact is widespread in the general karrenfield evolution in the Serra de Tramuntana (A. Ginés, 1990, 1995a; Ginés and Ginés, 1995), as will be argued later. In some particular sites (for example, near Ses Basses de Mortitx, Escorca) there are fully-rounded runnels (*rundkarren*) separated by metric-sized smooth ridges, which have little or no superimposition of bare karren features such as rillenkarren. Finally, it must be pointed out that the walls of grikes and pinnacles are intensely sculptured by diverse vertical runnels and wide flutes, such as *regenrinnenkarren* (solution flutes of the second order, after Bögli, 1980) and *wandkarren*; these forms contribute strongly to the isolation of big pyramidal units of spitzkarren or pinnacles.

Generally speaking, runnels are well developed at elevations from 200 to 800 metres a.s.l., where the best karren sites of the Serra occur. At greater elevations some localities (e.g. Puig Major massif) show modest rinnenkarren and mänderkarren, developed on gentle slopes and associated with melting snow-patches.



**Figure 6:** Famous camel-like pinnacle – popularly known as Es Camell – existing in the karren-fields at the surroundings of Lluc monastery (Escorca). Carbonate rocks are Lower Miocene in age.



**Figure 7:** Spectacular vertical runnels in Jurassic limestones from the Es Castellots massif (Escorca). Elevation of this locality is around 500 m a.s.l.

### Pinnacles and grikes

Undoubtedly the most spectacular karren examples in Mallorca are on the limestone ranges of Escorca municipality, at the central part of Serra de Tramuntana. In that area, karrenfields like those situated between Lluc monastery and Menut farmhouse (inside a cleared holm oak forest setting) or other localities such as Mortitx and Sa Calobra (in totally deforested conditions) form almost impassable areas, because an impressive pinnacle or *spitzkarren landscape* is the dominant feature (Figure 6). The sites referred to are always located below 700 metres a.s.l., being chiefly developed on the Lower Miocene coarse limestones and conglomerates.

The solutional forms which comprise these karrenfields consist of large pyramidal pinnacles – frequently more than 200 m<sup>2</sup> in plan and exceeding 10 metres of height – separated by deep clefts or grikes whose walls are sculptured by abundant vertical runnels (Figure 7). The pinnacle flanks are cut by large stepped runnels, such as those previously described. In detail, the ridges of pinnacles

(and rock crests in general) exhibit an extensive sculpturing by very sharp rillenkarren, making an extremely jagged and uninhabitable environment. The hydrological efficiency of karrenfields of this kind is noteworthy, since rain is almost completely infiltrated through solutionally widened fissures (*grikes* or *kluftkarren*). The spot known as Sa Mitjania – also in Escorca municipality – is a typical example of landscape with minimized surface run-off due to karren development; it has large solutionally sculptured pinnacles separated by small dolines, grikes and even deep shafts (J. Ginés, 1990).

The individual features that constitute the spitzkarren or pinnacle extensions in Serra de Tramuntana show clear evidences of subsoil dissolution (Figure 8), which took place during the first stages of the evolution of these karrenfields (A. Ginés, 1990a, 1995a, 1998b). Such *cryptolapiaz* (subcutaneous) inheritance is evident from the roughly rounded appearance of the ridges forming the emergent pinnacles and even in the rather rounded appearance of most of the rinnenkarren. Modern subsoil sculpturing can be seen at the bottom of the clefts between the pinnacles. These subsoil inheritances become progressively masked, in many cases almost totally, by bare surface solutional types (rainpits, kamenitzas, rillenkarren, regenrinnenkarren, wandkarren, etc.) as has been described at Son Marc site – between Lluc and Polença village – by Smart and Whitaker (1996).

### Other minor solutional sculpturing

Non-linear forms are represented by a wide range of types whose distribution patterns can be quite different to the solutional features described above. For example, whereas *solution pans* (or *kamenitzas*) may be considered ubiquitous in relatively flat limestone outcrops, *rainpits* show a geographical distribution restricted to the more arid spots of Serra de Tramuntana. Specifically, centimetric cup-like rainpits are abundant in the periphery of the mountain range, that is to say in the



Figure 8: Clearly smoothed and rounded karren features (rundkarren) observable in Lower Miocene rocks at Ses Basses de Mortitx (Escorca).

areas located at low altitudes (< 200 metres a.s.l.; annual precipitations < 700 mm) and in particular at its SW and NE extremes, such as the famous tourist place of Formentor.

Another karren microform linked in some manner to arid locations are *rillensteine* (*micro-rills*). These very tiny millimetric rills and spikes can be found in abundance at the drier ends of the range, frequently related to marine spray during heavy storms. However, that *rillensteine* also occur in more humid conditions (karrenfields situated from 500 to 800 metres a.s.l.) but associated with water supplies in the form of dew. At greater elevations, lichen colonization can competitively hinder the generation of microkarren features, such as *rillensteine* or even larger flutes such as *rillenkarren* (Ginés, 1999a). In the highest summits, subvertical or very steeply dipping rock surfaces become sculptured by forms transverse to the water flow, consisting of *horizontal cockling patterns* which produce concave shapes resembling ripples. These last features are located at elevations above 1,000 metres a.s.l., with mean annual precipitation that exceeds 1,000 mm and includes occasional snowfalls.

An interesting aspect is related to the roughness of the rock surfaces, a topic investigated in depth by Crowther (1996, 1997). That author



measured the so-called *Mean Gradient Change* of rocky surfaces with an approximate 1 mm resolution, finding the lowest roughness values (MGC = 6°) in smooth features such as the stepped flats (trittkarren) embedded inside the rinnenkarren channels. On the other hand, the highest roughness is related to rillenkarren and rinnenkarren forms, with MGC values of 8.8° and 11° respectively; these high values were attributed to the turbulent flow occurring in runnels and flutes, compared with the laminar flow on flatter slopes. Finally, strongly *etched surfaces* characterized by a sharp microtopography can be observed in the more arid parts of the Serra, together with abundant rainpits and microrills. In some sites these etched rock surfaces appear associated with marine spray in the supralittoral zone. No data are available on roughness in these specific coastal and arid environments, but Crowther (1996) refers to very high MGC values, between 15° and 25°, from supralittoral karren on the eastern coast of the island.

## The karren assemblages and their ecological significance

Observation of karst landscapes throughout the study area allows recognition of several distinctive karren assemblages, whose distribution clearly shows strong regularities. For example, it has already been reported in the literature that the solutional forms present in the highest summits of the range are very different to those at the lowest elevations, where a semi-arid climate occurs. Likewise, any journey through the Serra shows that the best developed karrenfields in Mallorca are found in quite specific environmental conditions: precipitation > 800 mm/yr; elevation between 200 and 700 metres a.s.l.; and other factors such as the presence of suitable lithologies.

A first approximation aimed at defining the karren assemblages observable in Serra de Tramuntana was developed by Ginés (1996a). That author sampled 100 sites, along the whole range,

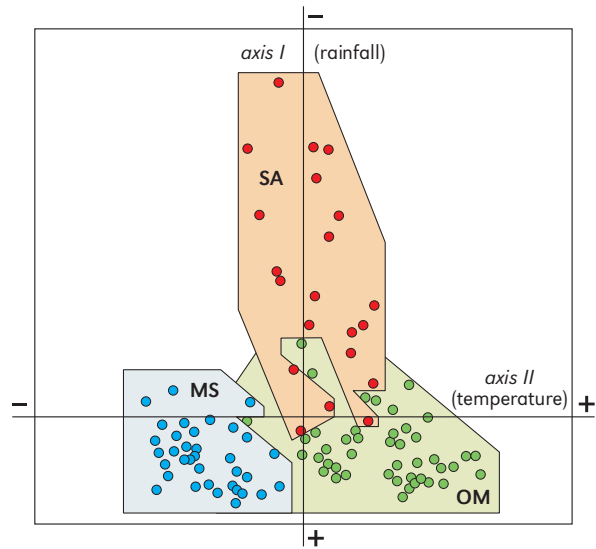


Figure 9: Results of the geo-ecological factorial analysis of karren assemblages, performed using 20 morphological karren-descriptors as well as the characteristic plant species from 100 sampled sites. The distinguished assemblages are: OM. optimum mediterranean mid-mountain karren; MS. mountain summits karren; SA. semi-arid karren.

using a semi-quantitative method which takes into account both the abundance of 20 karren types as well as the characteristic plant species found at each site. Vegetational descriptors were the presence/absence of some species considered good indicators of the environmental variability. The data were treated by factorial analysis (Figure 9) and the results support the distinction of the three main karren assemblages listed below:

- 1 **semi-arid karren**, characterized by common rainpits, rillensteine and irregularly etched surfaces, located on southern exposures at the periphery of the range (usually < 200 metres a.s.l.), where rainfall do not reach 800 mm/yr and xeric plant associations are dominant;
- 2 **optimum mediterranean mid-mountain karren**, exhibiting long rillenkarren and rinnenkarren, together with other types such as trittkarren, regenrinnenkarren, etc., all integrated into a spectacular spitzkarren landscape (Figure 5). This is found in mid-mountain lo-

calities (200 to 800 metres a.s.l.) with precipitation ranging from 800 to 1,000 mm/yr, mainly on southern exposures and associated in many cases with cleared holm-oak forests;

- 3 **mountain summit karren**, present at high elevations (> 800 m a.s.l. on northern exposures, and > 1,100 m on southern ones), where more than 1,000 mm/yr of precipitation occur including some winter snowfalls. This assemblage is defined by the dominance of small decantation flutes (wider than rillenkarrén), kluftkarrén and transversal cockling patterns, together with a few runnels and mäanderkarrén (Figure 10). From the vegetational point of view, this appears linked to the peculiar shrub formations of the so-called “balearic stage”.

The above assemblages are complemented by two more karren associations related to small scale climatic variability linked – for instance – to differences in temperature and humidity between sunny and shady exposures, or to the availability of rock surfaces for colonization by lichens. Therefore, two more karren assemblages must be taken into account both characterized by biokarstic weathering:

- 1b **semi-arid biokarstic karren**, on localities with



Figure 10: Special karren assemblage of the highest summits of Mallorcan mountains (> 800 m a.s.l.). At localities such as Puig de Massanella (Escorca) the predominant forms are a type of solution flute wider than rillenkarrén (decantation flutes) as well as kluftkarrén (scale bar = 20 cm).

annual rainfall less than 800 mm, showing poorly developed solutional features and rock surfaces extensively colonized by xeric lichens, as happens in the Andratx area at the SW end of the range;

- 3b **wet mountain biokarstic karren**, restricted

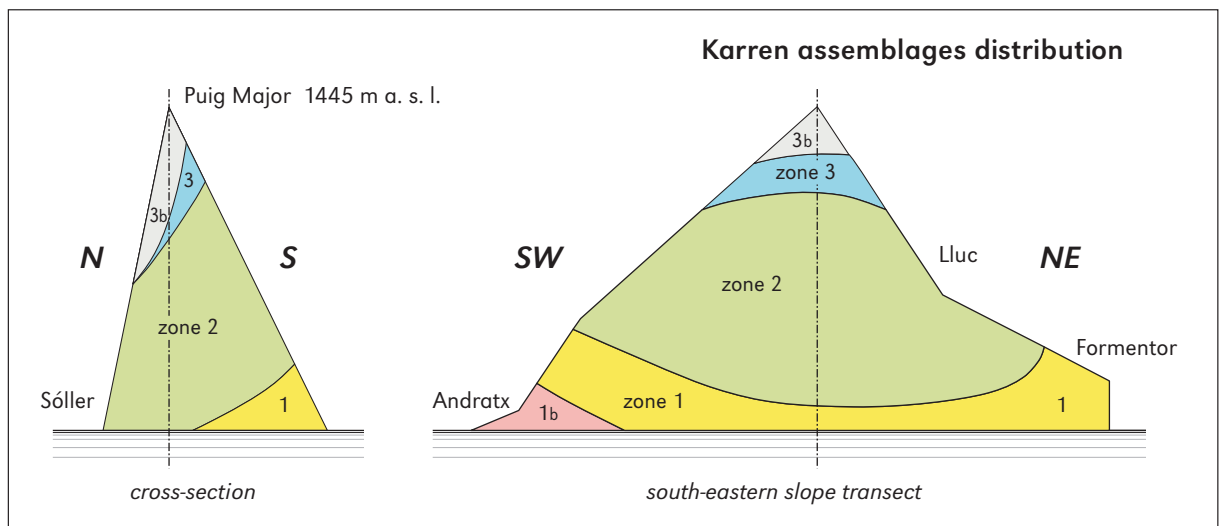


Figure 11: Distribution of the existing karren assemblages, shown on two idealized profiles of Serra de Tramuntana. 1. semi-arid karren; 2. optimum mediterranean mid-mountain karren; 3. mountain summits karren; 1b. semi-arid biokarstic karren; 3b. wet mountain biokarstic karren.



**Figure 12:** Pinnacle landscape at Míner locality (Pollença). These karrenfields evolved from subcutaneous forms through progressive and diverse deforestation and soil loss mechanisms.

to moist and shady northern exposures in the high peaks of the Serra (precipitation > 800 mm/yr), sites where intense colonization by lichens takes place.

The spatial distribution of these five karren assemblages is represented in Figure 11 using two idealised cross-sections of Serra de Tramuntana. This diagram shows how the location of the most spectacular karrenfields (2) corresponds to the mid-altitude parts of the range; it is also evident that climatic gradients related to topographical relief are controlling the distribution of other well differentiated assemblages both around the periphery of the area (1, 1b) and on the highest summits of the mountain chain (3, 3b).

## Karrenfield evolution

When describing the different solutional forms represented in Serra de Tramuntana, the subsoil origin of most karrenfields was emphasized. This is true in almost all of the environmental situations distinguished in this range, being evident a first morphogenetic stage characterized by a

strong development of subcutaneous karren features corresponding to a former vegetal cover adapted to the regional and local climatic conditions (Ginés, 1998b, 1999a). A subsequent phase consists of the progressive exhumation of the previously generated cryptolapiaz (Figure 12), as a result of the negative balance between generation and loss of soil (A. Ginés, 1995); this second stage includes the superimposition of a great variety of bare solutional forms (rillenkarren, rainpits, kamenitzas, etc.).

Smart and Whitaker (1996) followed that approach in a case study on the karren assemblages encountered at distinct elevations above the valley floor in Son Marc site, near Pollença. In that locality, exokarst development is characterized by the differential lowering of the soil-covered rock surface, which preferentially occurs along subvertical joints initially to form stripped rock ridges. Soil losses linked to incision of stream courses indicate the advance of bedrock exposure, with the formation of incipient kamenitzas and rillenkarren. Later, rinnenkarren features are increasingly developed on the steep-sided ridge flanks, at the same time that differential relief is created be-

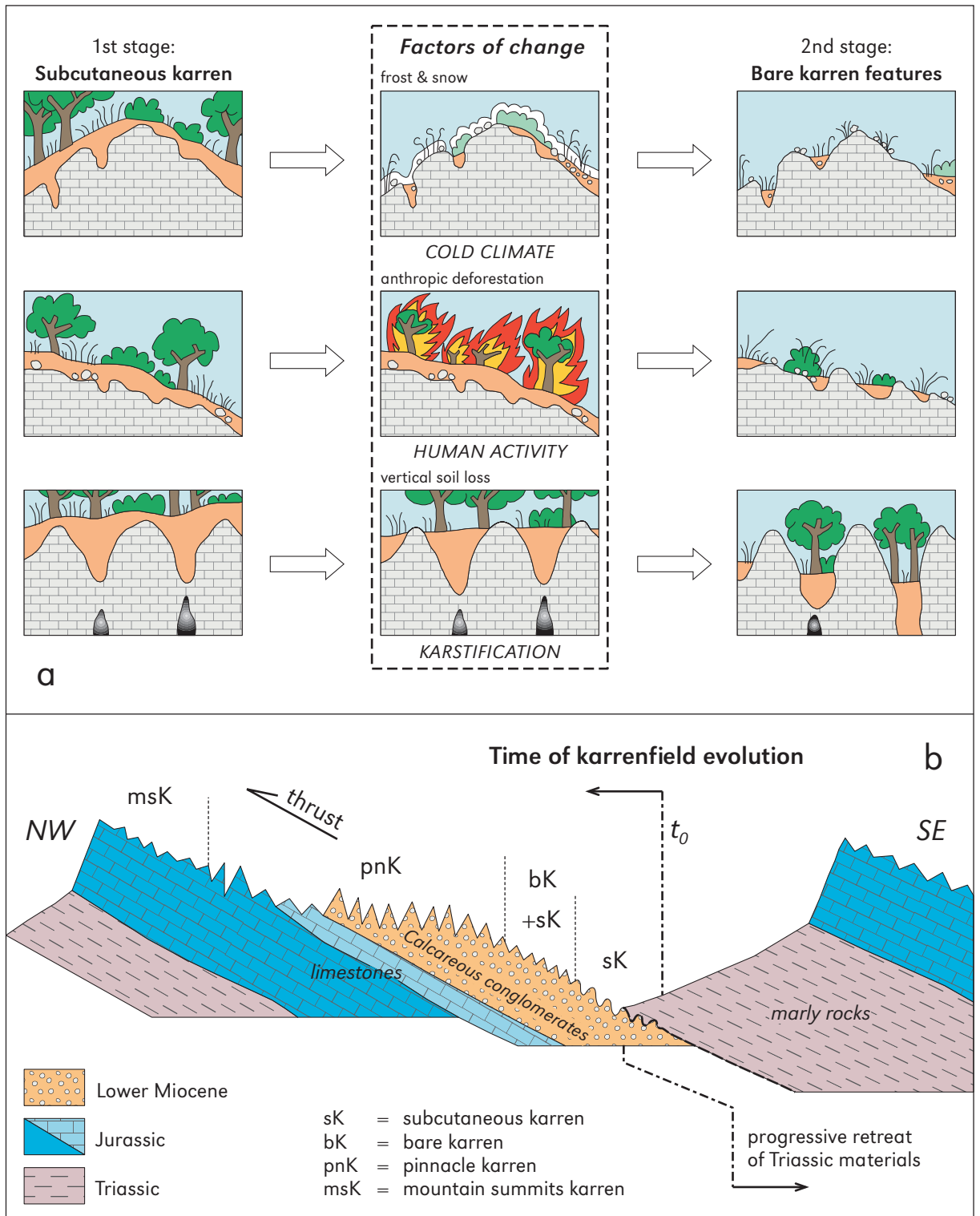
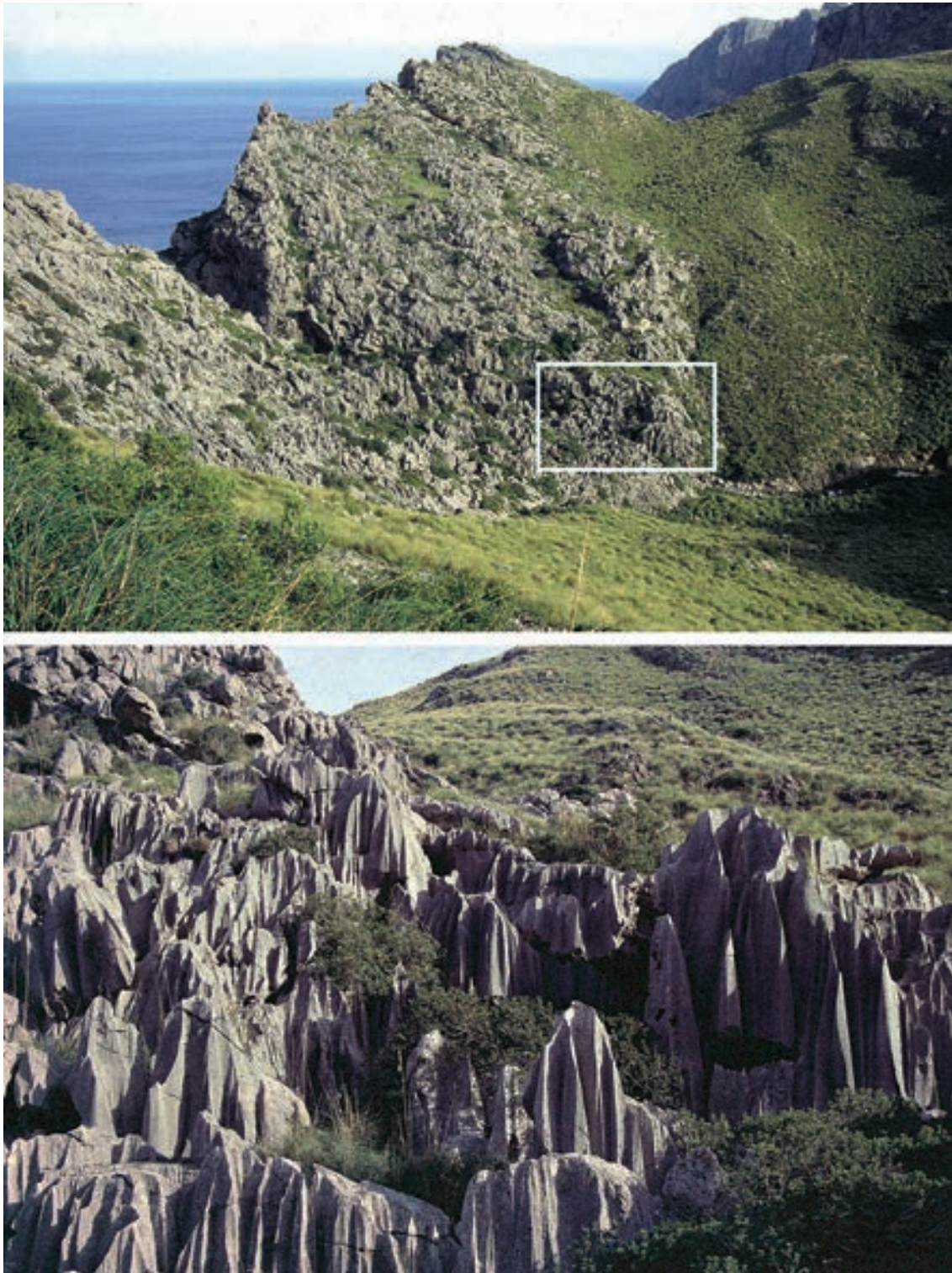


Figure 13: Patterns observed in the evolution of Serra de Tramuntana karrenfields: a. two-stage model of karren development and possible factors responsible for deforestation and soil loss processes; b. karren features distribution related to the retreat of Triassic non-karstifiable materials from above the limestone, occurring at the front of main thrust sheets.



**Figure 14:** Karrenfield evolution associated with the fronts of thrust sheet structures. Both images are from Coma des Truges (Escorca). Above: pinnacle features in Lower Miocene rocks (left side of the photo) progressively emerging with increasing distance from the contact with overlying Triassic marly materials (grassy slopes at the right side of the image); below: detail of the resulting spitzkarren landscape (square in the upper photo).

tween the rock crests and the rounded soil-filled grikes.

Related to this two-stage model of karren development (subcutaneous solutional shaping followed by bare karren features), the main problem lies in deducing the factors responsible for the negative soil balance which causes the continuous stripping of these subsoil sculptured solutional forms. A. Ginés (1995) proposed three distinct – but not mutually exclusive – causes that can produce a complex karrenfield, starting from cryptolapiaz features and leading to the bare expanses nowadays present in Serra de Tramuntana (Figure 13a). The proposed mechanisms are:

- pleistocene cold-climate periods might have stressed the existing forest communities, as well as severely damaging the soil mantle. The replacement of forests by scrub and grass communities stimulated the natural degradation of soil profiles, mainly in the highest parts of the range;
- human activity during the last five millennia has undoubtedly contributed to the regression of holm oak and pine forests in the island. The traditional practice of burning brushwoods, in order to renew the grazing lands for cattle pasturing, is a very effective historical cause of plant cover reduction in the Mallorcan karst;
- the striking pinnacle landscapes found in the central part of Serra de Tramuntana, seem to result from a mechanism of “subsidence” of the natural soil and forest mantle as a whole, rather than corresponding to an authentic deforestation process. It could be a general tendency of forest subsidence promoted by the progress of karstification, which produces important vertical soil losses occurring down through the karst massif. The lowering of both soil and plant cover has resulted in a relative steady rise of karren pinnacles above the level of the forest.

In addition to this last point, it is worth pointing out that loose marl and clay particles, derived from the weathering of the Upper Triassic rocks,

play an important role in providing material for the subsoil evolution of the karrenfields during the first stage of their formation (Figure 14). The retreat of these beds – which frequently overlie the Jurassic and/or the Lower Miocene carbonate rocks – allows the progressive exhumation of the subsoil solutional features and the subsequent superimposition of bare karren forms; the end of this evolutionary sequence is shown by the pinnacle karrenfields that occur in the areas furthest from the Triassic cover, which have been longest exposed to subaerial conditions (Figure 13b).

## Conclusions

Mallorca island is a representative location for the Mediterranean environment, including a mid-altitude mountain range – the Serra de Tramuntana – that is notable for its spectacular karst landforms. Jurassic and Lower Miocene limestones, folded during the alpine tectonic event, have experienced an intense exokarstic sculpturing which produces extensive karrenfields with a remarkable richness in solutional micro- and meso-forms. The distribution and morphometry of the different karren types is controlled by the climatic gradients existing over the range which are in turn linked to elevation, since the mountain heights span from sea level to 1,445 metres above. Biokarst incidence is remarkable, particularly in some specific ecological situations: the semi-arid periphery of the range and, particularly, the northern exposures of the highest summits. Current karrenfields have evolved from previous subsoil types, being later exhumed by various deforestation and soil-loss processes until reaching the conspicuous karren pinnacles landscape, characteristic of the central part of the area.

The Serra de Tramuntana is an excellent location for karren investigation in mid-latitudes, owing to the great variety of environmental conditions as well as to the important – but relatively recent – human impact on the area.

## **Acknowledgement**

We gratefully acknowledge Ken Grimes (Hamilton, Australia) for the helpful review of this paper

as well as for the improvement of the English text. This work was partially supported by the research fund of *Ministerio de Educación y Ciencia* – FEDER, CGL2006–11242–C03–01/BTE.

Ken G. GRIMES

Karren in tropical Australia are strongly developed at all scales from microkarren to giant grikes and pinnacled towers, but with decreasing intensity and variety as one moves into the drier climates of the interior. However, the local effects of lithology, structure, cover and denudation history can create considerable variation.

## The tropical karsts of Australia

### Distribution

The tropical karst of Australia can be divided into

two structurally distinct provinces in the east and the north-west of the continent (Figure 1). A third province, the coastal dune limestones of southern Australia extends a short distance into the dry tropics of western Australia but is not discussed here as the karren are poorly developed, and poorly documented (see chapter 42). There are also many areas of well-developed silicate karst, both as surface landforms (grikefields, “stone cities” and pinnacles) and as caves, which will not be discussed here (see bibliography in Wray, 1997). Recent reviews of Australia’s tropical karst are provided in Spate and Little (1995) and Gillieson and Spate (1998).

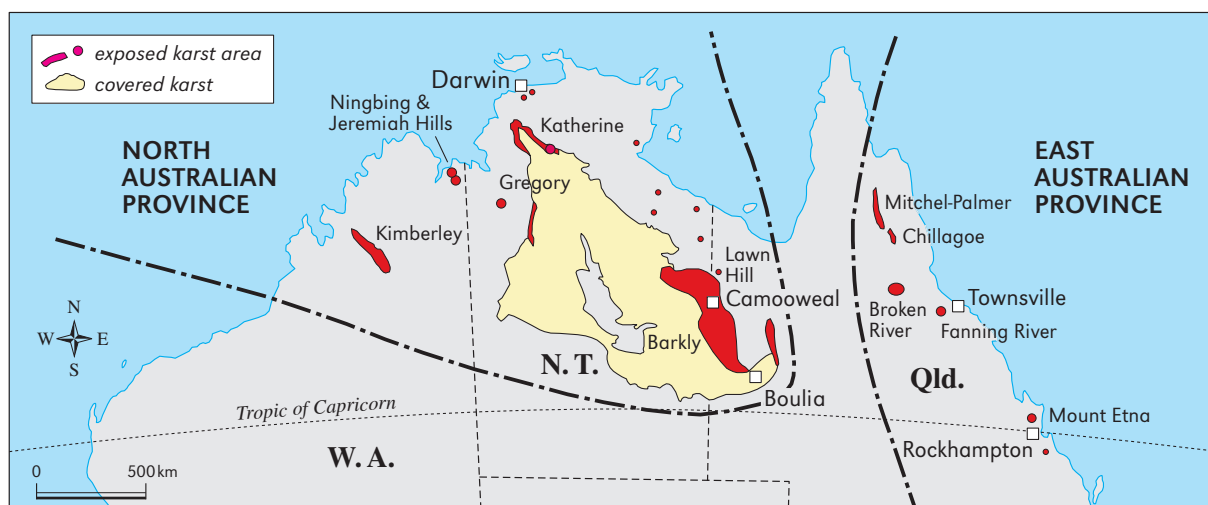


Figure 1: Location map of tropical karsts in Australia, showing the two main structural provinces. Karrenfields occur in the exposed karst, but not in the covered karsts.



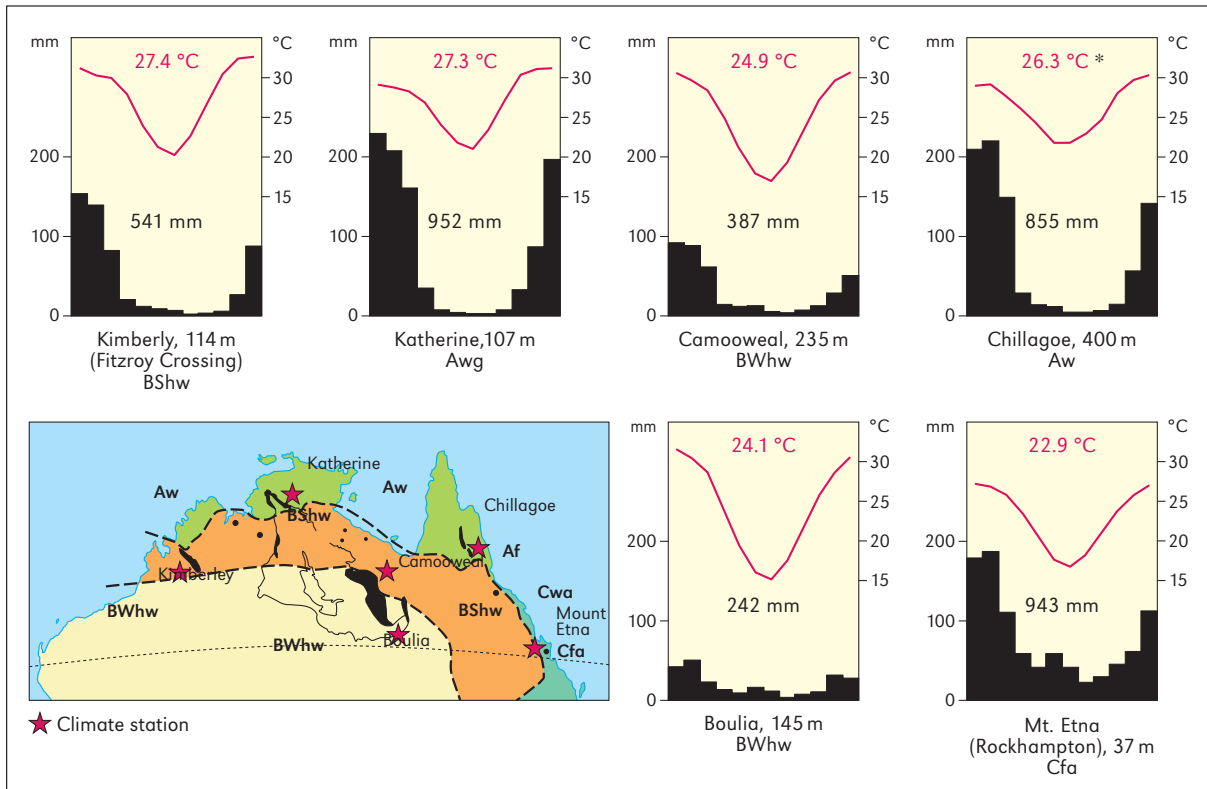


Figure 2: Monthly and annual mean temperatures and rainfall, and elevations for selected climate stations on tropical karsts. Station names are shown in parenthesis where this differs from the karst name. The Köppen climates for north Australia are also shown. Data from BOM (2005). \*Temperature data for Chillagoe is from 3 years only (Robinson, 1982).

### Geological setting

The East Australian Karst Province (Figure 1) is formed on strongly-folded, generally steep-dipping, Palaeozoic limestones and occasional marbles. These usually form narrow linear outcrops. They are *impounded karst* (Jennings, 1985), in which the drainage is largely controlled by allo-genic streams which cross over, or cut through, the limestone belts with little loss of water underground. In the tropical part of this province the limestone beds tend to stand above the surrounding rocks as ridges and towers.

In the North Australian Karst Province the host rocks are flat-lying to gently folded Proterozoic dolomites and Palaeozoic limestones and dolomites. These form extensive regions, but in some

the depth of the carbonate rock is limited to a few tens of metres. In some areas the carbonate rocks are well-exposed, with strongly karstified outcrops; others have extensive covers of Mesozoic and Tertiary sediments and younger soils (Figure 1). There are also laterite and silcrete capped deep weathering profiles. Chert nodules and beds are common in some of the carbonates and this can influence the degree of karst.

### Climate

Northern Australia has a tropical monsoon climate. The Köppen climate classes range from humid Aw southwards through drier BShw to arid BWhw. The rainfall has a pronounced seasonal-



Figure 3: Aerial view of the crest of a tower at Chillagoe showing large sculptured pinnacles and vertical wandkarren.

ity with a five-month summer “wet” and a longer winter dry season (see Figure 2, and BOM, 2005, for further details). On the east coast the seasonality decreases southwards and the climate grades to the Cfa type. Most rain in the wet season falls either in short intense thunderstorms, or in occasional cyclonic events lasting several days. Significant variation in rainfall between years is a consequence of the “El Niño southern oscillation” effect. Potential evapotranspiration is substantially greater than actual rainfall throughout the region, giving a deficit in excess of 1,000 mm per annum.

### Vegetation

Most of the region has a savanna woodland: denser and with more understory in the wetter parts, and more open in the arid regions. Open grassland is found in the drier areas or where there is a heavy clay soil cover. Deep-rooted deciduous vine thicket may grow on the rocky limestone towers and karrenfields.

## Steep-dipping limestones, east Australia

### Chillagoe and Mitchell-Palmer

The Chillagoe area is one of the better documented tropical karren in Australia (e.g. Lundberg, 1977a; Ford, 1978; Pearson, 1982; Jennings, 1982; Dunkerley, 1983). The area is best known for its serrated limestone towers - or "bluffs" as they are locally called (Figure 3) - which can reach up to 90 m high, though most are less than 50 m, and are from 100 m to over a kilometre long. The overall size and distribution of the towers are structurally controlled by the narrow lenses or fault-blocks of steep-dipping limestone which alternate with insoluble chert and other sedimentary rocks that are less resistant to erosion in this setting (Figure 4) - thus they are a special type of structural "tower karst" (Ford, 1978; Jennings, 1981, 1982). Some towers are surrounded by a limestone pediment (Figure 5) or by alluvium, but others rise immediately beside the (commonly faulted) contact with the surrounding rocks. The Mitchell-Palmer karst is similar to Chillagoe, but more remote and has larger towers but fewer pediments.

Jennings (1981, 1982) discussed the *pediments*, which, along with climatic control of tower form,

had been given considerable emphasis in earlier work. He noted that, in fact, the pediments constitute less than half the tower perimeters. However, they are still active in many places and have cut back the tower flanks, in some cases reducing the tower to a scatter of fragments and ruins. The lower "scree" slopes of the towers are partly bedrock with a thin cover and Jennings (1982) referred to these ramps as "*Richer denudation slopes*" (Figures 4, 5). Some towers have marginal depressions, with active subsidence of the soil into the epikarst, which are the result of aggressive water runoff from tower surface (Pearson, 1982).

The towers may be quite old. Robinson (1978), Jennings (1982), Webb (1996) and Gillieson et al. (2003), all discuss the age of the karst, noting the presence of isolated outcrops of quartz sandstone of possible Mesozoic age both on the tower tops, and around their bases. The conclusion is that the towers were already well-formed at the time of their burial during the early Cretaceous transgression, and were exhumed and further dissected during the Cenozoic.

#### KARREN FORMS

While the climate would seem to be important for the overall abundance of karren forms in the area, lithology has been an important control on

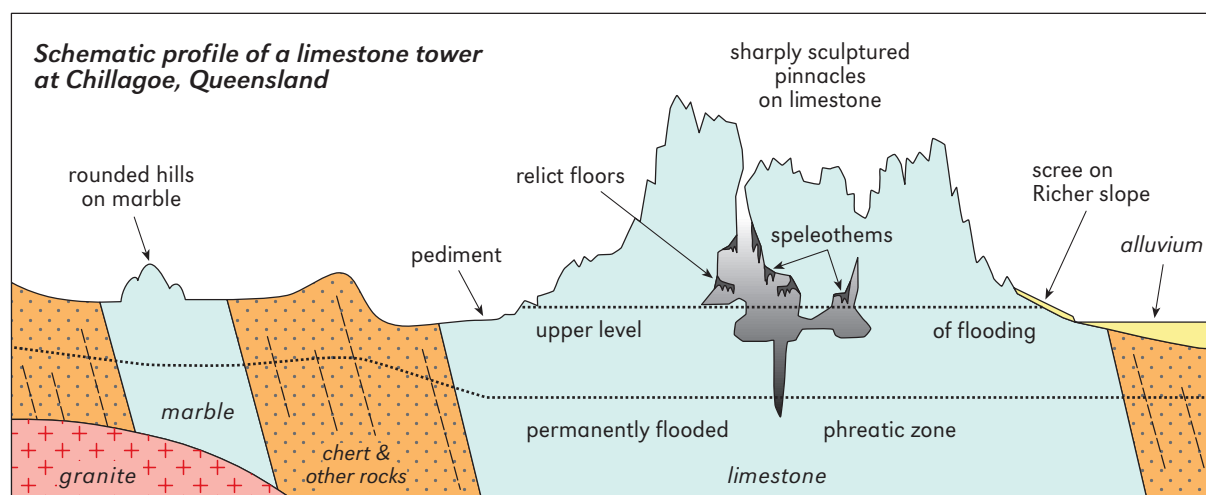


Figure 4: Schematic profile of a limestone tower at Chillagoe, Queensland, based partly on a diagram in Robinson (1978).

**Figure 5:** Pediment (P) with clints and soil-filled grikes at Chillagoe. In background is a small tower with a debris-covered Richer slope (R).



the detailed sculpturing of individual towers. This was recorded quite early (e.g. Daneš, 1911) and has been discussed by many authors (Wilson, 1975; Marker, 1976b; Lundberg, 1977a, b; Ford, 1978; Pearson, 1982; Jennings, 1982; and Dunkerley, 1983, 1988). Unfortunately, there has been a lack of consistency in the lithological subdivisions recognized, and in the terminology used.

Jennings (1982) summarized the lithological control as producing poorly developed karren on the coarse-grained “sugarstones” (a crumbly coarse-grained marble) and heterogeneous limestones, and a much wider range of well-developed karren on the fine-grained uniform limestones – known variously as “sparite”, “fossil” or “reef” limestone. He also noted that areas of excessive fracturing inhibit those karren that result from water flow over large surface areas.

Dunkerley (1988) measured the chemistry of runoff water and kamenitza waters from rock surfaces on three lithological groups (coarse and fine-grained marble, and fine-textured “fossil” limestone) and found that the “fossil” limestone (water of 41.9 ppm total hardness) and the fine-grained

marble (41.3 ppm) were dissolving more rapidly than the coarse marble (34.1 ppm). His detailed results have not yet been published.

The following description draws mainly on Pearson (1982) and Jennings (1982). The white, coarsely-crystalline, marbles (“sugarstone”) form smoothly rounded domes with exfoliation sheets that occasionally are raised to form *A-tents*. Some surfaces show a crazed pattern of fine cracks. *Rillenkarren* do occur on the marble, but are less well developed. Lundberg (1977a) tabulated the differences in character between the *rillenkarren* on the “sugarstone” and those on the “sparite” limestones (see also summary in Jennings, 1982). The “sugarstone” differed from the “sparite” limestone in having pits and flutes that were narrower, shallower, more constant in form and less close-set and had more rounded ribs between them.

The finer-grained marbles have karren forms that are more similar to the “sparite” limestone. However, the grain size of the marble can be quite variable over short distances, so the above distinctions need to be applied with some care.

The more widespread “sparite” or “reef” lime-

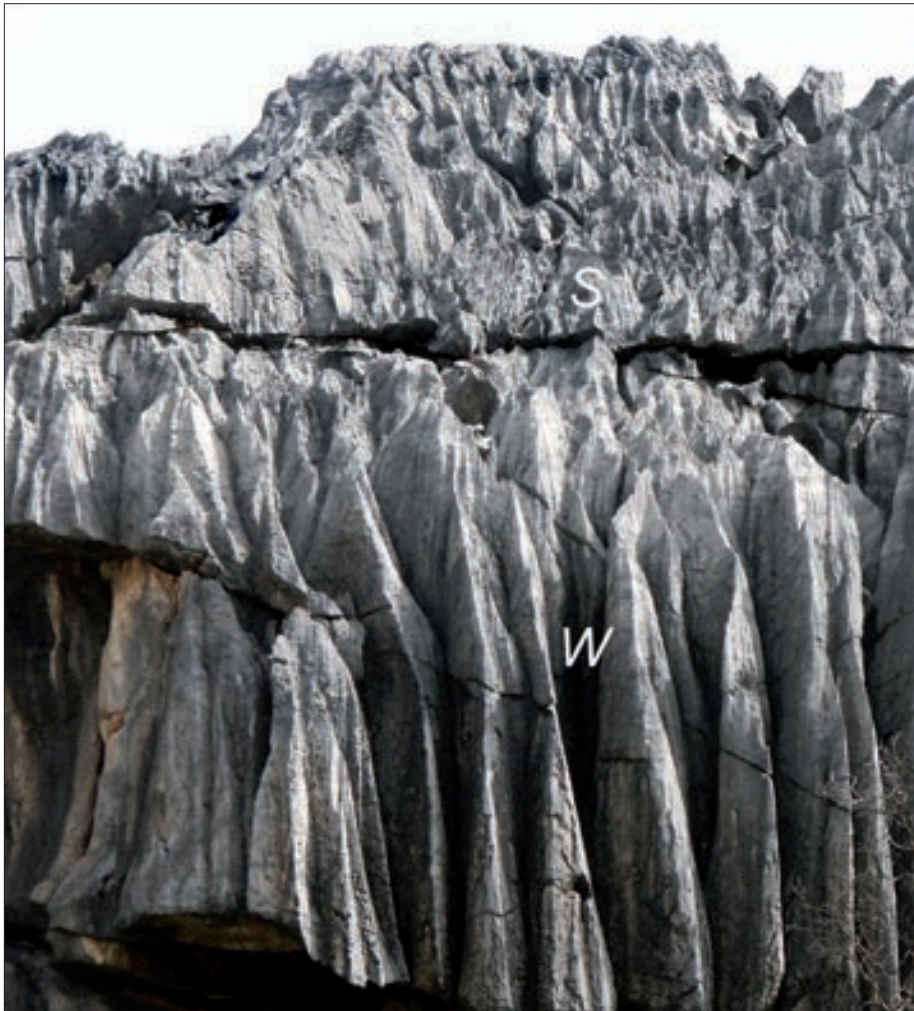


**Figure 6:** Spitzkarren (S) grading down to deep vertical wandkarren (W), on a tower in the Mungana area, Chillingoe. View is about 8 m high.

stone towers are strongly dissected by solution and contain large *grikes*, vertical sculptured walls, fields of spitzkarren and large sharp-sculptured pinnacles which make access difficult (Figure 3). The following description refers mainly to these limestones (Jennings, 1982). Note that the term “*spitzkarren*” is used here for small to medium-sized pointed pinnacles that are sculptured by rillenkarren. In my usage these range from incipient rosettes of rillenkarren a few decimetres high to large pinnacles several metres high. However, I do not use the term for the “large sculptured pinnacles” which have more complex walls (with wandkarren) and are big enough to have clusters of smaller spitzkarren pinnacles on their crests.

Within the towers, *giant grikes* up to 10 m wide and 30 m deep connect to fissure-maze caves with

numerous daylight holes. In places the grikes open out into *karst corridors* or deep steep-walled *dolines* of both solutional and collapse origin. The grikes combine with rillenkarren and wandkarren to form intricately sculptured patterns of sharp pointed *pinnacles* 5 m or more high (Figure 3). Solution dolines on the tower tops tend to be irregular forms with fields of spitzkarren and internal drainage via grikes. Some towers have a stepped relief with risers and treads.

On the sides of the towers and the giant grikes extensive rillenkarren feed via steep runnels, 10–20 cm deep, into vertical *wandkarren* that can be up to a metre deep (into the wall) and 40 m long (Figures 3, 6). On steep slopes the rillenkarren are modified by *cockling* patterns (Sweeting, 1973). *Rinnenkarren* (runnels) are listed by several

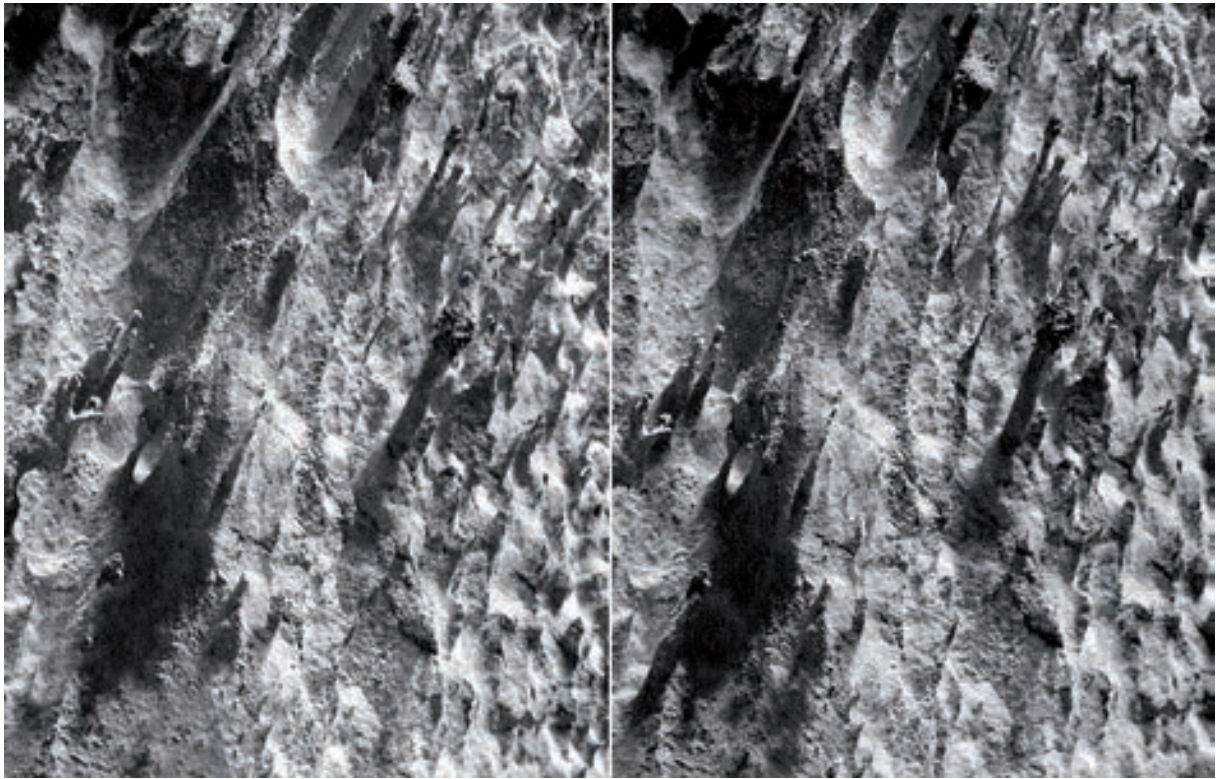


Figure 7: Stereopair of phototropic spikes with coralloid overgrowths, a result of light-oriented algal corrosion, in the twilight zone of a cave entrance. Width of view is 65 cm.

authors but some appear to use this term for *regenrinnenkarren* or *wandkarren*. Occasional *decantation runnels* occur below horizontal joints cutting into vertical walls.

On the more gentle slopes, which include steps and bevels, there are *rainpits*, localized rosettes of rillenkarren which grade to incipient spitzkarren, short irregular runnels, and small (up to 1 m wide) *solution pans* (*kamenitzas*). Wilson (1975) reported that flat-floored solution pans are common on tops of the towers, and noted that these always have an outlet drain.

The rillenkarren have been studied morphometrically by Lundberg (1977a, b), Jennings (1982) and Dunkerley (1983). Jennings (1982) measured rillenkarren lengths on the “sparite” that averaged 95–100 cm at three sites, with a SD of 48. Dunkerley (1983) summarized the results in Lundberg’s (1977a) thesis, and also reported additional measurements giving flute lengths averaging between

17.3 and 29.8 cm and widths of 16.9 to 18.5 mm at three sites on the marble, whereas two “sparite” sites had lengths of 31.3 and 35.6 cm and widths of 18.5 and 23 mm.

Two types of *horizontal solution ripple* were described by Jennings (1982): on underhangs and in the twilight walls of cave entrances there are sharp-ribbed and deeply recessed symmetrical forms; whereas on steep surfaces exposed by soil erosion of the pediment grikes there are more rounded and asymmetrical ripples that might have resulted from subsoil solution.

Jennings (1982) described *phototropic karren* which are grooves, sticks and spines oriented towards the light and found in the twilight zone of the caves and deep grikes (Figure 7). These are a type of *phytokarst* eroded by algae. Individual spikes and grooves are between 2–50 mm across, but can be up to 400 mm long! Some spikes have *coralloid* growths on their tips, or along their full



**Figure 8:** Solution pan on a pediment near Racecourse Tower, Chilla-goe. It is formed from coalescence of smaller circular pans with central pits. Width of view is 50 cm.

length. Jennings (1982) described *small needles*, 10 mm high and 1–2 mm thick, on the side of a rather deep solution pan on top of one tower.

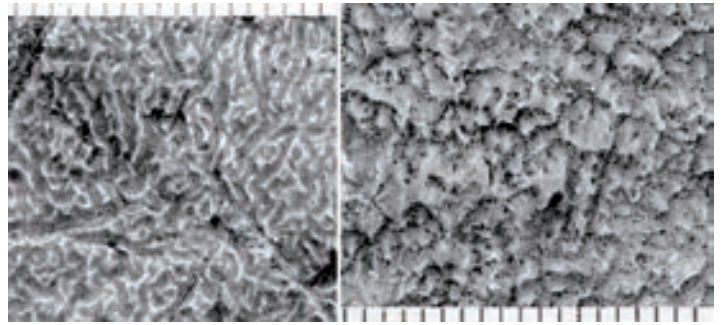
*Microkarren* are more extensive than suggested by earlier reports (Jennings, 1981, 1982; Dunkerley, 1983). The terminology used here is that suggested by Grimes (2007). The microkarren are most common on the flatter surfaces, especially on the gently rounded “clints” of the pediments and on the steps of the towers. However, I found microrills and other forms on slopes up to 60 degrees. Some microkarren are superimposed on rillenkarrren or rainpits (e.g. see photos 1–3 in Dunkerley, 1983); these appear to be secondary features modifying the initial coarser form. Linear *microrills* grade to *micro-networks* of irregular, discontinuous ridges which in turn break up into arrays of tiny rasp-like *micro-teeth* (Figure 9). I measured the following size ranges from a set of enlarged photographs: the microrills range from 0.2 to 2.8 mm wide, averaging 1.1 mm; the micro-teeth were spaced 0.5 to 3 mm apart, averaging 1.5 mm. Vertical relief is generally less than 1 mm; some microrills and micro-networks are extremely shallow and visible mainly by a slight bleaching of the crests. Circular micro-pits also occur as small as 1 mm across,

but show a greater size range and all gradations up to normal rainpits (10 mm or greater) can occur on one outcrop. There is also a very fine *etching* of structures such as irregular cracks, the crystal boundaries of the marbles, or the skeletal structure of fossil corals.

These small features have been under-reported because of their cryptic nature. They are most visible in areas lacking the ubiquitous thin grey algal coating, e.g. in the bare areas used by wallabies. However, they seem too extensive to be solely a consequence of corrosion by wallaby urine or dung, as suggested by Jennings (1981, 1982). Solution by thin films of water, dew or light rain, seems the most likely origin (see chapter 7).

On the pediments there are smoothly rounded *clints* between soil-filled grikes (Figure 5). The clint surfaces may carry small areas of rillenkarrren, but rainpits or smooth surfaces are more common, along with a range of microkarren. Solution pans (*kamenitzas*) are less common. In one area, which appears to be flooded regularly, there were composite pans formed from coalescing smaller circular pans with small deep conical holes in their centres (Figure 8). It would appear that these small pans have been draining downwards through fine

**Figure 9:** Microkarren on a pediment at Chillagoe. Left: micro-network of small furrows and bleached ridges; right: rasp-like micro-teeth. Scales in mm.



cracks. Subsoil solution pipes also occur, typically elongated along a joint. In places soil erosion has exposed the grikes and other, generally rounded, *rundkarren* and *subsoil karren*.

### Broken River

This region is similar to Chillagoe, but differs in that the limestones here are not as steeply dipping, typically 50-70 degrees, and rather than high abrupt towers, they form long linear ridges dissected by grikes, spitzkarren and larger sculptured pinnacles. Microkarren here are restricted to bleached patches which are mainly the result of wallaby defecation. They comprise well-developed microrills, micro-networks and micro-pits superimposed on rillenkarren and rainpits.

The Turtle Creek Tower has some features of special interest. This broad, but steep-sided tower is topped by a bare plateau, including several *broad solutional basins* up to 100 m across, that are dissected into low spitzkarren and smoother areas of kamenitzas, rainpits and rillenkarren.

An unusual set of “*interconnected solution rivulets*” was first recorded within the basins by Godwin (1988). The rivulets are *large runnels* that form a branching contributory system of small flat-floored, and locally meandering, stream channels incised into the limestone floors of the basins (Figure 10). The drainage of the largest basin leaves the tower via an increasingly deep channel with some 2 m waterfalls; in the smaller basins the runnels sink underground into small shafts. The channels have flat floors and steep sides which

may be slightly undercut. Commonly they are from 0.3 to 2 m wide and from 10 to 80 cm deep. The floor is generally bare limestone, with a thin (1-5 mm) coating of clay and organic material. There are several terraces visible on the channel floors with the presently active channel in places being a narrow slot within a broader channel. The higher terraces, which are commonly paired, now have small rillenkarren, rainpits and kamenitzas developing on them.

These channels appear to be dominantly solutional in origin. The wet season storms could produce sufficient runoff to allow some hydraulic erosion, though there is no sediment to provide abrasive tools. The clay and algal material on the floors may have favoured undercutting of the walls over down-cutting of the floor – as happens in kamenitzas.

### Fanning River

This is a small karst area inland from Townsville that is developed on a 1 km wide low ridge of gently dipping Devonian limestone. The rock occurs in alternating zones of thick-bedded limestone with good karst development and poorly exposed belts of interbedded limestone, sandstone and shale with no karst features (Grimes, 1990). Dips vary from 10 to 70 degrees. The thick-bedded limestone has some grikes, rillenkarren, and kamenitzas. However, surface solution sculpturing is not as well developed as in the Chillagoe and Broken River areas.

An unusual, dipping limestone pavement occurs





Figure 10: Meandering and branching flat-floored solutional runnels in a shallow bedrock basin on the crest of the Turtle Creek Tower, Broken River. Width of view is 5 m, at the lower edge.

in one place. This is a 12 degree dip surface formed by the stripping of a thinner-bedded muddy limestone from above a thicker-bedded calcirudite. The pavement has scattered grikes (0.5–2 m deep and 2–20 m long), some of which connect with caves, some relatively deep kamenitzas with overflow channels on the downslope side, and small patches of rillenkarren and rainpits; but otherwise it is essentially undissected. This may be a similar situation to that described below at the Gregory Karst – where a surface has not been exposed for long enough to develop deep sculpturing.

### Mount Etna

Mount Etna, rising 190 m above the surrounding plain, is the largest of several limestone ridges and hills that lie near the coast, just north of the Tropic of Capricorn (Shannon, 1970). These provide a

borderline example of tower karst as the hills tend to be conical with a scree-covered base, and vertical cliffs are rare. The steep sides of the mountain are bare or covered with vine thicket and are strongly sculptured by a combination of rillenkarren and larger runnels to form spitzkarren. Large rubble-choked grikes cut across the karrenfields. Cave entrances are associated with the grikes or with large, vertical, solution pipes.

### Other eastern areas

Mount Etna is at the southern limit of the tropical region, and lies just within the northern limit of the Cfa climate type. However, well-developed spitzkarren are found as far south as Kempsey, latitude 31°S, in northern New South Wales, which has a Cfa climate with an annual rainfall of about 1,700 mm.

## Flat-lying carbonates, north-west Australia

### West Kimberley region, western Australia

The West Kimberley Karst Region of northwestern Australia is also referred to in reports as the "Limestone Ranges", "Napier Ranges" and "Fitzroy Basin" regions. It is an extensive belt of exposed Devonian reef that has had little folding (Playford, 1980). It lies at the junction between the rugged Proterozoic ranges of the Kimberley region and the flat plains of the Mesozoic Canning Basin to the south. Limestone ridges and plateau rise abruptly 30–90 m above the plains and extend for 290 km with a maximum width of 30 km. The plateau top is a dissected planation surface that may date back to the Permian – Playford (2002) suggests that an Early Permian glacial palaeokarst, exhumed during the Cenozoic, has been incorporated into the modern karst topography in many areas. Dissection of the plateau in the late Tertiary and Quaternary has created the present karst landforms, along with gorges of superimposed drainage that cut across the limestone ranges.

#### LARGE-SCALE KARST LANDFORMS (MACROKARREN)

The surface karst landforms have been described in detail by Jennings and Sweeting (1963) and summarized in later papers by Jennings (1967, 1969), Williams (1978), Goudie et al. (1989, 1990) and Gillieson and Spate (1998). The main scarp is an abrupt wall or cliff, deeply sculptured by various karren forms, as are the steep walls of the gorges, *box valleys* (*bogaz*) and *giant grikes* which extend into the plateau. In detail, the steepness and character of these walls are controlled by the lithology and structure of the different reef facies (Allison and Goudie, 1990). In particular, Jennings (1967) noted that the backreef facies tends to be impure (due to terrigenous components) and that reduces the degree of karstification so that one finds more rounded hills and valleys typical of fluvial erosion. Jennings and Sweeting (1963) called these areas

"merokarst" and excluded them from their main discussion.

Jennings and Sweeting (1963) described an evolutionary sequence of dissection for the pure and well-jointed limestones (but not the merokarst). Progressive dissection and pediplanation has produced the following landforms on the pure limestones. Stripping of the original clay soil cover of the plateau leaves a relatively smooth rock surface with minor small karren features and scattered large, deep grikes ("giant grikeland", Figure 11). Widening of the giant grikes forms box valleys, with flat floor and vertical walls, which in turn coalesce to leave isolated towers and large sculptured pinnacles within a broad pediment. Dolines are relatively uncommon.

#### MESOKARREN FORMS

The surface sculpturing can be quite intense to form inhospitable jagged ridges and spires. In the undissected parts of the plateau the smooth surface has kamenitzas, rainpits and small patches of rillenkarrren. This pavement is cut by a widely spaced network of deep grikes with fluted vertical walls (Figure 11). The giant grikes are up to 7 m wide, 33 m deep and hundreds of metres long and extend underground into fissure caves. As dissection becomes greater a rugged terrain of spitzkarren and larger sculptured pinnacles develops (cf. Figure 18). Rillenkarrren are ubiquitous, but their intensity and character are controlled by the local lithology, structure and slope (see below). On the vertical walls there are large vertical solution runnels (*wandkarren*), 1–2 m deep and wide and running vertically for 30–60 m (Figure 11). The pediments have kamenitzas and occasional shallow dolines and subsoil solution pipes.

Goudie et al. (1989) discuss some lithological and other factors controlling the development of the *rillenkarrren*, which are only well-developed on certain beds. The limestones are all hard and have little primary porosity, but, of the factors which Goudie and others studied, the important control on the occurrence of rillenkarrren appeared to be the purity (insoluble residue) and the



**Figure 11:** A giant grike, at least 5 metres wide, with collapsed blocks and deep vertical wandkarren, above Mimbi Cave, West Kimberley region. Note the relatively undissected plateau in the background (photo by J. Jennings).

homogeneity (as revealed by thin section study). The difference is mainly one of the fabric and the cement type: in particular, rillenkarren develop best in the absence of fabrics characterised by bioclasts, ooids, and an excess of ooids over intraclasts. They are also related to an absence of micritic cement. Other factors statistically associated with rillenkarren were low levels of dolomite and a sparite cement that is less equant than elsewhere. In addition to the factors measured by Goudie et al. (1989), Jennings and Sweeting (1963) noted the influence of bedding in disrupting rillenkarren development and breaking it into pagoda-like stacks of conical spitzkarren (cf. Figure 18).

Goudie et al. (1989) also recorded that the karren types vary with gradient of slope: shallow

slopes ( $0-30^\circ$ ) tend to be pitted and have kamenitzas. Grikes are scattered across these “pavements” and some may be filled with tufa deposits. Moderate slopes ( $30-55^\circ$ ) have bifurcating rillenkarren which become parallel as the slope steepens ( $55-80^\circ$ ). The steepest slopes ( $> 80^\circ$ ) are described by Goudie and others as having “boxy forms”.

Within the major river gorges which cross the karst, wet season floods rise to heights of 10 m (Gillieson et al., 1991). The flooded sections of the gorge walls show well-developed *scallops* and strong etching of bedding and vertical joints to form cavernous slots (*splitkarren*, sensu Ford and Williams, 1989) and vertical grikes, along with spongework.

There is no information on the occurrence of microkarren in this area.

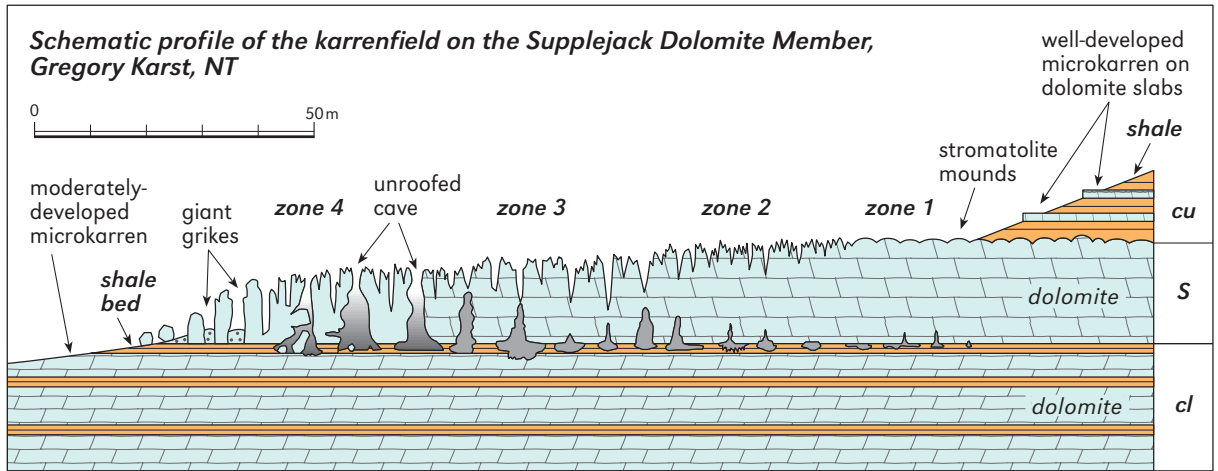


Figure 12: Schematic profile of a karrenfield in the Gregory Karst, Northern Territory. cu. upper Skull Creek formation; S. Supplejack dolomite member; cl. lower Skull Creek formation; zone 1. incipient karren; zone 2. moderately-developed grikes and spitzkarren; zone 3. deep grikes and large spitzkarren; zone 4. giant grikes, unroofed caves, sculptured pinnacles.

### Ningbing and Jeremiah Hills

There have been no karst-specific reports published on this area of gently-dipping Devonian and Carboniferous reef limestones, which is also known as the East Kimberley. However, the geological report by Veevers and Roberts (1968) has photographs of outcrops of the different carbonates which show the distinctive fluted, pinnacled and cavernous tower structure seen in other areas. There is also a suggestion of both lithological and structural control on the character of the solutional sculpturing. A photo of the fore-reef breccia of the gently dipping (10–20°) Westwood member shows unusual smooth-surfaced cones and pinnacles from 1 to 4 m high. These could be uncovered subsoil features, but as the outcrop is in an area of low relief in a prograding coastal plain the potential for soil erosion seems limited.

### Gregory Karst

In this area karst and karren are largely restricted to a thin (10–18 m) but extensive dolomite unit, the Supplejack member, within the flat-ly-

ing late Proterozoic Skull Creek formation. The Skull Creek formation is also dominantly carbonate, but less pure and thinner bedded (Sweet et al., 1974; Bannink et al., 1995). Apart from the Supplejack member, the Skull Creek formation has only poorly developed mesokarren, but it has well-developed microkarren, especially in the upper part. Figure 12 illustrates the geological structure and the resulting karren. Extensive maze caves underlie the dissected surface (Storm and Smith, 1991; Bannink et al., 1995). There is obvious joint and bedding control of both the karren and the underlying caves.

Only brief descriptions of the karren have been published previously (Dunkley, 1993; Bannink et al., 1995). The *karrenfields* on the Supplejack member show a zonation which results from progressively longer periods of exposure at the surface. This starts with incipient karren development on recently exposed surfaces adjacent to the contact with the overlying Skull Creek formation and continues through progressively deeper dissected karren to a final stage of “stone cities” of isolated pinnacles at the outer edge (zones 1 to 4 on Figures 12, 13). The zones are gradational and the boundaries shown on Figure 13 are only ap-

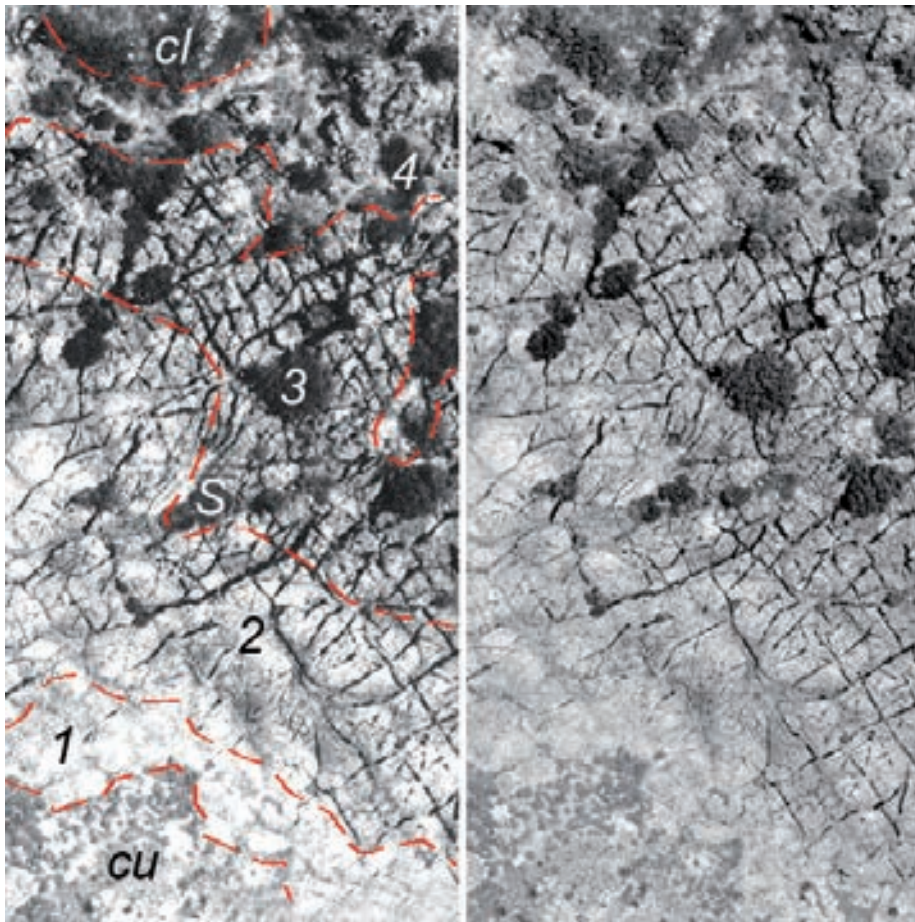


**Figure 13:** Aerial stereo-pair of a karrenfield in the Gregory Karst. Numbers 1–4 refer to the zones shown on Figure 12. The main karrenfield is on the Supplejack member; cl and cu are outcrops of the lower and upper Skull Creek formation, respectively. Note subsided areas in centre (S) – a result of cave undermining. Width of view is 100 m. Original air-photos copyright Northern Territory Government, 1989.

proximate. This developmental sequence has similarities to that described by Jennings and Sweeting (1963) in the West Kimberley region, but at a smaller scale.

Zone 1 has well-preserved *stromatolite domes* (up to 12 m wide and 2 m high) exposed by stripping of the overlying rock. The surfaces are smooth or sculptured by incipient rainpits and rillenkarren with superimposed microkarren (Figure 14). Etching of joints and bedding forms splitkarren. There are scattered kamenitzas and small grikes.

Away from the contact, increasing dissection produces small spitzkarren up to 0.3 m high, and grades to zone 2. There the stromatolite domes are still recognizable locally, but are strongly dissected by a variety of mesokarren, including numerous kamenitzas (up to 2 m wide and 0.4 m deep) and spitzkarren up to 1 m high. Grikes are wider

and deeper, averaging 2 m deep, but with considerable variation, including occasional narrow connections to the cave passages below.

The transition to zone 3 is quite gradual. Zone 3 has wider and deeper grikes, and connections to the cave become more common, though still narrow. Traversing the surface becomes difficult. Spitzkarren are dominant and up to 2 m high. Wandkarren appear on the grike walls and the sides of the larger spitzkarren.

In zone 4 the surface has become completely dissected. Giant grikes 1–5 m wide penetrate to the cave floors 10–15 m below and separate blocks of rock with strong spitzkarren on the tops and wandkarren, rillenkarren and cockles on the walls. As the grikes widen, one gets a “stone city” topography of isolated blocks, many of which are tilted, and finally an abrupt change to a broad flat floored valley on the lower Skull Creek formation

with only scattered blocks and sculptured pinnacles (Figure 15).

*Kamenitzas* are common in zones 2 and 3 but also found in the other zones, reaching up to several metres wide and 0.4 m deep. These can form chains linked by short runnels. The flat floors have two types of surface associated with different algal types: smooth, bare rock floors are associated with curled fragments of black algae, and pitted floors are coated by the usual thin, grey, hard film of algae that covers most of the rock surface. The pitted floors comprise both pits and cones, 2–5 mm wide and 2 mm deep/high. Larger rainpits form *hackly* floors in places. Etched stromatolite structures make small ridges on some floors.

In the twilight zone of cave entrances and at the base of the giant grikes there are *phototropic spikes* and solution ripples similar to those described at Chillagoe (cf. Figure 7).

*Microkarren* occur within the main karrenfield. They are common in zone 1, but also occur in the other zones, usually at the tops of spitzkarren and associated with rillenkarren and rainpits. However, the best development of microkarren in the Gregory Karst is on the flaggy to slabby outcrops of dolomite in the upper Skull Creek formation, where there is little competition from mesokarren. This formation has the best array of microkarren found anywhere in tropical Australia; nearly every outcrop has examples.

Microkarren are best developed on gentle slopes. They include *microrills* up to 60 cm long, typically 1–2 mm wide, and straight to sinuous (Figure 14) or locally tightly meandering (Figure 16). *Micro-pits* have a full size range from less than 1 mm wide and deep up to 20 mm (i.e. they grade to rainpits). A broad range of sizes can occur within a single outcrop. On gently-domed surfaces micro-pits occur on the crest and grade to microrills on the slopes. Micro-teeth and micro-networks (as seen at Chillagoe, Figure 9) are less common. Small shallow *micro-pans* are 2.5–8 mm wide but only 1–2 mm deep and are superimposed on pre-existing microrills (Figure 17). These have

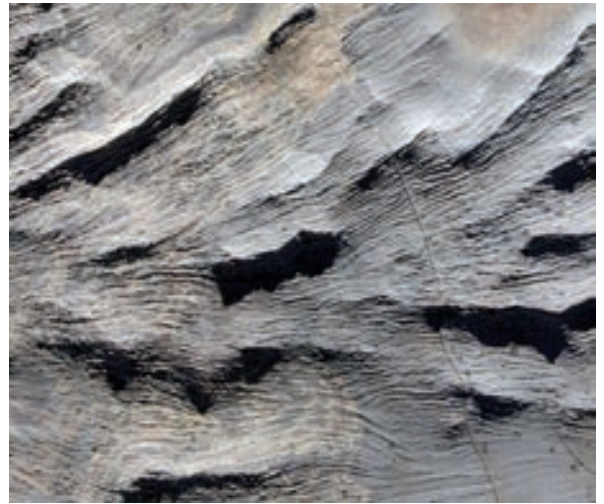
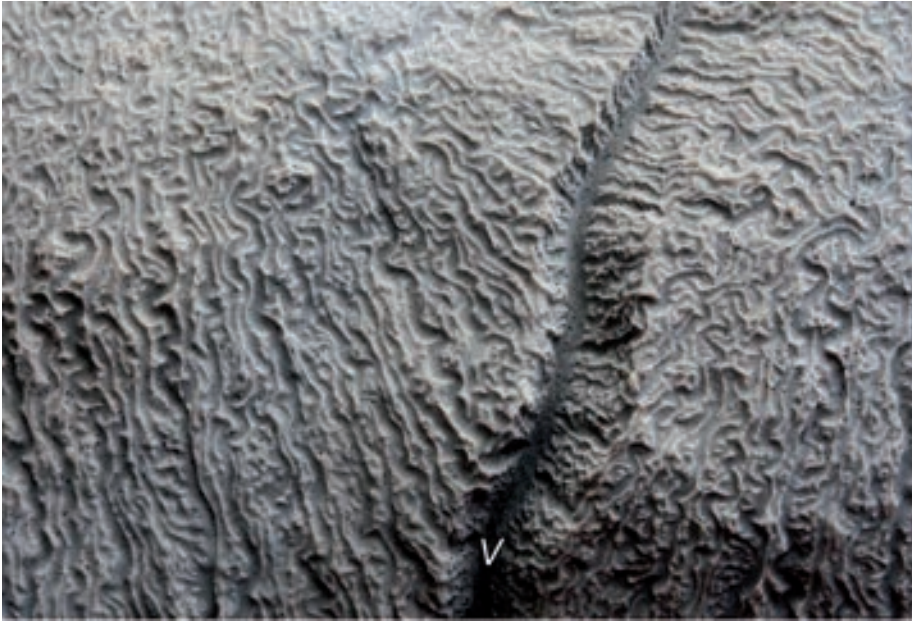


Figure 14: Microrills superimposed on shallow rillenkarren on a horizontal slab in the upper Skull Creek formation, Gregory Karst region. Width of view is 15 cm.

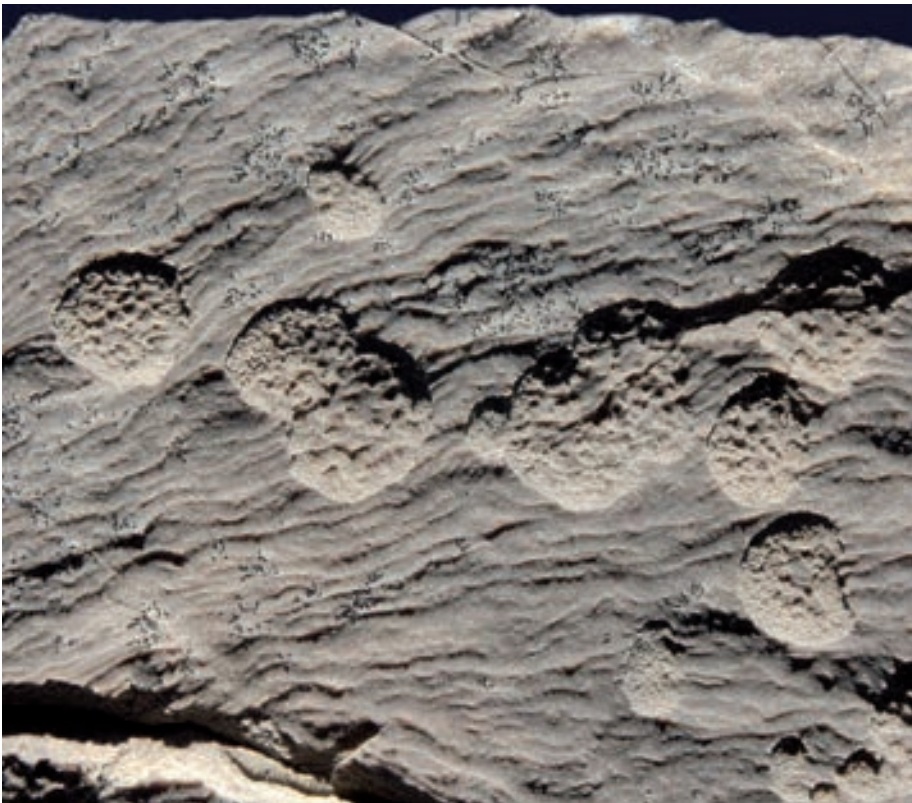


Figure 15: Isolated pinnacle, about 5 m high, at outer edge of zone 4 in the Gregory Karst (photo by N. White, 1992).

finely pitted or toothed floors. *Micro-tessellations* (spaced networks of shallow etched cracks; see photo 3 in Grimes, 2007) are also superimposed on other microkarren.



**Figure 16:** Tightly meandering microrills and a v-notch (V) following a joint, on a cobble in the upper Skull Creek formation, Gregory Karst region. Width of view is 50 mm.



**Figure 17:** Shallow micropans, with finely pitted and toothed floors, superimposed on microrills, Gregory Karst region. Width of view is 50 mm.

### Katherine (Daly Basin)

The Katherine area is at the northern end of the Daly Basin, a broad area of flat-lying early Palaeozoic limestone that has an extensive cover of

Cretaceous sandstone and claystone and younger alluvium (Figure 1). Karst features are mainly restricted to the exposed limestones at the northern and western margins of the basin.

Most outcropping limestone forms pavements

of grikes and clints or, in more strongly dissected areas, widening and deepening of the grikes has converted the clints to pinnacles and small towers that are typically 1-3 m high, but up to 30 m in places (Hamilton-Smith et al., 1989; Lauritzen and Karp, 1993; Karp, 2002). The surfaces of the pinnacles and towers are sculptured by deep rainpits and rillenkarren grading to spitzkarren in the more dissected areas. Locally the pitting becomes very intense to form a sharp fretted surface analogous to coastal *phytokarst* (Hamilton-Smith et al., 1989). Kamenitzas up to two metres across are also common and some have outlet channels.

Microkarren occur but are not common. They appear local patches of bleached outcrop or on occasional distinctive thin beds of finer-grained, cream-coloured limestone – in contrast to the usual more massive and coarser-grained grey limestone.

Beneath the sandy cover there is a well-developed *epikarst* surface of narrow smooth-surfaced

pinnacles and deep shafts, which is exposed within the occasional soil-subsidence doline.

Further south, the rainfall is lower, and outcrops around the edge of the basin have only hackly surfaces with deep rainpits ranging in width from 3 mm to 20 mm.

### Barkly Karst region (Georgina Basin)

This is the easternmost of the large covered karst basins (Figure 1). The rocks are mainly Palaeozoic flat-lying dolomite with some gently folded limestones around the basin margins which have the best exposures of surface karst (Grimes, 1988). The climate ranges from semi-arid in the north to arid in the south (Figure 2) and karren are best developed in the wetter northern part.

#### THE DISSECTED NORTHEASTERN EDGE

Much of the northeastern edge of the karst region



**Figure 18:** The Colless Creek karrenfield, Barkly Karst, Queensland. In the foreground a thick-bedded limestone is dissected into deep grikes and spitzkarren. Beyond the gorge of Colless Creek is a plateau developed on a less pure and thinner-bedded limestone. This photo is typical of many outcrops of flat-lying thick-bedded carbonates in tropical Australia.



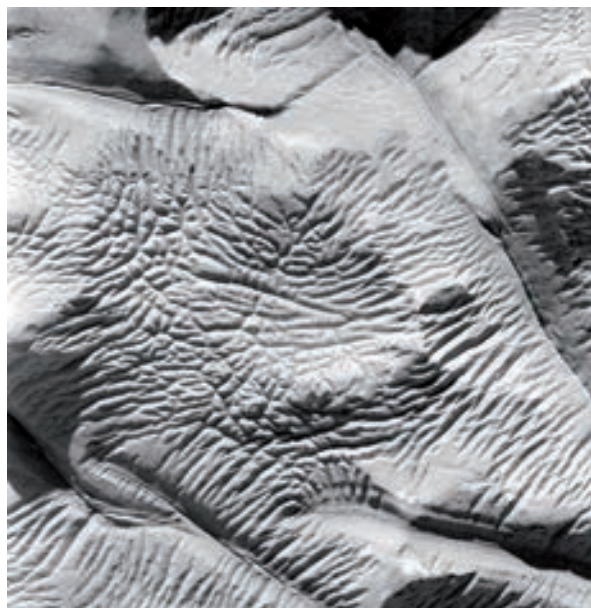


Figure 19: Fine etching of cracks (splitkarren) in dolomite near Camooweal, Barkly Karst, Queensland. Width of view is 20 cm.

is a dissected Tertiary plateau (Grimes, 1988; Williams, 1978) with the major streams incised as a superimposed drainage pattern. Between these is a dense pattern of modern dendritic surface drainage with v-section valleys and rounded interflues which is developed on impure limestone and dolomite with abundant chert as nodules and thin beds. This is equivalent to the “merokarst” of the West Kimberley region (Jennings and Sweeting, 1963) and lacks significant karst or karren, though there are scattered caves and dolines. Within this terrain occasional distinctive dark bands show up on the air photos – these are karrenfields developed on belts of pure, thick-bedded and well-jointed limestone (Figure 18).

One of the more accessible of these karrenfields is on the north side of Colless Creek a kilometre above its junction with Lawn Hill Creek, just west of Lawn Hill Gorge (Grimes, 1978, 1988). There, the flat-lying, thick-bedded, pure limestone bed is about 45 m thick and large grikes connect down to joint-controlled fissure caves. The structure is similar to that at Gregory (Figure 12). The surface

between the deep grikes is strongly dissected by rillenkarrren, steep runnels and spitzkarren (Figure 18). Kamenitzas and rainpits also occur on flatter surfaces.

Gale et al. (1997) described another karrenfield 12 km further west which had relatively thin (about 2 m) beds of pure and thick-bedded limestone interbedded with less pure, closer-jointed and medium-bedded cherty limestone beds. There, the grikes have widened to form small flat-floored “box valleys” (their usage) a few metres across and a “Lost City” of narrow walls and small “towers” up to 4.5 m high. The “towers” and walls are capped by the thick-bedded limestone, but the grikes have cut below this several metres into the underlying thinner bedded and less pure limestone. Gale et al. (1997) interpret the flat floors as corresponding to an impermeable bed which converted the downward erosion of the joints to lateral corrosion which widened the grikes.

#### THE SOUTHERN, ARID REGION

The more arid and less dissected parts of the Barkly Karst have relatively poor karren development. Possibly this is partly because much of this country is developed on dolomite.

Camooweal lies at the boundary between the semi-arid BShw and arid BW hw climates (Figure 2). Here, the dolomite strata are horizontal and thick to medium and occasionally thin bedded. They have well developed vertical joints that result in a blocky to slabby outcrop with narrow grikes and clints. Other karren are common rainpits and fine etching of structures and occasional poorly-developed rillenkarrren and runnels, usually only a few decimetres long. The *rainpits* occur mainly on slopes and vertical faces, and tend to follow the bedding structure. Sizes are variable, typically ranging from 4 to 25 mm across and they can form hackly surfaces. The flat tops of beds are generally smooth or finely etched or have various sizes of rainpits. The etching can be quite detailed, following nets of very fine cracks, and forming deeper v-notches (*splitkarren*) in larger joints or the bedding planes (Figure 19). Colour variations

in the cream-coloured dolomite indicate that weathering has penetrated a few mm in from the major cracks.

Apart from etching and fine pitting, *microkarren* are rare at Camooweal, but Reto Zollinger (personal comments, 2003) found a variety of well-developed microkarren in a more dissected area 80 km to the north-east. These included microrills, micro-networks and rasp-like micro-teeth, as well as fine pitting. Micro-pans and micro-tessellations were superimposed on the microrills and micro-teeth.

Further south, in the drier area near Boulia (Figure 2), I found some well-developed *microkarren* on cobbles of thin-bedded limestone. The upper, horizontal surface had radiating microrills 0.5–2.0 mm wide and linear microrills also ran down the vertical sides, but became less pronounced downward suggesting a decantation process. The underside of a loose specimen had fine pits (0.5–2 mm) where it had been in contact with the soil. In this arid region larger mesokarren are restricted to grikes and rainpits (Andy Spate, personal comments).

## Conclusion

Australia's tropical monsoon karst have a number of surface features in common (Spate and Little, 1995). There are extensive areas of bare limestone. The macrokarren have a positive relief with up-standing limestone towers, pinnacles, scarps and ridges, sometimes with adjoining pediments. The mesokarren are very well developed and include extensive and deep grikes, spitzkarren, rillenkarrren, kamenitzas, a variety of sharply-fretted pittings, and other forms. However, all these become less well-developed in the drier areas. Subsoil forms such as subsoil grikes, rundkarren, and smooth-surfaced pinnacles are locally exposed by soil erosion to form surface fields, as at Chillagoe. Directional phytokarst structures and solution ripples occur in the twilight zones of the caves and giant grikes. Microkarren have been recorded

recently from a number of areas, and are particularly well-developed in the Gregory Karst, but because of their cryptic nature it is too early yet to make deductions about their true distribution.

However, the local effects of lithology, structure, cover and denudation history can create considerable variation within that broad tropical theme.

## A semi-arid tropical monsoon model?

Jennings and Sweeting (1963), and Jennings in later papers, described a sequence of development for the West Kimberley karst region, with gradation from undissected plateau through giant-grikes, box valleys, and towers to pediment. Jennings (1967) said "it may be that here there is a semi-arid tropical monsoonal karst type". Some later writers have taken this sequence to be a purely climatic model, arguing for or against it on that basis (e.g. Williams, 1978; Gale et al., 1997). But Jennings and Sweeting (1963) also noted local lithological and structural controls and specifically excluded the impure limestones from their discussion as those formed a quite different "merokarst" terrain. The Jennings and Sweeting sequence is only applicable to areas of hard, pure, thick-bedded, jointed and flat-lying limestones in a tropical monsoon climate. Other constraints may also apply: e.g. time for the full sequence to evolve, and a dissected plateau with limited vertical relief. Even within such areas, variation in lithological and structural factors and the history of denudation can result in quite distinctive landforms and karren styles.

When considering climate, Jennings (1967, 1983) noted that although many of these areas are semi-arid the rainfall is concentrated into a short wet season and frequently falls as brief intense storms. So intense solutional sculpturing of the surfaces, comparable to that of more humid climates, is not inexplicable - one would not need to invoke past wetter climates. However, this idea is opposed by theoretical modelling by Szunyogh (2005) which suggests that long periods of gentle rain should be more effective for denudation than

short intense falls. Higher temperatures in tropical regions could also speed the reaction rates, and there may be a greater input from biological activity - including micro-organisms and algal coatings. However, in Australia what is probably more important is the history of long periods of exposure of many of the tectonically stable limestone areas, which could compensate for the slower rates of sculpturing.

However, Jennings (1981) argued for moderation in applying both climatic and other (e.g. lithological) influences to karst morphology. The truth will usually lie between the extreme views; climate, lithology and structure have all contributed to greater or lesser degree to the character of Australia's tropical karst. Each area needs to be interpreted according to its local setting.

## **Acknowledgements**

Andy Spate reviewed an early draft and provided information and photos of many of the areas. He also made available a collection of photos taken by Joe Jennings. Susan and Nicholas White, Mick Godwin and Reto Zollinger provided information, photos and specimens from several areas. Les Pearson commented on the Chillagoe text. Angel Ginés discussed the nomenclature and Bernie Smith discussed etchings and rainpits. Jacques Martini discussed the karren zones in the Gregory Karst. Sources of photographic figures are acknowledged in the captions, all unacknowledged photos are my own.

Jean-Noël SALOMON

*Giant pointed karren forms, or tsingy, figure among the most extraordinary karstic landscapes of the planet. Because of their distinctiveness, special tsingy areas have been developed for tourism or scientific purposes, mainly as nature reserves. Madagascar has several tsingy karsts and those of Bemaraha in particular have been included in the Unesco World Natural Heritage list. This kind of giant karren or megalapies, to be found only in tropical zones, is restricted to rigid and highly pure limestone outcrops that are more often than not fractured. They require, moreover, a good deal of time to acquire sizeable dimensions. The study of different tsingy karrenfields in Madagascar and their comparison makes it possible to address the mechanisms of their genesis and their preservation. In other respects, the extreme environments that make up tsingy karsts have allowed the development of both vegetal and animal endemic forms which make them extremely rich reserves of biodiversity which should at all costs be protected.*

## The tsingy karsts of Madagascar

Madagascar is an extraordinary country for the study of tropical karst phenomena since karst covers more than 30,000 km<sup>2</sup>, stretching 200 km from the north of the island to the south. All

these karsts develop on monoclinical, slightly sloping limestone plateaus with rocks dating from the Jurassic to the Miocene.

Rainfall (from 2,200 mm in the north, to less than 300 mm in the south) is concentrated over a period of a few months. The Madagascar karst areas are essentially famous for their extraordinary fields of tsingy, that is to say, giant, extremely pointed and spectacular karren or megalapies (Figure 1). Those of the Bemaraha are registered on the Unesco World Natural Heritage list and those of the Ankarana are worthy of inclusion in this list. Altogether, tsingy karsts cover about 800 km<sup>2</sup>.

## Tsingy karsts

According to the people of Madagascar, the term of tsingy (invariable noun) refers to a type of karren landform that is particularly pointed and which is said to “sing” when hit with a hammer, producing a sound transformed into an onomatopoeia: “tsingy”!

Not all the karsts of Madagascar include tsingy. Only a few have this particularity. They number from north to south: the Ankarana, the Namoroka karst and the Bemaraha (Figure 2). Elsewhere, tsingy are only present in rare and confined areas (Narinda, the Kasinge Forest in the Kelifely, the



Figure 1: Extremely jagged karrenfield, called tsingy, in Madagascar.

north of the Mikoboka). We shall, see further, on the reasons why.

Other karstic regions have karren landforms as tsingy, and apart from China (Ford et al., 1996; Salomon, 1997) let us mention the best known: certain parts of Cameroon, the Kouilou (Congo), the coastal area near Mombassa (Kenya and

Tanzania), Bom Jesus da Lapa (Brazil), Ta Khli (Thailand), Mount Api (Mulu, Sarawak), Mount Kaijende (Papouasia-New Guinea), the Chillagoe massif and the Fitzroy Limestone Ranges (Australia), etc. Tsingy are great karren forms which are extremely pointed (Figure 3) and which develop in groups, engendering extraordinary land-



Figure 2: Location of tsingy karsts in Madagascar.

scapes. In my opinion, the word “pinnacle” often used to describe them is not suitable: it is far too inaccurate and qualifies countless morphologies that are often outside the domain of karst.

Tsingy shapes do not greatly vary: they are always nose cone-, turret-, or needle-shaped. The acute angles of the needle-shaped ones are always between 15 and 20 degrees, which, on a large scale, produces a certain uniformity in an otherwise chaotic landscape (Figure 4). In detail, tsingy



Figure 3: Tsingy are characterized by great karren forms which are extremely pointed.

are grooved with vertical scores and are studded with a *honeycomb of cupola or micro cavities*. As the crests separating two grooves are often intersected, there result sharp reliefs which stand out clearly. Chiselling makes for edges that are extremely sharp and jagged (Figure 5), and dangerous in the case of a fall. The sizes of the tsingy differ and range from a few metres to over 30 m for the biggest.

### The Ankarana

The Ankarana massif is situated about 30 km to the north of Ambilobe and 75 km south/south west of Antsiranana (formerly Diego Suarez). It is



Figure 4: A typical appearance of tsingy karrenfields.

composed of a set of limestone dating to the middle Jurassic (Bajocian and Batonian) measuring about 30 km in length and 8 km in width, sometimes intruded upon by quite recent basalt (Plio-Pleistocene). The whole area covers around 150 km<sup>2</sup>. It is bordered on its north-western side by a subvertical 200 m high fault scarp, the “Ankarana Wall”, which is over twenty kilometres long.

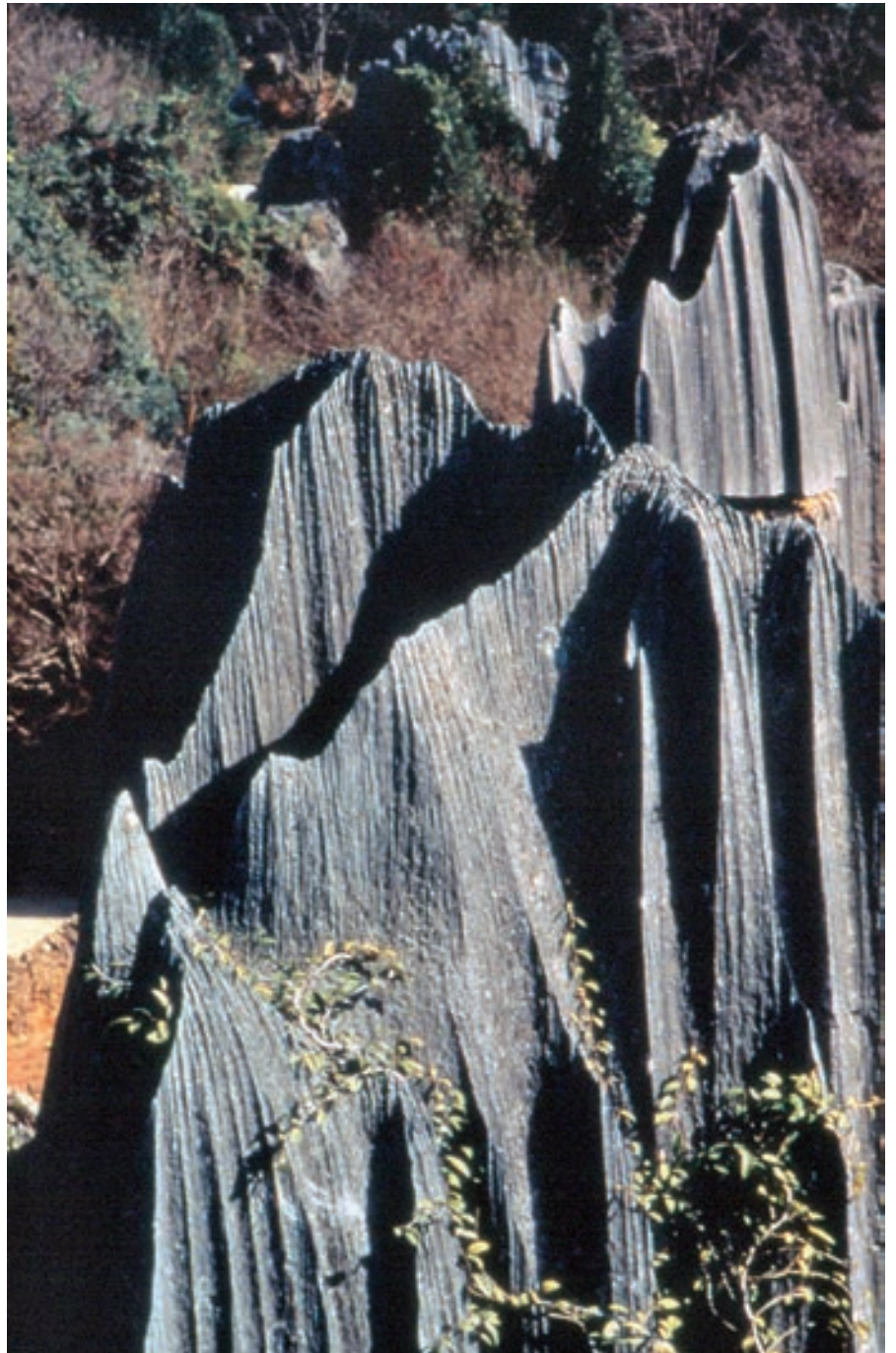
The Ankarana massif was not recognized as a special reserve until 1956, undoubtedly due to the lack of knowledge about the area, for it is in fact unique, with its speleological network of more than 100 km (Radofilao, 1977; Adamson et al., 1984), the largest in Africa, its wealth of tsingy and a unique cave-dwelling fauna (*Crocodilus niloticus*, bats, etc. (Wilson, 1985, 1987). However, the most visible caves (Andriabe, Ambatomanjamana and the underground waterway of the Mahajamba) have long been known, as can be seen in the

traces of smoke on the walls and the abandoned fireplaces in the galleries.

The surface of the plateau is made up of limestone capping rock on which lithology plays a fundamental part. The upper limestone layers, which are the most chalky, tend to produce reliefs with residual mounds and slightly depressed dolines. However, there is very soon evidence of crystalline limestone with a change of morphology. The surface then becomes pockmarked with deep collapse dolines, cluttered with block fields and forming islands of xerophytic vegetation.

From a tectonic point of view, the Ankarana behaves like a rigid block. As early as the Jurassic period, tectonic movements led the block to shift towards the west and this tendency continued in the Cretaceous as is shown in the general incline of the slopes in a westward direction. At the same time, the massif was affected by a slight synclinal

Figure 5: Chiselling by rillenkarren produces sharp reliefs on the tsingy pinnacles.



tendency (four-degree slopes both in the east and the west) with an axis situated approximately one kilometre to the east of the cliffs. The consequence of these movements is the presence of a series of fault scarps, more or less parallel to the Great Wall (Figure 6).

The actual tsingy karst which rises about 200

m above the surrounding savannah and canyon beds corresponds to summit areas and zones of intense joint pattern. Indeed, the massif is crossed with deep bogaz and narrow, vertically-walled gorges, oriented on the mainly NW-SE fracturing. Some of them (the Forestier canyon) can be flooded up to a height of 30 m during periods



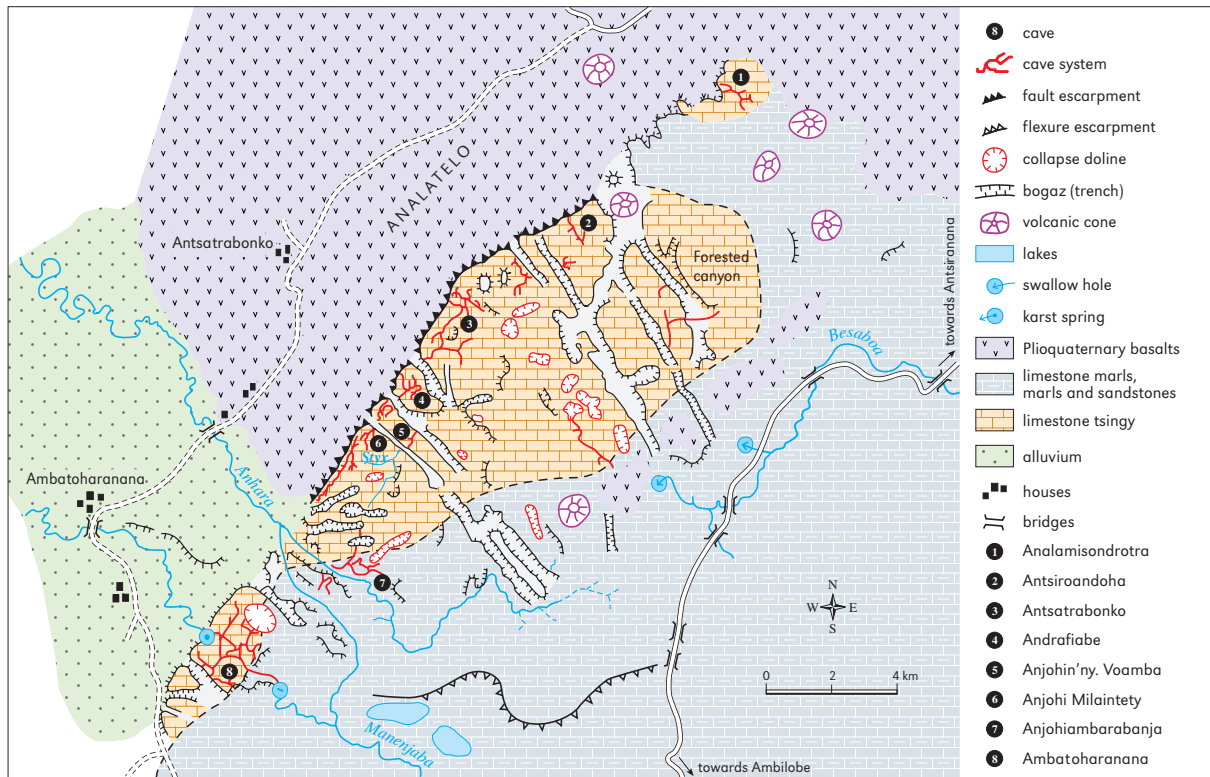


Figure 6: Morphologic sketch of the tsingy massif of Ankarana.

of cyclonic rainfall. One part of these corridors corresponds to the collapsing of the roofs of underground galleries oriented by faults; others are simply open fractures of tectonic origin that dissolving and collapsing processes of the walls have consequently widened. Some peaks, separated by profound crevices, measure over 20 m in height and the landscape may look as if it is a turret karst.

All in all, it should be remembered that, on the one hand, these tectonic movements can account for a strong NW–SE joint pattern and that, on the other hand, the tsingy as well as the general configuration of the cavities and the karst have been considerably influenced by the rigid nature of brittle limestone.

### The karst of Namoroka

The karst of Namoroka (about 160 km<sup>2</sup>) is situated at 150 km to the south-west of Majunga, between

latitude 16°20' and 16°30'S. This 100 m thick table of crystalline limestone (but with variations tending towards dolomitic) in many ways evokes the Ankarana and contains anastomosed speleological networks (the Ambovonomby one has a development of several kilometres). It is extremely marked by often circular fracturing as can be seen in the numerous corridors that cut through the massif, being colonized by xerophilous forest. In detail, a network of open joints and grikes divides the surface of these massifs into blocks. Because of this, an overhanging position of the upper blocks is often to be found, giving to the landscape a very spectacular aspect.

The tsingy chisel most of the Namoroka towers (some of which reach a height of 80 m) and some are more than 10 metres wide. They correspond again to highly pure crystalline limestone (99.2% CaCO<sub>3</sub> with only slight porosity: < 3%). As soon as the limestone becomes more dolomitic (that is to say, near the base), they disappear.

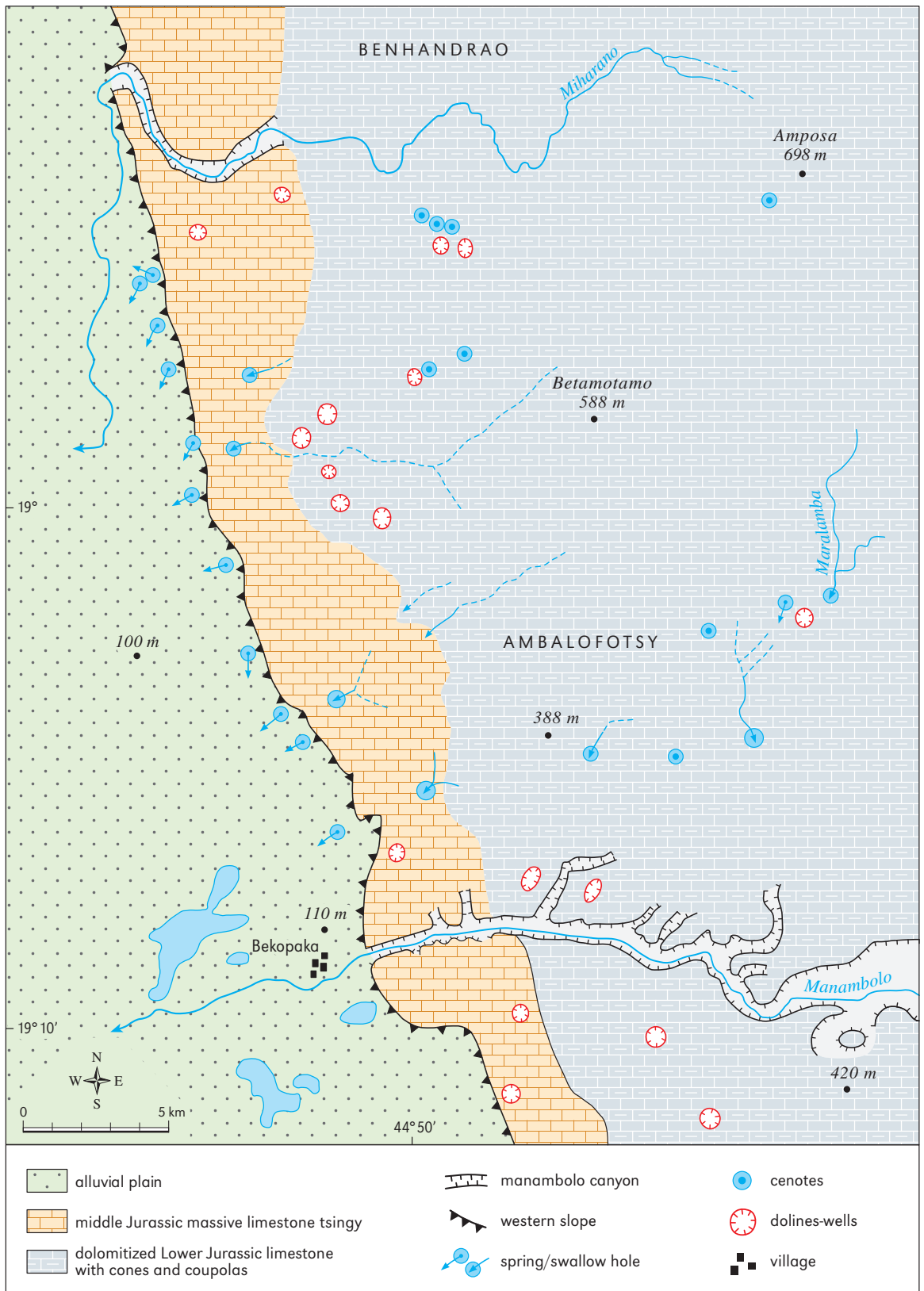


Figure 7: Morphologic sketch of the tsingy plateau of Bemaraha.

## The Bemaraha

The Bemaraha karst lies on the west coast of Madagascar and covers a surface of about 4,000 km<sup>2</sup>, between latitude 17° and 20°S. It stretches from the Ranobe in the north as far as the great Tsiribihina river in the south. Its width varies from 4 to 5 km in the north to 25 km in the south, between the canyons of the Manambolo and the Tsiribihina where the plateau is the most spectacular. The region is situated in a tropical climate area with a long dry season, but rainfall in season can be heavy and concentrated.

From a geological point of view, the plateau corresponds to limestone outcrops of the Middle Jurassic. To the west, it is covered by marl and marly-limestone of the Upper Jurassic and by the Cretaceous continental sandstone. Its eastern and western frontiers are well-defined since to the east there is a scarp face and to the west a scarp partly delimited by faults. On the south side, it is bordered by the deeply embanked Tsiribihina valley, whilst in the north it fades into small mounds of ever decreasing height (Figure 7). Rossi (1980) distinguishes several areas according to lithology:

- the north of the plateau with its scattered large conical cupola-shaped mounds and its steep slopes (mogotes). The smaller ones have a diameter of around 100 m and are 20 to 30 m tall; the larger can have a major axis reaching 2 km and a height of around 100 m. Between the mogotes, collapse-dolines are regularly present. Some summits are affected by tsingy but the latter do not make up continuous tables. Much of the karst has been covered with red clay coming from the breakdown of basalt. Today, erosion causes the disappearance of this cover and reveals crypto-corrosion shapes: limestone blocks with smooth ovoid or ogival shaped sides (rundkarren, small “stone teeth” or “dragon teeth”) that are sometimes pierced with cavities corresponding to what was once an opening made by roots. The limestone here is very pure (> 95% CaCO<sub>3</sub>; 1 to 2% MgCO<sub>3</sub>) with low porosity (1 to 3%);
- the central plateau is dotted with kuppen and dolines. The kuppen correspond to hard limestone with a thickness of some tens of metres situated above levels of marly-limestone. The tops of the mounds are trenched with tsingy from which a number of trees emerge, whereas the marly-limestone floors are more water-resistant and are covered in savannah. The actual centre of Bemaraha is made up of a huge field of kuppen separated by closed depressions which are usually shallow since they are trapped on a more impermeable level. They are large mounds (up to 80 m high) with steep slopes (20 to 30°) laid out in groups of several individuals;
- the Antsingy. The whole western border of the plateau which overhangs the western scarp is the realm of an extraordinary landscape: tsingy entablatures. The heart of the area, the Tsingy Nature Reserve of Bemaraha, covers 152,000 hectares of a typical tsingy natural biotope with caves, springs, a primary forest and calci-xerophilous growing formations inhabited by a rich endemic fauna. It is actually a limestone table of about 400 km<sup>2</sup> that has been subjected to fracturing and is jointed in all directions (main directions: N20°W to N30° to N40°). They are open fractures that have cut out tsingy blocks, engendering a landscape that is not unlike that of the Ankarana but with a greater scope. The sight when flying over the sharp blades of the tsingy is unforgettable: knife blades, turrets, needles and tsingy follow each other in an endless succession, separated by deep corridors in which decalcification clay and vegetal products pile up. Similarly to the Ankarana, the relief of these tsingy corresponds to a thick table (150 to 200 m) of very pure, non-dolomitic and non-porous (2 to 4%) micro-crystalline massive limestone. The density of fracturing would seem to be the fundamental element as it is from the thick network of joints that the dissolving process carves out tsingy. Even if some main directions may easily be identified (they are underlined by the appearance of volcanic seams) the density of the

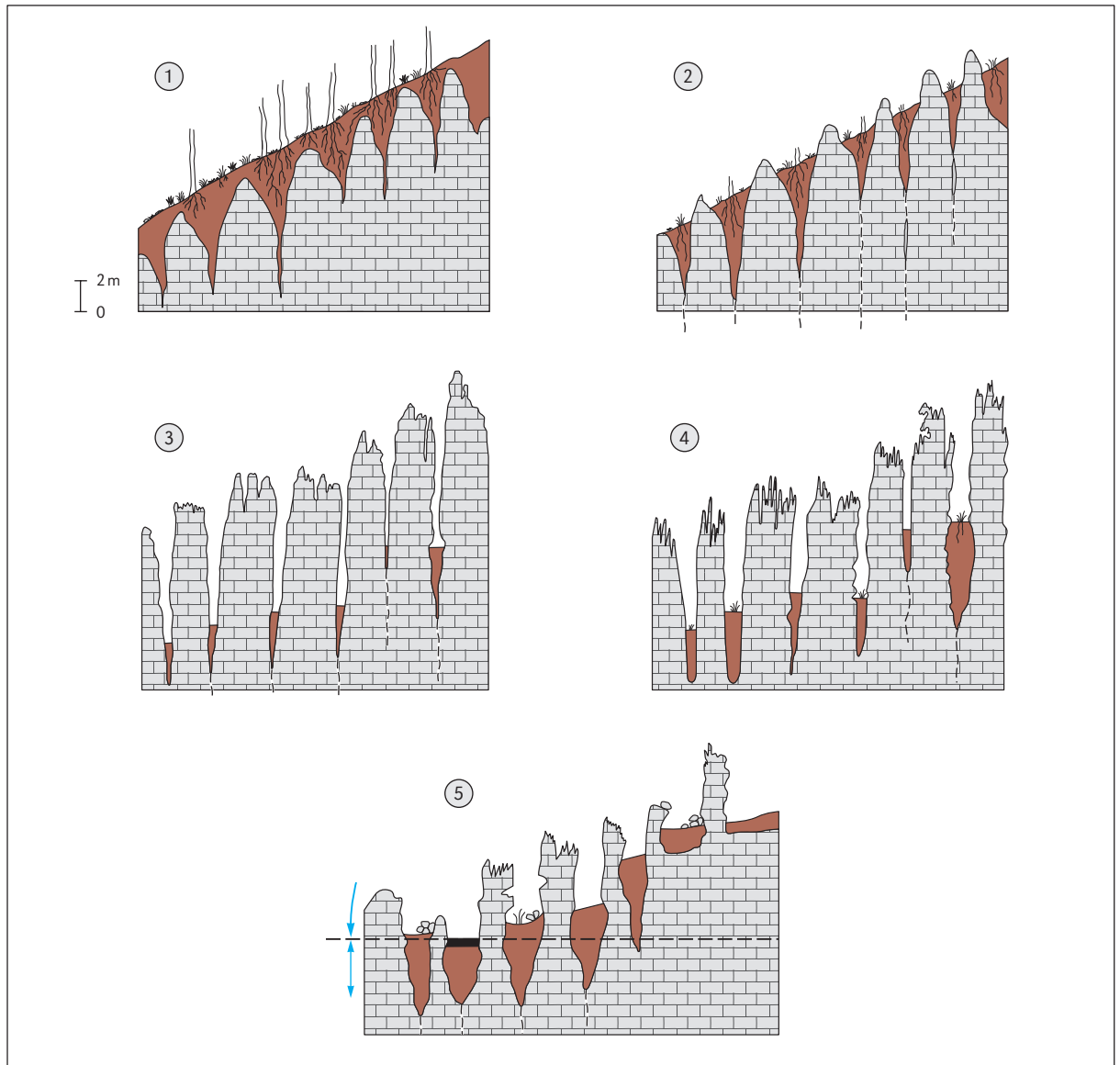


**Figure 8:** Evolution of the various stages leading to the formation of tsingy, then to their deterioration: 1. crypto-karst stage below the soil and lateritic soil. Possible presence of forest. Karst develops due to diaclasses and primary fractures; 2. dragon teeth stage. Upper layer removed by erosion, limestone is shaped (rundkarren); 3. pinnacle stage. Single towers and pillars appear, rillenkarren and dissolution coupolas develop. Gorges and bogaz along the fractures and diaclasses filled up by clay; 4. tsingy stage. This stage occurs when the limestone summits are very pure and massive and exposed to meteoric waters for a long time. In enlarged and developed bogaz some vegetation occurs; 5. developed stage. Landscape of isolated towers, enlarged gorges filled by breakdown and sediments. At certain low points phreatic zone appears.

joints and grikes is such that all directions are represented as orienting the networks. Among the latter, the Ming network extends to 1,050 m of galleries, that of Zohy Siramany to 1,950 m

and the AnjoHy Kibojeny network to 4,972 m. In all, more than a hundred cavities (Zohy in the Sakalaka language, or local language) have been counted (of which 12 are more than 1 km

long) and more than 53 km have been mapped (Delaty, 2000).

Since 1996, several circuits have been developed starting out from Antsalova (“Petits tsingy”, “Grands tsingy”). These circuits make it possible to visit this magnificent karst and the gorges of the Manambolo river.

## The genesis of the tsingy

A comparison of the tsingy karsts described above makes it possible to identify a number of common factors accounting for the genesis of the tsingy.

### The role of the climate and the time factor

In the case of Madagascar, most karst landforms, including therefore the tsingy, developed in a tropical climate with alternating seasons (rainfall exceeding 1,000 mm and a pronounced dry season). The observation of other areas of the planet featuring tsingy karsts shows that the situation is the same and this would seem to indicate that tsingy are subjected to tropical climates. Moreover, the tropical climate atmosphere has long affected these regions, often since the Jurassic at least. Traces of this are numerous: tropical red soils, strong weathered coverings and rubble (from broken up ferroaluminous crusts and so on). Only a few variations, such as the lengthening or shortening of the dry season or else of the total annual rainfall have played a part. It can be said that the main features of karst massifs that are visible today (tectonic movements, division into large compartments, the development of networks and so on) were established at the end of the Tertiary. The Plio-Pleistocene period brought only slight alterations (volcanic intrusion, incision of valleys and surface stripping) but which are not without importance as far as detailed minor forms are concerned, an example being the tsingy. The time factor also plays a part in so far as that, through gradation neomorphism and enrichment

in calcite, limestone becomes less and less porous as time goes by.

In Madagascar, it is the older (Jurassic) limestone that has tabular surfaces featuring tsingy. All this should be set in the context of the permanence of a great structural stability of limestone bastions, limiting mechanical erosion with time.

Whatever the case, we must acknowledge a relatively ancient evolution in which water has always played an essential part and in which the temperature factor has always been secondary, being subequal throughout the year. In particular, the absence of frost accounts for the fact that tsingy have been preserved and have reached a considerable height (up to 20–30 m in the Bemaraha). It can be observed that if tsingy are not present in temperate or cold countries, it is because they are destroyed by frost as soon they reach a certain height. There are some outstanding pointed karren (lapies) in the Pyrenees (Arres d’Anie) and in the Alps (Désert de Platée) but they only very seldom exceed 2–3 m in height: they do not have the time to develop further. In arid and semi-arid countries, drought and the predominance of mechanical erosion over chemical erosion account for the absence of tsingy.

### The role of the structure: lithology and fracturation

The part played by lithology is clearly demonstrated in the development of different types of pointed karren, from the stage of *dragon teeth* (Ford et al., 1996) to the true tsingy (Figure 8).

As a general rule, morphologies (rundkarren, dragon teeth) established under laterite (clay and colluvium silt) and a soil cover are similar whatever the lithology. However, once they are exposed to the open air, the teeth formed in pure limestone gradually acquire pointed or ogival shapes caused by superficial dissolving. This can go as far as to produce the formation of the pointed pinnacles, that are chiselled and carved of rillenkarren and honeycomb cupola. In detail, the reliefs are very

sharp. On the other hand, in impure and more porous limestone (dolomitic) the forms that develop are more rounded and of ruiniform type or sometimes mushroom shaped. The sharpest and most spectacular shapes form tsingy which often supply the finishing touch on the tops of columns. In the end, the formation of tsingy requires conditions which are specific and always the same:

- very pure crystalline or microcrystalline limestone (more than 95 or even 98% of  $\text{CaCO}_3$ ) with low porosity (always less than 1 to 2%), which is the case of the tsingy formations of the Ankarana and of the Bemaraha but also of the “Stone Forest” of Lunan (China) and the karren spires of Mulu (Sarawak). The nearly complete absence of porosity results in water being unable to penetrate the rocky mass and causes it all to run over the walls of the tsingy. Dissolving, facilitated by the extreme pureness of the limestone, is only superficial and laminar: this results in the high development of the tsingy and the vertical cracks which form ridges on their sides. It also accounts for the absence of decalcification residues. However, differences in porosity of the subhorizontal shelves can explain the development of stratification joints and the many overhangs that are visible along the walls and that are often unstable, as well as the presence of collapsed blocks at the base of the latter when evolution goes back a long time. The thickness of the limestone is of course an important element in explaining the height of the tsingy;
- a very strong fracturation producing *bogaz* and *corridors* lined up on the fracture as well as a great many intersections of vertical fractures that are often more than a metre wide and have an intense joint pattern. The fracturation network is a prerequisite for the organization of the patterns of the tsingy. This fracturation was furthered in Madagascar by the intervention of recent volcanic activity (intrusions) and the rigid nature of the limestone tables. The widening of the cracks can also be explained by consecutive dissolving by water running after heavy rainfall;
- a relatively slight dip ( $< 5^\circ$ ). Indeed, a more pronounced dip would influence the flow of water and would limit the vertical penetration by the joint pattern;
- heavy and concentrated rainfall (everywhere more than 1,200 mm). When it rains, water flows over the rock faces as limestone has low porosity and is too water-resistant for rain to penetrate. Often the water will not get as far as the base of the tsingy since it evaporates beforehand in contact with the overheated rock face. Dissolving is just superficial and is decreasingly effective from top to bottom. The rate of dissolution depends first of all on the quantity of rain falling on a given limestone surface (surface and sides of the tsingy) and secondly on how aggressive the rain is (with a decrease from top to bottom due to the saturation and evaporation). Dissolution only occurs on the surface. But in fact, as the water is concentrated in cracks, the latter deepen more rapidly than the peaks of the tsingy. This leads to the formation of tsingy which are higher and higher the older they get as well as to the genesis of shapes that are more and more pointed, in some cases with an angle of 10 to  $20^\circ$ . Once this angle has been established, the faces seem to recede parallel to themselves in such a way that the angle consequently remains the same.

The total absence of vegetation, or at least its rareness, linked to the absence of soil or the weakness of the corrosion in contact with the latter. Tsingy develop in an environment of bare karst. But is this absence not a consequence of the presence of the tsingy (the steepness of the slopes prevents any soil accumulation)? On the other hand bogaz soils may hold well grown vegetal formations (e.g. xerophytic dry forests).

However, the broadening of joints makes it possible for organic debris to be trapped and sometimes flowing water will reach the base of the tsingy, thus accounting for the corrosion features that may sometimes be observed there. Once the deepening stops (sometimes because of blocking at a more impermeable level), the bogaz widens

and it is possible to make one's way without any problem along the clay bottom stuffed with vegetal debris, as is the case in the Bemaraha.

## **Conclusions**

The comparison of the various karsts of Madagascar (as well as those of other regions of the world) makes it possible to underline the rareness of such landscapes (Salomon, 1997). The pureness of the limestone, its lack of porosity and the intense formation fracturing of the latter in addition to the permanence of a tropical climate atmosphere, are

the main factors accounting for their genesis. On a relatively reduced time scale, tsingy require some millions or even tens of millions of years to develop. However, they are fragile forms, sensitive to tectonics and to gravity (overhangs and collapses).

These exceptional landscapes, which in Madagascar harbour treasures of biodiversity as far as both flora and fauna are concerned, are likely to be of increasing interest to the tourist industry as their existence becomes more widely known (through television programmes, sightseeing circuits, books of photographs, and so on). For this reason, it is necessary to take immediate protective measures.

Mick DAY and Tony WALTHAM

The *pinnacles* on the northwestern flanks of Gunung Api, in the Gunung Mulu National Park, in northern Sarawak, are perhaps the world's largest individual *spitzkarren* and certainly among the most impressive pinnacle or *shilin karrenfields* in any karst landscape. They were first described by Wilford and Wall (1965), but remained virtually unknown until 1977–1978. They are now recognized as the “type example” of *pinnacle karst*, but their precise morphology, their exact distribution, and their mode of formation are still known only broadly, and they certainly warrant further study. These “classic” pinnacles represent a dramatic subset within the overall pinnacle assemblage within the Gunung Mulu Park, and their relationship to the broader *karrenfield* also warrants further research.

### Setting

The Gunung Mulu National Park has a relatively simple geological structure expressed by striking topography that rises from less than 100 m a.s.l. to over 2,400 m within a distance of less than 10 km (Sweeting, 1980). The western 38% of the Park is lowland with some ridges, but the eastern portion is mountainous, and about 25% of this is karst terrain. Essentially, the geology consists of a broadly conformable Paleocene-Miocene sedimentary

sequence that has been folded into an anticlinorium and partially metamorphosed. At the core of the anticlinorium and occupying the highest elevations are the slates, slaty shales and quartzitic sandstones of the Mulu formation (Liechti et al., 1960). These are overlain sequentially by the Melinau limestone, which crops out as a belt on the northwestern flanks of Gunung Mulu and by the Setap Shale, which forms the bulk of the western lowlands and ridges.

The Mulu pinnacles are formed in the Melinau limestone (Upper Eocene-Lower Miocene), which forms a dissected karst escarpment about 30 km long and < 5 km wide, rising to 1,600 m from the alluvial lowlands on the northwest flank of the metasedimentary spine of Gunung Mulu itself. The limestone is lenticular, 1,500 to 2,000 m thick, massively bedded, and dips steeply at 40–50°, more in some locations, to the west-north-west, though bedding planes are rarely visible in surface exposures (Osmaston and Sweeting, 1982; Waltham and Webb, 1982; Waltham, 1997a). The limestone is dominantly a white to blue-grey calcilutite that includes some fine calcarenite, is locally recrystallised to resemble a marble, and has a dolomite content ranging from 2 to 20%. The carbonate is predominantly lagoonal, and the macrofauna is sparse, with the most prolific fossils being foraminiferal tests (Adams, 1965; Waltham and Webb, 1982).

The limestone belt is cut into several distinct



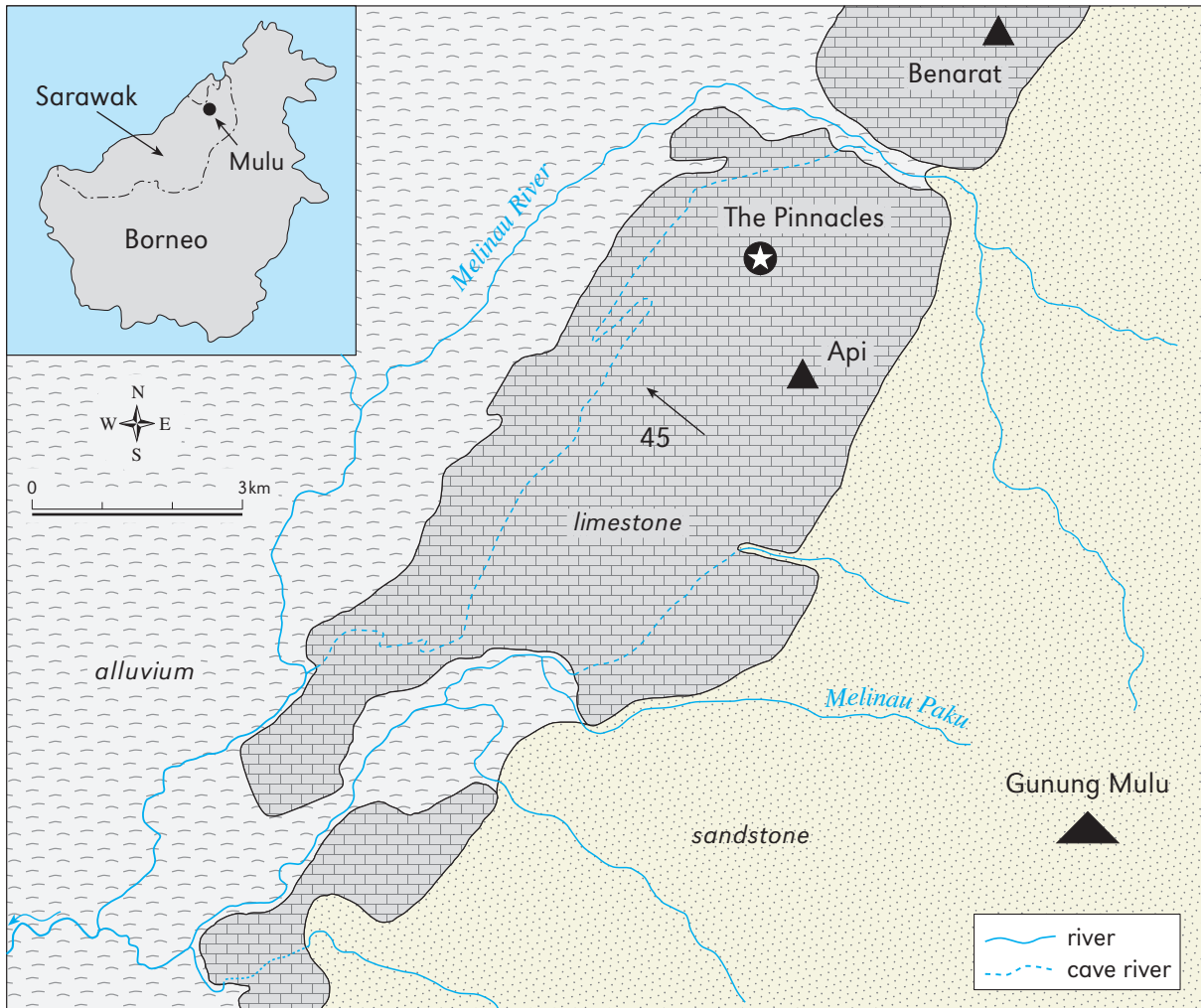


Figure 1: Location of The Pinnacles on the limestone ridge of Gunung Api, within the Gunung Mulu National Park, Sarawak.

blocks by the through-flowing allogenic rivers of the Melinau, Melinau Paku and Medalam (Figure 1). Within the karst blocks between the three river gorges, the peaks of Gunung Api and Gunung Benarat rise to elevations of about 1,700 m above very steep, vertical or undercut flanks. All the karst blocks are drained internally by massive and complex cave systems that are still not completely mapped (Eavis, 1980; Waltham, 1997b). Their surfaces are ubiquitous jagged pinnacle karrenfields, shrouded in dense rain forest and punctured by open shafts, large collapsed dolines, and a few dismembered large dry valleys (Osmaston and

Sweeting, 1982; Brook et al., 1982; Waltham, 1995, 1997a, b; Waltham and Brook, 1980a, b).

It is uncertain whether the limestone also extends below the alluvial Melinau plain (Wilford, 1961; Osmaston, 1980). Bordering the karst massifs, a series of gravel terraces are the outer portions of massive alluvial fans that head in the gorges where they are fed by denudation of the non-carbonates of Gunung Mulu itself. These gravels have been transported largely above ground through the breaches in the limestone escarpment, aggrading during wetter interglacial periods and being incised during drier glacial epi-



Figure 2: Aerial view of pinnacles along the ridge of Gunung Api (photo Malaysian Tourist Board).

sodes (Rose, 1982, 1984a, b). They also extend into the caves, and Farrant et al. (1995) have used them to date cave wall notches, which correlate with resurgence levels defined by interglacial aggradation intervals, to demonstrate a mean base level lowering rate of 0.19 m per 1,000 years over the past 2 million years. Interpreting the rate of base level lowering as the rate of isostatic uplift in response to regional denudation indicates that internal erosion of the karst blocks has been minimal, and the present karst topography has evolved over the past 10 million years.

The Mulu karst experiences an equatorial monsoonal climate, at a latitude of 4°N. Temperatures range within 20–30°C, and mean annual rainfall is about 5,000 mm, distributed evenly throughout the year (Walsh, 1982a). Vegetation is generally dense rain forest, but that on the limestone is distinctive, with numerous endemic calcicolous species exhibiting altitudinal zonation (Anderson and Chai, 1982). Osmaston (1980) pointed out in-

tersecting rectilinear patterns in the vegetation that appear to correspond to fracture patterns in the limestone itself. The limestone soils are lithosols thin, skeletal, highly organic silt or clay loams with limestone rubble (Baillie et al., 1982; Anderson and Chai, 1982).

The climate accelerates contemporary carbonate dissolution within the karst, producing an inhospitable, sharply fretted surface that is very difficult to traverse or investigate in detail. Many of the lower slopes are mantled by talus, much of which is cemented by calcite. Soil carbon dioxide levels may be locally high, but measurements are generally less than 0.1% (Friederich, 1980; Laverty, 1980). Provisional data from limestone weight loss tablets (Day, 1981a) indicate that limestone weathering rates within soils and in riverine locations are ca. 100 mm/ka, within the range measured elsewhere in tropical karst, but that rates on steep rock faces are much lower, at around 10 mm/ka. Solute loads in the rapid run-off are low (Fried-



Figure 3: The Pinnacles, the classic site seen from the overlook high on Gunung Api.

erich, 1980) and regional solute loads similarly are unremarkable by tropical karst standards, generally falling within the 80 to 150 mg/l range (Walsh, 1982b). By contrast, annual runoff is considerable, probably near 4,000 mm, and the chemical denudation rate is about 125 mm/ka (Walsh, 1982b).

## Pinnacle morphology and development

Pinnacle karrenfields are widespread within the Mulu karst, occupying at least 30% of the limestone surface on the Gunung Api and Gunung Benarat blocks. Adequate sampling is almost impossible on the inaccessible and forest-clad mountains, but observations and limited, non-random sampling suggest that about half the pinnacles throughout the area are less than 5 m tall, with 30% less than 2 m tall, while about 20% reach more than 20 m in height, and the type examples on the flanks of Gunung Api may reach to 50 m. This suggests that the size distribution is not normally distributed, and supports previous observations about the size distribution (Osmaston, 1980; Waltham, 1995, 1997a). The available evidence also suggests that the larger pinnacles generally are at the higher elevations, but this may be due to their prominence on the

more gently sloping terrain of the summit ridges. Further investigation is needed, with larger sized random samples. Ley (1980) measured some of the “classic” pinnacles at 35 m tall, and estimated that some individuals might be up to 100 m in height, though this would seem to be an overestimation, and such individuals would certainly represent statistical outliers. Many of the seriously inaccessible high regions of the karst blocks have only been observed from helicopters. Giant pinnacles protrude from the forest canopy over areas of the Api and Benarat ridges (Figure 2) far beyond the well-known classic pinnacles on Api, and some of the very steep (but not vertical) mountain flanks are almost ladders of tall pinnacles half-hidden by the very large trees that grow between them.

The pinnacles’ type example is a cluster known as The Pinnacles high on the northwestern flank of the Gunung Api ridge (Figure 3). This site lies in a shallow, steeply inclined valley aligned north-east-southwest at about 1,200 m, and contains perhaps no more than 100 individual pinnacles, within an area of just a few hectares (Osmaston, 1980; Waltham, 1995, 1997a). Between 30 and 50 m in height, these enormous individuals protrude 10–20 m above the forest canopy. Many pinnacles are connected to form contiguous but dissected *arêtes* or lines of summits (Ley, 1980) and others

Figure 4: Pinnacles that appear to be clustered around deep shafts, on the edge of The Pinnacles group.



are grouped in circular pattern, resembling the remnants of near-vertical shaft margins (Figure 4). The dominant pinnacle summit alignment is close to north-south, so that the pinnacles cut across the minor valley, with their summit elevations decreasing towards the valley axis. Osmaston (1980) reported that the dominant fracture sets over most of Gunung Api are orientated at  $22^\circ$  and  $85^\circ$ , but that these were displaced by about  $10^\circ$  clockwise near The Pinnacles.

Although surface run-off down the pinnacles has not been documented, by inference and analogy it occurs frequently, rapidly, and with dissolution limited by the restricted residence time. Thus water reaching the pinnacle bases remains aggressive, and may be rendered more so by contact with the suspended organic root mat, and dissolution is focused within the epikarst below the pinnacle bases, though this is still far above the known active cave systems (Brook et al., 1982).



Figure 5: Immature rillenkarren grooves cut into the rounded flanks of a rundkarren dome since the latter was exhumed from its soil cover, beside the trail up to The Pinnacles.

Ley (1980) postulated the potential role of high humidity, cloud condensation and mist in maintaining the sharpness of the pinnacles. Noting that mists often wetted pinnacle summits, and that rainfall run-off registered solute loads of only 10 mg/l, compared to 60 mg/l for condensation run-off, Ley suggested that the *rillenkarren* themselves were produced by torrential stormwater run-off, but that their razor-sharp edges were maintained by condensation corrosion. Although this contention provoked initial skepticism (Ley, 1980; Osmaston, 1980), it is noteworthy that the role of condensation in carbonate dissolution has since received increased attention (e.g. Dublyansky and Dublyansky, 2000), and its role in shaping the pinnacles may warrant further attention.

The remnant limestone blocks have sides too



Figure 6: Deeply fretted honeycomb karren near the crest of one of the Gunung Api pinnacles.

steep to maintain any cover of macro-vegetation, and even algae may be scoured by run-off and desiccated under the hot sun in intervening dry periods. The lack of blue-green algae is evident in the stark whiteness of the largest pinnacles, in contrast to the blackened surfaces that characterise most smaller pinnacles in China and elsewhere. Given the significant role of organic agencies in other tropical karst environments (Viles, 1984, 1988), it would be surprising if the pinnacles did not have at least some biogenic component, but this requires further investigation. At the transition from the fluted upper pinnacles to their more blocky and rounded pedestals, there is a suspended organic mat where vegetation thrives on a tangled root mass of skeletal organic soils, besides rooting in soils that clog the diminishing widths

Figure 7: Razor-sharp crests on some of the smaller pinnacles on Gunung Api.



of the intervening fissures. From the root mass, trees rise to heights in excess of 20 m, with the white-grey fluted pinnacle spires emergent above the canopy with their rock faces inclined at 70–85°. The precise role that the suspended organic root mat plays in pinnacle evolution has to date been conjectural, and there remain questions, such as

what controls the position of the mat, and whether it marks a formerly less dissected surface between the individual pinnacles themselves.

At their bases, although generally obscured by soil and vegetation, the pinnacles have broadly blocky, sometimes rounded and often densely pitted margins (Figure 5), and typical sub-soil *rund-*

*karren* are widespread where the vegetation mat has been stripped away from the rock by micro-earthslides (Waltham, 1995, 1997a). Above their bases, however, the pinnacles are upward tapering and with a grossly blade-like morphology, which Osmaston (1980) attributed to a tendency for the two upper corners of elongate pinnacle blocks to be eroded. The upper portions of the pinnacles, above the vegetation mat, are deeply fluted by dissolutional *runnels*, producing exaggerated rillenkarren with razor-sharp edges. Osmaston and Sweeting (1982) recorded a range of flute sizes, between 16 and 590 mm in width, 2 to 500 mm in depth, and up to 15 m in length. Ley (1980) noted that rillenkarren were particularly well developed on the more exposed southern and western faces of the “classic” pinnacles.

At their uppermost extremities, above the rillenkarren zone, most pinnacles have sharp, pointed *spires*, but some have grotesque, labyrinthine shapes reflecting assemblages of what Osmaston (1980) terms *honeycomb karren* (Figure 6). These have received little attention, and it would seem that the *pitting* could be due to either *biokarstic processes* or to variations within the rock lithology. It would be interesting to compare their morphology to that of the karren developed on the pedestals beneath the vegetative mat. Another unresolved issue is the role of bedding, if any, in influencing pinnacle micromorphology. Osmaston (1980) noted that there were “faint signs of bedding on the pinnacles and only occasional fracture planes with moderate easterly dips”, and that the latter “typically show as an undercut ledge with a rough surface that is suggestive of a *stylolitic pressure contact*.”

There has been only limited research on the broader array of pinnacles within Gunung Mulu, but Osmaston (1980) made some general observations and reported on a grouping that had been investigated by Hans Friederich (Friederich, 1980) in a small doline low on the southwestern slopes of Gunung Api. There, too, were “sharp crested monoliths, but much smaller, due to the closer fractures, and at the bottom of the doline many

had collapsed” (Osmaston, 1980). Fallen limestone blocks occur elsewhere too, especially close to steep, undercut cliffs along the flanks of the limestone belt, and some of these appear as isolated pinnacle rising out of the alluvial soil cover. All across the forested limestone slopes, small pinnacles project from the soil and understory vegetation, and many are distinguished by razor-sharp edges (Figure 7) - sharp enough to slice to the bone the thigh of a falling walker. Many of the pinnacles in the shadows of the forest lack the dramatic proportions of their larger equivalents, but details of their morphology need further investigation.

## Pinnacle geology

Other factors may have played some role in pinnacle development, particularly in enlargement of the classic site of The Pinnacles on the north-western flank of Gunung Api. Frost action during the Pleistocene is unlikely to have occurred, much less had a pronounced influence, and surface profiles mean that unloading stress relief can only have had some local influence on joint accessibility. Local focusing of surface drainage, either on the early limestone surface or from an overlying non-carbonate surface (developed on the Tertiary setap shales) may also have been a factor. In many areas of mature fluviokarst, deep fissures on joints that parallel the contours of steep valley sides have a jagged morphology that emulates pinnacles. Consideration of comparisons with the developmental history of the Lunan shilin promoted the conjecture that “there is a clear possibility that these shales overlay a Tertiary fossil karst, which was exhumed to provide an initial stage of development of the modern pinnacles” (Waltham, 1995). Alternatively, the apparent location of the largest pinnacles at relatively high elevations may suggest that they are simply the oldest such features; it is difficult to assess the age of The Pinnacles, but a realistic timescale is within 10–100 ka (Waltham, 1995).

One factor in the development and maintenance of the dramatic pinnacle morphology is the mechanical strength of the limestone itself (Day, 1980, 1981b, 1982b). Schmidt hammer hardness, a surrogate for compressive strength, is 56 (Day, 1980) - but this is within the upper end of the range for limestones that support many other karst terrains. The limestone is very massive, facilitating the formation and persistence of pinnacles within very thick individual beds; the singularly massive structure of the Melinau limestone appears to account for it containing some of the world's largest cave chambers, in addition to some of the world's tallest pinnacles. The limestone also has a very low primary permeability, and is extremely pure, with non-carbonate contents less than one percent (Waltham and Webb, 1982). Osmaston (1980) suggested that the "classic" pinnacles might be formed in an area of particularly pure calcite, but this suggestion has not yet been investigated further.

The pinnacles are assumed to have developed by dissolution focused on nearly vertical joints - though definitive evidence of this awaits access to, and mapping within, cave passages immediately beneath some of the taller pinnacles. Mean spacing of the defining joints at right angles to each other in the "classic" Pinnacles area has been estimated at between 10 and 20 m (Osmaston, 1980). It may be somewhat less elsewhere, thereby restricting formation of the larger pinnacles to locations where wider spacing results in the focusing of larger volumes of rainwater into each fracture (Osmaston and Sweeting, 1982). Ley (1980) invoked bedding planes dipping at about 60° to the northwest and joints dipping at 45° to the east in explaining the shape of the pinnacles, but also portrayed vertical development (presumably down another set of joints) in his developmental model. The role of vertical joint sets was raised in subsequent debate (Waltham, in Ley, 1980) and in other reports (Osmaston, 1980), but the issue has not been fully resolved. Osmaston (1980) presented a simplified model of pinnacle evolution suggesting that, given sufficient stabil-

ity and time and an adequate rate of dissolution, pinnacles will be derived from the walls of deepening wedge-shaped fissures, with the slopes of the walls depending on the ratio of the rates of vertical and lateral dissolution; his model has the intersections of fissures producing wedge-shaped pinnacles, the heights of which are proportional to the fracture spacing, and whose relationship to the initial form of the upper surfaces of the limestone blocks is minimal.

Osmaston considered two aspects of Mulu's pinnacles: 1) the general formation of such sharp-crested protrusions, and 2) the specific development of the exceptionally large "classic" pinnacles. With respect to the latter, he concluded that "...the local factor which is responsible for the formation of The Pinnacles is the exceptionally widely spaced, rectangular, vertical fracture pattern coupled with an absence of other fractures or bedding. This has a threefold importance: it leaves strong intact blocks that are large in plan; it leaves wide fissures between them; and, because the blocks are stable, they have time to assume a profile of dynamic equilibrium which can descend with the general landscape surface" (Osmaston, 1980).

## Analogous features

The Mulu pinnacles are broadly analogous to giant *spitzkarren* karst at various other locations. The *shilin* (stone forests) of China, including the type locality at Shilin, Yunnan (Song et al., 1997), tend to cover much larger areas with unbroken seas of pinnacles that do not reach the heights of those in Mulu. The *tsingy* of Madagascar (Rossi, 1974; Salomon, 1997) are even more extensive, but only small areas have pinnacles heights comparable to those in shilin karst. The *assegai* landforms of Palawan, Philippines (Longman and Brownlee, 1980) are larger than shilin, and similar terrains forming the *arête karst* around Mount Kaijende, New Guinea (Jennings and Bik, 1962; Beck, 2003) appear to have pinnacles that equal or exceed the



dimensions of those in Mulu. Waltham (1995, 1997a) draws a distinction between normal pinnacle karst, such as that in Mulu, which has formed on steep slopes in high limestone mountain rain forests, and the shilin sub-type, which has evolved through multiple phases on gently dipping limestones. There are also more distant analogies to the pinnacles formed in indurated calcareous aeolianites in the Nambung National Park in western Australia (Ford and Williams, 1989), and to non-karstic pinnacles formed in soils and other rocks (James, 1997).

## **Context**

The Mulu pinnacles are landforms of significance to geomorphology on a world scale. They are protected both by their inaccessibility and by the establishment (since 1974) of the Gunung Mulu National Park, which was inscribed as a U.N. Natural World Heritage Site in 2000. Along with the caves and other karst features, they represent a significant attraction of the park, and deserve appropriate attention in the development of future management strategies (Anderson et al., 1982; Day, 1979, 1982a, 1983).

# ARÊTE AND PINNACLE KARST OF MOUNT KAIJENDE

Paul W. WILLIAMS

Mount Kaijende is located in the Western Highlands district of Papua New Guinea (Figure 1) between the settlements of Laiagam and Porgera at latitude 5°30'S. *Arête and pinnacle karst* occurs near its summit, which rises to about 3,500 m above sea level, the regional tree-line being at around 3,800 m a.s.l. The karst of the area was first brought to the attention of scientists through the work of Jennings and Bik (1962) and investigated further by Williams (1971, 1972). Other occurrences of arête and pinnacle karst have been observed from aircraft further west in Papua New Guinea and Papua, but these sites have not been scientifically investigated. This account draws on the work cited above and on a recent review by Williams (2004).

Although Jennings and Bik named the morphology "*arête-and-doline karst*", Williams (1972) considered it misleading to imply that the enclosed depressions resemble dolines as they are normally understood, because of their very steep rock sides and intimate connection to the arête ridges; so he preferred to omit the term doline from the description of the terrain, which he described as "*arête and pinnacle karst*" (Figure 2).

## Bioclimatic environment

In Papua New Guinea climates vary from tropical

humid or seasonally humid at sea level to glacial above the snow line at about 4,600 m a.s.l. Mean annual temperatures decrease with elevation at a rate of about 5.8°C/1,000 m, consequently the upper slopes of Mount Kaijende are cool with a mean annual temperature near the summit of about 10°C and the tropical location implies little seasonal variation. Nevertheless, there is a significant diurnal variation, with a range of about 12°C being measured at 2,800 m a.s.l. Night time frosts are common above 2,430 m, so freezing conditions must often affect the arête and pinnacle terrain. The mountain is almost always cloud covered, thus fog-drip must make a large contribution to annual precipitation. Rainfall at Porgera, which is 8 km to the west and at 2,200 m a.s.l. in a nearby valley, has been measured at about 3,700 mm, so it is likely to be considerably more at the summit. The arête surfaces are essentially bare on their crests, being in an exposed hostile environment near the upper limit of montane forest. Frost shattering was probably common during the Last Glacial Maximum, because at that time the snow-line was at about 3,550 m (Löffler, 1977).

At an elevation of about 3,200 m a.s.l., Williams (1971) commented that "thick, virtually impenetrable moss-forest, swirling in mist, clings like a sodden cloak to the rugged slopes". Daytime temperature at that height was 11°C and water dripping from moss-draped branches had a pH of 3.9.

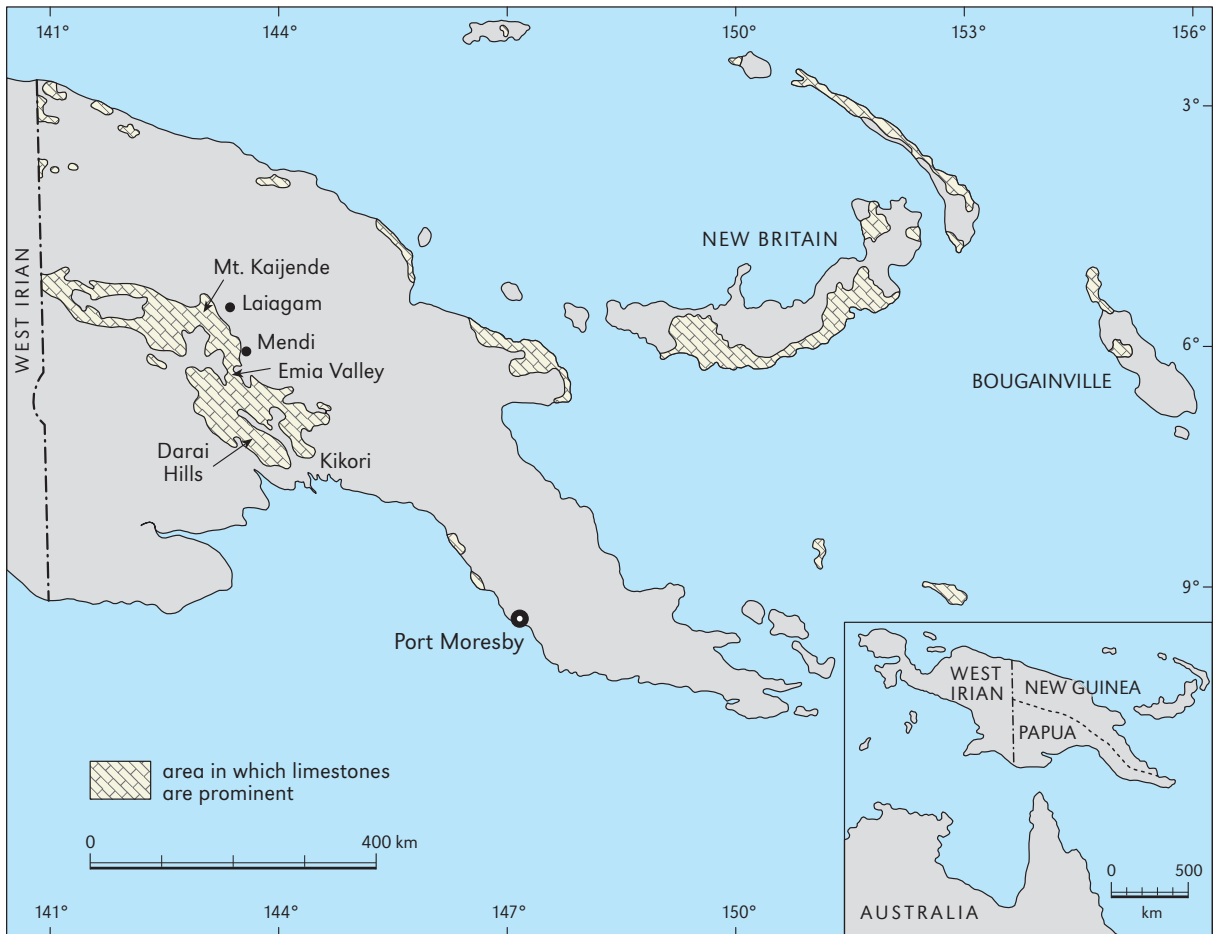


Figure 1: Location of Mount Kaijende in Papua New Guinea (from Williams, 1972).

Solutional denudation rates have not been measured, but must be at the upper end of international estimates. *Glacial pedestals* on mountain Jaya in neighbouring Irian Jaya indicate surface lowering rates on limestones of 32 mm/ka over the last 9.5 ka (Peterson, 1982).

On the lower slopes of the mountain at around 2,900 m a.s.l. *arête* and *pinnacle karst* progressively gives way to *polygonal karst*. This is completely clothed in rainforest except for the bottoms of some of the larger depressions which are covered with coarse *kunai* grassland and tree-ferns, temperature inversion and associated frost drainage having excluded the forest.

## Geological setting

Karst in the southern fold belt of Papua New Guinea is developed mainly in Oligocene to Miocene limestones and covers an area of about 20,000 km<sup>2</sup> (Löfler, 1977). Around Mount Kaijende it is developed in Lower Miocene limestone of more than 1,000 m stratigraphic thickness. Exposures in cliff faces show it to be extremely massively bedded (order of tens of metres). Mount Kaijende is a triangular block faulted on its NW, SW and E sides, and tilted gently to the SSE. Fault scarps vary in height, some attaining almost 1,500 m. Thus local relief is considerable and the vadose zone is deep. The region was probably first uplifted and exposed



Figure 2: Sketch of arête and pinnacle karst on Mount Kaijende (from Williams, 1972).

to denudation in the early Pliocene, but the region is still tectonically active.

## Regional morphology

The altitudinal zonation of karst forms in Papua New Guinea was discussed by Williams (1973). Arête and pinnacle karst occurs between 2,600 and 3,500 m a.s.l., but its occurrence appears to have more to do with structural-topographic considerations than climate. Arête and pinnacle terrain is known in three small localities at the northern extremity of the limestone country in the neighbourhood of Mount Kaijende, and occurs mostly within an area of 8–10 km<sup>2</sup> around the summit. The arêtes are naked, reticulated, saw-topped ridges with spires, and with practically vertical side slopes that have a local relief of up to about 120 m. A good photograph of the area is available in Löffler (1977). The ridges are crudely aligned, dominantly NNE–SSW, and are determined by master joints striking at 25° crossed by other sets at 110° and 155°. These lineaments

isolate large blocks, the edges of which have been incised by huge sub-vertical *solution gutters*. The converging heads of these solution channels from different flanks of the blocks impart a sinuosity to the arête ridges. The bare pinnacle tops are probably sharp and fluted with rillenkarren, but investigation has not been close enough to determine details. There are no measurements of the height of the pinnacles, but they are of the order of 100 m or more and the near vertical solution gutters are several metres wide. Drainage down the gutters converges in deep shaft-like enclosed basins (Williams, 2004).

Although the arêtes are bare along their crests, the limestone faces gradually obtain an increasingly dense plant cover as the surfaces descend into the more sheltered environment of joint canyons, along which the bottoms of closed depressions are aligned. Thus most depressions within the arête and pinnacle terrain are vegetated at their base. However, authoritative observations are unavailable, because the terrain is extremely inaccessible (Figure 3) and so has never been penetrated very far and subjected to a field survey.



**Figure 3:** General aerial view from the south of arête and pinnacle karst on Mount Kaijende.



**Figure 4:** Oblique aerial view of arête and pinnacle karst on Mount Kaijende.



Figure 5: View of Mount Kaijende from the southeast with arête and pinnacle karst on the skyline.

## Discussion

The landforms described are an extreme case of *karrenfield* (Figure 4); extreme because of their height and steepness. This is made possible by the combination of considerable local relief, the strength of very massive and widely jointed limestones, and the rapid dissolution engendered by the very humid environment. The tropical context has no special significance, except that occasional frosts are not severe enough to destroy the karren and Pleistocene glaciers have not eroded the area; however, glaciation has affected other karsts in the region (Hope, 1976). Similar landforms are found in Sarawak in the pinnacles of Gunung Api

in Mulu National Park. On Gunung Api the pinnacles are sharper than observed on Mount Kaijende, but long arête ridges are less common. The gradual clothing with vegetation of the pinnacle sides as they descend into the forest is a feature of both areas (Figure 5). The tsingy of Madagascar also have some similarity to the karren landforms of Mount Kaijende, but the lowland context is different and the extent of the tsingy area is greater. The shilin (stone forest) of Lunan in China also has tall sharp spire features that resemble those found in Madagascar, although the pinnacled ridge relief of Mount Kaijende is much higher and more dramatic. Ford et al. (1996) compare the features of these three areas.



# LITHOLOGICAL CHARACTERISTICS, SHAPE, AND ROCK RELIEF OF THE LUNAN STONE FORESTS

Martin KNEZ and Tadej SLABE

The Lunan *stone forests* – *shilin* are a unique form of karst karren (Chen et al., 1998; Knez and Slabe, 2001a, b, 2002; Kogovšek et al., 1999). The karren, which is criss-crossed by fissures along the fractures, is composed of *rock pillars* (Song, 1986; Habič, 1980) or *stone teeth* (Song, 1986; Song and Liu, 1992). Stone teeth are smaller protuberances less than five metres tall; “high” teeth are taller than three metres, and “low” teeth are less than one metre tall (Song and Liu, 1992). According to their shape, they are divided (Song and Liu, 1992) into conical, angular, and oblong. The pillars are between five and fifty metres high and are of various shapes. Large stone forests are a characteristic feature of subtropical climate conditions (Song, 1986).

According to their location, Song (1986) distinguishes three types of stone forests: valley, hill top and hill slope. In lowlands and valleys, large stone forests occur with intermediate dolines and depressions. Underground waters flow beneath them, so they are periodically flooded or water flows through them. Stone forests on the tops of the hills are lower (10–30 metres), their pillars grow from a common foundation, and the cover of sediment above them was thin. Stone forests on hillslopes are an intermediate form between the other two types.

The Lunan stone forests are often described as a form of covered karst (Chen et al., 1986; Maire

et al., 1991; Sweeting, 1995). The carbonate rock on which karren developed was covered by thick layers of sediment that decisively influenced the occurrence and shape of the stone forest. According to the thickness of the sediment, a stone forest can be barren, covered, or buried. Hantoon (1997) describes the stone forests as an epikarst form. Mangin (1997) believes that epikarst of the stone forests extends to a depth of 100 metres.

The Lunan stone forests were formed predominantly through the dissolving of rock below the soil and sediments. The water increases the width of the fissures and separates rocks. Under sediment with acidic water, wide and deep cracks developed between the pillars with deep channels on their walls (Yuan, 1997). Uncovered carbonate rock is transformed by rainwater. Teeth develop first and from them, the forests form (Song, 1986).

Originally, the limestone, which was already in the process of karstification (Yu and Yang, 1997; Song and Wang, 1997), was covered by Permian basalt and tuff that influenced its shaping and in places metamorphosed the rock (Song and Li, 1997; Ford et al., 1996). Water permeated through the basalt and tuff, and underground karst began to develop. In the Mesozoic, part of the limestone was exposed (Song and Wang, 1997). In the Oligocene and Miocene, rock blocks rose and lowered, and in lower parts the karst relief was transformed by erosion (Yu and Yang, 1997). In





Figure 1: Major stone forest.

the Eocene, the Lunan graben subsided, and thick layers of lake sediments were deposited (Chen et al., 1986; Zhang, Geng et al., 1997; Song and Wang, 1997). In the tropical climate, thick layers of laterite soil developed on the sediment (Sweeting, 1995; Ford et al., 1997). In the Pliocene, the current stone forests began to develop (Yu and Yang, 1997). In the Quaternary, a great part of the sediment was removed but some remained in the fissures.

The level of the underground water played an important role in the development of the stone forests (Ford et al., 1997). With the development of underground water courses, pillars began to develop from teeth (Zhang, Geng et al., 1997). The fluctuating underground water widened the fissures (Yuan, 1991). Below the forests today is a comprehensive and diverse system of water caves (Zhang et al., 1997). Tectonic action resulted in lowering the level of the underground water, the

removal of sediments from the surface, and the more rapid growth of the stone forests.

The Major stone forest spreads over 80 hectares, while the other larger and smaller stone forests cover some 350 square kilometres (Chen et al., 1986; Zhang, Geng et al., 1997). The Major stone forest lies at 1,625–1,875 metres above sea level and is located in a valley system. The underground water, which is just below the surface, rises ten metres following abundant precipitation. Most (70–80%) of the annual precipitation of 936.5 mm falls between June and October (Chen et al., 1986). The average temperature is 16.3°C, with a range between –2°C and 39°C. The pillars are tallest in the central part of the valley system where the surface waters flow into the underground and there is more sediment at the edges of the forest (Sweeting, 1995). Habič (1980) calls this “shallow karst.” In the lower part of the stone forest, waters also run on the surface.



Figure 2: Naigu stone forest.

The tourist areas of the Lunan stone forests are visited annually by more than a million people. This is a unique and integral natural and cultural landscape where the Sani minority lives, many of whom work in the tourist industry (Figure 1).

The shape of the pillars in the stone forests and their height are characteristic of certain types of rock and their topographical position (Zhang, Geng et al., 1997).

Numerous examples of stone forests that have developed in almost identical conditions confirm that the diverse shapes of the pillars are primarily the consequence of the distribution and density of the joints and fissures that cut the carbonate rock and the rock's varying stratification and texture. We must also add the importance of the efficiency of their formation by underground factors and their reshaping by rainwater that determined the course of their development in different periods.

## Selected examples of stone forests

### Naigu stone forest

The Naigu stone forest (Figure 2) lies twenty kilometres east of the Major stone forest and is an important tourist site. This stone forest is composed of larger rock masses (Figure 3) and smaller pillars that stand together or individually. The unique form of the forest is defined primarily by the fracturedness and texture (Figure 4) of the various beds of rock from which the stone forest formed at different levels. The dimensions of the pillars are dictated by the joints and fissures that vertically criss-cross the layers of rock. The shape of the pillars, which are frequently undercut, and their *rock relief* clearly reflect the importance of *subsoil formation* and the *reshaping by rainwater* progressing slowly down the pillars.

The stone forest lies alongside two ridges slight-



Figure 3: Larger stone masses of Naigu stone forest.

ly elevated by tectonics. The joints that border the joint zone are extremely strong, and the intermediate joints that largely run in a northwest-southeast direction are several kilometres long and deep. The pillars formed on a package of Lower Permian carbonate rock of Qixia formation more than one hundred metres thick. The properties of rock throughout the geological cross-section are very different, and from the morphogenic viewpoint we therefore divide the groups of layers into three groups from the bottom up: a) layered micrite and non-porous limestone, b) porous and heavily dolomitized limestone (Figure 5), and c) massive and striped dolomitized limestone.

The pillars developed on different levels of the described rock beds and their shapes correspond to this rock variation. The most characteristic shape of the pillars is mushroom-like, and there are distinct *notches* along the porous and heavily dolomitized beds (Figure 4). This notching is the consequence of faster underground corrosion

and hollowing of the most porous part of the rock, whose surface disintegrates relatively quickly. The pillars whose tops are in porous and heavily dolomitized beds are narrower and mostly without characteristic or regular shapes dictated by the factors of their development. Stratified and non-porous limestone often forms wider bases of the pillars composed of porous and heavily dolomitized and massive and striped dolomitized limestone. The shape of subsoil rock teeth as a rule does not reflect the different texture of the rock.

The most distinctive rock forms are subsoil and composed. *Subsoil rock forms* include large channels on the walls of pillars and channels on the broader tops. Composed forms include the channels leading from the *subsoil channels* or *subsoil cups* found on the tops. The deepening of subsoil cups and water flowing along the channels caused the dissection of the tops of the pillars, particularly the larger ones, into points with *funnel-like notches* between them (Figures 4, 5).

Figure 4: Individual pillars in Naigu.



Subsoil rock forms, as a rule the larger ones, developed on all types of rock in the Naigu stone forest. The rock influenced their shape, especially that of the smallest, which on dolomitized rock often have jagged edges. *Flutes* hollowed by rain drops are a less distinctive rock form in Naigu. Their occurrence and development is primarily

influenced by the texture of the rock. Subsoil rock forms developed on the majority of beds of different rock, but only a few are found on porous and heavily dolomitized beds. Here we find *subsoil tubes*. When these beds of rock are found at the tops of pillars, smaller rock forms hollowed by rainwater hardly occur. In places these



Figure 5: Dolomitized beds of Naigu stone forest. Width of view is 1.5 m, in the middle.

are only *rainpits* or the rainwater shapes larger subsoil rock forms. The rock relief therefore developed relative to the position of the beds in the pillars.

The gradual and diverse development of the stone forest, which of course is connected with

the development of the caves below them, is also confirmed by the traces of the development in the Bayun cave in its central part. From the cave sediments and the rock relief we can distinguish several periods of development in the epiphreatic part of the aquifer, then a rapid drop of the un-



Figure 6: The top of Pu Chao Chun stone forest.

derground water that probably caused the faster growth of the stone forest (Šebela et al., 2001).

### Pu Chao Chun stone forest

The Pu Chao Chun (Figure 6) is a smaller stone forest located fifteen kilometres south of the Major stone forest. Its rock pillars are located on a ridge, where their network is the densest, and on the hillslope below. Its shape is defined primarily by the unique distribution of variously thick beds of rock, mostly thin in the upper parts, on which the stone forest developed at different levels. The dimensions and oblong form of the pillars were dictated by the joints and fissures that vertically criss-cross the rock beds. The shape of the pillars and its subsoil rock forms clearly reflect their subsoil formation and their transformation by rain-water slowly progressing down the pillars.

The rock changes little across the geological profile. Throughout, we trace mainly biomicroparitic limestone with an almost hundred per cent proportion of  $\text{CaCO}_3$ , limestone that in this profile shows similar sedimentation conditions and that regardless of the thickness of the beds shows the same response to the influence of erosion and corrosion processes. The thickness of the beds has a decisive influence and clearly reflects the morphological appearance of the individual rock pillars.

In the upper part of the stone forest, the pillars are mostly individual and of smaller diameters, and the rock beds are the thinnest here. The lower parts of the pillars, which are formed on the thicker beds of the rock, are stouter and stand closer together. Along the thinner beds (Figure 7) there are distinct notches. Here, the beds disintegrated faster and the tops left beneath them are often flat, while if the beds above them were thicker, the



Figure 7: Characteristical pillars of Pu Chao Chun stone forest.

tops are sharp. In the lower part of the stone forest, where there are fewer rock pillars, the pillars formed on thick beds of rock and as a rule therefore are wider at the bottom and narrower toward the top.

All the types of subsoil rock forms that reveal the evolution of the stone forest are well developed. These include large subsoil channels and *subsoil scallops*, as well as channels and *subsoil cups* on the wider tops. The latter channels often developed from subsoil tubes along bedding planes and were uncovered when the upper beds disintegrated. Subsoil notches developed where long-lasting layers of soil surrounded the walls. A distinct proportion of the rock relief consists of *composed rock forms*. These are divided into those that occurred due to direct interaction of subsoil factors and rainwater and those whose unique shape is the consequence of transformation of subsoil forms

by rainwater. The composed rock forms are channels that lead from subsoil channels and cups at the tops and hollows between the bedding planes of the rock. *Funnel-shaped mouths* formed on the edges. Exposed subsoil rock forms were transformed by rainwater that hollowed flutes, channels, and rainpits, and on vertical and overhanging walls *rain scallops* are present that occurred due to water trickling down the rough surface of the rock. *Solution pans* most often occur on the bottoms of exposed subsoil rock forms.

### Lao Hei Gin stone forest

The Lao Hei Gin stone forest (Figure 8) lies eighteen kilometres north of the Major stone forest. Individual and clustered rock pillars and larger blocks of rock transformed by corrosion and ero-



Figure 8: Lao Hei Gin stone forest.

sion occupy about two square kilometres. Where the pillars are clustered, there are only cracks or fissures between them. The pillars developed on various levels of almost horizontal rock beds, and their shapes correspond to this. The larger clusters of stone pillars are composed of several dozen pillars. On the relatively large area of the stone forest, there are only individual pillars and rock teeth. Some pillars have the shape of square towers and others of mushrooms. They are often composed of several blocks (Figure 9), the remains of rock beds between bedding planes and fissures. The individual pillars are either relatively large, wide, and high or low (1–2 m) and wide.

In the area of the Lao Hei Gin stone forest, the original limestone is heavily diagenetically altered: under the microscope, we can observe subhedral to euhedral grains of dolomite in the rock that form hipidiotopic to idiotopic structures. With the exception of the upper part, the rock pil-

lars are roughly built of dolosparites and dolomicrosparites of the grainstone type.

An important difference in individual packages of layers was in the determination of various degrees of secondary porosity and recrystallization, which are also reflected in the morphological appearance of the stone pillars. The lower parts of the pillars are composed of dolosparites to dolomicrosparites of the grainstone type in which secondary porosity is barely noticeable. The central part of the pillars is composed of very secondary-porous dolomites. On average, the crystals of dolomite are smaller than the crystals in the lower package of the layers and at the same time are less pure. The upper parts of the pillars are again composed of secondary almost non-porous limestone and dolomites. Only the tops are composed of recrystallized secondary non-porous limestone. Dolomite rock disintegrates mostly into grains.

The strongly secondary porous central parts of





Figure 9: Mushroom-like pillars in Lao Hei Gin stone forest.

pillars below the ground as well as on the surface weather and disintegrate faster. As a rule, tall pillars therefore have a distinct mushroom shape because the non-porous beds are more durable and extensive. In places, the upper parts of pillars no longer exist, and only low pillars that formed

in the lower non-porous rock and protrude from the ground remain. The heavily porous rock in the central part of the pillars is often hollowed by subsoil tubes that have been formed by rainwater trickling down the pillars. The rare tops of pillars formed on such rock have non-uniform shapes in most cases.

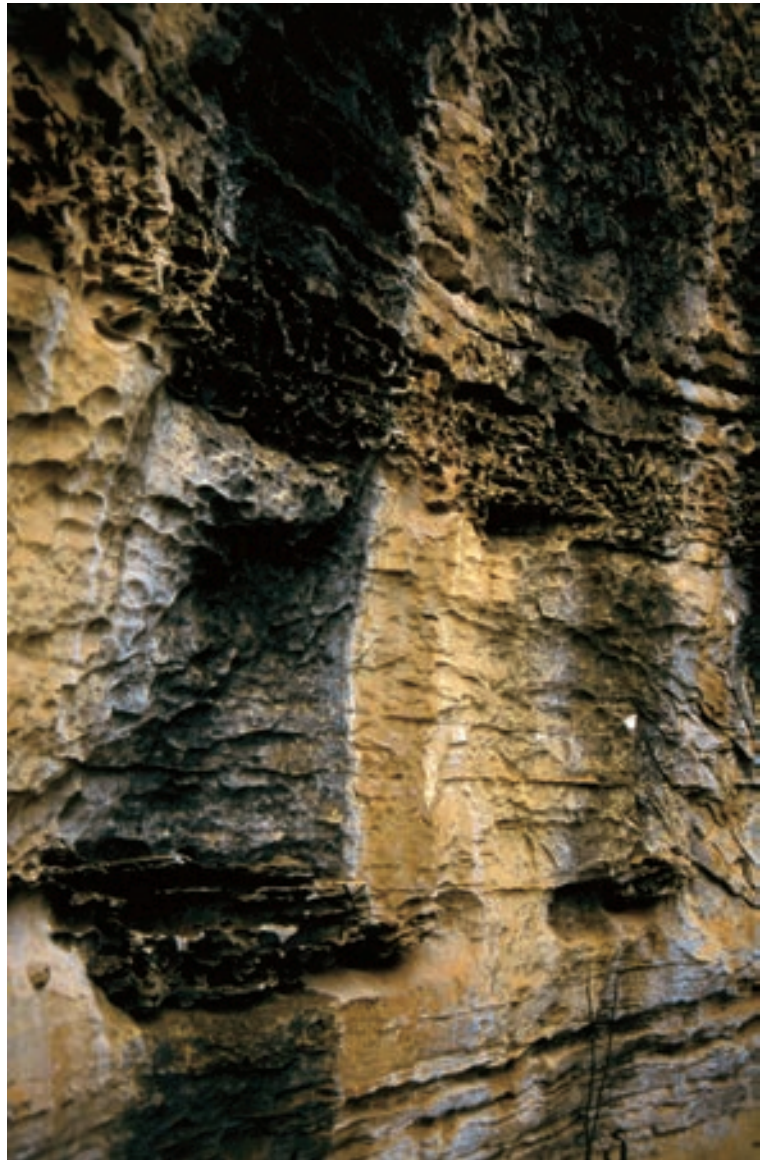
The rock relief is composed of all the characteristic groups of subsoil rock forms, forms hollowed by rainwater, and composed rock forms. To a considerable extent, the texture of the various rock beds determines their features.

The first complex of subsoil forms includes various subsoil channels that occurred due to the continuous flowing of water along the contact of the wall and the sediment that covered the rock and filled cracks along the vertical fissures. The diameter of the largest channels reaches several metres. They dissect all four different complexes of beds. On the tops of the tallest pillars, they were



Figure 10: Rough surface of the dolomitized rock in Lao Hei Gin stone forest. Width of view is 50 cm.

Figure 11: Chert nodules from Naigu stone forest. Height of view is 2.5 m.



transformed by rainwater, while the porous middle beds weathered too quickly for the channels to remain on them for a longer time. Thus the channels are mostly a characteristic of lower pillars and rock teeth. Subsoil scallops, which occur at relatively permeable contacts between the rock and sediments, are also preserved as a rule on the nonporous beds or on only recently uncovered heavily porous beds.

The wider tops of pillars and teeth are dissected by medium-sized and smaller subsoil channels and subsoil cups (Slabe, 1999) that developed under the soil that partially covered the rock, that

is, due to the permeation of water through the soil and its flowing along the contact with the rock. The larger channels on the upper parts of pillars are composed rock forms. They occur due to the water flowing from subsoil channels on the wide tops of pillars or lead from funnel-shaped notches. At the bottoms of the latter there are or used to be subsoil cups. At the edges of the tops are therefore larger or smaller funnel-shaped mouths most frequently reshaped by rainwater. They are especially distinct on the non-porous beds, or when the top is in a limestone rock, reaching to lower lying heavily porous beds. Their distribution and shape



- relatively narrow and deep - are determined by the fracturedness of the rock and the indentation of the rock circumference by the texture of the rock.

*Half-bells* occur at the longer lasting levels of soil and sediments surrounding the pillars (Slabe, 1998, 1999).

Rock forms hollowed by rainwater, especially smaller ones like flutes and rainpits, do not occur on the rock described above. The rock is coarsely rough, and only those rock forms whose size exceeds individual elements of texture and structure occur on it (Figure 10). The exception is the smaller, highest-lying part of the stone forest where flutes occurred on the tops of limestone teeth. The dissection of most of the tops is therefore determined by the texture and fracturedness of the rock. From subsoil cups distinctly dissected and rough *solution pans* occur, and only the bottoms of those covered by a thin layer of sediment and are overgrown remain flat and relatively smooth. On the upper part of steep walls, there are rough features similar to channels, which in most cases are very narrow and relatively deep, of angular shape; their diameters measure one to ten centimetres and they are two to three metres long.

## Lithological and morphological characteristics and rock relief

The area of the stone forests is composed of Lower Permian carbonates of the Qixia and Maokou formations. These formations are two of the more important basal formations on which numerous stone forests developed in the southern Yunnan region of Lunan. Characteristics of the Qixia formation are micrite limestone with intercalations of dolomite and dololimestone with intermediate sheets of schist. In the lower part of the Maokou formation, the limestone alternates with dolomite and dolomitic limestone. In the upper part, we trace the sequence of limestone, which is thinly bedded in places and elsewhere composed of several metres thick beds, as well as massive lime-

stone, which in individual horizons contains up to several decimetres of thick quartz chert nodules (Figure 11). The main lithological features of the Maokou formation are roughly similar to the Qixia formation, the only difference being that in the Maokou carbonates we do not trace any major impact of late diagenetic dolomitization and in some places there is considerable secondary porosity. In both formations, we notice heavy diagenetic variability of the foundation rock, which is undoubtedly the consequence of the intensive volcanic (basalt lava) activity during the transition from the Paleozoic to the Mesozoic. The rock has an exceptionally high percentage of carbonate.

In the area studied, we found considerable variations in the thickness, porosity, degree and manner of dolomitization, containment of inclusions, and colour of individual layers reflected in the formation of the stone forests (Knez, 1998).

Morphological characteristics (Figure 12) are the reflection of various factors, of which the most important are geological factors. One of the basic factors is undoubtedly the fissuring of the rock, which influences the shape of the forest and the dimensions of the stone pillars. The distribution of the pillars (ground-plan of the stone forests) matches the fracturedness of the rock. The pillars can be joined in rows between distinct joint sections and stand closely side by side, or the stone forests or their parts are composed of individual wide or narrow pillars. Pillars with smaller diameters as a rule occur along dense networks of fissures, while larger rock masses with broader tops occur along thinner networks.

An especially important factor is the stratification of rock, which affects the shape of the stone pillars. The beds have virtually no impact on pillars that developed on thicker beds and beds with an even rock texture. However, the vertical cross-sections of pillars on thin beds of rock are often jagged because they are dissected by the notches that occur along bedding planes, and the unequal resistance of different beds of rock is reflected in their external shape.

Enumerating geological factors, we should not



Figure 13: Stone teeth.

forget the texture of the rock. The rock texture, especially if it is diverse, can decisively influence the shaping of stone pillars, as much the shape of their vertical cross-sections as the size of the cross-sections. Porous beds are often hollowed and disintegrate faster, while beds of rock with less soluble components most often protrude from the walls.

For better understanding both the regional and local development of stone pillars, we must also point out the influence of subsoil processes that fostered the development of pointed tops of subsoil teeth (Figure 13) and the undercut shape of the pillars. Rainwater sharpens the tops of pillars and transforms the traces of their original subsoil formation. The unique development of the stone forests is reflected in their rock relief. Rainwater gradually transforms subsoil rock relief. Subsoil and composed rock forms, especially the largest, are the most distinctive. Subsoil rock forms include scallops, large channels, notches, and half-

bells and subsoil channels and cups on broader tops, while composed rock forms include the channels leading from subsoil channels or solution cups and they dissect the walls of the pillars. Many pillars are subsoil undercut, and their tops are transformed by secondary subsoil rock forms and shapes hollowed by rainwater. A unique rock relief is found on the larger rock pillars, especially those that have wide tops, either on thick beds of rock where secondary subsoil rock forms occur or on the tops that developed due to the disintegration of thin rock beds, where the subsoil tubes that occurred along bedding planes are transformed into subsoil forms or large channels reshaped by rainwater. Both features also indirectly influence the shaping of the pillar sides due to the flowing of the water and the hollowing of channels. As a rule, smaller rock forms do not occur on dolomite rock, on very porous rock, or on rock with large inclusions.

# TWO IMPORTANT EVOLUTION MODELS OF LUNAN SHILIN KARST

Linhua SONG and Fuyuan LIANG

The Shilin National Park, with a total area of 350 km<sup>2</sup>, is located in Lunan, 80 km east of Kunming, the capital of Yunnan Province. The shilin landscape is a special type of *pinnacle karst* developed in thick, gently dipping, and mostly pure Lower Permian carbonate rocks in a humid, tropical climate. It includes *subadjacent karst*, *subsoil karst* and *subaerial karst*. The main shilin karst landscape consists of *stone columns* or *pillars*, and *stone teeth*, with extensive subsoil solution features such as *through caves*, *wall niches*, and *solution grooves*, as well as subaerial solution forms like different types of *karren*, *vertical solution columns*, *depressions*, and *pits*. The most typical joint-oriented features, both subsoil and subaerial, are vertical wells about 10 m deep.

Field studies show two evolutionary types for the shilin landscape. In the Shilin National Park the area was covered by basalts in the Late Permian, and by conglomerates and mudstones in the Tertiary period. When the basalt covered the Lower Permian limestone, the basalt fractured as it cooled and solidified, and intense weathering took place. Rainwater was able to penetrate through the basalt into the limestone and cause intense dissolution of the limestone. This process produced the high and magnificent shilin landscape beneath the basalt cover. Another type of shilin landscape developed in the carbonate area that has not been covered by non-carbonate rocks.

The karst features were formed by subsoil dissolution. On hilltops, the limestone blocks have been corroded by rainwater dissolution along fractures and other openings, with a result that is similar to the *tsingy karst* landforms of Madagascar. On slopes, most rainwater runs off and washes the soil and insoluble materials onto lower land such as depressions and basins. On the slopes, isolated stone columns or pillars and stone teeth with subsoil solution features are displayed. In the depressions and basins, the soil thickness reaches several metres to tens of metres. The subsoil solution that formed the stone columns was highly irregular, and the distance between stone columns varies from 10 to 50 m. The lower parts of the columns are buried by fluvial deposits.

## Development of the Shilin Park

The shilin landscape is the special type of karst landscape in the Lunan Area, Yunnan. The name shilin is from the Chinese, shi = stone or rock, and lin = forest. The term applies only to stone pillars that stand above the ground at least 5 m like a stone forest (Yuan, 1982; Song, 1986). Three thousand years ago, Qiu Yuan searched for the Shilin, but nobody could tell him the location (Wang et al., 1994). Four hundred years ago, Xiu Xiake, the great geographer of the Ming Dynasty,

traveled through 11 provinces from the east to the southwest of China for about 50 years to visit karst landforms, caves, springs and minority societies. He summed up his great learning in his “Travels of Xiu Xiake”. But there is no specific description of the shilin landscape in his diary, although he wrote about similar features. In 1931, Lu Yun, the president of Yunnan Province, visited Shilin, and used the term “shilin” to describe the stone forest landscape. The Shilin Park was approved and directly managed by the Yunnan government. To develop the wild karst park into a tourist site, the government developed a brief plan and allocated money to build trails, a small visitors’ centre, and a sightseeing pavilion overlooking the Shilin landscape. Since then, the Shilin Karst Park has become well known in China. The first scientific study of the shilin landforms was conducted by Ma (1936). Since then, with the development of tourism in China, many scientists have studied their origin and evolution (Qing, 1977; Song, 1986; Zhang, 1984; Waltham, 1984; Ford, 1997; Lin, 1997; Song and Li, 1997).

In the 20<sup>th</sup> century, people recognized that the shilin was the result of rainwater dissolution (Qing, 1977). That point of view predominated throughout China. In 1979, in cooperation between the Chinese Academy of Sciences and the Yugoslavian Academy of Arts and Sciences, Dr. Peter Habič and Dr. Rado Gospodarič visited China. We carefully observed the characteristics of the shilin karst and discovered that subsoil solutional features such as through holes solutional conduits, spongework, and benches are typical. We learned that subsoil dissolution is the main process by which the shilin landscape forms. In 1982, when Dr. Marjorie Sweeting visited Shilin, we studied the karren on the tops of stone teeth and pillars, the gullies and flutes on their sides, the contact between the limestone teeth and the surrounding red mud, and the subjacent karst (Chen et al., 1986). In 1984, Prof. Shouyue Zhang published a paper that described the characteristics of subsoil dissolution that forms the shilin landscape. During visits in 1983 and 1984, Paul

Williams, Derek Ford, Timothy Atkinson and Anthony Waltham, also confirmed that the shilin karst is mainly caused by subsoil solution (Song, 1986).

How the shilin karst formed by subsoil solution, has been systematically studied since 1999. The Institute of Geography, Chinese Academy of Sciences, and administration of Shilin National Park coordinated in establishing the Shilin Research Center and Shilin Research Foundation to support the scientific study of the karst evolution, ecosystem, and environment. This paper describes some of the studies of how subsoil dissolution has produced the shilin scenery.

## Field studies

During field trips since 1984, two contrasting types of landscape have been distinguished in the Lunan shilin karst area:

### Type 1: Naigu shilin and Puduocun

Naigu shilin is located in the northern Shilin National Park. The Lower Permian Qixia limestone and the thick Maokou limestone, both with siliceous soil and residuum, extend throughout the area. The Maokou limestone block is elevated about 50 m above the ground surface and is cross-cut by NE and NW joint sets. Karren and rocky dolines controlled by joint intersections are well developed on the tops of limestone blocks.

On the slopes of limestone hills, isolated pillars about 10-15 m high, as well as stone teeth, are well developed. Subsoil solution features include *through holes conduits*, *solutional furrows* and *spongework*. Red soil up to 0.5 m thick covers the limestone, and it fills the limestone fissures to depths of more than 1 metre.

Depressions are floored by red and brown soil with a thickness of 2 m or more. A few isolated stone pillars about 7-10 m high stand on the depression floors (Figure 1). Some depressions are

floored only by red soil with no protruding columns or teeth.

## Type 2: Songmaoshan karst and Major shilin karst

About 1.5 km south of the Major shilin, basalt tuff constitutes the upper part of Songmaoshan hill. On the southeastern hillslope, intense soil erosion has removed the brown red weathered soil, loose tuff and debris. It is clear that the basalt and tuff once covered the limestone and filled the limestone fissures. Stone teeth 3-5 m high and small pillars 5-7 m high stand above the fractured basalt tuff. *Solution holes, pits, and karren rills* have developed on the upper parts of the stone teeth, whereas the columns are distinguished by smooth surfaces. The lower parts remain as truncated features surrounded by coarse black debris and rhombic calcite crystals 50 mm in diameter in small solutional holes. The limestone has been metamorphosed to marble. About 30 m eastward from the metamorphosed stone teeth and columns, limestone pillars 10-15 m high and stone teeth are very well developed in depressions. In the opposite direction, limestone fissures also retain basalt.

It should be mentioned that the Major shilin was also developed in relation to the basalt. The basalt is distributed on the top and southern slope of Shilin Hotel hill, which is the Major shilin on the south side. The magnificent Major shilin, 10-40 m high, is characterized by blocks of limestone separated by narrow vertical fissures. Pinnacles are well developed on the tops of the columns, whereas *vertical rills* are common on the sides. *Solution pockets, benches, conduits, and niches* are developed in the lower parts of the columns. Landform development in the Shi-



Figure 1: Evolution of the shilin karst landscape from the hills to the depressions: a. on hill tops; b. on slopes; c. in depressions.



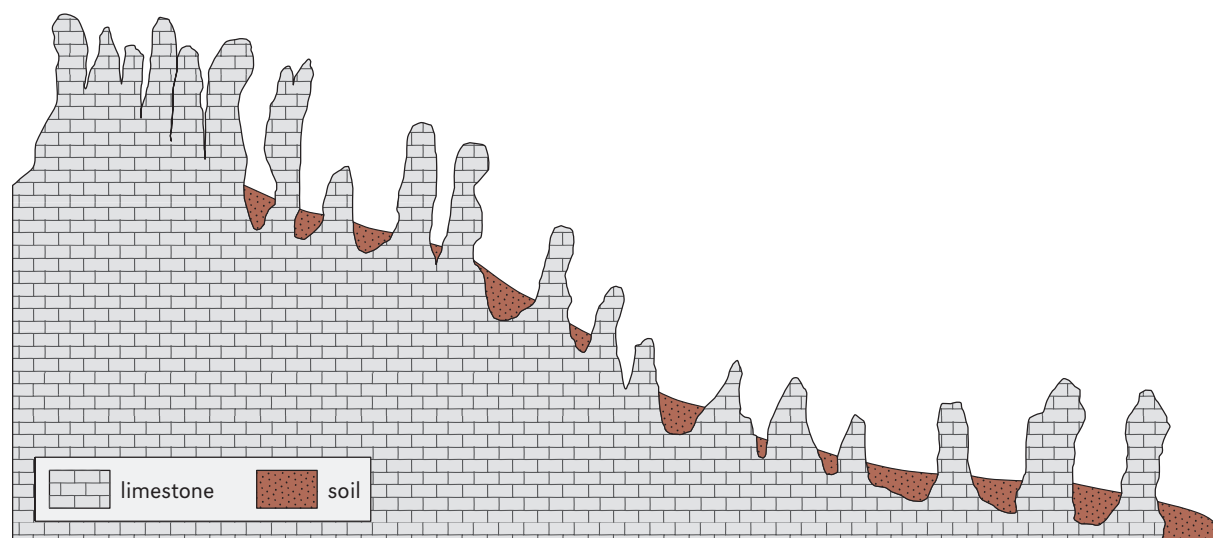


Figure 2: Sketch of karst geomorphological profile in Naigu Shilin Park.

lin Hotel zone is very similar to that in the Songmaoshan.

## Two models of shilin karst development

### Developmental model of the shilin landscapes

The development of Type 1 shilin karst is summarized in Figure 2. The limestone block on the high plateau is assumed to be cut by joints and other fractures and to have suffered mechanical and chemical weathering. Soluble materials such as  $\text{Ca}^{+2}$ ,  $\text{Mg}^{+2}$  and  $\text{HCO}_3^-$  are carried away with the water on and/or in the limestone, while residual materials are transported by water to lower sites such as dolines and depressions.

The  $\text{CO}_2$  content in soil air varies with the depth of soil and the type of vegetation (Figure 3). The  $\text{CO}_2$  in irrigated loam is much higher than in other soil and vegetative covers. The lowest  $\text{CO}_2$  is in soil with no vegetal cover – only 2,400 ppm at the depth of 120 cm.

Soil thickness also strongly affects the soil  $\text{CO}_2$  (Table 1).  $\text{CO}_2$  was measured down to the soil/

limestone contact. In thin soil, the  $\text{CO}_2$  value is low (e.g. A1, at 1,000 ppm). If the nearby soil is thick, the  $\text{CO}_2$  content will be affected by the  $\text{CO}_2$  content of the thick soil (e.g. A2, with 2,200 ppm). Table 1 also shows that the maximum  $\text{CO}_2$  content occurs at depths of 40–60 cm below the surface, with the highest value reaching 17,820 ppm. The effect of vegetation on  $\text{CO}_2$  content decreases in the following order: irrigated lawns, cypress, rare grassland, pine, bush and cultivation, and land without vegetation.

Experimental results with standard limestone tablets with diameters of 50 mm and thickness of 5 mm, made from the Maokou limestone in Shilin Park, show that they lost  $0.04 \text{ mg}\cdot\text{cm}^{-2}\cdot 100\text{d}^{-1}$  in soil 20 cm thick by dissolution. The dissolution rates in the soil on slopes was 0.58, 0.16, and  $0.04 \text{ mg}\cdot\text{cm}^{-2}\cdot 100\text{d}^{-1}$  at 20, 60, and 100 cm depths in the soil, respectively. However, the average dissolution rates in wet soil reached  $4.46 \text{ mg}\cdot\text{cm}^{-2}\cdot 100\text{d}^{-1}$  at depths of 20–80 cm.

The shilin landscape on karst hilltops is guided by the spacing of fractures, where soil and residuum are very thin. But the soil and residuum may also enhance the limestone dissolution along fractures, even though it may be slow. The soil on the slope varies from 0 to 0.5 m on the limestone,

**Table 1:** Soil air CO<sub>2</sub> between stone teeth near the Stone Screen spot (Liang et al., 2000).

No.	Soil CO <sub>2</sub> (ppm) at different depths (cm)								
	10	20	30	40	50	60	70	80	100
A1	1,000								
A2	2,200								
B1	3,820	10,180		11,200		18,840			
B2			13,340		9,420	14,260	12,730		
B3	3,820								
C1	6,370			16,240		17,820		8,150	7,640
C2	6,110		12,220		15,280	15,780		5,600	9,670

**Table 2:** Properties and contents of microbes and CO<sub>2</sub> in weathered basalt (D) and limestone soils.

No.	Soil depth (cm)	Soil temperature (°C)	pH	Humidity (%)	Microbes (x10 <sup>4</sup> /g dry soil)	Soil CO <sub>2</sub> (ppm)
D1-6-1	-20	10.4	6.71	33.092	20.8	18,000
D1-5-2	-40	10.8	6.87	33.636	12.6	12,000
D1-4-1	-60	11.4	7.33	32.593	28.5	20,000
D1-3-1	-80	11.9	7.51	34.084	24.4	14,000
D1-2-1	-100	12.3	6.85	40.805	7.55	12,000
D1-1-1	-120	15.5	6.95	46.697	20.2	20,000
S1-5-1	-20	9.6	7.06	40.813	20.6	3,400
S1-4-1	-40	10.3	7.24	40.746	15.3	4,500
S1-3-1	-60	10.6	7.37	45.614	18.3	3,000
S1-2-1	-80	11.1	7.48	46.355	6.56	4,500
S1-1-1	-100	11.4	7.68	43.888	8.70	4,000

**Table 3:** The subsoil dissolution rate (mg·cm<sup>-2</sup>·y<sup>-1</sup>) on limestone tablets in shilin.

Soil depth (cm)	D1	D2	S1	X1	B1	E1	T1
-20	5.9495	2.117	2.117	15.111	0.146	1.1315	6.0225
-40	5.6575	1.898	0.5475	20.367			
-60	6.424	1.679	0.584	13.870			
-80	5.2925		0.219	15.768			
-100	9.6725		0.146				
-120	10.1105						
Mean rate	7.1832	1.898	0.7227	16.279	0.146	1.1315	6.0225

and beneath it the limestone can corrode at a rate of 0.16–0.58 mg·cm<sup>-2</sup>·100d<sup>-1</sup>. The isolated stone pillars with the solution pockets, benches, conduits and niches may appear on the slope. After heavy rain, the slope flow carries detrital materials into depressions. Many depressions form temporary lakes after storms. Their sediments cover the underlying karst features. The wet soil will strongly dissolve the stone teeth and pillars at the rate of 4.46 mg·cm<sup>-2</sup>·100d<sup>-1</sup>, after the experiments. In this

case, the pillars become smaller, evolve into stone teeth, and finally disappear completely.

### Subjacent development model of the shilin landscape

After the development of palaeokarst in the early Permian, basaltic lava of Late Permian age covered the karst features and filled fissures. Karst

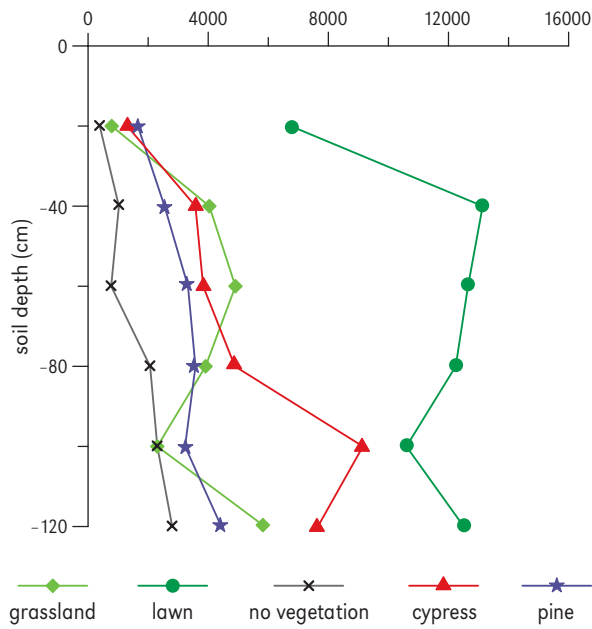


Figure 3: CO<sub>2</sub> concentration in the atmosphere of soil covered by various types of vegetation.

features that developed beneath the non-carbonate rocks have been defined as *subadjacent karst* (Chen et al., 1986).

Measurements show that the water penetrating into basalts has a low pH value of about 7. Microbes reproduce vigorously in the weathered materials (Liang et al., 2003). Table 2 shows that the microbes and CO<sub>2</sub> concentrations in weathered basaltic soil are much richer than in the limestone soil.

The high CO<sub>2</sub> content in the weathered basalt soil air causes strong corrosion of the underlying limestone (Song and Liang, 2001). Table 3 demonstrates that the subsoil dissolution rate in weathered basalt is 4–6 times of the rates on soil-covered limestone or in soil-filled limestone fissures. It is clear the karst development in limestone under the basalt is stronger than in soil-covered limestone.

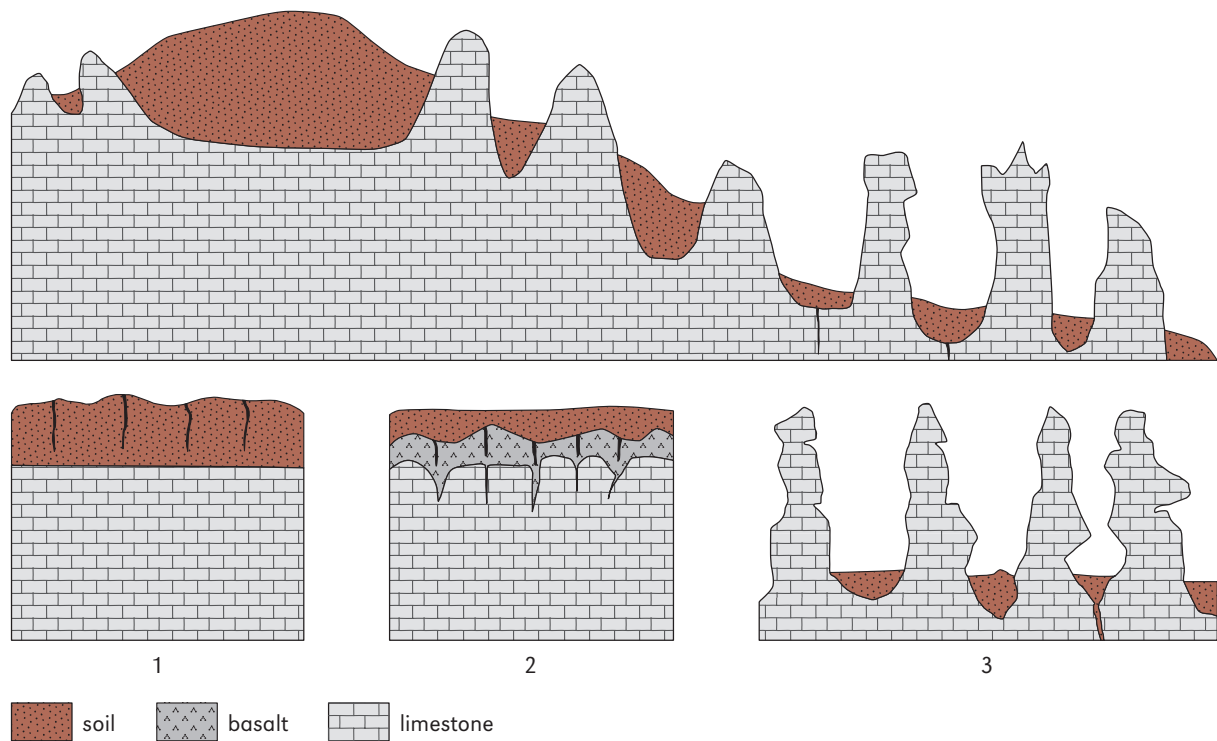


Figure 4: Subjacent karst evolution model for the limestone covered by basalt in Songmaoshan region. The upper diagram shows the status of the shilin landscape in relation to the basalt. 1. shows the basalt cover on the limestone; 2. subjacent karst developed beneath the basalt; 3. basalt weathered away and the shilin landscape developed.

The shilin development in the basalt area is summarized by Figure 4. The upper part shows the relations between the basalt and the palaeokarst features (stone teeth and pillars). The lower three diagrams illustrate the evolution of karst features covered by the basalt.

After the basalt lava flows covered the limestone, fractures, especially vertical ones, developed during the cooling process. The basalt became a fractured aquifer. During and after rainfall, water penetrates through the fractured basalt aquifer and into the underlying limestone along fractures. The water absorbs  $\text{CO}_2$  from the weathered material, so that it can rapidly dissolve the underlying limestone. The water retains its solution capacity for limestone, as the basalt is relatively insoluble. The limestone tablet experiments show that water in loose weathered material on the rims of basalt depressions can dissolve limestone at the rate of  $0.46\text{--}0.58 \text{ mg}\cdot\text{cm}^{-2}\cdot 100\text{d}^{-1}$ .

The water in the deep weathered materials in depressions dissolves the limestone tablets at a mean rate of  $1.968 \text{ mg}\cdot\text{cm}^{-2}\cdot 100\text{d}^{-1}$ , with a range of  $1.45$  to  $2.77 \text{ mg}\cdot\text{cm}^{-2}\cdot 100\text{d}^{-1}$ . In this case, the fissures in limestone were enlarged and began to partition the limestone beneath the basalt. The initial phase of development of the stone teeth and pillars were as shown in Figure 4.

With this manner of subjacent karst development, the shilin landscape rapidly develops along fractures. As the basalt on the proto-shilin is eroded away, the proto-shilin landscape is exposed. Vegetation grows on the basalt soil and the strong subsoil solution greatly increases the rate of development of the shilin landscape. *Subsoil solution features* are developed on the buried parts of the shilin landforms, and subaerial solution features such as rillenkarren, solution pans, and pinnacles are developed on the exposed shilin. This evolutionary stage is shown in Figure 4, diagram 3.



# SOLUTION RATES OF LIMESTONE TABLETS AND CLIMATIC CONDITIONS IN JAPAN

Kazuko URUSHIBARA-YOSHINO, Naruhiko KASHIMA, Hiroyuki ENOMOTO,  
Takehiko HAIKAWA, Masahiko HIGA, Zenshin TAMASHIRO,  
Tokumatsu SUNAGAWA and Eisyo OOSHIRO

Many karstologists have been interested in karst terrain, which is the surface which has been formed over a long period through the dissolution of the rock by physical-chemical processes. However, this feature *per se* cannot inform us of the time scale of the dissolution process. So many karstologists have tried to clarify the rates at which this process of limestone dissolution had occurred, and so identify it as the main factor causing karstification. Measurements of *solution rates* using limestone tablets were made by Trudgill (1975) and Jennings (1977).

Since 1980 the denudation commission of the International Speleological Union has measured solution rates globally using the Slovenian Cretaceous limestone (Gams, 1985). Similar *limestone tablets* made of Guilin Permian limestone were measured in China (Yuan, 1991). The solution rates of Slovenian Cretaceous limestone in Japan were measured from 1989 to 1990 by Urushibara-Yoshino (1991). In addition the solution rates of Slovenian Cretaceous limestone, Guilin Permian limestone and Japanese limestone have been measured since 1992. The results of these observations during the three years 1993, 1994 and 1995 were published (Urushibara-Yoshino et al., 1998) as they were during the five years from 1993 to 1997 by Urushibara-Yoshino et al. (1999b). The solution rates of limestone tablets from 1992 to 2001 in Minamidaito island is discussed in an article

by Urushibara-Yoshino (2003). In this paper, the results of 10 years from 1992 to 2002 will be discussed.

## Methods and study areas

Limestone areas occupy only 1,764 km<sup>2</sup> (less than 0.05% of the land) in Japan (Urushibara-Yoshino, 1996). The limestone areas are distributed from north to south and developed under different climatic conditions. Seven limestone areas were selected for study (from 1992-1997), from Hokkaido in northern Japan to Okinawa southwest Japan. They were in Toma, Abukuma, Chichibu, Akiyosidai, Shikoku, Ryugado and Minamidaito. From 1998 to 2002, the observations continued at all limestone sites except Chichibu. The locations of these sites are shown in Figure 1 and their environmental conditions in Table 1.

The tablets used at these sites measured 40 mm in diameter with a thickness of 4 mm. Before placing the tablets, their surface was ground to 300 meshes and weighted after dry up in 7 days in sili-cagel. The weights of tablets ranged from 12.5-13.5 g. Every 10 years, the tablets were cleaned, dried and weighted. The *weight loss* was measured to be in the range of 10<sup>-5</sup> g. At all observation sites, the upper surfaces of the tablets were corroded more than the bottom surfaces. From the air, rain water



Figure 1: Limestone areas and location of observation sites in Japan.

drops onto the upper surface, and water in the soil also percolates through to the upper surface. Because of this, there is a differential rate of lime-

stone dissolution between the upper and lower surface, the decrease in thickness was not measured. Only the loss of weight was measured. At each site



Figure 2: The observation site at Abukuma in the air (1.5 m).

the tablets were made from Slovenian Cretaceous limestone, Guilin Permian limestone, Chichibu Triassic limestone and the local limestone. These four tablets, made from different lithologies, were set in the air 1.5 m above the ground (Figure 2) and in the  $A_3$  and  $B_2$  horizons of local soils. The depth of the buried tablets at each site was different. This was because of the different thickness of soil horizons found at each site.

The  $CO_2$  concentrations in the soils were meas-

ured because their solution rates are extremely high in soils. In this study, the  $CO_2$  in  $A_3$  and  $B_2$  horizons, where the tablets were set, was measured for at least 4 seasons at each locality over a period of 10 years. The following three methods were used: namely, the *Non Dispersive Infrared Gas Analyzer*, *Gastec* (Urushibara-Yoshino et al., 1998) and the *Dräger method* (Miotke, 1974).

For an understanding of the limestone solution processes, the *water balance* in each year from 1993 to 2002 was calculated using the method of Thornthwaite (1948). This method was chosen because it considers the soil moisture in the water balance.

## Results

### Solution rates of limestone tablets

The original weight of the tablets was in the range of 12.5–13.5 g. The mean annual solution rate of the four tablets was used for the discussion of differences between location, and year-to-year fluctuation. The correlation matrix for 5 years (1993–1997) between the solution rates of limestone and the climatic factors of annual precipitation, *water surplus* ( $WS$ ), *water surplus – water deficit* ( $WS-WD$ ) and *precipitation – evapotranspiration* ( $P-E$ ) was examined (Urushibara-Yoshino et al., 1999). In the air, the correlation coefficient is high between the solution rate and

Table 1: Location and environment of observation sites of limestone areas.

	ASAHIKAWA (TOMA)	ABUKUMA	AKIYOSHI	SHIKOKU (ONOGA-HARA)	RYUGADO	MINAMI-DAITO
Location	43°49'30" N 142°37'30" E	37°20' 30" N 140°40'40" E	31°14'50" N 131°17'40" E	33°28' 24" N 132°52'51" E	33° 54'54" N 133°44'53" E	25°30'7" N 131°14' 1" E
Geology	Permian limestone	Cretaceous marble	Carboniferous and Permian limestone	Permian limestone	Triassic limestone	Quaternary limestone
Vegetation	needle and deciduous forest	deciduous forest and grassland	evergreen deciduous forest and grassland	deciduous forest and grassland	evergreen forest grassland	subtropical evergreen tree and grassland
Annual mean temperature (°C)	7.0	10.5	13.7	9.1	14.9	23.3
Annual precipitation (mm)	1118.2	1216.2	1913.1	2262.9	2291.7	1727.2
10 years mean water surplus (mm)	558	552	1192	1645	1504	615



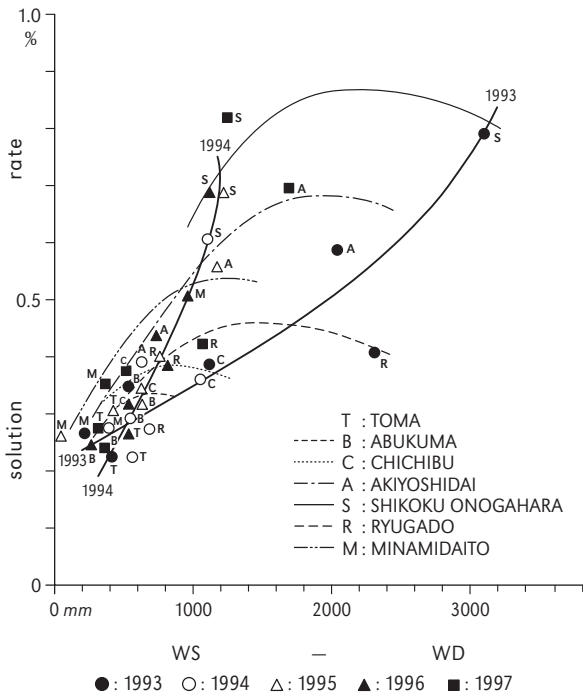


Figure 3: Trends of solution rates at 1.5 m above the ground from 1993 to 1997.

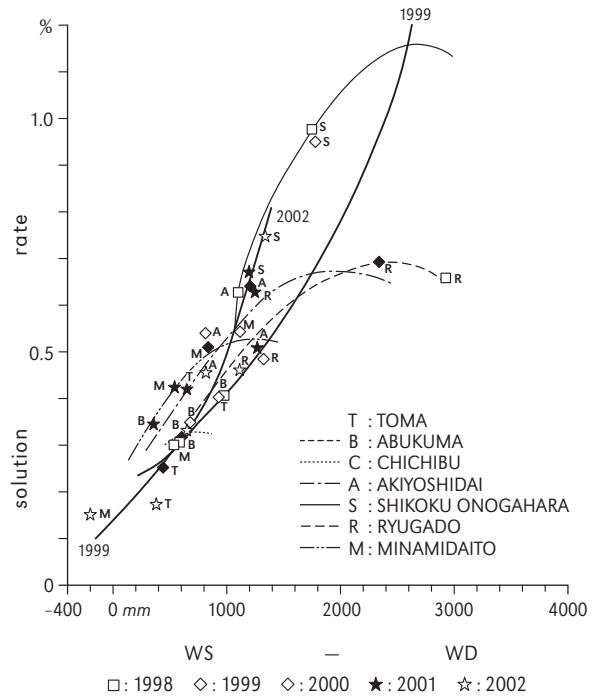


Figure 4: Trends of solution rates at 1.5 m above the ground from 1998 to 2002.

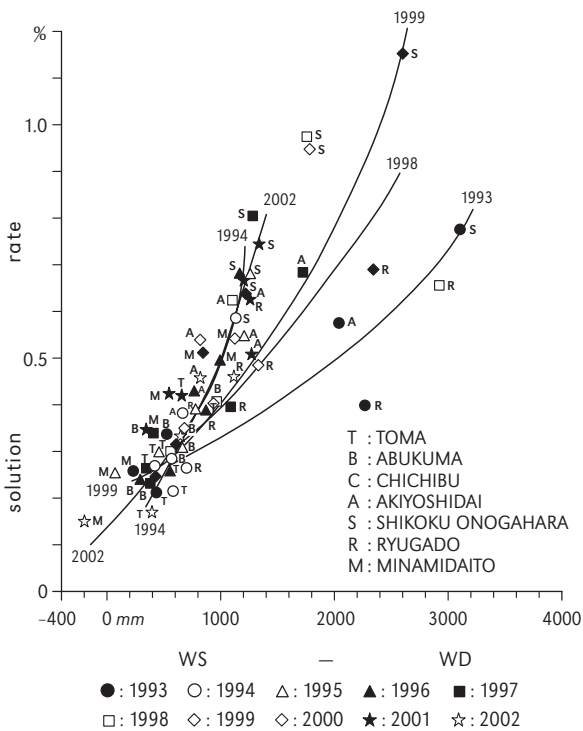


Figure 5: Trends of solution rates at 1.5 m above the ground at each observation site. Extreme cases of dry year and wet year are shown.

WS–WD. In A<sub>3</sub> horizon and in B<sub>2</sub> horizon in the soil, the correlation coefficients are highest between solution rate and annual precipitation. This means that the degree of dry condition (WS–WD) affects the difference of the solution rate in the air. However, the *annual precipitation* (total wet condition) of the area effects to the solution rates in the soils. The same correlation matrix for the 5 years (1998–2002) has also been examined. The correlation coefficient was highest with the same factor as the case with the results for 1993–1997. The solution rates of limestone tablets were plotted in Figure 3 from 1993 to 1997 and Figure 4 from 1998 to 2002. The solution rates of the tablets in the air showed the highest correlation coefficient between WS–WD during the two periods. And the solution rates at the observation sites show strong year-to-year fluctuations. In Figure 3, the tendency curves of the solution rates during the five years are shown by several lines. Fur-



Figure 6: The CO<sub>2</sub> measurement in Minamidaito island (upper Dräger method, lower Gastec method).

thermore, the driest year 1994 and the wettest year 1993 are shown by heavy lines from north to south during the five years (1993–1997). In Figure 4, the same tendency curves at the observation sites and the wettest years line (1999), as well as the driest year (2002), are also shown by heavy lines during 5 years (1998–2002). Only the Asahikawa (Toma) values are too small to fit into the tendency curve for those years. During these 10 years, the driest examples are 2002 and 1994 and the wettest examples are in the years 1999 and 1993.

These tendency curves are combined in Figure 5. In Figure 5 the tendency curves of solution rates of the driest year 2002 and wettest year 1993 in the 10 years period are shown. In 2002 WS–WD are extremely low, this was a dry year, especially in southern part of Japan, therefore the solution rates show the smallest values. In 1993, WS–WD are high in the air, this was an extremely wet year, and therefore the solution rates were high at every site.

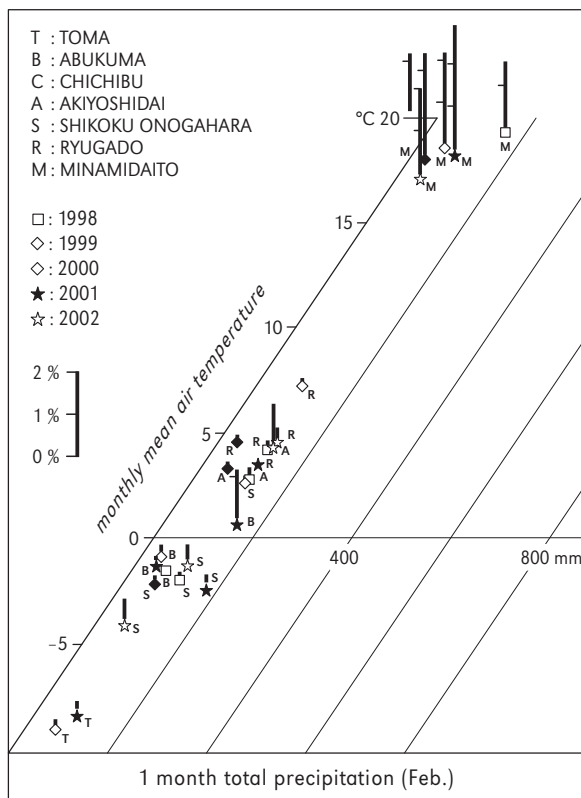
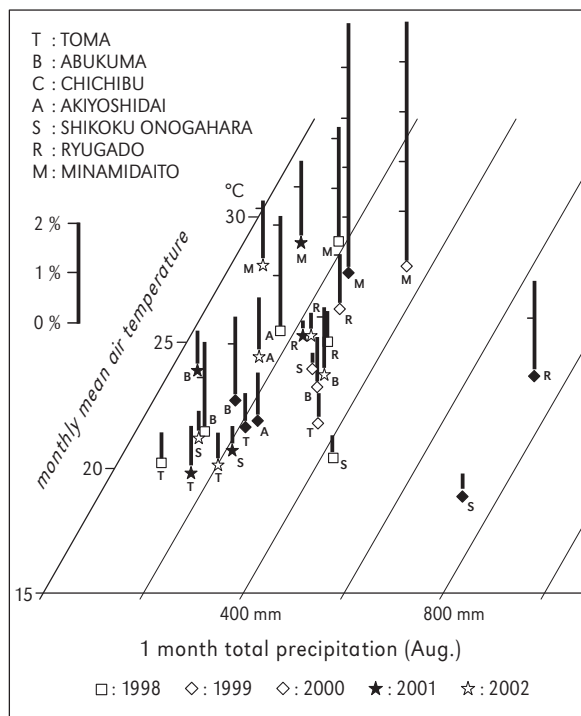


Figure 7: The CO<sub>2</sub> in B<sub>2</sub> horizon in August and in February from 1998–2002.



Figure 8: The tablets inserted in  $A_3$  and  $B_2$  horizons of soil in Minamidaito island.

### CO<sub>2</sub> in soils

In this part of the study, carbon dioxide in  $A_3$  and  $B_2$  horizons was measured at 7 sites in 1993–1997 and at 6 sites in 1998–2002. At all sites, the concentrations of carbon dioxide values were higher in the  $B_2$  horizons than in the  $A_3$  horizons. The reason why in the  $B_2$  horizon, the concentrations of carbon dioxide were higher than in the  $A_3$  horizon, is that the density of soils is higher in the  $B_2$  horizon than in the  $A_3$  horizon. At all the sites where measurements were taken, a high concentration of carbon dioxide occurs in the spaces be-

tween the soils particles after heavy rain (over 20 mm). However, this gas cannot escape into the air or into the underground water. This is because the pressure is higher in  $B_2$  horizon than in the  $A_3$  horizon. Carbon dioxide concentrations of the  $B_2$  horizon in summer (August) and in winter (February) are shown in the article by Urushibara-Yoshino et al. (1999b). The carbon dioxide, being measured by the Dräger and Gastec method in Minamidaito, is shown in Figure 6. Carbon dioxide concentrations of the  $B_2$  horizon in summer (August) and in winter (February) are shown for the 5 years (1998–2002) in Figure 7. The high CO<sub>2</sub>

concentration in the B<sub>2</sub> horizon during the warm periods of the year can support higher solution rates of limestone tablets in soils. However, solution activity in winter is extremely low, because of the low CO<sub>2</sub> in the B<sub>2</sub> horizon.

Figure 8 shows the four tablets in the A<sub>3</sub> and in B<sub>2</sub> horizons. The solution rates of limestone tablets were 3 to 5 times higher in B<sub>2</sub> horizon than in the air in Minamidaito Island (Urushibara-Yoshino et al, 2003). One of the reasons why in B<sub>2</sub> horizon high solution rates could be obtained, might be high concentration of carbon dioxide in B<sub>2</sub> horizon.

## Conclusion

Over the 10 years period, the correlation coefficients between the solution rates and WS–WD are highest in the air. On the other hand, correlation coefficients between the solution rate and the annual precipitation are highest in the A<sub>3</sub> and B<sub>2</sub> horizons in the 10 years observed.

Over the 10 years period, solution rate of limestone at the 6 sites showed annual fluctuations. The solution rates in the air 1.5 m above the ground show a clear trend with WS–WD. At each observation site, the solution rate increased in accordance with WS–WD, over the range 1,000–1,600 mm. Solution rates then decreased above 1,600 mm in WS–WD.

At the observation sites, the trend of the solu-

tion rates in the air 1.5 m above the ground shows the smallest range with WS–WD in 1994 and 2002, but the largest range with WS–WD during the 10 years in 1993 and 1999.

From these observations, the sites in Shikoku and Akiyoshidai, in the monsoonal temperate zone, have the best water balance conditions for solution of limestone in the air. Because of these good water balance conditions, the karstification of the limestone plateau with a dense pattern of dolines developed to a greater extent in these regions of Japan. Of course, for the development of dolines, beddings planes, the thickness of layers and the fissure pattern of limestone also assist karstification.

In the soil, the solution rates are 3 to 5 times higher than in the air. One reason might be high concentration of carbon dioxide in the soil. This means that the surface covered soils will be denuded much faster than limestone outcrop areas in Japan.

## Acknowledgement

This study was supported by the Ministry of Education, Science and Culture in Japan (No 0768090 1995–1997). We would like to express our sincere thanks to Prof. I. Gams and Prof. D. Yuan who supplied the tablets of Slovenian limestone, and Guillin limestones, respectively.



# THE ROCK CITIES OF ROSSO AMMONITICO IN THE VENETIAN PREALPS

Ugo SAURO

In the Venetian Prealps there are characteristic rocky landscapes developed in a thin formation of micritic limestone, dissected by a system of widely spaced fractures. These structurally controlled forms produce *rock cities* or *giant limestone pavements* (Figures 1, 2, 3) which contrast strongly with the soil-covered, smooth surfaces developed

on contiguous thicker rock units. The Rosso Ammonitico formation plays a very important role in the control of the subterranean hydrology and in the development of both dolines and lithological contact caves. The rocky landscapes of the Rosso Ammonitico with their associated features (Fig-



**Figure 1:** A typical rock city developed in the upper Rosso Ammonitico unit (Val Marisa, Monti Lessini). Note the system of corridors isolating large blocks.



**Figure 2:** The upper and lower units of the Rosso Ammonitico exert a strong structural control on slope evolution (Costeggioli, Monti Lessini). The “corridor karst” is better developed in the upper unit. The large blocks to the right have been involved during the last cold phases of Pleistocene by solifluction.



**Figure 3:** Detail of the Valle delle Sfingi (La Busa di Camposilvano, Monti Lessini). The relict blocks developed in the lower Rosso Ammonitico are widely spaced and similar to mushrooms.

ure 4) are the consequence of both karst and periglacial processes.

### **A structurally controlled rocky landscape**

A scenic landscape in the Venetian Prealps, especially of the Monti Lessini and the Altopiano dei

Sette Comuni (also called the Asiago plateau), is that which developed on the limestone formation called “Rosso Ammonitico” (ammonitic red). On this limestone are structurally controlled rocky landscapes of the “rock city” or “giant limestone pavement” types, contrasting with the soil-covered, smooth surfaces developed on contiguous rock units (Figures 1, 2) (Corrà and Benetti, 1966; Sauro, 1973c, 1977; Perna and Sauro, 1978, 1981).

**Figure 4:** The Ponte di Veja (Val della Marchiora, Monti Lessini), developed in the lower Rosso Ammonitico, is the remnant of the roof of a large cave, now partially collapsed.



The Rosso Ammonitico formation, which is about 30 m in thickness and mostly made up of pink, nodular, micritic limestones rich in iron oxides, was deposited during the Middle and Upper Jurassic in an oxidizing marine environment, at a slow sedimentation rate (about 1 m per million years). The Rosso Ammonitico formation is very massive in its lower part, well stratified, cherty and more clayey in its intermediate part and again relatively massive in its upper part. The rock formation is crossed by systems of widely spaced fractures (with meshes ranging between a few metres and some tens of metres).

Above the Rosso Ammonitico is the Maiolica (also called Biancone), a marly limestone similar to chalk, about 150 m in thickness, closely stratified and densely fractured. Below is the Calcari del Gruppo di San Vigilio (San Vigilio Group limestone), a pure, diffusely fractured limestone, up to 200 m in thickness.

The Rosso Ammonitico is much more resistant to denudation than the adjacent formations and outcrops over relatively large areas mostly as structural and sub-structural surfaces: small

tabular summits, structural terraces and rocky benches on the slopes, bedding slopes and wide valley bottoms. Due to the lower resistance to erosion of the intermediate beds, in the slopes where horizontal or infacing strata are exposed the Rosso Ammonitico extends in two superimposed lines of benches corresponding to the lower and upper parts of the sequence (Sauro, 1973c).

The vertical succession of rocks with different characteristics influences the evolution of karst landforms and caves (Sauro, 1973c, 1974). Underground water flowing diffusely in the dense network of discontinuities of Maiolica encounters a barrier with only a few main fractures when it comes into contact with the Rosso Ammonitico. The focused flow through the Rosso Ammonitico results in the development of discrete caves. In specific morpho-structural settings following the lowering of the topographical surface, funnel shaped dolines develop in the lower Maiolica just above the points of focused drainage within the underlying Rosso Ammonitico. Collapse dolines in the lower Rosso Ammonitico are caused by the breakdown of cave roofs.





Figure 5: Karren developed on bedding surfaces in the upper Rosso Ammonitico unit (Monte Grolla, Monti Lessini). Both rounded karren and runnels are present.

## Evolution of the rocky landscape of the Rosso Ammonitico

The rocky landscape of the Rosso Ammonitico is the consequence both of the much greater resistance of this rock in comparison with the confining rock units (Maiolica and Calcari del Gruppo di San Vigilio) and of the opening and widening of the main fractures which evolved as *dissolution grikes* and *corridors*. These dissolution features isolate large blocks with tabular bedding plane upper surfaces, delimited laterally by the rims of nearly vertical rock faces. These rocky landscapes may be considered special types of rock cities where the large clint blocks are delimited by a geometrical pattern of corridors corresponding to the network of fractures.

The early widening of the fractures in the Rosso

Ammonitico takes place within the epikarst, by underground dissolution, before the rock is exposed by denudation. Recently outcropping surfaces are characterized by bedding planes intersected by networks of grikes and corridors, which have greatly varying widths, between a few centimetres and several metres and are partially filled with soil and sediment.

The upper surfaces of the isolated blocks present different situations due to the lithological control and the character of the local slope. Some surfaces are made up of bare rock (Figure 5), others are characterized by a weathered layer of rock where the nodular structure of the limestone is evident and a thin soil cover has developed. Many of the nodules isolated by dissolution and biokarstic processes are ammonite moulds. On the bare surfaces it is possible to find *rundkarren*, *rinnen-*



Figure 6: Detail of the moved parallelepipedal blocks (Costeggioli, Monti Lessini).

*karren*, *kamenitzas*, and other karren features. *Rillenkarren* are relatively rare, probably because of the nodular structure of the rock.

The evolution of the rocky landscapes of the Rosso Ammonitico is the consequence not only of dissolution but also of periglacial processes such as cryoclastic weathering and solifluction. These processes operated very effectively during the cold phases of the Pleistocene. On bedding slopes of 10°–15° (Sauro, 1976a), both isolated blocks and “isles” of the Rosso Ammonitico moved by soli-

fluction (Figures 2, 6). These isles evolved as a peculiar type of rock glacier following the filling of the grikes and other discontinuities caused by the ice (Sauro, 2002). These forms no longer appear to be active.

To conclude, the rocky landscapes of the Rosso Ammonitico with their associated features may be classified as rock cities or giant limestone pavements, which are strongly controlled by the geological structure and evolved mainly by karst and periglacial processes.



# COASTAL EOGENETIC KARREN OF SAN SALVADOR ISLAND

John E. MYLROIE and Joan R. MYLROIE

Analysis of eogenetic coastal karren on Holocene and late Pleistocene eolianites from San Salvador island, Bahamas, indicates that the *karren* develop quickly, and similarly, on all outcrops studied. The Holocene eolianites provide a tight time window to overall karren development, and major storm-erosion features indicate that karren are routinely removed and re-initiated. Comparison of lagoonal versus ocean-exposed outcrops indicate that higher wave energies create a faster recycle time for the ocean-exposed karren. Both the Holocene and late Pleistocene eolianites are eogenetic in nature, and their overall rock youth is the single most important aspect of coastal karren development, over-riding both the age and ocean exposure differences among the study sites. The *coastal karren* are expressed as *pitting* and *surface irregularity* produced in the sea-spray zone; rocks in coastal settings but protected from sea spray are smoothed by storm events and show little *meteoric karren* development. The presence of coastal *sea-spray produced karren*, and the paucity of meteoric karren indicate both the rapidity with which coastal sea-spray karren can develop, and also the cycle time of major storm events, which must be faster than meteoric karren production.

## Geographic and geologic setting

The Bahama islands are a 1,400 km long portion of a NW–SE trending archipelago that extends from Little Bahama bank east of the coast of Florida to Great Inagua island, just north of the coast of Cuba (Figure 1). The archipelago extends farther southeast as the Turks and Caicos islands, and Mouchoir, Silver, and Navidad banks that are a separate political entity. The northeastern Bahama islands are isolated landmasses that project above sea level from two large carbonate platforms, Little Bahama bank and Great Bahama bank. To the southeast, beginning in the area of San Salvador island (Figure 2), the Bahamas comprise small isolated platforms, many of which are capped by islands that make up a significant portion of the available platform area. The Bahamian platforms have been sites of carbonate deposition since at least the Cretaceous, with a minimum thickness of 5.4 km (Meyerhoff and Hatten, 1974) and perhaps as much as 10 km (Uchupi et al., 1971). The large platforms to the northwest are dissected by deep channels and troughs, and the isolated platforms of the southeastern Bahamas are surrounded by deep water (Melim and Masa-

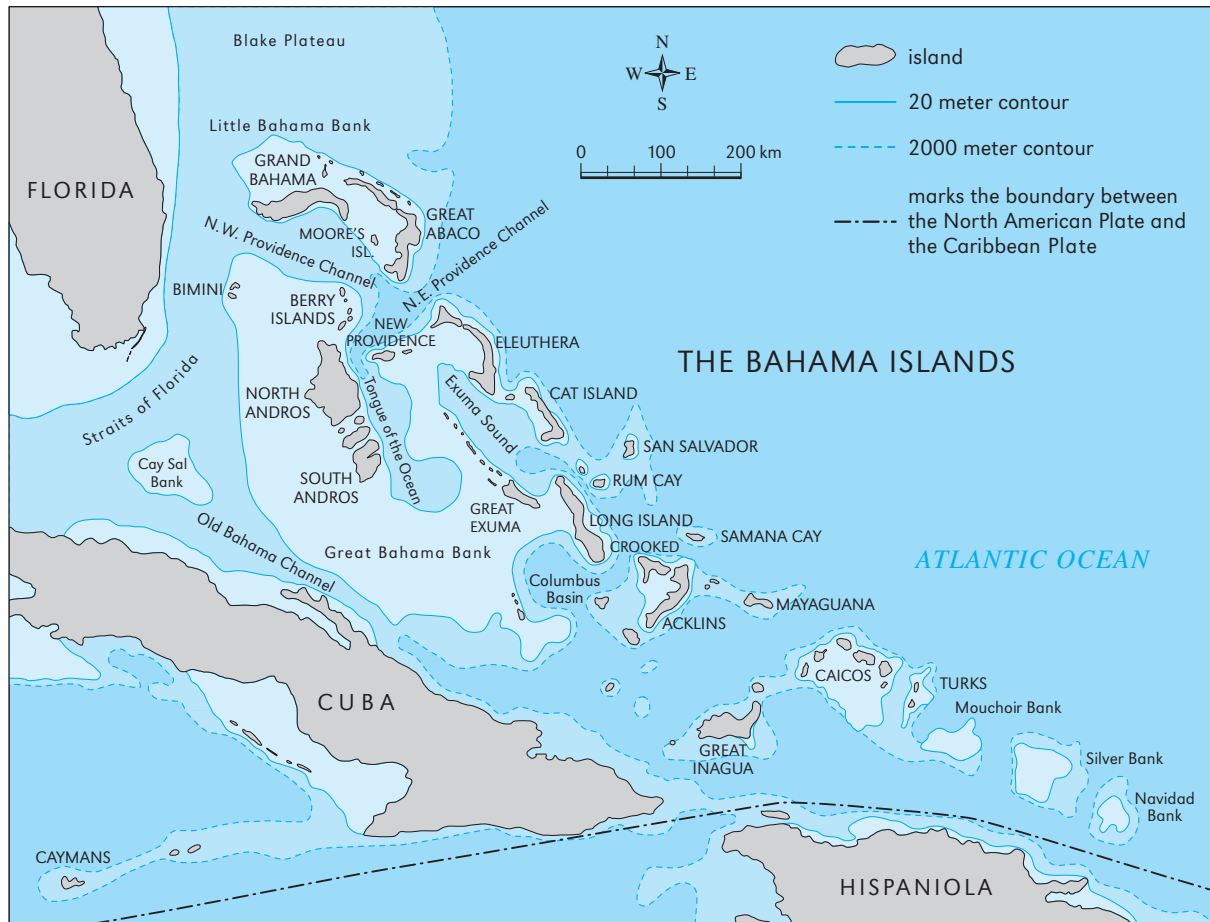


Figure 1: A map of the Bahamas, showing the location of San Salvador island.

ferro, 1997). Water depth on the platforms is generally less than 10 metres. There is no evidence for active tectonics in the Bahamas (Carew and Mylroie, 1995a).

## Stratigraphy

The exposed carbonates of San Salvador island consist of late Quaternary limestones that were deposited during glacio-eustatic highstands of sea level. Each highstand event produced transgressive-phase, stillstand-phase, and regressive-phase units. Because of slow platform subsidence, Pleistocene carbonates deposited on highstands prior to the last interglacial (Marine Isotope substage 5e,

ca. 125,000 years ago) are represented solely by eolianites (Carew and Mylroie, 1995a, 1997). These oldest eolianites form the Owl's Hole formation (Figure 3) and are made of biopelsparites on San Salvador. The Owl's Hole formation contains eolianites of at least two sea level highstands prior to the last interglacial (Panuska et al., 1999), as has been noted elsewhere in the Bahamas (Kindler and Hearty, 1995).

Overlying the Owl's Hole formation, and separated from it by a palaeosol or other erosion surface are deposits of the last interglacial (Marine Isotope substage 5e), the Grotto Beach formation (Figure 3). The Grotto Beach formation contains a complete sequence of subtidal, intertidal, and eolian carbonates, consisting of two members. The



Figure 2: A map of San Salvador island, showing major features and location of the sample sites (at the north and south ends of the island, in large type).

age	lithology	member	formation	magnetotype
H o l o c e n e		Hanna bay member	Rice bay formation	
		North point member		
P l i s t o c e n e		Cockburn town member	Grotto beach formation	Fernandez bay
		French bay member		
				Gaulin cay
		Upper Owl's hole formation		Sandy point pits
		Lower Owl's hole formation		

Figure 3: Stratigraphic column for surface rocks on San Salvador island (from Panuska et al., 1999).

French Bay member is a transgressive eolianite. In some places, transgressive eolianites are marked by an erosional platform on which later still-stand fossil corals are found (Carew and Mylroie, 1995b, 1997; Halley et al., 1991). The Cockburn Town member is a complex arrangement of still-stand subtidal and intertidal facies overlain by regressive eolianites. During Grotto Beach time ooids were produced in great numbers, and the vast majority of eolianites in the Grotto Beach formation are either oolitic (up to 80–90% ooids) or contain appreciable ooids.

Overlying the Grotto Beach formation, and separated from it by a palaeosol or other erosion surface is the Rice Bay formation (Figure 3) that has been deposited during the Holocene. The Rice Bay formation is divided into two members, based on their depositional history relative to Holocene sea level. The North Point member consists en-

tirely of eolianites, whose foreset beds can commonly be followed at least 2 m below modern sea level. Whole rock carbon-14 measurements from the North Point member indicate particle ages centred around 5,000 years BP. Laterally adjacent, but rarely in an overlying position, is the younger Hanna Bay member. This unit consists of intertidal facies and eolianites deposited in equilibrium with modern sea level. The eolianite grains have radiocarbon ages that range from approximately 3,300 to 400 years BP (Carew and Mylroie, 1987; Boardman et al., 1989). While weakly-developed ooids have been reported from the early stages of North Point member deposition (Carney and Boardman, 1991), the Rice Bay formation is predominantly peloidal and bioclastic on San Salvador. The North Point member is currently being attacked by wave erosion. Sea caves, inland cliff-line talus, and coral-encrusted wave-cut benches of the North Point member exist. The relationship of the deposits to sea level, and the carbon-14 ages, indicate that the North Point member was deposited as a transgressive unit after sea level rose at the end of the last glaciation, but that deposition was complete prior to sea level reaching its current elevation. Sea level must have been about 10 m or less below current sea level, as the platform had to be partially flooded to allow allochem production that later became the source material for the eolianites. But sea level must have been below modern position, as evidenced by the foreset beds of the North Point member eolianites dipping ~2 m below modern sea level. Given the tectonic stability of the Bahamas, the time and sea-level position window for the North Point member rocks is tightly constrained. By the time of the Hanna Bay eolian deposition, beginning ~3,000 years ago, sea level had reached and stabilized at its current position.

The three formations are separated from one another by well-developed palaeosols and other erosion surfaces that formed during sea-level lowstands; however, as previously noted, the Owl's Hole formation contains at least one palaeosol within its section representing a glacioeustatic

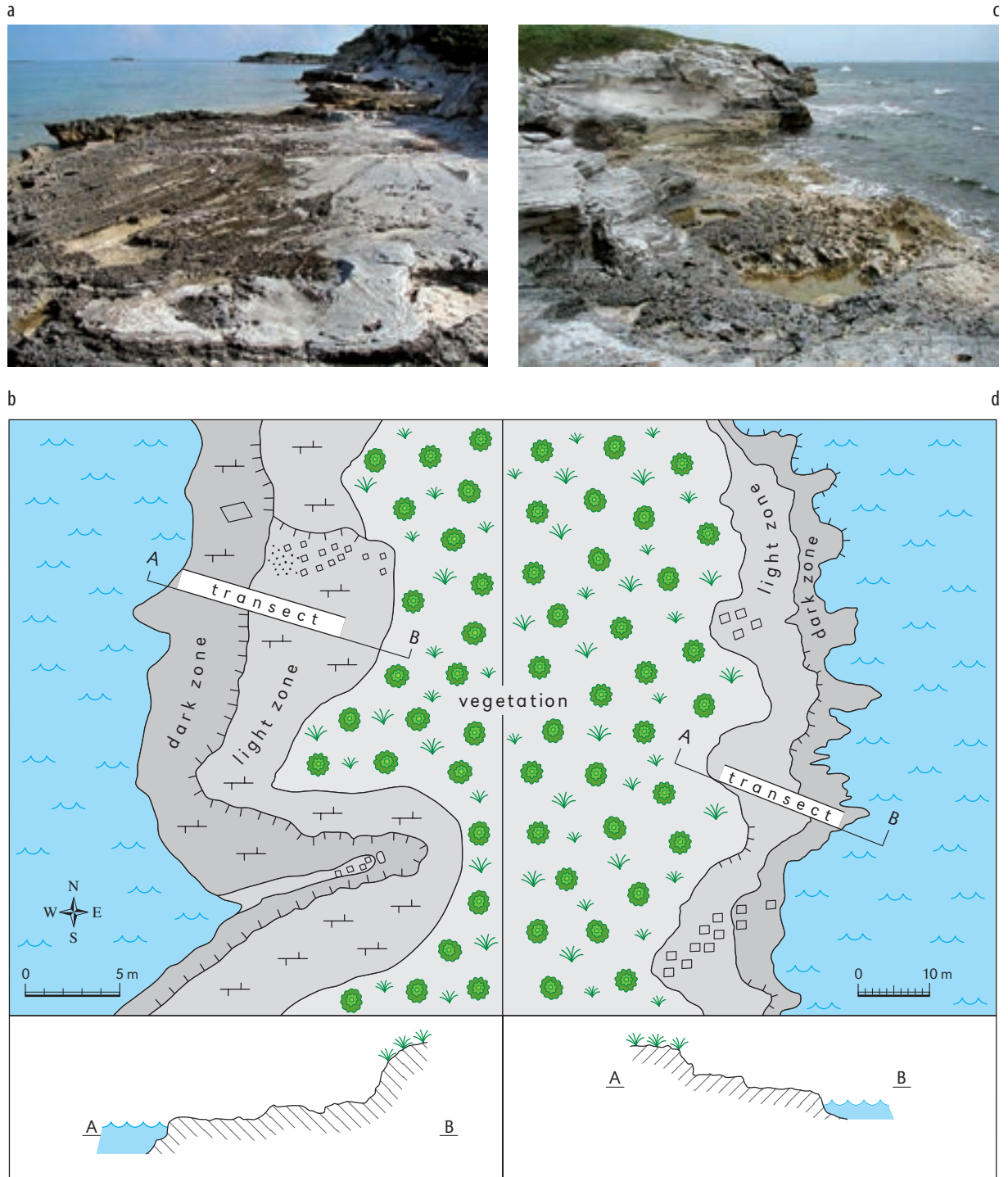


**Figure 4:** a. overview of the Grahams Harbour side of North Point. Note the “dark zone” at the shore and the “light zone” farther inland on the low, wide bench; b. diagrammatic representation of the view in a, showing transect location; c. overview of the Atlantic side of North Point. The steep topography makes the “dark zone” and “light zone” bands less obvious than in a; d. diagrammatic representation of the view in c, showing transect location.



sea-level lowstand (Panuska et al., 1999). The stratigraphic column shown in Figure 3 contains magnetozones that allow palaeosols of different ages to be identified based on the signal of secular variation contained in their palaeomagnetic record (the rocks are too young to display magnetic reversals). Despite the subdivisions made above, the carbonates of the Bahamas are remarkably uniform in texture and petrography, especially when compared to ancient rocks found in continental settings. For a further review of Bahamian geology and stratigraphy see Carew and Mylroie (1995b, 1997), and Melim and Masferro (1997), and the references therein.

## Eogenetic coastal karren of San Salvador island, Bahamas

### Eogenetic karren

The karren of carbonate islands and coasts are distinct from karren of inland settings of continents or large islands. Reef, lagoonal and eolian limestones that form most young carbonate islands are eogenetic, meaning they have not undergone significant diagenesis and still exhibit high primary porosity and extreme heterogeneity (Mylroie and Vacher, 1999; Vacher and Mylroie, 2002). These lithologic qualities appear to favour the development of highly irregular and *composite karren*, and preclude the development of many other types, particularly the hydrodynamically-shaped forms (Taboroši et al., 2004). These coastal karren contain *deep pits*, extremely *sharp points*, *knife-edge ridges*, and completely *penetrating holes*.

Despite being the characteristic karren type on young eogenetic limestones, there is not yet a unique and accurate geomorphic term for this type of sculpturing, both the centimetre-scale karren, and metre-scale *pinnacles*, found on youthful, or eogenetic, carbonate coasts. Taboroši et al. (2004), have reviewed the situation, as follows. The terms applied to the most intensely corroded variant of this karren, often reported from

tropical limestone coasts, include *champignon surface* (Stoddard et al., 1971), *phytokarst* (Folk et al., 1973), *lacework morphology* (Bull and Laverty, 1982), *biokarst* (Viles, 1988) and *coastal karren* (Mylroie and Carew, 1995). Considered one of the most variable and least understood karren types (White, 1988), its appearance is thought to be largely influenced by endolithic and epilithic organisms (Jones, 1989). This was first reported by Folk et al. (1973), who named the features “phytokarst” based on the assumption that boring by filamentous algae is responsible for observed morphology. However, the impact of organisms on topography has never been unequivocally demonstrated (Viles, 2001) and this karren is most likely polygenetic, affected by a variety of concurrently operating processes in addition to biological corrosion. In coastal areas, these mechanisms can include abrasion by marine invertebrates (Schneider and Torunski, 1983; Trudgill, 1987), wave action, wetting and drying, salt weathering and hydration (Ford and Williams, 1989), and salt spray and rain water mixing. This great variety of processes is superimposed on the highly heterogeneous texture and high primary porosity of young limestones, which may be the crucial factors controlling the development of this type of karren by making the rocks predisposed to the development of multitudes of *irregular pits and hollows*.

Taboroši et al. (2004) report that while the impact of endolithic microorganisms on rock morphology, for example, may be considerable at small scales, the *large scale pinnacles* and pits are more likely a result of differential erosion due to metre-scale heterogeneities, such as variations in mineralogy and cementation (Trudgill, 1976b) and structural weaknesses (Viles and Spencer, 1986). Thus, the term “phytokarst” is inappropriate not simply because the organisms originally thought to be responsible are not plants (Jones, 1989), but also because a variety of other processes are involved, and their relative contributions vary by location and scale. The terms “*eogenetic karren*” for this type of small-scale dissolutional morphology, and “*eogenetic karrenfeld*” for result-

ant metre-scale topography has been proposed by Taboroši et al. (2004). We believe that these terms proposed by Taboroši et al. (2004) are most appropriate because they emphasize the eogenetic nature of host limestone as the common factor controlling the development of all karren forms of this type, while avoiding references to genetic mechanisms (which are too numerous, variable, and poorly known) as well as settings (which are not necessarily island nor coastal). Placing “coastal” in front of the general term “eogenetic karren” provides a location indicator that does not predispose a genetic mechanism for the karren development. Thus, this paper will discuss *coastal eogenetic karren* of Holocene coastal rocks on San Salvador island.

### Coastal eogenetic karren: the Holocene of San Salvador island

San Salvador island has the most complete published geologic record of any of the Bahamian islands, and perhaps of any carbonate island in the world, as a result of the Gerace Research Centre (formally the Bahamian Field Station) on the island, which has hosted scientific enquiry for over 30 years. The geologic map of San Salvador (Carew and Mylroie, 1995b) shows that Holocene rocks, primarily eolianites, are found in numerous coastal locations. Two areas of the Holocene North Point member of the Rice Bay formation (Figure 3) were examined at the type section of North Point (Figures 2, 4). An additional area of late Pleistocene-aged Cockburn Town member of the Grotto Beach formation (Figure 3) at the south end of the island, called West of Gulf for its location just west of a landmark called The Gulf, was studied as a control for the work (Figures 2, 5). At all three locations the bedrock is eolian in origin.

The North Point locations are divided into an ocean-facing outcrop, the Atlantic side (Figure 4c, d) and a lagoon-facing outcrop, Grahams Harbor (Figure 4a, b), to help differentiate wave and spray magnitude issues in a uniform lithology.

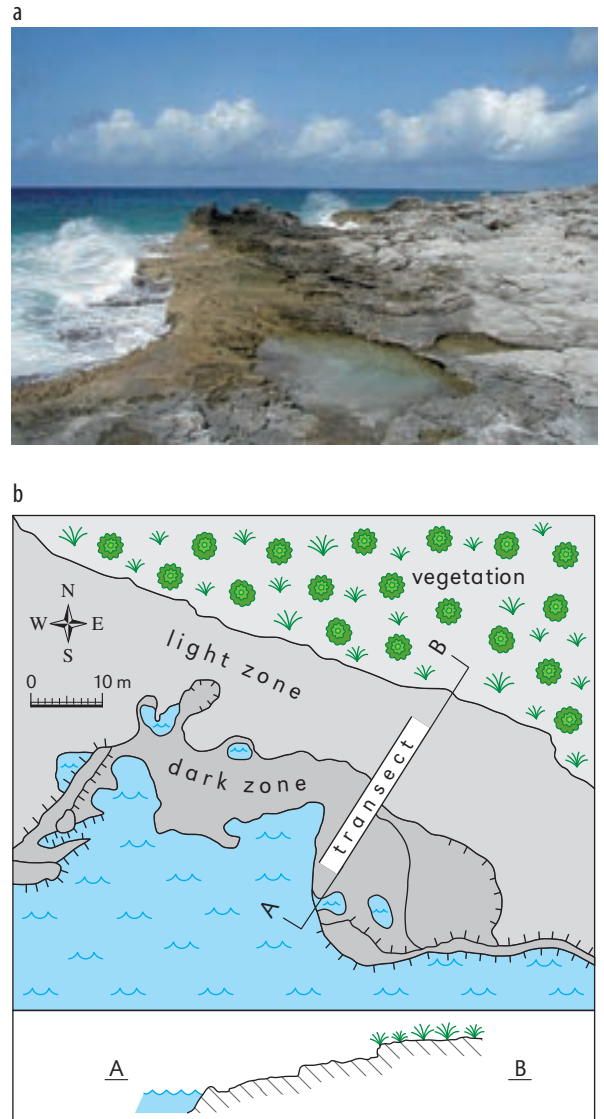


Figure 5: a. overview of the West of Gulf area; b. diagrammatic representation of the view in a, showing transect location.

The southern coast location, West of Gulf, being in an ocean-facing, but late Pleistocene aged outcrop (Figure 5a, b), was selected to determine if any age-related differences might be discernable.

Examination of the three sample outcrops demonstrates that they contain a suite of etched and pitted surfaces (Figure 6) that are blackened by endolithic algal growth (“dark zone” of Figures 4b, d, 5b), with a sharp boundary with a relatively

**Table 1:** Summary numerical data from the transect measurements.

Location	Small pits					
	width SD	width confidence	width mean	depth SD	depth confidence	depth mean
Atlantic side North Point	0.865	0.159	1.35	0.590	0.108	0.68
Graham's Harbour	1.057	0.198	1.71	0.902	0.169	0.81
West of Gulf	0.690	0.116	1.17	0.451	0.076	0.65
	Large pits					
	width SD	width confidence	width mean	depth SD	depth confidence	depth mean
Atlantic side North Point	11.039	3.122	17.39	6.412	0.814	9.68
Graham's Harbour	9.575	4.845	26.46	4.104	2.077	8.36
West of Gulf	13.564	4.203	24.55	4.702	1.457	6.20
All measurements are in cm.						

smooth, grey limestone inland of the pitted surface (“light zone” of Figures 4b, d and 5b). The boundary between the light and dark coloured zones is very abrupt. This abrupt boundary, while sometimes coincident with local relief, commonly is not. Field observations indicate that the boundary coincides with the margin of sea-spray wetting during normal wave conditions. The Bahamas are in a low-amplitude tidal environment, with tides ranging ~1 m. As a result, sea spray is scattered over a very similar range during the tidal cycle. Small pits are the dominant karren feature in the dark zone.

Measurements of the pitted surface indicate that the pits fall into two arbitrary categories, small (0.5–6 cm width) and large (6–65 cm width). At each outcrop location, a transect made up of grid boxes was placed perpendicular to the shoreline, from the shoreline inland into the grey or light limestone area (Figures 4, 5, 6d). Circles of 15 cm diameter were dropped into each grid box at random and the small pits in each circle measured in terms of width and depth, and catalogued. All large pits in each grid box were measured in terms of width and depth, and catalogued. The results from these measurements are shown in Table 1 and in Figure 7. None of the width-to-depth distributions have any statistical correlation ( $r^2 < 0.4$ ), although the large pits at West of Gulf had a width to depth  $r^2 = 0.52$ . The width to depth ratio for almost all pits, however, is less than one, indicating that they are wider than they are deep (Figure

7). The mean values for the small pit widths and depths from the protected Grahams Harbour location on North Point were wider and deeper than for the less protected Atlantic side at North Point, and at West of Gulf.

As shown in Figure 4, the Atlantic side of North Point is steep and rugged in its gross morphology. The Grahams Harbour side of North Point has a broad erosional bench separating the coast from a cliff of erosionally-truncated eolianites. The West of Gulf site (Figure 5) is in a basin-like feature flanked by higher rocky outcrops. The Grahams Harbour bench indicates that while normal waves do not cross it, major storm and hurricane waves must do so, as the bench has been carved since the stabilization of sea level at its current position ~3,000 years ago. Both the Atlantic side at North Point, and West of Gulf at the south end of the island, have more rugged coasts reflecting their exposure to wave energies routinely higher than that found in the sheltered Grahams Harbour site.

## Conclusions

The first major conclusion that can be reached is that the pitted surface found at North Point is Holocene in origin, as it must be younger than the Holocene rocks on which that surface is developed. The similarity of pitting seen at the late Pleistocene section at West of Gulf indicates that those pits are also Holocene in age, and have not



**Figure 6:** a. closer view of scene in Figure 4a, note smooth “light zone” to the right, and pitted, “dark zone” to the left; b. close up view of the pitted surface found in the “dark zone” areas on San Salvador island, top to bottom lineations are bedding of the eolianite; c. rock hammer sits on surface that had covering rock peeled off by a storm in the winter of 2003. The peeled surface is white and unpitted, but as this surface is in the spray zone, it will soon become dark and pitted; d. transect being measured on the Graham Harbour site. Note that it extends from the dark zone into the light zone.

been inherited from an earlier time (such as the last interglacial sea-level highstand). The age difference in the rocks at North Point and West of Gulf is expressed most obviously in the more irregular large-scale topography at West of Gulf, which most likely reflects differential cementation and diagenesis in those rocks since their deposition 120,000 years ago. At the small scale, however, the rocks at all sites appear to behave similarly, reflecting their overall eogenetic nature. The larger depth and width of the small pits at the protected Grahams Harbour site, relative to the other two

ocean-exposed sites, may indicate that the recycle time is longer in the protected lagoon, allowing the pitting to progress more completely before a storm strong enough to agitate the lagoon occurs.

The occasional major storm event that has carved the Grahams Harbour bench must at the same time strip the pitted surface. After the storm passes, sea spray begins to re-initiate pitting on those surfaces within spray reach, while the wave-polished surface farther inland, away from sea spray, remains unaltered. Given that the eolianite high ground has been eroded inland at least 10 m

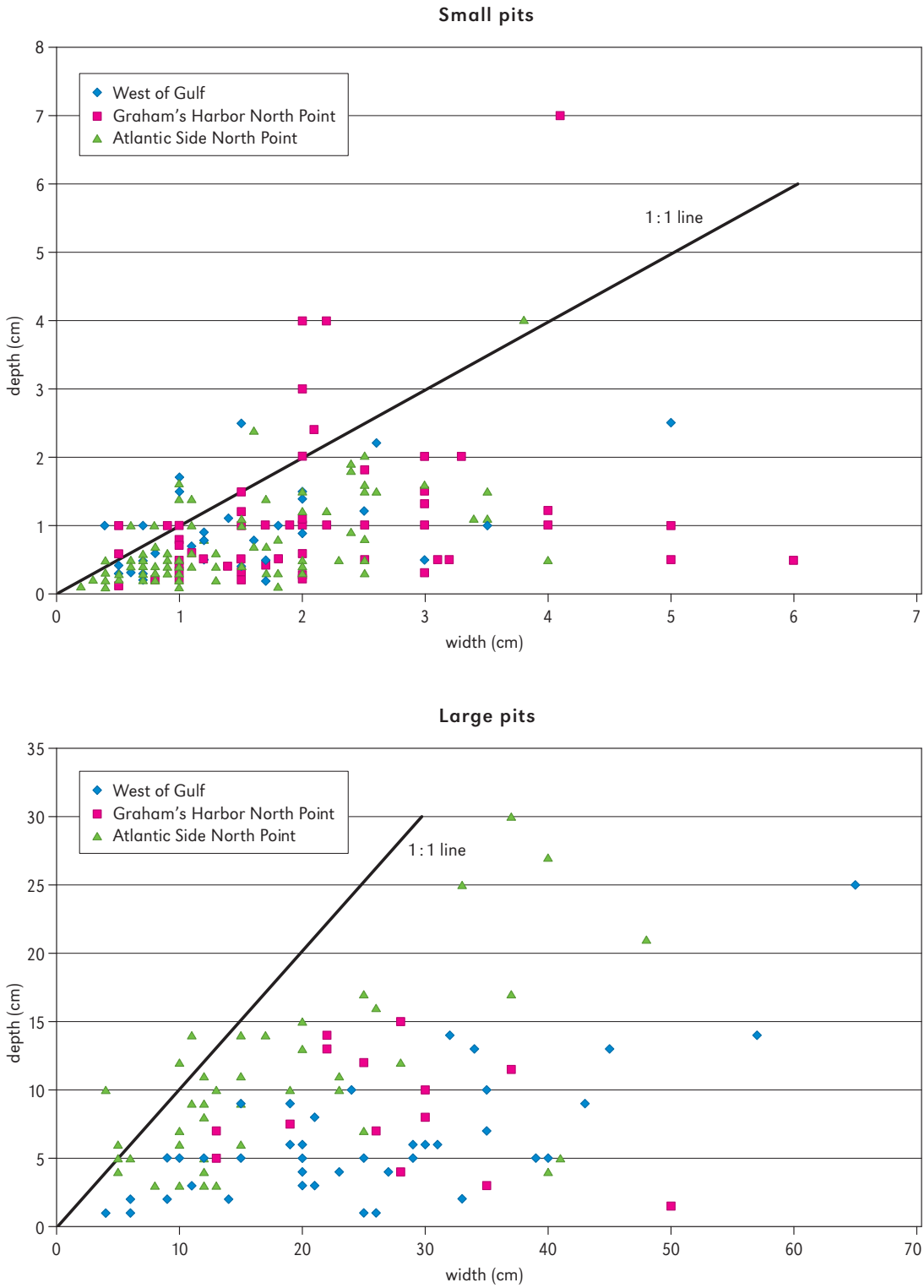


Figure 7: Plots of width versus depth data for pits measured in the transects at the three sites: above. small pits; below. large pits.

in the last 3,000 years, the outcrop must be routinely, in geologic time terms, swept and eroded by storm waves. Therefore, the pitting seen on the coastal “dark zone” must develop relatively quickly.

Most studies reported in the literature of young coastal carbonate outcrops deal with rocks that are Pleistocene in age. The work presented here from San Salvador, using Holocene rocks, provides time constraints not available in those other localities. While age differences of a hundred thousand years manifest themselves on the large scale, they do not do so at the small scale. Rather, exposure to wave energies seems to be more important. The data further reinforce the idea that it is the eogenetic aspect of the rocks that is critical. The data also indicate that these coastal eogenetic karren forms develop quickly, and rapidly renew their micro-morphology as major erosion events reshape the overall coastal landscape. The presence of coastal sea-spray produced karren, and the paucity of meteoric karren indicate both the

rapidity with which coastal sea-spray karren can develop, and also the cycle time of major storm events, which must be faster than meteoric karren production.

## **Acknowledgments**

The authors wish to thank the Gerace Research Centre for assistance with the field research, conducted under GRC Research Number G-102. Field assistance by the Teachers in Geoscience Bahamian Field Class of 2003 (Christene Anderson, Tracy Brown, Neal Becker, Deborah Buffingham, Melissa Kellerman, Patrick Leonard, Lisa Keith-Lucas, Rebecca Murray, Debra Neuhaus-Palmer, Christine Oxenford, Thomas Rozycki, Tricia Schafebook, Patti Jean Simpson and Rebecca Vowell) is greatly appreciated. Data reduction by Lica Ersek, Monty Keel, Nono Lascu and Monica Roth was extremely valuable. Discussions with Larry Davis and Jim Carew were helpful.



Lluís GÓMEZ-PUJOL and Joan J. FORNÓS

*Coastal karren*, understood as an assemblage of small (down to millimetres) to large-scale (up to several metres) mainly dissolutional features developed on carbonate coasts, is a topic with a large but not with an abundant tradition in geomorphological literature. Since Wentworth (1939), one of the earliest papers concerned with coastal

karren features, the approach to the study of this topic has changed significantly. Earlier workers focused their effort on morphological descriptions and spatial zonations across the coast profiles (Emery, 1946; Corbel, 1952; Guilcher, 1953; Dalongeville, 1977; Mazzanti and Parea, 1979), whereas modern ones put their effort into try-

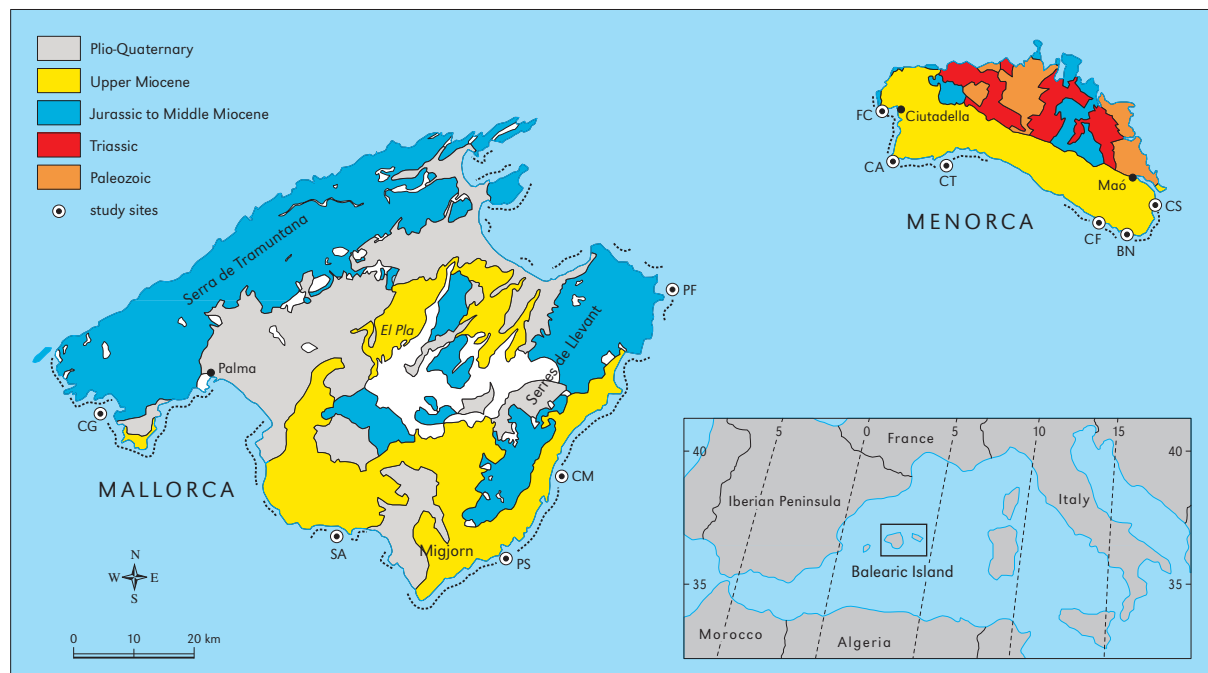


**Figure 1:** Location inset and geological map of Balearic islands. Dotted line indicates coastline with conspicuous coastal karren features. CG. Cala d'en Guixar; SA. S'Alavern; PS. Punta des Savinar; CM. Cala Murada; PF. Punta des Faralló; FC. Far de Ciutadella; CA. Cap d'Artrutx; CT. Cala Turqueta; CF. Cap d'en Font; BN. Binibèquer; CS. Cala Sant Esteve.



ing to identify and understand which processes and agents operate on carbonate coasts (Folk et al., 1973; Schneider, 1976; Trudgill, 1976a, 1987; Viles et al., 2000; Lundberg and Lauritzen, 2002; Moses, 2003).

The earliest references to the coastal karren of the Balearic islands appear in a nineteenth-century naturalist's works (Habsburg-Lorena, 1884-1891), although the first description from a scientific point of view is developed by Walter-Levy et al. (1958). Butzer (1962), Butzer and Cuerda (1962) and Ginés (2000) consider briefly Mallorcan coastal karren forms in their Quaternary stratigraphy research, but the first paper exclusively concerned with these forms is published by Rosselló (1979) who attempts to assess the type of forms and their spatial organization in the south-eastern Mallorca coast. More specific studies linking coastal karren forms and *bioerosion* are developed by Kelletat (1980, 1985) in the north-eastern coast of Mallorca. Moses and Smith (1994) characterize the spatial domain of inorganic processes – salt weathering and solution – operating on Mallorca's southern coasts, by means of SEM and XRD analysis. Since 1998 there has been an increase in coastal karren knowledge related to investigations on limestone rock coast evolution in the Balearic islands. Recent works characterize these features from an integrated approach linking forms and morphological zonation to different processes, agents and their erosion rates (Fornós and Gómez-Pujol, 2002). The most detailed inventory of coastal karren forms and their organization is by Gómez-Pujol and Fornós (2001) who link forms to hydrodynamic and biological gradients as well as to major features of cliff profiles. Recently, Gómez-Pujol and Fornós (2004b) have assessed Menorcan coastal karren through morphometrical, SEM and mineralogical studies.

The aim of this paper is to review and summarize the characteristic assemblages, organization and processes involved in coastal karren development in the Balearic islands.

## Study area

Mallorca and Menorca are the two biggest islands of the Balearic archipelago, which is located at the centre of the Western Mediterranean (Figure 1). They have a typical mediterranean climate with hot dry summers and mild wet winters. The mean annual temperature is approximately 17°C, with mean winter and summer values of 10 and 25°C respectively; the mean annual precipitation is about 500 mm and is mostly concentrated in autumn (Guijarro, 1986). The Western Mediterranean presents a temperate, oligotrophic, clear sea environment. Waves rarely exceed 8 m in height and 50 m in wavelength; these values are considerably reduced near the shore where a maximum height of 4 m is achieved only during 6-8 Beaufort scale gales (Butzer, 1962). Forcing by tides is almost negligible in the Mediterranean with a spring tidal range of less than 0.25 m, although changes in atmospheric pressure and wind stress can account for a considerable portion of sea level fluctuations (Basterretxea et al., 2004).

These islands are the eastern emergent parts of the Balearic promontory; a thickened continental crustal unit forming the NE continuation of the Alpine Betic thrust and fold belt (Alonso-Zarza et al., 2002; Gelabert et al., 1992) built during the Middle Miocene. The major topographic heights of both islands are horsts formed during post-Middle Miocene extension and expose deformed Palaeozoic to Middle Miocene carbonate rocks. The intervening grabens are flat areas, filled by an Upper Miocene carbonate shelf and Quaternary alluvial fan and aeolianite deposits (Gelabert, 1998, 2003). Cliff coasts are characteristic of a large part of the Mallorcan and Menorcan littoral. They are almost exclusively associated with deeper water offshore, and the -20 m isobath is generally found at distances considerably less than 500 m from the shoreline. Cliff form is closely related to the main characteristics of the large-scale morphostructural units of each island. Abrupt cliff faces are characteristic of horsts, and grabens host the major beach-barrier systems. Tabular

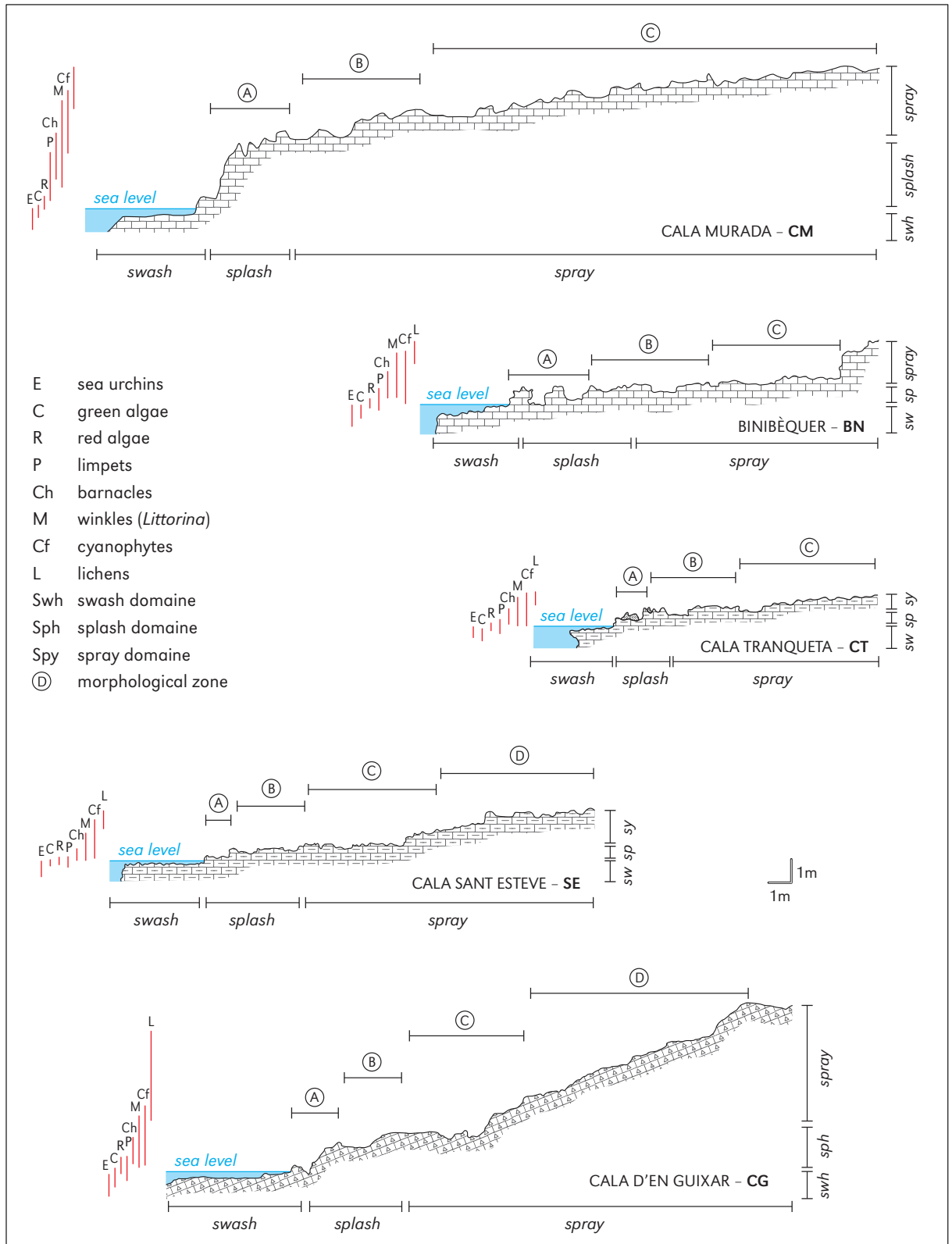


Figure 2: Balearic islands coastal karren selected cross-section profiles showing main morphological features, hydro-dynamic gradient and biological zonation. See locations in Figure 1.

relief added to the major horsts and grabens are bounded by Upper Miocene-Quaternary listric faults (Gelabert, 1998), which result in medium to low vertical sea cliffs. Thus the general picture is one of plunging and composite cliffs that affect from Palaeozoic to Middle Miocene folded outcrops. Cliff faces vary locally from 3 to 30 m in height and extend from 5 to 10 m below sea level. In these folded outcrops shore platforms and rock coasts sculptured by coastal karren appear patchily and are closely related to lithology and structure control. On the other hand, in post-orogenic Upper Miocene outcrops, cliffs present a composite profile with a step-like form closely related to higher Pleistocene sea levels (Butzer, 1962). These steps are enhanced by the geometry of the Upper Miocene tabular strata and differences in geomechanical properties between depositional levels (Pomar and Ward, 1999). Where cliffs fall vertically, their height range is 3 to 30 m. Shore platforms, although, patchily distributed, are here more continuous than in the folded rock coasts. Coastal karren forms are more common and continuous in the Upper Miocene outcrops.

## Method

The coastal karren was surveyed from low water mark at the shore platforms up to the terrestrial transition zone using a tachometer TOPCOM® CTS210. On each profile the extent of hydrodynamic and biological zonation (Figure 2) was marked according to colouration and key-species presence (Torunski, 1979; Schneider, 1976). The surveys documented the size and shape of karren features as well as comments focusing on any biological action. The morphometrical approach designed by Johansson et al. (2001) has been developed just for basin pools. It consists of taking the major morphometrical parameters – length, width, and depth – and classifying the shape according to a set of shape types; of assessing the connectivity degree between different basin pools; and of evaluating the number of joints that con-

trol the geometry of each karren feature. SEM observations according to Viles (1987) and Taylor and Viles (2000) have been developed at each coast profile.

## Classification of coastal karren forms

The classification adopted here is based on morphologies with some subdivision based on genetic factors. Although generic classification of karren forms is to be preferred, the genesis of many forms is not completely understood. Much of the variety in karren occurs because two or more differing processes combine to produce a *polygenic form* (Ford and Williams, 1989). This is especially true for coastal karren where different processes, such as salt weathering, inorganic solution or bioerosion, contribute to the final shape of forms like basins or pinnacles.

### Negative forms

#### CIRCULAR PLAN FORMS

*Micropits:* A wide variety of small depressions and differential etching forms commonly less than 1.0 cm in characteristic dimension. Micropit walls are smooth and are partly or entirely covered by cyanophytes, fungi or lichens. They may be isolated, in coalescence, or aligned following a microfracture. Micropits cover other major forms such as pinnacles, and also are present on bare and vertical rock surfaces. These depressions do not present any kind of preferred orientation, and gravitational control is not dominant. For this reason, although a recognized solution microtopography, it is believed that biological agents also play an important role on micropit development (Folk et al., 1973; Danin et al., 1982). Most species of cyanophytes, fungi and lichens are surface dwellers (epiliths), but in stressful environments – such as rock coasts – some of them bore into rocks to depths of ~1.0 mm (Jones, 1989; Viles et al., 2000). They contribute to micropit creation or enlarge-



**Figure 3:** a. basin pools isolated and coalesced at Binibèquer (BN). Note the control of joints on biggest basin pool shape and limits, width of view is 7 m; b. big basin pools developed on supratidal zone of the profile of Cala Sant Esteve (CS). Inside the basin remnants of former basin pool walls can be identified; c. fretted pinnacle completely covered by microscopic algae at Cap d'en Font (CF), width of view is 15 cm; d. zone of pinnacles just above the notch and shore platform at Cap d'Artrutx (CA); e. splitkarren perpendicular to the coastline at Punta des Savinar (PS), width of view is 1.5 m; f. rillenkarrren developed on Jurassic breccia in the splash zone at Cala d'en Guixar (CG), width of view is 15 cm; g. microrills on a fine grained limestone located in the spray domain, Punta Prima (Menorca), width of view is 5.5 cm. Order of pictures from top: a, b, c, d, e, f, g.

ment by organic acid excretion or CO<sub>2</sub> production (Pomar et al., 1975; Gehrmann et al., 1992; Peyrot-Clausade et al., 1995) or by the physical action of lichen hyphae (Moses and Smith, 1993; Chen et al., 2000). Larger borers, such as gastropods, can create pits directly by physical and chemical action and indirectly by forcing cyanophytes and lichen to bore more deeply in order to avoid being consumed (Torunski, 1979; Spencer, 1988). It is quite common in the Balearic islands to find snails such as *Melaraphe neritoides* or *Melaraphe punctata* inside micropits. Their densities in areas intensively colonized by cyanobacteria can reach 200 to 2,000 individuals per m<sup>2</sup> (Gómez-Pujol et al., 2002; Kelletat, 1980). Some depressions seem to have a proportional relation between snail body size and micropit dimensions.

**Pits:** Small, closely spaced, roughly circular to elliptical depressions of a few centimetres in diameter and depth. Such features are attributed to a number of origins including those described for *micropits*. Mechanical weathering has been argued in combination with inorganic and organically induced dissolution. Salt crystallisation has been observed by scanning electron microscopy and X-R diffraction analysis on carbonate rock coasts in Japan (Matsukura and Matsuoka, 1991) and in Mallorca (Balearic islands) by Moses and Smith (1994). Pits appear in the zone subjected to the salt-laden spray; depressions of diameter 1.0 to

10 cm and depth 1.0 to 5.0 cm occur on both vertical and horizontal surfaces between pinnacles and pans.

**Basin pools:** These depressions display an elliptical or irregular plan view and a flat or nearly flat bottom that is usually horizontal (Figure 3a, b). The walls are steep and may display a basal *corrosion notch*. Individual basin pools attain diameters of several metres and depths greater than one metre. Coalescence of adjoining pools is common, creating larger features with crenulated or irregular plan form. The origin of these features is largely attributed to dissolution (Ford and Williams, 1989), but biochemical processes are really important in their formation by causing undersaturation of water in basins with respect to CaCO<sub>3</sub> at night (Emery, 1946; Schneider, 1976; Trudgill, 1976a) or directly as a result of biological corrosion and erosion of the substrate by cyanophytes (Dalongeville et al., 1994; Torunski, 1979) and snails, limpets or sea urchins which also attack the rock mechanically (Hodgkin, 1970; Trudgill et al., 1987; Andrews and Williams, 2000).

In the Balearic islands basin pools range in width from 1.0 dm to 6.0 m and in depth from 4 cm to 1.6 m (Table 1). But considerable differences between morphometrical parameters can be identified across the coast profile. Thus basin pools nearest to the sea are narrower than those that are far away; for instance, in the southern

**Table 1:** Summary of reported basin pool form properties measurement in Balearic islands.

Location	Lithology	Width range	Depth range	Source
Cala Pudent (Mallorca)	Quaternary carbonate aeolianite	0.90 to 2.30 m	0.07 to 0.38 m	Rosselló (1979)
Cala d'en Guixar (Mallorca)	Jurassic limestone breccia	0.45 to 1.20 m	0.12 to 0.33 m	Gómez-Pujol and Fornós (2001)
Cala d'en Guixar (Mallorca)	Quaternary carbonate aeolianite	0.48 to 1.58 m	0.22 to 0.43 m	Gómez-Pujol and Fornós (2001)
S'Alavern (Mallorca)	Miocene reefal calcarenites	0.30 to 1.70 m	0.04 to 0.35 m	Gómez-Pujol and Fornós (2001)
Cala Figuera (Mallorca)	Miocene reefal calcarenites	0.30 to 4.00 m	0.25 to 0.70 m	Gómez-Pujol and Fornós (2001)
Punta des Sivinar (Mallorca)	Miocene reefal calcarenites	0.10 to 6.00 m	0.20 to 1.20 m	Gómez-Pujol and Fornós (2001)
S'Estret des Temps (Mallorca)	Quaternary carbonate aeolianite	0.40 to 2.00 m	0.17 to 0.50 m	Gómez-Pujol and Fornós (2001)
Es Caló (Mallorca)	Quaternary carbonate aeolianite	0.50 to 1.30 m	0.14 to 0.47 m	Gómez-Pujol and Fornós (2001)
Far de Ciutadella (Menorca)	Miocene reefal calcarenites	0.40 to 4.00 m	0.11 to 0.67 m	Gómez-Pujol and Fornós (2004)
Cap d'Artrutx (Menorca)	Miocene reefal calcarenites	0.56 to 3.20 m	0.10 to 0.53 m	Gómez-Pujol and Fornós (2004)
Cala Turqueta (Menorca)	Miocene reefal calcarenites	0.54 to 1.30 m	0.16 to 0.53 m	Gómez-Pujol and Fornós (2004)
Cap d'en Font (Menorca)	Miocene reefal calcarenites	0.49 to 3.12 m	0.12 to 0.45 m	Gómez-Pujol and Fornós (2004)
Cala Sant Esteve (Menorca)	Miocene reefal calcarenites	0.38 to 3.20 m	0.10 to 1.60 m	Gómez-Pujol and Fornós (2004)

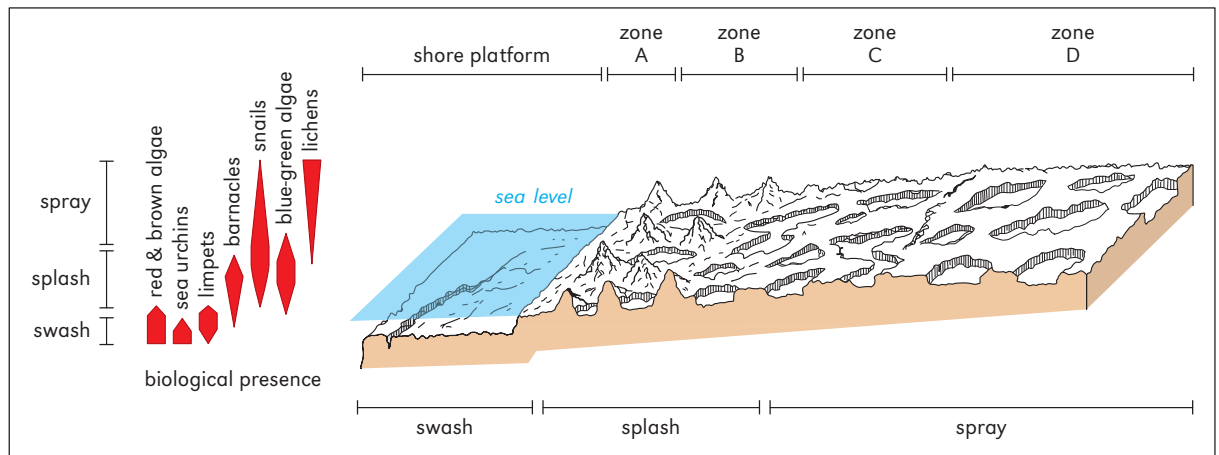


Figure 4: Morphological, biological and hydrodynamic zonation at coastal karren systems in Balearic islands.

Menorca Miocene calcarenites, the mean diameter for basin pools nearest to the sea is 0.62 m and landward this parameter rises to the 1.66 m. If we compare maximum values between seaward and landward basin pools, the same pattern applies: at Cap d'Artrutx study site near the sea, basin pools have a maximum width of 2.20 m and landward of 3.20 m; the same couple for Cala Sant Esteve is 1.23 m and 3.20 m. This pattern is also clear in the Mallorca coast: in Jurassic limestone, seaward basin pools reach 0.9 m in mean width and 2.30 m at landward. The same is true for Upper Miocene calcarenites and Quaternary carbonate aeolianites where width increases from 0.7 to 4.0 m and from 0.4 to 1.2 m respectively. Basin pool depth is quite variable, and although all features are characteristically tapered, depth values change from one basin to another according to changes in facies and lithology. Basin pools can be isolated (more likely close to the land) or coalesced (more likely close to the sea): close to the sea basin pools are connected in 60% to 90% of cases; far away from the sea, basin pools are isolated in 70% to 90% of cases (Figure 4).

**Subsoil tubes or shafts:** These features are deeper than wide, and in plan form rounded or elliptical. Tubes evolve under gravitational control enhanced by rock discontinuities and joints systems. Their vertical walls are smooth and sinuous, and

at the bottom of tubes thin layers of soils or beach sands may accumulate. Subsoil tubes measured in the Balearic islands range from a minimum of 4 x 4 x 9 cm to a maximum of 26 x 26 x 50 cm. Ford and Williams (1989) and A. Ginés (1995) identify this kind of form as a feature developed beneath soil and vegetation cover and exposed after soil erosion. In coastal profiles exposed to sea waves, subsoil tubes only appear landward, sometimes between isolated basin pools; on bare surfaces close to the soil layer similar forms partially exposed can be observed.

### Linear plan forms fracture controlled

**Microfissures:** Small channels guided by *microjoints*, tapering with depth. Microfissures in the Balearic islands limestone rock coast may be some centimetres wide but rarely exceed more than 5 mm in depth. They are more common in the landward areas. Ford and Lundberg (1987) understand microfissures as a typical inorganic solution form.

**Splitkarren:** Depressions that are elongated along joints, veins or fractures. These features range in length from one centimetre to several metres and down to 20 cm in width; with the same magnitude scale order for the depth (Figure 3e). If a rock outcrop displays several families of joints,

splitkarren can result in a pseudo-meandering channel. Solution is the main process operating in these features (Ford and Williams, 1989) although the splitkarren walls are carpeted by cyanobacteria and may also be related to microkarren forms such as pits or micropits.

### Linear plan forms hydrodynamically controlled

**Microrills:** Small channels ~1.0 mm in width normally rounded in cross-section with depth. They are sinuous or anastomizing on gentle slopes and straighter on steep slopes. Lengths are up to a few centimetres. In the Balearic islands microrills in coastal karren environments occur landward in coastal profiles; they are widespread in the spray domain (Figure 3g). They are associated with fine grained limestones. Capillary flow is believed to explain these features, although wind or gravity forces also may play a significant role (Laudermilk and Woodford, 1932; Ford and Lundberg, 1987). Microrills have been identified in different localities, both in fine-grained Miocene calcarenite and on Jurassic mudstones from Mallorca and Menorca (see chapter 7).

**Rillenkarren:** Shallow channels with round-bottomed troughs, packed side by side, separated by sharp crested ridges, and commencing at crest of slope (Ford and Williams, 1989) (Figure 3f). They are not really frequent in Balearic coastal karren assemblages, although they appear on different rock types such as Miocene calcarenite or Jurassic breccias. They show width ranges from 0.7 to 1.4 cm, and length from 4 to 12 cm. They may occur on dissected relief, between discrete *basin pools* or on *splitkarren* walls and in splash and swash rush domain.

### Positive remnant forms

**Pinnacles:** Upward-pointing pyramid or projectile-shaped bodies of rock separated by widened

fractures or basin pools. Their walls appear dissected with nested concavities bounded by knife-edges that often penetrate the rock (Figure 3c, d). Micropits are not gravitationally oriented, giving to the pinnacles a spongy appearance and the rock surface is coated by a layer of blue-green algae. Pinnacles are the only coastal karren form positive in topographic terms; Trudgill (1979) argues that the rugged topography could be related to the differential solubility of clasts and cements mainly in bioclastic limestone. So rock structure has an overriding importance and microorganism processes just enhance surface irregularities produced by inorganic dissolution. Alternatively, other authors (e.g. Jones, 1989) point out that biological processes outweigh solutional disintegration while at the same time lithological variations control microfloral growth. Moses (2003) links biological and salt weathering to pinnacle development. Pinnacles in the Balearic islands range in height from 20 cm to 1.3 m and are better developed on carbonate aeolianite and also on Miocene calcarenite outcrops. They do not appear on Jurassic breccia outcrops, nor in marls.

## Organization of coastal karren forms

The sequence of coastal karren development in the Balearic islands is a general picture where in a meso-scale order of analysis four morphological domains can be separated (Figure 4). After a sub-horizontal shore platform, 1 to 6 m wide, sculptured by sea-urchin hollows and completely carpeted by green and brown algae and sometimes preceded by a notch profile, we find the coastal karren forms from the swash domain to inland until the transition to fully terrestrial environments.

**Zone A:** This domain is characterized by the transition from the swash to the splash hydrodynamic zone in quiet conditions. Waves reach this surface during storms. From a morphological point of view the presence of isolated pinnacles is the clearest feature, those near to the sea are sharper

than those that are far away. Their surface is completely fretted by micropits and the rock surface has a dark brown to blue-black coloration due to the intense colonization by cyanophytes and lichens (*Rivularia* sp., *Pynerocollema* sp.). It is easy to find individuals of *Melaraphe neritoides* or *Melaraphe punctata*; limpets (mainly *Patella rustica* and *Patella caerulea*) are abundant at horizontal surfaces between pinnacles or vertical walls just above the scarp after the shore platform as well as snails such as *Monodonta turbinata* and/or *Monodonta articulata*. Joints widened by solution (splitkarren) that remain in zone A are colonized by filtering barnacles (*Chthamalus depressus* and *Chthamalus stellatus*) specially where waves and run-off water flow. The rock surface is very rough and abundant salt efflorescence occurs during dry periods.

**Zone B:** This area corresponds to the extension affected by wave splash. Pinnacles are the dominant feature although they are not isolated. Pinnacles are joined at their bases by a small wall, resulting in a configuration of shallow basins flanked by triangular bodies of pinnacles. The general aspect, although a different order of magnitude, is reminiscent of “cockpit” karst. Densities of *Melaraphe neritoides* and *M. punctata* winkles increase and limpets and barnacles decrease.

**Zone C:** This is a zone when sea spray is the dominant hydrodynamic condition, only subjected to splash in storms. Basin pools have a greater degree of connectivity, between 60 to 90% of cases; and those nearest to Zone B share walls between them. Many of them show overhanging sidewalls, usually fretted by micropits, where densities of *Melaraphe neritoides* reach the most dense of the profile. Some localities can reach between 200 to 600 ind/m<sup>2</sup>, although on lithologies such as carbonate aeolianites, densities of 1,700 ind/m<sup>2</sup> have been counted (Palmer et al., 2003; Kelletat, 1980). All basin pools have basal coverings of cyanophytes while some also contain a layer of salt crystals. The rock surface between basins presents a rough texture and much of it is colonized also by cyanophytes giving to the rock a characteristic blue to grey color.

**Zone D:** Here basin pools are the characteristic feature. They are generally isolated (around 85% of cases). The rock surface between them is smooth or rounded inland where lichens (mainly *Verrucaria* sp.) are present. A smooth rock surface is common on basin walls and floors. Winkles such as *Melaraphe neritoides* are abundant; densities of 271 to 897 ind/m<sup>2</sup> on basin walls are common. *M. neritoides* individuals in Zone D show bigger sizes than in the other zones (Gómez-Pujol et al., 2002), this fact is related to physical resistance to seawater impact and also to their reproduction strategy (Bosch and Moreno, 1982). Beyond the upper limit of Zone D, where micro-relief is not conspicuous, forms such as microrills or subsoil tubes appear. These last features lie in the zone of lichen and halophytes, just in the transition to the spray domain to the fully terrestrial environments.

## Major controls on coastal karren forms

Coastal karren landforms are complex systems; many agents and factors act on morphologies configuration and erosion processes. The process magnitude, order and frequency is quite variable according to the focus of interest (Goudie and Viles, 1999); different controls can be identified if the investigation is concerned with bioerosion or with distribution of forms along the coast. So, scale issues are fundamental to the study the coastal karren assemblages, being a fundamental key to identify the controls of the system under analysis (Viles, 2001).

### Macro-scale controls

The chemical nature of the carbonate rock is the main key for coastal karren development, but texture and structure are also important. Structure plays a double role because it guides the outcrop of lithologies susceptible to coastal karren development, and also governs the shape of the profile.



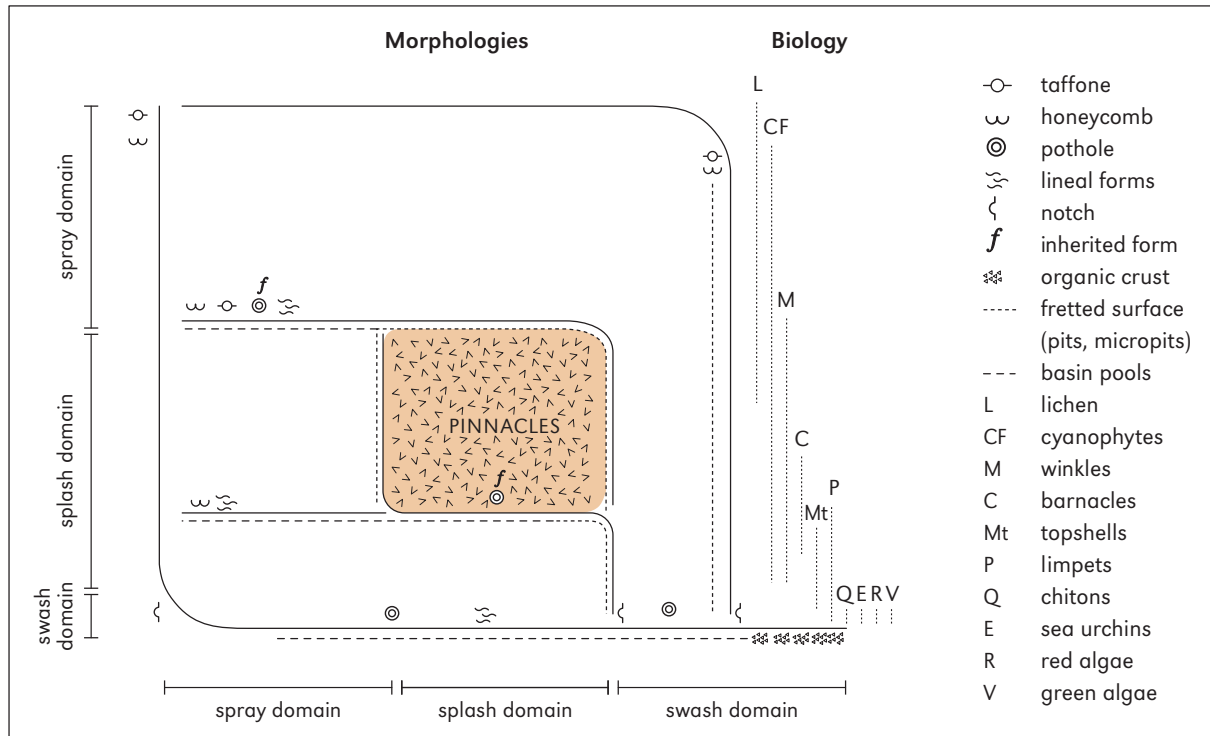


Figure 5: Typology of coast profiles in Balearic islands and coastal karren associated forms.

This last feature is also enhanced by lithology and discontinuities.

The map of coastal karren distribution along coast of Mallorca and Menorca (Figure 1) shows that there is not a homogeneous presence of coastal karren assemblages between and within geological units. The interplay of structure and lithology can explain much of this patchy distribution. For instance, in southern Menorca most rock outcrops affected by coastal karren appear eastward and westward, the central sector of the island being poor in this kind of micro-relief. Southern Menorca is built of Miocene limestone which is affected by a gentle anticline (Gelabert, 2003; Gelabert et al., 2005); for this reason lower Miocene units (Lower Bar unit) appear in the central southern coast of the island and Upper Miocene bodies (Reefal unit) appear to the east and west. Muddy calcarenites are the most important bulk constituent of the Lower Bar unit and erode more easily than the red-algae rud-

stone and grainstones that are characteristic of Reefal unit (Pomar et al., 2002). So, vertical cliffs are dominant on Lower Bar unit while there are abundant examples of coastal karren assemblages on the Reefal unit.

The control of tectonics and lithology on coastal karren development is also quite evident in Mallorca. For instance the south-eastern coast is built of Upper Miocene reefal and oolitic calcarenites affected by a pre-Holocene tectonic tilting towards the SE (Fornós et al., 2002). This fact explains the presence of vertical low cliffs in the north-east cut into Reefal unit rocks alone, and on stepped profiles in the south-east built by the succession of Reefal unit calcarenites to oolitic and mangrove calcarenites.

Based on macro-scale controls, an array of possible profiles can be drawn (Figure 5). Completely vertical or subhorizontal profiles just allow the development of micropits or pits and some basin pools; however, stepped profiles display the clas-

sical succession of forms described above and are the necessary condition for pinnacle development.

### Meso-scale controls

The hydrodynamic gradient also plays a role as a meso-scale control. It is largely responsible for the morphological zonation: differences in sea water input and contact with rock control the amount of physical impact, dissolution or salt deposition (Moses and Smith, 1994). For instance, the pinnacle domain is closely related to the extent of profile extension affected by splash; micropits and fretted hollows, that overlie rock surfaces in this domain, contain a layer of salt crystals. Exposed profiles tend to present bigger areas of rock outcrop affected by karren sculpturing than sheltered ones. On Mallorcan Cala d'en Guixar (CG on Figure 1) Jurassic folded limestones, exposed profiles show karren development for 24 m inland, whereas in sheltered profiles coastal karren landforms extend only 4 to 10 m landward. This also applies to Menorcan coastal karren. In exposed profiles such as in Cap Artrutx (CA) or Cap d'en Font (CF), coastal karren development extends more than 20 m inland. In sheltered profiles such as Cala Turqueta (CT) or Binibèquer (BN), sculptured surfaces extend only 8 to 10 m inland. Obviously seawater is essential for basin pool development. The hydrodynamic gradient is also important for biological colonization and zonation. Palmer et al. (2003) demonstrate that rock surface wetness is a significant control on both biological film (endo and epilithic algae, lichens and fungi) and grazing organisms (limpets, snails, etc.), the greatest density of organisms or biomass being near the sea edge of the profile. This means that bioerosion can be greater seaward than landward; thus biotic and abiotic factors, such as the hydrodynamic gradient, reinforce the same pattern maximizing the erosion rate at sites exposed and located just above the sea level.

From a meso-scale control the role of texture and composition differences on lithology due to

the sedimentary environment are also important. This is quite evident in coastal karren assemblages developed on Upper Miocene sediments in both Menorca and Mallorca. Upper Miocene is composed of bioclastic calcarenites and coral reefs growths interlayered with levels of oolitic limestones and stromatolites (Fornós and Gelabert, 1995; Pomar et al., 2002). These materials correspond to the development of a coral reef barrier type with wide lagoon, which evolves to a more littoral environment. Although the extent of the outcrops are built up by calcarenites or calcisiltites, there are considerable lateral variations according to the depositional environment (Fornós, 1999). This fact can imply that in the same profile some features can evolve easily because the rock facies enhances the differential erosion.

### Micro-scale controls

SEM examination showed abundant evidence for biological weathering processes along coastal karren profiles of Mallorca and Menorca limestone coasts. Viles and Moses (1998) note that circular etch pit and tunnel *nanomorphologies*, as well as lichen hyphae and biological patinas, are related to biological weathering action; whereas crystal boundary widening, V-in-V etching, blocky etching, grain rounding and deposition of salts or crystal growth are related to inorganic solution (Figure 6). Thus, studying the relative abundance of nanomorphologies can assess the relative magnitude of these processes across the profile. For instance, in Menorcan coastal karren (Table 2) there are abundant examples of circular etching in the pinnacles domain and connected basin pools (zones A and B). These forms are the morphological result of cyanophyte biological activity (Jones, 1989; Schneider, 1976) and affect both the rock grains and the cement between them. Cyanophyte activity increases rock porosity; so there is a major effective surface attack where additional agents and processes (e.g., salt weathering or wave impact) can act (Fiol et al., 1996). This fact can help to explain the fretted surface of coast-

al karren seaward forms. Differential dissolution between grains aid detachment by seawater impact, and rain or wind action leaves depressions on the rock surface. Landward (zones C and D), biological action appears by means of lichen action. Some act as protective agents because they carpet the rock surface, and others may play an erosive role because their hyphae grow between grains voids (Moses and Smith, 1993; Chen et al., 2000). Dissolution due to inorganic processes or biochemically-driven processes increases landward (shown by the rounding of grains). It is less important in the pinnacle zone than on surfaces between isolated basin pools or in most terrestrial environments. However, not all surfaces are fretted: smooth rock surface is also a feature in mm to cm scale. Dissolution processes act, in spatial terms, in a more homogeneous fashion than the processes and agents described above. In fact, the spatial continuity of the thin boundary layer of static water on rock surface and their low turbulence and laminar behaviour favours the development of smooth surfaces, at least at the nanoscale (Ford and Williams, 1989; Trudgill, 1985). This fact can explain much of the smooth rock surface behaviour in the spray domain.

### Processes, zonation and evolution of coastal karren

Of the many sites documented, a general zonation may be delineated using morphologies distribution and attributes. Evidence for “classical” dissolution processes was limited to rounded and smooth rock surface and subsoil tubes. These fea-

tures are related to the chemical dissolution that occurs below the soil (Ginés, 1999a). When the soil is eroded, these forms become exposed to the weathering agents that slowly give to the rock surface a roughened appearance (e.g. microrills, cockling). If the rock surface remains free of soil cover, then it is colonized by lichen and blue-green algae, which carpet the rock and protect it from the physical action of rain drops and sea splash and spray. At the same time the lichen texture increases surface roughness, allowing the retention of thin water films, which contribute to chemical weathering. In addition, weathering is enhanced by physicochemical action of lichens closely related to their physiological activity (Chen et al., 2000; Viles, 1987). Basin pools have been described simply as typical solution forms (Trudgill, 1987), but this is not necessarily true. Although these depressions are often filled up by fresh water, aggressive enough for calcium carbonate dissolution, this is not the habitual situation. Most of the time basin pools are filled by seawater that is saturated with carbonate, so dissolution is not possible by means of inorganic processes. Schneider (1976) and Trudgill (1987) point out that in basin pools, undersaturation may occur during darkness hours caused by the physiological activity of blue-green algae colonizing rock surfaces. During the day, the biological cover consumes CO<sub>2</sub> by means of photosynthesis; when sunlight decreases and there is not enough light for photosynthesis, this process stops and CO<sub>2</sub> content increases in basin pool standing water. So the basin pool water becomes undersaturated with CaCO<sub>3</sub>. Thus the solution potential increases and inorganic solution by itself can clearly be excluded as the ge-

**Table 2:** Summary of nanomorphology abundances at different zones of coastal karren profiles. 0 form not evident; + form evident; ++ form well developed; +++ abundant form.

Zone	Morphological feature	Circular etch pits and tunnels	Crystal boundary widening	V – in – V etching	Blocky etching	Rounding	Deposition, crystal growth	Biological patina
A	Pinnacle edge	+++	+	0	+	+	0	0
A	Pinnacle base	+++	++	0	+	+	+++	+
B	Horizontal surface	++	+	+	+	++	+	+
B	Basin pool floor	+	++	0	0	++	+++	++
C	Horizontal surface	+	++	0	+	+++	+	+++

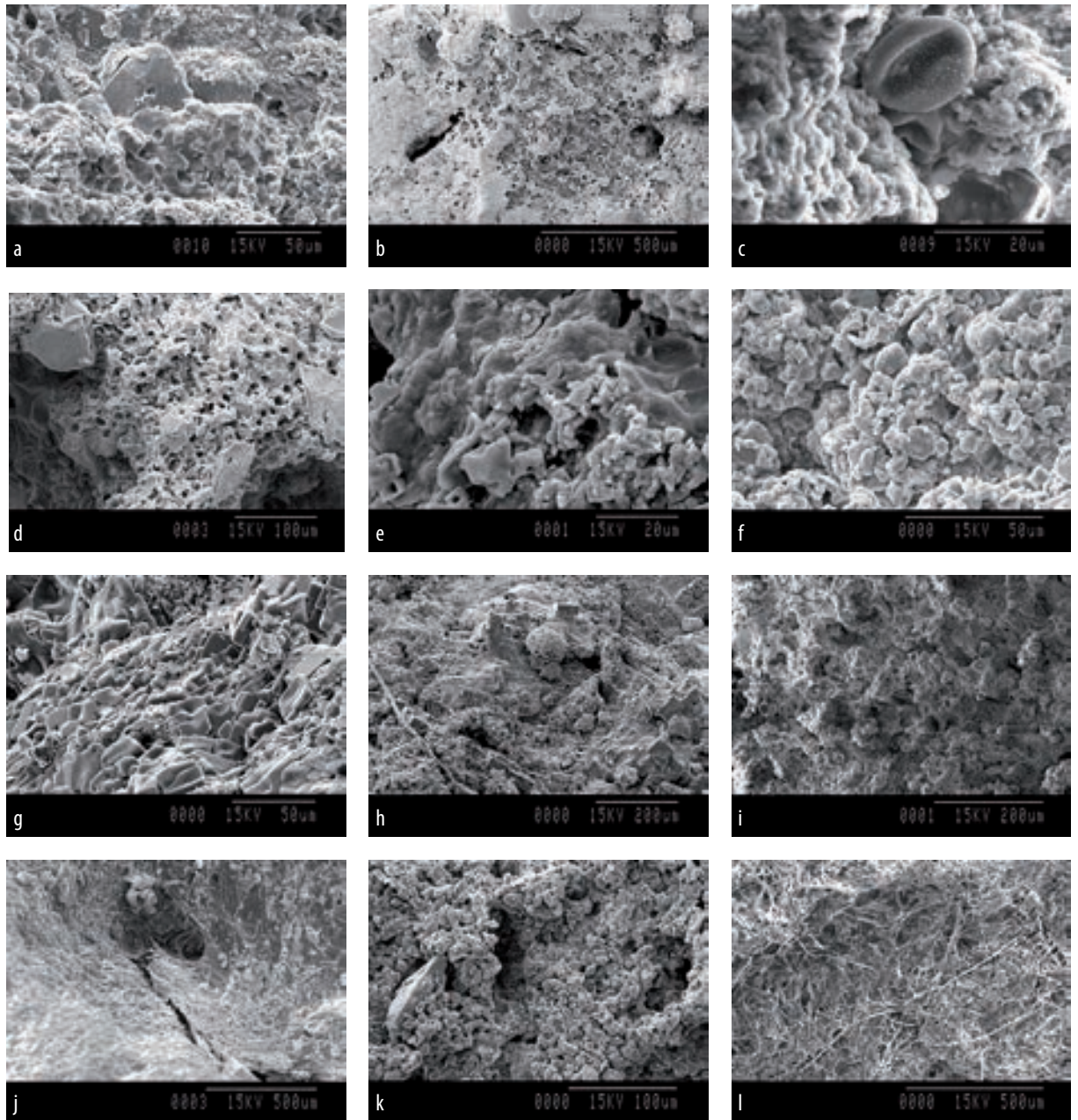


**Figure 6:** Scanning electron micrographs: a. fracture surface showing circular etch pits, attributed to boring algae activity. Note the “V in V” disolution etching of calcite crystal; b. detail of pitted surface of pinnacle with two generations of solution pittings. Surface is overlaid by case-hardened limestone. This is sculptured by larger hollows which host smaller pits that also appear on the crusted surface; c. detail of endolithic algal cell; d. circular etch pits developed on rock cement and calcite crystals affected by typical solution and crystallographically controlled nanomorphologies; e. biological patina covering rock surface in spray domain; f. blocky etching of the rock cement grains. Note the rounding of the grains; g. salt and gypsum deposition inside rock pores at base of pinnacles; h. combination of salt action, biological patina and filament shaped trenches on a surface between basin pools; i. biological circular etch pits affecting rock cement on a basin pool wall surface; j. high magnification view of base of individual etch pit showing a biological patina carpeting the depression surface; k. blocky etching and “V in V” solution of calcite crystals. Note the widening of the contact between cement grains that enhances rock granular disintegration; l. lichen hyphae and circular etch pits on a basin pool floor sample.

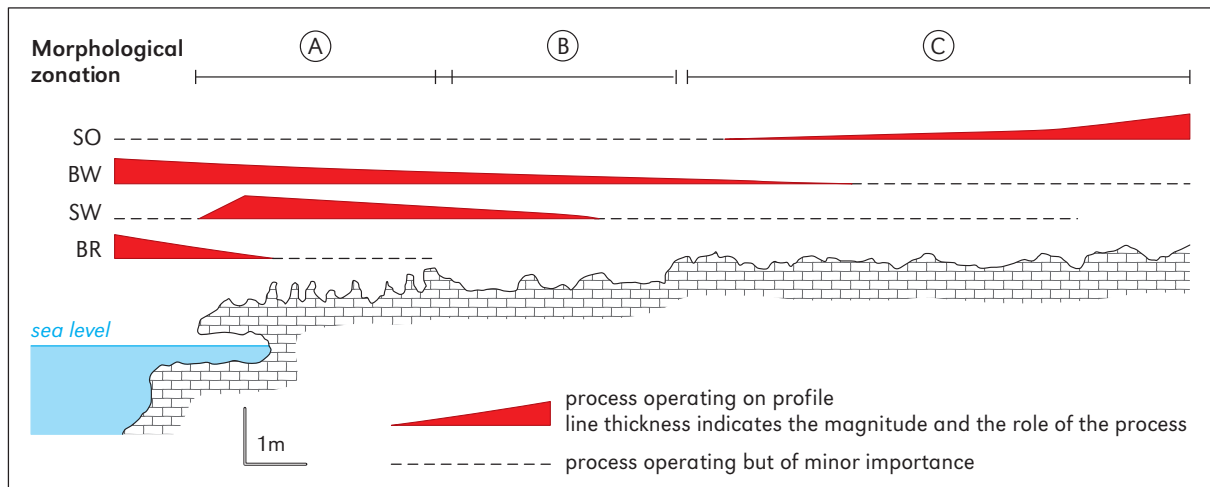


Figure 7: Suggested process zonation in the Balearic islands according to SEM observations and morphological organization. SO. dissolution; BW. biological weathering; SW. salt weathering; BR. bioerosion.

netic mechanism of basin pool formation (Schneider, 1976; Trudgill, 1987). This biologically-driven process is probably responsible for the gross form of micropits and pinnacles, although salt weathering (Moses, 2003; Moses and Smith, 1994) and the biological action should not be forgotten (Jones, 1989). On the seaward edge, the region of major biological colonization (Palmer et al., 2003), grazing erosion and biochemical weathering play a major role, while the physical action of waves contributes to rock physical erosion.

At least four main weathering and/or erosion vectors can be drawn on coastal karren systems according to the organization of coastal karren forms and the controls exerted by structure, geological history and hydrodynamic gradient (Figure 7). The first of these corresponds to dissolution weathering understood as inorganically-driven dissolution. This vector decreases seaward and has its main morphological expression in subsoil exhumed forms. It is especially important in zones D and in C. Biological weathering or biologically-driven dissolution is the second vector and the most important weathering agent along coastal karren profiles. Because the biochemical action of organisms controls the chemical properties of water standing in basin pools, biological

weathering affects most of the profile, although it is really important and intensive in zones A and B and with a minor role in C. The third vector, biological erosion, caused mainly by grazers (limpets, sea urchins and snails), is constrained mainly to zone A and to the vertical walls of sea edge profiles. Finally, salt weathering affects mainly zone A and decreases landward according to the extent of the splash and spray domains.

A general model for coastal karren development in the Balearic islands is proposed below (Figure 8). We consider a first stage (T1 on Figure 8) when the rock surface is not yet affected by marine agents and still suffers mainly terrestrial weathering processes. The soil layer retreats gradually, extending the surface exposed to marine agents (Figure 8.T1). The second stage represents the initial development of basin pools by means of some inorganic dissolution (fresh rainwater and run-off) but mainly by biological control of blue-green algae that colonizes rock surfaces. Basin pool development may be enhanced by rock joints and discontinuities (Figure 8.T2). In stage 3, the soil retreats landward and leaves smooth depressions to be colonized where seawater is added by wave splash. At the same time older basin pools become wider and deeper and some of them share

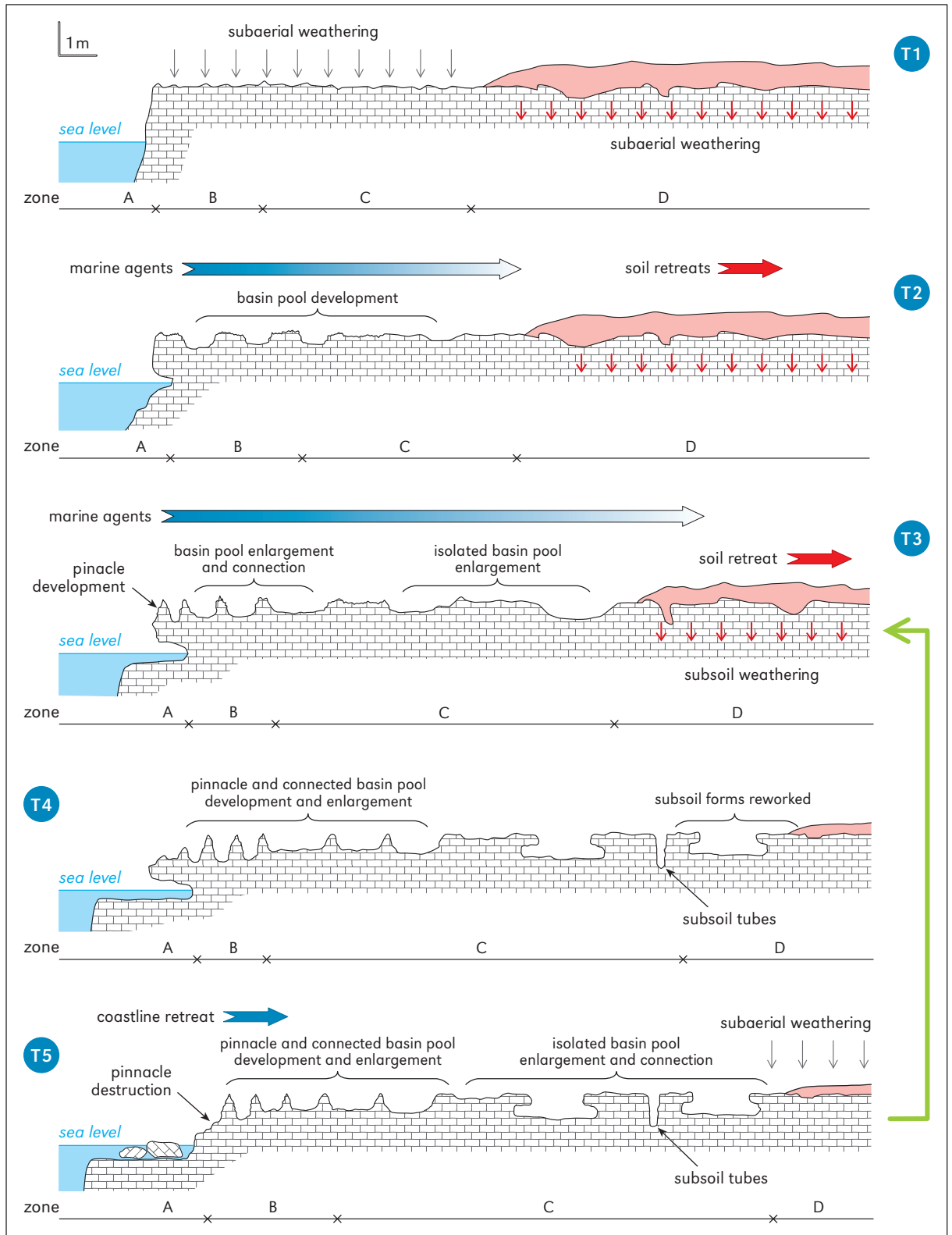


Figure 8: Evolution model for coastal karren landforms in Balearic islands.

their walls. Those basin pools, that are nearest to the sea edge suffer the physical action of wave impact during storms and their thinner walls break down. According to the density of joints and to rock properties some points or basin pools walls may be more resistant and will remain as pyramidal bodies; this is the initial pinnacle development (Figure 8.T3). Generally the rock surfaces nearest to the sea increase their roughness due to biological weathering and erosion combined with salt weathering. Previous basin pools developed in zone B have evolved to isolated pinnacles, and those previously isolated basin pools become wider and share the walls between them. Some of them coalesce and initial elliptical plan forms evolve to complex forms. In stage 4 landward, isolated basin pools enlarge. Soil retreat allows the interaction between marine forms and subsoil forms. At the seaward edge a narrow shore platform and a notch develop and those former isolated pinnacles nearest to the sea edge are destroyed, leaving some irregular topography on the notch roof (Figure 8.T4). The following stage corresponds to the visor break and this fact implies the displacement of the coastal karren system landward at the same time that the shore platform enlargement occurs (Figure 8.T5). The model follows in a cycle as the evolution of the coastal karren system follow, as we are once again in the third described stage.

Two features should be pointed out from this model that combines morphological zonation and controls on coastal karren systems at different scales. The first is that pinnacles are not a morphological feature by themselves because they are the remnant of the basin pool evolution. In fact they are just the only one topographically positive form described in the coastal karren forms classification. Also the hydrodynamic gradient creates,

from landward to seaward zones, different stages of basin pool evolution in the same profile.

Despite the major imprints of geological history and structural control on profiles, coastal karren systems are organized according to the biological zonation and the hydrodynamic gradient; thus it is an ecological zonation. The ecosystems present along the coast profile control and in some cases govern by their ethology the rock morphology and it may occur at different scales and orders of magnitude; from facts as the fluctuation of water chemical properties in basin pools to rock fatigue caused by the physical erosion enhancement by boring and biological increase in porosity. Thus, the coastal karren cannot be understood as classical exokarstic landforms. Dissolution is the dominant process on limestone rocks, but this is induced directly or indirectly by biological activity. So, coastal karren should be understood as a complex example of biokarst in the sense of Viles (1984).

## Acknowledgements

We would like to thank Angel Ginés, Joyce Lundberg, Guillem X. Pons and Lluís Fiol for helpful comments, as well as the work of the technical staff of the SEM unit of the Balearic islands University. Also we are in debt to Pau Balaguer, Joan Miquel Carmona, Marta Asensi and Mariana Baldo for the logistical support during fieldwork. Financial support was received from DGI-FED-ER project of the Spanish Government BTE2002-04552-C03-02 and CGL2006-1242-C03-01/BTE. L. Gómez-Pujol was in receipt of a FPI scholarship from the Direcció General de R+D+I, Govern de les Illes Balears.

# COASTAL AND LACUSTRINE KARREN IN WESTERN IRELAND

David DREW

More than 40% of the island of Ireland is underlain by karstifiable limestone rocks almost all of which are of Carboniferous age. The limestones form the bedrock along the coast in comparatively restricted zones (Figure 1). However, limestone coasts do exist, especially in the east of Ireland, north of Dublin; in the west of Ireland on the eastern and southern shores of Galway Bay and on the Atlantic coast of County Clare, and in isolated parts of the south coast. Littoral (inter-tidal zone) karren are developed to some extent in many of these areas of coastal limestone outcrop.

*Littoral karren* have been investigated by Burke (1994) on the low-lying limestone coast of north County Dublin. The zone occupied by karren forms is wide as tidal range is some 3 m. In this area karren development is correlated with the purity of the limestone. However, the features are considerably smoothed and modified by sand abrasion and this, together with the lesser biodiversity, mean that the littoral karren are less well developed than those found on the Atlantic coast of Ireland described below.

Some 2% of the land area of Ireland is occupied by lakes, many of which are located on the limestone floored central plain of Ireland (Figure 1). The origin of the lakes is presumed to be due in part to glacial erosion and deposition and in part to solution. The waters of most of these lakes are saturated with respect to calcium carbonate

yet some of them, particularly those in the west of Ireland, exhibit karren forms in the zone of seasonal fluctuation of lake water levels. Two lakes, Muckross and Leane, in County Kerry in the extreme southwest of Ireland, are located on steeply dipping limestone bedrock but are fed by streams with acidic waters derived from adjacent non-carbonate rocks. Inorganic dissolution has generated *notches*, small caves, *dissolution platforms* and limited areas of *scallops*, but not the zone of intense karren development found on lakes with saturated water (Priesnitz, 1985).

The best developed and best documented examples of littoral and *lacustrine karren*, in Counties Clare and Mayo respectively, are described in this chapter.

## Coastal karren, Burren, County Clare

The Burren karst plateau of County Clare is bounded to the north by Galway Bay and to the west by the open Atlantic Ocean. Over a 20 km long stretch of shoreline, mainly on the western-facing Atlantic coast, pure, highly karstifiable Viséan limestones comprise the bedrock. The tidal range along this high-energy coastline is in excess of 4 m. The extent of the inter-tidal zone varies. The limestones dip to the south at 2–5° and on dip-slope coastal exposures the littoral zone may



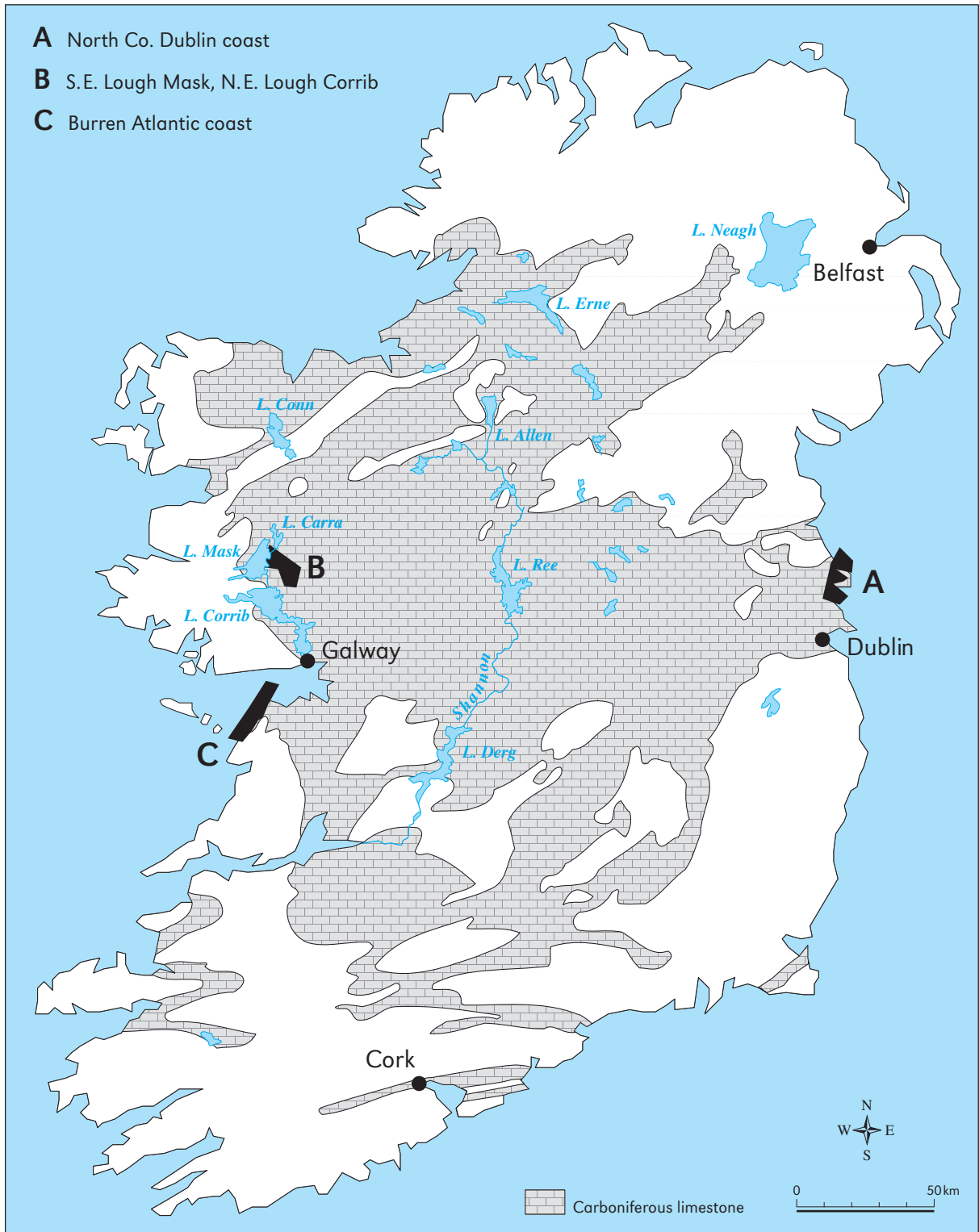


Figure 1: The distribution of Carboniferous limestone in Ireland and the locations of the main coastal and lacustrine karren zones.

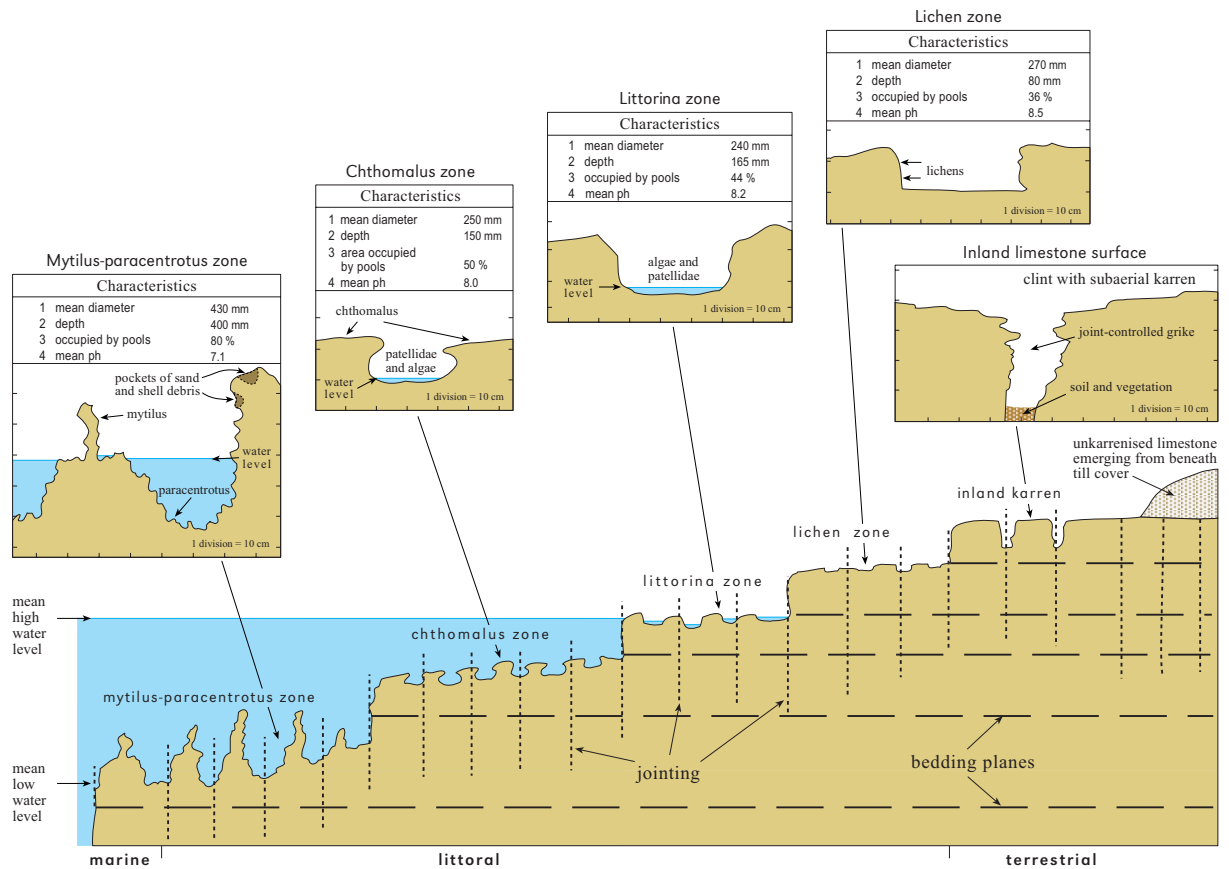


Figure 2: Idealized transect of karren forms in the inter-tidal zone on the County Clare coast (adapted from Lundberg, 1977c).

be more than 100 m in extent, whereas on up-dip exposures the intertidal zone may be compressed into less than 10 m horizontally.

The karren zones were first described by Lundberg (1977c), with subsequent studies by Trudgill (1987), Trudgill and Crabtree (1987) and Trudgill et al. (1987) focussing upon the role of marine organisms in forming the karren features. The typical sequence of karren forms in the littoral zone is shown in Figure 2 (Drew 2001, adapted from Lundberg, 1977c). At the type site shown in Figure 2, at Poulsallagh Bay, morainic deposits blanket the limestone bedrock (Figure 3). The moraine has been eroded by wave action to a level above high tide and the limestone bedrock is being progressively exposed. The calcareous nature of the till has prevented solutional ero-

sion of the bedrock beneath and thus the newly exposed limestone surface is smooth and wholly lacking in dissolution features. At a distance of less than a metre from the till margin subaerial solution has already enlarged the joints and *solution hollows* are beginning to form. The wave-splash zone is characterized by isolated, shallow *pans* with lichens being the dominant life form. Within the intertidal zone *Littorina*, *Chthamalus* and *Mytilus-Paracentrotus* dominated zones at successively lower levels have been distinguished (Figures 4, 5, 6). The mean depth of the hollows increases from 80 mm to 400 mm and the percentage of the area of limestone occupied by hollows increases from 36% to 80% from the uppermost to the lowest zone.

Lateral erosion is eroding away the remnants of



**Figure 3:** A general view of the limestone foreshore at Poulsallagh, County Clare. In the background is a morainic deposit which is gradually being eroded, exposing intact limestone which is then occupied by karren under sub-aerial conditions. In the centre of the picture is the sloping limestone surface in the inter-tidal zone with the suite of bio-erosion karren, and to the right is an isolated limestone block with *Chthamalus* zone karren on its top surface.



**Figure 4:** The upper *Mytilus* zone in which remnants of the original rock surface are still preserved.

**Figure 5:** The lower *Chthamalus-Mytilus* zone in which almost all of the original limestone surface has been destroyed, leaving only residual stumps of rock.



the original limestone surface in each zone and that process, combined with the vertical erosion, means that the zones are progressively migrating landwards. Enlarged joints which are a prominent feature of the uppermost zones are not apparent in any of the lower zones where *bio-erosion* and the development of *kamenitzas* are all-important. Examples of the littoral karren zones are given in Figures 3, 4, 5 and 6. The karren suite shown in Figure 2 is that which occurs on sections of coast where the limestone dip slope is stepped with successively lower bedding planes hosting the different karren assemblages. On uniformly sloping coastal sections the zones grade into one another whilst on cliffed sections of coast some or most of the zones may be absent. Lundberg (1977c) regarded solution as being of great importance in developing the pits in the littoral zone. Trudgill (1987) regarded *boring* by marine organisms as being of greatest significance, especially in the lower zones where he records boring rates of 1.2-10 mm per annum. Simms (1990), discussing the existence of *photokarren* in caves on the foreshore and its relation to the *karren zonations*, also favours boring as the primary mechanism.

### Lacustrine karren, Lough Mask, County Mayo

Loughs Corrib (190 km<sup>2</sup> in area), Mask (90 km<sup>2</sup> in area), and Carra (20 km<sup>2</sup> in area) are located in the east of Counties Galway and Mayo (Figure 1). Loughs Corrib and Mask occur on the boundary between limestone to the east and non-calcareous rocks to the west whilst Lough Carra is located wholly on limestone. Lough Mask, up to 60 m deep in its western part, has a catchment area of approximately 1,000 km<sup>2</sup>, 60% of which is limestone floored. Over the greater part of the limestone shoreline of these lakes the bedrock is blanketed beneath till, peat or marl. However, such deposits are absent along part of the shoreline of Lough Carra, the northeastern shore of Lough Corrib and the southeastern shore of Lough Mask and gently dipping Carboniferous limestone forms the lake margins. Loughs Mask and Corrib are linked by subterranean channels; numerous sink in the southeastern part of Lough Mask draining to a series of very large springs in the village of Cong on the shores of Lough Corrib (Drew and Daly, 1993). It is in this 8-10 km long reach of the shoreline of Lough Mask, including the swal-



Figure 6: A large pool near low tide level, occupied by and eroded by *Paracentrotus lividus* which is enlarging laterally to consume the higher *Chthamalus-Mytilus* dominated zone of pools and spires.

low hole zone, that the lacustrine karren are best developed. The strata dip at 2-5° to the southeast and comprise mainly pure bioclastic limestones with some dolomites. The development of karren does not appear to be noticeably influenced by lithology. In places on the dip slopes the width of the karren-bearing limestones exceeds 50 m but there are also numerous scarps 1-5 m in height.

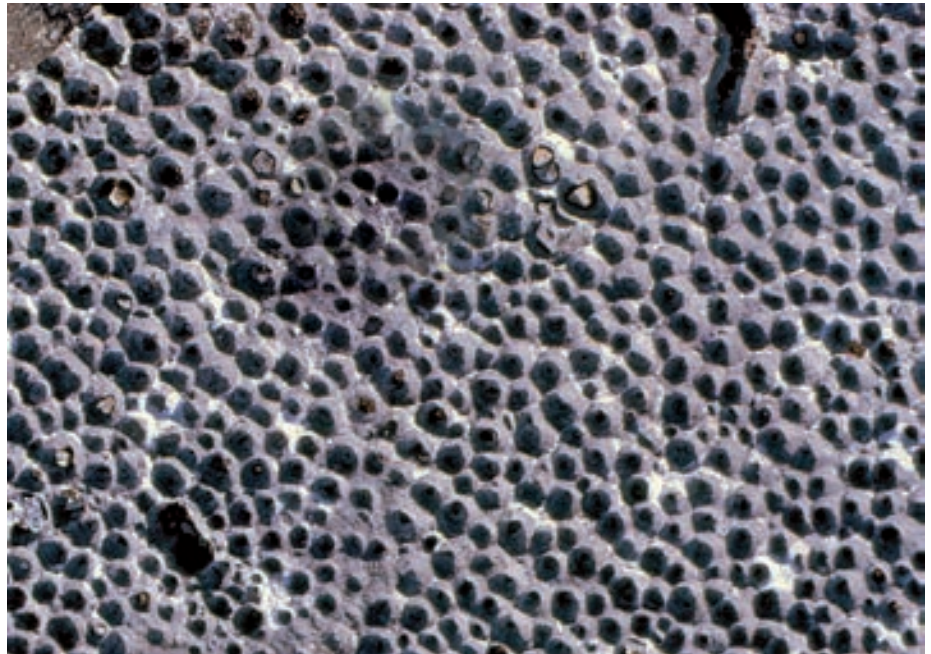
The lake-shore karren have developed within

the zone of seasonal fluctuation of lake water level. This fluctuation, originally averaging some 2.9 m, is associated with the capacity of the underground drainage system from Lough Mask in comparison to the inflow to the lake from surface rivers. A complicating factor is that in 1855 a canal (the Cong canal) was completed linking Loughs Mask and Corrib via a surface channel, which had the effect of lowering the height of maximum water

**Figure 7:** The lakeshore of southeastern Lough Mask at low summer water level. In the foreground the limestone is covered by sediment derived from till and karren have not developed. The centre-background shows the gently inclined bedrock surfaces covered with small solution pits. The isolated boulders have pits on their upper surfaces and rohrenkarren on the underhangs.



**Figure 8:** Small solution pits on 350 x 500 mm area of limestone bedrock in the zone of seasonal inundation on the shore of Lough Mask.



levels in Lough Mask in winter and allowing summer lake levels to fall lower than hitherto. At a certain lake water level the canal becomes dry. Thus since 1855 the zone of active karren development associated with seasonal lake level fluctuations has been shifted down by ca. 1 m, allowing previously permanently inundated areas of limestone to experience water level oscillations but placing the highest levels of the zone of former karren

growth beyond the reach of lake water throughout the year. The karren phenomena were first noted in passing by Kinahan and Nolan (1870) and subsequently by Ford and Williams (1989). However, the only scientific studies of the phenomena are those made by Quigley (1984) and Simms (2002).

Two distinct karren forms occur in the zone of seasonal inundation (Figure 7). On horizontal or gently sloping surfaces, whether of bedrock or on

boulders, every bare limestone surface is pitted with hollows, 20–120 mm in diameter and 10–120 mm in depth (*lacustrine pittings*). On overhanging surfaces, whether on the underside of isolated boulders or on the upper surfaces of enlarged bedding planes on the small scarps, are found tubular features, tapering upwards to a rounded apex. These features, termed *rohrenkarren* (*tube karren*) by Simms (2002), occur at the same density as the solution hollows. The occurrence of the karren forms is summarized in Table 1.

According to Quigley (1984), the smaller *pittings* (Figure 8) range from conical to cylindrical hemispherical in shape. When they are closely spaced they coalesce leaving a surface of sharp residual pinnacles. As the pits enlarge so they become more variable in size within a particular area. There is a good correlation between altitude (a surrogate for inundation duration) and morphology (depth and diameter) except for the pits at the lowest levels (longest periods of inundation) which may not have had time to attain their final form. The pits are essentially sub-aerial features – the pittings at higher levels contain algae (*Cyanophyta* and *Chlorophyta* predominantly) whose presence must enhance erosion in the hollows.

Rohrenkarren are described by Simms (2002) as commonly having diameters of less than 30 mm, but with lengths of hundreds of mm (Figures 9, 10). They occur at densities comparable to those of the solution pits. The two may coalesce where rohrenkarren penetrate a limestone bed to a surface above occupied by pits. Simms regards the development of rohrenkarren as being purely physico-

chemical, taking place when water vapour in the air trapped by rising lake levels, condenses at times when the rock is colder than the water. He argues that the condensate trickles downwards and corrodes the limestone. Initiation of these features requires calm and saturated lake water.

In the lake-shore zones where the karren forms are best developed, individual limestone beds may have coalesced pits on their upper surface and rohrenkarren coalesced to develop downward pointing spires, on their lower surfaces with some rohrenkarren having penetrated the full thickness of the bed to form tubes linking the upper and lower surfaces of the bed.

The effects of the lowering of water levels in Lough Mask due to the construction of the canal (Figure 11) are evident in the pittings at the highest levels – those levels that are not now inundated in winter. The pits have developed into pans (Figure 12) with lateral erosion outstripping vertical erosion. They are mutating into wholly subaerial forms of kamenitza. It is probable that in post-glacial times the drainage channels that link Lough Mask with Lough Corrib have become progressively enlarged and that this increased transmissivity has further lowered the inundation zone of Lough Mask. However, no research has been undertaken to determine if ancient solution pits can be detected at elevations above the pre-canal inundation level. The location of rohrenkarren means that their development will effectively have ceased within zones that are no longer seasonally inundated. All of these karren features are almost certainly Holocene in age – some 15 ka ± 1 in this area.

**Table 1:** Zonation of lacustrine karren forms on the shores of Lough Mask in relation to lake water level before and since the lowering of lake water levels in 1855.

Inundation regime	Karren forms	Lake water levels
Never submerged	Wholly subaerial runoff, pit and pan karren types.	
Seasonal under original conditions	Former lacustrine solution pits now being modified subaerially into pans, vegetated pits and runoff karren. Decaying rohrenkarren.	22.65 m a.s.l. (original max.)
	Well developed small solution pits on the upper surfaces of all exposed bedding planes and boulders. Rohrenkarren well developed on lower surfaces of undercut bedding planes.	21.21 m a.s.l. (present day max.)
Seasonal under present day conditions	Incipient solution pits and possibly incipient rohrenkarren on bare rock surfaces.	19.72 m a.s.l. (original min.)
		18.41 m a.s.l. (present day min.)
Always submerged	Few or no karren forms. Slight solution enlargement of some joints on bare rock surfaces.	

**Figure 9:** Rohrenkarren on the lower surface of an enlarged bedding-plane. Many of the tubes have coalesced to form downward projecting spires. Southeastern shore of Lough Mask. Width of view is 70 cm.



**Figure 10:** Rohrenkarren developed on the underside of a boulder which has subsequently been tilted from its original position. South-eastern shore of Lough Mask.



## Discussion

As is apparent from the paper by Lundberg (see chapter 20), *coastal karren* are well documented from a wide variety of limestone coastal environments and different climatic zones. The littoral karren on the Atlantic coast of County Clare,

described above, are consistent in their morphology and in the existence of zonation with those described from elsewhere. It remains uncertain as to the relative importance that should be attached to corrosion as against dissolution in explaining their origin. Although the present evidence emphasizes the primacy of bioerosion, the con-



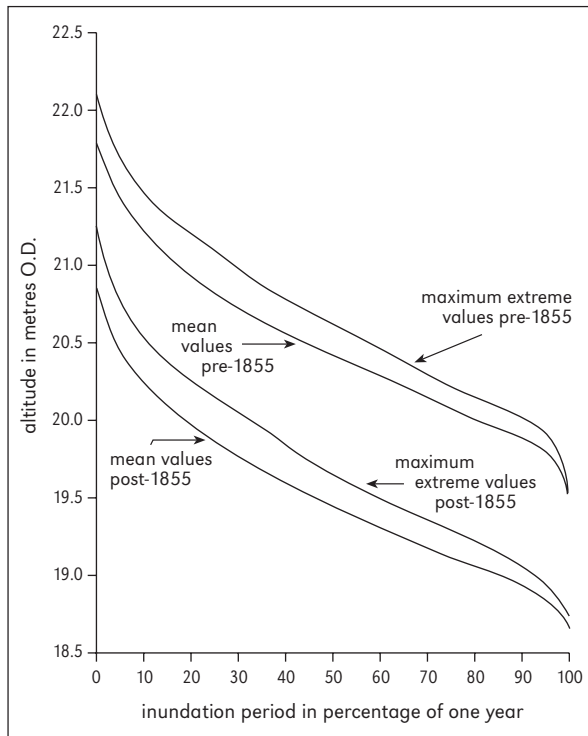


Figure 11: Seasonal inundation durations for the lake-shore of southeast Lough Mask.

trast between the limestone foreshore in County Clare with its high degree of karren development and nearby shorelines located on non-calcareous rocks with few kamenitzas is striking.

Far less common, certainly as far as descriptions in the literature are concerned, are the lake-shore karren (the features on the shores of Lake Huron in Canada being one of the few other examples; Vajoczki and Ford, 2000). The initiation of both the solution pits and the rohrenkarren is uncertain but their subsequent development is complementary - both require alternating sub-aerial and submerged conditions, though for rohrenkarren the period of emergence can be brief as they do not develop subaerially whilst for the pits the period of submergence can be brief as they do not develop subaqueously.



Figure 12: Solution pits on the shore of Lough Mask in the zone that has not been subject to seasonal inundation since lake levels were lowered by drainage in 1855. The pits are now enlarging laterally and forming pans.

Of the karren forms considered: one is wholly physico-chemical in origin (rohrenkarren), one is largely bioerosional - direct or indirect - (coastal karren), and one is the result of both biologically and physically driven solution (lacustrine pittings). Both the coastal and the lacustrine karren seem to require oscillations in water level to develop, though in the case of the coastal site the inundation cycle is on a diurnal scale whilst for the lacustrine site the cycle is annual.

# SOLUTION PIPES AND PINNACLES IN SYNGENETIC KARST

Ken G. GRIMES

*Solution pipes* (or dissolution pipes), as described here, are the small, vertical, smoothly cylindrical pipes found in soft (poorly cemented) porous *calcarenites*, and usually associated with a modern or ancient soil or a calcrete band. They are typically about 0.5 m wide and 2–5 m deep, though there is significant variation. Pinnacles are associated features, but less common. A recent detailed review of solution pipes was given by Lundberg and Taggart (1995) – who advocated “dissolution pipe” as being a more correct term.

Solution pipes are also known as *solution chimneys*, *shafts*, *pits*, *geological organs*, and Lundberg and Taggart (1995) list other names. The confusion of terminology is increased by many of those terms also being used for similar features in the epikarst of hard telogenetic limestones, where the lack of matrix porosity and greater structural control require a different genesis.

## Syngenetic and eogenetic karst

This chapter deals with solution pipes formed in soft, porous limestones. These limestones form a special type of karst that has been referred to as syngenetic or eogenetic karst (Jennings, 1968; Mylroie et al., 2001; Grimes, 2002, 2006; White et al., 2007). *Syngenetic karst* occurs in dune limestone (*aeolianite*) and other *calcarenites* (e.g.

beach or shallow marine sands), in finer-grained material such as chalk and in coarser coquina or reef rubble. It is distinguished from the classic (telogenetic) karsts in that the host limestone has never been deeply buried and indurated by mesogenetic diagenesis (Choquette and Pray, 1970). Apart from being only weakly cemented, a critical feature of these limestones is that most of them still have a significant primary matrix porosity – up to 30%. Within these soft sediments many of the karst features, including the pipes, have formed at the same time as the sand was being cemented into a rock and the term syngenetic karst has been applied to that process (Jennings, 1968; Grimes, 2002, 2006). White et al. (2007) discuss the usage of the terms syngenetic and eogenetic karst, which overlap in most situations, and suggest that “syngenetic” be used as the general term, and that “*eogenetic karst*” be restricted to the subset of syngenetic karst which postdates the depositional cycle in which the sediments were formed.

## The development of syngenetic karst

In calcareous dunes, percolating rain water gradually converts the unconsolidated sand to limestone by dissolution and redeposition of calcium carbonate. Initial solution at the surface forms a *terra rossa* or similar soil depleted in carbonate

but enriched in the insoluble grains (e.g. quartz). At the base of the soil, precipitation of carbonate forms a cemented and locally brecciated *calcrete* layer or *hard-pan*, also known as a *cap-rock*. Within and below this the downward percolating aggressive water becomes focussed to dissolve characteristic vertical solution pipes, and simultaneously the carbonate dissolved at the surface and within the pipes cements the surrounding sand. Calcrete hard-pans and solution pipes both appear quite early in the syngenetic sequence, long before the sand is sufficiently cemented to support a cave roof (Bastian, 1964). However, the pipes continue to develop and deepen as cementation of the host sand continues. Early cementation tends to be localized about roots to form distinctive rhizomorphs or rhizocretions.

Surface karren forms are rare in syngenetic karst, mainly because there is little hard rock available for their formation. Where soil stripping exposes the calcrete hard-pan, *rainpits* and small *grikes* may form, and sharply pitted *phytokarst* occurs in coastal exposures. *Subsoil karren* are also uncommon, apart from the pipes and pinnacles discussed in this chapter. The top of the hard-pan may show irregular hollows, but it is difficult to be sure whether these are solutional, or merely irregularities in the top of the cemented zone. Rhizomorphs are common.

## Occurrence of solution pipes

Solution pipes have been reported from porous limestones in many parts of the world, in particular from the *dune limestones*, also known as dune calcarenite or aeolianite (Gardner, 1983; McKee and Ward, 1983). Examples include: the western and southern coasts of Australia (Fairbridge, 1950; Boutakoff, 1963; Jennings, 1968; Grimes, 1994, 2004, 2006; White, 2000), southern Africa (Coetzee, 1975), the Mediterranean (Day, 1928; Marsico et al., 2003), the Caribbean (Lundberg and Taggart, 1995; Mylroie and Carew, 1995) and Bermuda (Herwitz, 1993). Similar pipes also occur

in the *chalk* of Europe, which is finer grained, but still relatively soft and porous (Burnaby, 1950; Ford, 1984; Rodet, 1992).

Climate appears to be less important than the nature of the host rock, although the global distribution of dune calcarenites seems to be partly controlled by climate and oceanography (Gardner, 1983; McKee and Ward, 1983). Many aeolianites occur between 20–40 degrees of latitude, either in coastal “mediterranean” climates that have cool wet winters and hot dry summers, or in hotter or more arid settings. However, there are exceptions in cooler and wetter climates.

## The nature of solution pipes

### Form

Typically, *solution pipes* form smooth vertical cylinders which may narrow towards a rounded base (“cigar shaped” is a common description) or terminate abruptly in a hemisphere (Figures 1, 2). Conical pipes are less common. The pipes have a range of widths, averaging about 0.5 m, but can be smaller than 0.2 m or over 1 m, although the wider ones tend to be less regular, and some may be due to coalescence of several smaller pipes. Depths are typically 2–5 m, but they can be up to 20 m deep and some may connect with underlying caves (Figure 3). They can occur as isolated individuals, widely spaced sets (e.g. 5–10 m spacing) or in dense fields with spacings that can be closer than one metre (Figure 1). At Cape Bridgewater, Victoria, Webster (1996) measured densities of 0.7 to 2.8 pipes per m<sup>2</sup> (average 1.8) in ten 3 x 3 m quadrats; and pipe diameters ranging from 0.27 m to 0.54 m (average 0.40 m). In one 5 x 5 m quadrat at the same site Grimes (2004) measured a density of 2.1 pipes per m<sup>2</sup>, a mean inside diameter of 0.27 +/- 0.09 m, and mean distance to nearest neighbour of 0.46 +/- 0.013 m. Herwitz (1993) reported mean diameters between 0.2 and 0.37 m from sites at Bermuda, however his densities were much less at between 0.33 and 0.60 per m<sup>2</sup>, though

**Figure 1:** Stereopair of a cluster of pipes at “The Petrified Forest”, Cape Bridgewater, western Victoria. Note the cemented rims. Width of view is 6 m.

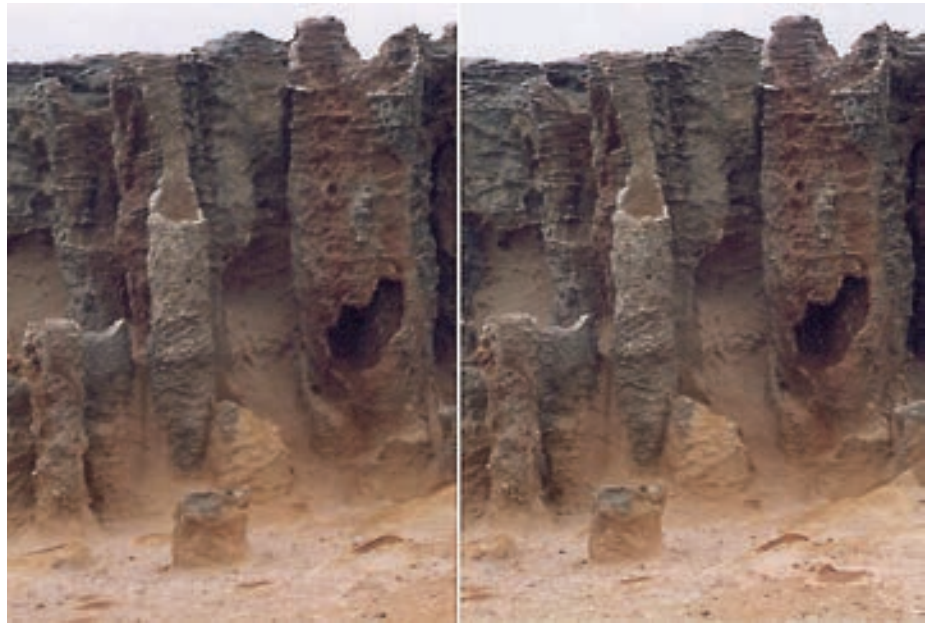


**Figure 2:** Stereopair of the cigar-shaped base, with thin cemented rim, of a pipe near “The Petrified Forest”, Victoria. Width of view is 60 cm.



he mentioned densities in localised areas exceeding 1.2 per m<sup>2</sup>.

Solution pipes are commonly associated with a present or past soil horizon; either descending from it (Figure 4), or cutting through a hard band of pedogenic calcrete that could be a subsoil hardpan. In stacked dune sequences one commonly sees several levels of *palaeosoils*, each with a set of associated soil-filled solution pipes. Where closely

spaced sequences occur, solution pipes may terminate on reaching the underlying palaeosoil, or may drill through it and continue through the underlying dune unit.

#### Related features

In the Bahamas the term *pit cave* has been applied



Figure 3: A deep, open solution pipe that forms a cave entrance. Ladder rungs are spaced 30 cm; photo by R. K. Frank.

both to solution pipes, and to larger pits, up to 7 m in diameter and 10 m depth, that have less-regular forms (Pace et al., 1993; Mylroie and Carew, 1995; González et al., 1997). Some of these have horizontal or inclined extensions at depth. In some cases these larger pits appear to be due to coalescence of smaller solution pipes, but many are too irregular to have that origin.

Pinnacles, such as those at Nambung in western Australia, may be an extreme case resulting from the coalescence of closely spaced solution pipes in a calcrete band, or they may be due to focussed cementation. They are discussed later in this chapter.

### Rims and fill material

Solution pipes commonly, but not always, have a *calcareous cemented rim* around them that is a few centimetres thick. Thin concentric micritic calcrete laminae can also line the pipes. Lundberg and Taggart (1995) describe in detail the *rims, fills* and host rocks at two sites in Puerto Rico: the rims there were of micrite and microspar, and there was also replacement of bioclasts



Figure 4: A red palaeosol and soil-filled pipes beneath a younger sand dune exposed in a cliff at Canunda National Park, south Australia. These pipes lack a cemented rim. Width of view is 10 m.

by those cements. Porosities were much less than in the host rock, typically 0–5%. Cemented rims and fills can be etched out by erosion of the surrounding softer sands (Figure 1).

Some pipes appear to be filled with a modified version of the original host sediment, and relict structures of the original bedding may be preserved (the “ghost tubes” of Pace et al., 1993). Most, however, are filled with a downward extension of the overlying red or pale brown soil (typically a *terra rossa* that has been enriched in insoluble components of the host sediment). Some of the associated soils are partly allogenic rather than entirely residual (e.g. Herwitz, 1993). Pipes can be emptied by loss of their fill downward into an underlying (younger) cave, where they may form soil cones, or by erosional undermining, or by excavation by sea water or a stream. These empty pipes may later be refilled by younger allogenic material, for example by a younger dune, or during a subsequent marine transgression. Secondary fills are common in *palaeokarst* exposures, where complex multi-generation fills can occur (e.g. see Figure 3 of Mylroie and Carew, 1995). Fills can be massive, or crudely bedded, or have concentric cemented layers or calcrete laminae (Figure 5). Brecciated material and calcareous veins occur in some pipes. Many pipe fills have traces of thin calcareous root structures (rhizomorphs) embedded in them; as does the surrounding host sand.

### Rhizomorphs

*Rhizomorphs* (or *rhizocretions*) are hard calcified root structures that are commonly associated with the pipes. Rhizomorphs are common in calcareous dunes and have an obvious branching root structure. They form from carbonate that has been precipitated around the root, and are thus thicker than the original root – which may be identifiable as a thin hollow core if that has not been infilled by younger cement.



Figure 5: Concentric laminae in the partly cemented fill of a solution pipe near “The Petrified Forest”, Victoria. Width of view is 40 cm.

### Palaeokarst

Solution pipes can be preserved in *palaeokarsts* and are an important clue to the existence of sub-aerial disconformities and hardgrounds in the geological record (e.g. Ford, 1984; Wright, 1988; Sandler, 1996). The fill material in *palaeokarst* pipes may be an important record of deposition events that have been destroyed elsewhere during the subsequent transgression (e.g. Walkden and Davies, 1983).

### Mode of formation

An early suggestion, by Boutakoff (1963) among others, was that the pipes were *petrified forests*; that is, moulds of buried tree trunks. This had some initial support from workers in Bermuda, where the pipes were regarded as moulds of palmetto stumps; however, recent work has discredited this (Herwitz, 1993; Grimes, 2004).

Lundberg and Taggart (1995) note that dissolution by focussed vertical vadose flow of under-saturated rain or soil water through the porous sedi-

ment can explain all the features of the pipes: the uniform, vertical cylindrical form, the dense clustering in places, and the cemented rims (where dissolved material is re-precipitated at the edges of the pipe). The associated rhizomorphs are formed around rootlets that have penetrated the sands from above, possibly following the soil-filled pipes by preference and radiating out from them. As the pipes are developing downward from the surface or from a soil cover the overlying material can progressively fill them as they deepen.

But why is the downward water flow focussed into narrow routes rather than travelling evenly throughout the uniformly porous sand? In hard, non-porous, limestone pipes usually form where flow is concentrated along the intersections of joints or steeply-dipping bedding planes. But in soft sandy limestone there are no vertical joints, and the inter-granular porosity is uniform apart from occasional horizontal hard-bands – the dune cross-bedding seems to have little effect on flow directions. Three methods of concentrating the flow have been suggested by Lundberg and Taggart (1995), drawing on earlier authors: surface hollows, roots and stem-flow; to those Grimes (2004) added a fourth: areas of higher porosity within the developing soil hard-pan (Figure 6).

In passing, it is worth noting that similar vertical pipes occur in the giant podsoils that develop on the porous quartz sand dunes of the Queensland coast (e.g. Thompson and Bowman, 1984). These have a deep, leached, white A2 horizon over a dark, humic-rich, less permeable B horizon. Pipes of the leached A2 material from a few centimetres to nearly half a metre wide penetrate several metres down into the enriched B horizon. Spontaneous focussing of downward water flow through the porous sand seems to be involved in that setting also. Solution pipes also occur in laterite karsts, as discussed in the section on pinnacles.

### Stem-flow

*Stem-flow* is the process whereby the leaves of a

tree intersect rain, and direct it down the branches so that it is concentrated at the base of the trunk. The concentrated inflow would cause localized solution and pipe development (Figure 6a). Herwitz (1993) measured stem-flow under a variety of trees in Bermuda and showed that it could generate significant concentrations of water and noted that multiple generations of trees could produce the dense spacing of pipes which is observed in places.

### Roots

The influence of tree roots was suggested by Jennings (1968) and Brink and Partridge (1980). Roots generate organic acids and raised CO<sub>2</sub> levels that enhance solution in their vicinity (Figure 6b). A vertical tap-root could therefore form an initial thin pipe which would enhance water flow and enlarge with time. This is a self-perpetuating process as a pipe, with soil fill, would be a preferred place for continuing root growth and organic activity.

### Surface hollows

Surface hollows were suggested by Coetzee (1975) as a way of concentrating inflow (Figure 6c). If hollows exist (on a partly indurated surface, or on the top of the soil hard-pan) then water will accumulate in these and the base of the hollows will be lowered by solution at a faster rate than the surrounding higher areas – the process becomes self-perpetuating.

### Variations in hard-pan porosity

Uneven cementation of the developing hard-pan is a possible fourth process (Grimes, 2004). Rain dissolves carbonate grains as it penetrates the soil, and some of this is re-precipitated lower down to form a hard-pan or calcrete band near the base of the soil. In the initial stages this cemented band

**Figure 6:** Alternative ways in which the downward flow of water can become focussed to generate solution pipes (see text). Black arrows are aggressive water flow and red arrows are saturated water. Note, the alternatives are not mutually exclusive, they could all contribute in different settings.

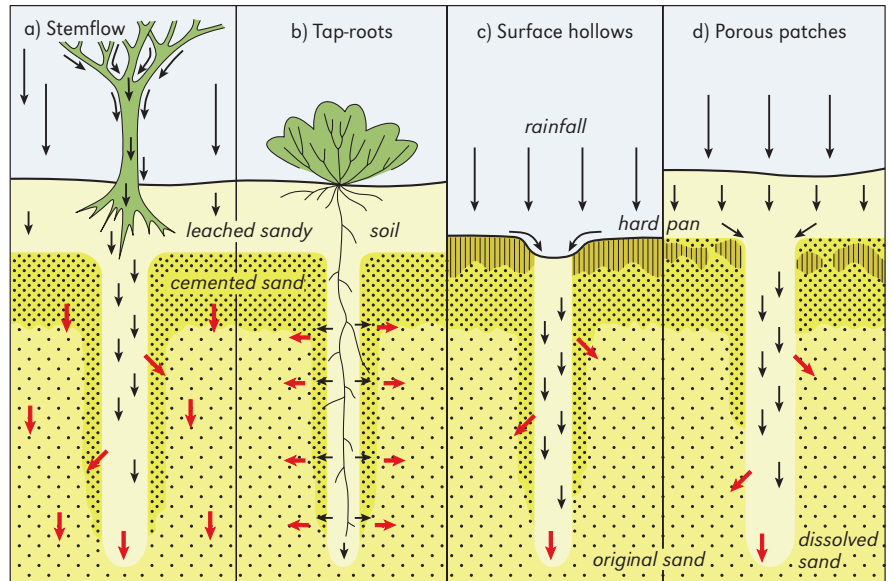
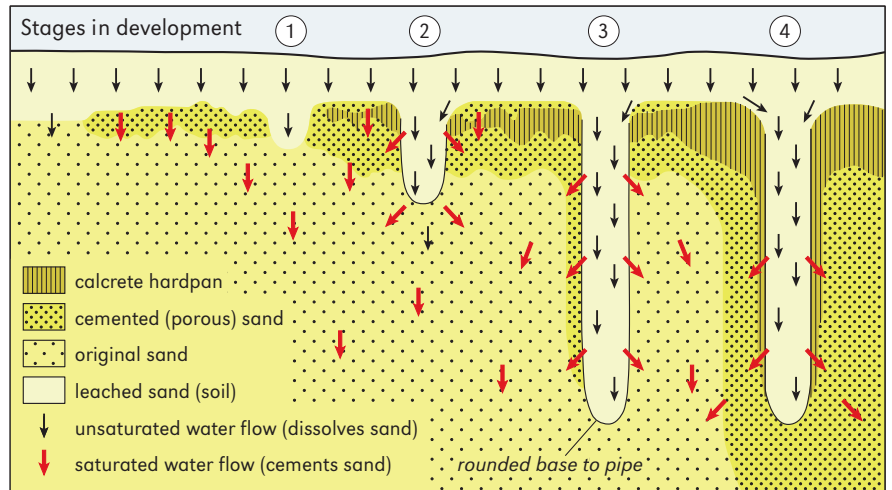


**Figure 7:** Stages in which a solution pipe deepens and develops a cemented rim. A possible further stage in which the fill is cemented is not shown.



would not develop evenly (Figure 6d). The better-cemented areas would tend to deflect flow laterally to places which retained more of their original porosity and concentrated inflow would occur there, inhibiting further cementation, and allowing solution pipes to form below.

### Ongoing evolution of the pipe

In all four cases, once the inflow is concentrated at a point, solution will progressively deepen a vertical pipe beneath the focal point. Lateral movement

of saturated water out of the pipe would form the cemented rim and also contribute to the general cementation of the sand body (Figure 7). Lundberg and Taggart (1995) noted that the linings have many features of pedogenic calcretes. Where pipes become emptied, case-hardening of the exposed pipe walls would also contribute to rim cementation. Some fills show “ghost structures” which indicate that the host sand has had its porosity enhanced, without being actually removed. Most fills are associated soils that have subsided into the pipe as it formed, or later allogenic material that has entered an empty pipe. These fills





**Figure 8:** A composite conical pinnacle at Nambung, western Australia, that shows the dune cross-bedding and sections of several small filled solution pipes that have been intersected by the pinnacle. Height is about 2 m.

can also be cemented and may show structures of pedogenic calcretes.

### Special cases

Some special cases include the larger of the pit caves of the Bahamas and the pinnacles of the Nambung area in western Australia. The larger pit caves are distinguished by their less regular form. Instead of smooth cylinders they have irregular outlines and may be inclined or bell out at depth. Pace et al. (1993) attributed the Bahamas pit caves to the “concentration of meteoric water by surface and subcutaneous channelization”; the same process described above. However, the more complex forms of these larger pits do not agree with the concept of simple focussed flow through a uniformly porous sand. Possibly the larger pit caves are late syngenetic features where the more strongly cemented limestone exerts structural controls on the

shape of the pit. For example, the inclined pits may be following indurated dune cross-bedding, and the irregular vertical profiles may reflect various degrees of cementation in the host rock. Some pit caves seem to show joint control.

### Pinnacles

The *pinnacles* at Nambung and other parts of the coastal dune limestone in western Australia may be an extreme case resulting from the coalescence of closely spaced solution pipes in a calcrete band (Lowry, 1973; McNamara, 1995), or they may be due to focussed cementation.

These are generally discrete pinnacles with a conical form (Figure 8), or are cylindrical with a round top (Figure 9). A few are hollow. They are up to 3 m high and 0.5 to 3 m wide. The broader pinnacles are composite structures with multiple peaks (Figure 8). They are the dissected remnants



Figure 9: Smooth cylindrical pinnacles at Nambung developed in the hard calcrete band. Height of the pinnacles is about 2 m.

of a cemented band. The upper part of this band is a hard pedogenic calcrete in which the primary depositional structures have been obliterated, but it grades down into a cemented dune sand where the dune bedding is still visible. At the base cemented rhizomorphs extend downward into the soft parent sand. Those pinnacles developed in the calcrete have smooth surfaces (Figure 9), but those developed below have rough surfaces resulting from the fretting of the dune bedding and rhizomorphs (Figure 8). Where both types occur

together the calcrete may form a phallic bulb at the top of the pinnacle. Sections of an earlier generation of small solution pipes (0.1 to 0.4 m wide) with a hard concentric fill are exposed in both the calcrete and the bedded material (Figure 8). The tops of the pinnacles show a summit conformity which would be the sharp upper surface of the original calcrete band. Where exposed, their bases may end abruptly or, more usually, grade downward into less-cemented material characterised by abundant rhizomorphs (Figure 10).



Figure 10: A fallen pinnacle shows a smooth, strongly cemented, upper part and a rougher area below that is less cemented, and mainly composed of rhizomorphs. Width of view is 4 m.

## Genesis

Lowry (1973) and McNamara (1995) suggested that the pinnacles at Nambung may be residual features resulting from coalescence of densely spaced solution pipes that dissected a cemented calcrete band. The genesis is complicated by the presence of an earlier generation of solution pipes, with cemented concentric-banded fill, that is exposed in the sides of the later pinnacles (Figure 8). Lowry (1973) suggested the following stages in development of the Nambung pinnacles:

- formation of the dunes as loose calcareous sand;
- development of a hard cap-rock (hard-pan) comprising cemented calcarenite, recrystallised micritic limestone and banded secondary limestone (calcrete). Solution pipes develop and become filled with concentric layers of calcrete;
- continued leaching sculpts the cemented limestone into pinnacles up to 4–5 m high, which cut across the earlier structures of dune bedding, rhizomorphs, cemented solution pipes, and calcrete. The pinnacles are covered by 4–5 m of loose yellow quartz sand;
- erosion of the loose sand has exposed the pinnacles.

McNamara (1995) extended Lowry's model to suggest that some of the more cylindrical pinnacles might have formed by cementation around tap roots in zones up to 1 m wide. He also noted that some of the small pinnacles could be the cemented fill of prior solution pipes.

An alternative origin for the pinnacles could be as a result of focussed cementation – the focussing would be in a similar way to that described for solution pipes, but in this case instead of the down-flowing water being aggressive, it was saturated and so cemented the sand in vertical cylindrical patterns. The source of the saturated water would be the topsoil of the dune, or possibly younger dune sands which buried the initial dune. The latter situation could explain the earlier generation of solution pipes exposed within the pinnacles at Nambung. Alternatively, the change from unsaturated water that produced the earlier generation of

pipes, to saturated water flow might reflect a climate change.

Supporting evidence of this process is given by some calcrete hard-pans which have bulbous cemented pendants descending from them into the softer sand below (Figure 11). These inverted pinnacles could result from focussed cementation.

The focussed cementation process differs from that of the solution pipes in that the pipes are self-perpetuating and can drill down to great depths, whereas the vertical cemented zones would reduce the permeability and deflect the flow so that the cemented area spreads horizontally and eventually cements the whole dune. Perhaps pinnacles are less common than pipes because we only see them where the cementation is incomplete.

Both of the suggested processes, coalescing solution pipes and focussed cementation, could be valid. The cylindrical pinnacles (Figures 9, 10) might have formed by focussed cementation, as would the hollow pinnacles which would be due to cementation around a solution pipe. However, the composite pinnacles (Figure 8) might be the result of coalescing pipes.

## Other pinnacles

In France, Rodet (1992) described subsoil pinnacles in the *chalk*, exposed at the coast and known as *bonshommes de craie*. He attributed these to coalescence of conical solution pipes, his *racines du manteau d'altération*. Waltham (2001) described 2–4 m high pinnacles in chalk in the Egyptian desert and attributed them to the same solution processes that produce stone teeth in hard limestones. The Egyptian chalk pinnacles have been modified by sand-blasting and thermal shattering and are larger than those at Nambung, so it is difficult to compare the two areas.

Pinnacles are also reported as *epikarst* features buried beneath phosphate deposits on several oceanic islands (e.g. Jacobson et al., 1997), but unfortunately there is generally insufficient information on the character of the host limestone (in particu-



Figure 11: Cemented lobes descending from a hard-pan layer at Naracoorte, south Australia, suggest focussed cementation by downward moving water. Width of view is 5.5 m.

lar, its matrix porosity and cement) to allow comparison with the Nambung pinnacles. On Christmas island, in the Indian Ocean (Grimes, 2001), the pinnacles beneath the phosphate are formed on a hard, micritic limestone that has minimal matrix porosity. Those pinnacles are best classed with epikarst features on hard, telogenetic limestones; they are not the same as the syngenetic pinnacles on the calcarenites at Nambung.

There are analogies with *laterite karsts*. In northern Australia deep weathering profiles and associated ferruginous and siliceous cemented duricrusts show both pinnacles and solution pipes (Grimes and Spate, 2008). These are also “syngenetic” in that they formed at the same time as the weathering profile, and they also appear to have formed by focussed cementation (the pinnacles) and solution (the pipes). A significant number of laterite pinnacles are hollow, which suggests cementation adjacent to a pipe.

## Conclusion

Solution pipes are distinctive features of soft porous limestones, in particular dune calcarenites. They are syngenetic karst features, developing in the early stages of cementation of the loose sand,

but continuing to deepen and evolve after the sand has been converted to a soft limestone. They can contain a variety of fill materials, which may give clues to the history of the karst surface and are particularly useful in the interpretation of palaeokarst exposures.

Solution by focussed vertical vadose seepage through the porous sand can account for both isolated pipes, and the dense fields of pipes. Note that the four alternative modes of focussing water flow discussed above are not presented as mutually exclusive hypotheses – all could act, either together or separately, according to the local situation in any area. The associated pinnacles may be an extreme case in which solution pipes cutting through a cemented band have coalesced to leave residual areas of hard limestone; or they may be the result of focussed cementation by down-flowing saturated vadose water.

## Acknowledgements

My colleague, Susan White, has contributed to many discussions on the nature of these and other features of the calcareous dunes. Andy Spate commented on an early draft of this paper. I also thank my wife, Janeen Samuel, for assistance in the field.



# THE KARREN LANDSCAPES IN THE EVAPORITIC ROCKS OF SICILY

Giuliana MADONIA and Ugo SAURO

The karren in the evaporitic rocks of Sicily show wide distribution and variety of shapes relating to the large extension of the rocky outcrops, to the different lithofacies and to the climate. Karren features are largely present in all kinds of evaporites: macrocrystalline selenitic gypsum, detritic gypsum with various grain size, microcrystalline gypsum and in salts such as halite and kainite. Both the origin and the evolution of the karren are controlled by the dynamics of several processes such as solution and recrystallization, granular disintegration, carbonation, and phenomena linked to biological activity.

The karren features have different dimensions, ranging from the nano- and the micro-forms to very large forms, and develop both on the exposed surfaces and under permeable covers. Karren are present on extensive outcrops, such as denuded slopes and hilly summits, and even on the exposed faces of little stones and isolated blocks. Peculiar environments where some specific types of karren have been recognized are the fluvial and coastal geo-ecosystems, some artificial and semi-artificial geo-ecosystems such as quarries, the dumps of mines and dry walls.

Generally several analogies can be drawn between the gypsum karren in Sicily and limestone karren, despite important differences.

## Setting

The most complete and extensive sequence of evaporitic rocks in the Mediterranean basin outcrops in Sicily, covering a total area of more than 1,000 km<sup>2</sup> (Macaluso et al., 2003). This series consists mostly of gypsum rocks of Messinian age showing nearly all the possible lithological varieties such as selenitic (or macro-crystalline), alabastrine, laminated balatino and various detritic lithofacies. The range of crystal sizes is really wide, from tenths of millimetres to several decimetres, and the porosity of the rocky mass also varies widely.

The gypsum rocks present a multiplicity of morphostructural settings and natural environments. From the morphostructural point of view it is possible to distinguish tabular plateaux, homoclinal ridges, fault scarps and faulted blocks, folded ridges, isolated large gypsum blocks floating on clays, and different types of landslides. From the point of view of the natural environments, the slope geo-ecosystems, the fluvial geo-ecosystems, the lacustrine geo-ecosystems, the coastal geo-ecosystems and the hypogean geo-ecosystems can be distinguished. High mountain environments do not exist, because the highest gypsum outcrops do not reach 1,000 m a.s.l.

The climate regime is of mediterranean type with a rainy season (autumn–winter, where 80% of the precipitation amount occurs) and a summer dry season, even lasting in some southern areas up to 7 months. The annual temperature range is moderate, especially in the coastal areas. The highest summer temperatures (more than 42°C) have been recorded in the southern-central areas.

## Gypsum karren in Sicily

In nearly all environments exposed rock surfaces are common, due both to the gradient of many

slopes and to the consequences of human impact on the fragile environments characterized by the typical mediterranean climate. The land use of the steeper slopes, as pasture for sheep and goats, has caused desertification starting in prehistoric times (Figure 1). Soil erosion has been effective and total also on relatively gentle slopes and hilly summits, due to the scarcity of grikes and holes normally acting as traps for soil sediments. On the other hand, inside most of the closed depressions such as dolines there are consistent amounts of fillings, made up of clays and other residual materials present on the gypsum surfaces (Sauro, 1996).

On the exposed gypsum surfaces there is a



Figure 1: Desertified gypsum slope exposing pseudo-bedding planes resulting by tensional relaxation (Palma di Montechiaro, Agrigento).



Figure 2: Pavements with runnels and rills in macro-crystalline gypsum (Palma di Montechiaro, Agrigento). Width of view is 5 m.



Figure 3: Association of different types of karren developed on alabastrine gypsum: rillenkarren, heelprint karren and solution levels (Montallegro, Agrigento).



Figure 4: Mini-craters (rainpits) with slopes interested by the development of microrills.

great density of karren-like features ranging from the nano- and the micro-forms to very large forms. Even if large forms are present only on the extensive outcrops, such as on the denuded slopes and hilly summits, it is possible to identify micro- and small karren, often covering nearly all the surface, on the exposed faces of little stones and isolated blocks. The karren are often organized in complex associations in which different forms, shapes and dimensions overlap over one and other (Figures 2, 3, 4). In particular, on *solution level-like meso-forms*, *rills*, *heelprints* and *small runnels* are present; on the exposed faces of little stones and isolated blocks *rain craters* and *rills* are common; on the minute rain craters and on the rills, *micro-rills*, *micro-meanders* and *micro-ridges* can be observed.

Besides the gypsum karren, assemblages of *salt karren* are present, developed on some salt outcrops related to the evaporitic series, of which only one is natural. The others are linked to salt mines. Here solution forms may even develop during a single rainfall, but these karren are ephemeral forms. The more frequent features are rills, *minute spitz*, *heelprints* and small solution levels (Figures 5, 6).

Almost every type of karren already recognized in limestone is present here (Table 1) but some are much better expressed, others are relatively rarer,

and some present significant differences (Macaluso and Sauro, 1996a; Macaluso et al., 2001).

In particular, most of the spotted, linear and small planar forms are hydrodynamically controlled, like the minute rain craters or rainpits (Figure 4), the *micro-karren* (*microrills*, etc; Figures 4, 7), the solution rills (*rillenkarren*), the *meandering rills*. Some types of heelprint karren and of *scallop-like karren* are very well expressed in the fine grained gypsum lithofacies. Beside these forms, on macro and microcrystalline gypsum and salt, solution levels can be easily observed. These forms are produced by diffuse solution from a homogeneous water sheet flowing slowly on the surface or by water stagnation (Figures 3, 6) (Macaluso and Sauro, 1996a, b); their extent ranges from some decimetres to several metres. The largest of these forms may be considered meso-forms.

Among the relatively rare or uncommon forms both the covered type forms, like the *covered karren* (*rundkarren*) and the linear forms (fracture controlled) like the *grikes*, are worthy of note.

Typical *rundkarren*, which have evolved in a covered environment, are relatively rare. In fact, they do not develop under common soil which acts as a protective cover, but only below permeable covers made up of insoluble clastic material. The best developed hidden forms (*crypto-karren*) have been found on the Ciminna plateau (Paler-



**Figure 5:** Short rills organized in a comb pattern, associated with summit minute craters, developed on salt blocks (dump of Case Ranieri Mine, Caltanissetta). Width of view is 45 cm.

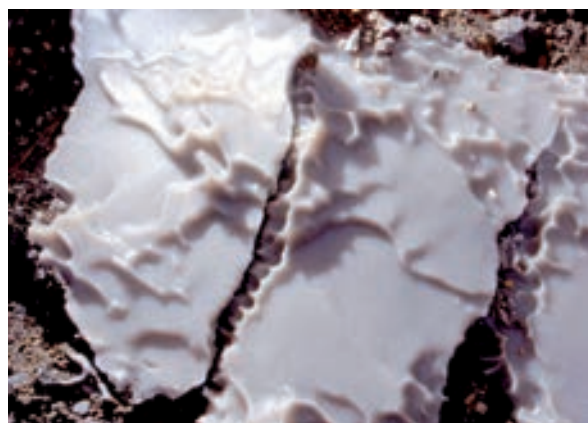


**Figure 6:** Small solution levels delimited by small scarps and crests developed on salt blocks (dump of Case Ranieri Mine, Caltanissetta). Width of view is 80 cm.



**Table 1:** The main types of karren present in the evaporitic rocks of Sicily (after Macaluso and Sauro, 1996a, modified). mf = meso-forms; mc = micro-forms; sf = small forms; b, d, l = width x depth x length; diam. = diameter; d. = depth; div. = divers; al. = alabastrine; bal. = laminated balatino; disint. = disintegration; tensl. = tensional slackening; biocon = biological control; diffsol = differential solution.

Size	Nomenclature	Relief	Dimensions (b,d,l) mm	Lithology	Geometry	Processes	Control	Environment
mc	micro-rills	negative	1, 1, 50-200	al. bal. gypsum	linear	solution	hydrodynamical	bare rock
mc	micro-ridges	positive	0.5-2, 1, 5	al. bal. gypsum	linear	solution	hydrodynamical	bare rock
mc	micro-meanders	negative	1-4, 2, 50-400	al. bal. gypsum, salt	linear	solution	hydrodynamical and decantation	semicovered rock
mc	micro-loops	negative	0.2, 0.2, 2-5	al. bal. gypsum, salt	linear	solution	hydrodynamical and decantation	semicovered rock
mc	micro-pits	negative	3-10, 3-6 (diam., d.)	div. gypsum	planar circular	solution	hydrodynamical	bare rock
mc	micro-conduits	negative	1-5, variable	bal. gypsum	planar circular	solution	structural (fractures)	various
sf	minute rain craters	negative	10-20, 5-30	al. bal. gypsum, salt	planar circular	solution	hydrodynamical	rocky spikes
sf	rills	negative	3-30, 2-20, 200-1000	div. gypsum, salt	linear	solution	hydrodynamical	bare rock
sf	minute-spitz	positive	20, 10-30	al. bal. gypsum, salt	linear	solution	hydrodynamical	bare rock
sf	solution levels	negative	large variability	al. bal. gypsum, salt	planar	solution	hydrodynamical	bare rock
sf	heelprint karren	negative	50-200, 5-30, 50-200	div. gypsum	planar	solution	hydrodynamical	bare rock
sf	scallops	negative	10-80, 5-20, 20-100	gypsum al., bal.	circular	solution	hydrodynamical	bare rock
sf	meandering rills	negative	large variability	gypsum al., bal.	linear	solution	hydrodynamical and decantation	semicovered rock
sf	runnels	negative	30-300, 30-150, 200-400 m	div. gypsum	linear	disint. and solution	hydrodynamical and decantation	semicovered rock
sf	meandering runnels	negative	4-20, 5-15, 50-700	gypsum al., bal.	linear	solution	hydrodynamical and decantation	semicovered rock
sf	small knobs	positive	10-500, 20-200	div. gypsum	planar circular	biocon; diffsol	complex	various
sf	pans in knobs	negative	5-30, 10-200	div. gypsum	planar circular	biocon; diffsol	complex	various
sf	pans in boxes	negative	10-200, 5-30, 10-300	div. gypsum, salt	planar circular	diffsol	lithological (veins of calcite)	various
sf, mf	grikes	negative	large variability	div. gypsum	linear	tensl., solution	structural (fractures)	various
sf, mf	pits	negative	30-500 (diam.)	div. gypsum	planar circular	solution, disint.	structural (fractures)	various
mf	rundkarren	positive	large variability	div. gypsum	areal	solution and weathering	structural (fractures)	covered and semicovered rock
mf	pavements	positive	large variability	div. gypsum	areal	solution and weathering	complex	various
mf	pinnacle karst	positive	large variability	div. gypsum	areal	interface solution	complex	covered surface

mo) where permeable sediments cover a macro-crystalline gypsum. Along slopes where the cover has been eroded there are many deep and wide cutters with rounded bottoms isolating small pinnacles (Figure 8). In the Siculiana area (southern Sicily) a more typical “stone forest” is present which evolved under a permeable cover, which favoured the development of an interface karst. Where later erosion, also due to quarrying activity, exhumed this karst, unusual landforms have been revealed like upstanding rocky peaks (Forti

and Sauro, 1996; Macaluso et al., 2001) separated by deep trenches (Figure 9).

The rarest solution features in the gypsum are the grikes and all the *minute-shafts* penetrating inside the mass of the rock. Because of the dynamic of the outer gypsum layer (see below), these last forms only evolve under a permeable cover of insoluble materials and are exposed after its removal.

In terms of karren presenting significant differences in comparison with limestone karren, the



Figure 7: Small block of arenitic gypsum engraved by numerous radially arranged microrills (S. Caterina Villarmosa, Caltanissetta). Width of view is 2 m.



Figure 8: Crypto-karren with deep and wide cutters often with rounded bottoms isolating small pinnacles, developed under permeable covers subsequently eroded (Ciminna basin, Palermo).



Figure 9: Crypto-karren of stone forest type developed under permeable covers exposed by quarrying activity near Siculiana (Agrigento). Width of view is 8 m.



Figure 10: Runnels oriented according to the slope on a surface in selenitic gypsum in the Santa Ninfa area (Archivio R.N.I. Grotta di Santa Ninfa).

*solution runnels (rinnenkarren), the small closed basins, selective solution forms* and in general all the solution forms influenced by biological processes are worthy of note. In effect, the runnel-like features are not so common and not always so clearly defined as those of the limestones (Figure 2). These forms mainly develop on selenitic gypsum or on detritic macro-crystalline gypsum, sometimes occupying the whole slope (Figure 10). Their development is frequently influenced by the crystalline structure or by the bedding planes. In particular, runnels on gypsum with iso-oriented

crystals tend to lengthen along the direction of the long axes of the crystals and thus to stray from the



Figure 11: Runnels and scallops by wave splashing and surf erosion developed on a coastal scarp in pelitic gypsum (Marina di Palma di Montechiaro, Agrigento).

slope. They also tend to lengthen along the direction of the bedding on gypsum with subvertical bedding planes (Gatani et al., 1989; Macaluso et al., 2001).

On coastal cliffs runnels develop downslope of the belts affected by wave splashing and the subsequent decantation of the water. They are small

parallel runnels, which are often associated with rills, meandering rills and scallop-like forms (Figure 11).

On gypsum surfaces, classical solution pans originated by biological processes, like the *kamenitzas*, do not exist. However closed basins with diameters ranging from some centimetres to

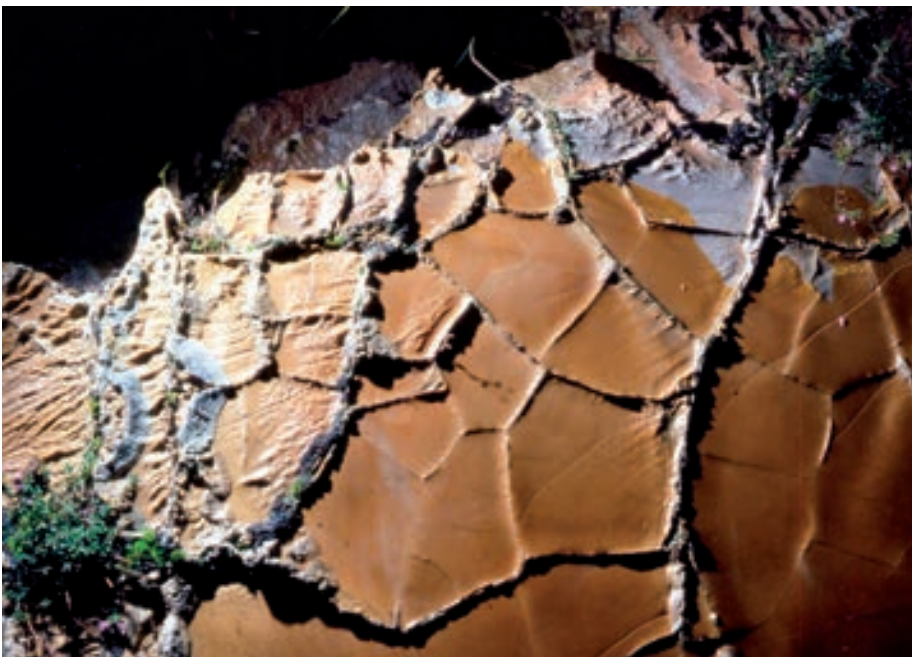


Figure 12: Boxwork and polygon pans evolved by selective solution on a surface of arenitic gypsum. The fissures are filled by calcite (S. Caterina Villarmosa, Caltanissetta). Width of view is 90 cm.

a few decimetres and, usually, depths of less than one decimetre are frequent. These basins can be isolated or arranged in groups to form a *honeycomb karst-like mini-relief*. Their evolution is due to the combination of solution by water stagnation, bio- and thermoclastic phenomena and slow draining of the water through the intra-crystalline porosity (Macaluso and Sauro, 1996a).

Among the selective solution forms some result from the rock structure, others from differential covers of some species of lichens. *Boxwork-like forms* are present on gypsum outcrops containing veins of less soluble materials, like calcite resulting from carbonation (precipitation of calcite). Between these forms, polygon basins and solution levels delimited by enclosures of calcite veins may be easily found. These forms are common on microcrystalline gypsum and on salt outcrops (Figure 12). Between the forms originated by the protective influence of lichen colonies small knobs and enclosures are common on surfaces of microcrystalline gypsum. The enclosures present a circular pattern and surround closed depressions.

The ample variability of gypsum karren is also linked with the wide range of environmental conditions. According to the local micro-environments it is possible to find gypsum surfaces with very different conditions of soil or detritus cover, also changing in time. These are: clay as a residuum of the solution processes; clay and soil sediments transported by the overland flow on the gypsum slopes; gypsum crystals originating from the granular disintegration of the rock; and, in the coastal environment, also sand brought by the breakers. The presence of these thin and often scattered covers influences the evolution of the karren (Macaluso and Sauro, 1996a; 1998b), especially of the sinuous linear forms, like the meandering rills and runnels (Figures 13, 14).

On the bare gypsum surfaces a phenomenon that interferes in some way with the morphological evolution is the development of a *weathering crust* linked with the cycles of the pore water hosted inside the rock (Ferrarese et al., 2002). During wet winters the rock becomes saturated with water,



Figure 13: Minute rills and sinuous meandering rills developed on steep surfaces fed by slow and protracted water decantation from soil patches (Montallegro, Agrigento).

while during dry summers the oversaturated solution migrates upwards and causes the precipitation of gypsum crystals or the growth of pre-existing crystals. This results in an increase of volume of the outer layer with a rearrangement of its crystal structure. This in turn causes a plastic deformation of the rock causing the closure of nearly all the plan discontinuities, like the fissures and consequently impeding the development of the grikes. In fact, the grikes are present only on the rocky surfaces previously buried under covers of permeable materials. The forms resulting from the dynamic processes of the gypsum crust are the *gypsum bubbles (tumulos)*, the *pressure ridges*, the *pressure humps*, etc., and also larger forms, like the *dome-like hills* (Macaluso and Sauro, 1998a; Ferrarese et al., 2002;



Figure 14: Meandering rills developed on balatine gypsum in the coastal scarp where the wave splashing feeds water decantation (Marina di Palma di Montechiaro, Agrigento). Width of view is 40 cm.

Sauro, 2003). On the surfaces of these “pressure” forms solution forms are uncommon probably because of both the rearrangement of the gypsum crystals and the detachment of some of these.

## Conclusions

The presence on the gypsum surfaces of nearly

all the elementary types of karren, already recognized on the limestones (Perna and Sauro, 1978), proves that the development of these karren is mostly controlled by the dynamics of the water flowing above the rocky surfaces (Macaluso and Sauro, 1996a). In fact, the differences in the solution processes between the gypsum and the limestones are insignificant from the point of view of the genesis of the free surface karren.

Only the kamenitzas and the rounded karren which have developed in the limestones at the soil/rock interface, are strongly influenced by the hydrochemical environment. Anyway, here we do not find typical forms except for those which are structurally controlled.

The areas of evaporitic rocks in Sicily represent really extraordinary environments both for their original landscapes and for the observation and study of the solution forms. They are also ideal for carrying out experiments on the development of

these forms. The Sicilian Region Authority has already set up some small natural reserves in these areas, mostly linked to the presence of show caves. But the exceptional nature of these landscapes is worthy of the creation of a special park devoted both to the natural aspects and to the characteristic nature of the human landscapes (Bianco et al., 2003). In the park it would be possible to maintain or to revive some of the traditional human activities linked to the use of these distinctive natural resources.



# REFERENCES

- Abensperg-Traun M., Wheaton G. A., Eliot I. G., 1990: Bioerosion, notch formation and micromorphology in the intertidal and supratidal zones of calcareous sandstone stack. *Journal of the Royal Society of Western Australia* 73: 47–56.
- Adams C. G., 1965: The Foraminifera and stratigraphy of the Melinau Limestone, Sarawak, and its importance in Tertiary correlation. *Quarterly Journal of the Geological Society of London* 121: 283–338.
- Adamson A. P., Boase M. J., Howarth C. J., Wilson J. M., Wilson M. E., 1984: Southampton University Madagascar Expedition. University of Southampton, 136 p.
- Alexandersson T., 1976: Actual and anticipated petrographic effects of carbonate undersaturation in shallow water. *Nature* 262: 653–658.
- Allen J. R. L., 1972: The origin of cave flutes and scallops by enlargement of inhomogeneities. *Rassegna Speleologica Italiana* 24, 1: 3–20.
- Allison R. J., Goudie A. S., 1990: The form of rock slopes in tropical limestone and their associations with rock mass strength. *Zeitschrift für Geomorphologie* 34, 2: 129–148.
- Alonso-Zarza A. M., Armenteros I., Braga J. C., Muñoz A., Pujalte C., Ramos E., Aguirre J., Alonso-Gavilán G., Arenas C., Baceta J. I., Carballeira J., Calvo J. P., Corrochano A., Fornós J. J., González A., Luzón A., Martín J. M., Pardo G., Payros A., Pérez A., Pomar L., Rodríguez J. M., Villena J., 2002: Tertiary. In: Gibbons W., Moreno T. (Eds.), *The Geology of Spain*. The Geological Society, London, 293–334.
- Ameen M. S., 1995: Fracture characterization in the Chalk and the evolution of the Thanet monocline, Kent, southern England. In: Ameen M. S. (Ed.), *Fractography: Fracture topography as a tool in fracture mechanics and stress analysis*. Geological Society of London, Special Publication 92: 149–174.
- Anderson J. A. R., Chai P. P. K., 1982: Vegetation. In: Jermy A. C., Kavanagh K. P. (Eds.), *Gunung Mulu National Park, Sarawak*. Sarawak Museum Journal (Special Issue 2) 30, 51: 195–206.
- Anderson J. A. R., Jermy A. C., The Earl of Cranbrook, 1982: *Gunung Mulu National Park. A management and development plan*. Royal Geographical Society, London, 345 p.
- Andrews C., Williams R. B. G., 2000: Limpet erosion of chalk shore platforms in southeast England. *Earth Surface Processes and Landforms* 25: 1371–1382.
- Aubert D., 1969: Phénomènes et formes du Karst jurassien. *Eclogae Geologicae Helvetiae* 62, 2: 325–399.
- Audra P., 2000: Le karst haut alpine du Kanin (Alpes Juliennes, Slovénie-Italie). *Karstologia* 35: 27–38.
- Auerswald K., 1998: Bodenerosion durch Wasser. In: Richter G. (Ed.), *Bodenerosion. Analyse und Bilanz eines Umweltproblems*, Darmstadt, 31–42.
- Bahun S., 1974: Tektogeneza Velebita i postanak Jelenaslaga. *Geološki vjesnik* 27: 35–51.
- Baillie I. C., Liong T. Y., Pang L. C., Phang C. M. S., 1982: Soils. In: Jermy A. C., Kavanagh K. P. (Eds.), *Gunung Mulu National Park, Sarawak*, Sarawak Museum Journal (Special Issue 2) 30, 51: 183–193.
- Balogh Z., 1998: Saroknyomkarrok vizsgálata az ausztriai Totes-Gebirgében. *Karsztfejlődés* 2: 149–167.
- Bannink P., Bannink G., Magraith K., Swain B., 1995: Multi-level maze cave development in the Northern Territory. In: Baddeley G. (Ed.), *Vulcon Preceedings of the 20<sup>th</sup> Conference of the Australian Speleological Federation*. Victorian Speleological Association, Melbourne, 49–54.
- Bär W. F., Fuchs F., Nagel G., 1986: *Lluc/Sierra Norte*



- (Mallorca) – Karst einer mediterranen Insel mit alpidischer Struktur (UIS International Atlas of Karst Phenomena, sheet 5). *Zeitschrift für Geomorphologie*, Supplementband 59: 27–48.
- Bartrum J. A., Mason P. A., 1948: Lapiez and solution pits in basalts at Hokianga, New Zealand. *New Zealand Journal of Science Technology* 30, B: 165–172.
- Basterretxea G., Orfila A., Jordi A., Casas B., Lynett P., Duarte C. M., Tintoré J., 2004: Seasonal dynamics of a microtidal pocket beach with *Posidonia oceanica* seabeds (Mallorca, Spain). *Journal of Coastal Research* 20: 1155–1164.
- Bastian L., 1964: Morphology and development of caves in the southwest of Western Australia. *Helvétique* 2, 4: 105–119.
- Battistini R., 1981: La morphogenèse des plateformes de corrosion littorale dans les grès calcaires (plateforme supérieure et plateforme à vasques) et le problème des vasques, d'après des observations faites à Madagascar. *Revue de Géomorphologie Dynamique* 3: 81–94.
- Battistini R., Guilcher A., 1982: Les plates-formes littorales à vasques en roches calcaires: répartition dans le monde, mer Méditerranée non comprise. *Karst Littoraux*, Comité National Français de Géographie, May 1982, Actes du Colloquium de Perpignan 1: 1–11.
- Bauer F., 1962: Nacheiszeitliche Karstformen in den Österreichischen Kalkhochalpen. Actes du Deuxième Congrès International de Spéléologie 1: 299–328.
- Beck H. M., 2003: Beneath the Cloud Forests – a History of Caving in Papua New Guinea. *Caving Publications International*, Allschwil, 352 p.
- Bedi N., Rao K. L. V. R., 1984: Nature and evolution of a part of Saurashtra coast, Gujarat, India. *Zeitschrift für Geomorphologie* 28: 53–69.
- Beek W. J., Muttzall K. M. K., 1975: *Transport Phenomena*. Wiley, London, New York, 298 p.
- Belloni S., 1969: Alcune osservazioni sulle acque e sui depositi al fondo delle “vaschette di corrosione” (kamenitza) della località Borgo Grotta Gigante (Carso Triestino). *Atti e Memorie della Commissione Grotte “Eugenio Boegan”* 9: 33–62.
- Belloni S., Orombelli G., 1970: Osservazioni e misure su alcuni tipi morfologici nei campi solcati del Carso Triestino. *Atti della Società Italiana di Scienze Naturali e Museo Civico di Storia Naturale Milano* 110, 4: 317–372.
- Bernot F., 1985: Podnebnje. In: Fabjan I. (ed.), *Triglavski narodni park*. Vodnik, Bled, 57–61.
- Bianco D., Panzica La Manna M., Sauro U., 2003: Tutela e valorizzazione delle aree carsiche italiane nelle rocce evaporitiche: problemi e prospettive. In: Madonia G., Forti P. (Eds.), *Le aree carsiche gessose d'Italia*. *Memorie Istituto Italiano di Speleologia* 2, 14: 115–120.
- Biese W. B., 1956: Über Karstvorkommen in Chile. *Die Höhle* 7, 4: 91–96.
- Biese W. B., 1957: Auf der Marmor-Insel Diego de Almagro (Chile). *Natur und Volk* 87, 4: 123–132.
- Bird E. C. F., Guilcher A., 1982: Observations préliminaires sur les récifs frangeants actuels du Kenya et les formes littorales associées. *Revue de Géomorphologie Dynamique* 31: 113–125.
- Bird J. B., Richards A., Wong P. P., 1979: Coastal subsystems of Western Barbados, West Indies. *Geografiska Annaler* 61A, 3–4: 221–236.
- Boardman M. R., Neumann A. C., Rasmussen K.A., 1989: Holocene sea level in the Bahamas. In: Mylroie J. E. (Ed.), *Proceedings of the 4<sup>th</sup> Symposium on the Geology of the Bahamas*. Port Charlotte, Bahamian Field Station, Florida, 45–52.
- Bögli A., 1951: Probleme der Karrenbildung. *Geographica Helvetica* 3: 191–204.
- Bögli A., 1960a: Kalklösung und Karrenbildung. *Zeitschrift für Geomorphologie*, Supplementband 2: 4–21.
- Bögli A., 1960b: Les phases de dissolution du calcaire et leur importance pour les problèmes karstiques. *Rassegna Speleologica Italiana* 4: 16 p.
- Bögli A., 1961: Karrentische, ein Beitrag zur Karstmorphologie. *Zeitschrift für Geomorphologie* 5, 3: 185–193.
- Bögli A., 1964: Le Schichttreppenkarst. Un exemple de complexe glaciokarstique. *Revue Belge de Géographie* 1, 2: 64–82.
- Bögli A., 1970: Le Hölloch et son karst [Das Hölloch und sein Karst]. *Baconnière*, Neuchâtel, 109 p.
- Bögli A., 1972: Gips in Höhlen. *Uerner Mineralienfreund* 10, 6: 77–84.
- Bögli A., 1973: Der alpine Karst in der Zentralschweiz. *Proceedings of the 6<sup>th</sup> International Congress of Speleology*, Olomouc. *Academia*, Praha, 39–42.
- Bögli A., 1976: Die wichtigsten Karrenformen der Kalkalpen. In: *Karst Processes and Relevant Landforms*. Department of Geography, Philosophical Faculty, Ljubljana, 141–149.
- Bögli A., 1978: *Karsthydrographie und physische Speläologie* [Karst hydrology and physical speleology]. Springer-Verlag, Berlin, Heidelberg, New York, 292 p.
- Bögli A., 1980: *Karst Hydrology and Physical Speleology*. Springer-Verlag, Berlin, 284 p.
- Bögli A., 1981: Solution of limestone and karren formation. In: Sweeting M. M. (Ed.), *Karst Geomorphol-*

- ogy. Benchmark Papers in Geology 59, Hutchinson Ross Publishing Company, 64–89.
- Bögli A., 1987: Der Karst der Innerschweiz. *Mitteilungen Naturforschende Gesellschaft Luzern* 29: 225–235.
- Bognar A., 1992: Pedimenti južnog Velebita. *Geografski glasnik* 54: 19–32.
- Bognar A., Blazek I., 1986: Geomorfološka karta područja V. Paklenice 1:25.000. Simpozij o kraškem površju. *Acta Carsologica* 14, 15: 19–206.
- BOM (Bureau of Meteorology, Australia), 2005: Climate. <http://www.bom.gov.au/climate/averages>.
- Bordoy M., Ginés A., 1990: Observaciones morfométricas sobre la profundidad de estrías de lapiaz (Riltenkarren) en Mallorca. *Endins* 16: 21–25.
- Bosch M., Moreno I., 1982: Estructura de las poblaciones y crecimiento de *Littorina neritoides* (L. 1758) (Mollusca, Gastropoda) en las costas de las Islas Baleares. *Bolletí de la Societat d'Història Natural de Balears* 31: 57–66.
- Boutakoff N., 1963: The geology and geomorphology of the Portland area. *Geological Survey of Victoria, Memoir* 22: 52–58.
- Bradley W. C., Hutton J. T., Twidale C. R., 1978: Role of salts in development of granitic tafoni, south Australia. *Journal of Geology* 86: 647–654.
- Brandt C. J., 1989: The size distribution of throughfall drops under vegetation canopies. *Catena* 16: 507–524.
- Brandt C. J., 1990: Simulation of the size distribution and erosivity of raindrops and throughfall drops. *Earth Surface Processes and Landforms* 15: 687–698.
- Brink A. B. A., Partridge T. C., 1980: The nature and genesis of solution cavities (Makondos) in Transvaal cave breccias. *Palaeontology Africa* 23: 47–49.
- Bromley R. G., 1978: Bioerosion of Bermuda Reefs. *Palaeogeography, Palaeoclimatology, Palaeoecology* 23: 169–197.
- Brook D. B., Eavis A. J., Lyon M. K., Waltham A. C., 1982: Caves in the limestone. In: Jermy A. C., Kavanagh K. P. (Eds.), *Gunung Mulu National Park*. Sarawak Museum Journal (Special Issue 2) 30, 51: 95–119.
- Brown M. A., 1990: Regional lithofacies and depositional environments of the Salem Limestone (Valmeyeran, Mississippian), south-central Indiana. In: Thompson T. A. (Ed.), *Architectural elements and paleoecology of carbonate shoal and intershoal deposits in the Salem Limestone (Mississippian) in south-central Indiana*. Indiana Geological Survey, Guidebook 14: 1–12.
- Bryan K., 1920: Origin of Rock Tanks and Charcos. *American Journal of Science* 50, 4: 163–174.
- Buhmann D., Dreybrodt W., 1985: The kinetics of calcite dissolution and precipitation in geologically relevant situations of karst areas: 1. Open system. *Chemical Geology* 48: 189–211.
- Bull P. A., Laverty M., 1982: Observations on phytokarst. *Zeitschrift für Geomorphologie* 26: 437–457.
- Burke M. A., 1994: A quantitative analysis of marine kamenitza on the Carboniferous limestone between Skerries and Loughshinny, Co. Dublin. Thesis submitted as part of B. A. degree, Geography Department, Trinity College, Dublin, 198 p.
- Burnaby T. P., 1950: The tubular chalk stacks of Sheringham. *Proceedings of the Geological Association* 61: 226–241.
- Buser S., 1976: Geological, geomorphological and hydrogeological investigations of Kanin Mts. *Archives of Geological Institute of Slovenia, Ljubljana*, 56 p.
- Buser S., 1986a: The basic geological map 1:100.000, L 33–64, L 33–63, Tolmin in Videm (Udine). Beograd.
- Buser S., 1986b: Commentary to the map Tolmin and Videm (Udine), L 33–64, L 33–63. Beograd, 103 p.
- Butzer K. W., 1962: Coastal geomorphology of Majorca. *Annals of the Association of American Geographers* 52: 191–212.
- Butzer K. W., Cuerda J., 1962: Coastal stratigraphy of southern Mallorca and its implications for the Pleistocene chronology of the Mediterranean Sea. *Journal of Geology* 70: 398–416.
- Calaforra J. M., 1996: Some examples of gypsum karren. In: Fornós J. J., Ginés A. (Eds.), *Karren Landforms*. Universitat de les Illes Balears, Palma de Mallorca, 253–260.
- Calder I. R., 1996: Dependence of rainfall interception on drop size: 1. Development of the two-layer stochastic model. *Journal of Hydrology* 185: 363–378.
- Cardell C., Delalieux F., Roumpopoulos K., Moropoulou A., Auger F., Van Grieken R., 2003: Salt-induced decay in calcareous stone monuments and buildings in a marine environment in SW France. *Construction and Building Materials* 17: 65–179.
- Carew J. L., Mylroie J. E., 1987: A refined geochronology for San Salvador Island, Bahamas. In: Curran H. A. (Ed.), *Proceedings of the 3<sup>rd</sup> Symposium on the Geology of the Bahamas*. Fort Lauderdale, CCFL Bahamian Field Station, Florida, 35–44.
- Carew J. L., Mylroie J. E., 1995a: Quaternary tectonic stability of the Bahamian Archipelago: Evidence from fossil coral reefs and flank margin caves. *Quaternary Science Reviews* 14, 2: 145–153.
- Carew J. L., Mylroie J. E., 1995b: Depositional model and stratigraphy for the Quaternary geology of the Bahama Islands. In: Curran H. A., White B. (Eds.), *Terrestrial and Shallow Marine Geology of the Baha-*

- mas and Bermuda. Geological Society of America, Special Paper 300: 5–32.
- Carew J. L., Mylroie J. E., 1997: Geology of the Bahamas. In: Vacher H. L., Quinn T. M. (Eds.), *Geology and Hydrogeology of Carbonate Islands*. Elsevier, Amsterdam, 91–139.
- Carney C., Boardman M. R., 1991: (abstract), Oolitic sediments in a modern carbonate lagoon, Graham's Harbor, San Salvador, Bahamas. Geological Society of America Abstracts with Programs 23, 5: A 225.
- Carter N. E. A., Viles H. A., 2003: Experimental investigations into the interactions between moisture, rock surface temperatures and an epilithic lichen cover in the bioprotection of limestone. *Building and Environment* 38: 1225–1234.
- Cecioni G., 1982: El fenómeno cárstico en Chile. *Informaciones geográficas* 29: 57–79.
- Cerdá A., 1997: Rainfall drop size distribution in the Western Mediterranean basin, Valencia, Spain. *Catena* 30, 2–3: 169–182.
- Chaix E., 1895: Topographie du Désert de Platé. *Le Globe, Société de Géographie de Genève* 34: 44 p.
- Chen J., Blume H. P., Beyer L., 2000: Weathering of rocks induced by lichen colonization, a review. *Catena* 38: 121–146.
- Chen X., Gabrovšek F., Huang C., Jin Y., Knez M., Kogovšek J., Liu H., Petrič M., Mihevc A., Otoničar B., Shi M., Slabe T., Šebela S., Wu W., Zhang S., Zupan Hajna N., 1998: South China Karst I. Založba ZRC, Ljubljana, 247 p.
- Chen Z., Song L., Sweeting M. M., 1986: The pinnacle karst of the stone forest, Lunan, Yunnan, China: an example of a subjacent karst. In: Paterson K, Sweeting M. M. (Eds.), *New Directions in Karst*. Geobooks, Norwich, 597–607.
- Choppy J., 1996: Les cannelures et rigoles sont des indicateurs climatiques. In: Fornós J. J., Ginés A. (Eds.), *Karren Landforms*. Universitat de les Illes Balears, Palma de Mallorca, 137–148.
- Choquette P. W., Pray L. C., 1970: Geologic Nomenclature and Classification of Porosity in Sedimentary Carbonates. *American Association of Petroleum Geologists, Bulletin* 54: 207–250.
- Čílek V., 1989: Rosná koroze rápencu z pustrich oblasti Iránu a Pákistánu. *Československý Kras* 40: 135–137.
- Coetzee F., 1975: Solution pipes in coastal aeolianites of Zululand and Moçambique. *Transactions of the Geological Society of South Africa* 78: 323–333.
- Conca J. L., Rossman G. R., 1985: Core softening in cavernous weathered tonalite. *Journal of Geology* 93: 59–73.
- Cooke R. C., 1977: Factors regulating the composition, change, and stability of phases in the calcite-seawater system. *Marine Chemistry* 5: 75–92.
- Corbel J., 1952: Les lapiaz marins. *Revue Géographique de Lyon* 37: 379–380.
- Corbel J., 1959: Érosion en terrain calcaire (Vitesse d'érosion et morphologie). *Annales de géographie* 366: 97–120.
- Corrà G., 1972: Morfologie carsiche nella zona di Canale in Val Lagarina (Val d'Adige meridionale). *Studi Trentini di Scienze Naturali A* 49, 2: 127–160.
- Corrà G., Benetti A., 1966: Morfologie carsiche nella zona lessinea compresa tra il M. Purga di Velo e il M. Bellocca. *Natura Alpina* 17: 115–129.
- Crowther J., 1996: Roughness (mm-scale) of limestone surfaces: examples from coastal and mountain karren features in Mallorca. In: Fornós J. J., Ginés A. (Eds.), *Karren Landforms*. Universitat de les Illes Balears, Palma de Mallorca, 149–159.
- Crowther J., 1997: Surface roughness and the evolution of karren forms at Lluc, Serra de Tramuntana, Mallorca. *Zeitschrift für Geomorphologie* 41, 3: 393–407.
- Crowther J., 1998: New methodologies for investigating rillenkarrén cross-sections: a case study at Lluc, Mallorca. *Earth Surface Processes and Landforms* 23, 4: 333–344.
- Cucchi F., Forti F., Finocchiaro F., 1987: Carbonate surface solution in the Classical Karst. *International Journal of Speleology* 16, 3–4: 125–138.
- Cucchi F., Forti F., Marinetti E., 1996: Surface degradation of carbonate rocks in the karst of Trieste (Classical Karst, Italy). In: Fornós J. J., Ginés A. (Eds.), *Karren Landforms*. Universitat de les Illes Balears, Palma de Mallorca, 41–51.
- Cucchi F., Radovich N., Sauro U., 1990: I campi solcati di Borgo Grotta Gigante nel Carso Triestino. *International Journal of Speleology* 18, 3–4: 117–144.
- Curl R. L., 1966: Scallops and flutes. *The Transaction of Cave Research Group of Great Britain* 7, 2: 121–160.
- Cvijić J., 1924: The evolution of lapiés. A study in karst physiography. *Geographical Review* 14: 26–49.
- Cvijić J., 1926: *Geomorfologija* 2. Beograd, 505 p.
- Cvijić J., 1927: Škrape. *Glasnik Srpskog geografskog društva* 13: 17–29.
- Dalongeville M., 1977: Formes littorales de corrosion dans les roches carbonatées au Liban: Étude Morphologique. *Méditerranée* 3: 21–33.
- Dalongeville M., Guilcher A., 1982: Les plates-formes à vasques en Méditerranée, notamment leur extension vers le nord. *Karst Littoraux*, Comité National Français de Géographie, May 1982, Actes du Colloquium de Perpignan 1: 13–22.
- Dalongeville R., Le Champion T., Fontaine M. F., 1994: Bilan bioconstruction-biodestruction dans les

- roches carbonatées en mer Méditerranée: étude expérimentale et implications géomorphologiques. *Zeitschrift für Geomorphologie* 38: 457–474.
- Daneš J. V., 1911: Physiography of some limestone areas in Queensland. *Proceedings of the Royal Society of Queensland* 23: 75–86.
- Danin A., 1983: Weathering of limestone in Jerusalem by cyanobacteria. *Zeitschrift für Geomorphologie* 27: 413–421.
- Danin A., Caneva G., 1990: Deterioration of limestone walls in Jerusalem and marble monuments in Rome caused by cyanobacteria and cyanophilous lichens. *International Biodeterioration* 26: 397–417.
- Danin A., Gerson R., Garty J., 1983: Weathering patterns on hard limestone and dolomite by endolithic lichens and cyanobacteria: Supporting evidence for eolian contribution to Terra Rossa soil. *Soil Science* 136: 213–217.
- Danin A., Gerson R., Marton K., Garty J., 1982: Patterns of limestone and dolomite weathering by lichen and blue-green algae and their paleoclimatic significance. *Palaeogeography, Palaeoclimatology, Palaeoecology* 37: 221–233.
- Darabos G., 2003: Observation of microbial weathering resulting in peculiar “exfoliation” features in limestone from Hirao-dai karst, Japan. *Zeitschrift für Geomorphologie, Supplementband* 131: 33–42.
- Davies T. T., Sutherland A.J., 1980: Resistance to flow past deformable boundaries. *Earth Surface Processes* 5, 2: 175–179.
- Davis W. E., 1957: Rillenstein in Northwest Greenland. *National Speleological Society Bulletin* 19: 40–46.
- Day A. E., 1928: Pipes in the Coast Sandstone of Syria. *Geological Magazine* 65: 412–415.
- Day M. J., 1979: The contribution of geomorphology to the formulation of a management plan for the Gunong Mulu National Park, Sarawak, East Malaysia. *Applied Geography Conferences* 2: 193–202.
- Day M. J., 1980: Rock hardness: Field assessment and geomorphic importance. *Professional Geographer* 32, 1: 72–81.
- Day M. J., 1981a: Limestone hardness and tropical karst terrain. *Proceedings of the 8<sup>th</sup> International Congress of Speleology* 1, Bowling Green, 327–329.
- Day M. J., 1981b: Rock hardness and landform development in the Gunong Mulu National Park, Sarawak, East Malaysia. *Earth Surface Processes and Landforms* 6, 2: 165–172.
- Day M. J., 1982a: Geomorphological considerations in a management plan for the Gunong Mulu National Park. In: Frazier J. W. (Ed.), *Applied Geography: Selected Perspectives*. Prentice-Hall International, 197–218.
- Day M. J., 1982b: The influence of some material properties on the development of tropical karst terrain. *Transactions of the British Cave Research Association* 9, 1: 27–37.
- Day M. J., 1983: Karst-related management considerations in the Gunong Mulu National Park, Sarawak, East Malaysia. In: Dougherty P. H. (Ed.), *Environmental Karst*. GeoSpeleo Publications, Cincinnati, 55–76.
- Day M. J., 1997: Conservation issues in Stone Forest karst. In: Song L., Waltham T., Cao N., Wang F. (Eds.), *Stone Forest: A Treasure of Natural Heritage*. *Proceedings of the International Symposium for Lunan Shilin to Apply for World Natural Heritage Status*. China Environmental Science Press, Beijing, 17–21.
- Delaty J. N., 2000: Expédition Bemaraha 1998. *Expedition Malagasy* 1999. *Spelunca* 78: 11.
- Doornkamp J. C., Brunnsden D., Jones D. K. C., 1980: *Geology, Geomorphology and Pedology of Bahrain*. Geobooks, Norwich, 443 p.
- Drew D. P., 2001: *Classic Landforms of the Burren Karst*. The Geographical Association, Sheffield, 51 p.
- Drew D. P., Daly D., 1993: *Groundwater and Karstification in Mid Galway, South Mayo and North Clare*. Report Series, Geological Survey of Ireland RS 93, 3: 86 p.
- Dreybrodt W., 1988: *Processes in Karst Systems. Physics, Chemistry and Geology*. Springer Series in Physical Environments 4, Berlin, New York, 288 p.
- Dreybrodt W., 1990: The role of dissolution kinetics in the development of karst aquifers in limestone: A model simulation of karst evolution. *Journal of Geology* 98: 639–655.
- Dreybrodt W., 1996: Principles of early development of karst conduits under natural and man-made conditions revealed by mathematical analysis of numerical models. *Water Resources Research* 32: 2923–2935.
- Dreybrodt W., Gabrovšek F., Romanov D., 2005: *Processes of speleogenesis: a modeling approach*. Založba ZRC, Ljubljana, 375 p.
- Dreybrodt W., Kaufmann G., 2007: Physics and chemistry of dissolution on subaerially exposed soluble rocks by flowing water films. *Acta Carsologica* 36, 3: 357–367.
- Duane M. J., Al-Mishwat A. T., Rafique M., 2003: Weathering and biokarst development on marine terraces, Northwest Morocco. *Earth Surface Processes and Landforms* 28: 143–144.
- Dubljanskij J. V., 1987: Teoreticheskoje modelirovanije dinamiki formirovanija gidrotermokarsztovüh polosztvej – Metodi i izucssenyija geologicszkikh javlenij [Теоретическое моделирование

- динамики формирования гидротермокарстовых полостей - Методы и изучения геологических явлений]. Novosibirsk, 97–111.
- Dublyansky V. N., Dublyansky Y. V., 2000: The role of condensation in karst hydrogeology and speleogenesis. In: Klimchouk A. B., Ford D. C., Palmer A. N., Dreybrodt W. (Eds.), *Speleogenesis: Evolution of Karst Aquifers*. National Speleological Society, Huntsville, Alabama, 100–112.
- Dunkerley D. L., 1979: The morphology and development of rillenkarren. *Zeitschrift für Geomorphologie* 23, 3: 332–348.
- Dunkerley D. L., 1983: Lithology and micro-topography in the Chillagoe karst, Queensland, Australia. *Zeitschrift für Geomorphologie* 27, 2: 191–204.
- Dunkerley D. L., 1988: Solution and precipitation of limestone in the Chillagoe karst and opportunities for dating landscape development. 17<sup>th</sup> Biennial Conference of the Australian Speleological Federation, Sydney, 112–117.
- Dunkley J. N., 1993: The Gregory Karst and Caves, Northern Territory, Australia. Proceedings of the 11<sup>th</sup> International Congress of Speleology, Beijing, 17–18.
- Dzulynski S., Gil E., Rudnicki J., 1988: Experiments on kluftkarren and related lapis forms. *Zeitschrift für Geomorphologie* 32, 1: 1–16.
- Eavis A. J., 1980: *Caves of Mulu '80*. Royal Geographical Society, London, 52 p.
- Eckert M., 1898: Die Karren oder Schratzen. *Petermanns Mitteilungen*, Gotha, 69–71.
- Eckert M., 1902: Das Gottesackerplateau. Ein Karrenfeld im Allgäu. Studien zur Lösung des Karrenproblems. Wissenschaftliche Ergänzungshefte zur Zeitschrift des Deutschen und Österreichischen Alpenvereins 1, 3: 1–108.
- Elert G., 2001: Diameter of a Raindrop. <http://hypertextbook.com/facts/2001/IgorVolynets.shtml>.
- Emery K. O., 1946: Marine Solution Basins. *The Journal of Geology* 54: 209–228.
- Emery K. O., 1962: Marine geology of Guam. U.S. Geological Survey Professional Paper 403-B, 76 p.
- Emmett W. W., 1970: The hydraulics of overland flow on hillslopes. U.S. Geological Survey Professional Paper 662-A, 45 p.
- Escobar F., 1980: Mapa Geológico de Chile. 1:1.000.000 (feuille sud). Servicio Nacional de Geología y Minería, Departamento de Geología General, Santiago.
- Ewers R. O., 1966: Bedding plane anastomoses and their relation to cavern passages. *Bulletin of the National Speleological Society* 28, 3: 133–141.
- Ewers R. O., 1972: A model for the development of sub-surface drainage routes along bedding planes. A thesis submitted in partial fulfilment of the requirement for the degree of Master of Science, M. Sc. Thesis, University of Cincinnati, Cincinnati, 84 p.
- Ewers R. O., 1982: Cavern Development in the Dimension of Length and Breadth. Ph. D. Thesis, McMaster University, Hamilton, Ontario, 398 p.
- Fabre G., Nicod J., 1982: Lapiés, modalités et rôle de la corrosion crypto-karstique. *Mémoires et documents de géographie, Phénomènes karstiques* 3: 115–131.
- Fairbridge R. W., 1950: The geology and geomorphology of Point Peron, Western Australia. *Journal of the Royal Society of Western Australia* 34: 35–72.
- Farrant A. R., Smart P. L., Whittaker F. F., Tarling D. H., 1995: Long-term Quaternary uplift rates inferred from limestone caves in Sarawak, Malaysia. *Geology* 23: 357–360.
- Favre A., 1867: *Recherches géologiques dans les parties de la Savoie, du Piémont et de la Suisse voisine du Mont Blanc* 3, 71 p.
- Ferrarese F., Macaluso T., Madonia G., Palmeri A., Sauro U., 2002: Solution and re-crystallization processes and associated landforms in gypsum outcrops of Sicily. *Geomorphology* 49: 25–43.
- Fiol L., Fornós J., Ginés A., 1992: El Rillenkarren: un tipus particular de Biocarst? Primeres dades. *Endins* 17, 18: 43–49.
- Fiol L., Fornós J., Ginés A., 1996: Effects of biokarstic processes on the development of solutional rillenkarren in limestone rocks. *Earth Surface Processes and Landforms* 21, 5: 447–452.
- Focke J. W., 1977: The effect of a potentially reef-building Vermetid-coraline algal community on an eroding limestone coast, Curaçao, Netherlands Antilles. Proceedings of the 3rd International Coral Reef Symposium 1: 239–245.
- Focke J. W., 1978a: Limestone cliff morphology on Curaçao (Netherlands Antilles) with special attention to the origin of notches and vermetid/coraline algal surf benches (“cornices”, “trottoirs”). *Zeitschrift für Geomorphologie* 22: 329–349.
- Focke J. W., 1978b: Limestone cliff morphology and organism distribution on Curaçao (Netherlands Antilles). *Leidse Geologische Mededelingen* 51, 1: 131–150.
- Folk R. L., Roberts H. H., Moore C. H., 1973: Black phytokarst from Hell, Cayman Islands, British West Indies. *The Geological Society of America Bulletin* 84: 2351–2360.
- Ford D. C., 1980: Threshold and limit effects in karst geomorphology. In: Coates D. L., Vitek J. D. (Eds.), *Thresholds in Geomorphology*. Allen Unwin, London, 345–362.
- Ford D. C., 1996: Features of karren development on

- dolostones in Canada. In: Fornós J. J., Ginés A. (Eds.), *Karren Landforms*. Universitat de les Illes Balears, Palma de Mallorca, 161–162.
- Ford D. C., 1997: Preface. In: Song L., Waltham T., Cao N., Wang F. (Eds.), *Stone Forest: A Treasure of Natural Heritage*. Proceedings of the International Symposium for Lunan Shilin to Apply for World Natural Heritage Status. China Environmental Science Press, Beijing, 1–4.
- Ford D. C., Lundberg J., 1987: A review of dissolutional rills in limestone and other soluble rocks. *Catena Supplement* 8: 119–140.
- Ford D. C., Salomon J. N., Williams P. W., 1996: Les Forêts de Pierre ou Stone forests de Lunan (Yunnan, Chine). *Karstologia* 28: 25–40.
- Ford D. C., Salomon J. N., Williams P. W., 1997: The Lunan Stone forest as a potential world heritage site. In: Song L., Waltham T., Cao N., Wang F. (Eds.), *Stone Forest: A Treasure of Natural Heritage*. Proceedings of the International Symposium for Lunan Shilin to Apply for World Natural Heritage Status. China Environmental Science Press, Beijing, 107–123.
- Ford D. C., Williams P. W., 1989: *Karst Geomorphology and Hydrology*. Unwin Hyman, London, 601 p.
- Ford D. C., Williams P. W., 2007: *Karst Hydrogeology and Geomorphology*. Wiley, Chichester, 576 p.
- Ford T. D., 1978: Chillagoe – a tower karst in decay. *Trans British Cave Research Association* 5: 61–84.
- Ford T. D., 1984: Palaeokarsts in Britain. *Cave Science* 11, 4: 246–264.
- Fornós J. J., 1999: Karst collapse phenomena in the Upper Miocene of Mallorca (Balearic Islands, Western Mediterranean). *Acta Geologica Hungarica* 42: 237–250.
- Fornós J. J., Gelabert B., 1995: Lithology and tectonics of the Majorcan karst. In: Ginés A., Ginés J. (Eds.), *Karst and caves in Mallorca*. *Endins* 20, Monographs of the Natural History Society of the Balearic Islands 3: 27–43.
- Fornós J. J., Gelabert B., Ginés A., Ginés J., Tuccimei P., Vesica P., 2002: Phreatic overgrowths on speleothems: a useful tool in structural geology in littoral karstic landscapes. The example of eastern Mallorca (Balearic Islands). *Geodinamica Acta* 15: 113–125.
- Fornós J. J., Ginés A., 1996: *Karren Landforms*. Universitat de les Illes Balears, Palma de Mallorca, 450 p.
- Fornós J. J., Gómez-Pujol L., 2002: Estudio integrado del lapiaz costero de Mallorca dentro del Proyecto ESPED: metodología y resultados preliminares. *Boletín de la Sociedad Española de Espeleología y Ciencias del Karst* 3: 106–107.
- Fornós J. J., Pomar L., 1983: Mioceno Superior de Mallorca: Unidad Calizas de Santanyí (Complejo Terminal). In: *El Terciario de las Islas Baleares. Guía de las excursiones del 10<sup>th</sup> Congreso Nacional de Sedimentología*, Menorca. Universidad de Palma de Mallorca, 177–206.
- Forsythe R., 1981: Geological investigations of pre-Late Jurassic terranes in the Southernmost Andes. Ph. D. Thesis, Columbia University, New York, 298 p.
- Forsythe R., Mpodozis C., 1983: Geología del basamento pre-jurásico superior en el archipiélago Madre de Dios, Magallanes, Chile. *Servicio Nacional de Geología y Minería, Boletín No. 39*, 63 p.
- Forti F., 1972: Le “vaschette di corrosione”. *Atti e Memorie della Commissione Grotte “Eugenio Boegan”* 11: 37–65.
- Forti P., 1996: Erosion rate, crystal size and exokarst microforms. In: Fornós J. J., Ginés A. (Eds.), *Karren Landforms*. Universitat de les Illes Balears, Palma de Mallorca, 261–276.
- Forti P., Cucchi F., Ayub S., 2001: Le “marmitte di corrosione” della Grotta Perolas (San Paolo, Brasile). *Le Grotte d’Italia* 5, 2: 15–24.
- Forti P., Sauro U., 1996: Gypsum karst of Italy. In: Klimchouk A., Lowe D., Cooper A., Sauro U. (Eds.), *Gypsum Karst of the World*. *International Journal of Speleology* 25, 3–4: 239–250.
- Fras F. J., 1835: *Vollständige Topographie der Karlstädter Militärgrenze*. Državna štamparija, Zagreb.
- Friederich H., 1980: The water chemistry of the unsaturated zone in the Melinau Limestone. *Geographical Journal* 146, 2: 246–258.
- Fry E. J., 1927: The mechanical action of crustaceous lichens on substrata of shale, schist, gneiss, limestone and obsidian. *Annals of Botany* 41: 437–460.
- Fry J. C., Swineford A., 1947: Solution features on cretaceous sandstone in central Kansas. *American Journal of Science* 245: 366–379.
- Gabrovšek F., 2000: Evolution of early karst aquifers: from simple principles to complex models. *Inštitut za raziskovanje krasa ZRC SAZU, Postojna*, 150 p.
- Gale S. J., Drysdale R. N., Scherrer N. C., Fischer M. J., 1997: The Lost City of North-west Queensland: a test of the model of giant grikeland development in semi-arid karst. *Australian Geographer* 28, 1: 107–115.
- Gams I., 1971: Podtalne kraške oblike [Subsoil karst forms]. *Geografski vestnik* 43: 27–45.
- Gams I., 1974: *Kras*. Slovenska matica, Ljubljana, 358 p.
- Gams I., 1976: Forms of subsoil karst. In: *Proceedings of the 6<sup>th</sup> International Congress of Speleology*, Olo-mouc. Academia, Praha, 169–179.
- Gams I., 1985: Mednarodne primerjalne meritve površinske korozije s pomočjo standardnih apneniških tablet [International comparative measurements of

- surface solution by means of standard limestone tablets]. In: Grafenauer S., Pleničar M., Drobne K. (Eds.), *Zbornik Ivana Rakovca*. Slovenska akademija znanosti in umetnosti, 361–386.
- Gams I., 1990: Depth of rillenkarren as a measure of deforestation age. *Proceedings of the International Conference on Anthropogenic Impact and Environmental Changes in Karst*. *Studia Carsologica* 1: 29–36.
- Gams I., 1997: Climatic and lithological influence on the cave depth development. *Acta Carsologica* 26, 2: 321–336.
- Gams I., Kunaver J., Radinja D., 1973: Slovenska kraška terminologija [Slovene Karst Terminology] (in Slovene, English, French and German). *Kraška terminologija jugoslovanskih narodov*, knjiga I. Oddelek za geografijo Filozofske fakultete, Ljubljana, 76 p.
- Gardner R. A. M., 1983: Aeolianite. In: Goudie A. S., Pye K. (Eds.), *Chemical sediments and geomorphology*. Academic Press, London, 265–300.
- Gatani M. G., Laureti L., Madonia P., Pisano A., 1989: Caratteri e distribuzione delle microforme carsiche nel territorio di S. Ninfa (Trapani). In: Agnesi V., Macaluso T. (Eds.), *I gessi di Santa Ninfa: studio multidisciplinare di un'area carsica*. *Memorie Istituto Italiano di Speleologia* 2, 3: 49–58.
- Gavrilović D., 1964: Kamenice – mali korozivni oblici na krečnjaku. *Glasnik Srpskog geografskog društva* 44, 1: 53–60.
- Gavrilović D., 1968: Kamenice, kleine Korrosionsformen im Kalkstein. 4<sup>th</sup> International Congress of Speleology 3: 127–133.
- Gehrmann C. K., Krumbein W. E., Petersen K., 1992: Endolithic lichen and the corrosion of carbonate rocks, a study of biopitting. *International Journal of Mycology and Lichenology* 5: 37–48.
- Gelabert B., 1998: La estructura geológica de la mitad occidental de la isla de Mallorca. *Instituto Tecnológico GeoMinero de España, Colección Memorias*, Madrid, 129 p.
- Gelabert B., 2003: La estructura geológica de Menorca: las zonas de Tramuntana y Migjorn. In: Rosselló V., Fornós J. J., Gómez-Pujol L. (Eds.), *Introducción a la Geografía Física de Menorca*. *Monografía de la Societat d'Història Natural de Balears* 10: 39–48.
- Gelabert B., Fornós J. J., Pardo J. E., Rosselló V. M., Segura F., 2005: Structurally controlled drainage basin development in the south of Menorca (Western Mediterranean, Spain). *Geomorphology* 65: 139–155.
- Gelabert B., Sàbat F., Rodríguez-Perea A., 1992: A structural outline of the Serra de Tramuntana of Mallorca (Balearic Islands). *Tectonophysics* 203: 167–183.
- George T. N., Johnson G. A. L., Mitchell M., Prentice J. E. I., Ramsbottom W. H. C., Sevastopulo G. D., Wilson R. B., 1976: A correlation of Dinantian Rocks in the British isles. *Geological Society of London Special Report* 7, 87 p.
- Gèze B., 1973: Lexique des termes français de spéléologie physique et de karstologie. *Annales de Spéléologie* 28, 1: 1–20.
- Gil M. V., 1992: Quantitative analysis of solution flutes in La Safor karst, Valencia, Spain. *Zeitschrift für Geomorphologie, Supplementband* 85: 89–100.
- Gillespie P. A., Walsh J. J., Watterson J., Bonson C.G., Manzocchi T., 2001: Scaling relationships of joint and vein arrays from The Burren, Co. Clare, Ireland. *Journal of Structural Geology* 23: 183–201.
- Gillieson D. S., Nethery J., Webb J., Godwin M., O'Keefe C., Atkinson A., 2003: *Field Guidebook: Limestone and Lava*. 15<sup>th</sup> Australasian Conference on Cave and Karst Management, Chillagoe and Undara, Queensland. *Australasian Cave and Karst Management Association*, 43 p.
- Gillieson D. S., Smith D. I., Greenaway M., Ellaway M., 1991: Flood history of the limestone ranges in the Kimberley region, Western Australia. *Applied Geography* 11: 105–123.
- Gillieson D. S., Spate A. P., 1998: Karst and caves in Australia and New Guinea. In: Yuan D., Liu Z. (Eds.), *Global Karst Correlation*. Science Press, Beijing PRC and VSP Press, Utrecht, 229–256 p.
- Ginés A., 1990: Utilización de las morfologías de lapiaz como geoindicadores ecológicos en la Serra de Tramuntana (Mallorca). *Endins* 16: 27–39.
- Ginés A., 1993: Morfologies exocàrstiques. In: Alcover J. A., Ballesteros E., Fornós J. J. (Eds.), *Història Natural de l'Arxipèlag de Cabrera*. *Monografia de la Societat d'Història Natural de les Balears* 2: 153–160.
- Ginés A., 1995: Deforestation and karren development in Majorca, Spain. *Acta Universitatis Szegediensis, Acta Geographica* 34: 25–32.
- Ginés A., 1996a: An environmental approach to the typology of karren landform assemblages in a Mediterranean mid-mountain karst: the Serra de Tramuntana, Mallorca, Spain. In: Fornós J. J., Ginés A. (Eds.), *Karren Landforms*. *Universitat de les Illes Balears, Palma de Mallorca*, 163–176.
- Ginés A., 1996b: Quantitative data as a base for the morphometrical definition of rillenkarren features found on limestones. In: Fornós J. J., Ginés A. (Eds.), *Karren Landforms*. *Universitat de les Illes Balears, Palma de Mallorca*, 177–191.
- Ginés A., 1998a: Dades morfomètriques sobre les estries de lapiaz dels Alps calcaris suïssos i la seva

- comparació amb les estries de la Serra de Tramuntana. *Endins* 22: 109–118.
- Ginés A., 1998b: L'exocarst de la serra de Tramuntana de Mallorca. In: Fornós J. J. (Ed.), *Aspectes geològics de les Balears*, Universitat de les Illes Balears, Palma de Mallorca, 361–389.
- Ginés A., 1999a: Morfología kárstica y vegetación en la Serra de Tramuntana. Una aproximación ecológica. Unpublished Ph. D. Thesis, Departament de Biologia Ambiental, Universitat de les Illes Balears, Palma de Mallorca, 581 p.
- Ginés A., 1999b: Agriculture, grazing and land use changes at the Serra de Tramuntana karstic mountains. *International Journal of Speleology* 28 B, 1–4: 5–14.
- Ginés A., 2004: Karren. In: Gunn J. (Ed.), *Encyclopedia of Caves and Karst Science*. Fitzroy Dearborn, New York, London, 470–473.
- Ginés A., Ginés J., 1995: The exokarstic landforms of Mallorca Island. In: Ginés A., Ginés J. (Eds.), *Karst and caves in Mallorca*. *Endins* 20, Monographs of the Natural History Society of the Balearic Islands 3: 59–70.
- Ginés J., 1990: El modelat càrstic de sa Mitjania (Escorca, Mallorca). *Endins* 16: 17–20.
- Ginés J., 1995: Mallorca's endokarst: the speleogenetic mechanisms. *Endins* 20: 71–86.
- Ginés J., 2000: El karst litoral en el Levante de Mallorca: una aproximación al conocimiento de su morfogénesis y cronología. Unpublished Ph. D. Thesis, Universitat de les Illes Balears, Palma de Mallorca, 595 p.
- Ginés J., Fornós J.J., 2004: Caracterització del carst del Migjorn. La seva contribució al modelat del territori. *Monografia de la Societat d'Història Natural de les Balears*, 11: 259–274.
- Ginsburg R. N., 1953: Intertidal erosion on the Florida Keys. *Bulletin of Marine Science Gulf and Caribbean* 3, 1: 55–69.
- Gladysz K., 1987: Karren on the Quatsino Limestone, Vancouver Island. B. Sc. Thesis, McMaster University, Hamilton, Ontario.
- Glew J. R., 1976: The simulation of rillenkarrren. Unpublished M. Sc. Thesis, McMaster University, Hamilton, Ontario, 116 p.
- Glew J. R., Ford D. C., 1980: A simulation study of the development of rillenkarrren. *Earth Surface Processes* 5, 1: 25–36.
- Godwin M., 1988: Broken River Karst: a speleological field guide, North Queensland. Unpublished report by Chillagoe Caving Club and Queensland National Parks and Wildlife Service, Cairns, 134 p.
- Goldie H. S., 1976: Limestone pavements: with special reference to North West England. Unpublished Ph. D. Thesis, Oxford University, Oxford.
- Goldie H. S., 1986: Human influences on landforms: the case of limestone pavements. In: Paterson K., Sweeting M. M. (Eds.), *New Directions in Karst*. Geobooks, Norwich, 515–540.
- Goldie H. S., 1993: The legal protection of limestone pavements in Great Britain. *Environmental Geology* 21: 160–166.
- Goldie H. S., 1995: Major protected sites of limestone pavement in Great Britain. *Acta Geographica Szegeiensis, Special Issue T 34*: 61–92.
- Goldie H. S., 1996: The limestone pavements of Great Asby Scar, Cumbria, U.K. *Environmental Geology* 28, 3: 128–136.
- Goldie H. S., 2005: Erratic judgments: re-evaluating solutional erosion rates of limestones using erratic-pedestal sites, including Norber, Yorkshire. *Area* 37, 4: 433–442.
- Goldie H. S., 2006: Mature intermediate-scale surface karst landforms in NW England and their relations to glacial erosion. In: Kiss A., Mezösi G., Sümeghy Z. (Eds.), *Táj, Környezet és Társadalom [Landscape, Environment and Society]*. Studies in Honour of Prof. Ilona Bárány-Kevei, Szeged, 225–238.
- Goldie H. S., Cox N. J., 2000: Comparative morphometry of limestone pavements in Switzerland, Britain and Ireland. *Zeitschrift für Geomorphologie, Supplementband* 122: 85–112.
- Golubić S., Friedmann E., Schneider J., 1981: The lithobiotic niche, with special reference to microorganisms. *Journal of Sedimentary Petrology* 51: 475–478.
- Golubić S., Perkins R. D., Lukas K. J., 1975: Boring micro-organisms and microborings in carbonate substrates. In: Frey R. W. (Ed.), *The Study of Trace Fossils*. Springer-Verlag, Berlin, 229–259.
- Gómez-Pujol L., Balaguer P., Baldo M., Fornós J. J., Pons G. X., Villanueva G., 2002: Patronos y tasas de erosión de Melaraphe neritoides (Linneo, 1875) en el litoral rocoso de Mallorca: resultados preliminares. In: Pérez-González A., Vegas J., Machado J. (Eds.), *Aportaciones a la Geomorfología de España en el Inicio del Tercer Milenio*. ITGE, Madrid, 351–354.
- Gómez-Pujol L., Fornós J. J., 2001: Les microformes de meteorització del litoral calcari de Mallorca: aproximació a la seva sistematització. *Endins* 24: 169–185.
- Gómez-Pujol L., Fornós J. J., 2004a: Forma, procesos y zonación en el lapiaz-karren-litoral del Sur de Menorca, 1: aproximación morfométrica. In: Benito G., Díaz A. (Eds.), *Contribuciones Recientes sobre Geomorfología*. SEG, CSIC, Madrid, 347–355.
- Gómez-Pujol L., Fornós J. J., 2004b: Les microformes litorals del Migjorn. In: Fornós J. J., Obrador A.,



- Rosselló V. M. (Eds.), *Història Natural del Migjorn de Menorca*. Bolletí de la Societat d'Història Natural de Balears 11: 245–258.
- González L. A., Ruiz H. M., Taggart B. E., Budd A. F., Monell V., 1997: Geology of Isla de Mona, Puerto Rico. In: Vacher H. L., Quinn T. (Eds.), *Geology and Hydrogeology of Carbonate Islands*. *Developments in Sedimentology* 54, Elsevier Science BV, 327–358.
- Goodchild M. F., Ford D. C., 1971: Analysis of scallop pattern by simulation under controlled conditions. *Journal of Geology* 79, 1: 52–62.
- Gosden M. S., 1968: Peat deposits of Scar Close, Ingleborough, Yorkshire. *Journal of Ecology* 56, 1: 345–353.
- Goudie A. S., 1974: Further experimental investigation of rock weathering by salt and other mechanical processes. *Zeitschrift für Geomorphologie, Supplementband* 21: 1–12.
- Goudie A. S., 1990: *The Landforms of England and Wales*. Blackwell, Oxford, 394 p.
- Goudie A. S., 1999: Experimental salt weathering of limestones in relation to rock properties. *Earth Surface Processes and Landforms* 24: 715–724.
- Goudie A. S., Bull P. A., Magee A. W., 1989: Lithological control of rillenkarrren development in the Napier Ranges, Western Australia. *Zeitschrift für Geomorphologie, Supplementband* 75: 95–114.
- Goudie A. S., Migon P., Allison R. J., Rosser N., 2002: Sandstone geomorphology of the Al-Quwayra area of south Jordan. *Zeitschrift für Geomorphologie* 46: 365–390.
- Goudie A. S., Viles H. A., 1997: *Salt Weathering Hazards*. Wiley, Chichester, 241 p.
- Goudie A. S., Viles H. A., 1999: The frequency and magnitude concept in relation to rock weathering. *Zeitschrift für Geomorphologie, Supplementband* 115: 175–189.
- Goudie A. S., Viles H. A., Allison R. J., Day M. J., Livingstone I. P., Bull P. A., 1990: The geomorphology of the Napier Range, Western Australia. *Transactions of the Institute of British Geographers* 15, 3: 308–322.
- Granger D. E., Fabel D., Palmer A. N., 2001: Pliocene-Pleistocene incision of the Green River, Kentucky, determined from radioactive decay of cosmogenic  $^{26}\text{Al}$  and  $^{10}\text{Be}$  in Mammoth Cave sediments. *Geological Society of America Bulletin* 113, 7: 825–836.
- Grimes K. G., 1978: Colless Creek and Lawn Hill Gorge, Down Under. *Newsletter of the University of Queensland Speleological Society* 17, 2: 45–49.
- Grimes K. G., 1988: The Barkly Karst Region, North-west Queensland. 17<sup>th</sup> Biennial Conference of the Australian Speleological Federation, Sydney, 16–24.
- Grimes K. G., 1990: Fanning River Karst Area: Notes on the geology and geomorphology. Queensland Department of Mines, Record 1990/7 (unpublished), 31 p.
- Grimes K. G., 1994: The South-East Karst Province of South Australia. *Environmental Geology* 23: 134–148.
- Grimes K. G., 2001: Karst features of Christmas Island (Indian Ocean). *Helictite* 37, 2: 41–58.
- Grimes K. G., 2002: Syngenetic and Eogenetic Karst: an Australian Viewpoint. In: Gabrovšek F. (Ed.), *Evolution of karst: from prekarst to cessation*. Karst Research Institute ZRC SAZU, Postojna, 407–414.
- Grimes K. G., 2004: Solution Pipes or Petrified Forests? Drifting sands and drifting opinions! *The Victorian Naturalist* 121, 1: 14–22.
- Grimes K. G., 2006: Syngenetic Karst in Australia: a review. *Helictite* 39, 2: 27–38.
- Grimes K. G., 2007: Microkarren in Australia – a request for information. *Helictite* 40, 1: 21–23.
- Grimes K. G., Spate A. P., 2008: Laterite Karst (Andysez No 53). *Australasian Cave and Karst Management Association Journal* 73: 49–52.
- Gross M. R., Fischer M. P., Engelder T., Greenfield R. J., 1995: Factors controlling joint spacing in interbedded sedimentary rocks: integrating numerical models with field observations from the Monterey Formation, USA. In: Ameen M. S. (Ed.), *Fractography: fracture topography as a tool in fracture mechanics and stress analysis*. Geological Society of London, Special Publication 92: 215–233.
- Guijarro J. A., 1986: *Contribución a la bioclimatología de las Baleares*. Unpublished Ph. D. Thesis, Universitat de les Illes Balears, Palma de Mallorca.
- Guijarro J. A., 1995: Bioclimatic aspects of karst in Mallorca. In: Ginés A., Ginés J. (Eds.), *Karst and caves in Mallorca*. *Endins* 20, Monographs of the Natural History Society of the Balearic Islands 3: 17–26.
- Guilcher A., 1952: Formes et processus d'érosion sur les récifs coralliens du nord du banc Farsan (Mer Rouge). *Revue de Géomorphologie Dynamique* 6: 261–274.
- Guilcher A., 1953: Essai sur la zonation et la distribution des formes littorales de dissolution du calcaire. *Annales de Géographie* 62: 161–179.
- Guilcher A., 1958: Coastal Corrosion Forms in Limestones Around the Bay of Biscay. *The Scottish Geographical Magazine* 74, 3: 137–149.
- Gunn J., 2004: *Encyclopedia of Caves and Karst Science*. Fitzroy Dearborn, New York, 902 p.
- Gustavson T. C., Holliday V. T., Hovorka S. D., 1995: Origin and Development of Playa Basins, Source of Recharge to the Ogallala Aquifer, Southern High

- Plains, Texas and New Mexico. Report of Investigations 229, Bureau of Economic Geology. University of Texas at Austin, 45 p.
- Habič P., 1980: S poti po kitajskem krasu. Summary: From the way to the Chinese karst. *Geografski vestnik* 52: 107–122.
- Habsburg-Lorena L. A., 1884–1891: Die Balearen in Wort und Bild Geschildert. Brockhaus, Leipzig.
- Hacquet B., 1785: Physikalisch-politische Reise aus den Dinarischen, durch die Julischen, Carnischen, Rhätischen in die Nordischen Alpen, im Jahre 1781 und 1783 unternommen. Böhme, Leipzig, 377–380.
- Hall R. L., Calder I. R., 1993: Drop size modification by forest canopies: measurements using a disdrometer. *Journal of Geophysical Research* 90: 465–470.
- Halley R. B., Muhs D. R., Shinn E. A., Dill R. F., Kindinger J. L., 1991: [abstract], A +1.5-m reef terrace in the southern Exuma Islands, Bahamas. *GSA Abstracts with Programs* 23, 1: 40.
- Halpern M., 1973: Regional geochronology of Chile, south of 50° latitude. *Geological Society of America, Bulletin* 84, 7: 2407–2422.
- Hamilton S. E., Holland E., Mott K., Spate A., 1989: Cutta Cutta Caves Nature Park – Draft Plan of Management. Unpublished report by the Australasian Cave Management Association for the Conservation Commission of the Northern Territory.
- Hantke R., 1961: Tektonik der helvetischen Kalkalpen zwischen Obwalden und dem St. Galler Rheintal. *Vierteljahresschrift Naturforschende Gesellschaft Zürich* 106, 1: 210 p.
- Hantoon P. W., 1997: Definition and characteristics of Stone forest epikarst aquifers in south China. *Proceedings of the 12<sup>th</sup> International Congress of Speleology* 1, 8: 311–314.
- Hartlieb M., 1999: Der oberirdische Karst im Gebiet des Dachsteins. <http://www.sbg.ac.at/geog/studenten/roth/se/manfred/manfred.html>.
- Haserodt K., 1965: Untersuchungen zur Höhen- und Altersgliederung der Karstformen in den Nördlichen Kalkalpen. *Münchener Geographische Hefte* 27, 114 p.
- Hauer F., 1867–1871: Geologische Übersichtskarte Österreichisch-Ungarischen Monarchie. Geologischen Reichsanstalt, Wien.
- Heim A., 1878: Über die Karrenfelder. *Jahrbuch des Schweizer Alpenclub* 13: 421–433.
- Heinemann U., Kaaden K., Pfeffer K. H., 1977: Neue Aspekte zum Phänomen der Rillenkaren. *Abhandlungen zur Karst- und Höhlenkunde, Reihe A*, 15: 56–80.
- Helgeson D. E., Aydin A., 1991: Characteristics of joint propagation across layer interfaces in sedimentary rocks. *Journal of Structural Geology* 13, 8: 897–911.
- Herwitz S. R., 1993: Stemflow influences on the formation of solution pipes in Bermuda eolianite. *Geomorphology* 6: 253–271.
- Higgins C. G., 1980: Nips, notches and the solution of coastal limestone: an overview of the problem with examples from Greece. *Estuarine and coastal marine science* 10: 15–30.
- Hinsinger P., Fernandes Barros O. N., Benedetti M. F., Noack Y., Callot G., 2001: Plant-induced weathering of a basaltic rock: Experimental evidence. *Geochimica et Cosmochimica Acta* 65: 137–152.
- Hobléa F., Jaillet S., Maire R., 2001: Érosion et ruissellement sur karst nu en context subpolaire sur les îles calcaires de Patagonie. *Karstologia* 38: 13–18.
- Hodgkin E. P., 1964: Rate of erosion of intertidal limestone. *Zeitschrift für Geomorphologie* 8, 4: 385–392.
- Hodgkin E. P., 1970: Geomorphology and biological erosion of limestone coasts in Malaysia. *Bulletin of the Geological Society of Malaysia* 3: 27–51.
- Holbye U., 1989: Bowl-karren in the littoral karst of Nord-Arnøy, Norway. *Cave Science* 16: 19–25.
- Hope G. S., 1976: Vegetation. In: Hope G. S., Peterson J. A., Radok U., Allison I. (Eds.), *Equatorial Glaciers of New Guinea*. Balkema, Rotterdam, 113–172.
- Hopley D., Mackay M. G., 1978: An investigation of Morphological Zonation of Beach Rock erosional features. *Earth Surface Processes* 3: 363–377.
- Horbury A. D., 1987: The relative roles of tectonism and eustasy in the deposition of the Urswick Limestone in South Cumbria and North Lancashire. In: Arthurton R. S., Gutteridge P., Nolan S. C. (Eds.), *The Role of Tectonism in Devonian and Carboniferous Sedimentation in the British Isles*. Yorkshire Geological Society, Occasional Publication 6: 153–169.
- Horoí V., 2001: L'influence de la Géologie sur la Karstification: Étude Comparative Entre le Massif Obarisia Closani – Piatra Mare (Roumanie) et le Massif d'Arbas (France). Thèse, Laboratoire souterrain de Moulis (CNRS) and Institut Emile Racovitz de Bucarest, 174 p.
- Humbert S. E., Driese S. G., 2001: Phased development of a subaerial paleokarst plane in upper Pennington Formation limestones (upper Mississippian) and associated paleokarst features. Poster presented during G. S. A. Big South Fork National Recreation Area, Tennessee, Annual Meeting, M. S. November 5–8, 2001. M. Sc. Thesis, 143 p.
- Hume W. F., 1925: *Geology of Egypt*. Government Press, Cairo, 408 p.
- Hunt C. O., 1996: Tafoni (pseudokarst) features in the Maltese Islands. *Cave and Karst Science* 23, 2: 57–62.

- Hutchinson D. W., 1996: Runnels, rinnenkarren and mäanderkarren: form, classification and relationships. In: Fornós J. J., Ginés A. (Eds.), *Karren Landforms*. Universitat de les Illes Balears, Palma de Mallorca, 209–223.
- Ivanović A., Sakač K., Marković S., Sokač B., Šušnjar M., Nikler L., Šušnjara A., 1973: Osnovna geološka karta SFRJ 1:100.000, List Obrovac L 33–140. Institut za geološka istraživanja, Zagreb, Savezni geološki zavod, Beograd.
- Jacobson G. J., Hill P. J., Ghassemi F., 1997: Geology and Hydrogeology of Nauru Island. In: Vacher H. L., Quinn T., (Eds.), *Geology and Hydrogeology of Carbonate Islands*. Developments in Sedimentology 54, Elsevier Science HV, 707–742.
- Jaillet S., Hobléa F., and l'équipe Ultima Patagonia, 2000: Une morphologie originale liée au vent: les "fusées" ou "crêtes éoliennes de lapiaz" de l'île Madre de Dios (Archipel Ultima Esperanza – Patagonie – Chili). Actes 10ème rencontre d'octobre du Spéléo-Club de Paris.
- Jakucs L., 1977: Morphogenetics of karst regions. Akadémiai Kiadó, Budapest, 284 p.
- Jakucs L., Keveiné-Bárány I., Mezősi G., 1983: A karsztkorrózió korszerű értelmezése. *Földrajzi Közlemények* 31, 107, 3–4: 213–217.
- Jakucs P., 1956: Karrosodás és növényzet. *Földrajzi Közlemények* 3: 241–249.
- James J., 1997: A comparison of the Stone Forest of Lunan with pinnacle karsts of the World. In: Song L., Waltham T., Cao N., Wang F. (Eds.), *Stone Forest: A Treasure of Natural Heritage*. Proceedings of the International Symposium for Lunan Shilin to Apply for World Natural Heritage Status. China Environmental Science Press, Beijing, 22–29.
- Jennings J. N., 1967: Some karst areas of Australia. In: Jennings J. N., Mabbutt J. A. (Eds.), *Landform Studies from Australia and New Guinea*. Australian National University Press, Canberra, 256–292.
- Jennings J. N., 1968: Syngenetic Karst in Australia. In: Williams P. W., Jennings J. N. (Eds.), *Contributions to the study of karst*. Australian National University, Department of Geography Publication G 5: 41–110.
- Jennings J. N., 1969: Karst of the seasonally humid tropics in Australia. In: Štelcl O. (Ed.), *Problems of the Karst Denudation*. Supplement for the 5<sup>th</sup> International Speleological Congress, Institute of Geography, Brno, 149–158.
- Jennings J. N., 1971: *Karst*. Australian National University Press, Canberra, 252 p.
- Jennings J. N., 1973: *Karst*. The M. I. T. Press, Cambridge, Massachusetts, London, 253 p.
- Jennings J. N., 1977: Limestone tablets experiments at Cooleman Plains, New South Wales, Australia, and their implications. *Abhandlungen zur Karst- und Höhlenkunde*, Reihe A, 15: 26–38.
- Jennings J. N., 1981: Morphoclimatic control: a tale of piss in the wind or a case of the baby out with the bath water? *Proceedings of the 8<sup>th</sup> International Congress of Speleology 1*, Bowling Green, 61–73.
- Jennings J. N., 1982: Karst of northeastern Queensland reconsidered. *Tower Karst*, Chillagoe Caving Club, Occasional Paper 4: 13–52.
- Jennings J. N., 1983: The disregarded karst of the arid and semiarid domain. *Karstologia* 1: 61–73.
- Jennings J. N., 1985: *Karst Geomorphology*. Basil Blackwell, New York, 293 p.
- Jennings J. N., Bik M.A., 1962: Karst morphology in Australian New Guinea. *Nature* 194: 1036–1038.
- Jennings J. N., Sweeting M. M., 1963: The limestone ranges of the Fitzroy Basin, Western Australia, a tropical semi-arid karst. *Bonner Geographische Abhandlungen* 32: 1–60.
- Jeschke A. A., Vosbeck K., Dreybrodt W., 2001: Surface controlled dissolution rates of gypsum in aqueous solutions exhibit nonlinear dissolution kinetics. *Geochimica et Cosmochimica Acta* 65: 27–34.
- Johansson M., Migon P., Olvmo M., 2001: Development of joint controlled rock basins in Bohus granite, SW Sweden. *Geomorphology* 40: 145–161.
- Jones B., 1989: The role of microorganisms in phytokarst development on dolostones and limestones, Grand Cayman, British West Indies. *Canadian Journal of Earth Sciences* 26: 2204–2213.
- Jones B., Hunter I. G., 1992: Very large boulders on the coast of Grand Cayman: the effects of giant waves on rocky coastlines. *Journal of Coastal Research* 8, 4: 763–774.
- Jones B., Pemberton S. G., 1987: The role of fungi in the diagenetic alteration of spar calcite. *Canadian Journal of Earth Sciences* 24: 903–914.
- Jones R. J., 1965: Aspects of the biological weathering of limestone pavements. *Proceedings of the Geologists' Association* 76: 421–433.
- Jones W. K., Culver D. C., Herman J. S., 2004: *Epikarst*. Karst Waters Institute, Charles Town, Special Publication 9, 160 p.
- Karp D., 2002: Land degradation associated with sink-hole development in the Katherine region. Resource Assessment Branch, Northern Territory Department of Infrastructure, Planning and Environment, Technical Report No. 11/2002, 53 p.
- Kashima N., Urushibara-Yoshino K., 1996: Karren development. Solutional erosion measurements by the limestone-tablet method in Shikoku Island, South-West Japan. In: Fornós J.J., Ginés A. (Eds.),

- Karren Landforms. Universitat de les Illes Balears, Palma de Mallorca, 65–73.
- Kaufmann G., Dreybrodt W., 2007: Calcite dissolution kinetics in the system  $\text{CaCO}_3\text{-H}_2\text{O-CO}_2$  at high undersaturation. *Geochimica et Cosmochimica Acta* 71, 6: 1398–1410.
- Kaye C. A., 1959: Shoreline features and Quaternary shoreline changes, Puerto Rico. U. S. Geological Survey Professional Paper 317-B: 49–140.
- Kelletat D., 1980: Formenschatz und Prozessgefüge des "Biokarstes" an der Küste von Nordost-Mallorca (Cala Guya). *Berliner Geographische Studien* 7: 99–113.
- Kelletat D., 1985: Bio-destruktive und bio-konstruktive Formelemente an den spanischen Mittelmeerküsten. *Geodynamik* 6: 1–20.
- Kelletat D., 1991: The 1550 B.P. tectonic event in the Eastern Mediterranean as a basis for assessing the intensity of shore processes. *Zeitschrift für Geomorphologie, Supplementband* 81: 181–194.
- Kerr A., 1983: Rock temperature measurements from southeast Morocco, and their implications for weathering and weathering forms. Unpublished B. Sc. Thesis, Queen's University, Belfast, 136 p.
- Kershaw S., Guo L., 2001: Marine notches in coastal cliffs: indicators of relative sea-level change, Parachora Peninsula, Central Greece. *Marine Geology* 179: 213–228.
- Kinahan G. H., Nolan J., 1870: Explanation to accompany map sheet 95 of the Geological Survey of Ireland. *Memoirs of the Geological Survey of Ireland*, Dublin.
- Kindler P., Hearty P. J., 1995: Pre-Sangamonian eolianites in the Bahamas? New evidence from Eleuthera Island. *Marine Geology* 127: 73–86.
- Kinnell P. I., 1987: Rainfall Energy in Eastern Australia: Intensity-Kinetic Energy Relationships. *Australian Journal of Soil Research* 25: 547–553.
- Kirchhofer W., 1982: Mittlere Jahrestemperaturen. *Klimaatlas der Schweiz*, sheet 6.1.
- Kirchhofer W., Sevruck B., 1991: Mittlere jährliche korrigierte Niederschlagshöhen 1951–1980. *Hydrologischer Atlas der Schweiz*, sheet 2.2.
- Kirigin B., 1967: Klimatske karakteristike Sjevernog Velebita. *Zbornik radova X kongresa klimatologa Jugoslavije*, Kopaonik, Beograd, 189–206.
- Klimchouk A. B., 2000a: Dissolution and conversion of gypsum and anhydrite. In: Klimchouk A. B., Ford D. C., Palmer A. N., Dreybrodt W. (Eds.), *Speleogenesis: Evolution of Karst Aquifers*. National Speleological Society, Huntsville, Alabama, 160–168.
- Klimchouk A. B., 2000b: Types of karst and evolution of hydrogeologic sections. In: Klimchouk A. B., Ford D., Palmer A., Dreybrodt W. (Eds.), *Speleogenesis: Evolution of Karst Aquifers*. National Speleological Society, Huntsville, Alabama, 45–53.
- Klimchouk A. B., 2000c: The formation of epikarst and its role in vadose speleogenesis. In: Klimchouk A. B., Ford D. C., Palmer A. N., Dreybrodt W. (Eds.), *Speleogenesis: Evolution of Karst Aquifers*. National Speleological Society, Huntsville, Alabama, 91–99.
- Klimchouk A. B., Ford D. C., Palmer A. N., Dreybrodt W., 2000: *Speleogenesis: Evolution of Karst Aquifers*. National Speleological Society, Huntsville, Alabama, 527 p.
- Knez M., 1998: Lithologic Properties of the Three Lunan Stone Forests (Shilin, Naigu and Lao Hei Gin). In: Chen X., Gabrovšek F., Huang C., Jin Y., Knez M., Kogovšek J., Liu H., Petrič M., Mihevc A., Otoničar B., Shi M., Slabe T., Šebela S., Wu W., Zhang S., Zupan Hajna N., 1998: *South China Karst I*. Založba ZRC, Ljubljana, 30–43.
- Knez M., Slabe T., 2001a: Oblika in skalni relief stebrov v Naigu kamnitem gozdu (JZ Kitajska). *Acta Carsologica* 30, 1: 13–24.
- Knez M., Slabe T., 2001b: The lithology, shape and rock relief of the pillars in the Pu Chao Chun stone forest (Lunan stone forests, SW China). *Acta Carsologica* 30, 2: 129–139.
- Knez M., Slabe T., 2002: Lithologic and morphological properties and rock relief of the Lunan stone forests. In: Gabrovšek F. (Ed.), *Evolution of karst: from prekarst to cessation*. Karst Research Institute ZRC SAZU, Postojna, 259–266.
- Kogovšek J., Kranjc A., Slabe T., Šebela S., 1999: *South China Karst 1999*, Preliminary research in Yunnan. *Acta Carsologica* 28, 2: 225–240.
- Komac B., 2001: The karst springs of the Kanin massif [Kraški izviri pod Kaninskim pogorjem]. *Geografski zbornik* 41: 7–43.
- Kondic L., 2003: Instabilities in Gravity Driven Flow of Thin Fluid Films. *Society for Industrial and Applied Mathematics Review* 45, 1: 95–115.
- Körner C., 1999: *Alpine Plant Life – Functional Plant Ecology of High Mountain Ecosystems*. Springer-Verlag, Berlin, Heidelberg, 343 p.
- Kunaver J., 1973a: O razvoju slovenske terminologije za mikroreliefne kraške oblike [On the development of the Slovene terminology of the Karst microrelief]. In: Gams I., Kunaver J., Radinja D. (Eds.), *Slovenska kraška terminologija [Slovene Karst Terminology]*. Oddelek za geografijo Filozofske fakultete, Ljubljana, 68–76.
- Kunaver J., 1973b: The High Mountainous Karst of the Julian Alps in the System of Alpine Karst. *IGU*

- European regional conference, Symposium on karst-morphogenesis, Papers, Budapest, 209–225.
- Kunaver J., 1976: Kotlič – a Specific Depression Form of Subnival Alpine Karst. Proceedings of the 6<sup>th</sup> International Congress of Speleology, Academia, Praha, 223–230.
- Kunaver J., 1983: Geomorphology of the Kanin Mountains with special regard to the glaciokarst. *Geografski zbornik* 22: 197–346.
- Kunaver J., 1984: The high mountains karst in the Slovene Alps. *Geographica Yugoslavica* 5, Ljubljana, 15–22.
- Kunaver J., 1985: Relief. In: "Fabjan I. (ed.), Triglavski narodni park. Vodnik, Bled, 29–56.
- Kunaver J., 1991: Corrosion terraces as geoecological response to postglacial development of glaciokarstic rock surface. In: Proceedings of the International conference on environmental changes in karst areas. 13 Quaderni del dipartimento di geografia, Università di Padova, 325–331.
- Kunaver J., 1998: Karst of the Kanin-mountain. Alpine Karst, Guide-booklet for the excursions and abstracts of the papers. 6<sup>th</sup> International Karstological School, Classical karst. Speleological Association of Slovenia and Karst Research Institute ZRC SAZU, Postojna, 12–16.
- Kurtz H. D., Netoff D. I., 2001: Stabilization of friable sandstone surfaces in a desiccating, wind-abraded environment of south-central Utah by rock surface microorganisms. *Journal of Arid Environments* 48: 89–100.
- Kuščer I., Kodre A., 1994: Matematika v fiziki in tehniki. Društvo matematikov, fizikov in astronomov Slovenije, Ljubljana, 194–199.
- Laczay L., 1982: A folyószabályozás tervezésének morfológiai alapjai. *Vízügyi Közl* 25: 235–254.
- Langridge D., 1971: Limestone pavement patterns on the island of Inishmore, County Galway. *Irish Geography* 3: 282–293.
- Laudermilk J. D., Woodford A. O., 1932: Concerning rillensteine. *American Journal of Science* 223: 135–154.
- Lauritzen S. E., 1981: Simulation of Rock Pendants – Small Scale Experiments on Plaster Models. Proceedings of the 8<sup>th</sup> International Congress of Speleology, Georgia, 407–411.
- Lauritzen S. E., Karp D., 1993: Speleological assessment of karst aquifers developed within the Tindall Limestone, Katherine N.T., Power and Water Authority, NT. Report 63/1993 (unpublished).
- Laverty M., 1980: Water chemistry in the Gunung Mulu National Park, including problems of interpretation and use. *Geographical Journal* 146, 2: 232–245.
- Ley R. G., 1977: The Influence of Lithology on Marine Karren. *Abhandlungen zur Karst- und Höhlenkunde, Reihe A*, 15: 81–100.
- Ley R.G., 1979: The Development of Marine Karren Along the Bristol Channel Coastline. *Zeitschrift für Geomorphologie, Supplementband* 32: 75–89.
- Ley R. G., 1980: The pinnacles of Gunung Api. *Geographical Journal* 146, 1: 14–21.
- Liang F., Song L., Tang T., 2003: Microbial production of CO<sub>2</sub> in red soil in Stone Forest National Park. *Journal of Geographical Sciences* 13, 2: 250–256.
- Liang F., Song L., Wang F., Zheng B., Zhang L., 2000: The case study of subsoil solution features and soil CO<sub>2</sub> concentration in Stone Forest Region, Lunan, Yunnan, China. *Carsologica Sinica* 19: 187–193.
- Liechti P., Roe R. W., Haile N. S., 1960: The geology of Sarawak, Brunei and the western part of North Borneo British Territory of Borneo. *Bulletin of the Geological Survey Department* 3 (2 volumes), 360 p.
- Lin J., 1997: Genesis of Lunan Stone Forest and its Geomorphological Significance. In: Song L., Waltham T., Cao N., Wang F. (Eds.), *Stone Forest: A Treasure of Natural Heritage*. Proceedings of the International Symposium for Lunan Shilin to Apply for World Natural Heritage Status. China Environmental Science Press, Beijing, 30–33.
- Linton D. L., 1963: The Forms of Glacial Erosion. *Transactions of the Institute of British Geographers* 33: 1–28.
- Linton D. L., 1964: The origin of the Pennine tors – an essay in analysis. *Zeitschrift für Geomorphologie* 8: 5–24.
- Löffler E., 1977: Geomorphology of Papua New Guinea. Scientific and Industrial Research Organization in association with Australian National University Press, Canberra, 195 p.
- Longman M. W., Brownlee D. N., 1980: Characteristics of karst topography, Palawan, Philippines. *Zeitschrift für Geomorphologie* 24: 299–317.
- Louis H., 1968: *Allgemeine Geomorphologie*. Walter de Gruyter, Berlin, 522 p.
- Lowry D. C., 1973: Origin of the Pinnacles. *Australian Speleological Federation Newsletter* 62: 7–8.
- Lozano R., 1884: *Anotaciones físicas y geológicas de la Isla de Mallorca*. Excm. Diputación Provincial de Baleares. Imprenta de la Casa de Misericordia, Palma de Mallorca, 68 p.
- Lundberg J., 1974: The karren of the littoral zone, Burren District, Co. Clare, Ireland. Unpublished B. Sc. Thesis, Trinity College, Dublin.
- Lundberg J., 1977a: The geomorphology of Chillagoe limestones: variations with lithology. Unpublished

- M. Sc. Thesis, Australian National University, Canberra, 175 p.
- Lundberg J., 1977b: An analysis of the form of rillenkarrren from the tower karst of Chillagoe, Northern Queensland, Australia. Proceedings of the 7<sup>th</sup> International Congress of Speleology, Sheffield, 294–296.
- Lundberg J., 1977c: Karren of the littoral zone, Burren District, Co. Clare, Ireland. Proceedings of the 7<sup>th</sup> International Speleological Congress, Sheffield, 291–293.
- Lundberg J., 2004: Coastal Karst. In: Gunn J. (Ed.), Encyclopedia of Cave and Karst Science. Fitzroy Dearborn, New York, London, 231–233.
- Lundberg J., Lauritzen S. E., 2002: The search for an arctic coastal karren model in Norway and Spitzbergen. In: Hewitt K., Byrne M. L., English M., Young G. (Eds.), Landscapes of Transition: Landform assemblages and transformations in cold regions. Kluwer Academic Publishers, The GeoJournal Library 68: 183–203.
- Lundberg J., Taggart B. E., 1995: Dissolution pipes in northern Puerto Rico: an exhumed paleokarst. Carbonates and Evaporites 10, 2: 171–183.
- Ma X., 1936: Preliminary investigation on the Lunan stone forest, Yunnan, from the geomorphological view. Theoretical Review 1, 1.
- Macaluso T., Madonia G., Palmeri A., Sauro U., 2001: Atlante dei karren nelle evaporiti della Sicilia [Atlas of the karren in the evaporitic rocks of Sicily]. Quaderni del Museo Geologico "G.G. Gemmellaro" 5, Dipartimento di Geologia e Geodesia, Università degli Studi di Palermo, 143 p.
- Macaluso T., Madonia G., Sauro U., 2003: Le forme di soluzione nei gessi. In: Madonia G., Forti P. (Eds.), Le aree carsiche gessose d'Italia. Memorie Istituto Italiano di Speleologia 2, 14: 55–64.
- Macaluso T., Sauro U., 1996a: The karren in evaporitic rocks: a proposal of classification. In: Fornós J. J., Ginés A. (Eds.), Karren Landforms. Universitat de les Illes Balears, Palma de Mallorca, 277–293.
- Macaluso T., Sauro U., 1996b: Weathering crust and karren on exposed gypsum surfaces. International Journal of Speleology 25, 3–4: 115–126.
- Macaluso T., Sauro U., 1998a: Aspects of weathering and landforms evolution on gypsum slopes and ridges of Sicily. Geografia Fisica Dinamica Quaternaria, Supplement 3, 4: 91–99.
- Macaluso T., Sauro U., 1998b: I Karren nei gessi di Verzino. In: Ferrini G. (Ed.), L'area carsica delle Vigne di Verzino. Memorie Istituto Italiano di Speleologia 2, 10: 35–45.
- Macfayden W. A., 1930: The undercutting of coral reef limestone on the coasts of some islands in the Red Sea. Geographical Journal 75: 27–34.
- Maire R., 1990: La haute montagne calcaire. Karsts, cavités, remplissages, quaternaire, paleoclimats. Karstologia-Mémoires 3, Association Française de Karstologie et Fédération Française de Spéléologie, La Ravoire, 731 p.
- Maire R., 1999: Les glaciers de marbre de Patagonie. Un karst subpolaire océanique de la zone australe. Karstologia 33: 25–40.
- Maire R., 2004: Patagonia marble karst (Chile). In: Gunn J. (Ed.), Encyclopedia of Cave and Karst Science. Fitzroy Dearborn, New York, 57–577.
- Maire R., Pernet J. F., Fage L. H., 1999: Les "glaciers de marbre" de Patagonie, Chili; un karst subpolaire océanique de la zone australe [The "marble glaciers" of the Chilean Patagonia; example of a subpolar oceanic karst in the austral zone]. Karstologia 33: 25–40.
- Maire R., Zhang S., Song S., 1991: Génese des karsts subtropicaux de Chine du sud (Guizhou, Sichuan, Hubei). Grottes et karsts tropicaux de Chine Méridionale, Karstologia mémoires 4: 162–186.
- Malis C. P., 1997: Littoral karren along the western shore of Newfoundland. Unpublished M. Sc. Thesis, McMaster University, Hamilton, Ontario, 310 p.
- Malis C. P., Ford D. C., 1995: Littoral karren along the western shore of Newfoundland. Geological Society of America, Abstracts with Programs 27, 6: A 9–56.
- Malott C. A., 1945: Significant features of the Indiana karst. Indiana Academy of Science Proceedings 54: 8–24.
- Mamužić P., Milan A., Korolija B., Borović I., Majcen Ž., 1969: Osnovna geološka karta SFRJ 1:100.000, List Rab L 33–114. Institut za geološka istraživanja, Zagreb, Savezni geološki zavod, Beograd.
- Mangin A., 1997: Some features of the Stone forest of Lunan, Yunnan, China. In: Song L., Waltham T., Cao N., Wang F. (Eds.), Stone Forest: A Treasure of Natural Heritage. Proceedings of the International Symposium for Lunan Shilin to Apply for World Natural Heritage Status. China Environmental Science Press, Beijing, 68–70.
- Mariko S., Bekku Y., Koizumi H., 1994: Efflux of carbon dioxide from snow covered forest floors. Ecological Research 9: 343–350.
- Marker M. E., 1976a: Note on some South African pseudokarst. Bollettino Sociedad Venezolana Espeleologia 7: 5–12.
- Marker M. E., 1976b: A Geomorphological Assessment of the Chillagoe Karst Belt, Queensland. Helictite 14, 1: 31–49.
- Marker M. E., 1985: Factors controlling micro-solu-

- tional karren on carbonate rocks of the Griqualand West sequence. *Cave Science* 12, 2: 61–65.
- Marsico A., Selleri G., Mastronuzzi G., Sanso P., Walsh N., 2003: Cryptokarst: a case-study of the Quaternary landforms of southern Apulia (southern Italy). *Acta Carsologica* 32, 2: 147–159.
- Martel E. A., 1921: *Nouveau traité des eaux souterraines*. Doin, Paris, 838 p.
- Martini I. P., 1978: Tafoni weathering with examples from Tuscany, Italy. *Zeitschrift für Geomorphologie* 22: 44–67.
- Matičec D., Fuček L., Oštrić N., Sokač B., Velić I., Vlahović I., Ženko T., 1999: Geološka građa Velebita duž trase cestovnog tunela “Sv. Rok”. Field-trip guidebook. Geotrip, Hrvatsko geološko društvo, Zagreb, 1–20.
- Matsukura Y., Matsuoka N., 1991: Rates of tafoni weathering on uplifted shore platforms in Nojima-zaki, Boso Peninsula, Japan. *Earth Surface Processes and Landforms* 16: 51–56.
- Matsukura Y., Matsuoka N., 1996: The effect of rock properties on rates of tafoni growth in coastal environments. *Zeitschrift für Geomorphologie, Supplementband* 106: 57–72.
- Mazari R. K., 1988: Himalayan karst – karren in Kashmir. *Zeitschrift für Geomorphologie* 32, 2: 163–178.
- Mazzanti R., Parea G. C., 1979: Erosione della “panchina” sui litorali di Livorno e di Rosignano. *Bolletino Società Geologica Italiana* 96: 457–489.
- McCabe A. M., 1987: Quaternary deposits and glacial stratigraphy in Ireland. *Quaternary Science Reviews* 6: 259–299.
- McKee E. D., Ward W. C., 1983: Eolian Environment. In: Scholle P. A., Bebout D. E., Moore C. H. (Eds.), *Carbonate depositional environments*. American Association of Petroleum Geologists Memoir 33: 131–170.
- McNamara K. J., 1995: *Pinnacles* (revised edition). Western Australian Museum, Perth, 24 p.
- Melim L. A., Masaferrro J. L., 1997: Geology of the Bahamas: Subsurface geology of the Bahamas banks. In: Vacher H. L., Quinn T. M. (Eds.), *Geology and Hydrogeology of Carbonate Islands*. Elsevier, Amsterdam, 161–182.
- Mensingh H., 1955: Karst und Terra-Rossa auf Mallorca. *Erdkunde* 9: 188–196.
- Meyerhoff A. A., Hatten C. W., 1974: Bahamas salient of North America: Tectonic framework, stratigraphy, and petroleum potential. *American Association of Petroleum Geologists, Bulletin* 58: 1201–1239.
- Migon P., Dach W., 1995: Rillenkarrren on granite outcrops, S.W. Poland, age and significance. *Geografiska* 77 A, 1–2: 1–9.
- Mihevc A., 2001: *Speleogeneza Divaškega krasa*. Zbirka ZRC 27, Založba ZRC, Ljubljana, 180 p.
- Mikulas R., 1999: The protective effect of lichens and the origin of modern bulge-like traces on weakly lithified sandstones (Hilbre Islands, Wirral Peninsula, Great Britain). *Ichnos* 6: 261–268.
- Miotke F. D., 1974: Carbon dioxide and the soil atmosphere. *Abhandlungen zur Karst- und Höhlenkunde, Reihe A*, 9: 1–49.
- Moe D., Johannessen P. J., 1980: Formation of cavities in calcareous rocks in the littoral zone of northern Norway. *Sarsia* 65: 227–232.
- Monroe W. H., 1970: *A Glossary of Karst Terminology*. Geological Survey Water-Supply Paper, 1899-K: 1–26.
- Moseley F., 1972: A tectonic history of northwest England. *Journal of the Geological Society of London* 128: 561–598.
- Moses C. A., 2003: Observations on coastal biokarst, Hells Gate, Lord Howe Island, Australia. *Zeitschrift für Geomorphologie* 47: 83–100.
- Moses C. A., Smith B. J., 1993: A note on the role of *Collema auriforma* in solution basin development on a Carboniferous limestone substrate. *Earth Surface Processes and Landforms* 18: 363–368.
- Moses C. A., Smith B. J., 1994: Limestone weathering in the supra-tidal zones: an example from Mallorca. In: Robinson D. A., Williams R. B. G. (Eds.), *Rock Weathering and Landform Evolution*. John Wiley and Sons, Chichester, 433–451.
- Moses C., Spate A. P., Smith D. I., Greenaway M. A., 1995: Limestone weathering in eastern Australia. Part 2: Surface micromorphology study. *Earth Surface Processes and Landforms* 20: 501–514.
- Moses C. A., Viles H. A., 1996: Nanoscale morphologies and their role in the development of karren. In: Fornós J. J., Ginés A. (Eds.), *Karren Landforms*. Universitat de les Illes Balears, Palma de Mallorca, 85–96.
- Mottershead D. N., 1996a: A study of solution flutes (Rillenkarrren) at Lluc, Mallorca. *Zeitschrift für Geomorphologie, Supplementband* 103: 215–241.
- Mottershead D. N., 1996b: Some morphological properties of solution flutes (Rillenkarrren) at Lluc, Mallorca. In: Fornós J. J., Ginés A. (Eds.), *Karren Landforms*. Universitat de les Illes Balears, Palma de Mallorca, 225–238.
- Mottershead D. N., Lucas G. R., 2000: The role of lichens in inhibiting erosion of a soluble rock. *Lichenologist* 2000: 601–609.
- Mottershead D. N., Lucas G. R., 2001: Field testing of Glew and Ford's model of solution flute evolution. *Earth Surface Processes and Landforms* 26: 839–846.

- Mottershead D. N., Lucas G. R., 2004: The role of mechanical and biotic processes in solution flute development. In: Smith B. J., Turkington A. V. (Eds.), *Stone decay: its causes and control*. Donhead Publishing, London, 273–291.
- Mottershead D. N., Moses C. A., Lucas G. R., 2000: Lithological control of solution flute form: a comparative study. *Zeitschrift für Geomorphologie* 44, 4: 491–512.
- Mottershead D. N., Pye K., 1994: Tafoni on coastal slopes, South Devon, U. K. *Earth Surface Processes and Landforms* 19: 543–563.
- Mottershead D. N., Viles H. A., 2004: Experimental studies of rock weathering by plant roots: Updating the work of Julius Sachs (1832-1897). In: Mitchell D. J., Searle D. E. (Eds.), *Stone Deterioration in Polluted Urban Environments*. Scientific Publishing, Plymouth, 61–72.
- Murphy P. J., Lord T., 2003: *Victoria Cave, Yorkshire, UK: new thoughts on an old site*. *Cave and Karst Science* 30, 2: 83–88.
- Murray A. N., Love W. W., 1930: Action of organic acids upon limestone. *The American Association of Petroleum Geologists Bulletin* 13: 1467–1475.
- Mustoe G. E., 1983: Cavernous weathering in the Capitol Reef Desert, Utah. *Earth Surface Processes and Landforms* 8: 517–526.
- Myers T. G., 2002: Modelling laminar sheet flow over rough surfaces. *Water Resources Research* 38, 11: 1230.
- Myroie J. E., Carew J. L., 1995: Karst development on carbonate islands. In: Budd D. A., Harris P. M., Saller A. (Eds.), *Unconformities and Porosity in Carbonate Strata*. American Association Petroleum Geologists, Memoir 63: 55–76.
- Myroie J. E., Jenson J. W., Taboroši D., Jocson J. M. U., Vann D. T., Wexel C., 2001: Karst Features of Guam in Terms of a General Model of Carbonate Island Karst. *Journal of Cave and Karst Studies* 63, 1: 9–22.
- Myroie J. E., Vacher H. L., 1999: A conceptual view of carbonate island karst. In: Palmer A. N., Palmer M. V., Sasowsky I. D. (Eds.), *Karst Waters*. Karst Waters Institute Special Publication 5: 48–57.
- Narr W., Suppe J., 1991: Joint spacing in sedimentary rocks. *Journal of Structural Geology* 3, 9: 1037–1048.
- Naylor L. A., Viles H. A., 2002: A new technique for evaluating short-term rates of coastal bioerosion and bioprotection. *Geomorphology* 47: 31–44.
- Nelhans G., Svensson P., 1997: Some small-scale weathering structures in the Sidi Bouzid area, central Tunisia. *The virtual Geomorphology*, <http://user.tninet.se/~bgb354w/home/Tunisien.htm>.
- Neumann A. C., 1966: Observations on coastal erosion in Bermuda and measurements of the boring rate of the sponge *Cliona lampa*. *Limnology and Oceanography* 11: 92–108.
- Newell N. D., 1961: Recent terraces of tropical limestone shores. *Zeitschrift für Geomorphologie, Supplementband* 3: 87–106.
- Newell N. D., Imbrie J., 1955: Biogeological reconnaissance in the Bimini area, Great Bahama Bank. *Transactions of the New York Academy of Sciences* 18: 3–14.
- Newson M. D., 1970: *Studies in chemical and mechanical erosion by streams in limestone terrains*. Ph. D. Thesis, University of Bristol, Bristol.
- Nicod J., 1976: Corrosion de type crypto-karstique dans les karst méditerranéens. In: *Karst Processes and Relevant Landforms*. Department of Geography, Philosophical Faculty, Ljubljana, 171–179.
- Ogorelec B., 1996: Dachstein Limestone from Krn in Julian Alps (Slovenia). *Geologija* 39: 133–157.
- Ollier C., 1984: *Weathering*. Longman, London, New York, 270 p.
- Oluic M., Grandić S., Haček M., Hanich M., 1972: Tektonska građa vanjskih Dinarida Jugoslavije. *Nafta* 23, 1–2: 3–16.
- Osmaston H. A., 1980: Patterns in trees, rivers and rocks in the Mulu Park, Sarawak. *Geographical Journal* 146, 1: 33–50.
- Osmaston H. A., Sweeting M. M., 1982: Geomorphology. In: Jermy A. C., Kavanagh K. P. (Eds.), *Gunung Mulu National Park, Sarawak*. Sarawak Museum Journal (Special Issue 2) 30, 51: 75–93.
- Pace M. C., Myroie J. E., Carew J. L., 1993: Investigation and review of dissolution features on San Salvador Island, Bahamas. In: White B. (Ed.), *Proceedings of the 6th Symposium on the Geology of the Bahamas*. Bahamian Field Station, Port Charlotte, Florida, 109–123.
- Palmer A. N., 1975: The origin of maze caves. *National Speleological Society Bulletin* 57: 56–76.
- Palmer A. N., 1991: Origin and morphology of limestone caves. *Geological Society of America Bulletin* 103: 1–21.
- Palmer M., Fornós J. J., Balaguer P., Gómez-Pujol L., Pons G. X., Villanueva G., 2003: Spatial and seasonal variability of the macro-invertebrate community of a rocky coast in Mallorca (Balearic Islands): implications for bioerosion. *Hydrobiologia* 501: 13–21.
- Palmer M., Palmer A. N., 1975: Landscape development in the Mitchell Plain of southern Indiana. *Zeitschrift für Geomorphologie* 19, 1: 1–39.
- Panuska B. C., Myroie J. E., Carew J. L., 1999: Paleomagnetic evidence for three Pleistocene paleosols on San Salvador Island, Bahamas. In: Curran H. A.,



- Mylroie J. E. (Eds.), Proceedings of the 9<sup>th</sup> Symposium on the Geology of the Bahamas, Bahamian Field Station, San Salvador Island, Bahamas, 93–100.
- Papida S., Murphy W., May E., 2000: Enhancement of physical weathering of building stones by microbial populations. *International Biodeterioration and Biodegradation* 46: 305–317.
- Paradise T., 1997: Disparate sandstone weathering beneath lichens, Red Mountain, Arizona. *Geografiska Annaler* 79: 177–184.
- Parry J. T., 1960: Limestone pavements of North West England. *Canadian Geographer* 15: 41–21.
- Paterson K., Sweeting M. M. (Eds.), 1986: *New Directions in Karst*. Geobooks, Norwich, 613 p.
- Pearson L. M., 1982: Chillagoe karst solution and weathering. Tower Karst, Chillagoe Caving Club, Occasional Paper 4: 58–70.
- Perica D., 1998: *Geomorfologija krša Velebita*. Doctoral Thesis, University of Zagreb, Zagreb, 251 p.
- Perica D., Kukić B., 1992: Karren on the South Velebit Range. International Symposium “Geomorphology and Sea”, Mali Lošinj. Zagreb, 153–157.
- Perica D., Kukić B., Trajbar S., 1995: Egzokrške osobine Nacionalnog parka Paklenica. *Paklenički zbornik* 1, Starigrad-Paklenica, 65–69.
- Perica D., Marjanac T., Aničić B., Mrak I., Juračić M., 2004: Small karst features (karren) of Dugi Otok island and Kornati Archipelago coastal karst (Croatia). *Acta Carsologica* 33: 117–130.
- Perica D., Marjanac T., Mrak I., 1999: Vrste grizina i njihov nastanak na području Velebita. *Acta Geographica Croatica* 34: 31–58.
- Perica D., Orešić D., 1997: Prilog poznavanju klimatskih obilježja Velebita. *Acta Geographica Croatica* 32: 45–68.
- Perica D., Orešić D., 1999: Klimatska obilježja Velebita i njihov utjecaj na oblikovanje reljefa. *Senjski zbornik* 26: 1–50.
- Perna G., Sauro U., 1978: Atlante delle microforme di dissoluzione carsica superficiale del Trentino e del Veneto. *Memorie del Museo Tridentino di Scienze Naturali* 22, Trento, 176 p.
- Perna G., Sauro U., 1981: Types morphologiques du Rosso Ammonitico dans le Trentino et le Veneto. In: Farinacci A., Elmi S. (Eds.), *Rosso Ammonitico Symposium Proceedings*. Tecnoscienza, Roma, 541–546.
- Peter C., 2001: Deep into the land of extremes. Probing Chile's wild coast. *National Geographic*, 2–19.
- Peterson J. A., 1982: Limestone pedestals and denudation estimates from mountain Jaya, Irian Jaya. *Australian Geographer* 15: 170–173.
- Petterson O., 2001: The development of a technique to measure water film thickness and the study of flow hydraulics and dissolutional characteristics on plaster of Paris rillenkarren channels. B. Sc. Thesis, School of Geographical Sciences, University of Bristol, Bristol.
- Peyrot-Clausade M., Le Campion T., Harmelin M., Romano J. C., Chazottes V., Pari N., Le Campion J. L., 1995: La bioérosion dans le cycle des carbonates: essais de quantification des processus en Polynésie française. *Bulletin de la Société Géologique de France* 1: 85–94.
- Phelps H. O., 1975: Shallow laminar flows over rough granular surfaces. *Journal of the Hydraulics Division* 101, 3: 367–384.
- Pigott C. D., 1962: Soil formation and development on the carboniferous limestone of Derbyshire. I. Parent materials. *Journal of Ecology* 50: 145–156.
- Pigott C. D., 1970: Soil formation and development on the carboniferous limestone of Derbyshire. II. The relation of soil development to vegetation on the plateau near Coombs Dale. *Journal of Ecology* 58: 528–541.
- Pirnat J., 2002: Speleology on Kanin. Soški razgovori 1, Proceedings for Regional Studies of the History Section of the Cultural Association Golobar, Bovec, 77–98.
- Playford P. E., 1980: Devonian “Great Barrier Reef” of Canning Basin, Western Australia. *American Association of Petroleum Geologists, Bulletin* 64, 6: 814–840.
- Playford P. E., 2002: Palaeokarst, pseudokarst, and sequence stratigraphy in Devonian reef complexes of the Canning Basin, Western Australia. In: Keep M., Moss S. J. (Eds.), *The Sedimentary Basins of Western Australia 3*. Petroleum Exploration Society of Australia, Symposium, Perth, W. A., 763–793.
- Pluhar A., Ford D. C., 1970: Dolomite karren of the Niagara Escarpment, Ontario, Canada. *Zeitschrift für Geomorphologie* 14, 4: 392–410.
- Plummer L. N., Wigley T. M. L., 1976: The dissolution of calcite in CO<sub>2</sub>-saturated solutions at 25°C and 1 atmosphere total pressure. *Geochimica et Cosmochimica Acta* 40: 191–202.
- Plummer L. N., Wigley T. M. L., Parkhurst D.L., 1978: The kinetics of calcite dissolution in CO<sub>2</sub>-water systems at 5° to 60°C and 0.0 to 1.0 atm CO<sub>2</sub>. *American Journal of Science* 278: 179–216.
- Poljak J., 1929a: Geomorfološki oblici krednih kršnika Velebita. *Vijesti Geološkog zavoda* 3: 53–85.
- Poljak J., 1929b: *Planinarski vodič po Velebitu*. Hrvatsko planinarsko društvo, 277 p.
- Pomar L., Esteban M., Llimona X. M., Fontarnau R., 1975: Acción de líquenes, algas y hongos en la telodi-

- agénesis de las rocas carbonatadas de la zona prelitoral catalana. Instituto de Investigaciones Geológicas 30: 83–117.
- Pomar L., Obrador A., Westphal H., 2002: Sub-wase-base cross-bedded grainstone on distally steepened carbonate ramp, Upper Miocene, Menorca, Spain. *Sedimentology* 49: 139–169.
- Pomar L., Ward W. C., 1999: Reservoir-scale heterogeneity in depositional packages and diagenetic patterns on a reef-rimmed platform, Upper Miocene, Mallorca, Spain. *American Association of Petroleum Geologists, Bulletin* 83: 1579–1773.
- Powell R. L., 1961: Caves of Indiana. *Indiana Geological Survey* 8: 1–127.
- Powell R. L., 1964: The origin of the Mitchell Plain. *Indiana Academy of Science, Proceedings* 73: 177–182.
- Priesnitz K., 1985: Nichtbiogene Kalklösung am Lough Leane und am Mackross Lake (SE-Irland). *Berliner Geographische Studien* 16: 55–69.
- Pye K., Mottershead D. N., 1995: Honeycomb weathering of carboniferous sandstone in a sea wall of Weston-Super-Mare, UK. *Quarterly Journal of Engineering Geology* 28: 333–347.
- Qing S., 1977: Lunan stone forest – a spectacular karst geomorphology. *Geographical Knowledge* 4.
- Quigley M., 1984: A study of micro-solution pits on the limestone pavements at Lough Mask, Co. Mayo. M. Sc. Thesis, Geography Department, University College, Dublin, 225 p.
- Quinif Y., 1973: Contribution à l'étude morphologique des coupoles. *Annales de Spéléologie* 28, 4: 565–573.
- Radofilao J., 1977: Bilan des explorations spéléologiques dans l'Ankarana. *Annales de l'Université de Madagascar*, 14: 159–204.
- Raistrick A., 1947: Malham and Malham Moor. Dalesman, Clapham, 122 p.
- Rasmusson G., 1959: Karstformen im Granit des Fichtelgebirges. *Die Höhle* 1: 1–4.
- Ray J.A., 1996: Fluvial features of the karst-plain erosion surface in the Mammoth Cave region. *Proceedings of the 5<sup>th</sup> Annual Science Conference, Mammoth Cave National Park, Kentucky*, 137–156.
- Revelle R., Emery K. O., 1957: Chemical erosion of beach rock and exposed reef rock. *U.S. Geological Survey Professional Paper* 260-T: 699–706.
- Richmond I. A., 1933: Castle Folds, by Great Asby. *Transactions of the Cumberland and Westmorland Antiquarian and Archaeological Society*, 233–237.
- Ridanović J., 1964: Glacijalni relikti kao kriterij za kronološko određivanje morfogeneze prevladavajućih oblika krša. *Zbornik VII. kongresa geografa SFRJ, Zagreb*, 279–290.
- Ridanović J., 1966: Orjen. *Radovi Geografskog instituta u Zagrebu* 5: 5–103.
- Robinson T., 1978: A question of age. *Tower Karst, Chillagoe Caving Club, Occasional Paper* 2: 18–36.
- Robinson T., 1982: Limestone solution experiment at Chillagoe. *Tower Karst, Chillagoe Caving Club, Occasional Paper* 4: 71–76.
- Rodet J., 1992: La Craie et ses Karsts. *Centre de Géomorphologie du Centre National de la Recherche Scientifique, Caen*, 560 p.
- Rodríguez-Navarro C., Doehne E., Sebastián E., 1999: Origins of honeycomb weathering: The roles of salt and wind. *Bulletin of the Geological Society of America* 111: 1250–1255.
- Rodríguez-Navarro C., Rodríguez-Gallego M., Ben Chekroum K., González-Muñoz M. T., 2003: Conservation of ornamental stone by *Myxococcus xanthus*-induced carbonate biomineralization. *Applied and Environmental Microbiology* 69: 2182–2193.
- Rodríguez-Perea A., 1984: El Mioceno de la Serra Nord de Mallorca. *Estratigrafía, Sedimentología e Implicaciones Estructurales*. Ph. D. Thesis, University of Barcelona, Barcelona, 532 p.
- Rogić V., 1958: Velebitska primorska padina. *Radovi Geografskog Instituta u Zagrebu* 2: 1–114.
- Rögner K., 1986: Temperature measurements of rock surfaces in hot deserts (Negev, Israel). *International Geomorphology* 2: 1271–1286.
- Rose J., 1982: The Melinau River and its terraces. *Cave Science* 9, 2: 113–127.
- Rose J., 1984a: Contemporary river landforms and sediments in an area of equatorial rain forest, Gunung Mulu National Park, Sarawak. *Transactions of the Institute of British Geographers* 9: 345–363.
- Rose J., 1984b: Alluvial terraces of an equatorial river, Melinau drainage basin, Sarawak. *Zeitschrift für Geomorphologie* 28, 2: 155–177.
- Rose L., Vincent P. J., 1986a: Some aspects of the morphometry of grikes; a mixture modeling approach. In: Paterson K., Sweeting M. M. (Eds.), *New Directions in Karst*. Geobooks, Norwich, 497–514.
- Rose L., Vincent P. J., 1986b: The kamenitzas of Gait Barrows National Nature Reserve, north Lancashire, England. In: Paterson K., Sweeting M. M. (Eds.), *New Directions in Karst*. Geobooks, Norwich, 473–496.
- Rosselló V. M., 1979: Algunas formas kársticas litóralas de Mallorca. In: Barceló B. (Ed.), *Actas del VI Coloquio de Geografía*. AGE, Palma de Mallorca, 115–121.
- Rossi G., 1974: Morphologie et évolution d'un karst en milieu tropical: l'Ankarana. In: *Phénomènes Karstiques II. Mémoires et Documents* 14, Centre National de la Recherche Scientifique, 279–298.

- Rossi G., 1980: L'Extrême-Nord de Madagascar. Edisud, Aix-en-Provence, 440 p.
- Rubić I., 1936: Mali otoci na obalnom reljefu istočnog Jadrana. *Geografski vestnik* 12, 13: 3–53.
- Rudnicki J., 1960: Experimental work on flutes development. *Speleologia* 2, 1: 17–30.
- Rust D., Kershaw S., 2000: Holocene tectonic uplift patterns in northeastern Sicily: evidence from marine nocthes in coastal outcrops. *Marine Geology* 167: 105–126.
- Sachs J., 1865: *Handbuch der experimental Physiologie der Pflanzen*. Verlag von Wilhelm Engelmann, Leipzig, 514 p.
- Safriel U. N., 1966: Recent vermetid formation on the Mediterranean shore of Israel. *Proceedings of the Malacological Society London* 37: 27–34.
- Sakač K., Benić J., Fuček L., Miknić M., Vlahović I., 1993: Stratigraphic and tectonic position of paleogene Jelar beds in the Outer Dinarides. *Natura Croatica* 2, 1: 55–72.
- Salles C., Poesen J., Sempere-Torres D., 2002: Kinetic energy of rain and its functional relationship with intensity. *Journal of Hydrology* 257, 1–4: 256–270.
- Salomon J. N., 1997: Comparaison entre les “Stone Forests” du Lunan (Yunnan–Chine) et les karsts a “tsingy” de Madagascar. In: Song L., Waltham T., Cao N., Wang F. (Eds.), *Stone Forest: A Treasure of Natural Heritage*. Proceedings of the International Symposium for Lunan Shilin to Apply for World Natural Heritage Status. China Environmental Science Press, Beijing, 124–136.
- Salopek I., 1952: O gornjem permu Velike Paklenice u Velebitu. *Rad Jugoslavenske akademije znanosti i umjetnosti* 289: 5–26.
- Sandler A., 1996: A Turonian subaerial event in Israel: karst, sandstone and pedogenesis. *Geological Survey of Israel, Bulletin* 85, 56 p.
- Sauro U., 1973a: Forme di corrosione su rocce montonate nella Val Lagarina meridionale. *L'Universo* 53, 2: 309–344.
- Sauro U., 1973b: Observations on some great solution runnels with nested pans of the Venetian Prealps. *Proceedings of the 6<sup>th</sup> International Congress of Speleology, Olomouc*. Academia, Praha, 353–361.
- Sauro U., 1973c: Il paesaggio degli Alti Lessini. *Studio geomorfologico*. Memorie del Museo Civico di Storia Naturale di Verona, Memorie fuori serie 6, 161 p.
- Sauro U., 1974: Aspetti dell'evoluzione carsica legata a particolari condizioni litologiche e tettoniche negli Alti Lessini. *Bollettino Società Geologica Italiana* 93: 945–969.
- Sauro U., 1976a: Aspects et influences de la Formation du Rosso Ammonitico sur l'évolution des versants des Hauts Lessini Veronais. *Actes du Symposium sur les versants en Pays Méditerranéens – Aix en Provence, Centre d'Études de Géographie et Écologie de la Region Mediterraneenne* 5: 43–47.
- Sauro U., 1976b: The geomorphological mapping of “Karrenfelder” using very large scales: an example. In: Gams I. (Ed.), *Karst Processes and Relevant Landforms*. Department of Geography, Philosophical Faculty, Ljubljana, 189–199.
- Sauro U., 1977: Le città di roccia. *Economia Trentina* 26, 1: 73–80.
- Sauro U., 1996: Geomorphological aspects of gypsum karst, with special emphasis on exposed karst. In: Klimchouk A., Lowe D., Cooper A., Sauro U. (Eds.), *Gypsum Karst of the World*. *International Journal of Speleology* 25, 3–4: 105–114.
- Sauro U., 2002: Quando in Lessinia c'era il grande gelo. *Quaderno Culturale – La Lessinia ieri oggi domani*, Verona, 85–94.
- Sauro U., 2003: Aspetti evolutivi del paesaggio carsico nei gessi in Italia. In: Madonia G., Forti P. (Eds.), *Le aree carsiche gessose d'Italia*. *Memorie dell'Istituto Italiano di Speleologia* 2, 14: 41–45.
- Schmalz R. F., Swanson F. J., 1969: Diurnal variations in the carbonate saturation of seawater. *Journal of Sedimentary Petrology* 39: 255–267.
- Schneider J., 1976: Biological and inorganic factors in the destruction of limestone coasts. *Contributions to Sedimentology* 6: 1–112.
- Schneider J., Le Champion Alsumard T., 1999: Construction and destruction of carbonates by marine and freshwater cyanobacteria. *European Journal of Phycology* 34: 417–426.
- Schneider J., Torunski H., 1983: Biokarst on limestone coasts, morphogenesis and sediment production. *Marine Ecology* 4: 45–63.
- Schoeneich Ph., Reynard E., Pierrehumbert G., 1998: Geomorphological mapping in the Swiss Alps and Prealps. *Wiener Schriften zur Geographie und Kartographie, Band* 11: 145–153.
- Sellier D., 1997: Utilisation des mégalithes comme marqueurs de la vitesse de l'érosion des granites en milieu tempéré: enseignements apportés par les alignements de Carnac (Morbihan). *Zeitschrift für Geomorphologie* 41, 3: 319–356.
- Shannon C. H. C., 1970: Geology of the Mt. Etna area. In: Sprent J. K. (Ed.), *Mount Etna Caves*. University of Queensland Speleological Society, Brisbane, 11–21.
- Simeonović R., 1921: O škrapama. *Glasnik Srpskog geografskog društva* 5: 142–155.
- Simms M. J., 1990: Phytokarst and photokarren in Ireland. *Cave Science* 17: 131–133.

- Simms M. J., 2002: The origin of enigmatic, tubular, lake-shore karren: a mechanism for rapid dissolution of limestone in carbonate saturated waters. *Physical Geography* 23, 1: 1–20.
- Slabe T., 1992: Naravni in poskusni obnoplavinski jamski skalni relief [Natural and experimental cave rocky relief on the contact of water and sediments]. *Acta Carsologica* 21: 7–34.
- Slabe T., 1994: Dejavniki oblikovanja jamske skalne površine [The factors influencing on the formation of the cave rocky surface]. *Acta Carsologica* 23: 369–398.
- Slabe T., 1995a: Cave Rocky Relief and its Speleogenetical Significance. Zbirka ZRC 10, Založba ZRC, Ljubljana, 128 p.
- Slabe T., 1995b: Experimental modelling of cave rocky forms in Paris plaster. *Atti e Memorie della Commissione Grotte "Eugenio Boegan"* 32: 65–83.
- Slabe T., 1996: Karst features in the motorway section between Čebulovica and Dane. *Acta Carsologica* 25: 221–240.
- Slabe T., 1998: Rock relief of pillars in the Lunan Stone Forest. In: Chen X., Gabrovšek F., Huang C., Jin Y., Knez M., Kogovšek J., Liu H., Petrič M., Mihevc A., Otoničar B., Shi M., Slabe T., Šebela S., Wu W., Zhang S., Zupan Hajna N., 1998: South China Karst I. Založba ZRC, Ljubljana, 51–67.
- Slabe T., 1999: Subcutaneous rock forms. *Acta Carsologica* 28, 2: 255–271.
- Slabe T., 2005: Two experimental modelings of karst rock relief in plaster: subcutaneous "rock teeth" and "rock peaks" exposed to rain. *Zeitschrift für Geomorphologie* 49, 1: 107–119.
- Smart P. L., Dawans J. M., Whitaker F., 1988: Carbonate dissolution in a modern mixing zone. *Nature* 335: 811–813.
- Smart P. L., Whitaker F. F., 1996: Development of karren landform assemblages – a case study from Son Marc, Mallorca. In: Fornós J. J., Ginés A. (Eds.), *Karren Landforms*. Universitat de les Illes Balears, Palma de Mallorca, 111–122.
- Smith B. J., 1978: The origin and geomorphic implications of cliff foot recesses and tafoni on limestone hamadas in the North West Sahara. *Zeitschrift für Geomorphologie* 22: 21–43.
- Smith B. J., 1986: An integrated approach to the weathering of limestone in an arid area and its role in landscape evolution: a case study from south-east Morocco. In: Gardiner V. (Ed.), *International Geomorphology* 2. John Wiley and Sons, London, 637–657.
- Smith B. J., 1988: Weathering of surficial limestone debris in a hot desert environment. *Geomorphology* 1: 355–367.
- Smith B., McAllister J. J., 1986: Observations on the occurrence and origins of salt weathering phenomena near Lake Magadi, southern Kenya. *Zeitschrift für Geomorphologie* 30: 445–460.
- Smith B., Moses C. A., Warke P. A., 1996: Modification of karren in arid environments: a case study from southern Tunisia. In: Fornós J. J., Ginés A. (Eds.), *Karren Landforms*. Universitat de les Illes Balears, Palma de Mallorca, 123–134.
- Smith D. I., 1969: The solutional erosion of limestone in an arctic morphogenetic region. In: Stell O. (Ed.), *Problems of Karst Denudation*. Proceedings of the 5<sup>th</sup> International Speleological Congress, Brno, Czechoslovakia. *Studia Geographica* 5.
- Sokač B., 1973: *Geologija Velebita*. Ph. D. Thesis, University of Zagreb, Zagreb, 151 p.
- Song L. H., 1986: Origination of stone forest in China. *International Journal of Speleology* 15, 1–4: 3–33.
- Song L. H., Liu H., 1992: Control of geological structures over development of cockpit karst in south Yunnan, China. *Tübingen Geographische Studien* 109: 57–70.
- Song L., Li Y., 1997: Definition of Stone forest and its evolution in Lunan County, Yunnan, China. In: Song L., Waltham A. C., Cao N., Wang F. (Eds.), *Stone Forest: A Treasure of Natural Heritage*. Proceedings of the International Symposium for Lunan Shilin to Apply for World Natural Heritage Status, China Environmental Science Press, Beijing, 37–45.
- Song L., Liang F., 2001: Distribution of CO<sub>2</sub> in Soil Air Affected by Vegetation in the Shilin National Park. *Acta Geologica Sinica* 75, 3: 288–293.
- Song L., Waltham A. C., Cao N., Wang F. (Eds.), 1997: *Stone Forest: A Treasure of Natural Heritage*. Proceedings of the International Symposium for Lunan Shilin to Apply for World Natural Heritage Status, China Environmental Science Press, Beijing, 136 p.
- Song L., Wang F., 1997: Lunan Shilin Landscape in China. *Proceedings of 12<sup>th</sup> International Congress of Speleology, Symposium* 8, 1: 433–435.
- Spate A. P., Little L., 1995: Is the conventional approach to karst area management appropriate to tropical Australia. In: Henderson K., Houshold I., Middleton G. (Eds.), *Proceedings of the 11<sup>th</sup> Australasian Conference on Cave and Karst Management*. Australasian Cave and Karst Management Association, Carlton South, 68–84.
- Spencer T., 1985a: Marine erosion rates and coastal morphology of reef limestones on Grand Cayman Island, West Indies. *Coral Reefs* 4: 59–70.
- Spencer T., 1985b: Weathering rates on a Caribbean

- Reef limestone: results and implications. *Marine Geology* 69: 195–201.
- Spencer T., 1988: Limestone coastal morphology: the biological contribution. *Progress in Physical Geography* 12: 66–101.
- Spencer T., Viles H., 2002: Bioconstruction, bioerosion and disturbance on tropical coasts: coral reefs and rocky limestones. *Geomorphology* 48: 23–50.
- Stanton W. I., 1984: Snail holes in Mendip limestones. *Proceedings of the Bristol Naturalists' Society* 44: 15–18.
- Stenson R. E., Ford D. C., 1993: Rillenkarren on gypsum in Nova Scotia. *Géographie Physique et Quaternaire* 47, 2: 239–243.
- Stoddart D. R., Taylor J. D., Farrow G. R., Fosberg F. R., 1971: The geomorphology of Aldabra. In: Westoll T. S., Stoddart D. R. (Eds.), *A discussion on the results of the Royal Society expedition to Aldabra, 1967–1968*. *Philosophical Transactions of the Royal Society of London*, London, 31–65.
- Storm R., Smith D. I., 1991: The caves of Gregory National Park, Northern Territory, Australia. *Cave Science* 18, 2: 91–97.
- Svensson U., Dreybrodt W., 1992: Dissolution kinetics of natural calcite minerals in CO<sub>2</sub>-water-systems approaching calcite equilibrium. *Chemical Geology* 100: 129–34.
- Sweet I. P., Mendum J. R., Bultitude R. J., Morgan C. M., 1974: The geology of the southern Victoria River Region, Northern Territory. Bureau of Mineral Resources, Australia, Report 167, 143 p.
- Sweeting M. M., 1955: Landforms in North-West County Clare, Ireland. *Transactions of the Institute of British Geographers* 21: 218–249.
- Sweeting M. M., 1966: The weathering of limestones. In: Dur G. H. (Ed.), *Essays in Geomorphology*. Heinemann, London, 177–210.
- Sweeting M. M., 1972: Karst landforms. MacMillan Press, London, 362 p.
- Sweeting M. M., 1973: Karst Landforms. Columbia University Press, New York, 362 p.
- Sweeting M. M., 1980: The geomorphology of Mulu: an introduction. *Geographical Journal* 146, 1: 1–7.
- Sweeting M. M., 1995: Karst in China. Its Geomorphology and Environment. Springer-Verlag, Berlin, New York, 265 p.
- Sweeting M. M., Lancaster N., 1982: Solutional and wind erosion forms on limestone in the Central Namib Desert. *Zeitschrift für Geomorphologie* 26, 2: 197–207.
- Sweeting M. M., Sweeting G. S., 1969: Some aspects of the Carboniferous limestone in relation to its landforms with particular reference to NW Yorkshire and Co. Clare. *Étude de Travaux de Méditerranée* 7: 210–209.
- Szunyogh G., 2000a: Differential Equations Describing the Changes of Shape Caused by Karst Corrosion of any Arbitrary Limestone Surface. *Karsztfejlődés* 4: 151–174.
- Szunyogh G., 2000b: The Theoretical-Physical Study of the Process of Karren Development. *Karsztfejlődés* 4: 125–150.
- Szunyogh G., 2005: Theoretical investigation of the duration of karstic denudation on bare, sloping limestone surfaces. *Acta Carsologica* 34, 1: 9–23.
- Szunyogh G., Lakotár K., Szigeti I., 1998: Nagy területet lefedő karrvályúrendszer struktúrájának elemzése. *Karsztfejlődés* 2: 125–147.
- Šebela S., Slabe T., Kogovšek J., Liu H., Pruner P., 2001: Baiyun Cave in Naigu Shilin, Yunnan Karst, China. *Acta Geologica Sinica* 75, 3: 279–287.
- Šušnjar M., Bukovac J., Nikler L., Crnolatic I., Milan A., Šikić D., Grimani I., Vulić Z., Blašković I., 1970: Osnovna geološka karta SFRJ 1:100.000, List Crikvenica L 33–102. Institut za geološka istraživanja, Zagreb, Savezni geološki zavod, Beograd.
- Taboroši D., Jenson J. W., Mylroie J. E., 2004: Karren features in island karst: Guam, Mariana Islands. *Zeitschrift für Geomorphologie* 48, 3: 369–389.
- Tari Kovačić V., Mrinjek E., 1994: The role of Paleogene clastics in the tectonic interpretation of northern Dalmatia (southern Croatia). *Geologia Croatica* 47, 1: 127–138.
- Taylor M. P., Viles H. A., 2000: Improving the use of microscopy in the study of weathering: sampling issues. *Zeitschrift für Geomorphologie, Supplementband* 120: 145–158.
- Thomas T. M., 1970: The limestone pavements of the North Crop of the South Wales coalfield with special reference to solution rates and processes. *Transactions of the Institute of British Geographers* 50: 87–105.
- Thompson C. H., Bowman G. M., 1984: Subaerial denudation and weathering of vegetated coastal dunes in eastern Queensland. In: Thom B. G. (Ed.), *Coastal Geomorphology in Australia*. Academic Press, Sydney, 263–290.
- Thorntwaite C. W., 1948: An approach toward a rational classification of climate. *Geographical Review* 38: 55–94.
- Tjia H. D., 1985: Notching by abrasion on a limestone coast. *Zeitschrift für Geomorphologie* 29, 3: 367–372.
- Toledo X., Zapater E., 1991: *Geografía General y Regional de Chile*. Editorial Universitaria, Colección Imagen de Chile, Santiago, 443 p.
- Tomaselli L., Lamenti G., Bosco M., Tiano P., 2000: Bio-

- diversity of photosynthetic micro-organisms dwelling on stone monuments. *International Biodeterioration and Biodegradation* 46: 251–258.
- Torunski H., 1979: Biological erosion and its significance for the morphogenesis of limestone coasts and for nearshore sedimentation (Northern Adriatic). *Senckenbergiana Maritima* 11: 193–265.
- Tóth G., 2003: Karrenmorphologische Forschungen im Dachstein und im Toten-Gebirge – Gmundner Geostudien 2. Beiträge zur Geologie des Salzkammerguts, 191–198.
- Tóth G., 2007: A mérsékeltövi mészkő magashegységek fedetlen karros celláinak osztályozása és fejlődése [Classification and development of bare karren cells in calcareous high mountains]. BDF Természetföldrajzi Tanszék Kiadó, Szombathely, 116 p.
- Tóth G., Balogh Z., 2000: Karrmeanderek lefűződésének vizsgálata a Júliai-Alpok Héttő-völgyének egy karsztos térszíne alapján. *Karsztfejlődés* 5: 139–142.
- Trenhaile A. S., 1987: *The Geomorphology of Rocky Coasts*. Clarendon Press, Oxford, 384 p.
- Trenhaile A. S., 2002: Rock coasts, with particular emphasis on shore platforms. *Geomorphology* 48: 7–22.
- Trenhaile A. S., Pepper D. A., Trenhaile R. W., Dalimonte M., 1998: Stacks and notches at Hopewell rocks, New Brunswick, Canada. *Earth Surface Processes and Landforms* 23: 975–988.
- Tricart J., 1972: *Landforms of the Humid Tropics: Forests and Savannas*. Longman, London, 306 p.
- Trimmel H., 1965: *Speläologisches Fachwörterbuch*. Landesverein für Höhlenkunde in Wien und Niederösterreich, Wien, 109 p.
- Trudgill S. T., 1975: Measurement of erosional weight-loss of rock tablets. *British Geomorphological Research Group, Technical Bulletin* 17: 13–19.
- Trudgill S. T., 1976a: The marine erosion of limestones on Aldabra Atoll, Indian Ocean. *Zeitschrift für Geomorphologie, Supplementband* 26: 164–200.
- Trudgill S. T., 1976b: The subaerial and subsoil erosion of limestones on Aldabra Atoll, Indian Ocean. *Zeitschrift für Geomorphologie, Supplementband* 26: 201–210.
- Trudgill S. T., 1979: Spitzkarren on calcarenites, Aldabra Atoll, Indian Ocean. *Zeitschrift für Geomorphologie, Supplementband* 32: 67–74.
- Trudgill S. T., 1983: Preliminary estimates of intertidal limestone erosion on Tree island, Southern Great Barrier Reef, Australia. *Earth Surface Processes and Landforms* 8: 189–193.
- Trudgill S. T., 1985: *Limestone geomorphology*. Longman, London, New York, 196 p.
- Trudgill S. T., 1986: Limestone weathering under a soil cover and the evolution of limestone pavements, Malham District, north Yorkshire. In: Paterson K., Sweeting M. M. (Eds.), *New Directions in Karst*. Geobooks, Norwich, 461–471.
- Trudgill S. T., 1987: Bioerosion of intertidal limestone, Co. Clare, Eire 3: zonation, process and form. *Marine Geology* 74: 111–121.
- Trudgill S. T., Crabtree R. W., 1987: Bioerosion of intertidal limestone, Co. Clare, Eire 2: *Hiatella arctica*. *Marine Geology* 74: 99–109.
- Trudgill S. T., Inkpen R., 1993: Impact of Acid Rain on Karst Environments. *Catena Supplement* 25: 199–218.
- Trudgill S. T., Smart P. L., Friederich H., Crabtree R. W., 1987: Bioerosion of intertidal limestone, Co. Clare, Eire 1: *Paracentrotus lividus*. *Marine Geology* 74: 85–98.
- Tučan F., 1911: Die Oberflächenformen bei Carbonatgesteinen in Karstgegenden. *Centr. F. Min. Geol. und Paleont.*, 343–350.
- Uchupi E., Milliman J. D., Luyendyk B. P., Brown C. O., Emery K. O., 1971: Structure and origin of the southeastern Bahamas. *American Association of Petroleum Geologists, Bulletin* 55: 687–704.
- Udden J. A., 1925: Etched Potholes. *University of Texas Bulletin* 2509: 5–9.
- Uijlenhoet R., Stricker J. N. M., 1999: A consistent rainfall parameterization based on the exponential raindrop size distribution. *Journal of Hydrology* 218: 101–127.
- Underhill J. R., Gayer R. A., Woodcock N. H., Donnelly R., Jolley E. J., Stimpson I. G., 1988: The Dent Fault System, Northern England – reinterpreted as a major oblique slip zone. *Journal of the Geological Society of London* 145, 2: 303–316.
- Urushibara-Yoshino K., 1991: The regionality of solution rate of limestone tablets in karst areas of Japan (in Japanese). *Institute for Applied Geography, Komazawa University, Regional Views* 4: 107–117.
- Urushibara-Yoshino K., 1996: Karst – environment and human activities (in Japanese). *Taimeido Ltd.*, Tokyo, 325 p.
- Urushibara-Yoshino K., 2003: Karst terrain of raised coral islands, Minamidaito and Kikai in the Nansei Islands of Japan. *Zeitschrift für Geomorphologie, Supplementband* 131: 17–31.
- Urushibara-Yoshino K., Miotke F. D. and Research Group of Solution Rates in Japan, 1998: Solution rates of limestone tablets and CO<sub>2</sub> measurement in soils in limestone areas of Japan. *Geografia Fisica e Dinamica Quaternaria, Supplement* 4: 35–39.
- Urushibara-Yoshino K., Research Group of Solution Rates in Japan, 1999a: Interannual variation of lime-

- stone solution rates in Japan. In: Bárány-Kevei I., Gunn J. (Eds.), *Essays in the ecology and conservation of karst*. Special Issue of *Acta Geographica Szegediensis*, *Acta Geographica* 36: 201–211.
- Urushibara-Yoshino K., Miotke F. D., Research Group of Solution Rates in Japan, 1999b: Solution Rate of Limestone in Japan. *Physics and Chemistry of the Earth A* 24, 10: 899–903.
- Uzdowski E., 1982: Reactions and equilibria in the systems  $\text{CO}_2\text{-H}_2\text{O}$  and  $\text{CaCO}_3\text{-CO}_2\text{-H}_2\text{O}$  (0–50° C), a review. *Jahrbuch für Mineralogie, Abhandlungen* 144: 148–171.
- Vacher H. L., Mylroie J. E., 2002: Eogenetic karst from the perspective of an equivalent porous medium. *Carbonates and Evaporites* 17: 182–196.
- Vajoczki S., Ford D., 2000: Underwater dissolutional pitting on dolostones, Lake Huron-Georgian Bay, Ontario. *Physical Geography* 21, 5: 418–432.
- Vanstone S. D., 1998: Late Dinantian palaeokarst of England and Wales: implications for the exposure surface development. *Sedimentology* 45: 19–37.
- Veevers J. J., Roberts J., 1968: Upper Palaeozoic rocks, Bonaparte Gulf Basin of Northwestern Australia. Bureau of Mineral Resources, Australia, *Bulletin* 97, 155 p.
- Veni G., 1994: Hydrogeology and evolution of caves and karst in the southwestern Edwards Plateau. In: Elliot W. R., Veni G. (Eds.), *The Caves and Karst of Texas*. National Speleological Society, Huntsville, Alabama, 13–30.
- Veress M., 1993: Egy Totes Gebirge-i nagy karrvályú kioldódástörténeti vázlat. *Karszt és Barlang* 1–2: 21–28.
- Veress M., 1995: Karros folyamatok és formák rendszerezése Totes Gebirge-i példák alapján. *Karsztfejlődés* 1: 7–30.
- Veress M., 1998: Adatok karrvályúk meanderfejlődéséhez. *Karsztfejlődés* 2: 75–90.
- Veress M., 2000a: Karrformák összeoldódása. *Karsztfejlődés* 5: 143–158.
- Veress M., 2000b: The main types of karren development of limestone surfaces without soil covering. *Karsztfejlődés* 4: 7–30.
- Veress M., 2000c: Adalékok karrványúk működéséhez. *Hidrológiai Közöny* 80, 4: 207–209.
- Veress M., 2000d: The morphogenetics of karren meander and its main types. *Karsztfejlődés* 4: 41–76.
- Veress M., 2002: Talaj nélküli sziklafelszínnek néhány karros jelensége és ezek hatására képződő karrformák. *Földr Értesítő*, 51: 41–71.
- Veress M., 2003: Adalékok a homokkő anyagú kőtengerek (Káli-medence) pszeudokarrjainak morfofenetikájához – Zirci Természettud. Múzeum Közleményei 20: 7–46.
- Veress M., Barna J., 1998: Karrmeanderek morfológiai térképezésének tapasztalatai. *Karsztfejlődés* 2: 59–73.
- Veress M., Kocsis Z. S., 1996: A Szentbékállai kőtenger madáritatóinak morfofenetikai csoportosítása. *Proceedings of the 6<sup>th</sup> International Symposium on Pseudokarst*, Galyatető, 90–97.
- Veress M., Lakotár K., 1995: Saroknyom karrok morfofenetikai csoportosítása Totes Gebirge-i példák alapján. *Karsztfejlődés* 1: 89–102.
- Veress M., Nacsa T., 1998: The study of the history of dissolution of karren ground surfaces developing to karren monadocks and inselbergs – with some examples. *Karsztfejlődés* 4: 77–108.
- Veress M., Nacsa T., Széles Gy., Dombi L., 1995: Néhány totesi karros forma domborzatrাজي ábrázolása. *Karsztfejlődés I. (Totes Gebirge karrjai)* Pauz Kiadó, Szombathely, 31–40.
- Veress M., Szabó L., 1996: Adatok a velemi Kalapos-kő morfofenetikájához. *Vasi Szemle*, 50: 211–234.
- Veress M., Szabó L., Zentai Z., 1996: Evolution of hats on the greenschist terrain of Kőszegi Mountain. In: Eszterhás I., Sárközi Sz. (Eds.), *Proceedings of the 6<sup>th</sup> International Symposium on Pseudokarst*, Galyatető, 98–104.
- Veress M., Szunyogh G., Tóth G., Zentai Z., Czöpek I., 2006: The effect of the wind on karren formation on the Island of Diego de Almagro (Chile). *Zeitschrift für Geomorphologie* 50: 425–445.
- Veress M., Tóth G., 2001: Formes et micro-reliefs de lapiés: Approche morphométrique, application au massif de Totes-Gebirge (Autriche). *Karstologia* 37, 1: 47–53.
- Veress M., Tóth G., 2002: Egy dachsteini réteglapos térszínrészlet karros fejlődéstörténete. *Karsztfejlődés* 7: 187–204.
- Veress M., Tóth G., 2004: Types of meandering karren. *Zeitschrift für Geomorphologie* 48, 1: 53–77.
- Veress M., Tóth G., Czöpek I., 2003: Falikarrok morfofenetikája dachsteini példák alapján. *Karsztfejlődés* 8: 197–212.
- Veress M., Tóth G., Péntek K., 2001b: Adalékok karrformák kialakulási korához és fejlődési sebességéhez a Hallstatt-gleccser jégmentes völgytalpán. *Karsztfejlődés* 6: 161–169.
- Veress M., Tóth G., Zentai Z., Kovács G., 2001a: Study of a new method for characterising karren surfaces based on alpine researches. *Revue de Géographie Alpine* 89: 49–62.
- Veres V., 1985: Solution and associated features of

- limestone fragments in calcareous soil (lithic calcixeroll) from southern France. *Geoderma* 36: 109–122.
- Viles H. A., 1984: Biokarst: Review and Prospect. *Progress in Physical Geography* 8: 523–542.
- Viles H. A., 1987: Blue-green algae and terrestrial limestone weathering on Aldabra Atoll: a SEM and light microscope study. *Earth Surface Processes and Landforms* 12: 319–330.
- Viles H. A., 1988: Organisms and karst geomorphology. In: Viles H. A. (Ed.), *Biogeomorphology*. Blackwell, Oxford, 319–350.
- Viles H. A., 1995: Ecological perspectives on rock surface weathering: towards a conceptual model. *Geomorphology* 13: 21–35.
- Viles H. A., 2001: Scale issues in weathering studies. *Geomorphology* 41: 63–72.
- Viles H.A., Moses C.A., 1998: Experimental production of weathering nanomorphologies on carbonate stone. *Quarterly Journal of Engineering Geology* 31: 347–357.
- Viles H. A., Spencer T., 1986: Phytokarst, blue-green algae and limestone weathering. In: Paterson K., Sweeting M. M. (Eds.), *New directions in Karst*. Geobooks, Norwich, 115–140.
- Viles H. A., Spencer T., Teleki K., Cox C., 2000: Observations on 16 years of microfloral recolonization data from limestone surfaces, Aldabra Atoll, Indian Ocean: Implications for biological weathering. *Earth Surface Processes and Landforms* 25: 1355–1370.
- Viles H. A., Trudgill S. T., 1984: Long term remeasurements of micro-erosion meter rates, Aldabra Atoll, Indian Ocean. *Earth Surface Processes and Landforms* 9: 89–94.
- Vincent P. J., 1983a: The morphology and morphometry of some arctic Trittkarren. *Zeitschrift für Geomorphologie* 27, 2: 205–222.
- Vincent P., 1983b: The dissolving landscape: step karren. *Geographical Magazine* 55: 508–510.
- Vincent P. J., 1995: Limestone pavements in the British Isles: a review. *Geography Journal* 161: 265–274.
- Vincent P., 1996: Rillenkarrren in the British Isles. *Zeitschrift für Geomorphologie* 40, 4: 487–497.
- Vincent P., 2004: Loess on the Burren. *North Munster Antiquarian Journal* 44: 59–67.
- Vincent P., Lee M., 1981: Some observations on the loess around Morecambe Bay, North-West England. *Proceedings of the Yorkshire Geological Society* 43: 281–294.
- Vlahović I., Velić I., Tišljarić J., Matičec D., 1999: Lithology and Origin of Tertiary Jelar Breccia within the Framework of Tectogenesis of Dinarides. In: *Some Carbonate and Clastic Successions of the External Dinarides: Velebit Mountain, Island of Rab*. Harold Reading's IAS Lecture tour '99 (Croatia). Field-trip guidebook, Hrvatsko geološko društvo, Zagreb, 23–25.
- Wagner G., 1950: Rund um Hochifen Gottesackergebiet. *Öhringen*, 72–80.
- Walkden G. M., 1972: The mineralogy and origin of interbedded clay wayboards in the Lower Carboniferous of the Derbyshire Dome. *Geological Journal* 8: 143–160.
- Walkden G. M., 1974: Palaeokarstic surfaces of upper Viséan (Carboniferous) limestones of the Derbyshire Block, England. *Journal of Sedimentary Petrology* 44: 1232–1247.
- Walkden G.M., Davies J., 1983: Polyphase erosion of subaerial omission surfaces in the late Dinantian of Anglesey, North Wales. *Sedimentology* 30: 861–878.
- Walsh R. P. D., 1982a: Climate. In: Jermy A. C., Kavanagh K. P. (Eds.), *Gunung Mulu National Park, Sarawak*. Sarawak Museum Journal (Special Issue 2) 30, 51: 29–67.
- Walsh R. P. D., 1982b: Hydrology and water chemistry. In: Jermy A. C., Kavanagh K. P., (Eds.), *Gunung Mulu National Park, Sarawak*. Sarawak Museum Journal (Special Issue 2) 30, 51: 121–181.
- Walter-Levy L., Frécaut R., Strauss R., 1958: Contribution à l'étude de la zone littorale des îles Baléares. *Biologie et chimie des algues calcaires. Formes du relief qui leur sont liées*. *Revue Algologique* 3: 202–228.
- Waltham A. C., 1984: Some features of karst geomorphology in south China. *Cave Science* 11: 185–199.
- Waltham A. C., 1995: The pinnacle karst of Gunung Api, Mulu, Sarawak. *Cave and Karst Science* 22, 3: 123–126.
- Waltham A. C., 1997a: Pinnacle karst of Gunung Api, Mulu, Sarawak. In: Song L., Waltham A. C., Cao N., Wang F. (Eds.), *Stone Forest: A Treasure of Natural Heritage*. Proceedings of the International Symposium for Lunan Shilin to Apply for World Natural Heritage Status, China Environmental Science Press, Beijing, 52–55.
- Waltham A. C., 1997b: Mulu – the ultimate in cavernous karst. *Geology Today* 13, 6: 216–222.
- Waltham A. C., Brook D. B., 1980a: Cave development in the Melinau Limestone of the Gunung Mulu National Park. *Geographical Journal* 146, 2: 258–266.
- Waltham A. C., Brook D. B., 1980b: Geomorphological observations in the limestone caves of Gunung Mulu National Park, Sarawak. *Transactions of the British Cave Research Association* 7, 3: 123–139.
- Waltham A.C., Simms M. J., Farrant A. R., Goldie H. S., 1997: *Karst and Caves of Great Britain*. Chapman and Hall, London, 358 p.



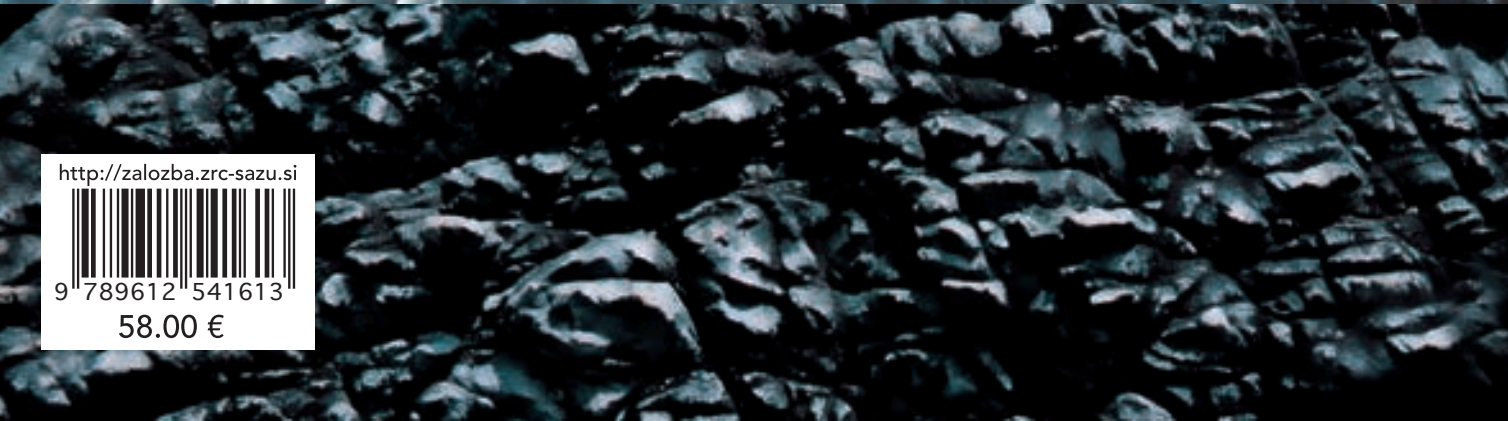
- Waltham A. C., Webb B., 1982: Geology. In: Jermy A. C., Kavanagh K. P. (Eds.), Gunung Mulu National Park, Sarawak. Sarawak Museum Journal (Special Issue 2) 30, 51: 68–74.
- Waltham T., 2001: Pinnacles and barchans in the Egyptian desert. *Geology Today* 17, 3: 101–104.
- Waltham T., Hamilton-Smith E., 2004: Ha Long Bay, Vietnam. In: Gunn J. (Ed.), *Encyclopedia of Cave and Karst Science*. Fitzroy Dearborn, New York, London, 413–414.
- Ward S. D., Evans D. F., 1976: Conservation assessment of British limestone pavements based on floristic criteria. *Biological Conservation* 9: 217–233.
- Webb J., 1996: Chillagoe Field Trip Excursion Guide. 7<sup>th</sup> Australia and New Zealand Geomorphology Group Conference, Cairns, 21 p.
- Webb S., 1995: Conservation of limestone pavement. *Cave and Karst Science* 21: 97–100.
- Weber H., 1967: *Die Oberflächenformen des festen Landes*. B. G. Teubner Verlagsgesellschaft, Leipzig, 367 p.
- Webster C. L., 1996: The Intrigue of the Question about the Bridgewater “Fossil Forest”, Victoria, Australia. *Origins* 23, 1: 50–60.
- Wentworth C. K., 1939: Marine bench-forming processes II, solution benching. *Journal of Geomorphology* 2: 3–25.
- Wentworth C. K., 1944: Potholes, pits and pans subaerial and marine. *Journal of Geology* 52: 117–130.
- Werner E., 1975: Solution of calcium carbonate and the formation of karren. *Cave Geology* 1: 3–28.
- White S., 2000: Syngenetic Karst in Coastal Dune Limestone: A Review. In: Klimchouk A. B., Ford D. C., Palmer A. N., Dreybrodt W. (Eds.), *Speleogenesis: Evolution of Karst Aquifers*. National Speleological Society, Huntsville, Alabama, 234–237.
- White S., Grimes K. G., Mylroie J. E., Mylroie J. R., 2007: The earliest time of karst cave formation. *Proceedings of the Time in Karst Conference*, Karst Research Institute, Postojna (on a CD-ROM), 5 p.
- White W. B., 1988: *Geomorphology and hydrology of karst terrains*. Oxford University Press, New York, 464 p.
- White W. B., Jefferson G. L., Haman J. F., 1966: Quartzite karst in Southeastern Venezuela. *International Journal of Speleology* 2: 309–314.
- Wilford G. E., 1961: The geology and mineral resources of Brunei and adjacent parts of Sarawak. Geological Survey Department (British Territories in Borneo), *Memoir* 10: 319 p.
- Wilford G. E., Wall J. R. D., 1965: Karst topography in Sarawak. *Journal of Tropical Geography* 21: 44–70.
- Williams P. W., 1966: Limestone pavements with special reference to western Ireland. *Transactions of the British Geographers* 40: 155–172.
- Williams P. W., 1971: Illustrating morphometric analysis of karst with examples from New Guinea. *Zeitschrift für Geomorphologie* 15: 40–61.
- Williams P. W., 1972: Morphometric analysis of polygonal karst in New Guinea. *Bulletin of the Geological Society of America* 83: 761–796.
- Williams P. W., 1973: Variations in karst landforms with altitude in New Guinea. *Geographische Zeitschrift* 32: 25–33.
- Williams P. W., 1978: Interpretations of Australasian Karsts. In: Davies J. L., Williams M. A. J. (Eds.), *Landform Evolution in Australia*. Australian National University Press, Canberra, 259–286.
- Williams P. W., 1983: The role of the subcutaneous zone in the karst hydrology. *Journal of Hydrology* 61: 45–67.
- Williams P. W., 2004: Mountain Kaijende arête and pinnacle karst, Papua New Guinea. In: Gunn J. (Ed.), *Encyclopedia of Caves and Karst*, Fitzroy Dearborn, New York, 467–468.
- Williams P. W., 2008: The role of the epikarst in karst and cave hydrogeology: a review. *International Journal of Speleology* 37, 1: 1–10.
- Wilson J. M., 1985: Ecology of the Crocodile Caves of Ankarana, Madagascar. *Cave Science* 12: 135–138.
- Wilson J. M., 1987: The Crocodile Caves of Ankarana: Expedition to Northern Madagascar. *Cave Science* 14: 107–119.
- Wilson P. A., 1975: Observations on the geomorphology of the Chillagoe limestones. *Proceedings of the 10<sup>th</sup> biennial conference of the Australian Speleological Federation*, Sydney, 69–73.
- Winkler E. M., 1979: Role of salts in development of granitic tafoni, South Australia: a discussion. *Journal of Geology* 87: 119–120.
- Woodruff C. D., Stoddard D. R., Harmon R. S., Spencer T., 1983: Coastal morphology and Late Quaternary history, Cayman Islands, West Indies. *Quaternary Research* 19: 64–84.
- Wray R. A. L., 1997: A global review of solutional weathering forms on quartz sandstones. *Earth-Science Reviews* 42: 137–160.
- Wright V. P., 1988: Paleokarsts and paleosoils as indicators of paleoclimate and porosity evolution: a case study from the Carboniferous of South Wales. In: James N. P., Choquette P. W. (Eds.), *Paleokarst*. Springer-Verlag, New York, 329–341.
- Yonge C. M., 1963: Rock-boring organisms. In: Sognnaes R. F. (Ed.), *Mechanics of soft tissue destruction*. American Association for the Advancement of Science 75: 19–24.

- Young A. R. M., 1987: Salt as an agent in the development of cavernous weathering. *Geology* 15: 962–966.
- Yu Y., Yang B., 1997: Paleoenvironment during formation of Lunan Stone Forest. In: Song L., Waltham A. C., Cao N., Wang F. (Eds.), *Stone Forest: A Treasure of Natural Heritage*. Proceedings of the International Symposium for Lunan Shilin to Apply for World Natural Heritage Status, China Environmental Science Press, Beijing, 63–67.
- Yuan D., 1982: Glossary of Karstology. Geological Publishing House, Beijing, 55p.
- Yuan D., 1991: Karst of China. Geological Publishing House, Beijing, 224 p.
- Yuan D., 1997: A global perspective of Lunan Stone forest. In: Song L., Waltham A. C., Cao N., Wang F. (Eds.), *Stone Forest: A Treasure of Natural Heritage*. Proceedings of the International Symposium for Lunan Shilin to Apply for World Natural Heritage Status, China Environmental Science Press, Beijing, 68–70.
- Zamora E., Santana A., 1979: Características climáticas de la costa occidental de la Patagonia entre las latitudes 46°40' y 56°30' S. *Anales del Instituto de la Patagonia* 10: 109–154.
- Zeller J., 1967: Meandering channels in Switzerland. International Union of Geodesy and Geophysics, International Association of Scientific Hydrology (IUGG/IASH), Symposium on River Morphology, Bern, 174–186.
- Zentai Z., 2000: Karrvályúk fejlődésének sajátosságai néhány Héttó-völgyi (Júliai-Alpok, Szlovénia) mintaterület adatainak felhasználásával. *Karsztfejlődés* 5: 127–137.
- Zeza F., 1994: Minoan palace of Knossos: weathering of gypsum stones. In: Fassina V., Ott H., Zeza F. (Eds.), *Proceedings of the 3<sup>rd</sup> International Symposium on the Conservation of Monuments in the Mediterranean Basin*, Venice, 635–646.
- Zhang D., 1994: Distribution of Tibetan karren and their morphogenetic analysis. *Carsologica Sinica* 13, 3: 270–280.
- Zhang F., Geng H., Li Y., Liang Y., Yang Y., Ren J., Wang F., Tao H., Li Z., 1997: Study on the Lunan stone forest karst, China. Yunnan Science and Technology Press, 155 p.
- Zhang F., Wang F., Wang H., 1997: Lunan Stone forest landscape and its protection and conservation. In: Song L., Waltham A. C., Cao N., Wang F. (Eds.), *Stone Forest: A Treasure of Natural Heritage*. Proceedings of the International Symposium for Lunan Shilin to Apply for World Natural Heritage Status. China Environmental Science Press, Beijing, 71–77.
- Zhang S., 1984: The development and evolution of Lunan stone forest. *Carsologica Sinica* 3: 78–87.
- Zotov V. D., 1941: Pot-holing of limestone by development of solution cups. *Journal of Geomorphology* 4: 71–73.
- Zseni A., 1999: A talaj szerepe a mészkőjárdák kialakulásában [The role of soil cover in the evolution of karrenfields]. CD proceeding of the 4<sup>th</sup> National Conference of Geographical Ph. D. Students, Szeged.
- Zseni A., 2002a: The role of soil cover in the evolution of karrenfelds. In: Gabrovšek F. (Ed.), *Evolution of karst: from prekarst to cessation*. Karst Research Institute ZRC SAZU, Postojna, 299–306.
- Zseni A., 2002b: Karrmezők talajainak vizsgálata magyarországi és angol területeken [Investigation of soils of karren fields in Hungarian and English karst]. *Karsztfejlődés* 7: 281–295.
- Zseni A., Goldie H., Bárány-Kevei I., 2003: Limestone pavements in Great Britain and the role of soil cover in their evolution. *Acta Carsologica* 32, 1: 57–67.
- Zseni A., Bárány-Kevei I., 2000: Nagy-Britannia mészkőjárdái és a talaj hatása azok fejlődésében [Limestone pavements of Great Britain and the influence of soil in the evolution of them]. *Karsztfejlődés* 5: 181–194.





Franco Cucchi Mick Day David Drew Wolfgang Dreybrodt  
Hiroyuki Enomoto Joan J. Fornós Franci Gabrovšek Angel Ginés  
Joaquín Ginés Helen S. Goldie Lluís Gómez-Pujol Andrew S. Goudie  
Ken G. Grimes Takehiko Haikawa Masahiko Higa Fabien Hobléa  
Stéphane Jaillet Naruhiko Kashima Georg Kaufmann Martin Knez Jurij  
Kunaver Fuyuan Liang Hong Liu Joyce Lundberg Giuliana Madonia  
Richard Maire Tihomir Marjanac Michel Monbaron Joan R. Mylroie  
John E. Mylroie Eisyo Ooshiro Arthur N. Palmer Dražen Perica  
Matija Perne Jean-Noël Salomon Ugo Sauro Tadej Slabe Linhua  
Song Tokumatsu Sunagawa Zenshin Tamashiro Gábor Tóth Kazuko  
Urushibara-Yoshino Márton Veress Heather Viles Peter Vincent  
Tony Waltham Andres Wildberger Paul W. Williams Anikó Zseni



<http://zalozba.zrc-sazu.si>



9 789612 541613

58.00 €